



*foods*

# The Health Benefits of the Bioactive Compounds in Foods

---

Edited by

Laura Jaime and Susana Santoyo

Printed Edition of the Special Issue Published in *Foods*

# **The Health Benefits of the Bioactive Compounds in Foods**



# The Health Benefits of the Bioactive Compounds in Foods

Editors

**Laura Jaime**

**Susana Santoyo**

MDPI • Basel • Beijing • Wuhan • Barcelona • Belgrade • Manchester • Tokyo • Cluj • Tianjin



*Editors*

Laura Jaime  
Universidad Autónoma de Madrid  
Spain

Susana Santoyo  
Universidad Autónoma de Madrid  
Spain

*Editorial Office*

MDPI  
St. Alban-Anlage 66  
4052 Basel, Switzerland

This is a reprint of articles from the Special Issue published online in the open access journal *Foods* (ISSN 2304-8158) (available at: [https://www.mdpi.com/journal/foods/special\\_issues/Health\\_Benefits](https://www.mdpi.com/journal/foods/special_issues/Health_Benefits)).

For citation purposes, cite each article independently as indicated on the article page online and as indicated below:

LastName, A.A.; LastName, B.B.; LastName, C.C. Article Title. *Journal Name* **Year**, *Volume Number*, Page Range.

**ISBN 978-3-0365-1156-6 (Hbk)**

**ISBN 978-3-0365-1157-3 (PDF)**

© 2021 by the authors. Articles in this book are Open Access and distributed under the Creative Commons Attribution (CC BY) license, which allows users to download, copy and build upon published articles, as long as the author and publisher are properly credited, which ensures maximum dissemination and a wider impact of our publications.

The book as a whole is distributed by MDPI under the terms and conditions of the Creative Commons license CC BY-NC-ND.

# Contents

About the Editors . . . . .	vii
<b>Laura Jaime and Susana Santoyo</b> The Health Benefits of the Bioactive Compounds in Foods Reprinted from: <i>Foods</i> <b>2021</b> , <i>10</i> , 325, doi:10.3390/foods10020325 . . . . .	1
<b>Qi Lu, Lu Li, Shujin Xue, De Yang and Shaohua Wang</b> Stability of Flavonoid, Carotenoid, Soluble Sugar and Vitamin C in ‘Cara Cara’ Juice during Storage Reprinted from: <i>Foods</i> <b>2019</b> , <i>8</i> , 417, doi:10.3390/foods8090417 . . . . .	5
<b>Patricio Orellana-Palma, Guisella Tobar-Bolaños, Nidia Casas-Forero, Rommy N. Zúñiga and Guillermo Petzold</b> Quality Attributes of Cryoconcentrated Calafate ( <i>Berberis microphylla</i> ) Juice during Refrigerated Storage Reprinted from: <i>Foods</i> <b>2020</b> , <i>9</i> , 1314, doi:10.3390/foods9091314 . . . . .	21
<b>Katarzyna Janda, Karolina Jakubczyk, Irena Baranowska-Bosiacka, Patrycja Kapczuk, Joanna Kochman, Ewa Rębacz-Maron and Izabela Gutowska</b> Mineral Composition and Antioxidant Potential of Coffee Beverages Depending on the Brewing Method Reprinted from: <i>Foods</i> <b>2020</b> , <i>9</i> , 121, doi:10.3390/foods9020121 . . . . .	41
<b>Eric Banan-Mwine Daliri, Fred Kwame Ofosu, Ramachandran Chelliah, Joong-Hark Kim, Jong-Rae Kim, Daesang Yoo and Deog-Hwan Oh</b> Untargeted Metabolomics of Fermented Rice Using UHPLC Q-TOF MS/MS Reveals an Abundance of Potential Antihypertensive Compounds Reprinted from: <i>Foods</i> <b>2020</b> , <i>9</i> , 1007, doi:10.3390/foods9081007 . . . . .	57
<b>Cong Teng, Zhenxing Shi, Yang Yao and Guixing Ren</b> Structural Characterization of Quinoa Polysaccharide and Its Inhibitory Effects on 3T3-L1 Adipocyte Differentiation Reprinted from: <i>Foods</i> <b>2020</b> , <i>9</i> , 1511, doi:10.3390/foods9101511 . . . . .	71
<b>Reda Derdak, Souraya Sakoui, Oana Lelia Pop, Carmen Ioana Muresan, Dan Cristian Vodnar, Boutaina Addoum, Romana Vulturar, Adina Chis, Ramona Suharoschi, Abdelaziz Soukri and Bouchra El Khalfi</b> Insights on Health and Food Applications of <i>Equus asinus</i> (Donkey) Milk Bioactive Proteins and Peptides—An Overview Reprinted from: <i>Foods</i> <b>2020</b> , <i>9</i> , 1302, doi:10.3390/foods9091302 . . . . .	87
<b>Amira Mohammed Ali and Hiroshi Kunugi</b> Apitherapy for Age-Related Skeletal Muscle Dysfunction (Sarcopenia): A Review on the Effects of Royal Jelly, Propolis, and Bee Pollen Reprinted from: <i>Foods</i> <b>2020</b> , <i>9</i> , 1362, doi:10.3390/foods9101362 . . . . .	105
<b>Qian-Qian Mao, Xiao-Yu Xu, Shi-Yu Cao, Ren-You Gan, Harold Corke, Trust Beta and Hua-Bin Li</b> Bioactive Compounds and Bioactivities of Ginger ( <i>Zingiber officinale</i> Roscoe) Reprinted from: <i>Foods</i> <b>2019</b> , <i>8</i> , 185, doi:10.3390/foods8060185 . . . . .	143

<b>Shiqi Yang, Wenlai Fan and Yan Xu</b> Melanoidins from Chinese Distilled Spent Grain: Content, Preliminary Structure, Antioxidant, and ACE-Inhibitory Activities In Vitro Reprinted from: <i>Foods</i> <b>2019</b> , <i>8</i> , 516, doi:10.3390/foods8100516 . . . . .	165
<b>Juan Antonio Nieto, Susana Santoyo, Marin Prodanov, Guillermo Reglero and Laura Jaime</b> Valorisation of Grape Stems as a Source of Phenolic Antioxidants by Using a Sustainable Extraction Methodology Reprinted from: <i>Foods</i> <b>2020</b> , <i>9</i> , 604, doi:10.3390/foods9050604 . . . . .	181
<b>Soad Taha, Ibrahim El-Sherbiny, Toshiki Enomoto, Aida Salem, Emiko Nagai, Ahmed Askar, Ghada Abady and Mahmoud Abdel-Hamid</b> Improving the Functional Activities of Curcumin Using Milk Proteins as Nanocarriers Reprinted from: <i>Foods</i> <b>2020</b> , <i>9</i> , 986, doi:10.3390/foods9080986 . . . . .	199
<b>Sara Ramos-Romero, Daniel Martínez-Maqueda, Mercè Hereu, Susana Amézqueta, Josep Lluís Torres and Jara Pérez-Jiménez</b> Modifications of Gut Microbiota after Grape Pomace Supplementation in Subjects at Cardiometabolic Risk: A Randomized Cross-Over Controlled Clinical Trial Reprinted from: <i>Foods</i> <b>2020</b> , <i>9</i> , 1279, doi:10.3390/foods9091279 . . . . .	213

## About the Editors

**Laura Jaime** (Ph.D. in Chemistry, Autonomous University of Madrid (UAM), 2000) is currently an Associate Professor at the Autonomous University of Madrid (UAM), where she develops her research within the Department of Production and Characterization of New Foods at the Institute of Food Science Research (CIAL), a combined institute of UAM and the Spanish Higher Scientific Research Council (CSIC). She is co-author of numerous research papers in international journals with high impact within the area of food science and technology. She has been involved in various national and international research projects on the development of functional ingredients and foods through a sustainable approach. Her research activities mainly include obtaining bioactive ingredients from natural and side streams sources, highlighting the design of extraction and purification processes of health food ingredients through advanced technologies, studying the biological activities of functional ingredients, conducting chemical analysis of bioactive extracts, and designing formulations that increase the *in vitro* bioaccessibility and/or bioavailability of these bioactive ingredients. She has also mentored many research projects of undergraduate and graduate students.

**Susana Santoyo** graduated in Pharmacy in 1991 at the University of Navarra, and in 1996, she received her Ph.D. degree at the same university. She completed her postdoctoral studies at the University of Paris VII (1996–1998). Currently, she is an Associate Professor at the Universidad Autónoma of Madrid in the Department of Applied Physical Chemistry (Food Science Section), where she has been developing her teaching and research activities for the last 18 years. In 2010, she joined the Institute in Food Science Research (CIAL). She has published more than 68 articles in International Journals, among them 29 in Q1 journals. As a researcher, she has participated in 13 national and European research projects. Seven of these projects were research and development (R&D) agreements with pharmaceutical companies. She is also co-author of four patents in the field of development of functional food ingredients, two of which are currently being used by pharmaceutical companies.



Editorial

# The Health Benefits of the Bioactive Compounds in Foods

Laura Jaime \* and Susana Santoyo \*

Institute of Food Science Research (CIAL), Universidad Autónoma de Madrid (CEI, UAM-CSIC),  
28049 Madrid, Spain\* Correspondence: laura.jaime@uam.es (L.J.); susana.santoyo@uam.es (S.S.); Tel.: +34-910017925 (L.J.);  
+34-910017926 (S.S.)**Keywords:** bioactive compounds; biological activities; isolation; analysis; mechanism of action; bioaccessibility; intestinal absorption; bioavailability

The health benefits of consuming certain foods have been commonly known since ancient times. However, the study of foods as a source of healthy bioactive compounds has been gaining interest over recent decades. At present, numerous research papers have been focused on the beneficial role played by certain food components in the close relationship between food intake and health status. In this sense, many foods, including fruits, vegetables, fish, seaweeds, herbs, etc., are known to be excellent sources of bioactive compounds such as carotenoids, phenolic compounds, terpenoids, fatty acids, peptides, and saponins, among others.

On the other hand, the development of new foods or nutraceuticals with health benefits is a current topic today and represents an appealing opportunity for the food and/or pharmaceutical industries. However, this launch of new products should be endorsed by strong scientific support on the health benefits attributable to the intake of these bioactive food ingredients. To this end, an enlightenment about the most suitable source of a specific bioactive compound is required. This study should include the most suitable sources of bioactive compounds, the development of the most sustainable extraction techniques, isolation, and also an accurate analysis of the bioactive compounds by using the most adequate techniques. Moreover, the biological activities of these compounds should be elucidated in vitro, in cells, and also in clinical trials. Studies focusing on changes during storage, the digestion process, intestinal absorption rates, bioaccessibility, bioavailability, biological mechanisms of action, or bioactivity of their metabolites are also required to establish the real contribution of these compounds to the health status.

Within this context, food is usually exposed to various temperatures throughout the food supply chain. Thus, research aimed at changes in bioactive compounds that occur during food storage at different temperatures is a topic of interest. In this context, Lu et al. [1] carried out a pilot study to investigate the changes of carotenoids, flavonoids, and vitamin C in a “Cara-Cara” juice during 16 weeks of storage at 4, 20, 30, and 40 °C. The results indicated that total flavonoids and carotenoids studied showed slight degradation at each temperature, while vitamin C degraded intensively, especially at 40 °C storage. Another work [2] also studied the bioactive compounds, antioxidant activity, and sensory analysis of a cryoconcentrated calafate (*Berberis microphylla*) juice during refrigerated storage. This study indicated that under a refrigerated storage time of 35 days, the cryoconcentrate samples retained bioactive compounds and the antioxidant components naturally presented in calafate juice.

On the other hand, food processing techniques could also be related with the amount of bioactive compounds present in foods. Thus, Janda et al. [3] determined the mineral content, antioxidant activity, and acidity of coffee beverages depending on the brewing technique. Their findings showed that the brewing method had a significant effect on the antioxidant potential, polyphenol content, and redox potential of the beverage obtained.



**Citation:** Jaime, L.; Santoyo, S. The Health Benefits of the Bioactive Compounds in Foods. *Foods* **2021**, *10*, 325. <https://doi.org/10.3390/foods10020325>

Academic Editor: Joana S. Amaral  
Received: 29 January 2021  
Accepted: 1 February 2021  
Published: 4 February 2021

**Publisher’s Note:** MDPI stays neutral with regard to jurisdictional claims in published maps and institutional affiliations.



**Copyright:** © 2021 by the authors. Licensee MDPI, Basel, Switzerland. This article is an open access article distributed under the terms and conditions of the Creative Commons Attribution (CC BY) license (<https://creativecommons.org/licenses/by/4.0/>).

Use of the AeroPress coffee maker was the brewing method that resulted in the highest content of health-promoting compounds in a coffee beverage. Besides, there are other processes such as enzyme treatment and fermentation of cereals that enhance the release of bound bioactive compounds and make them available for bioactivity. Authors of [4] found that enzyme-treated destarched rice samples with subsequent fermentation contained known antihypertensive phenolic compounds and peptides that make these samples a promising material for developing cheap antihypertensive foods.

Moreover, many foods have been described to possess different biological activities beyond their nourishing properties, linked to the presence of some constituents. In this Special Issue, the health benefits of donkey milk, quinoa, bee products, and ginger have been included. In that way, quinoa is known to contain some constituents (saponins or dietary fiber polysaccharides, among others) that exert an anti-obesity activity. Nevertheless, its mechanism of action needs to be ascertained. Teng et al. [5] characterized an anti-obesity polysaccharide from quinoa using gas chromatography coupled to mass spectrometry, the structure of which was confirmed by nuclear magnetic resonance. Moreover, they demonstrated that this fructose- and glucose-based polysaccharide inhibited 3T3-L1 adipocyte differentiation by suppressing specific genes' expression. In other work [6], *Equus asinus* is presented as a novel and improved alternative to cow's milk due to its great similarity with human milk and its low allergenic properties. However, the properties of donkey milk are not limited to its provision of valuable nutrients, as a wide range of biological activities such as antioxidant, antimicrobial, anti-tumoral, anti-proliferative and anti-diabetic activities compared to other sources of milk have been described, especially associated to whey protein fraction. Moreover, these promising activities might be used by the food industry for the production of novel foods with healthy properties, contributing to immune system stimulation, regulation of intestinal flora, or prevention of inflammatory-based diseases. Regarding foods based on bee products such as royal jelly, propolis, or bee pollen, they have been used since a long time ago to ameliorate some chronic physical states involving increased muscle weakness. In that respect, Ali and Kunugi [7] reviewed that numerous mechanisms at many different levels could be related to a beneficial effect on sarcopenia, including an improvement of inflammation and oxidative damage, enhancement of satellite stem cell responsiveness and muscle blood supply, or promotion of peripheral neuronal regeneration, without ruling out other promising mechanisms. Mao et al. [8] present an up-to-date review concerning the biological activities of ginger, a commonly used spice, that are mainly related to the presence of phenolic compounds such as gingerol and shogaols. In this sense, there are numerous activities that have been described for this spice, from the most known antioxidant or anti-inflammatory activities to anti-diabetic, anti-obesity, or anti-emetic activities. Moreover, the different mechanisms of action to exert these health benefits have been illustrated in this review.

Currently, the valorization of by-products derived from food processing is considered a hot topic. Thus, distilled spent grain, the main residue of baijiu making, is presented as a potential source of melanoidins with antioxidant and antihypertensive activity [9]. In this context, the sequential extraction of melanoidins using water and NaOH at different extraction conditions from dry distilled spent grain, and the subsequent ultrafiltration of the most enriched fraction, makes up a useful technique to obtain fractions enriched in melanoidins with different molecular weights and activities. Melanoidins of high molecular weight (>100 kDa) showed a high antioxidant activity, whereas low molecular weight (3–10 kDa) melanoidins exhibited a high antihypertensive activity against the angiotensin-converting enzyme. Nieto et al. [10] proposed the use of pressurized liquid extraction with green solvents (ethanol:water mixtures) in order to use grape stems as a source of antioxidant phenolics. They optimized the extraction conditions by using an experimental design along with response surface methodology to obtain an extract with high antioxidant activity and high phenolic content. The results pointed out the presence of 42 phenolic compounds, mainly polymer procyanidins, in the optimal extract, where the antioxidant activity was mainly attributed to the presence of the latter. Therefore, this

study valorizes this side stream as a source of natural and antioxidant phenolics as part of a sustainable food system.

On the other hand, the encapsulation of bioactive compounds as a strategy to improve their solubility and preserve their chemical integrity and successful delivery in physiological targets has been proposed recently. In that regard, Taha et al. [11] evaluate the efficacy of different milk proteins as nanocarriers for curcumin. Their results revealed that the developed nanoparticles presented an antimicrobial activity much higher compared to curcumin and the native milk proteins.

Nowadays, the colonic microbiota has emerged as a factor in the relationship between diet and health, since increasing evidence connects imbalances in the gut microbiota (dysbiosis) with pathologies. Consequently, there is growing interest in exploring the potential modifications of the gut microbiota by bioactive compounds in foods and their relationship with some pathologies. The study carried out by Ramos-Romero et al. [12] explored the potential modifications in the microbiota profile induced by grape pomace (a product rich in both dietary fiber and polyphenols) supplementation. The authors explored the possible ways in which grape pomace supplementation might have differentially induced a reduction in insulin secretion in responder individuals—specifically changes in representative gut bacterial populations. However, the results obtained in this study indicated that the decrease in insulin levels in subjects at cardiometabolic risk upon supplementation appeared not to be related to modifications in the major subgroups of gut microbiota.

In conclusion, this Special Issue comprises nine original research papers and three review articles addressing recent advances in the health benefits of the bioactive compounds of foods, including new sources of bioactive compounds, valorization of side streams as sources of bioactive compounds, molecular mechanisms of these bioactive compounds, their analysis, isolation, food processing influence on bioactive compounds of food, or the influence of intestinal microbiota, among other related aspects.

**Author Contributions:** Conceptualization, L.J. and S.S.; validation, L.J. and S.S.; resources, L.J. and S.S.; writing—original draft preparation, L.J. and S.S.; writing—review and editing, L.J. and S.S.; visualization, L.J. and S.S.; supervision, L.J. and S.S.; funding acquisition, L.J. and S.S. All authors have read and agreed to the published version of the manuscript.

**Funding:** Authors gratefully recognize the Spanish Ministry of Science and Innovation for funding project PDI2019-110183RB-C22/AEI/10.13039/501100011033 within which this editorial has been prepared.

**Institutional Review Board Statement:** Not applicable.

**Informed Consent Statement:** Not applicable.

**Data Availability Statement:** Not applicable.

**Conflicts of Interest:** The authors declare no conflict of interest.

## References

- Lu, Q.; Li, L.; Xue, S.; Yang, D.; Wang, Y. Stability of Flavonoid, Carotenoid, Soluble Sugar and Vitamin C in 'Cara Cara' Juice during Storage. *Foods* **2019**, *8*, 417. [[CrossRef](#)] [[PubMed](#)]
- Orellana-Palma, P.; Tobar-Bolaños, G.; Casas-Forero, N.; Zúñiga, R.N.; Petzold, G. Quality Attributes of Cryoconcentrated Calafate (*Berberis microphylla*) Juice during Refrigerated Storage. *Foods* **2020**, *9*, 1314. [[CrossRef](#)] [[PubMed](#)]
- Janda, K.; Jakubczyk, K.; Baranowska-Bosiacka, I.; Kapczuk, P.; Kochman, J.; Rębacz-Marón, E.; Gutowska, I. Mineral Composition and Antioxidant Potential of Coffee Beverages Depending on the Brewing Method. *Foods* **2020**, *9*, 121. [[CrossRef](#)] [[PubMed](#)]
- Daliri, E.B.-M.; Ofosu, F.K.; Chelliah, R.; Kim, J.-H.; Kim, J.-R.; Yoo, D.; Oh, D.-H. Untargeted Metabolomics of Fermented Rice Using UHPLC Q-TOF MS/MS Reveals an Abundance of Potential Antihypertensive Compounds. *Foods* **2020**, *9*, 1007. [[CrossRef](#)] [[PubMed](#)]
- Teng, C.; Shi, Z.; Yao, Y.; Ren, G. Structural Characterization of Quinoa Polysaccharide and Its Inhibitory Effects on 3T3-L1 Adipocyte Differentiation. *Foods* **2020**, *9*, 1511. [[CrossRef](#)] [[PubMed](#)]
- Derdak, R.; Sakoui, S.; Pop, O.L.; Muresan, C.I.; Vodnar, D.C.; Addoum, B.; Vulturar, R.; Chis, A.; Suharoschi, R.; Soukri, A.; et al. Insights on Health and Food Applications of Equus asinus (Donkey) Milk Bioactive Proteins and Peptides—An Overview. *Foods* **2020**, *9*, 1302. [[CrossRef](#)] [[PubMed](#)]

7. Ali, M.A.; Kunugi, H. Apitherapy for Age-Related Skeletal Muscle Dysfunction (Sarcopenia): A Review on the Effects of Royal Jelly, Propolis, and Bee Pollen. *Foods* **2020**, *9*, 1362. [[CrossRef](#)] [[PubMed](#)]
8. Mao, Q.-Q.; Xu, X.-Y.; Cao, S.-Y.; Gan, R.-Y.; Corke, H.; Beta, T.; Li, H.-B. Bioactive Compounds and Bioactivities of Ginger (*Zingiber officinale* Roscoe). *Foods* **2019**, *8*, 185. [[CrossRef](#)] [[PubMed](#)]
9. Yang, S.; Fan, W.; Xu, Y. Melanoidins from Chinese Distilled Spent Grain: Content, Preliminary Structure, Antioxidant, and ACE-Inhibitory Activities in Vitro. *Foods* **2019**, *8*, 516. [[CrossRef](#)] [[PubMed](#)]
10. Nieto, J.A.; Santoyo, S.; Prodanov, M.; Reglero, G.; Jaime, L. Valorisation of Grape Stems as a Source of Phenolic Antioxidants by Using a Sustainable Extraction Methodology. *Foods* **2020**, *9*, 604. [[CrossRef](#)] [[PubMed](#)]
11. Taha, S.; El-Sherbiny, I.; Enomoto, T.; Aida Salem, S.; Nagai, E.; Askar, A.; Abady, G.; Abdel-Hamid, M. Improving the Functional Activities of Curcumin Using Milk Proteins as Nanocarriers. *Foods* **2020**, *9*, 986. [[CrossRef](#)] [[PubMed](#)]
12. Ramos-Romero, S.; Martínez-Maqueda, D.; Hereu, M.; Amézqueta, S.; Torres, J.L.; Pérez-Jiménez, J. Modifications of Gut Microbiota after Grape Pomace Supplementation in Subjects at Cardiometabolic Risk: A Randomized Cross-Over Controlled Clinical Trial. *Foods* **2020**, *9*, 1279. [[CrossRef](#)]

Article

# Stability of Flavonoid, Carotenoid, Soluble Sugar and Vitamin C in ‘Cara Cara’ Juice during Storage

Qi Lu <sup>1,2</sup>, Lu Li <sup>1</sup>, Shujin Xue <sup>1</sup>, De Yang <sup>1</sup> and Shaohua Wang <sup>1,\*</sup>

<sup>1</sup> Institute of Agro-Products Processing and Nuclear Agricultural Technology, Hubei Academy of Agricultural Sciences, Wuhan 430064, China; luqihzau@126.com (Q.L.); Lulilu2662@163.com (L.L.); xsj2000@163.com (S.X.); yde0537@163.com (D.Y.)

<sup>2</sup> College of Food Science and Technology, Huazhong Agricultural University, Wuhan 430070, China

\* Correspondence: shaohuawangfood@sina.com

Received: 5 August 2019; Accepted: 10 September 2019; Published: 16 September 2019

**Abstract:** In view of understanding the stability of sterilized ‘Cara Cara’ juice during storage, the changes of specific quality parameters (flavonoid, carotenoid, vitamin C, soluble sugar and antioxidant activities) of ‘Cara Cara’ juice were systematically investigated over the course of 16 weeks in storage at 4, 20, 30 and 40 °C. Total flavonoid and carotenoid indexes showed slight degradation at each temperature, while vitamin C and soluble sugar degraded intensively, especially at 40 °C storage with a great amount of HMF (5-hydroxymethylfurfural) accumulated. There were 29 carotenoids detected during storage, including carotenes and carotenoid esters. Carotenes were kept stable, while the degradations of carotenoid esters were fitted by biexponential function. Carotenoid ester group 2 contained epoxy structures that quickly decreased in the first four weeks at all storage temperatures, while the ester group 1 (belonged to  $\beta$ -cryptoxanthin ester) was degraded gradually. The 13- or 15-cis-lycopene, isomerized from all-(trans)-lycopene, increased with storage time at each temperature. Total flavonoid and carotenoid indexes in stored ‘Cara Cara’ juice were positively correlated with hydrophilic and lipophilic antioxidant abilities.

**Keywords:** ‘Cara Cara’ juice; storage; hydrophilic and lipophilic antioxidant; carotenoid; flavonoid; degradation

## 1. Introduction

Citrus juice possesses an attractive natural color, with a sweet and sour taste, making it popular with food consumers around the world [1]. Intake of citrus juice is confirmed to be effective for prevention of human chronic-degenerative diseases [2,3], and micronutrients of carotenoids, flavonoids and ascorbic acid are responsible for the physiological function of citrus juice [4,5]. Orange cv. ‘Cara Cara’, a bud mutation of navel orange (*Citrus sinensis* L. Osbeck) originating in Venezuela in the 1980s, displays an attractive bright red color due to the accumulation of lycopene [6], and it has been widely planted in China [7]. Changes of food sensorial and nutritional quality during storage limits the date of food consumption. ‘Cara Cara’ juice products have not been commercially available in China, and the nutritional changes of ‘Cara Cara’ juice during storage have not been investigated.

Citrus juice products are usually exposed to various temperatures in the food supply chain. It is necessary to investigate the changes of carotenoid, flavonoid and ascorbic acid during storage at different temperatures, since these components play an important role in the healthy function of citrus juice. Rapisarda reported that the flavanone in sweet orange juice decreased about 50% after storage at 4 °C for 20 days [8], while Klimczak found that the flavanone in commercial pure orange juice was rather stable during storage with only minor changes observed [9]. Apigenin-6,8-di-C-glucoside, narirutin-4'-O-glucoside, narirutin, hesperidin and didymi were confirmed as typical flavonoids in

'Cara Cara' juice [10]. There is little information on the influence of storage temperature and duration on flavonoid content in 'Cara Cara' juice.

Due to the complex composition of carotenoids in oranges, the saponification procedure has typically been applied to simplify the analysis, by transferring esterified carotenoids into free carotenoids [11,12]. The stability of carotenoids can be influenced by temperature, time, and the availability of light and oxygen [13]. Previous studies have mainly focused on the degradation of free carotenoids during storage [12,14], while the change of carotenoid esters in citrus juice during storage has not been reported. There have been 19 carotenoid esters inferred in 'Cara Cara' fruit, with the 9-cis-violaxanthin ester confirmed as the dominant component [7], and esterified  $\beta$ -cryptoxanthin considered to be the most stable ester during thermal treatment [15]. The change of free and esterified carotenoids in 'Cara Cara' juice needs to be further explored.

Non-enzymatic browning, frequently observed in citrus juice, plays an important role in the color, flavor and nutritional quality of the stored citrus juice [1]. Non-enzymatic browning is also strongly connected to the degradation of ascorbic acid and sugar, with HMF (5-hydroxymethylfurfural) detected as the indicator [1]. A previous report confirmed that vitamin C in citrus juice was affected by the storage temperature and duration [9]. However, changes of flavonoid, carotenoids, vitamin C and sugar in 'Cara Cara' juice during storage at different temperatures have been not investigated, especially in terms of carotenoid esters.

We, therefore, carried out a pilot study to investigate the changes of carotenoid, flavonoid and vitamin C in 'Cara Cara' juice during 16 weeks of storage at different temperatures. In addition, the lipophilic and hydrophilic antioxidant abilities of stored 'Cara Cara' juice were analyzed.

## 2. Materials and Methods

### 2.1. Sample Preparation

'Cara Cara' juice (15.3 °Brix, pH 3.70, titratable acidity 0.93%) was obtained from commercial matured fruit of Orange cv. Cara Cara, harvested from the Fujian province of China in December 2017. The fresh 'Cara Cara' fruit (50 kg) was immediately peeled and squeezed with a fruit extruder. Half of the crude juice was stored at  $-80\text{ }^{\circ}\text{C}$  and half was directly subjected to a rapid thermal sterilization. Specifically, 'Cara Cara' juice was boiled in a stainless-steel container with an electronic thermometer (F1, invisible, Guangdong, China) monitoring the internal temperature of the 'Cara Cara' juice ( $98\text{ }^{\circ}\text{C}$ , 16 s). The sterilized juice was immediately filled into glass bottles (50 mL). These bottles and their caps were disinfected before use. After cooling, the juice was stored at 4, 20, 30 and  $40\text{ }^{\circ}\text{C}$  for 16 weeks without lights. At each sampling time, three bottles of juice were taken and frozen at  $-80\text{ }^{\circ}\text{C}$  until use.

### 2.2. Chemicals and Reagents

The standards of narirutin, hesperidin, didymin, lycopene,  $\beta$ -carotene, fructose, glucose and sucrose were acquired from Yuanye Bio-Technology Co., Ltd (Shanghai, China). Phytoene and violaxanthin were purchased from CaroteNature (Lupsingen, Switzerland) and Sigma (St. Louis, MO, USA), respectively. ABTS<sup>+</sup> (2,2'-azino-bis(3-ethylbenzothiazoline-6-sulfonic acid)) and 2,2-diphenyl-1-picrylhydrazyl (DPPH) were purchased from Yuanye Bio-Technology Co., Ltd (Shanghai, China). High performance liquid chromatography purity solvents, including methyl tert-butyl ether (MTBE), methanol and hexane were obtained from Thermo Fisher Scientific (Leicestershire, UK). Other analytical grade chemicals, such as ethanol, hexane and sodium hydroxide were bought from Sinopharm Chemical Reagent Co., Ltd (Shanghai, China).

### 2.3. Extraction of Carotenoid from 'Cara Cara' Juice

The extraction of carotenoids from 'Cara Cara' juice was performed according to our previous study [15]. Briefly, 'Cara Cara' juice (10 mL) was homogenized with 10 mL ethanol/hexane (4:3, *v/v*, 0.1% butylated hydroxytoluene) by stirring at 700 rpm for 0.5 h. The mixture was subsequently centrifuged

(19,360× g, 4 min) to obtain the liquid phase. After extraction of the residue twice, all the liquid phases were combined, and then washed by separatory funnel to collect the non-polar supernatants. The obtained supernatant was evaporated to dryness, then re-dissolved by methyl tert-butyl ether and filtered (0.22 μm polytetrafluoroethylene filter) for the analysis of carotenoids.

#### 2.4. Extraction of Flavonoid from 'Cara Cara' Juice

Flavonoids in 'Cara Cara' juice were extracted based on our previous study, with minor modification [15]. Briefly, 'Cara Cara' juice (1 mL) was homogenized with the extract solvent (85% aqueous ethanol containing 0.1% HCl, 4 mL) by an ultrasonic cleaner (KQ-500E, Kun Shan Ultrasound Instrument Co., Jiangsu, China) at 40 kHz for 30 min. The mixture was centrifuged (9680× g for 5 min) and filtered through 0.22 μm PTFE filter for further analysis.

#### 2.5. Antioxidant Assays

Based on a previous study [16], the antioxidant abilities of hydrophilic and lipophilic extracts in 'Cara Cara' juice were measured by DPPH and ABTS<sup>+</sup> assays. The DPPH activity was evaluated as previously described [10], and the final results were expressed as μmol ascorbic acid equivalent (AAE) per milliliter 'Cara Cara' juice (μmol AAE/mL,  $y = 0.0012x + 0.0438$ ,  $R^2 = 0.9902$ ). The ABTS<sup>+</sup> assay was conducted according to the existing protocol [17], while the final results were expressed as μmol Trolox equivalent (TE) per milliliter 'Cara Cara' juice (μmol TE/mL,  $y = 0.3025x + 0.076$ ,  $R^2 = 0.9807$ ). The hydrophilic and lipophilic capacities of stored 'Cara Cara' juice were calculated every four weeks (0, 4, 8, 12, 16 weeks).

#### 2.6. Analysis of Carotenoids and Flavonoids in 'Cara Cara' Juice

The analysis of carotenoids was performed on HPLC (2695 system, Waters Corp., Milford, MA, USA) using a C<sub>30</sub> reversed phase column (250 × 4.6 mm, 5 μm; YMC, Inc. Wilmington, NC, USA) and flavonoids were separated on the Waters Acquity UPLC system (Waters Corp., Milford, MA, USA) with a BEH C<sub>18</sub> column (100 mm × 2.1 mm, 1.7 μm). Their chromatographic separation, identification and quantification procedures were conducted based on our previous study [15]. The content of flavonoids in 'Cara Cara' juice during storage were analyzed every four weeks (0, 4, 8, 12, 16 weeks), and the sampling times for carotenoids quantification in stored 'Cara Cara' juice were set at 0, 2, 4, 6, 8, 12 and 16 weeks.

#### 2.7. Ascorbic Acid Measurement

The ascorbic acid was determined by the titration method, using 2,6-dichlorophenolindophenol dye [18].

#### 2.8. Sugar Measurement

Modified from a previous study [19], the soluble sugar in 'Cara Cara' juice was determined by HPLC (2695 system, Waters Corp., Milford, MA, USA) with 2414 refractive index detector (Waters, Milford, MA, USA), and an inertsil NH<sub>2</sub> column (250 × 4.6 mm, 5 μm; Dikma Technologies Inc., Beijing, China) was used for sugar separation. Zinc acetate solution (21.9%, 0.1 mL) and potassium ferrocyanide solution (10.6%, 0.1 mL) were added in 'Cara Cara' juice (1 mL) to precipitated proteins. Afterwards, distilled water was added to 2 mL, and centrifuged to obtain the supernatant for HPLC analysis. Mobile phase was acetonitrile/water (75/25) and the HPLC operating conditions were set as: injection volume 20 μL; column temperature 40 °C; detector temperature 40 °C; flow rate 1 mL/min. The contents of sugar in 'Cara Cara' juice during storage were detected every two weeks (0, 2, 4, 6, 8, 10, 12, 14, 16 weeks).

## 2.9. Statistical Analysis

All the experiments were conducted in triplicate, and the data were presented as mean  $\pm$  standard deviation of triplicate independent experiments. One-way analysis of variance (ANOVA) was applied to compare the means, and the differences between the means were analyzed by Duncan's multiple range tests at a significance level of 0.05. Correlation analysis of the matrix was analyzed by Pearson correlation coefficient (*t*-test). All statistical analyses were processed by IBM SPSS Statistics version 20.0. Carotenoid compounds were quantified in 'Cara Cara' juice during the 16 weeks of storage at different temperatures. The data were arranged to have carotenoid components at different temperatures as objects (rows) and storage weeks as variables (columns) and processed by principal component analysis (XLSTAT 2016, Addinsoft, New York, NY, USA). The results were presented with graphs plotting the projections of the units onto the components, and the loadings of the variables. Correlation between variables was evaluated by Pearson's correlation coefficient [20].

## 3. Results and Discussion

### 3.1. Changes of Flavonoids in 'Cara Cara' Juice

Based on our previous study [10,15], flavonoids were confirmed to be the dominant phenolic compounds in 'Cara Cara' juice, including apigenin-6,8-di-C-glucoside, narirutin-4'-O-glucoside, narirutin, hesperidin and didymin. The content changes of individual flavonoids are shown in Table 1. Compared with a previous study [21], the contents of narirutin and hesperidin reported in this study were relatively higher. Each individual flavonoid was not significantly changed during storage at 4 °C. Didymin and narirutin were stable with no significant decrease observed at all storage temperatures, while other flavonoids (apigenin-6,8-di-C-glucoside, narirutin-4'-O-glucoside, hesperidin) were significantly degraded during storage at 20, 30 and 40 °C. The degradation of flavonoids in fruit juice was probably associated with the peroxidase activity, which might not be completely inactive by sterilization [22].

**Table 1.** Changes in the content of flavonoids ( $\mu\text{g/mL}$ ) in 'Cara Cara' juice during 16 weeks of storage at different temperatures.

Weeks	Apigenin-6,8-di-C-Glucoside	Narirutin-4'-O-Glucoside	Narirutin	Hesperidin	Didymin	Total Flavonoid Index
4 °C						
0	30.37 $\pm$ 2.47 a	30.43 $\pm$ 1.69 a	140.62 $\pm$ 6.47 a	620.22 $\pm$ 22.86 a	76.15 $\pm$ 3.24 a	897.79 $\pm$ 36.73 a
4	26.46 $\pm$ 0.48 a	27.41 $\pm$ 1.93 a	137.64 $\pm$ 12.29 a	618.98 $\pm$ 29.43 a	76.45 $\pm$ 2.67 a	886.94 $\pm$ 46.80 a
8	27.48 $\pm$ 1.36 a	26.77 $\pm$ 2.38 a	136.84 $\pm$ 13.91 a	601.63 $\pm$ 16.38 a	76.16 $\pm$ 5.33 a	868.88 $\pm$ 39.39 a
12	25.49 $\pm$ 1.56 a	25.93 $\pm$ 2.58 a	134.51 $\pm$ 6.17 a	583.72 $\pm$ 5.90 a	74.34 $\pm$ 3.85 a	843.99 $\pm$ 20.06 a
16	25.04 $\pm$ 0.47 a	25.52 $\pm$ 1.42 a	129.25 $\pm$ 4.35 a	567.65 $\pm$ 13.95 a	72.91 $\pm$ 1.34 a	820.37 $\pm$ 21.53 a
20 °C						
0	30.37 $\pm$ 2.47 a	30.43 $\pm$ 1.69 a	140.62 $\pm$ 6.47 a	620.22 $\pm$ 22.86 a	76.15 $\pm$ 3.24 a	897.79 $\pm$ 36.73 a
4	25.63 $\pm$ 2.35 ab	26.86 $\pm$ 3.25 ab	136.82 $\pm$ 4.57 a	614.16 $\pm$ 8.56 ab	75.28 $\pm$ 4.47 a	878.75 $\pm$ 23.20 a
8	25.35 $\pm$ 1.30 ab	24.66 $\pm$ 0.92 ab	133.32 $\pm$ 1.82 a	592.5 $\pm$ 17.68 ab	72.73 $\pm$ 2.45 a	848.56 $\pm$ 24.17 a
12	23.37 $\pm$ 0.53 b	24.65 $\pm$ 0.62 ab	125.89 $\pm$ 10.60 a	574.42 $\pm$ 10.99 ab	74.45 $\pm$ 1.34 a	822.78 $\pm$ 24.08 a
16	21.25 $\pm$ 1.24 b	21.77 $\pm$ 1.45 b	126.78 $\pm$ 5.32 a	556.75 $\pm$ 12.03 b	71.42 $\pm$ 1.38 a	797.95 $\pm$ 21.42 a
30 °C						
0	30.37 $\pm$ 2.47 a	30.43 $\pm$ 1.69 a	140.62 $\pm$ 6.47 a	620.22 $\pm$ 22.86 a	76.15 $\pm$ 3.24 a	897.79 $\pm$ 36.73 a
4	27.33 $\pm$ 3.03 a	26.35 $\pm$ 1.65 ab	133.14 $\pm$ 6.59 a	603.28 $\pm$ 17.21 ab	74.15 $\pm$ 1.27 a	864.25 $\pm$ 29.75 a
8	26.25 $\pm$ 1.73 a	27.06 $\pm$ 1.25 ab	128.52 $\pm$ 12.45 a	569.28 $\pm$ 8.79 ab	73.10 $\pm$ 5.83 a	824.21 $\pm$ 30.05 a
12	23.71 $\pm$ 0.66 a	22.91 $\pm$ 0.92 b	121.33 $\pm$ 5.08 a	567.69 $\pm$ 10.58 ab	73.92 $\pm$ 0.75 a	809.56 $\pm$ 17.99 a
16	22.35 $\pm$ 2.62 a	23.26 $\pm$ 2.98 b	122.57 $\pm$ 9.82 a	550.59 $\pm$ 16.56 b	70.70 $\pm$ 3.23 a	789.47 $\pm$ 35.21 a
40 °C						
0	30.37 $\pm$ 2.47 a	30.43 $\pm$ 1.69 a	140.62 $\pm$ 6.47 a	620.22 $\pm$ 22.86 a	76.15 $\pm$ 3.24 a	897.79 $\pm$ 36.73 a
4	24.63 $\pm$ 1.45 ab	26.19 $\pm$ 1.55 ab	131.68 $\pm$ 10.37 a	594.84 $\pm$ 14.22 ab	74.07 $\pm$ 4.63 a	851.41 $\pm$ 32.22 a
8	25.48 $\pm$ 0.93 ab	26.58 $\pm$ 1.12 ab	132.44 $\pm$ 4.75 a	579.33 $\pm$ 15.21 ab	72.25 $\pm$ 2.24 a	836.08 $\pm$ 24.25 a
12	23.36 $\pm$ 1.23 b	24.88 $\pm$ 1.69 ab	130.66 $\pm$ 8.46 a	570.12 $\pm$ 11.13 ab	73.33 $\pm$ 1.68 a	822.35 $\pm$ 24.19 a
16	23.59 $\pm$ 2.43 ab	24.09 $\pm$ 1.35 b	127.59 $\pm$ 10.68 a	552.17 $\pm$ 12.54 b	71.29 $\pm$ 3.36 a	798.73 $\pm$ 30.36 a

Values are expressed as mean  $\pm$  SD,  $n = 3$ . Values followed by different letters in the columns are significantly different (Duncan's multiple range tests,  $p < 0.05$ ). Total flavonoid index represents the sum of individual quantified flavonoid concentrations.

HMF eluted with flavonoids on UPLC was only detected at 40 °C storage, with a slow accumulation in the first 12 weeks ( $y = 0.006x + 0.012$ ,  $R^2 = 0.778$ ) and a rapid increase was found in the last four weeks ( $y = 0.071x + 0.833$ ,  $R^2 = 0.871$ ), with the final content reaching 285.74 µg/mL. HMF is generated from the decomposition of vitamin C or sugar degradation, and it is typically used to evaluate the deterioration severity of juice [23,24].

### 3.2. The Changes of Carotenoids in ‘Cara Cara’ Juice

#### 3.2.1. Carotenoid Composition

Citrus was reported as a natural carotenoids source [25]. A total of 29 peaks were detected by HPLC-DAD (Figure 1), and they were identified according to our previous studies [7,15]. Peaks 1 to 27 existed in the sterilized ‘Cara Cara’ juice before storage, and they were inferred as mutatoxanthin, zeaxanthin, β-cryptoxanthin, luteoxanthin-C14:0, 9-cis-violaxthin-C18:1, ζ-carotene, violaxthin-C16:0, luteoxanthin-C16:0, β-carotene, unknown ester, 9-cis-antheraxanthin-C16:0, 9-cis-violaxthin-C12:0-C14:0, β-cryptoxanthin-C12:0, β-cryptoxanthin-C16:1, 9-cis-violaxthin-C14:0-C14:0, β-cryptoxanthin-C14:0, 13- or 15-cis-β-cryptoxanthin-C18:1, a mixture of 9-cis-violaxthin-C14:0-C16:0 and 9-cis-violaxthin-C16:0-C18:1, 13- or 15-cis-lycopene, β-cryptoxanthin-C16:0, antheraxanthin-C14:0-C16:0, 9-cis-antheraxanthin-C16:0-C16:0, lycopene, phytoene, cis-phytofluene 1, cis-phytofluene 2 and cis-phytofluene 3, respectively. Peaks 28 and 29 were the newly formed compounds, in trace amounts, during storage at 40 °C for 8 weeks, and they were identified as 13- or 15-cis-β-cryptoxanthin and cis-phytofluene 4, based on their mass spectrometry, elution order and ultraviolet–visible spectra [15].

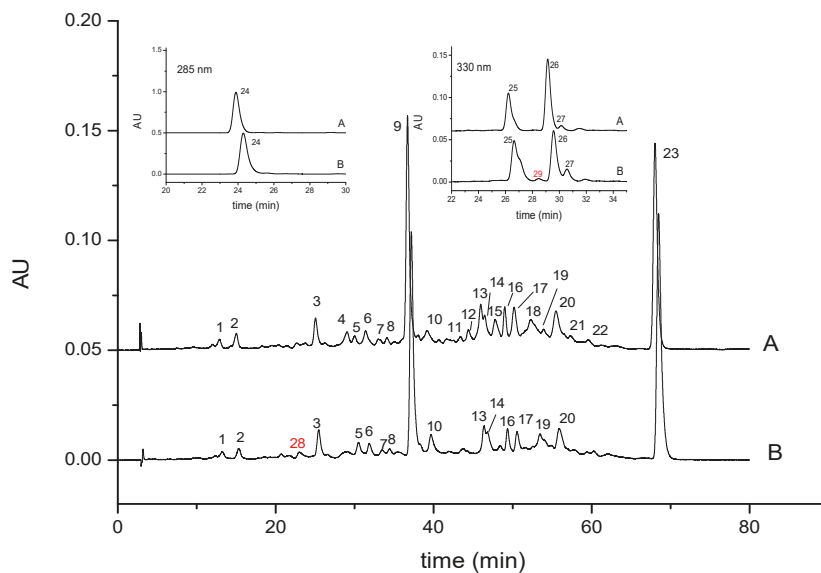


**Figure 1.** HPLC chromatograms (450 nm) of carotenoids detected in ‘Cara Cara’ juice before (A) and after 16 weeks of storage at 40 °C (B); Peaks 24–29 displayed no significant absorbance at 450 nm, while distinct absorption was detected at 285 nm (peak 24) and 350 nm (peak 25–29). AU represents the absorbance unit of carotenoid.

It was confirmed that β-cryptoxanthin esters were more stable than their corresponding free forms [26], whereas epoxy-carotenoid esters were liable to degrade in orange juice, since 5,6-epoxy

xanthophylls could be triggered into their 5,8-epoxy counterparts with a trace amount of acid [25,26]. Changes of carotenoids in 'Cara Cara' juice could be observed by comparing the HPLC chromatograms before and after the storage. Several epoxy-carotenoid esters (peaks 4, 11, 12, 15, 18, 21 and 22; luteoxanthin-C14:0, 9-cis-antheraxanthin-C16:0, 9-cis-violaxthin-C12:0-C14:0, 9-cis-violaxthin-C14:0-C14:0, a mixture of 9-cis-violaxthin-C14:0-C16:0 and 9-cis-violaxthin-C16:0-C18:1, antheraxanthin-C14:0-C16:0 and 9-cis-antheraxanthin-C16:0-C16:0) disappeared completely during the storage. The absence of epoxy-carotenoid esters in 'Cara Cara' juice was correlated with its long storage period [25]. Carotenoid esters in 'Cara Cara' juice were classified in different groups to simplify their quantification. Briefly,  $\beta$ -cryptoxanthin esters including peaks 13, 14, 16, 17 and 20 were categorized as ester group 1; epoxy carotenoid esters including peaks 4, 5, 7, 8, 11, 12, 15, 18, 21 and 22 were sorted as ester group 2; Peak 10 disappeared after saponification procedure, but its structure could not be inferred by MS fragments and UV-Vis spectra. Therefore, peak 10 was defined as unknown ester and was classified as ester group 3. The content of carotenoids in 'Cara Cara' juice during storage are presented in the Supplementary Materials (Table S1).

### 3.2.2. Carotenoid Degradation

The total carotenoid index in the sterilized 'Cara Cara' juice before storage was  $309.06 \pm 11.28 \mu\text{g/mL}$ , and the dominate compound was phytoene (69.78%), followed by total phytofluene (19.98%), carotenoid esters (4.15%),  $\beta$ -carotene (3.39%), lycopene (1.69%), and others (1.01%). The total carotenoids showed a declining trend at all storage temperatures, but their degradations did not reach a significant level. Carotenes of phytoene,  $\beta$ -carotene and lycopene were kept stable during storage, while all-trans-phytofluenes and cis-phytofluenes were irregularly fluctuated. Matrix protection might have been responsible for the stability of the carotenes in 'Cara Cara' juice [15,27,28]. Carotenoid ester, especially ester group 2, decreased dramatically during storage, and this might be related to their unstable xanthophyl structure which could be easily isomerized and degraded. The content changes of ester group 1 and ester group 2 in 'Cara Cara' juice are presented in Figure 2. Their degradation was fitted by biexponential function (Equation (1)) and the detailed kinetic parameters are presented in the Supplementary Materials (Figures S1 and S2).

$$y_t = y_\infty + A_1 \exp(-\alpha t) + A_2 \exp(-\beta t) \quad (1)$$

$y_t$ , is the carotenoid concentration at real time;  $y_\infty$ , is the theoretical concentration of carotenoid at infinite time.  $A_1$  and  $A_2$  represent the pre-exponential factors;  $\alpha$  and  $\beta$ , are the observed rate constants for fast and slow degradation. Biexponential degradation of carotenoid indicated both irreversible (degraded into volatiles or epoxides) and reversible (isomerization) degradation were involved, and this degradation form was also observed during thermal treatment of carotenoid juices [15,29]. Ester group 2 was quickly decreased in the first four weeks at all storage temperatures (Figure 2), while ester group 1 was degraded gradually. Therefore, the storage time of 'Cara Cara' juice could be estimated by combining the degrading rates of ester group 1 and ester group 2 at each temperature, and this issue will be explored in our future research.

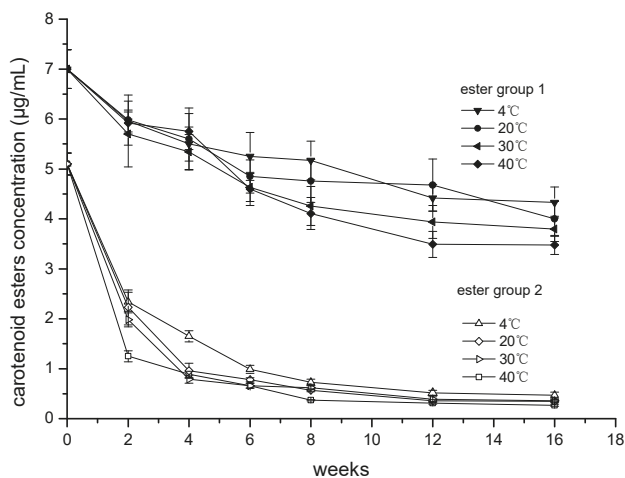
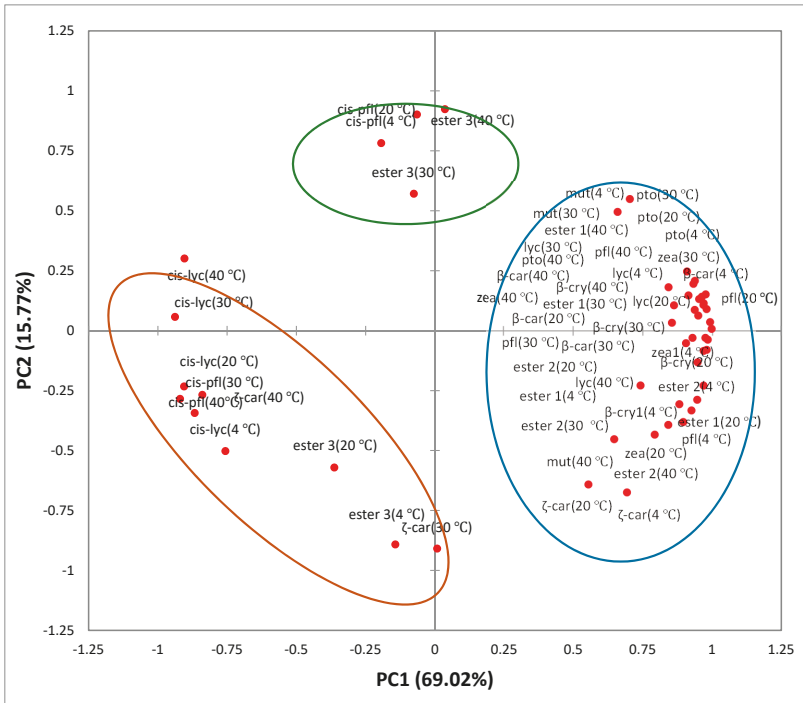


**Figure 2.** Changes in the content of ester group 1 and ester group 2 ( $\mu\text{g/mL}$ ) in 'Cara Cara' juice during 16 weeks of storage at different temperature.

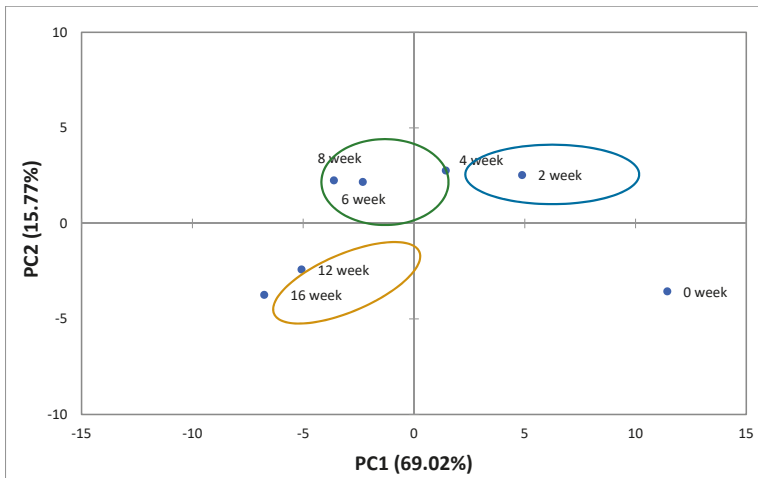
### 3.2.3. PCA Analysis

PCA was investigated to understand the segregation and correlation among carotenoid compounds in 'Cara Cara' juice at all storage temperatures. According to the PCA results, three principal components were obtained to account for the total variance. PC1 and PC2 accounted for 69.02% and 15.77% of the total variance, respectively. Carotenoid compounds, decreased with the storage time (Table S1), were sorted in the same group and they were strongly and positively correlated with PC1 (Figure 3A). Other compounds including 13- or 15-cis-lycopenes (4, 20, 30, 40 °C), cis-phytofluenes (4, 20, 30, 40 °C), ester groups 3 (4, 20, 30, 40 °C) and  $\zeta$ -carotenes (30, 40 °C) were classified into the other two groups. The 13- or 15-cis-lycopene, derived from all-(trans)-lycopene by isomerization, was increased with storage time at each temperature, and the contents of 13- or 15-cis-lycopenes (4, 20, 30, 40 °C) were strongly and negatively correlated with PC1. The contents of cis-phytofluene, ester group 3 and  $\zeta$ -carotene were irregularly changed in 'Cara Cara' juice during the overall storage period, and their contents at 4, 20, 30, 40 °C were sorted into different groups. Wibowo et al. proved that  $\zeta$ -carotene increased during juice storage at different temperatures, while Cortés presented the opposite view [12,30]. In this study, the increase of  $\zeta$ -carotene was just observed at 40 °C.

As presented in the PCA score plot (Figure 3B), the carotenoid profiles of 'Cara Cara' juice stored at different times were clearly divided into four groups. The sterilized juice at 0 week was grouped in the lower right quadrant, showing a positive correlation with PC1 and a negative correlation with PC2. Similarly, the other three groups (2 and 4 weeks, 6 and 8 weeks, 12 and 16 weeks) were distributed in the different quadrants, indicating that they have different correlations with PCs. Storage time of each group (2 and 4 weeks, 6 and 8 weeks, 12 and 16 weeks) had a similar impact on the change of carotenoid.



(A)



(B)

**Figure 3.** Principle component analysis (PCA) of carotenoid compounds in ‘Cara Cara’ juice during 16 weeks of storage at 4, 20, 30 and 40 °C. (A) Loading plot of PCA, (B) scores scatter plot of PCA. Note: mut for mutatoxanthin, zeax for zeaxanthin,  $\beta$ -cry for  $\beta$ -cryptoxanthin,  $\zeta$ -car for  $\zeta$ -carotene,  $\beta$ -car for  $\beta$ -carotene, cis-lyc for 13- or 15-cis-lycopene, lyc for lycopene, pto for phytoene, pfl for phytofluene, cis-pfl for cis-phytofluene, ester 1 for ester group 1, ester 2 for ester group 2, ester 3 for ester group 3. PC1 and PC2 represent the first principal component and the second principal component, respectively.

### 3.3. The Changes of Soluble Sugars in 'Cara Cara' Juice

Changes of soluble sugar are shown in Table 2. The total soluble sugars were gradually decreased with the improved temperature and prolonged storage. The total soluble sugars were decreased by 1.39%, 1.63%, 9.33% and 31.68% respectively when the juice was stored at 4, 20, 30 and 40 °C. It was reported that fructose, glucose and sucrose were greatly degraded in grapefruit juice during its storage at 37 °C for 16 weeks [19], and the loss of soluble sugars might be related to browning reactions. In the present study, sucrose in 'Cara Cara' juice was minorly hydrolyzed at 4, 20 and 30 °C, but it was completely degraded at 40 °C, with fructose and glucose being increased. It was shown that the hydrolysis of sucrose was followed by pseudo first-order reaction, and the hydrolysis progress was correlated with acid concentration and storage time [31]. The increased content of glucose and fructose in 'Cara Cara' juice stored at 40 °C was not stoichiometrically in line with the hydrolyzed sucrose (Table 2), indicating that hydrolyzate might be partly engaged in Maillard reactions [19].

**Table 2.** Changes in the content of soluble sugar concentrations (mg/mL) in 'Cara Cara' juice during 16 weeks of storage at different temperatures.

Weeks	Fructose	Glucose	Sucrose	Total
4 °C				
0	6.96 ± 0.17 a	15.15 ± 0.90 a	23.22 ± 1.85 a	45.33 ± 2.92 a
2	6.95 ± 0.31 a	15.09 ± 0.30 a	23.16 ± 1.25 a	45.21 ± 1.86 a
4	6.90 ± 0.42 a	14.92 ± 0.28 a	23.52 ± 1.36 a	45.40 ± 2.06 a
6	7.02 ± 0.36 a	15.36 ± 0.44 a	23.04 ± 1.33 a	45.36 ± 2.13 a
8	6.94 ± 0.55 a	15.08 ± 0.54 a	22.89 ± 0.83 a	44.93 ± 1.92 a
10	7.11 ± 0.43 a	15.58 ± 0.65 a	22.68 ± 1.42 a	45.22 ± 2.50 a
12	6.75 ± 0.56 a	14.98 ± 0.36 a	22.74 ± 1.88 a	44.68 ± 2.80 a
14	6.48 ± 0.38 a	15.97 ± 0.45 a	22.88 ± 1.76 a	45.81 ± 2.59 a
16	6.54 ± 0.25 a	15.72 ± 0.23 a	22.02 ± 1.42 a	44.70 ± 1.90 a
20 °C				
0	6.96 ± 0.17 a	15.15 ± 0.90 a	23.22 ± 1.85 a	45.33 ± 2.92 a
2	7.03 ± 0.12 a	15.13 ± 0.14 a	23.94 ± 1.67 a	46.03 ± 1.93 a
4	6.92 ± 0.42 a	15.29 ± 0.64 a	23.38 ± 1.79 a	45.63 ± 2.85 a
6	6.68 ± 0.88 a	15.23 ± 0.92 a	23.06 ± 1.15 a	45.25 ± 2.95 a
8	6.94 ± 0.37 a	15.11 ± 0.78 a	23.55 ± 1.84 a	45.62 ± 2.99 a
10	6.56 ± 0.21 a	15.64 ± 0.44 a	23.44 ± 1.38 a	46.04 ± 2.03 a
12	6.62 ± 0.54 a	15.79 ± 0.59 a	23.16 ± 1.47 a	45.91 ± 2.60 a
14	7.08 ± 0.52 a	16.07 ± 0.84 a	22.43 ± 1.15 a	45.46 ± 2.51 a
16	6.84 ± 0.35 a	16.13 ± 0.72 a	21.50 ± 1.55 a	44.59 ± 2.62 a
30 °C				
0	6.96 ± 0.17 a	15.15 ± 0.90 a	23.22 ± 1.85 ab	45.33 ± 2.92 a
2	6.75 ± 0.29 a	15.16 ± 0.85 a	23.60 ± 1.13 a	45.72 ± 2.27 a
4	6.79 ± 0.50 a	15.71 ± 0.78 a	22.12 ± 2.05 ab	44.79 ± 3.33 a
6	7.14 ± 0.61 a	15.85 ± 0.69 a	21.81 ± 1.28 ab	44.62 ± 2.58 a
8	7.18 ± 0.65 a	16.00 ± 1.36 a	21.03 ± 1.11 ab	43.99 ± 3.12 a
10	7.15 ± 1.85 a	16.20 ± 0.46 a	20.37 ± 0.64 ab	43.53 ± 2.95 a
12	6.88 ± 0.47 a	16.68 ± 0.96 a	19.54 ± 1.57 ab	43.18 ± 3.0 a
14	7.17 ± 0.28 a	16.85 ± 1.27 a	19.00 ± 1.42 ab	42.81 ± 2.97 a
16	7.18 ± 0.17 a	16.05 ± 0.47 a	18.09 ± 1.54 b	41.10 ± 2.18 a
40 °C				
0	6.96 ± 0.17 d	15.15 ± 0.90 c	23.22 ± 1.85 a	45.33 ± 2.92 a
2	8.10 ± 0.24 cd	17.32 ± 1.37 c	20.87 ± 1.59 a	45.15 ± 3.2 a
4	8.69 ± 0.22 bc	18.10 ± 1.04 cb	16.97 ± 1.21 b	42.03 ± 2.47 ab
6	9.05 ± 0.38 abc	21.89 ± 1.53 ab	9.77 ± 0.24 c	38.62 ± 2.15 abc
8	9.04 ± 0.81 abc	22.43 ± 1.38 a	5.82 ± 0.30 d	35.21 ± 2.49 bc
10	10.01 ± 0.66 ab	22.70 ± 0.79 a	4.06 ± 0.11 de	33.72 ± 1.56 bc
12	9.34 ± 0.75 abc	23.43 ± 1.50 a	2.77 ± 0.14 de	33.16 ± 2.39 c
14	9.45 ± 0.38 abc	23.42 ± 1.03 a	1.59 ± 0.06 e	31.88 ± 1.47 c
16	10.78 ± 0.38 a	24.01 ± 1.04 a	nd	30.97 ± 1.42 c

Values are expressed as mean ± standard deviation,  $n = 3$ . Values followed by different letters in the columns are significantly different (Duncan's multiple range tests,  $p < 0.05$ ).

### 3.4. The Changes of Vitamin C in 'Cara Cara' Juice

The percent retention of vitamin C in 'Cara Cara' juice during storage is shown in Figure 4, and vitamin C retention decreased with prolonged storage and increased temperature. No significant loss of vitamin C was detected in the 'Cara Cara' juice stored at 4 °C for 16 weeks. The concentration of vitamin C decreased by 23.93%, 35% and 69.58% respectively when 'Cara Cara' juice was stored at 20, 30 and 40 °C for 16 weeks. The degradation of vitamin C in citrus juice has been widely studied, and the degradation mode has been fitted to the first-order reaction [32,33]. A similar result was found in our study. The presence of vitamin C in citrus juice could protect carotenoids from oxidation, and a lower loss of carotenoid was confirmed in vitamin C fortified juice [34].

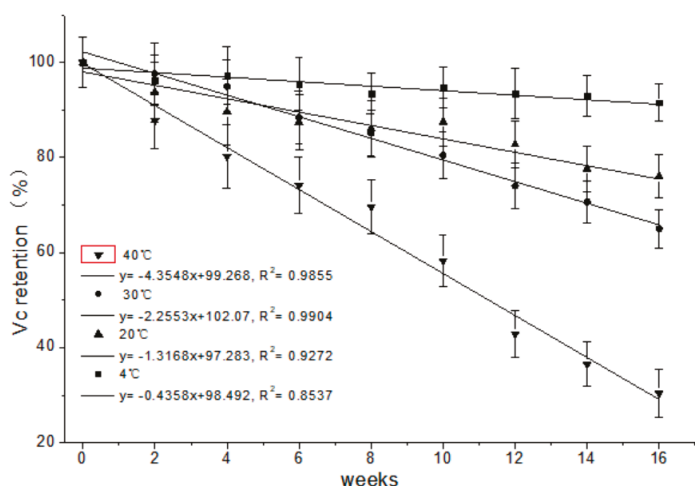


**Figure 4.** Percent retention of vitamin C in 'Cara Cara' juice during 16 weeks of storage at different temperatures.

### 3.5. The Changes of Antioxidants in 'Cara Cara' Juice

The antioxidants in 'Cara Cara' juice were evaluated in hydrophilic and lipophilic fractions, which represented the antioxidant ability of flavonoids and carotenoids, respectively. It was reported that lipophilic fractions usually displayed much lower antioxidant ability than the hydrophilic fraction in common fruits and vegetables [16,35]. A similar phenomenon was also found in our present study, which might be attributed to the higher content of total flavonoid index than that of the total carotenoid index (Table 1 and Table S1). The changes in both hydrophilic and lipophilic antioxidant abilities in 'Cara Cara' juice during the 16 weeks of storage at different temperatures are shown in Table 3.

**Table 3.** Changes of the hydrophilic and lipophilic antioxidant abilities in ‘Cara Cara’ juice during 16 weeks of storage at different temperatures.

Weeks	Hydrophilic ABTS <sup>1</sup>	Hydrophilic DPPH <sup>2</sup>	Lipophilic ABTS	Lipophilic DPPH
4 °C				
0	6.42 ± 0.44 a	2.14 ± 0.06 a	0.88 ± 0.03 a	0.76 ± 0.02 a
4	6.23 ± 0.12 a	2.09 ± 0.06 a	0.81 ± 0.02 ab	0.75 ± 0.03 a
8	5.89 ± 0.31 a	2.1 ± 0.06 a	0.87 ± 0.02 a	0.74 ± 0.05 a
12	5.71 ± 0.21 a	2.04 ± 0.06 a	0.80 ± 0.03 ab	0.74 ± 0.04 a
16	5.54 ± 0.24 a	1.94 ± 0.05 a	0.77 ± 0.05 ab	0.72 ± 0.02 a
20 °C				
0	6.42 ± 0.44 a	2.14 ± 0.06 a	0.88 ± 0.03 a	0.76 ± 0.02 a
4	5.84 ± 0.31 a	1.92 ± 0.05 b	0.82 ± 0.04 a	0.73 ± 0.06 a
8	5.89 ± 0.32 a	1.86 ± 0.05 b	0.87 ± 0.06 a	0.69 ± 0.02 a
12	5.81 ± 0.24 a	1.82 ± 0.04 b	0.76 ± 0.03 a	0.67 ± 0.03 a
16	5.48 ± 0.21 a	1.64 ± 0.03 c	0.75 ± 0.04 a	0.67 ± 0.04 a
30 °C				
0	6.42 ± 0.44 a	2.14 ± 0.06 a	0.88 ± 0.03 a	0.76 ± 0.02 a
4	6.19 ± 0.27 a	1.84 ± 0.05 b	0.83 ± 0.06 a	0.74 ± 0.03 ab
8	6.06 ± 0.32 a	1.82 ± 0.03 b	0.82 ± 0.04 a	0.66 ± 0.05 ab
12	5.76 ± 0.28 a	1.64 ± 0.04 c	0.76 ± 0.05 a	0.68 ± 0.03 ab
16	5.53 ± 0.34 a	1.56 ± 0.05 c	0.73 ± 0.03 a	0.62 ± 0.02 b
40 °C				
0	6.42 ± 0.44 a	2.14 ± 0.06 a	0.88 ± 0.03 a	0.76 ± 0.02 a
4	6.35 ± 0.31 cd	1.96 ± 0.06 ab	0.86 ± 0.03 ab	0.72 ± 0.01 ab
8	6.26 ± 0.32 bc	1.80 ± 0.05 bc	0.79 ± 0.02 ab	0.73 ± 0.03 ab
12	6.18 ± 0.24 abc	1.72 ± 0.03 c	0.75 ± 0.05 b	0.64 ± 0.05 ab
16	5.91 ± 0.26 abc	1.61 ± 0.06 c	0.74 ± 0.03 b	0.63 ± 0.04 b

<sup>1</sup> DPPH: expressed as ascorbic acid equivalent (μmol AAE/mL); <sup>2</sup> ABTS: expressed as Trolox equivalent (μmol TE/mL). Values are expressed as mean ± SD, *n* = 3. Values followed by different letters in the columns are significantly different (Duncan’s multiple range tests, *p* < 0.05).

The ABTS<sup>+</sup> and DPPH values for both hydrophilic and lipophilic antioxidants were decreased during storage at different temperatures. After storage for 16 weeks, ABTS<sup>+</sup> assay values for hydrophilic antioxidants decreased by 13.70%, 14.64%, 13.86% and 7.94% respectively, under 4, 20, 30, 40 °C, while DPPH assay values for hydrophilic antioxidants decreased by 9.34%, 23.36%, 27.10% and 24.76% at corresponding storage temperatures. The ABTS<sup>+</sup> and DPPH values for lipophilic antioxidants were relatively stable, and their significant decrease was only observed at the end of storage at 40 °C.

A correlation between flavonoid compositions and antioxidant activity in hydrophilic extracts from ‘Cara Cara’ juice was explored. A positive correlation was found between the total flavonoid index and hydrophilic antioxidant ability (Table 4), in accordance with a previous study [36]. Each individual flavonoid was significantly and positively correlated with tested antioxidant activities at *p* < 0.01 level (Table 4). Therefore, flavonoid compounds in ‘Cara Cara’ juice were the important contributions to the hydrophilic antioxidant ability. Correlations between carotenoid compositions and lipophilic antioxidant activities of ‘Cara Cara’ juice are presented in Table 5. Consisting of zeaxanthin, β-cryptoxanthin, lycopene, phytoene, phytofluene, ester group 1, ester group 2 and the total carotenoid index were significantly and positively correlated with the tested bioactivities at *p* < 0.01. β-carotene correlated with ABTS<sup>+</sup> capacity and DPPH scavenging at *p* < 0.01 level and *p* < 0.05 level, respectively. ζ-carotene, 13- or 15-cis-lycopene, cis-phytofluene and ester group 3 were negatively correlated with the tested bioactivities. The result suggested that zeaxanthin, β-cryptoxanthin, lycopene, phytoene, phytofluene, ester group 1 and ester group 2 were contributors to the lipophilic antioxidant ability of ‘Cara Cara’ juice.

**Table 4.** Correlation matrix between flavonoid compositions and antioxidant activity in hydrophilic extracts from stored ‘Cara Cara’ juice.

	Hydrophilic ABTS <sup>+</sup>	Hydrophilic DPPH
apigenin-6,8-di-C-glucoside	0.752 **	0.857 **
narirutin-4'-O-glucoside	0.808 **	0.870 **
narirutin	0.702 **	0.901 **
hesperidin	0.699 **	0.874 **
didymin	0.608 **	0.882 **
total flavonoid index	0.742 **	0.910**

\*\* indicated the correlated factors with each other reached significant level,  $p < 0.01$ .

**Table 5.** Correlation matrix between carotenoid compositions and antioxidant activity in lipophilic extracts from stored ‘Cara Cara’ juice.

	Lipophilic ABTS <sup>+</sup>	Lipophilic DPPH
mutatoxanthin	0.420	0.391
zeaxanthin	0.724 **	0.634 **
$\beta$ -cryptoxanthin	0.704 **	0.604 **
$\zeta$ -carotene	-0.178	-0.195
$\beta$ -carotene	0.640 **	0.558 *
13- or 15-cis-lycopene	-0.655 **	-0.666 **
lycopene	0.652 **	0.600 **
phytoene	0.698 **	0.619 **
phytofluene	0.760 **	0.848 **
cis-phytofluene	-0.629 **	-0.764 **
ester group 1	0.865 **	0.799 **
ester group 2	0.703 **	0.645 **
ester group 3	-0.225	-0.293
total carotenoid index	0.732 **	0.664 **

\* indicated the correlated factors with each other reached significant level,  $p < 0.05$ . \*\* indicated the correlated factors with each other reached significant level,  $p < 0.01$ .

#### 4. Conclusions

The micronutrients in ‘Cara Cara’ juice were investigated during storage at 4, 20, 30 and 40 °C for a period of 16 weeks. Total flavonoid and carotenoid indexes showed slight degradation at each temperature, while vitamin C and soluble sugar degraded intensively, especially at 40 °C storage. Although the total carotenoids were stable at each storage temperature, most carotenoid esters were significantly degraded and fitted by biexponential function. Specifically, the ester group 2 with epoxy structures quickly decreased in the first four weeks at all storage temperatures, while the ester group 1 (belonged to  $\beta$ -cryptoxanthin ester) degraded gradually. The combined degrading rates of the two type of esters might be further applied to estimate the storage time of ‘Cara Cara’ juice. Total flavonoid and carotenoid indexes in stored ‘Cara Cara’ juice were positively correlated with hydrophilic and lipophilic antioxidant abilities. This study provided information on changes of flavonoid, carotenoids, vitamin C and sugar in ‘Cara Cara’ juice during storage at moderate and elevated temperatures, which might be useful for the quality prediction of ‘Cara Cara’ juice during storage.

**Supplementary Materials:** The following are available online at <http://www.mdpi.com/2304-8158/8/9/417/s1>, Figure S1: Biexponential fitting with eq 1 of the experimental data obtained for the degradation of ester group 1 in Cara Cara juice during 16 weeks storage at 4 °C (A), 20 °C (B), 30 °C (C) and 40 °C (D), respectively. Figure S2: Biexponential fitting with eq 1 of the experimental data obtained for the degradation of ester group 2 in Cara Cara juice during 16 weeks storage at 4 °C (A), 20 °C (B), 30 °C (C) and 40 °C (D), respectively. Table S1: Changes in the content of carotenoids ( $\mu\text{g/mL}$ ) in ‘Cara Cara’ juice during 16 weeks of storage at different temperature.

**Author Contributions:** Data curation, L.L.; Methodology, S.X.; Project administration, S.W.; Supervision, D.Y.; Writing—original draft, Q.L.

**Funding:** National Natural Science Foundation of China: 31571847.

**Acknowledgments:** This work was supported by National Natural Science Foundation of China (grant number 31571847).

**Conflicts of Interest:** The authors declare no conflict of interest.

## References

1. Wibowo, S.; Grauwet, T.; Santiago, J.S.; Tomic, J.; Vervoort, L.; Hendrickx, M.; Van Loey, A. Quality changes of pasteurised orange juice during storage: A kinetic study of specific parameters and their relation to colour instability. *Food Chem.* **2015**, *187*, 140–151. [[CrossRef](#)] [[PubMed](#)]
2. Ghanim, H.; Sia, C.L.; Upadhyay, M.; Korzeniewski, K.; Viswanathan, P.; Abuaysheh, S.; Mohanty, P.; Dandona, P. Orange juice neutralizes the proinflammatory effect of a high-fat, high-carbohydrate meal and prevents endotoxin increase and Toll-like receptor expression. *Am. J. Clin. Nutr.* **2010**, *91*, 940–949. [[CrossRef](#)] [[PubMed](#)]
3. Aschoff, J.K.; Kaufmann, S.; Kalkan, O.; Neidhart, S.; Carle, R.; Schweiggert, R.M. In Vitro Bioaccessibility of Carotenoids, Flavonoids, and Vitamin C from Differently Processed Oranges and Orange Juices (*Citrus sinensis* (L.) Osbeck). *J. Agric. Food Chem.* **2015**, *63*, 578–587. [[CrossRef](#)] [[PubMed](#)]
4. Du, J.; Cullen, J.J.; Buettner, G.R. Ascorbic acid: Chemistry, biology and the treatment of cancer. *Biochim. Biophys. Acta Rev. Cancer* **2012**, *1826*, 443–457. [[CrossRef](#)]
5. Abuajah, C.I.; Ogbonna, A.C.; Osuji, C.M. Functional components and medicinal properties of food: A review. *J. Food Sci. Technol.* **2015**, *52*, 2522–2529. [[CrossRef](#)] [[PubMed](#)]
6. Lee, H.S. Characterization of Carotenoids in Juice of Red Navel Orange (Cara Cara). *J. Agric. Food Chem.* **2001**, *49*, 2563–2568. [[CrossRef](#)] [[PubMed](#)]
7. Lu, Q.; Huang, X.; Lv, S.; Pan, S. Carotenoid profiling of red navel orange “Cara Cara” harvested from five regions in China. *Food Chem.* **2017**, *232*, 788–798. [[CrossRef](#)] [[PubMed](#)]
8. Rapisarda, P.; Bianco, M.L.; Pannuzzo, P.; Timpanaro, N. Effect of cold storage on vitamin C, phenolics and antioxidant activity of five orange genotypes (*Citrus sinensis* (L.) Osbeck). *Postharvest Biol. Technol.* **2008**, *49*, 348–354. [[CrossRef](#)]
9. Klimczak, I.; Małeczka, M.; Szlachta, M.; Gliszczyńska-Świągło, A. Effect of storage on the content of polyphenols, vitamin C and the antioxidant activity of orange juices. *J. Food Compos. Anal.* **2007**, *20*, 313–322. [[CrossRef](#)]
10. Lu, Q.; Lv, S.; Peng, Y.; Zhu, C.; Pan, S. Characterization of phenolics and antioxidant abilities of red navel orange “Cara Cara” harvested from five regions of China. *Int. J. Food Prop.* **2018**, *21*, 1107–1116. [[CrossRef](#)]
11. Brasili, E.; Chaves, D.F.S.; Xavier, A.A.O.; Mercadante, A.Z.; Hassimotto, N.M.A.; Lajolo, F.M. Effect of Pasteurization on Flavonoids and Carotenoids in *Citrus sinensis* (L.) Osbeck cv. ‘Cara Cara’ and ‘Bahia’ Juices. *J. Agric. Food Chem.* **2017**, *65*, 1371–1377. [[CrossRef](#)] [[PubMed](#)]
12. Wibowo, S.; Vervoort, L.; Tomic, J.; Santiago, J.S.; Lemmens, L.; Panozzo, A.; Grauwet, T.; Hendrickx, M.; Van Loey, A. Colour and carotenoid changes of pasteurised orange juice during storage. *Food Chem.* **2015**, *171*, 330–340. [[CrossRef](#)] [[PubMed](#)]
13. Mezzomo, N.; Ferreira, S.R.S. Carotenoids Functionality, Sources, and Processing by Supercritical Technology: A Review. *J. Chem.* **2016**, *2016*, 16. [[CrossRef](#)]
14. Plaza, L.; Sánchez-Moreno, C.; De Ancos, B.; Elez-Martínez, P.; Martín-Belloso, O.; Cano, M.P. Carotenoid and flavanone content during refrigerated storage of orange juice processed by high-pressure, pulsed electric fields and low pasteurization. *LWT Food Sci. Technol.* **2011**, *44*, 834–839. [[CrossRef](#)]
15. Lu, Q.; Peng, Y.; Zhu, C.; Pan, S. Effect of thermal treatment on carotenoids, flavonoids and ascorbic acid in juice of orange cv. Cara Cara. *Food Chem.* **2018**, *265*, 39–48. [[CrossRef](#)] [[PubMed](#)]
16. Vallverdú-Queralt, A.; Arranz, S.; Casals-Ribes, I.; Lamuela-Raventós, R.M. Stability of the Phenolic and Carotenoid Profile of Gazpachos during Storage. *J. Agric. Food Chem.* **2012**, *60*, 1981–1988. [[CrossRef](#)] [[PubMed](#)]
17. Vallverdú-Queralt, A.; Medina-Remón, A.; Andres-Lacueva, C.; Lamuela-Raventós, R.M. Changes in phenolic profile and antioxidant activity during production of diced tomatoes. *Food Chem.* **2011**, *126*, 1700–1707. [[CrossRef](#)] [[PubMed](#)]

18. Stinco, C.M.; Fernández-Vázquez, R.; Escudero-Gilete, M.L.; Heredia, F.J.; Meléndez-Martínez, A.J.; Vicario, I.M. Effect of Orange Juice's Processing on the Color, Particle Size, and Bioaccessibility of Carotenoids. *J. Agric. Food Chem.* **2012**, *60*, 1447–1455. [[CrossRef](#)]
19. Lee, H.S.; Nagy, S. Quality Changes and Nonenzymic Browning Intermediates in Grapefruit Juice During Storage. *J. Food Sci.* **1988**, *53*, 168–172. [[CrossRef](#)]
20. Mohamed Ahmed, M.V.O.; Bouna, Z.E.O.; Mohamed Lemine, F.M.; Djeh, T.K.O.; Mokhtar, T.; Mohamed Salem, A.O. Use of multivariate analysis to assess phenotypic diversity of date palm (*Phoenix dactylifera* L.) cultivars. *Sci. Hortic.* **2011**, *127*, 367–371. [[CrossRef](#)]
21. Dhuique-Mayer, C.; Caris-Veyrat, C.; Ollitrault, P.; Curk, F.; Amiot, M.-J. Varietal and Interspecific Influence on Micronutrient Contents in Citrus from the Mediterranean Area. *J. Agric. Food Chem.* **2005**, *53*, 2140–2145. [[CrossRef](#)] [[PubMed](#)]
22. Persic, M.; Mikulic-Petkovsek, M.; Slatnar, A.; Veberic, R. Chemical composition of apple fruit, juice and pomace and the correlation between phenolic content, enzymatic activity and browning. *LWT Food Sci. Technol.* **2017**, *82*, 23–31. [[CrossRef](#)]
23. Dhuique-Mayer, C.; Tbatou, M.; Carail, M.; Caris-Veyrat, C.; Dornier, M.; Amiot, M.J. Thermal Degradation of Antioxidant Micronutrients in Citrus Juice: Kinetics and Newly Formed Compounds. *J. Agric. Food Chem.* **2007**, *55*, 4209–4216. [[CrossRef](#)] [[PubMed](#)]
24. Chen, P.X.; Tang, Y.; Zhang, B.; Liu, R.; Marcone, M.F.; Li, X.; Tsao, R. 5-Hydroxymethyl-2-furfural and Derivatives Formed during Acid Hydrolysis of Conjugated and Bound Phenolics in Plant Foods and the Effects on Phenolic Content and Antioxidant Capacity. *J. Agric. Food Chem.* **2014**, *62*, 4754–4761. [[CrossRef](#)] [[PubMed](#)]
25. Meléndez-Martínez, A.J.; Britton, G.; Vicario, I.M.; Heredia, F.J. The complex carotenoid pattern of orange juices from concentrate. *Food Chem.* **2008**, *109*, 546–553. [[CrossRef](#)]
26. Hadjal, T.; Dhuique-Mayer, C.; Madani, K.; Dornier, M.; Achir, N. Thermal degradation kinetics of xanthophylls from blood orange in model and real food systems. *Food Chem.* **2013**, *138*, 2442–2450. [[CrossRef](#)]
27. Cooperstone, J.L.; Francis, D.M.; Schwartz, S.J. Thermal processing differentially affects lycopene and other carotenoids in cis-lycopene containing, tangerine tomatoes. *Food Chem.* **2016**, *210*, 466–472. [[CrossRef](#)] [[PubMed](#)]
28. Nguyen, M.; Francis, D.; Schwartz, S. Thermal isomerisation susceptibility of carotenoids in different tomato varieties. *J. Sci. Food Agric.* **2001**, *81*, 910–917. [[CrossRef](#)]
29. Zepka, L.Q.; Mercadante, A.Z. Degradation compounds of carotenoids formed during heating of a simulated cashew apple juice. *Food Chem.* **2009**, *117*, 28–34. [[CrossRef](#)]
30. Cortés, C.; Torregrosa, F.; Esteve, M.J.; Frígola, A. Carotenoid Profile Modification during Refrigerated Storage in Untreated and Pasteurized Orange Juice and Orange Juice Treated with High-Intensity Pulsed Electric Fields. *J. Agric. Food Chem.* **2006**, *54*, 6247–6254. [[CrossRef](#)] [[PubMed](#)]
31. Akhavan, I.; Wrolstad, R.E. Variation of sugars and acids during ripening of pears and in the production and storage of pear concentrate. *J. Food Sci.* **1980**, *45*, 499–501. [[CrossRef](#)]
32. Tiwari, B.K.; O'Donnell, C.P.; Muthukumarappan, K.; Cullen, P.J. Ascorbic acid degradation kinetics of sonicated orange juice during storage and comparison with thermally pasteurised juice. *LWT Food Sci. Technol.* **2009**, *42*, 700–704. [[CrossRef](#)]
33. Burdurlu, H.S.; Koca, N.; Karadeniz, F. Degradation of vitamin C in citrus juice concentrates during storage. *J. Food Eng.* **2006**, *74*, 211–216. [[CrossRef](#)]
34. Choi, M.H.; Kim, G.H.; Lee, H.S. Effects of ascorbic acid retention on juice color and pigment stability in blood orange (*Citrus sinensis*) juice during refrigerated storage. *Food Res. Int.* **2002**, *35*, 753–759. [[CrossRef](#)]

35. Wu, X.; Beecher, G.R.; Holden, J.M.; Haytowitz, D.B.; Gebhardt, S.E.; Prior, R.L. Lipophilic and Hydrophilic Antioxidant Capacities of Common Foods in the United States. *J. Agric. Food Chem.* **2004**, *52*, 4026–4037. [[CrossRef](#)] [[PubMed](#)]
36. Miao, J.; Li, X.; Zhao, C.; Gao, X.; Wang, Y.; Gao, W. Active compounds, antioxidant activity and  $\alpha$ -glucosidase inhibitory activity of different varieties of Chaenomeles fruits. *Food Chem.* **2018**, *248*, 330–339. [[CrossRef](#)] [[PubMed](#)]



© 2019 by the authors. Licensee MDPI, Basel, Switzerland. This article is an open access article distributed under the terms and conditions of the Creative Commons Attribution (CC BY) license (<http://creativecommons.org/licenses/by/4.0/>).



Article

# Quality Attributes of Cryoconcentrated Calafate (*Berberis microphylla*) Juice during Refrigerated Storage

Patricio Orellana-Palma <sup>1,\*</sup>, Guisella Tobar-Bolaños <sup>2,3</sup>, Nidia Casas-Forero <sup>2,4</sup>, Rommy N. Zúñiga <sup>1,5</sup> and Guillermo Petzold <sup>2</sup>

<sup>1</sup> Department of Biotechnology, Universidad Tecnológica Metropolitana, Las Palmeras 3360, P.O. Box, 7800003 Ñuñoa, Santiago, Chile; rommy.zuniga@utem.cl

<sup>2</sup> Laboratory of Cryoconcentration, Department of Food Engineering, Universidad del Bío-Bío, Av. Andrés Bello 720, Casilla 447, 3780000 Chillán, Chile; guisella.tobar1901@alumnos.ubiobio.cl (G.T.-B.); nidia.casas1701@alumnos.ubiobio.cl (N.C.-F.); gpetzold@ubiobio.cl (G.P.)

<sup>3</sup> Magíster en Ciencias e Ingeniería en Alimentos, Universidad del Bío-Bío, Av. Andrés Bello 720, Casilla 447, 3780000 Chillán, Chile

<sup>4</sup> Doctorado en Ingeniería de Alimentos, Universidad del Bío-Bío, Av. Andrés Bello 720, Casilla 447, 3780000 Chillán, Chile

<sup>5</sup> Programa Institucional de Fomento a la I+D+i, Universidad Tecnológica Metropolitana, Ignacio Valdivieso 2409, San Joaquín, 8940577 Santiago, Chile

\* Correspondence: p.orellanap@utem.cl; Tel.: +56-2-2787-7032

Received: 28 August 2020; Accepted: 16 September 2020; Published: 18 September 2020

**Abstract:** This study aimed to evaluate the potential of centrifugal block cryoconcentration (CBCC) at three cycles applied to fresh calafate juice. The fresh juice and cryoconcentrate at each cycle were stored for five weeks at 4 °C and quality attributes were analyzed every 7 days. CBCC had significant effects in the calafate juice, since in the last cycle, the cryoconcentrate reached a high value of total soluble solids (TSS,  $\approx 42$  °Brix), with final attractive color, and an increase of approximately 2.5, 5.2, 5.1, 4.0 and 5.3 times in relation to the fresh juice values, for total bioactive compounds (TBC), 2,2-diphenyl-1-picrylhydrazyl (DPPH), 2,2'-azino-bis(3-ethylbenzothiazoline-6-sulfonic acid) (ABTS), ferric reducing antioxidant power (FRAP) and oxygen radical absorbance capacity (ORAC), respectively. However, at 35 days under storage, these values decreased by 5%, 13%, 15%, 19%, 24% and 27%, for TSS, TBC, DPPH, ABTS, FRAP and ORAC, respectively. Additionally, until the day 14, the panelists indicated a good acceptability of the reconstituted cryoconcentrate. Therefore, CBCC can be considered a novel and viable technology for the preservation of quality attributes from fresh calafate juice with interesting food applications of the cryoconcentrates due to their high stability during storage time in comparison to the fresh juice.

**Keywords:** cryoconcentration; calafate juice; storage time; physicochemical properties; bioactive compounds; antioxidant activity; sensorial analysis

## 1. Introduction

Calafate (*Berberis microphylla*) has presented unique properties due to the high variety of health associated compounds, such as phenols, vitamins, minerals and amino acids [1]. Calafate belongs to the family Berberidaceae, and the fruits are harvested in numerous Chilean and Argentinian Patagonian sectors [2]. However, calafate production is still low compared to other berries (2019: 0.2 hectares calafate versus 970.6, 9.0 and 2.9 hectares of blueberries (*Vaccinium corymbosum*), maqui (*Aristotelia chilensis*) and michay (*Berberis darwinii*), respectively). Therefore, different technologies have

been applied to keep this fruit available throughout the year. Thus, processed products from fresh calafate fruits such as juice, jellies, jams and wines can be found in local markets [3].

In recent decades, traditional thermal methods (evaporation, pasteurization and/or sterilization) have been used in fresh juice, and thus, the thermally treated concentrate products achieve a significant improvement in quality and prolonged shelf-life when compared to the fresh juice. Unfortunately, these technologies use high temperatures that cause undesirable changes on different properties (nutrients, flavor and color, among others), since these quality properties contain endless thermolabile and thermostable compounds that are degraded, and thus, the organoleptic properties are affected, resulting in possible rejection by consumers [4]. Hence, emerging non-thermal technologies have been investigated in the food processing sector to concentrate liquids, and thus, to retain their quality attributes [5].

Cryoconcentration (CC) is a non-thermal concentration technology which has demonstrated numerous advantages to preserve important properties in liquid foods [6]. Specifically, CC concentrates a liquid solution by total or partial freezing of water, and thus, as the temperature decreases the solutes are rejected from the ice phase and accumulate at the solid–liquid interphase, i.e., the cryoconcentrated (unfrozen liquid fraction) is between the ice crystals (solid water). Once the freezing process is finished, the cryoconcentrate is removed from the ice fraction, which allows lower energy consumption than thermal processing (0.33 versus 2.26 kJ/g, respectively) [7].

Different CC techniques can be found in the literature, with block CC (BCC) characterized by the easier fraction separation, equipment used and operation procedures [8]. Specifically, in BCC, a liquid solution is completely frozen, which is equivalent to a frozen block solution. Later, the block sample is thawed and separated by a natural (gravitational) method [9] or by employing assisted techniques to improve the process parameters involved in BCC, among them, efficiency, solute yield and percentage of concentrate [10–12].

Hence, BCC has proven to be an environmentally friendly emerging technology with great potential to retain various quality characteristics in fresh fruit juice, including physicochemical parameters [13], phenolic content [14], antioxidant activity [15] and volatile compounds [16]. In addition, sensory panelists did not find differences between reconstituted cryoconcentrate samples and fresh juice [17]. Nevertheless, to our knowledge, no researches have been published on quality characteristics obtained from a fresh native juice such as calafate juice by BCC. Therefore, the novelty of this study is the concentration of calafate juice, an endemic species of the Patagonian Andes of Chile and Argentina considered as a “superfruit” with high polyphenol content and high antioxidant capacity through a green and non-thermal technology called cryoconcentration.

Therefore, the aim of the study was to investigate the stability of fresh calafate juice and cryoconcentrate samples, in quality attributes terms, during 35 days of storage after applied centrifugal BCC (CBCC) technology. The physicochemical parameters, bioactive compounds content, antioxidant activity and sensory analysis were studied in each week of the storage period.

## 2. Materials and Methods

### 2.1. Calafate Juice Preparation

Fresh calafate (*Berberis microphylla*) were harvested in southernmost Chile (XI Región de Aysén) (December 2019), and the fruits were transferred in a refrigerated truck to Chillán (Región del Ñuble, Chile). The fruits were pressed, and then, the juice was filtered through nylon cloth (0.8 mm fine-mesh) to discard solid parts (peel and seeds) that might interfere with the CBCC process. The liquid sample was stored at 4 °C and processed within 24 h.

### 2.2. CBCC Protocol

The CBCC process was carried out as described in our previous study [18]. Thus, the prepared calafate juice (45 mL) was placed in plastic centrifugal tubes with foamed polystyrene (around the

tube) to produce an axial freezing. The samples were frozen at  $-20\text{ }^{\circ}\text{C}$  (overnight) in a vertical static freezer (280, M and S Consul, Sao Paulo, Brazil), and at the end of the freezing stage, the frozen samples were transported to centrifuge equipment (Eppendorf 5430R, Hamburg, Germany). Specifically, two centrifugation conditions (15 min with 4000 rpm and 20 min with 4000 rpm) were performed to determine the best separation condition, considering total soluble solids (TSS), efficiency (Eff, %) and final cryoconcentrate volume (mL). Thereby, the centrifugation was used as an assisted technique to force the extraction of the cryoconcentrated fraction ( $C_s$ ) from the frozen matrix ( $C_f$ ). The CBCC was performed at three cycles, i.e., the  $C_s$  at the first cycle was used as feed solution for the second cycle and the second  $C_s$  was used for the third cycle.

### 2.3. Physicochemical Analysis

The TSS was determined using a digital refractometer PAL-3 (range: 0–93 °Brix, precision:  $\pm 0.1\text{ }^{\circ}\text{Brix}$ , Atago Inc., Tokyo, Japan). The density ( $\text{kg}/\text{m}^3$ ) of the samples was determined by the pycnometric method at  $20\text{ }^{\circ}\text{C}$  using distilled water as a model liquid [19]. A digital pH meter HI 2221 (Hanna Instruments, Woonsocket, RI, USA) was used to determine the pH of the samples, and the mean pH values were calculated on the International Union of Pure and Applied Chemistry (IUPAC) recommendation [20]. The titratable acidity (TA) was measured by using 5 mL of sample mixed with 50 mL of degassed deionized water, pH of samples was adjusted to 8.2 with sodium hydroxide solution (0.1 M NaOH) and the TA was expressed as grams of malic acid (MA) per liter of sample (g MA/L). The color parameters were calculated on the International Commission on Illumination (CIE) with  $L^*$  (Lightness),  $a^*$  (Green–red axis) and  $b^*$  (Blue–yellow axis) space (CIELAB) using a spectrophotometer CM-5 (Konica Minolta, Osaka, Japan). The standard illuminant and observer angle were D65 and  $10^{\circ}$ , respectively. In addition, the total color difference ( $\Delta E^*$ ) between fresh calafate juice and cryoconcentrated samples was calculated according to Equation (1).

$$\Delta E^* = \sqrt{(\Delta L^*)^2 + (\Delta a^*)^2 + (\Delta b^*)^2} \quad (1)$$

where  $\Delta L^*$ ,  $\Delta a^*$  and  $\Delta b^*$  are differences between fresh calafate juice and cryoconcentrated samples at each week of the storage period.

TSS, pH, acidity, density and color determinations of fresh juice and cryoconcentrated samples were performed in triplicate at ambient temperature ( $\approx 22\text{ }^{\circ}\text{C}$ ). Three replicates for each treatment were analyzed.

### 2.4. Quantification of Total Bioactive Compound (TBC)

The total polyphenol content (TPC), total anthocyanin content (TAC) and total flavonoid content (TFC) of fresh calafate juice and cryoconcentrated samples were measured at each CBCC cycle and each storage period.

TPC was determined through the Folin–Ciocalteu method [21]. Wherein, 200  $\mu\text{L}$  of sample and 1500  $\mu\text{L}$  of diluted (1:10) Folin–Ciocalteu reagent were mixed. After 5 min, 1500  $\mu\text{L}$  of sodium carbonate solution (20% ( $w/v$ ),  $\text{Na}_2\text{CO}_3$ ) was added to the solution. After 90 min in the dark at room temperature (incubation), the absorbance was measured at 760 nm. Gallic acid (GA) was used for the standard curve construction, and the TPC results were expressed as mg of gallic acid equivalents (GAE) per grams (g) of dry matter (mg GAE/g d.m.).

TAC was quantified using the pH differential method [22]. Therefore, 200  $\mu\text{L}$  of sample was added to 1800  $\mu\text{L}$  of potassium chloride (pH 1.0, 0.025 M, KCl) and 1800  $\mu\text{L}$  of sodium acetate (pH 4.5, 0.4 M,  $\text{CH}_3\text{COONa}$ ). After 30 min in the dark at room temperature (incubation), the absorbance was measured at 520 and 700 nm. Cyanidin-3-glucoside (C3G) was used for the standard curve construction, and the TAC results were expressed as mg of C3G equivalent per grams (g) of dry matter (mg C3G/g d.m.).

TFC was measured by the aluminum chloride colorimetric method [23]. As such, 250  $\mu\text{L}$  of sample was mixed with 1000  $\mu\text{L}$  of distilled water and 75  $\mu\text{L}$  of sodium nitrite solution (5% ( $w/v$ ),

NaNO<sub>2</sub>). After 10 min, 75 µL of aluminum chloride (10% (*w/v*), AlCl<sub>3</sub>), 500 µL of sodium hydroxide (1 M, NaOH) and 600 µL of distilled water were added. After 30 min in the dark at room temperature (incubation), the absorbance was measured at 510 nm. Catequin (C) was used for the standard curve construction, and the results were expressed as mg of catechin equivalent (CE) per grams (g) of dry matter (mg CE/g d.m.).

All TBC determinations were evaluated using a spectrophotometer T70 UV-VIS (Oasis Scientific Inc., Greenville, SC, USA), and were done in triplicate at ≈22 °C.

### 2.5. Total Antioxidant Activity (TAA) Determinations

Four methods were used to quantify antioxidant activity, the 2,2-diphenyl-1-picrylhydrazyl (DPPH), 2,2'-azino-bis(3-ethylbenzothiazoline-6-sulphonic acid) (ABTS), ferric reducing antioxidant power (FRAP) and oxygen radical absorbance capacity (ORAC) assays, with minor modifications.

DPPH assay was determined using the protocol described by Brand-Williams et al. [24]. Thereby, 100 µL of sample was added to 2900 µL of DPPH solution (0.1 mM). The solution was incubated in the dark at room temperature (≈22 °C) for 30 min, and then, the absorbance was measured at 515 nm.

ABTS assay was performed according to Re et al. [25]. Therein, 10 µL of sample was added to 990 µL of ABTS solution. The sample was incubated in the dark at room temperature for 30 min, and then, the absorbance was measured at 734 nm.

FRAP assay was done according to the method described by Benzie and Strain [26]. As such, 100 µL of sample, 3000 µL of FRAP reagent and 300 µL of water were mixed. The sample was incubated in the dark at 37 °C for 10 min, and then, the absorbance was measured at 593 nm.

DPPH, ABTS and FRAP assays were quantified on a spectrophotometer T70 (UV-VIS spectrophotometer, Oasis Scientific Inc., Greenville, SC, USA).

ORAC assay was determined using the method reported by Ou et al. [27]. Specifically, 30 µL of sample and 20 µL of fluorescein solution (10 nM) were placed into black 96-well microplates and incubated at 37 °C for 30 min. Then, 50 µL of 2,2'-azobis(2-amidinopropane) dihydrochloride (AAPH, 600 mM) and 2900 µL of phosphate buffer (75 mM, pH 7.4) were added to the solution. The absorbance was measured every 1 min for 60 min at an excitation wavelength of 485 nm and an emission set of 520 nm using a multimode plate reader (Victor X3, Perkin Elmer, Hamburg, Germany).

For all assays, Trolox (T) (6-hydroxy-2,5,7,8-tetramethylchroman-2-carboxylic acid) was used for the standard curve construction, and the TAA results were expressed as mM Trolox equivalents (TE) per gram (g) of dry matter (mM TE/g d.m.) and the TAA determinations were performed in triplicate.

### 2.6. Storage Study

The fresh calafate juice and each cryoconcentrate sample were deposited in glass jars previously rinsed with distilled water and UV exposed for 1.5 h. All the samples were stored at 4 ± 1 °C in a refrigerated incubator (FOC 215E, Velp Scientific Inc., Milano, Italy) for 35 days. The physicochemical properties, TBC and TAA determinations were analyzed at day 0 (control) and after 7, 14, 21, 28 and 35 days, as previously described.

### 2.7. Sensory Evaluation

A sensorial analysis was done to measure the degree of acceptance or rejection between reconstituted cryoconcentrated samples (third cycle with similar TSS value than the fresh juice) and fresh calafate juice. The evaluations were performed at day 0, 7, 14 and 21 of the storage period by a trained sensory panel consisting of ten males and ten females with an average age of 33 years old (from 27 to 39 years old). The samples were rated according to a 5-score hedonic scale system, in which 1 = dislike extremely and 5 = like extremely. Thus, odor, aroma, flavor and overall acceptability were evaluated. Specifically, 20 mL of samples at 22 °C were placed in transparent cups, labeled with three random numbers. Cold water and crackers were supplied to each panelist in each test for rinsing their mouths between the samples. Three replicates were performed on each sample.

## 2.8. Statistical Analysis

The results were expressed as means  $\pm$  standard deviation. All statistical analysis was evaluated by analysis of variance (ANOVA) test and the treatment means were compared via least significant difference (LSD) or Student's t-test at level of significance ( $p \leq 0.05$ ). Statgraphics Centurion XVI software version 16.2.04 (StatPoint Technologies Inc. Warrenton, VA, USA) was used for analysis of data. Correlations between TBC, TAA and among them were evaluated by Pearson's correlation coefficient test.

## 3. Results and Discussion

### 3.1. Preliminary Centrifugation Results

In order to determine an adequate CBCC process, two centrifugation time conditions (15 min and 20 min) were used to identify the best separation performance. The other conditions were similar to that previously reported in our laboratory, i.e., 4000 rpm and 20 °C as centrifugation speed and separation temperature, respectively [16–18].

The centrifugation time had an important effect in TSS, efficiency and final cryoconcentrate volume, with significant differences ( $p \leq 0.05$ ) at each cycle (Table 1). Firstly, a gradual increase in TSS values was observed as cycles progressed, in both 15 min and 20 min conditions. However, at 15 min of centrifugation, the TSS values (27, 38 and 45 °Brix) were higher than those at 20 min (24, 31 and 37 °Brix), in the first, second and the third cycle, respectively. These results could be attributed to the centrifugation which remained relatively intact the ice fraction (without thawing and/or breaking) using 15 min as centrifugation time, and thus, only cryoconcentrate was extracted from the ice fraction.

**Table 1.** Preliminary results obtained at different centrifugation conditions.

Centrifugation Condition	Cycle	TSS (°Brix)	Efficiency <sup>1</sup> (Eff, %)	Cryoconcentrated Volume (CV, mL)
Fresh juice	0	14.6 $\pm$ 0.2 <sup>a</sup>	-	-
	1	27.2 $\pm$ 0.8 <sup>b</sup>	68.9 $\pm$ 0.9 <sup>a</sup>	28.6 $\pm$ 0.2 <sup>a</sup>
	2	37.6 $\pm$ 0.4 <sup>c</sup>	57.9 $\pm$ 0.4 <sup>b</sup>	22.4 $\pm$ 0.6 <sup>b</sup>
15 min, 4000 rpm, 20 °C	3	44.5 $\pm$ 0.5 <sup>d</sup>	52.3 $\pm$ 1.1 <sup>c</sup>	15.2 $\pm$ 0.8 <sup>c</sup>
	1	23.7 $\pm$ 0.7 <sup>b</sup>	75.7 $\pm$ 1.0 <sup>a</sup>	34.4 $\pm$ 0.6 <sup>a</sup>
	2	31.1 $\pm$ 0.6 <sup>c</sup>	69.7 $\pm$ 0.9 <sup>b</sup>	29.1 $\pm$ 1.0 <sup>b</sup>
20 min, 4000 rpm, 20 °C	3	36.6 $\pm$ 0.3 <sup>d</sup>	63.0 $\pm$ 0.5 <sup>c</sup>	21.6 $\pm$ 0.7 <sup>c</sup>

Total soluble solids (TSS), efficiency (Eff) and cryoconcentrate volume (CV). Different superscripts in a column are significantly different ( $p \leq 0.05$ ) according to least significant difference (LSD) test. <sup>1</sup> Eff(%) =  $((C_{cs} - C_{cf})/C_{cs}) * 100$ , where  $C_{cs}$  and  $C_{cf}$  are the solutes in cryoconcentrated and ice fraction, respectively.

An inverse behavior was observed in efficiency, since 20 min presented better results than 15 min, with 63% and 52%, in the last cycle, respectively. This phenomenon can be described by the TSS concentration values in the  $C_s$  and  $C_f$  fractions in each cycle, since a high TSS value produces an increase in viscosity and thus, an increase the difficulty of solute extraction from the ice matrix, which produces a reduction in the separation efficiency [28].

An important point to determine the best centrifugation condition is the cryoconcentrate volume (CV), which decreased as the cycles advanced. In our case, centrifugation for 20 min presented higher CV post-centrifugation by tube than 15 min, from  $\approx 34$  to  $\approx 22$  mL and  $\approx 29$  to  $\approx 15$  mL, respectively. These results can be correlated with the previously results obtained in TSS, since, as mentioned above, a high TSS value increases the viscosity, and this behavior influences the CV obtained due to the high viscosity preventing the solutes movement outside from the frozen phase.

Therefore, we defined 20 min as centrifugation time for the separation between  $C_s$  and  $C_f$  at each cycle, since it allows a higher CV extraction than 15 min. In addition, calafate (*Berberis microphylla*) is still a fruit with low production in Chile compared to other berries [29], and to date, these fruits present

a high price per kilogram due to recent knowledge acquired on different quality properties [1–3], which encourages the cryoconcentrated juice study and stability over time for the elaboration of different products such as fruit juice.

### 3.2. TSS Results

The fresh juice has an initial TSS value close to 13.9 °Brix (Figure 1), which is a value within the range established by Mariangel et al. [3], who studied the variability in numerous attributes of calafate fruit harvested from four sectors in Southern Chile, with TSS values between 9.3 to 22.9 °Brix, which reflects the influence of different agricultural and climatic conditions on the fruit growth pattern.

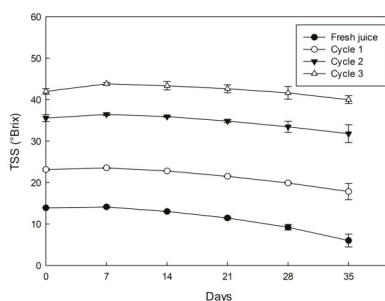


**Figure 1.** Effect of storage on TSS in fresh and cryoconcentrated calafate juice.

Firstly, in relation to day 0, the TSS in the fresh juice increased significantly cycle to cycle with values of 23.1, 35.6 and 42.0 °Brix in the first, second and third cycle, which is equivalent to a concentration index (CI, ratio  $C_s/C_0$ ) of 1.7, 2.6 and 3.0 times, compared to the initial TSS value (13.9 °Brix), respectively. Thus, the TSS results at each cycle have higher values than those achieved in previous investigations with other fresh fruit juice samples such as blueberry juice [18,30], orange juice [10] and pineapple juice [16] under similar conditions in our laboratory, with final concentration values (third cycle) close to 41, 33, 40 and 36 °Brix, respectively. Furthermore, the TSS values were superior to those described by Moreno et al. [31] and Ding et al. [32], who used BCC and suspension CC (SCC) to cryoconcentrate coffee extract and apple juice, respectively. Hence, the TSS values variation could be explained by the freezing conditions and sized tubes capacity used in the present study. Specifically, we used an axial freezing front propagation with moderate freezing rate temperature (−20 °C), which allows an improved counter-diffusion of solutes from the growing crystal surface. Additionally, the centrifugal equipment has a sized tubes capacity of 50 mL-tube, which favors the cryoconcentrate extraction from the ice frozen in the centrifugation step [18].

During the first week (day 7) under storage, the TSS in the fresh juice presented a slight increase (with statistical differences) compared with control juice (day 0). However, a continuous decline in TSS was observed in the next weeks, with a final value of approximately 6.0 °Brix at day 35 (week 5), which is equivalent to a decrease of more than 57% of the initial TSS value (day 0). A similar effect was observed for all CBCC cycles, with a slight increase until day 7, and then, TSS decreased significantly until day 35, where it reached values close to 17.8, 31.8 and 40.0 °Brix, for the first, second and third cycle, which indicates a decrease of 23%, 11% and 5%, with respect to the correspondent value at day 0, respectively.

The TSS decrease at each cycle under storage could be associated with sugar consumption by microorganisms, since as time progresses, there exists a possibility of microbial growth, and thus, as days passed, the microorganisms consume higher sugar amount than in the first days (first week), reflecting in a gradual TSS decrease [33]. Comparable results were described by Wahia et al. [34], who studied melon juice and their quality properties preservation at various days during storage. Additionally, Chia et al. [35] mentions that, in terms of consumption safety, the unpasteurized products

has a shelf life up to two weeks, since, in general, the fresh fruits have a microbial load close to 3 to 5 log CFU per mL and the limit is 6 log CFU per mL.

### 3.3. Physicochemical Analysis

Statistical differences ( $p \leq 0.05$ ) were found in density, pH and acidity values between the fresh juice and their respective CBCC cycle, and in turn, significant differences ( $p \leq 0.05$ ) were observed between the samples (at day 0) and their correspondent at each week under storage (Table 2).

Firstly, the initial pH and TA values in the calafate juice (day 0) were equivalent to those previously reported by Arena et al. [36], who studied the organic acids content of calafate in different growing seasons, specifying that the physicochemical properties of calafate depends on various aspects such as climate, place of growth, type of harvest and processing procedures.

Specifically, in the fresh juice (day 0) and as the cycles advanced, a gradual decrease in the pH values were observed, with a decrease close to 2.3%, 5.5% and 8.7% in relation to the initial pH value (pH  $\approx$ 3.09), for the cycle one, cycle two and cycle three, respectively. While, an opposite effect was denoted in TA values, since it presented a considerable increase, with values of approximately 2.1, 2.8, 4.1 and 4.6, from fresh juice to the final CBCC cycle, respectively. This contrary performance has been linked to the TSS and their values cycle by cycle, i.e., as TSS increased, an increase in the organic acid content was generated, affecting the pH and TA values [37]. Besides, the results are in accordance with those obtained in CC applied to pineapple juice [16], apple juice [17] and blueberry juice [38], in which all the cryoconcentrated juices had antagonistic values in pH and TA with the increase in solutes as the cycles passed.

On the days under storage, an opposite behavior was observed in each sample among pH and TA values, since a progressive increase was detected in pH and a significant decline was identified in TA, with values from 3.1 to 3.4 and 2.1 to 1.7 for fresh juice, 3.0 to 3.3 and 2.8 to 2.3 for cycle one, 2.9 to 3.2 and 4.1 to 3.6 for cycle two and 2.8 to 3.2 and 4.6 to 4.0 for cycle three, from the day 0 to day 35, respectively. In this case, this phenomenon has been attributed to the acid hydrolysis of various polysaccharides, in which the non-reducing sugars are transformed into reducing sugars, as well as the use of malic acid as an energy source by microorganisms [39].

In general terms, the fruit juices are a good media for microbial multiplication and spoilage, with a usual microbial increase during storage time. In these conditions, the microorganisms use nutrients and cause enzymatic changes, contributing to creating off-flavor by breakdown or synthesis of new compounds [40]. In the case of unpasteurized fruit juices, the microbial spoilage is most commonly the result of aciduric microbes such as lactic acid bacteria and yeasts that produce copious quantities of carbon dioxide and off-flavors [41].

Similar trends were perceived in fruit juices such as sugarcane juice [42], grape juice [43] and apple juice [44] during storage.

In terms of density, the values showed an overall increasing trend from the fresh juice to the last cycle at day 0, and thus, the density values presented an increase close to 5%, 8% and 12% in comparison to the respective initial value. This behavior can be justified by the TSS concentration reached post-centrifugation step at each cycle [45] and the performance was comparable with the results informed for different cryoconcentrated juices [16,17,38,45]. In addition, a similar behavior was observed throughout storage, since at day 35, the density showed an increment of approximately 12–14% to the respective sample at day 0. These trends might be explained by the water evaporation in the sample under storage period, which lead to a decrease in the volume of the sample, as it was explained in studies on physicochemical properties under storage conditions for watermelon juice [33] and grape juice [46].

Table 2. Physicochemical parameters of fresh calafate juice and cryoconcentrate samples during storage.

Day	pH			TA (g MA/L)			Density (kg/m <sup>3</sup> )					
	Fresh Juice	C1	C2	C3	Fresh Juice	C1	C2	C3	Fresh Juice	C1	C2	C3
0	3.09 ± 0.01 <sup>a,A</sup>	3.02 ± 0.01 <sup>b,A</sup>	2.92 ± 0.02 <sup>c,A</sup>	2.82 ± 0.02 <sup>d,A</sup>	2.07 ± 0.01 <sup>a,A</sup>	2.77 ± 0.05 <sup>b,A</sup>	4.10 ± 0.09 <sup>c,A</sup>	4.59 ± 0.06 <sup>d,A</sup>	1030 ± 3.55 <sup>a,A</sup>	1080 ± 5.92 <sup>b,A</sup>	1110 ± 9.01 <sup>c,A</sup>	1150 ± 3.77 <sup>d,A</sup>
7	3.15 ± 0.02 <sup>a,B</sup>	3.07 ± 0.02 <sup>b,B</sup>	3.00 ± 0.03 <sup>c,B</sup>	2.89 ± 0.00 <sup>d,B</sup>	2.03 ± 0.02 <sup>a,B</sup>	2.65 ± 0.02 <sup>b,B</sup>	3.97 ± 0.02 <sup>c,B</sup>	4.40 ± 0.08 <sup>d,B</sup>	1040 ± 2.74 <sup>a,B</sup>	1100 ± 10.14 <sup>b,B</sup>	1140 ± 5.74 <sup>c,B</sup>	1160 ± 4.58 <sup>d,B</sup>
14	3.24 ± 0.01 <sup>a,C</sup>	3.18 ± 0.00 <sup>b,C</sup>	3.05 ± 0.01 <sup>c,C</sup>	3.01 ± 0.01 <sup>d,C</sup>	1.98 ± 0.00 <sup>a,C</sup>	2.59 ± 0.01 <sup>b,C</sup>	3.90 ± 0.01 <sup>c,C</sup>	4.25 ± 0.05 <sup>d,C</sup>	1060 ± 3.01 <sup>a,C</sup>	1130 ± 6.63 <sup>b,C</sup>	1160 ± 2.10 <sup>c,C</sup>	1200 ± 10.15 <sup>d,C</sup>
21	3.30 ± 0.03 <sup>a,D</sup>	3.21 ± 0.01 <sup>b,D</sup>	3.09 ± 0.02 <sup>c,D</sup>	3.06 ± 0.00 <sup>d,D</sup>	1.84 ± 0.02 <sup>a,D</sup>	2.44 ± 0.00 <sup>b,D</sup>	3.82 ± 0.03 <sup>c,D</sup>	4.15 ± 0.03 <sup>d,D</sup>	1090 ± 10.75 <sup>a,D</sup>	1150 ± 11.25 <sup>b,D</sup>	1180 ± 11.52 <sup>c,D</sup>	1240 ± 12.00 <sup>d,D</sup>
28	3.36 ± 0.01 <sup>a,E</sup>	3.25 ± 0.02 <sup>b,E</sup>	3.17 ± 0.03 <sup>c,E</sup>	3.11 ± 0.01 <sup>d,E</sup>	1.79 ± 0.01 <sup>a,E</sup>	2.37 ± 0.01 <sup>b,E</sup>	3.75 ± 0.02 <sup>c,E</sup>	4.10 ± 0.01 <sup>d,E</sup>	1120 ± 9.95 <sup>a,E</sup>	1170 ± 4.12 <sup>b,E</sup>	1210 ± 3.58 <sup>c,E</sup>	1270 ± 6.83 <sup>d,E</sup>
35	3.40 ± 0.02 <sup>a,F</sup>	3.29 ± 0.01 <sup>b,F</sup>	3.22 ± 0.01 <sup>c,F</sup>	3.17 ± 0.02 <sup>d,F</sup>	1.72 ± 0.03 <sup>a,F</sup>	2.32 ± 0.01 <sup>b,F</sup>	3.62 ± 0.04 <sup>c,F</sup>	4.03 ± 0.04 <sup>d,E</sup>	1150 ± 12.10 <sup>a,F</sup>	1200 ± 6.58 <sup>b,F</sup>	1250 ± 4.50 <sup>c,F</sup>	1310 ± 4.45 <sup>d,F</sup>

a–d: Different small letters in the superscript in the same row denote differences at 5% between the fresh calafate juice and their cycles, according to the LSD test. A–F: Different capital letters in the superscript in the same column denote differences at 5% in the sample during storage time, according to the LSD test. C1, C2 and C3 represents cycle 1, cycle 2 and cycle 3, respectively.

Color parameters of fresh calafate juice and for each CBCC cycle during storage are shown in Table 3. The samples exhibited significant changes at each cycle, mentioning that the differences among the samples were quantitative and qualitative.

**Table 3.** CIELAB values of fresh calafate juice and cryoconcentrate samples during storage.

Day	Sample	L*	a*	b*	ΔE*
0	Fresh juice	33.95 ± 0.61 <sup>a</sup>	31.21 ± 2.72 <sup>a</sup>	3.11 ± 0.08 <sup>a</sup>	-
	C1	21.71 ± 1.01 <sup>b</sup>	39.58 ± 0.47 <sup>b</sup>	2.68 ± 0.24 <sup>b</sup>	14.84 ± 1.07 <sup>a</sup>
	C2	10.41 ± 0.51 <sup>c</sup>	43.40 ± 0.34 <sup>c</sup>	2.32 ± 0.21 <sup>b,c</sup>	26.52 ± 0.34 <sup>b</sup>
	C3	7.22 ± 0.19 <sup>d</sup>	46.71 ± 0.29 <sup>d</sup>	1.71 ± 0.08 <sup>d</sup>	30.92 ± 0.30 <sup>c</sup>
7	Fresh juice	32.05 ± 0.09 <sup>a</sup>	33.71 ± 1.00 <sup>a</sup>	3.04 ± 0.05 <sup>a</sup>	-
	C1	16.85 ± 0.23 <sup>b</sup>	41.44 ± 0.29 <sup>b</sup>	2.02 ± 0.02 <sup>b</sup>	17.08 ± 0.31 <sup>a</sup>
	C2	8.37 ± 0.14 <sup>c</sup>	44.85 ± 0.25 <sup>c</sup>	1.41 ± 0.13 <sup>c</sup>	26.22 ± 0.24 <sup>b</sup>
	C3	5.49 ± 0.26 <sup>d</sup>	48.45 ± 0.28 <sup>d</sup>	0.99 ± 0.03 <sup>d</sup>	30.44 ± 0.26 <sup>c</sup>
14	Fresh juice	31.12 ± 0.15 <sup>a</sup>	34.07 ± 0.13 <sup>a</sup>	3.00 ± 0.01 <sup>a</sup>	-
	C1	16.05 ± 0.05 <sup>b</sup>	41.94 ± 0.08 <sup>b</sup>	1.65 ± 0.06 <sup>b</sup>	17.05 ± 0.06 <sup>a</sup>
	C2	7.97 ± 0.03 <sup>c</sup>	45.07 ± 0.07 <sup>c</sup>	1.32 ± 0.01 <sup>c</sup>	25.68 ± 0.04 <sup>b</sup>
	C3	4.96 ± 0.02 <sup>d</sup>	49.18 ± 0.06 <sup>d</sup>	0.91 ± 0.02 <sup>d</sup>	30.28 ± 0.03 <sup>c</sup>
21	Fresh juice	25.84 ± 0.82 <sup>a</sup>	37.36 ± 0.32 <sup>a</sup>	2.79 ± 0.05 <sup>a</sup>	-
	C1	13.10 ± 0.60 <sup>b</sup>	43.41 ± 0.35 <sup>b</sup>	1.17 ± 0.04 <sup>b</sup>	14.20 ± 0.45 <sup>a</sup>
	C2	6.37 ± 0.16 <sup>c</sup>	46.48 ± 0.35 <sup>c</sup>	1.06 ± 0.06 <sup>c</sup>	21.58 ± 0.27 <sup>b</sup>
	C3	3.10 ± 0.05 <sup>d</sup>	50.46 ± 0.31 <sup>d</sup>	0.75 ± 0.05 <sup>d</sup>	26.32 ± 0.17 <sup>c</sup>
28	Fresh juice	20.25 ± 0.30 <sup>a</sup>	39.60 ± 0.33 <sup>a</sup>	2.33 ± 0.27 <sup>a</sup>	-
	C1	9.49 ± 0.14 <sup>b</sup>	45.30 ± 0.27 <sup>b</sup>	0.92 ± 0.04 <sup>b</sup>	12.26 ± 0.16 <sup>a</sup>
	C2	5.04 ± 0.07 <sup>c</sup>	48.31 ± 0.33 <sup>c</sup>	0.85 ± 0.04 <sup>c</sup>	17.58 ± 0.20 <sup>b</sup>
	C3	1.97 ± 0.02 <sup>d</sup>	52.34 ± 0.28 <sup>d</sup>	0.50 ± 0.05 <sup>d</sup>	22.36 ± 0.18 <sup>c</sup>
35	Fresh juice	13.57 ± 0.45 <sup>a</sup>	41.73 ± 0.24 <sup>a</sup>	1.99 ± 0.04 <sup>a</sup>	-
	C1	6.13 ± 0.02 <sup>b</sup>	47.67 ± 0.46 <sup>b</sup>	0.53 ± 0.03 <sup>b</sup>	9.63 ± 0.28 <sup>a</sup>
	C2	3.69 ± 0.15 <sup>c</sup>	51.00 ± 0.41 <sup>c</sup>	0.33 ± 0.03 <sup>c</sup>	13.65 ± 0.38 <sup>b</sup>
	C3	0.51 ± 0.37 <sup>d</sup>	55.00 ± 0.26 <sup>d</sup>	0.06 ± 0.01 <sup>d</sup>	18.72 ± 0.37 <sup>c</sup>

Different letters in the same column show significant differences at 5% between homogeneous groups in each variable to a LSD. C1, C2 and C3 represents cycle 1, cycle 2 and cycle 3, respectively. “-” corresponds to a control sample on the day of analysis.

At day 0, the fresh calafate juice presented a light reddish violet color ( $L^* \approx 34.0$ ,  $a^* \approx 31.2$  and  $b^* \approx 3.1$ ). However, to date, there are no studies that report the CIELAB color coordinates for calafate juice, but the color can be related to other fruit juices with comparable tonality such as strawberry juice [15], blueberry juice [18] and pomegranate juice [47]. Thus, at each CBCC cycle, a remarkable modification with respect to the fresh juice was observed, since  $L^*$  and  $b^*$  values decreased, i.e., the concentrate samples were darker with a slight brown tone, while  $a^*$  values had a significant increase, demonstrating a trend from the light red to dark red color (Figure 2). This behavior could be accredited to the increase in TSS values, since as the cycles advanced; more concentrated solute was separated from the ice fraction, leading to an intensification of the natural fruit juice color. These CIELAB values presented concordance with previous results for cryoconcentrated orange juice [10], strawberry juice [15], blueberry juice [18] and apple juice [48,49], in which the juices were darker with marked increase in  $a^*$  and/or  $b^*$  coordinates, depending on the initial juice color, as the cycles increased.

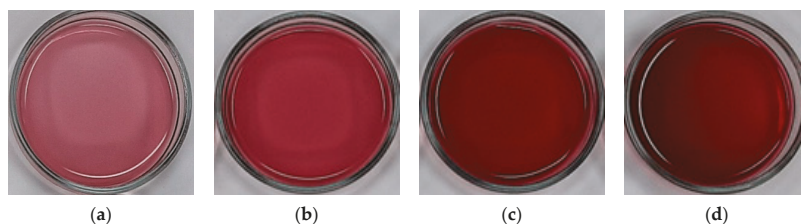


**Figure 2.** Visual appearance of samples: (a) fresh calafate juice; (b) cycle 1; (c) cycle 2; and (d) cycle 3.

In storage terms, at day 35, the fresh juice offered a considerable decrease in the  $L^*$  and  $b^*$  values by 60% and 36%, and  $a^*$  values had an increase by 34% with respect to the initial CIELAB values (day 0), respectively. Similarly, in the last cycle, a pronounced decrease by 93% and 97% was observed in  $L^*$  and  $b^*$  values in comparison to the values in the same cycle at day 0 ( $L^* = 7.22$  and  $b^* = 1.21$ ), respectively. On the contrary,  $a^*$  indicates an increase by 18% with respect to the third cycle at day 0 ( $a^* = 46.71$ ). Comparable performances, under different days of storage, were reported by Igual et al. [46] for grape juice, Yildiz and Aadil [50] for strawberry juice and Wurlitzer [51] for tropical fruit juices, specifying that the darkening and tendency to brown color is due to the compounds degradation by factors such as nonenzymatic Maillard reaction, exposure to air and light, pH changes and enzymatic activities, which leads to the oxidation in the sample that alters the visual appearance of the juice. Furthermore, the visual color of fresh calafate juice and each cycle during storage are presented in the Supplementary Materials (Figure S1), in which it is possible to observe the change from light reddish violet (fresh juice, day 0) to an attractive dark reddishness color due to the components concentration in the fresh calafate juice, as the cycles advanced. However, as the days passed, the color had a darker tone, which turned a brown color (cycle two) and a dark brown color (cycle three), which displays the degradation throughout the storage period, as mentioned above.

According to  $\Delta E^*$  evaluation (Table 3), at day 0, the values were over 14 CIELAB units, indicating that the human eye can find differences between fresh juice with each CBCC cycle, based on the scale proposed by Pankaj et al. [52] ( $\Delta E^* \geq 3$ , the color is humanly perceptible). The difference was more pronounced between fresh juice and the third cycle, since the  $\Delta E^*$  value was close to 31 units, indicating that the tendency to a dark reddish color generates a significant visual change to the fresh juice. As storage time passed, the  $\Delta E^*$  values were less noticeable than the samples at day 0. These  $\Delta E^*$  values were clearly depending on the TSS in the sample, since a high  $\Delta E^*$  between the fresh juice and cryoconcentrates was obtained by increasing the TSS cycle to cycle, and in turn, it can be related with the change in  $L^*$  values. As an important point, the decrease in the  $\Delta E^*$  values under storage time in comparison at day 0 is due to the progressive component degradation as days passed, with the color going from a light reddish violet to a red color, and from dark red to a dark brown, for the fresh juice and third cycle, from the day 0 to day 35, respectively, reducing the visual perception when the samples were compared.

### 3.4. TBC of Fresh and Cryoconcentrated Samples

TBC values at day 0 and during storage time of fresh juice and cryoconcentrated samples are presented in Table 4.

The TBC values (TPC, TAC and TFC) in fresh calafate juice (day 0) were close to 54.7 mg GAE/g d.m., 41.2 mg C3G/g d.m. and 31.9 mg CE/g d.m., respectively. These results were superior to those found by Brito et al. [53], who studied various bioactive components of native berries from VIII Region of Chile. The variations in TBC values could be due to the geographical characteristics in each Region, since there is a distance of approximately 1200 km between VIII Region and XI Region, which leads to diverse environmental conditions, genetic and species variabilities, affecting the time and form of fruit maturity and harvest-type method used by farmers, and thus, all these factors could explain the disparity between TBC values.

Table 4. Total bioactive compounds (TBC) values of fresh calafate juice and cryoconcentrates during 35 days of storage.

Day	TPC (mg GAE/g d.m.)			TAC (mg C3G/g d.m.)			TFC (mg CE/g d.m.)					
	Fresh Juice	C1	C2	C3	Fresh Juice	C1	C2	C3	Fresh Juice	C1	C2	C3
0	54.72 ± 0.02 aA	63.34 ± 0.66 bA	106.88 ± 0.77 cA	147.20 ± 0.04 dA	41.19 ± 0.07 aA	46.65 ± 0.65 bA	77.32 ± 0.48 cA	101.92 ± 0.53 dA	31.89 ± 0.45 aA	35.11 ± 0.58 bA	58.52 ± 0.34 cA	76.89 ± 0.41 dA
7	57.89 ± 0.20 aB	69.18 ± 0.38 bB	115.34 ± 1.25 cB	163.05 ± 2.30 dB	42.93 ± 0.50 aB	50.02 ± 0.40 bB	82.16 ± 0.59 cB	110.55 ± 5.35 dB	33.46 ± 1.29 aB	37.97 ± 1.05 bB	63.06 ± 0.55 cB	85.11 ± 0.08 dB
14	52.61 ± 0.38 aC	61.80 ± 0.31 bC	105.70 ± 4.34 cC	146.18 ± 3.73 dC	38.35 ± 0.59 aC	44.35 ± 0.21 bC	75.59 ± 0.53 cC	100.85 ± 4.28 dC	28.79 ± 0.52 aC	32.35 ± 1.27 bC	56.17 ± 0.56 cC	74.99 ± 1.25 dC
21	49.86 ± 0.39 aD	59.62 ± 0.39 bD	103.74 ± 0.97 cD	144.93 ± 0.77 dD	35.19 ± 0.66 aD	41.51 ± 0.73 bD	72.85 ± 0.06 cD	99.34 ± 3.59 dD	25.40 ± 0.51 aD	29.01 ± 0.55 bD	52.04 ± 0.34 cD	70.01 ± 0.64 dD
28	46.68 ± 0.17 aE	56.67 ± 1.09 bE	101.81 ± 1.79 cE	143.24 ± 1.23 dE	31.93 ± 0.44 aE	38.30 ± 0.18 bE	69.66 ± 0.12 cE	96.70 ± 0.93 dE	21.43 ± 0.39 aE	25.54 ± 0.27 bE	45.44 ± 0.85 cE	62.69 ± 1.08 dE
35	42.80 ± 0.56 aF	53.52 ± 1.85 bF	99.52 ± 1.64 cF	141.18 ± 1.71 dF	28.61 ± 0.31 aF	35.07 ± 0.47 bF	66.48 ± 0.38 cF	93.86 ± 4.29 dF	17.96 ± 0.28 aF	20.56 ± 1.23 bF	40.19 ± 0.06 cF	57.88 ± 0.80 dF

a–d: Different small letters in the superscript in the same row denote differences at 5% between the fresh calafate juice and their cycles, according to the LSD test. A–F: Different capital letters in the superscript in the same column denote differences at 5% in the sample during storage time, according to the LSD test. C1, C2 and C3 represents cycle 1, cycle 2 and cycle 3, respectively.

At day 0, the TBC values significantly increased as the cycles progressed, with an increase of approximately 1.2, 2.0 and 2.7, 1.1, 1.9 and 2.5 and 1.1, 1.8 and 2.4 times in relation to the initial TBC value, for TPC, TAC and TFC, for cycle 1, cycle 2 and cycle 3, respectively. Various studies showed a similar upward trend for TBC in the cryconcentration of orange juice [10], maqui juice [14], strawberry juice [15], pineapple juice [16], apple juice [17,32], blueberry juice [38] and broccoli extract [54], i.e., since as liquid food was concentrated at low temperatures, the thermolabile components were highly protected in comparison to high thermal concentration technology as evaporation, which seriously affects the bioactive composition of the liquid food due to the high processing temperatures [6].

In the first week of storage, all the samples presented a significant increase in TBC values, which exceeded the initial TBC value between 4% to 11%. This effect could be associated to the TSS behavior (Figure 1), since in the same week (day 7), the TSS values were higher than the initial results, and later, it decreased considerably during the weeks. Therefore, TSS and TBC are directly proportional. A clear and drastic decrease in TBC values was observed in the next weeks, and at the end of 35 days of storage, there was a reduction of up to 22%, 16%, 7% and 4% for TPC, 31%, 25%, 14% and 8% for TAC and 44%, 41%, 31% and 25% for TFC, with respect to the initial TBC value (day 0) for fresh juice, cycle one, cycle two and cycle three, respectively. This decline in the TBC values can be linked by factors as oxidation and/or polymerization of phenolic compounds with various proteins, and condensation of pigments with phenolic compounds present in the juice. Besides, the TBC degradation during storage time has been related to peroxidase enzyme activity [55]. However, to date, there are no studies on CC and enzymes that degrade bioactive components such as peroxidase, allowing the opening to future research.

### 3.5. TAA of Fresh and Cryoconcentrated Samples

The TAA values (mM TE in 100 g, on dry matter) in the fresh juice were approximately 6.9, 14.7, 23.0 and 21.4 for DPPH, ABTS, FRAP and ORAC, respectively (Table 5). These values are in line with values reported by Ruiz et al. [1], Mariangel et al. [3] and Brito et al. [53], who studied the antioxidant activity of calafate from different harvest seasons and geographical areas in Southern Chile, indicating that the variation in TAA values could be due to specific climatic and agricultural environments, since each Region presents endless characteristics that affect the genetic and growth of the fruits, pre-harvest phases, ripening, post-harvest processing, among other conditions, and thus, all these conditions impacts on the composition of the fruit.

As in TSS and TPC, as the cycles advanced, the differences in TAA values were statistically significant between the fresh juice and each cycle, with an increase of 2.5, 3.9 and 5.2-fold, 2.6, 3.9 and 5.1-fold, 1.9, 2.9 and 4.0-fold and 3.0, 4.1 and 5.3-fold, in comparison to the initial TAA values (fresh juice, day 0), for cycle one, cycle two and cycle three, for DPPH, ABTS, FRAP and ORAC, respectively. This upward behavior indicates a direct relationship with TSS and TBC values, since both values increased as the cycles progressed. The results are in agreement with CC reports applied to different liquid foods [15,48,56]. Hence, our results confirm that the conditions used to concentrate calafate juice allows an increase of TAA values, and thus, the sensitive components, as total anthocyanin content, are preserved, and these contribute to a high TAA [16,17,57,58].

As weeks passed, the TAA was progressively degraded, and at day 35, the fresh calafate juice was the sample most affected by storage time, with a decrease close to 40%, 42%, 48% and 50%, while, the third cycle gave lower TAA losses than the other samples, with reduction of approximately 15%, 19%, 24% and 27% in relation to the fresh juice value (day 0), for DPPH, ABTS, FRAP and ORAC, respectively. The downward trend of TAA values during the storage for several weeks are in agreement with other studies on fruit juices, which have described continuous TAA degradation such as sugarcane juice [42], grape juice [43,46], strawberry juice [50,59] and orange juice [60], which indicate that the oxidation of bioactive compounds and polymerization reactions of anthocyanins could be linked to the loss of antioxidant activity as the days passed.

**Table 5.** Total antioxidant activity (TAA) values of fresh calafate juice and cryoconcentrate samples during storage.

Day	Sample	DPPH *	ABTS *	FRAP **	ORAC **
0	Fresh juice	6.86 ± 0.51 <sup>a</sup>	14.74 ± 2.73 <sup>a</sup>	23.01 ± 1.87 <sup>a</sup>	21.40 ± 1.25 <sup>a</sup>
	C1	17.28 ± 1.47 <sup>b</sup>	38.91 ± 3.23 <sup>b</sup>	43.95 ± 3.04 <sup>b</sup>	63.77 ± 3.79 <sup>b</sup>
	C2	26.61 ± 1.51 <sup>c</sup>	57.04 ± 1.11 <sup>c</sup>	67.19 ± 2.57 <sup>c</sup>	87.95 ± 1.22 <sup>c</sup>
	C3	35.61 ± 2.04 <sup>d</sup>	75.47 ± 7.34 <sup>d</sup>	93.19 ± 5.74 <sup>d</sup>	113.21 ± 5.96 <sup>d</sup>
7	Fresh juice	7.11 ± 0.91 <sup>a</sup>	15.25 ± 0.77 <sup>a</sup>	23.91 ± 2.12 <sup>a</sup>	22.10 ± 1.77 <sup>a</sup>
	C1	18.36 ± 1.30 <sup>b</sup>	41.42 ± 2.15 <sup>b</sup>	46.64 ± 1.41 <sup>b</sup>	68.06 ± 1.14 <sup>b</sup>
	C2	28.95 ± 1.74 <sup>c</sup>	61.71 ± 4.39 <sup>c</sup>	72.51 ± 5.01 <sup>c</sup>	95.20 ± 2.65 <sup>c</sup>
	C3	39.51 ± 1.62 <sup>d</sup>	82.92 ± 2.55 <sup>d</sup>	102.23 ± 5.39 <sup>d</sup>	124.12 ± 3.24 <sup>d</sup>
14	Fresh juice	6.12 ± 0.25 <sup>a</sup>	12.02 ± 0.37 <sup>a</sup>	17.97 ± 1.71 <sup>a</sup>	15.96 ± 2.11 <sup>a</sup>
	C1	16.23 ± 0.91 <sup>b</sup>	35.41 ± 1.84 <sup>b</sup>	37.21 ± 3.27 <sup>b</sup>	52.18 ± 4.16 <sup>b</sup>
	C2	25.36 ± 1.01 <sup>c</sup>	53.62 ± 2.41 <sup>c</sup>	59.32 ± 4.91 <sup>c</sup>	74.63 ± 2.54 <sup>c</sup>
	C3	34.57 ± 2.21 <sup>d</sup>	72.36 ± 1.99 <sup>d</sup>	85.70 ± 3.22 <sup>d</sup>	101.12 ± 5.37 <sup>d</sup>
21	Fresh juice	5.33 ± 0.33 <sup>a</sup>	10.98 ± 0.78 <sup>a</sup>	16.34 ± 1.41 <sup>a</sup>	14.42 ± 1.24 <sup>a</sup>
	C1	15.08 ± 1.41 <sup>b</sup>	33.08 ± 1.02 <sup>b</sup>	35.28 ± 4.34 <sup>b</sup>	49.26 ± 2.04 <sup>b</sup>
	C2	24.24 ± 1.07 <sup>c</sup>	50.99 ± 2.01 <sup>c</sup>	56.76 ± 3.80 <sup>c</sup>	71.88 ± 1.95 <sup>c</sup>
	C3	33.41 ± 2.57 <sup>d</sup>	69.15 ± 2.07 <sup>d</sup>	83.43 ± 4.51 <sup>d</sup>	97.95 ± 3.35 <sup>d</sup>
28	Fresh juice	4.69 ± 0.40 <sup>a</sup>	9.81 ± 0.81 <sup>a</sup>	13.80 ± 1.71 <sup>a</sup>	12.36 ± 1.23 <sup>a</sup>
	C1	13.26 ± 1.02 <sup>b</sup>	29.14 ± 2.17 <sup>b</sup>	31.51 ± 2.36 <sup>b</sup>	42.99 ± 3.04 <sup>b</sup>
	C2	22.33 ± 2.14 <sup>c</sup>	45.48 ± 1.06 <sup>c</sup>	51.04 ± 3.25 <sup>c</sup>	62.45 ± 2.06 <sup>c</sup>
	C3	32.27 ± 0.43 <sup>d</sup>	65.73 ± 1.94 <sup>d</sup>	78.70 ± 2.74 <sup>d</sup>	92.52 ± 4.33 <sup>d</sup>
35	Fresh juice	4.11 ± 0.72 <sup>a</sup>	8.54 ± 1.99 <sup>a</sup>	12.04 ± 1.95 <sup>a</sup>	10.69 ± 2.54 <sup>a</sup>
	C1	12.33 ± 1.36 <sup>b</sup>	26.25 ± 0.77 <sup>b</sup>	28.49 ± 1.21 <sup>b</sup>	37.85 ± 1.74 <sup>b</sup>
	C2	20.96 ± 4.02 <sup>c</sup>	42.11 ± 1.67 <sup>c</sup>	45.38 ± 2.85 <sup>c</sup>	57.12 ± 3.23 <sup>c</sup>
	C3	30.22 ± 2.74 <sup>d</sup>	60.96 ± 7.25 <sup>d</sup>	71.18 ± 4.14 <sup>d</sup>	82.16 ± 4.47 <sup>d</sup>

Different letters in the same column show significant differences at 5% between homogeneous groups in each variable to a LSD. C1, C2 and C3 represents cycle 1, cycle 2 and cycle 3, respectively. \* Free radical scavenging capacity and \*\* Ferric reducing antioxidant power. All were determined as (mM TE/g d.m.)

### 3.6. Correlation between TBC and TAA

Correlation coefficients between TBC and TAA for cycle three are shown in Table 6. Furthermore, the correlation coefficients for fruit juice, cycle one and cycle two are presented in the Supplementary Materials (Tables S1–S3).

**Table 6.** Pearson's correlation coefficients (r) between biological active compounds content (TBC and TAA) obtained by centrifugal block cryoconcentration (CBCC) process (third cycle).

	TPC	TAC	TFC	DPPH	ABTS	FRAP	ORAC
TPC	1.00						
TAC	0.97 *	1.00					
TFC	0.96 *	0.96 *	1.00				
DPPH	0.94 *	0.99 *	0.98 *	1.00			
ABTS	0.90 *	0.98 *	0.99 *	1.00 *	1.00		
FRAP	0.91 *	0.97 *	0.98 *	0.99 *	1.00 *	1.00	
ORAC	0.90 *	0.96 *	0.97 *	0.98 *	0.99 *	1.00 *	1.00

\* Significant at 5%.

In all the samples, a positive and significant correlation was found between the biological active compounds content. The values (r) between 0.9 to 1.0, indicating the direct and proportional results between TBC and TAA, i.e., each component increased or decreased, as the cycles or the days under storage progressed, respectively. A similar trend was distinguished by Casas-Forero et al. [38] and

Correa et al. [57], who reported a high correlation (0.9 to 1.0) between antioxidant activity and bioactive compound in CC applied to blueberry juice and aqueous coffee extract, respectively.

### 3.7. Sensorial Analysis

The acceptance scores attributed by the panelists between fresh calafate juice and reconstituted cryoconcentrated juice (third cycle) are represented in Figure 3.

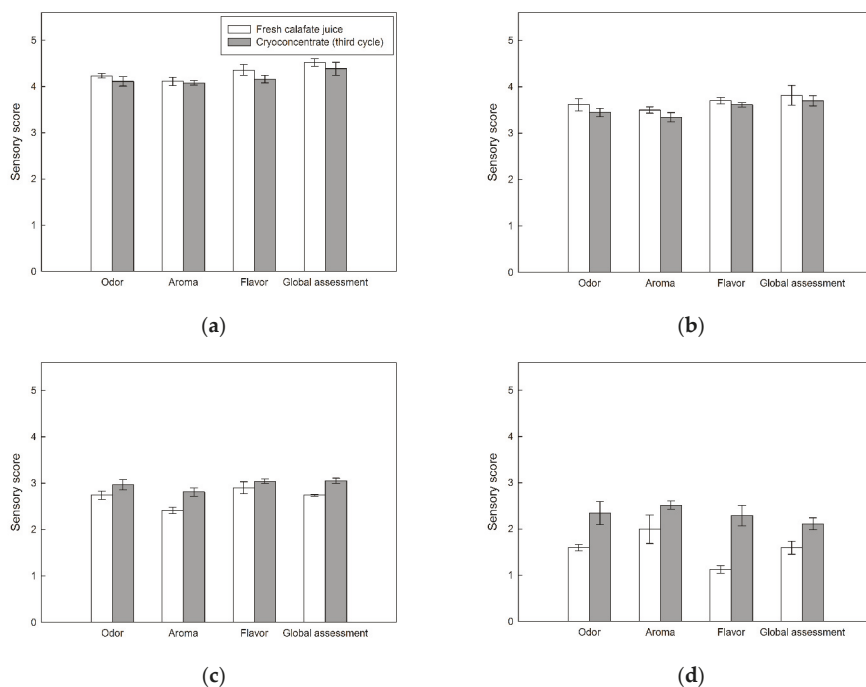


**Figure 3.** Sensory attributes between fresh calafate juice and reconstituted cryoconcentrated sample at the third cycle: (a) day 0; (b) day 7; (c) day 14; and (d) day 21.

In relation to the day 0, there were no significant differences in odor, aroma, flavor and global assessment between the fresh juice and reconstituted cryoconcentrated sample. Specifically, all the values were assessed as “like”, since the evaluations were superior to four points, i.e., the panelists specified a pleasure when tasting the fresh and cryoconcentrated juices, without finding differences when comparing the quality sensorial characteristics.

At day 7, the hedonic scale scores decreased significantly compared at day 0, with values between 3.0 and 3.8 points, which is equivalent to the category “liked slightly”. Therefore, the samples were considered as accepted for the sensorial panelists. Despite the decline, there were no statistical differences between the scores assigned by the panelists for the sensory attributes among the samples.

Nonetheless, as days advanced, the panelists reported an increase in the degree of rejection between samples, since the scores decreased considerably, and in addition, the points between the fresh juice and cryoconcentrated varied significantly. Specifically, the cryoconcentrated had better acceptance than the fresh juice, with scores of approximately 2.8–3.0 versus 2.4–2.9 and 2.1–2.5 versus 1.1–2.0, for day 14 and day 21, respectively. Thus, these scores designated a negative impression of the samples with respect to their sensorial characteristics. However, from 14 days in storage, the cryoconcentrates were more accepted to the sensory panel than the fresh juice, reinforcing that CC maintains better sensory attributes in the reconstituted concentrates than fresh juice during refrigerated storage.

Based on these results, at day 14 and day 21, the cryoconcentrated samples presented better scores than the fresh juice, since, as mentioned above, previous studies have shown that CC technology allowed the obtaining of high TSS values, and in turn, these increases the volatile compounds release [17]. Therefore, the reconstituted juice contains a high organoleptic acceptance that can be connected to taste and aroma, and thus, it resist storage time better than fresh juice, since the fresh juice possibly had a high fermentation level, generating more rancid odors and flavors on day 21 [61], i.e., the fresh juice was more vulnerable to external factors [62], which eventually led to a high degree of rejection. However, to date, there are no studies that compare a fruit juice with a reconstituted cryoconcentrated juice in terms of bioactive components, antioxidant capacity, volatile compounds and physicochemical properties. Therefore, a very interesting study about the commercialization of cryoconcentrated juice could be realized with similar concentration that a fresh juice.

Sensory analysis results on days 28 and 35 were not presented, since on day 21, the panelists indicated a high disgust and complete rejection, with values less than 2.5 point for all the characteristics evaluated.

Therefore, CC technology allows the preservation of different sensory attributes, and in turn, its concentration at low temperatures proves a high similarity in the reconstituted concentrate to the original sample. Analogous trends were observed in CC studies applied to apple juice [17], coffee extract [31], black currant juice [63] and Andes berry pulp [64].

#### 4. Conclusions

CBCC positively affects the quality properties of fresh calafate juice, as exemplified by the high TSS values obtained in the last cycle (42 °Brix). Additionally, this non-thermal technology intensifies the natural juice color to an attractive dark reddish color. Subjecting fresh calafate juice to CBCC resulted in high TBC content, with values over 2.4 times the initial TBC values. Moreover, the TAA presented a similar behavior, since these increased between 4.0 to 5.3 times, in comparison to the initial TAA values. These values indicate the advantages of CBCC application as a green technology to extract a high amount of concentrated liquid from the ice matrix without the use of high temperatures.

Under refrigerated storage time of 35 days, the CBCC samples showed better stability than the fresh juice, since the cryoconcentrated samples showed a low decreasing rate in their nutritional properties, inferring that CBCC allows to concentrate and to retain various bioactive and antioxidant components naturally present in calafate juice.

Additionally, until the day 21, sensory panelists reported acceptability of the reconstituted cryoconcentrated sample, while the fresh juice was totally rejected, reinforcing that CBCC also concentrate and preserve volatile components that are perceived by the panelists as an important quality parameter.

Therefore, CBCC can be considered a novel and viable technology for the preservation of quality attributes from fresh native juice with interesting food application of the cryoconcentrates due to its high stability during storage time and low bioactive components degradation in comparison to the fresh juice.

**Supplementary Materials:** The following are available online at <http://www.mdpi.com/2304-8158/9/9/1314/s1>, Figure S1: Visual appearance of fresh juice and concentrate samples at each cycle during storage., Table S1: Pearson's correlation coefficients (r) between biological active compounds content of fresh calafate juice., Table S2: Pearson's correlation coefficients (r) between biological active compounds content (TBC and TAA) obtained by CBCC process (first cycle), Table S3: Pearson's correlation coefficients (r) between biological active compounds content (TBC and TAA) obtained by CBCC process (second cycle).

**Author Contributions:** Conceptualization, P.O.-P., R.N.Z. and G.P.; methodology, P.O.-P., N.C.-F. and G.T.-B.; software, G.T.-B. and N.C.-F.; validation, G.T.-B., R.N.Z. and N.C.-F.; formal analysis, P.O.-P. and G.T.-B.; investigation, P.O.-P., N.C.-F. and G.P.; resources, P.O.-P.; data curation, P.O.-P., G.T.-B., N.C.-F. and G.P.; writing—original draft preparation, P.O.-P. and R.N.Z.; writing—review and editing, P.O.-P. and G.P.; visualization, P.O.-P.; supervision, R.N.Z. and G.P.; project administration, P.O.-P.; funding acquisition, P.O.-P. All authors have read and agreed to the published version of the manuscript.

**Funding:** This research was funded by ANID-Chile (Agencia Nacional de Investigación y Desarrollo de Chile) through the FONDECYT Postdoctoral Grant 2019 (Folio 3190420).

**Acknowledgments:** Patricio Orellana-Palma acknowledges the financial support of ANID-Chile (Agencia Nacional de Investigación y Desarrollo de Chile) through the FONDECYT Postdoctoral Grant 2019 (Folio 3190420).

**Conflicts of Interest:** The authors declare no conflict of interest.

## References

1. Ruiz, A.; Hermosin-Gutierrez, I.; Mardones, C.; Vergara, C.; Herlitz, E.; Vega, M.; Dorau, C.; Winterhalter, P.; von Baer, D. Polyphenols and antioxidant activity of calafate (*Berberis microphylla*) fruits and other native berries from Southern Chile. *J. Agric. Food Chem.* **2010**, *58*, 6081–6089. [\[CrossRef\]](#)
2. Schmeda-Hirschmann, G.; Jiménez-Aspee, F.; Theoduloz, C.; Ladio, A. Patagonian berries as native food and medicine. *J. Ethnopharmacol.* **2019**, *241*, 111979. [\[CrossRef\]](#) [\[PubMed\]](#)
3. Mariangel, E.; Reyes-Diaz, M.; Lobos, W.; Bensch, E.; Schalchli, H.; Ibarra, P. The antioxidant properties of calafate (*Berberis microphylla*) fruits from four different locations in southern Chile. *Cien. Investig. Agrar.* **2013**, *40*, 161–170. [\[CrossRef\]](#)
4. Sadilova, E.; Stintzing, F.C.; Kammerer, D.R.; Carle, R. Matrix dependent impact of sugar and ascorbic acid addition on color and anthocyanin stability of black carrot, elderberry and strawberry single strength and from concentrate juices upon thermal treatment. *Food Res. Int.* **2009**, *42*, 1023–1033. [\[CrossRef\]](#)
5. Hernández-Hernández, H.M.; Moreno-Vilet, L.; Villanueva-Rodríguez, S.J. Current status of emerging food processing technologies in Latin America: Novel non-thermal processing. *Innov. Food Sci. Emerg.* **2019**, *58*, 102233. [\[CrossRef\]](#)
6. Petzold, G.; Orellana, P.; Moreno, J.; Junod, J.; Bugueño, G. Freeze concentration as a technique to protect valuable heat-labile components of foods. In *Innovative Processing Technologies for Foods with Bioactive Compounds*, 1st ed.; Moreno, J.J., Ed.; CRC Press: Boca Raton, FL, USA, 2016; pp. 184–190.
7. Orellana-Palma, P.A. External Forces Assisted Cryoconcentration to Improve the Concentration Process and the Quality of Fruit Juices. Ph.D. Thesis, Universidad del Bío-Bío, Chillán, Chile, May 2018.
8. Amran, N.A.; Samsuri, S.; Safiei, N.Z.; Zakaria, Z.Y.; Jusoh, M. Review: Parametric study on the performance of progressive cryoconcentration system. *Chem. Eng. Commun.* **2016**, *203*, 957–975. [\[CrossRef\]](#)
9. Aider, M.; de Halleux, D. Passive and microwave-assisted thawing in maple sap cryoconcentration technology. *J. Food Eng.* **2008**, *85*, 65–72. [\[CrossRef\]](#)
10. Orellana-Palma, P.; Petzold, G.; Andana, I.; Torres, N.; Cuevas, C. Retention of ascorbic acid and solid concentration via centrifugal freeze concentration of orange juice. *J. Food Qual.* **2017**, *2017*, 5214909. [\[CrossRef\]](#)
11. Petzold, G.; Orellana, P.; Moreno, J.; Cerda, E.; Parra, P. Vacuum-assisted block freeze concentration applied to wine. *Innov. Food Sci. Emerg.* **2016**, *36*, 330–335. [\[CrossRef\]](#)
12. Kawasaki, K.; Matsuda, A.; Kadota, H. Freeze concentration of equal molarity solutions with ultrasonic irradiation under constant freezing rate; effect of solute. *Chem. Eng. Res. Des.* **2006**, *84*, 107–112. [\[CrossRef\]](#)
13. Petzold, G.; Aguilera, J.M. Centrifugal freeze concentration. *Innov. Food Sci. Emerg.* **2013**, *20*, 253–258. [\[CrossRef\]](#)
14. Bastías-Montes, J.M.; Martín, V.S.; Muñoz-Fariña, O.; Petzold-Maldonado, G.; Quevedo-León, R.; Wang, H.; Yang, Y.; Céspedes-Acuña, C.L. Cryoconcentration procedure for aqueous extracts of maqui fruits prepared by centrifugation and filtration from fruits harvested in different years from the same localities. *J. Berry Res.* **2019**, *9*, 377–394. [\[CrossRef\]](#)
15. Adorno, W.T.; Rezzadori, K.; Arend, G.D.; Chaves, V.C.; Reginatto, F.H.; Di Luccio, M.; Petrus, J.C. Enhancement of phenolic compounds content and antioxidant activity of strawberry (*Fragaria xananassa*) juice by block freeze concentration technology. *Int. J. Food Sci. Technol.* **2017**, *52*, 781–787. [\[CrossRef\]](#)
16. Orellana-Palma, P.; Zuñiga, R.N.; Takhar, P.S.; Gianelli, M.P.; Petzold, G. Effects of centrifugal block freeze crystallization on quality properties in pineapple juice. *Chem. Eng. Technol.* **2020**, *43*, 355–364. [\[CrossRef\]](#)
17. Orellana-Palma, P.; Lazo-Mercado, V.; Gianelli, M.P.; Hernández, E.; Zuñiga, R.; Petzold, G. Influence of cryoconcentration on quality attributes of apple juice (*Malus domestica* cv. Red Fuji). *Appl. Sci.* **2020**, *10*, 959. [\[CrossRef\]](#)
18. Orellana-Palma, P.; Petzold, G.; Guerra-Valle, M.; Astudillo-Lagos, M. Impact of block cryoconcentration on polyphenol retention in blueberry juice. *Food Biosci.* **2017**, *20*, 149–158. [\[CrossRef\]](#)

19. AOAC. *Official Methods of Analysis of the Association of Official Analytical Chemists (AOAC) International*, 19th ed.; Helrich, K., Ed.; AOAC: Washington, DC, USA, 1990; pp. 910–928.
20. Currie, L.A.; Svehla, G.Y.U.L.A. Nomenclature for the presentation of results of chemical analysis (IUPAC Recommendations 1994). *Pure Appl. Chem.* **1994**, *66*, 595–608. [CrossRef]
21. Singleton, V.L.; Orthofer, R.; Lamuela-Raventós, R.M. Analysis of total phenols and other oxidation substrates and antioxidants by means of Folin-ciocalteu reagent. *Methods Enzymol.* **1999**, *29*, 152–178. [CrossRef]
22. Lee, J.; Durst, R.W.; Wrolstad, R.E. Determination of total monomeric anthocyanin pigment content of fruit juices, beverages, natural colorants, and wines by the pH differential method: Collaborative study. *J. AOAC Int.* **2005**, *88*, 1269–1278. [CrossRef]
23. Dewanto, V.; Wu, X.; Adom, K.K.; Liu, R.H. Thermal processing enhances the nutritional value of tomatoes by increasing total antioxidant activity. *J. Agric. Food Chem.* **2002**, *50*, 3010–3014. [CrossRef]
24. Brand-Williams, W.; Cuvelier, M.E.; Berset, C. Use of a free radical method to evaluate antioxidant activity. *LWT-Food Sci. Technol.* **1995**, *28*, 25–30. [CrossRef]
25. Re, R.; Pellegrini, N.; Proteggente, A.; Pannala, A.; Yang, M.; Rice, C. Antioxidant activity applying an improved ABTS radical cation decolorization assay. *Free Radic. Biol. Med.* **1999**, *26*, 1231–1237. [CrossRef]
26. Benzie, I.F.F.; Strain, J.J. The ferric reducing ability of plasma (FRAP) as a measure of “Antioxidant Power”: The FRAP assay. *Anal. Biochem.* **1996**, *239*, 70–76. [CrossRef] [PubMed]
27. Ou, B.; Hampsch, M.; Prior, R.L. Development and validation of an improved oxygen radical absorbance capacity assay using fluorescein as the fluorescent probe. *J. Agric. Food Chem.* **2001**, *49*, 4619–4626. [CrossRef]
28. Petzold, G.; Orellana, P.; Moreno, J.; Valeria, P. Physicochemical properties of cryoconcentrated orange juice. *Chem. Eng. Trans.* **2019**, *75*, 37–42. [CrossRef]
29. ODEPA. *Catastro Frutícola Principales Resultados, Región de Los Lagos, Información Regional, Ministerio de Agricultura, Gobierno de Chile, Chile, 2019*. Available online: [https://www.odepa.gob.cl/wp-content/uploads/2019/09/catastro\\_aysen.pdf](https://www.odepa.gob.cl/wp-content/uploads/2019/09/catastro_aysen.pdf) (accessed on 12 July 2020).
30. Petzold, G.; Moreno, J.; Lastra, P.; Rojas, K.; Orellana, P. Block freeze concentration assisted by centrifugation applied to blueberry and pineapple juices. *Innov. Food Sci. Emerg.* **2015**, *30*, 192–197. [CrossRef]
31. Moreno, F.L.; Quintanilla-Carvajal, M.X.; Sotelo, L.I.; Osorio, C.; Raventós, M.; Hernández, E.; Ruiz, Y. Volatile compounds, sensory quality and ice morphology in falling-film and block freeze concentration of coffee extract. *J. Food Eng.* **2015**, *166*, 64–71. [CrossRef]
32. Ding, Z.; Qin, F.G.; Yuan, J.; Huang, S.; Jiang, R.; Shao, Y. Concentration of apple juice with an intelligent freeze concentrator. *J. Food Eng.* **2019**, *256*, 61–72. [CrossRef]
33. Lemos, A.T.; Ribeiro, A.C.; Delgado, I.; Saraiva, J.A. Shelf-life extension of watermelon juice preserved by hyperbaric storage at room temperature compared to refrigeration. *LWT-Food Sci. Technol.* **2020**, *117*, 108695. [CrossRef]
34. Wahia, H.; Zhou, C.; Mustapha, A.T.; Amanor-Atiemoh, R.; Mo, L.; Fakayode, O.A.; Ma, H. Storage effects on the quality quartet of orange juice submitted to moderate thermosonication: Predictive modeling and odor fingerprinting approach. *Ultrason. Sonochem.* **2020**, *64*, 104982. [CrossRef]
35. Chia, S.L.; Rosnah, S.; Noranizan, M.A.; Ramli, W.W. The effect of storage on the quality attributes of ultraviolet-irradiated and thermally pasteurised pineapple juices. *Int. Food Res. J.* **2012**, *19*, 1001–1010.
36. Arena, M.E.; Zuleta, A.; Dyer, L.; Constenla, D.; Ceci, L.; Curvetto, N. *Berberis buxifolia* fruit growth and ripening: Evolution in carbohydrate and organic acid contents. *Sci. Hortic.* **2013**, *158*, 52–58. [CrossRef]
37. Khajehei, F.; Niakousari, M.; Eskandari, M.H.; Sarshar, M. Production of pomegranate juice concentrate by complete block cryoconcentration process. *J. Food Process. Preserv.* **2015**, *38*, 488–498. [CrossRef]
38. Casas-Forero, N.; Orellana-Palma, P.; Petzold, G. Influence of block freeze concentration and evaporation on physicochemical properties, bioactive compounds and antioxidant activity in blueberry juice. *Food Sci. Technol.* **2020**, in press. [CrossRef]
39. Abid, M.; Jabbar, S.; Wu, T.; Hashim, M.M.; Hu, B.; Saeeduddin, M.; Zeng, X. Qualitative assessment of sonicated apple juice during storage. *J. Food Process. Preserv.* **2015**, *39*, 1299–1308. [CrossRef]
40. Bhardwaj, R.L.; Pandey, S. Juice blends—a way of utilization of under-utilized fruits, vegetables, and spices: A review. *Crit. Rev. Food Sci. Nutr.* **2011**, *51*, 563–570. [CrossRef]
41. Parish, M.E.; Worobo, R.W.; Danyluk, M.D. Juices and Juice-containing Beverages. In *Compendium of Methods for the Microbiological Examination of Foods*, 1st ed.; Salfinger, Y., Tortorello, M.L., Eds.; Apha Press: Philadelphia, PA, USA, 2015; pp. 115–156.

42. Zia, S.; Khan, M.R.; Zeng, X.A.; Shabbir, M.A.; Aadil, R.M. Combined effect of microwave and ultrasonication treatments on the quality and stability of sugarcane juice during cold storage. *Int. J. Food Sci. Technol.* **2019**, *54*, 2563–2569. [[CrossRef](#)]
43. Mesquita, T.C.; Schiassi, M.C.E.V.; Lago, A.M.T.; Careli-Gondim, Í.; Silva, L.M.; de Azevedo Lira, N.; Nunes Carvalho, E.E.; de Oliveira Lima, L.C. Grape juice blends treated with gamma irradiation evaluated during storage. *Radiat. Phys. Chem.* **2020**, *168*, 108570. [[CrossRef](#)]
44. Mezey, J.; Mezeyová, I. Changes in the levels of selected organic acids and sugars in apple juice after cold storage. *Czech J. Food Sci.* **2018**, *36*, 175–180. [[CrossRef](#)]
45. Orellana-Palma, P.; González, Y.; Petzold, G. Improvement of centrifugal cryoconcentration by ice recovery applied to orange juice. *Chem. Eng. Technol.* **2019**, *42*, 925–931. [[CrossRef](#)]
46. Igual, M.; Contreras, C.; Camacho, M.M.; Martínez-Navarrete, N. Effect of thermal treatment and storage conditions on the physical and sensory properties of grapefruit juice. *Food Bioprocess Technol.* **2014**, *7*, 191–203. [[CrossRef](#)]
47. Cano-Lamadrid, M.; Nowicka, P.; Hernández, F.; Carbonell-Barrachina, A.A.; Wojdyło, A. Phytochemical composition of smoothies combining pomegranate juice (*Punica granatum* L) and Mediterranean minor crop purées (*Ficus carica*, *Cydonia oblonga*, and *Ziziphus jujube*). *J. Sci. Food Agric.* **2018**, *98*, 5731–5741. [[CrossRef](#)] [[PubMed](#)]
48. Zielinski, A.A.; Zardo, D.M.; Alberti, A.; Bortolini, D.G.; Benvenuti, L.; Demiate, I.M.; Nogueira, A. Effect of cryoconcentration process on phenolic compounds and antioxidant activity in apple juice. *J. Sci. Food Agric.* **2019**, *99*, 2786–2792. [[CrossRef](#)] [[PubMed](#)]
49. Qin, F.G.; Ding, Z.; Peng, K.; Yuan, J.; Huang, S.; Jiang, R.; Shao, Y. Freeze concentration of apple juice followed by centrifugation of ice packed bed. *J. Food Eng.* **2020**, *291*, 110270. [[CrossRef](#)]
50. Yıldız, G.; Aadil, R.M. Comparison of high temperature-short time and sonication on selected parameters of strawberry juice during room temperature storage. *Int. J. Food Sci. Technol.* **2020**, *57*, 1462–1468. [[CrossRef](#)]
51. Wurlitzer, N.J.; Dionísio, A.P.; Lima, J.R.; dos Santos Garruti, D.; da Silva Araújo, I.M.; da Rocha, R.F.J.; Maia, J.L. Tropical fruit juice: Effect of thermal treatment and storage time on sensory and functional properties. *J. Food Sci. Technol.* **2019**, *56*, 5184–5193. [[CrossRef](#)]
52. Pankaj, B.P.; Umezuruike, L.O.; Fahad, A.A. Colour measurement and analysis in fresh and processed foods: A review. *Food Bioprocess Technol.* **2013**, *6*, 36–60. [[CrossRef](#)]
53. Brito, A.; Areche, C.; Sepúlveda, B.; Kennelly, E.J.; Simirgiotis, M.J. Anthocyanin characterization, total phenolic quantification and antioxidant features of some Chilean edible berry extracts. *Molecules* **2014**, *19*, 10936–10955. [[CrossRef](#)]
54. Azhar, A.N.; Panirselvam, M.; Amran, N.A.; Ruslan, M.S.; Samsuri, S. Retention of total phenolic content and antioxidant activity in the concentration of broccoli extract by progressive freeze concentration. *Int. J. Food Eng.* **2020**, in press. [[CrossRef](#)]
55. Feng, X.; Zhou, Z.; Wang, X.; Bi, X.; Ma, Y.; Xing, Y. Comparison of high hydrostatic pressure, ultrasound, and heat treatments on the quality of strawberry–apple–lemon juice blend. *Foods* **2020**, *9*, 218. [[CrossRef](#)]
56. Samsuri, S.; Li, T.H.; Ruslan, M.S.H.; Amran, N.A. Antioxidant recovery from pomegranate peel waste by integrating maceration and freeze concentration technology. *Int. J. Food Eng.* **2020**, in Press. [[CrossRef](#)]
57. Correa, L.J.; Ruiz, R.Y.; Moreno, F.L. Effect of falling-film freeze concentration on bioactive compounds in aqueous coffee extract. *J. Food Process Eng.* **2018**, *41*, e12606. [[CrossRef](#)]
58. Orellana-Palma, P.; Petzold, G.; Pierre, L.; Pensaben, J.M. Protection of polyphenols in blueberry juice by vacuum-assisted block freeze concentration. *Food Chem. Toxicol.* **2017**, *109*, 1093–1102. [[CrossRef](#)]
59. Tomadoni, B.; Cassani, L.; Viacava, G.; Moreira, M.D.R.; Ponce, A. Effect of ultrasound and storage time on quality attributes of strawberry juice. *J. Food Process Eng.* **2017**, *40*, e12533. [[CrossRef](#)]
60. Lu, Q.; Li, L.; Xue, S.; Yang, D.; Wang, S. Stability of flavonoid, carotenoid, soluble sugar and vitamin C in ‘Cara Cara’ juice during storage. *Foods* **2019**, *8*, 417. [[CrossRef](#)]
61. Rios-Corripio, G.; Guerrero-Beltrán, J.A. Physicochemical, antioxidant and sensory characteristics of black cherry (*Prunus serotina* subsp. *capuli*) fermented juice. *Int. J. Fruit Sci.* **2020**, in press. [[CrossRef](#)]
62. Walking-Ribeiro, M.; Noci, F.; Cronin, D.A.; Lyng, J.G.; Morgan, D.J. Shelf life and sensory evaluation of orange juice after exposure to thermosonication and pulsed electric fields. *Food Bioprod. Process.* **2009**, *87*, 102–107. [[CrossRef](#)]

63. Dette, S.S.; Jansen, H. Freeze concentration of black currant juice. *Chem. Eng. Technol.* **2010**, *33*, 762–766. [\[CrossRef\]](#)
64. Ramos, F.A.; Delgado, J.L.; Bautista, E.; Morales, A.L.; Duque, C. Changes in volatiles with the application of progressive freeze-concentration to Andes berry (*Rubus glaucus* Benth). *J. Food Eng.* **2005**, *69*, 291–297. [\[CrossRef\]](#)



© 2020 by the authors. Licensee MDPI, Basel, Switzerland. This article is an open access article distributed under the terms and conditions of the Creative Commons Attribution (CC BY) license (<http://creativecommons.org/licenses/by/4.0/>).



Article

# Mineral Composition and Antioxidant Potential of Coffee Beverages Depending on the Brewing Method

Katarzyna Janda <sup>1,\*</sup>, Karolina Jakubczyk <sup>1</sup>, Irena Baranowska-Bosiacka <sup>2</sup>, Patrycja Kapczuk <sup>2</sup>, Joanna Kochman <sup>1</sup>, Ewa Rębacz-Maron <sup>3</sup> and Izabela Gutowska <sup>4</sup>

<sup>1</sup> Pomeranian Medical University in Szczecin, Department of Human Nutrition and Metabolomics, 24 Broniewskiego Street, 71-460 Szczecin, Poland; jakubczyk.kar@gmail.com (K.J.); kochmaan@gmail.com (J.K.)

<sup>2</sup> Department of Biochemistry, Pomeranian Medical University in Szczecin, 71 Powstańców Wlkp. Street, 70-111 Szczecin, Poland; irena.bosiacka@pum.edu.pl (I.B.-B.); patrycja2510@o2.pl (P.K.)

<sup>3</sup> Department of Vertebrate Zoology and Anthropology, Institute of Biology, University of Szczecin, 13 Wąska Street, 71-415 Szczecin, Poland; ewa.rebacz-maron@usz.edu.pl

<sup>4</sup> Department of Medical Chemistry, Pomeranian Medical University in Szczecin, 71 Powstańców Wlkp. Street, 70-111 Szczecin, Poland; izagut@poczta.onet.pl

\* Correspondence: kjanda4@gmail.com

Received: 17 December 2019; Accepted: 21 January 2020; Published: 23 January 2020

**Abstract:** Coffee, being one of the world's most popular beverages, is a rich source of dietary antioxidants. The aim of this study was to determine the mineral content and antioxidant activity as well as acidity of coffee beverages depending on the brewing technique. We tested coffee brews made and served at a popular urban coffee shop (Szczecin, Poland). Five coffee brewing techniques were used: Aeropress, drip, espresso machine, French press, and simple infusion. Our findings showed that the brewing method had a significant effect on all parameters tested in the study. The antioxidant activity of the beverages was high (31%–42% inhibition of DPPH (2,2-diphenyl-1-picrylhydrazyl); reduction potential from 3435.06 mol Fe<sup>3+</sup>/mL to 4298.19 mol Fe<sup>3+</sup>/mL). Polyphenolic content ranged from 133.90 g (French press) to 191.29 g of gallic acid/L (Aeropress brew), depending on the coffee extraction method. Mineral content was also found to differ between brewing methods. Coffees prepared by simple infusion and Aeropress provided a valuable source of magnesium, manganese, chromium, cobalt, and potassium, whereas the drip brew was found to be a good source of silicon.

**Keywords:** beverages; brewing method; antioxidant potential; total polyphenols content; mineral composition

## 1. Introduction

Along with changes in modern society, as people's lives are getting faster and more intense, stimulant beverages are becoming increasingly popular. These products have been found to diminish fatigue, enhance concentration, boost productivity, and generally improve performance [1]. Coffee is one of such substances and, in parallel, is one of the most popular beverages [2]. For many people, coffee drinking is part of their lifestyle and a daily habit. Every day, millions of people—about 40% of the world population—begin their day with a morning cup of coffee [3]. Coffee beverages are consumed for various reasons, including their stimulatory effects resulting from the presence of caffeine, health benefits attributed to their rich phytochemistry, and, predominantly, due to excellent taste and aroma. Although flavor, aroma, and the content of caffeine (1,3,7-trimethylpurine-2,6-dione) play a role in its popularity, coffee (both beans and beverages) is a complex chemical mixture, reported to contain more than a thousand of different chemical compounds, including carbohydrates, lipids, nitrogen, vitamins, minerals, alkaloids, and phenolic compounds [2–4]. Various studies have suggested that coffee

consumption helps to reduce the risk of number of health conditions, including Alzheimer's disease, Parkinson's disease, heart disease, type 2 diabetes mellitus, liver cirrhosis, as well as certain types of disorders [3,4]. Regular consumption of coffee, both green and roasted, is recommended in order to lower the risk of metabolic syndrome [5]. These health-promoting properties of coffee have been linked with its antioxidant content. Indeed, coffee is one of the richest sources of these compounds [4]. Coffee beverages are also a dietary sources of minerals [2,4,6]. The concentrations of minerals and biologically active substances depend of the place of origin of the beans, the degree/intensity of roasting, as well as the brewing method [5–10].

There are no reports in the literature linking the brewing method to the antioxidant and mineral content. In this study, an attempt was made to determine the correlation between the antioxidant activity and the content of minerals in coffee brews.

## 2. Materials and Methods

In this study, we tested coffee brews (espresso blend—100% arabica) made and served at a popular urban coffee shop (an outlet in Szczecin, Poland).

### 2.1. Coffee Brewing Methods

Filtered water was used to make coffee beverages.

**Aeropress:** The Aeropress coffee maker was used. For 250.0 mL of the infusion, 18.0 g of quite coarsely ground coffee was used. The water had a temperature of 93 °C, and the pressure was 2–4 bars. The brewing lasted 2 min.

**Drip:** A drip coffee maker device was used. Medium ground coffee beans (18.0 g) were placed in a paper filter. A total of 300.0 mL of water at 92 °C was added to the tank and the machine was turned on. After 2.5 min, when the coffee was ready, samples were taken for measurement.

**Espresso:** An espresso machine was used. For 250 mL of the brew, 17.0 g of the most finely ground coffee was used. The water had a temperature of 92 °C. The coffee machine was set to 9 bars with regards to pressure.

**Simple infusion:** A total of 17.0 g of very finely ground coffee was placed inside the beaker, 250 mL of hot water (92 °C) poured inside, and it was left to steep. After 5 min, coffee samples were taken for analysis.

**French press:** A French press device, also called a press pot or a coffee plunger, was used. The pot was placed on a flat surface, with the plunger pulled out, and 17.0 g of medium ground coffee was added and then 300.0 mL of hot water (92 °C) was gently poured inside. Then the plunger was reinserted into the pot on the surface of the beverage and plunged down after 5 min. Under these conditions, a pressure of 1–2 bars was reached. Once the press plunger was pushed down, coffee samples were taken for analysis.

### 2.2. Spectrophotometric Assay

Determination of antioxidant activity, the reduction potential, and polyphenol content were determined using spectrophotometer Agilent 8453UV. All assays were performed in triplicate. For analysis, infusions were diluted 20 times.

#### 2.2.1. Determination of Antioxidant Activity

The antioxidant activity of samples was measured with spectrophotometric method using synthetic radical DPPH (2,2-diphenyl-1-picrylhydrazyl, Sigma Aldrich, Darmstadt, Germany). Antioxidant potential (antioxidant activity, inhibition) of tested solutions has been expressed by the percent of DPPH inhibition [6].

### 2.2.2. Determination of Total Polyphenol Content

Determination of polyphenols was performed according to ISO (International Organization for Standardization) 14502-1 using Folin–Ciocalteu reagent [11]. A total of 5.0 mL of a 10% Folin–Ciocalteu solution and 1.0 mL of test sample were successively introduced into the vial. The sample was shaken vigorously, and after 5 min, 4.0 mL of 7.5% Na<sub>2</sub>CO<sub>3</sub> solution was added. The prepared solution was incubated for 60 min at room temperature. Reference solution was prepared the same way, but distilled water was added instead of the tested sample. Absorbance at 765 nm was measured. Total polyphenols content (ppm) was determined from the calibration curve using gallic acid as the reference standard.

### 2.2.3. Determination of the Reduction Potential by the FRAP (Ferric Reducing of Antioxidant Power) Method

The FRAP method, used to determine the total reduction potential, is based on the ability of the test sample to reduce Fe<sup>3+</sup> ions to Fe<sup>2+</sup> ions. The FRAP unit determines the ability to reduce 1 mole Fe<sup>3+</sup> to Fe<sup>2+</sup> [12]. Absorbance at 593 nm was measured.

### 2.3. Determination of Total Acidity by Titration

The total acidity of coffee beverages subjected to analysis was determined by titrating the sample with a standard solution of NaOH in the presence of phenolphthalein until the color changed to light pink and stayed pink for at least 30 s [13]. The result was reported in grams per 100 mL of the infusion and expressed in units of malic acid.

### 2.4. Determination of Mineral Content

Samples (coffee beans:  $n = 3$ ; coffee beverages:  $n = 3$  of each type of coffee drink) were analyzed using inductively coupled plasma optical emission spectrometry (ICP-OES, ICAP 7400 Duo, Thermo Scientific (Waltham, MA, USA) equipped with a concentric nebulizer and cyclonic spray chamber to determine their Ca, Fe, Mg, K, Na, Sr, Zn, and P content. Analysis was performed in radial and axial mode. The samples were mineralized using microwave digestion system MARS 5 (CEM, Matthews, NC, USA). The weight of solid samples given to analysis was at least 0.1 g. The volume of liquid samples was 0.75 mL. The samples were transferred to clean polypropylene tubes. Then, 4 mL of 65% HNO<sub>3</sub> (Suprapur, Merck, Darmstadt, Germany) was added to each vial and each sample was allowed 30 min pre reaction time in the clean hood. After completion of the pre-reaction time, 1 mL of non-stabilized 30% H<sub>2</sub>O<sub>2</sub> solution (Suprapur, Merck, Darmstadt, Germany) was added to each vial. Once the addition of all reagents was complete, the samples were placed in special Teflon vessels and heated in a microwaved digestion system for 35 min at 180 °C (15 min ramp to 180 °C and maintained at 180 °C for 20 min). At the end of digestion, all samples were removed from the microwave and allowed to cool to room temperature. In the clean hood, samples were transferred to acid-washed 15 mL polypropylene sample tubes. A further 20-fold (for solids) and 5-fold (for liquids) dilution was performed prior to ICP-OES measurement. The samples were spiked with an internal standard to provide a final concentration of 0.5 mg/L yttrium, 1 mL of 1% Triton (Triton X-100, Sigma), and diluted to the final volume of 10 mL with 0.075% nitric acid (Suprapur, Merck). Samples were stored in a monitored refrigerator at a nominal temperature of 4 °C until analysis. Blank samples were prepared by adding concentrated nitric acid to tubes without sample and subsequently diluted in the same manner described above. Multielement calibration standards (ICP multi-element standard solution IV, Merck, Germany; phosphorus standard for ICP, Inorganic Ventures, United States) were prepared with different concentrations of inorganic elements in the same manner as in blanks and samples. Samples of reference material (NIST SRM (National Institute of Standards and Technology-Standard Reference Material) 1486 bone meal;  $n = 3$ ) were prepared in the same manner as the samples (Table 1). Deionized water (Direct Q UV, Merck Millipore Corporation, approximately 18.0 MΩ) was used for preparation

of all solutions. The wavelengths (nm) were P 178.284, K 766.490, Ca 315.887, Fe 239.562, Zn 213.856, Sr 421.552, Na 589.592, and Mg 285.213.

**Table 1.** Analysis of reference material bone meal NIST-SRM (National Institute of Standards and Technology-Standard Reference Material)1486 using inductively coupled plasma optical emission spectrometry (ICP-OES).

Chemical Element	NIST-SRM 1486 Certified (mg/kg)	NIST-SRM 1486 Measured (mg/kg)	Recovery (%)
P 178.284	123,000.00	131,500.00	107%
K 766.490	412.00	417.00	101%
Ca 315.887	265,800.00	247,021.00	93%
Fe 239.562	99.00	102.15	103%
Zn 213.856	147.00	143.60	98%
Sr 421.552	264.00	258.17	98%
Na 589.592	5000	4826.33	97%
Mg 285.213	4600	4382.13	95%

### 2.5. Statistical Analysis

In all the experiments, three individually extracted samples were analyzed and all the analyses were carried out at least in triplicate (nine replications). The statistical analysis was performed using Stat Soft Statistica 13.0 (StatSoft Polska Sp. z o.o., Kraków, Poland) and Microsoft Excel 2017 (Microsoft, Poland). The results are expressed as mean values and standard deviation (SD). To assess the differences between examined parameters, one-way analysis of variance (ANOVA) and Tukey's post-hoc test (StatSoft Polska Sp. z o.o., Kraków, Poland) were used. Differences were considered significant at  $p \leq 0.05$ .

### 3. Results

The content of mineral elements in ground coffee beans is shown in Table 2.

**Table 2.** Mineral composition of coffee beans.

Elements	Mineral Content (mg/kg)	
	Mean	SD
Ca	1441.20	49.49
Fe	48.36	3.30
Mg	2133.91	43.42
K	18,634.66	538.67
Na	83.75	10.01
Sr	16.25	0.80
Zn	9.93	0.42
P	2154.23	41.80

However, from a practical point of view, infusions are products that can be considered in terms of health-promoting properties, or as sources of minerals in the daily diet.

The brews included in the study underwent quantitative and qualitative analysis for mineral content, which showed that the highest level of calcium (Ca) was found in coffee from the espresso machine (25.71 mg/L), and the lowest level was found in the drip brew (16.34 mg/L) (Figure 1a). The Ca concentrations in individual coffee preparations were significantly different, except the comparison between the French press and simple infusion ( $p = 0.7552$ ).

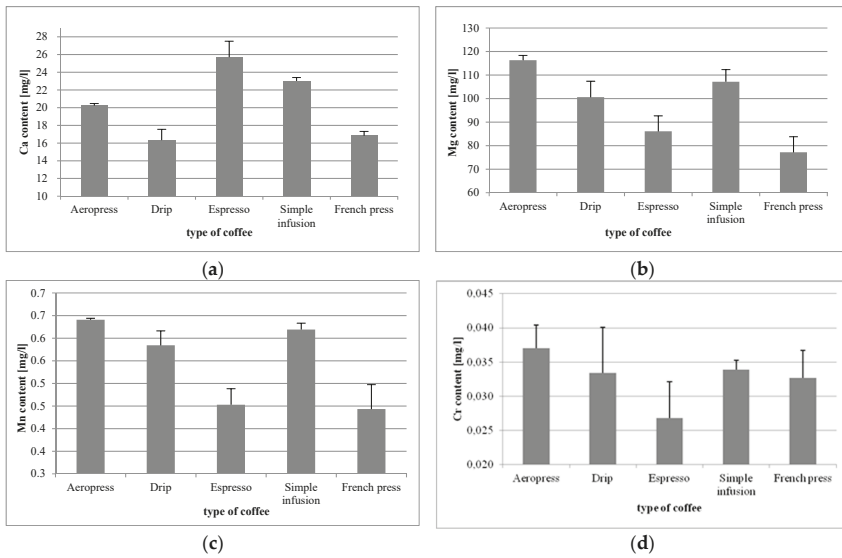


**Figure 1.** Concentrations of Ca (a), Mg (b), Mn (c), and Cr (d) in coffee beverages made using different methods.

Magnesium (Mg) content ranged from 77.15 mg/L (French press) to 116.30 mg/L (Aeropress) (Figure 1b). The differences in Mg content in the respective brews were statistically significant, except for drip vs. simple infusion ( $p = 0.0573$ ).

The highest level of manganese (Mn) was found in Aeropress coffee (0.640 mg/L), and the lowest was found in the coffee from the French press (0.443 mg/L) (Figure 1c). The differences were mainly statistically significant. The exceptions were in the simple infusion vs. Aeropress ( $p = 0.4960$ ), simple infusion vs. drip ( $p = 0.0878$ ), and in the French press vs. espresso ( $p = 0.9532$ ).

In the case of chromium (Cr), the highest content thereof was again found in Aeropress coffee (0.037 mg/L) (Figure 1d). The differences in the content of the mineral element between tested samples were statistically significant only regarding coffee from the espresso machine (vs. Aeropress,  $p = 0.0001$ ; vs. drip,  $p = 0.0077$ ; vs. simple infusion,  $p = 0.0039$ ; vs. French press,  $p = 0.0232$ ).

Coffee from the espresso machine was found to be the richest source of Zn (0.235 mg/L), the lowest level of which was determined in Aeropress coffee (0.123 mg/L) (Figure 2a). Statistically significant differences were observed for espresso vs. Aeropress ( $p = 0.0001$ ), espresso vs. drip ( $p = 0.0002$ ), espresso vs. simple infusion ( $p = 0.0002$ ), and in espresso vs. French press ( $p = 0.0001$ ).

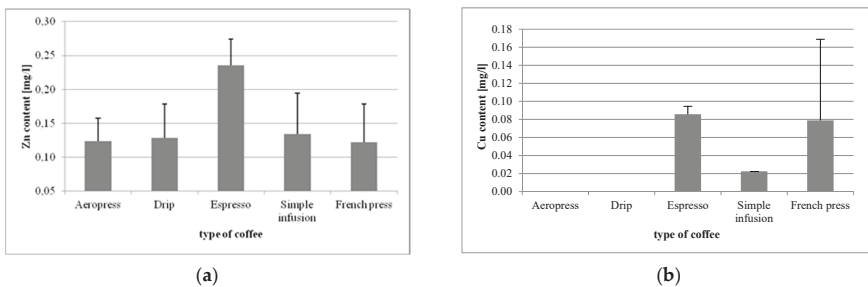


**Figure 2. Cont.**

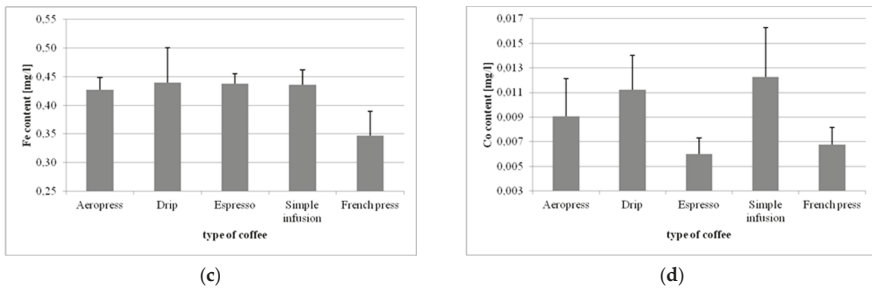


**Figure 2.** Concentrations of Zn (a), Cu (b), Fe (c), and Co (d) in coffee beverages made using different methods.

In the analysis of copper (Cu) levels, it was demonstrated that coffee from the espresso machine was the best source of that mineral (0.085 mg/L), whereas in Aeropress and drip brews its levels were below the detection limit (Figure 2b). Statistically significant differences in Cu levels were found in Aeropress vs. espresso ( $p = 0.000129$ ), Aeropress vs. simple infusion ( $p = 0.0072$ ), drip vs. espresso ( $p = 0.0001$ ), drip vs. simple infusion ( $p = 0.0072$ ), espresso vs. simple infusion ( $p = 0.0017$ ), and in French press vs. simple infusion ( $p = 0.0276$ ).

In the case of iron (Fe), the lowest levels were observed in coffee from the French press (0.346 mg/L), and the highest in the drip brew (0.439 mg/L) (Figure 2c). Significant differences were found between the coffee from the French press and the remaining methods (vs. Aeropress,  $p = 0.0002$ ; vs. drip,  $p = 0.0001$ ; vs. espresso,  $p = 0.0001$ ; vs. simple infusion,  $p = 0.0001$ ).

The highest content of cobalt (Co) was determined in the coffee made by simple infusion (0.012 mg/L), and the lowest in coffee from the espresso machine (0.006 mg/L) (Figure 2d). The differences were statistically significant for the following coffee preparations: espresso vs. drip ( $p = 0.00039$ ), simple infusion vs. Aeropress ( $p = 0.0494$ ), simple infusion vs. espresso ( $p = 0.000136$ ), French press vs. drip ( $p = 0.002342$ ), and in French press vs. simple infusion ( $p = 0.000271$ ).

The lowest levels of phosphorus (P) were observed in the coffee from the French press (49.64 mg/L), and the highest in the Aeropress coffee (81.58 mg/L) (Figure 3a). The differences between the respective coffee preparations were statistically significant, except for the difference between drip and simple infusion ( $p = 0.2176$ ).

The lowest level of silicon (Si) was observed in the coffee from the French press (2.55 mg/L), and the highest (3.44 mg/L) in the drip coffee (Figure 3b). The majority of differences between the observed results were statistically significant. The exception was the insignificant difference in silicon content between French press and espresso ( $p = 0.8914$ ).

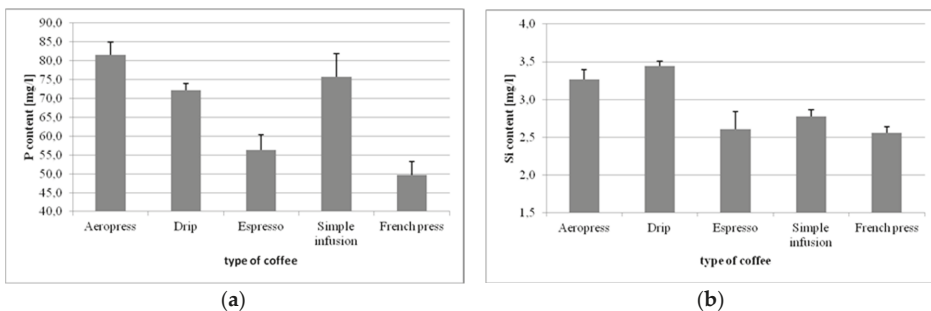


**Figure 3.** Cont.

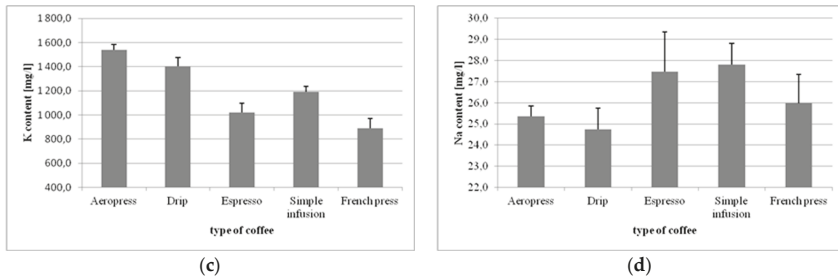


**Figure 3.** Concentrations of P (a), Si (b), K (c), and Na (d) in coffee beverages made using different methods.

Potassium (K) levels in coffee preparations ranged from 887.38 to 1540.70 mg/L (Figure 3c). The highest K content was found in Aeropress coffee, and the lowest was found in the coffee from the French press. All differences between these results were statistically significant ( $p = 0.0001$ ;  $p = 0.0003$ ).

In the case of sodium (Na), the highest levels were found in coffee made by simple infusion (27.810 mg/L), and the lowest were found in the drip brew (24.736 mg/L) (Figure 3d). Statistically significant differences in Na content were found for Aeropress vs. espresso ( $p = 0.00159$ ), Aeropress vs. simple infusion ( $p = 0.0003$ ), drip vs. espresso ( $p = 0.0002$ ), drip vs. simple infusion ( $p = 0.0001$ ), espresso vs. French press ( $p = 0.0421$ ), and simple infusion vs. French press ( $p = 0.0076$ ).

The coffee beverages made using different methods were also analyzed for the content of toxic elements (Figure 4). Starting with nickel (Ni), the drip brew was found to contain the highest levels thereof (0.0271 mg/L), and coffee from the French press had the lowest source of exposure (0.0213 mg/L). The following differences were statistically significant: simple infusion vs. drip ( $p = 0.0069$ ), simple infusion vs. Aeropress ( $p = 0.0402$ ), French press vs. drip ( $p = 0.0015$ ), French press vs. espresso ( $p = 0.0397$ ), and French press vs. Aeropress ( $p = 0.0098$ ).

In the case of strontium (Sr), coffee from the Espresso machine was the predominant source of exposure (0.734 mg/L), and the lowest concentrations were found in the drip brew (0.278 mg/L). The differences in Sr content were statistically significant between brewing methods ( $p = 0.0001$ ).

The highest exposure to aluminum (Al) came from the drip coffee (1.55 mg/L), and the lowest concentrations were found in the brew from the espresso machine (0.31 mg/L). Statistically significant differences were found only for the drip brew vs. the remaining brewing methods ( $p = 0.0001$ ).

The concentrations of molybdenum (Mo) and cadmium (Cd) in the coffee beverages were below the detection limit.

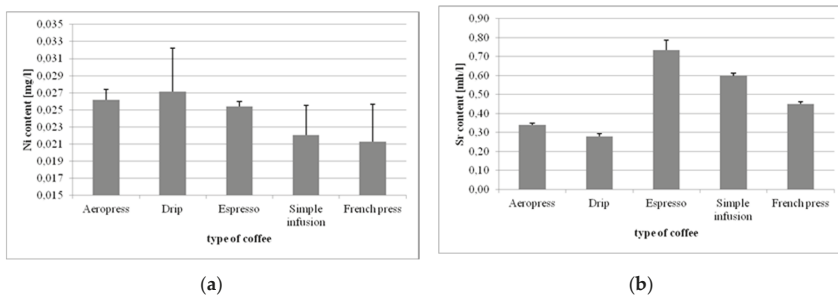
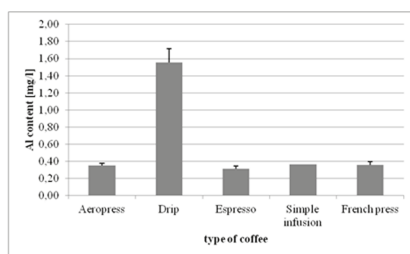


**Figure 4.** Cont.



(c)

**Figure 4.** Concentrations of Ni (a), Sr (b), and Al (c) in coffee beverages made using different methods.

### 3.1. Analysis of Antioxidant Properties of Coffee Preparations

The antioxidant potential of the coffee preparations included in the study, expressed as DPPH inhibition percentage, ranged from 31% to 42% (Figure 5a). The lowest figure is representative of coffee from the espresso machine, and the highest refers to the Aeropress brew. The differences were statistically significant for the following samples: Aeropress vs. espresso ( $p = 0.0001$ ), Aeropress vs. simple infusion ( $p = 0.0001$ ), and Aeropress vs. French press ( $p = 0.0001$ ), as well as drip vs. espresso, drip vs. simple infusion, and drip vs. French press ( $p = 0.0001$ ).

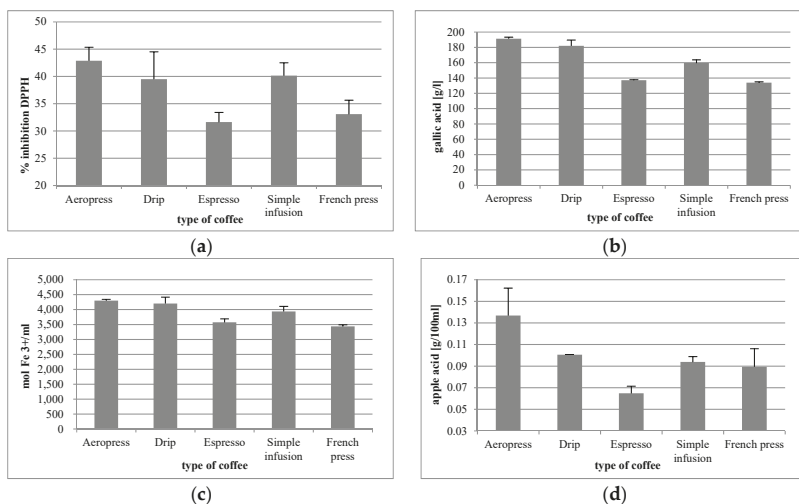


**Figure 5.** Antioxidant potential (a), total polyphenol content (b), reduction potential (c), and acidity (d) of coffee beverages made using different methods. DPPH: 2,2-diphenyl-1-picrylhydrazyl.

The lowest total polyphenol content was found in the coffee from the French press (133.90 g gallic acid/L) and the highest was observed in the Aeropress brew (191.29 g gallic acid/L) (Figure 5b). The differences between the respective coffee brews were statistically significant, except for the difference between the coffee from the French press vs. espresso ( $p = 0.4733$ ).

The reduction potential of the coffee brews ranged from 3435.06 mol Fe<sup>3+</sup>/mL for the coffee from the French press to 4298.19 mol Fe<sup>3+</sup>/mL in the Aeropress coffee (Figure 5c). The differences in the respective brews were statistically significant. The differences between Aeropress vs. drip ( $p = 0.5799$ ) and espresso vs. French press ( $p = 0.2392$ ) were demonstrated to be statistically insignificant.

The acidity of coffee brews ranged from 0.14% (espresso) to 0.6% (Aeropress) (Figure 5d). The only statistically insignificant differences in acidity were drip vs. French press ( $p = 0.4602$ ), drip vs. simple

infusion ( $p = 0.8514$ ), and simple infusion vs. French press ( $p = 0.9617$ ). The differences observed between the remaining brewing methods were statistically significant.

### 3.2. Correlations between the Analysed Parameters for Individual Brewing Methods

Statistical analysis of the results demonstrated significant positive correlations between the antioxidant potential parameters in the following brews:

- Between percentage DPPH inhibition and polyphenol content in Aeropress ( $r = 0.828$ ), drip ( $r = 0.949$ ), espresso ( $r = 0.752$ ), and French press ( $r = 0.731$ ).
- Between DPPH and FRAP for Aeropress ( $r = 0.919$ ), drip ( $r = 0.990$ ), and espresso ( $r = 0.932$ ).
- Between polyphenol content and FRAP for Aeropress ( $r = 0.972$ ), drip ( $r = 0.982$ ), and espresso ( $r = 0.972$ ).
- The only correlation found in simple infusion was between DPPH and FRAP ( $r = 0.914$ ).

A significant positive correlation between acidity and the levels of Mg, K, and P was observed in Aeropress, espresso, simple infusion, and French press brews (Table 3).

**Table 3.** Statistically significant (at  $p \leq 0.05$ ) correlation ( $r$ ) between elements in coffee: (a) Aeropress, (b) drip, (c) espresso, (d) simple infusion, and (e) French press.

<b>(a) Aeropress</b>		
<b>Correlations (<math>r</math>) between Elements</b>		
	<b>Positive</b>	<b>Negative</b>
Ca and	Zn; Co	Fe; Cr; Ni
Mg and	K; Na; Co; Sr; Si	Fe; Cr; Ni; Al
Mn and	Zn; Al	P; Na; Sr; Si
P and	K; Na; Sr; Si	Zn; Al
K and	Na; Co; Sr; Si	Fe; Cr; Ni; Al
Zn and		Fe
Fe and	Cr; Ni	Co
Na and	Co; Sr; Si	Cr; Al
Cr and	Ni; Al	Co; Sr; Si
Ni and		Co
Co and	Sr	
Sr and	Si	Al
Al and		Si
<b>(b) Drip</b>		
Ca and	Mg; Mn; P; K; Na; Co; Al; Si	
Mg and	Mn; P; K; Na; Co; Sr; Al; Si	
Mn and	P; K; Na; Co; Al; Si	Zn; Ni
P and	K; Na; Co; Sr; Al; Si	
K and	Na; Co; Sr; Al; Si	
Zn and	Fe; Cr; Ni	
Fe and	Cr; Ni; Sr	
Na and	Co; Al; Si	
Cr and	Ni; Sr	
Co and	Sr; Al; Si	
Sr and	Al; Si	
Al and	Si	

Table 3. Cont.

<b>(c) Espresso</b>		
Ca and	Mg; Mn; P; K; Na; Ni; Sr; Si	Zn; Cr; Co; Al
Mg and	Mn; P; K; Na; Ni; Sr; Si	Zn; Fe; Co; Al; Cu
Mn and	P; K; Na; Ni; S; Si	Zn; Cr; Co; Al
P and	K; Na; Ni; Sr Si	Zn; Fe Co; Al Cu
K and	Na; Ni; Sr; Si	Zn; Fe; Cr; Co; Al
Zn and	Cr; Al	Na; Ni; Sr; Si
Fe and	Co; Cu	Na; Sr
Na and	Ni; Sr; Si	Cr; Co; Al
Cr and	Al ( $r = 0.875$ )	Ni; Si
Ni and	Sr; Si	Al
Co and	Al; Cu	Sr; Si
Sr and	Si	Al
Al and		Si
<b>(d) Simple infusion</b>		
Ca and	Zn; Co	Fe; Cr; Ni
Mg and	K; Na; Co; Sr; Si	Fe; Cr; Ni; Al
Mn and	Zn; Al	P; Na; Sr; Si
P and	K; Na; Sr; Si	Zn; Al
K and	Na; Co; Sr; Si	Fe; Cr; Ni; Al
Zn and		Fe
Fe and	Cr; Ni	Co
Na and	Co; Sr; Si	Cr; Al
Cr and	Ni; Al	Co; Sr; Si
Ni and		Co
Co and	Sr	
Sr and	Si	Al
Al and		Si
<b>(e) French press</b>		
Ca and	Cr; N; Sr	
Mg and	P; K; Na; Ni; Si; Cu	
Mn and	P; K; Na	Zn; Fe; Cr; Sr
P and	K; Na; Ni; Si; Cu	Zn; Fe; Al
K and	Na; Ni; Si; Cu	Al
Zn and	Fe; Cr; Sr; Al	Na
Fe and	Cr; Al	
Na and	Ni; Si; Cu	
Cr and	Co; Sr; Al	
Ni and	Co; Si; Cu	
Co and	Sr	
Sr and	Al	
Si and	Cu	

No significant correlations with acidity were found for the drip coffee. The individual coffee brews were also examined for statistically significant correlations between mineral levels. Individual brews were characterized by diverse, both positive and negative, correlations between mineral levels. The results are presented in Table 4.

**Table 4.** Statistically significant (at  $p \leq 0.05$ ) correlation ( $r$ ) between mineral content and acidity in coffee infusions.

Correlations ( $r$ ) between Mineral Content and Acidity:		
	Positive	Negative
(a) in Aeropress coffee infusion		
acidity and	Mg; P; K; Na; Sr; S	Mn; Al
(b) in espresso coffee infusion		
acidity and	Mg; P; K; Na	Fe; Co; Cu
(c) in simple infusion coffee		
acidity and	Ca; Mg; P; K; Fe; Ni	Co
(d) in French press coffee infusion		
acidity and	Mg; Mn; P; K; Na	Zn; Fe; Cr; Sr; Al

#### 4. Discussion

Coffee is one of the most widely consumed beverages in the world. It is known for its organoleptic qualities and is appreciated by countless coffee aficionados [2]. Because of its popularity, it attracts the interest of researchers, who continue to examine its impact on human health. The body of research has so far pointed to the safety of coffee consumption by the majority of social groups, as well as its positive impact on health. Studies have highlighted the relationship between coffee consumption and reduced risk for certain cancers, cardiovascular diseases, type 2 diabetes, and Parkinson's disease [14]. However, the preparation method has a significant impact on many properties of the obtained brew [7]. For instance, it affects the aromatic compounds profile, acidity, fatty acid profile [15], caffeine and chlorogenic acid content [7,15], levels of diterpenic esters [16], furan [17], and isoflavones [18], as well as the extraction of biogenic and toxic elements into the coffee brew [10]. The biochemical properties of coffee preparations are determined by factors including brewing temperature, extraction time, and coffee grind size [7,16]. Recent research has indicated that the homogenization of the 30 ground coffee samples affected the extraction of lignans belonging to polyphenols. Comparison of lignan extraction yield in espresso coffee and ground coffee showed that these molecules seem to be completely extracted during espresso coffee percolation [19]. Judging by the present findings, it may be concluded that the levels of bioactive compounds and minerals in coffee also depend on the brewing method.

In present study, it was observed that the mineral composition changed depending on the brewing method, which may be of high importance from a nutritional point of view. The beverages included in the study were found to contain not only minerals that are essential for body functions, but also toxic elements.

Calcium plays a range of important functions in the body, and in order to maintain normal serum Ca levels, adults over the age of 25 require an intake of 750 mg/day for women and 950 mg/day for men [20]. Therefore, it seems that coffee may not be regarded as a significant source of Ca in the daily diet, as by consuming on average two cups of the beverage a day (approximately 360 mL) one can provide no more than about 1.3% and 1.0% (for women and men, respectively) of the daily requirement for that mineral (using the espresso machine). Magnesium acts as a cofactor for a vast number of enzymes, especially in energy metabolism. The daily requirement for Mg in an adult is 400 mg, and so consuming two cups of coffee provides about 7%–10% of the required amount [20]. Therefore, in nutritional terms, the coffee beverages included in the study may be regarded as a significant source of that mineral, predominantly prepared with simple infusion and Aeropress, with these being identified as the best brewing methods.

Taking into account the daily requirement for phosphorus, which in adults may be up to 550 mg [20], it was demonstrated that drinking Aeropress coffee provides approximately 3.2% of this mineral.

Silicon is not essential for humans. The estimated typical dietary intake (20–50 mg silicon/day) corresponds to 0.3–0.8 mg/kg body weight per day in a 60 kg person. These intakes are unlikely to cause adverse effects [21]. In this context, drinking two cups of drip coffee accounts for between 2.4% and 6.1% of the daily silicon intake.

Other elements found in considerable quantities in the coffee beverages included in the study were manganese, chromium, cobalt, and potassium, with the highest quantities determined in the Aeropress coffee and in simple infusion coffee. The recommended dietary allowance (RDA) for manganese amounts up to 3.0 mg/day [20], and thus drinking two cups of Aeropress coffee may deliver approximately 7.7% of the daily requirement for this mineral, which functions as a cofactor for a variety of enzymes, including arginase, glutamine synthetase (GS), pyruvate carboxylase, and manganese superoxide dismutase (Mn-SOD). Through these metalloproteins, Mn plays critically important roles in development, digestion, reproduction, antioxidant defense, energy production, immune response, and regulation of neuronal activities [22]. In the case of Cr, RDA guidelines differ from country to country [23]. According to the World Health Organization (WHO), the average requirement for this mineral amounts to 0.035 mg/day [24], and thus two cups of Aeropress coffee would correspond to approximately 38% of this amount, making it a potentially significant source of chromium.

The body of an adult person contains on average approximately 150 g potassium, and nearly 90% of that mineral is found inside cells. Potassium is responsible for maintaining normal water–electrolyte balance of the body and osmotic equilibrium in cells. Importantly, its functions include the activation of numerous enzymes and participation in carbohydrate and protein metabolism [25]. Serum levels of the mineral and overall body content make it impossible to determine its daily requirement, but it should be supplied in sufficient quantities to reduce the risk of diseases such as arterial hypertension, stroke, and ischaemic heart disease [19,23]. According to the experts from the European Food Safety Authority (EFSA) [20], the RDA for potassium should be 3500 mg/day, and thus coffee would provide approximately 15.8% of the daily K requirement for an adult. Considering the fact that potassium is present in practically all food products, with large quantities found in potatoes and cereal products, which are the most common food staples, the quantities supplied with coffee may account for a significant source of the mineral in the daily diet.

According to EFSA, evaluation of the average requirements for sodium and chloride is on-going [20]. The WHO, in turn, advises that the daily intake of sodium in adults should not exceed 2 g [24]. Consumption of two cups of the coffee brew that had the highest sodium content, that being the simple infusion, accounts for about 10.0% of that amount.

Cobalt and its compounds are widely distributed in nature and are part of numerous anthropogenic activities. Although cobalt plays a biologically necessary role as a metal constituent of vitamin B12 and is also needed to keep the body's nervous system healthy, excessive exposure has been shown to induce various adverse health effects [26]. The average adult intake of cobalt is 5–8 µg/day, and even a single cup of coffee (180 mL) prepared by simple infusion may supply approximately 2.16 µg of the mineral, which accounts for up to 43% of the daily intake. Although a safe RDA for cobalt has not been established to date [26], the lethal dose of cobalt (LD50) is thought to be about 150–500 mg/kg of body weight [27].

Coffee beverages in our study were also analyzed for the content of zinc and copper, with low quantities observed for both minerals. Considering the RDA for Zn, which amounts to approximately 11 mg/day [20], it may be concluded that two cups of coffee from the espresso machine would deliver up to 0.8% of the daily requirement for that mineral and up to about 2% RDA for copper, for which the daily requirement is 1.5 mg/day [20]. Iron levels in the analyzed beverages fell in a similar range. Taking into account the daily requirement for Fe, amounting to 11 mg [20], the intake of the mineral in the drip brew corresponded to approximately 1.4% RDA.

Some of the minerals supplied to the body with the diet are required in large amounts to ensure normal body function (e.g., Ca and Mg), whereas others, such as Cu, Zn, K, Na, Fe, Cr, and Co, are only needed in small concentrations. However, there are also some elements, for example, strontium or

aluminum, whose functions in the body are unknown [28]. In the case of toxic elements, their content in the diet should preferably stay below certain levels, due to the risk of adverse effects in response to excessive exposure. The presence of aluminum in soil is a natural phenomenon, but current studies suggest that the natural environment is significantly exposed to elevated levels of this mineral [29], whereas excessive accumulation of aluminum in brain tissue manifests itself primarily by memory deficit and posture dysfunction [29]. Vegetables cultivated in areas contaminated with heavy metals may include large amounts of aluminum, but it seems that the main source of human exposure comes from the public water supply [29,30]. For the general population, the intake of aluminum from food is 7.2 mg/day for females and 8.6 mg/day for males on average [31]. According to our findings, drinking two cups of coffee with the highest Al content, this being the drip brew (1.55 mg/L), supplies 0.55 mg of the mineral, and so the beverage does not constitute a significant source of aluminum in daily diet.

Nutritional requirements or RDA for nickel have not been established. The role and adverse health effects of nickel and nickel compounds have been assessed by several authors [32–34], but the role of nickel in the physiology of living organisms has not been fully explained. Most likely, Ni in animals and humans participates in erythropoiesis by influencing vitamin B12 metabolism and is regarded as a trace element in nutrition. Although there have been no reports in the literature to date on nickel deficiency, it is good to remember that nickel-rich foodstuffs include lentils, cocoa, chocolate, and nuts [35]. The daily intake of nickel from the average diet is about 150 µg, which corresponds to 2.5 µg/kg body weight per day in a 60 kg adult. Consumption of foods with a high nickel content and additional exposure from first-run drinking water and kitchen utensils may result in intake higher than the critical dose of this substance [21]. In terms of epidemiology, the most critical nickel-related issue to human health is nickel allergy. In those with a strong response, dermatitis may be caused by oral administration of 300 µg of nickel. This amount corresponds to doubled daily intake of this element [35]. In our study, Ni levels determined in coffee beverages made using different methods were more or less on a par. Two cups of coffee could supply about 6.5% of the daily intake of this element.

With respect to strontium, coffee from the espresso machine was the highest source of exposure (0.734 mg/L), and the lowest concentrations were found in the drip brew (0.278 mg/L). The Environmental Protection Agency (EPA) recommends that drinking water levels of stable strontium should not be more than 4 mg/L [36]. In the light of the aforementioned recommendation, coffee beverages contain considerable amounts of strontium, and the consumption of two cups a day may supply even 6.6% of this element.

The data obtained in this study are mostly consistent with other studies regarding elemental composition of coffees [10,37]. Potassium is the most abundant element in coffee beans and also in brews mainly due to its high water solubility [37,38]. Other studies show that the concentration of Ca in coffee beans is indeed high (about 1400 mg/kg); however, the percentage of this element travelling from the beans to the infusion is low, similarly to P and Mg. Debastiani et al. [37] reported that levels of Ca, K, P, and Mg in the drinking coffee were similar to our results, and the authors suggested that coffee is a good source of these substances [37]. Low levels of Si, Ca, Fe, Cu, and Zn in brews, despite their presence in coffee beans and their higher concentrations in spent coffee, suggest that coffee behaves as a sponge by absorbing part of these elements from the hot water [10,37]. The concentrations of Mn, Cu, Zn, and Fe in the present research were similar to other studies; however, we found lower levels of Al (except in drip coffee) in our coffee samples [37].

The very high polyphenolic content found in the studied coffee beverages suggests that they are a rich source of biologically active compounds. Polyphenolics are credited with a broad range of health-promoting properties, including antioxidant, antimicrobial, anti-inflammatory, prebiotic, and anticarcinogenic activity [39]. Phenolic acids have been also demonstrated to be inversely associated with hypertension [40]. The most abundant and important polyphenols found in coffee are chlorogenic acids [41]. According to research findings, these compounds have anti-diabetic, anti-inflammatory, anti-carcinogenic, and anti-obesity effects [42]. In our study, the lowest total polyphenol content was found in the coffee from the French press (133.90 g gallic acid/L) and the highest was observed in

the Aeropress brew (191.29 g gallic acid/L). These results are similar or lower than those reported by other authors but the infusions were made by traditional methods [43–45]. In soft and hard infusion, the total phenolic content for Arabica coffee was in the range of 94 to 96 mg QE/g of coffee, and in French Press was 100.78 mg QE/g of coffee [45]. Out of all coffee brewing methods investigated in the present study, the highest antioxidant potential, polyphenol content, and redox potential was observed in the brew made in the Aeropress. It was also characterized by the highest acidity. These findings lend themselves to the conclusion that this brewing method is responsible for the highest content of health-promoting compounds in a coffee beverage.

The antioxidant potential of coffee preparations is also affected by several factors, including the brewing method and bean variety. Wolska et al. [6] investigated percentage DPPH inhibition in Robusta, Arabica, and green coffee beans subjected to brewing using five different methods. The antioxidant activity of the beverages was high—71.97% to 83.21% inhibition of DPPH depending on bean type and extraction method. Ramadan-Hassanien [46] studied the antioxidant potential of instant coffee, Turkish coffee, and cappuccino. Cappuccino had the highest antioxidant activity—66.0% inhibition of DPPH—with instant coffee producing merely 14.0% inhibition of DPPH. A study by Caporaso et al. [47], which included a comparison of the antioxidant potential of coffee preparations made using different methods (espresso, moka, and American brews) demonstrated that the brewing technique has a significant effect on the chemical composition and quality of the resulting beverage. Please note that the literature is elusive regarding Aeropress brewing.

This study confirmed that the type of coffee preparation has a significant impact on the antioxidant potential of coffee beverages. According to Vicente et al. [48], coffee beverages can reduce the consequences of oxidative stress in the human body. Our results confirm that coffee infusions are a rich source of antioxidant compounds.

In conclusion, it was demonstrated that coffee brewing technique has a significant effect on both the antioxidant potential of the beverage and the levels of specific minerals. Coffee prepared by simple infusion and Aeropress provided a valuable source of magnesium, manganese, chromium, cobalt, and potassium, whereas the drip brew was found to be a good source of silicon. In addition, coffee was found to be a rich source of polyphenols with powerful antioxidant properties.

**Author Contributions:** K.J. (Katarzyna Janda): literature search and review, manuscript draft preparation, writing of the manuscript, and preparation of manuscript revision; K.J. (Karolina Jakubczyk): conducting the research and investigation process, and participation in writing the manuscript; I.B.-B.: carried out the experiment literature search and review; P.K.: conducted the research and investigation process; J.K.: participated in writing the manuscript; E.R.-M.: performed the analytic calculations; I.G.: prepared the manuscript revision and the final acceptance of the manuscript. All authors read and agreed to the published version of the manuscript.

**Funding:** The project was funded by the program of the Minister of Science and Higher Education under the name “REGIONALNA INICJATYWA DOSKONAŁOŚCI” in 2019–2020 (grant number 002/RID/2018/19, financing amount PLN 12.000.000).

**Acknowledgments:** We would like to extend our sincere gratitude to the Columbus coffee shop chain in Szczecin (Poland) for providing coffee preparations for the purposes of this study.

**Conflicts of Interest:** The authors declare no conflict of interest.

## References

1. Torquati, L.; Peeters, G.; Brown, W.J.; Skinner, T.L. A Daily Cup of Tea or Coffee May Keep You Moving: Association between Tea and Coffee Consumption and Physical Activity. *Int. J. Environ. Res. Public Health* **2018**, *15*, 1812. [[CrossRef](#)] [[PubMed](#)]
2. Lire Wachamo, H. Review on Health Benefit and Risk of Coffee Consumption. *Med. Aromat. Plants* **2017**, *6*, 4. [[CrossRef](#)]
3. Gaascht, F.; Dicato, M.; Diederich, M. Coffee provides a natural multitarget pharmacopeia against the hallmarks of cancer. *Genes Nutr* **2015**, *10*, 51. [[CrossRef](#)] [[PubMed](#)]
4. Zain, M.Z.M.; Shori, A.B.; Baba, A.S. Composition and Health Properties of Coffee Bean. *Eur. J. Clin. Biomed. Sci.* **2017**, *3*, 97–100. [[CrossRef](#)]

5. Sarriá, B.; Martínez-López, S.; Sierra-Cinos, J.L.; García-Diz, L.; Mateos, R.; Bravo-Clemente, L. Regularly consuming a green/roasted coffee blend reduces the risk of metabolic syndrome. *Eur. J. Nutr.* **2018**, *57*, 269–278. [CrossRef] [PubMed]
6. Wolska, J.; Janda, K.; Jakubczyk, K.; Szymkowiak, M.; Chlubek, D.; Gutowska, I. Levels of Antioxidant Activity and Fluoride Content in Coffee Infusions of Arabica, Robusta and Green Coffee Beans in According to their Brewing Methods. *Biol. Trace Elem. Res.* **2017**, *179*, 327–333. [CrossRef]
7. Caprioli, G.; Cortese, M.; Sagratini, G.; Vittori, S. The influence of different types of preparation (espresso and brew) on coffee aroma and main bioactive constituents. *Int. J. Food Sci. Nutr.* **2015**, *66*, 505–513. [CrossRef]
8. Dybkowska, E.; Sadowska, A.; Rakowska, R.; Dębowska, M.; Świdorski, F.; Świader, K. Assessing polyphenols content and antioxidant activity in coffee beans according to origin and the degree of roasting. *Rocz. Panstw. Zakł. Hig.* **2017**, *68*, 347–353.
9. Fuller, M.; Rao, N.Z. The Effect of Time, Roasting Temperature, and Grind Size on Caffeine and Chlorogenic Acid Concentrations in Cold Brew Coffee. *Sci. Rep.* **2017**, *7*, 1–9. [CrossRef]
10. Grembecka, M.; Malinowska, E.; Szefer, P. Differentiation of market coffee and its infusions in view of their mineral composition. *Sci. Total Environ.* **2007**, *383*, 59–69. [CrossRef]
11. Pérez-Burillo, S.; Mehta, T.; Esteban-Muñoz, A.; Pastoriza, S.; Paliy, O.; Ángel Rufián-Henares, J. Effect of in vitro digestion-fermentation on green and roasted coffee bioactivity: The role of the gut microbiota. *Food Chem.* **2019**, *279*, 252–259. [CrossRef] [PubMed]
12. Anesini, C.; Ferraro, G.; Filip, R. Total Polyphenol Content and Antioxidant Capacity of Commercially Available Tea (*Camellia sinensis*) in Argentina. *J. Agric. Food Chem.* **2008**, *56*, 9225–9229. [CrossRef] [PubMed]
13. Nielsen, S.S. Standard Solutions and Titratable Acidity. In *Food Analysis Laboratory Manual*; Nielsen, S.S., Ed.; Food Science Texts Series; Springer US: Boston, MA, USA, 2010; pp. 95–102. ISBN 978-1-4419-1463-7.
14. Grosso, G.; Godos, J.; Galvano, F.; Giovannucci, E.L. Coffee, Caffeine, and Health Outcomes: An Umbrella Review. *Annu. Rev. Nutr.* **2017**, *37*, 131–156. [CrossRef] [PubMed]
15. Gloess, A.N.; Schönbacher, B.; Klopffrogge, B.; D’Ambrosio, L.; Chatelain, K.; Bongartz, A.; Strittmatter, A.; Rast, M.; Yeretzyan, C. Comparison of nine common coffee extraction methods: Instrumental and sensory analysis. *Eur. Food Res. Technol.* **2013**, *236*, 607–627. [CrossRef]
16. Moenfarad, M.; Erny, G.L.; Alves, A. Variability of some diterpene esters in coffee beverages as influenced by brewing procedures. *J. Food Sci. Technol.* **2016**, *53*, 3916–3927. [CrossRef]
17. Pavesi Ariseto, A.; Vicente, E.; Soares Ueno, M.; Verdiani Tfouni, S.A.; De Figueiredo Toledo, M.C. Furan Levels in Coffee as Influenced by Species, Roast Degree, and Brewing Procedures. *J. Agric. Food Chem.* **2011**, *59*, 3118–3124. [CrossRef]
18. Alves, R.C.; Almeida, I.M.C.; Casal, S.; Oliveira, M.B.P.P. Isoflavones in coffee: Influence of species, roast degree, and brewing method. *J. Agric. Food Chem.* **2010**, *58*, 3002–3007. [CrossRef]
19. Angeloni, S.; Navarini, L.; Khamitova, G.; Sagratini, G.; Vittori, S.; Caprioli, G. Quantification of lignans in 30 ground coffee samples and evaluation of their extraction yield in espresso coffee by HPLC-MS/MS triple quadrupole. *Int. J. Food Sci. Nutr.* **2019**, 1–8. [CrossRef]
20. European Food Safety Authority (EFSA). Dietary Reference Values for nutrients. *EFSA Supporting Publ.* **2017**, *14*. [CrossRef]
21. European Food Safety Authority (Ed.) *Tolerable upper Intake Levels for Vitamins and Minerals*; European Food Safety Authority: Parma, Italy, 2006; ISBN 978-92-9199-014-6.
22. Chen, P.S.; Bornhorst, J.; Aschner, M. Manganese metabolism in humans. *Front. Biosci.* **2018**, *23*, 1655–1679. [CrossRef]
23. EFSA Panel on Dietetic Products, Nutrition and Allergies (NDA). Scientific Opinion on Dietary Reference Values for chromium. *EFSA J.* **2014**, *12*, 3845. [CrossRef]
24. World Health Organization. *Guideline*; WHO Press: Geneva, Switzerland, 2012; ISBN 978-92-4-150483-6.
25. Jarosz, M.; Rychlik, E.; Stoś, K.; Wierzejska, R.; Wojtasik, A.; Charzewska, J.; Mojska, H.; Szponar, L.; Sajor, I.; Klosiewicz-Latoszek, L.; et al. *Normy żywienia dla populacji Polski*; Instytut Żywności i Żywienia: Warszawa, Poland, 2017; ISBN 978-83-86060-89-4.
26. Leyssens, L.; Vinck, B.; Van Der Straeten, C.; Wuyts, F.; Maes, L. Cobalt toxicity in humans—A review of the potential sources and systemic health effects. *Toxicology* **2017**, *387*, 43–56. [CrossRef] [PubMed]
27. Cobalt in food. Cobalt Institute. Available online: <https://www.cobaltinstitute.org/food.html> (accessed on 22 January 2020).

28. Tchounwou, P.B.; Yedjou, C.G.; Patlolla, A.K.; Sutton, D.J. Heavy Metals Toxicity and the Environment. *EXS* **2012**, *101*, 133–164. [[PubMed](#)]
29. Kishima, K. Calmodulin Antagonists Differentiate between Nit<sup>+</sup>- and Mn<sup>2+</sup>-Stimulated Phosphatase Activity of Calcineurin. *J. Biochem.* **1991**, *110*, 402–406.
30. Matsui, H.; PallenSII, C.; Adachi, A.-M.; Wang, J. Demonstration of Different Metal Ion-induced Calcineurin Conformations Using a Monoclonal Antibody. *J. Biol. Chem.* **1985**, *260*, 4174–4179.
31. Krewski, D.; Yokel, R.A.; Nieboer, E.; Borchelt, D.; Cohen, J.; Harry, J.; Kacew, S.; Lindsay, J.; Mahfouz, A.M.; Rondeau, V. Human Health Risk Assessment for Aluminium, Aluminium Oxide, and Aluminium Hydroxide. *J. Toxicol. Environ. Healthpart B* **2007**, *10*, 1–269. [[CrossRef](#)]
32. Cempel, M.; Nickel, G. Nickel: A Review of Its Sources and Environmental Toxicology. *Polish J. Environ. Stud.* **2006**, *15*, 375–382.
33. Duda-Chodak, A. The Impact of Nickel on Human Health. *J. Elem.* **2008**, *13*, 685–693.
34. Kumar, S.; Trivedi, A.V. A Review on Role of Nickel in the Biological System. *Int. J. Curr. Microbiol. App. Sci.* **2016**, *5*, 719–727. [[CrossRef](#)]
35. Pizzutelli, S. Systemic nickel hypersensitivity and diet: Myth or reality? *Eur. Ann. Allergy Clin. Immunol.* **2011**, *1*, 1–18.
36. ATSDR—Public Health Statement: Strontium. Available online: <https://www.atsdr.cdc.gov/phs/phs.asp?id=654&tid=120> (accessed on 12 July 2019).
37. Debastiani, R.; Iochims dos Santos, C.E.; Maciel Ramos, M.; Sobrosa Souza, V.; Amaral, L.; Yoneama, M.L.; Ferraz Dias, J. Elemental analysis of Brazilian coffee with ion beam techniques: From ground coffee to the final beverage. *Food Res. Int.* **2019**, *119*, 297–304. [[CrossRef](#)] [[PubMed](#)]
38. Habte, G.; Hwang, I.M.; Kim, J.S.; Hong, J.H.; Hong, Y.S.; Choi, J.Y.; Nho, E.Y.; Jamila, N.; Khan, N.; Kim, K.S. Elemental profiling and geographical differentiation of Ethiopian coffee samples through inductively coupled plasma-optical emission spectroscopy (ICP-OES), ICP-mass spectrometry (ICP-MS) and direct mercury analyzer (DMA). *Food Chem.* **2016**, *212*, 512–520. [[CrossRef](#)] [[PubMed](#)]
39. Landete, J.M. Updated knowledge about polyphenols: Functions, bioavailability, metabolism, and health. *Crit. Rev. Food Sci. Nutr.* **2012**, *52*, 936–948. [[CrossRef](#)] [[PubMed](#)]
40. Godos, J.; Sinatra, D.; Blanco, I.; Mulè, S.; La Verde, M.; Marranzano, M. Association between Dietary Phenolic Acids and Hypertension in a Mediterranean Cohort. *Nutrients* **2017**, *9*, 1069. [[CrossRef](#)]
41. Ludwig, I.A.; Clifford, M.N.; Lean, M.E.J.; Ashihara, H.; Crozier, A. Coffee: Biochemistry and potential impact on health. *Food Funct.* **2014**, *5*, 1695–1717. [[CrossRef](#)]
42. Tajik, N.; Tajik, M.; Mack, I.; Enck, P. The potential effects of chlorogenic acid, the main phenolic components in coffee, on health: A comprehensive review of the literature. *Eur. J. Nutr.* **2017**, *56*, 2215–2244. [[CrossRef](#)]
43. Vignoli, J.A.; Viegas, M.C.; Bassoli, D.G.; Benassi, M. Roasting process affects differently the bioactive compounds and the antioxidant activity of arabica and robusta coffees. *Food Res. Int.* **2014**, *61*, 279–285. [[CrossRef](#)]
44. Cämmerer, B.; Kroh, L.W. Antioxidant activity of coffee brews. *Eur. Food Res. Technol.* **2006**, *223*, 469–474. [[CrossRef](#)]
45. Kaur, M.; Tyagi, S.; Kundu, N. Effect of Brewing Methods and Time on Secondary Metabolites, Total Flavonoid and Phenolic Content of Green and Roasted coffee Coffea arabica, Coffea canephora and Monsooned Malabar. *Eur. J. Med. Plants* **2018**, 1–16. [[CrossRef](#)]
46. Ramadan-Hassanien, M.F. Total antioxidant potential of juices, beverages and hot drinks consumed in Egypt screened by DPPH in vitro assay. *Grasas Y Aceites* **2008**, *59*, 254–259. [[CrossRef](#)]
47. Caporaso, N.; Genovese, A.; Canela, M.D.; Civitella, A.; Sacchi, R. Neapolitan coffee brew chemical analysis in comparison to espresso, moka and American brews. *Food Res. Int.* **2014**, *61*, 152–160. [[CrossRef](#)]
48. Vicente, S.J.V.; Queiroz, Y.S.; Gottlieb, S.L.D. Stability of Phenolic Compounds and Antioxidant Capacity of Regular and Decaffeinated Coffees. *Braz. Arch. Biol. Technol.* **2014**, *57*, 110–118. [[CrossRef](#)]



Article

# Untargeted Metabolomics of Fermented Rice Using UHPLC Q-TOF MS/MS Reveals an Abundance of Potential Antihypertensive Compounds

Eric Banan-Mwine Daliri <sup>1</sup>, Fred Kwame Ofofu <sup>1</sup>, Ramachandran Chelliah <sup>1</sup>, Joong-Hark Kim <sup>2,3</sup>, Jong-Rae Kim <sup>1,4</sup>, Daesang Yoo <sup>1,5</sup> and Deoghwan Oh <sup>1,\*</sup>

<sup>1</sup> Department of Food Science and Biotechnology, College of Agriculture and Life Sciences, Kangwon National University, Chuncheon 24341, Gangwon-do, Korea; ericdaliri@yahoo.com (E.B.-M.D.); fkofosu@gmail.com (F.K.O.); ramachandran@gmail.com (R.C.); jrkim@gmail.com (J.-R.K.); dsyoo@yahoo.com (D.Y.)

<sup>2</sup> Department of Medical Biotechnology, College of Biomedical Sciences, Kangwon National University, Chuncheon 24341, Gangwon-do, Korea; jhk@yahoo.com

<sup>3</sup> R&D, Erom, Co., Ltd., Chuncheon 24427, Gangwon-do, Korea

<sup>4</sup> R&D, Hanmi Natural Nutrition Co., LTD 44-20, Tongil-ro 1888 beon-gil, Munsan, Paju 10808, Gyeonggi, Korea

<sup>5</sup> R&D, H-FOOD, 108-66, 390 gil, Jingun Oh Nam-Ro, Nam Yang, Ju-Shi 12041, Gyung Gi-Do, Korea

\* Correspondence: deoghwa@kangwon.ac.kr

Received: 3 July 2020; Accepted: 24 July 2020; Published: 27 July 2020

**Abstract:** Enzyme treatment and fermentation of cereals are known processes that enhance the release of bound bioactive compounds to make them available for bioactivity. In this study, we tested the angiotensin converting enzyme (ACE) inhibitory ability of destarched rice, Prozyme 2000p treated destarched rice (DP), and fermented DP samples. Prozyme 2000p treatment increased the ACE inhibitory ability from  $15 \pm 5\%$  to  $45 \pm 3\%$ . Fermentation of the Prozyme 2000p treated samples with *Enterococcus faecium* EBD1 significantly increased the ACE inhibitory ability to  $75 \pm 5\%$ , while captopril showed an ACE inhibition of  $92 \pm 4\%$ . An untargeted metabolomics approach using Ultra-high-performance liquid tandem chromatography quadrupole time of flight mass spectrometry revealed the abundance of vitamins, phenolic compounds, antioxidant peptides, DPP IV inhibitory peptides, and antihypertensive peptides in the fermented samples which may account for its strong ACE inhibition. Although fermented DP had decreased fatty acid levels, the amount of essential amino acid improved drastically compared to destarched rice. Our results show that fermenting Prozyme-treated destarched rice with *Enterococcus faecium* EBD1 generates abundant bioactive compounds necessary for developing antihypertensive functional foods.

**Keywords:** bioactive peptides; hypertension; phenolic compounds; functional food

## 1. Introduction

In recent years, cereal grains such as rice have attracted much scientific attention [1] because they contain phenolic compounds such as quercetin, ferulic acid, and salicylic acid [2] which have strong antioxidant abilities [3]. Over the years, oxidative stress has been shown to play a key role in the pathogenesis of hypertension [4,5] since reactive oxygen species can cause endothelial dysfunction [6] leading to arterial stiffness in humans [7,8]. One popular physiological mechanism of hypertension is the renin-aldosterone-angiotensin system (RAAS) [9]. In the RAAS, renin cleaves angiotensinogen to release angiotensin I which is then hydrolyzed by angiotensin 1-converting enzyme (ACE) to generate angiotensin II (a vasoconstrictor) [10]. Interestingly, phenolic compounds have been shown to strongly inhibit angiotensin 1-converting enzyme (ACE) [11,12] and the strength of

inhibition is directly proportional to the number of hydroxyl groups they possess [13]. In addition to polyphenols, rice contains proteins which when hydrolyzed, generate bioactive peptides [10]. Many potent antihypertensive peptides such as IHRF [14], VNP, and VWP [15] have been identified in rice. These peptides may reduce hypertension by inhibiting ACE and/or renin activities [16], triggering nitric oxide production, or blocking angiotensin II receptors [17]. Antihypertensive peptides are usually generated in foods either by enzyme hydrolysis or fermentation of protein samples. Lactic acid bacteria have been effective in fermenting food materials to release polyphenols [18] and to generate antihypertensive peptides [19]. In recent years, metabolomic techniques such as  $^1\text{H-NMR}$  ( $^1\text{H}$ -nuclear magnetic resonance), GC-MS (gas chromatography-mass spectrometry), and LC-MS (liquid chromatography-mass spectrometry) have been used to identify metabolites in foods [20]. Among the techniques commonly used, LC-MS is the most used in metabolomic studies due to its detection sensitivity, high resolution, and nonderivatization of samples [21]. Ultra-high-performance liquid tandem chromatography quadrupole time of flight mass spectrometry (UHPLC-QTOF/MS) is a new approach in chromatography and was developed based on LC-MS to determine and quantify more metabolites [22]. In this study, we determined the ACE inhibitory ability of destarched rice before and after Prozyme 2000p treatment and after fermentation. We then used UHPLC-QTOF/MS to analyze the metabolite changes that occurred after Prozyme 2000p treatment and after fermentation to identify bioactive compounds generated by the processing methods.

## 2. Materials and Methods

### 2.1. Chemicals and Cultures

All chemical reagents were of analytical grade. ACE-1 Assay Kit (Fluorometric) was purchased from Biovision (Milpitas, CA 95035, USA). All other reagents, unless specified, were purchased from Sigma-Aldrich, Seoul, Korea. Two rice powder samples (*Oriza sativa* L. variety Japonica) were received from Erom Company Limited (Chuncheon-si, Kangwon-do, Korea). One sample (destarched rice) was composed of rice powder treated with  $\alpha$ -amylase to hydrolyze the starch present. The second sample (destarched rice + Prozyme (DP)) consisted of destarched rice treated with Prozyme 2000p.

*Enterococcus faecium* EBD1 was obtained from the Department of Food Science and Biotechnology, Kangwon National University, Korea to be used for fermentation. This bacterium was used in the current study because it demonstrated strong proteolytic ability in our previous study (data not shown). The bacteria stock culture was stored at  $-80\text{ }^\circ\text{C}$  in de Man, Rogosa and Sharpe (MRS) broth (Difco), containing 20% glycerol (*v/v*). The bacterium was spread on MRS agar and incubated at  $37\text{ }^\circ\text{C}$  overnight to obtain single colonies. MRS broth (10 mL) was then inoculated with a single bacteria colony and incubated at  $37\text{ }^\circ\text{C}$ . The cells were harvested at the exponential phase of growth. The number of viable bacterial cells was determined by the plate count on MRS agar.

### 2.2. Rice Fermentation

The bacteria growth medium for the lactic acid bacteria consisted of 10% (*w/v*) Prozyme 2000p treated destarched rice powder in distilled water. The growth media was sterilized by autoclaving at  $121\text{ }^\circ\text{C}$  for 15 min before inoculating with lactic acid bacteria. *E. faecium* EBD1 ( $2 \times 10^8$  cfu/mL) was transferred from an overnight culture to a 200 mL of autoclaved growth media (pH 6). The media was incubated at  $37\text{ }^\circ\text{C}$  with 150 rpm agitation for 48 h. The media was then centrifuged at  $10,000 \times g$  for 10 min and the supernatant was freeze-dried using TFD5505 table top freeze dryer (ilshinBioBase Co. Ltd., Gyeonggi-do, Korea) and the dried samples were stored at  $-20\text{ }^\circ\text{C}$  for further analysis. The final fermented product was labelled as Fermented DP.

### 2.3. Determination of Angiotensin 1-Converting Enzyme Inhibitory Ability

ACE inhibitory activities of destarched rice, Prozyme treated distarched rice (DP), and fermented Prozyme-treated rice (fermented DP) powder were measured using an ACE-1 Assay Kit according

to the manufacture's instructing with some modifications (Table S1). Briefly, 10  $\mu\text{L}$  of diluted ACE-1 solution was transferred to a 96 well plate and the volume was adjusted to 50  $\mu\text{L}$ /well with ACE-1 assay buffer. An aliquot of the rice samples (20  $\mu\text{L}$ , 5 mg/mL) was added to the wells and mixed thoroughly. Captopril (20  $\mu\text{L}$ , 5 mg/mL) was used as a positive control. ACE-1 substrate (50  $\mu\text{L}$ ) was added to the wells and mixed. Fluorescence (Ex/Em = 330/430 nm) was measured in a kinetic mode for 2 h at 37 °C. A standard curve was prepared using the Abz-standard solution. The ACE1 activity was calculated as:

$$\text{ACE1 activity} = B \times D / (\Delta T \times P) = \text{pmol/minute/mg},$$

where:

B = Abz in sample based on standard curve slope (pmol),

$\Delta T$  = reaction time (minutes),

P = sample used into the reaction well (in mg),

D = sample dilution factor.

One unit of ACE-1 activity is the amount of enzyme that catalyzes the release of 1 nmol of Abz per min from the substrate under the assay conditions at 37 °C. The extent of inhibition was calculated as  $100\% \times [(B - A)/B]$  where A is the ACE-1 activity in the presence of ACE and ACE inhibitor, B is the ACE-1 activity without ACE inhibitory component.

#### 2.4. Metabolomics Analysis

Each rice sample (1 g) was extracted with 20 mL of 50% methanol and placed on a mini rocker (Clinical Diagnostics, Gangnam, Korea) overnight. The samples were mixed completely for 30 s using a vortex and subsequently centrifuged at  $12,000 \times g$  for 12 min at 4 °C. Aliquots (1 mL) of the supernatants were filtered through 0.25  $\mu\text{m}$  pore size Millex syringe filters (Merck KGaA, Darmstadt, Germany) and transferred into LC-MS vials. LC-MS/MS analysis was carried out using a UHPLC (SCIEX ExionLC AD system, Framingham, MA, USA) connected to a controller, a pump, a degasser, an autosampler, column oven, and a photodiode array detector (ExionLC) coupled to a quadrupole time-of-flight mass spectrometer (Q-TOF-MS) (X500R QTOF). The analytical column used was a  $100 \times 3$  mm, Accucore C18 column (Thermo Fisher Scientific, Waltham, MA, USA). Solvent A consisted of water with 0.1% formic acid and solvent B was methanol. The chromatography was carried at a flow rate of 0.4 mL/min. A linear gradient was programmed for 25 min as follows: 0–3.81 min, 9% to 14% B; 3.81–4.85 min, 14% to 15% B; 4.85–5.89 min, 15% B; 5.89–8.32 min, 15% to 17% B; 8.32–9.71 min, 17% to 19% B; 9.71–10.40 min, 19% B; 10.40–12.48 min, 19% to 26% B; 12.48–13.17 min, 26% to 28% B; 13.17–14.21 min, 28% to 35% B; 14.21–15.95 min, 35% to 40% B; 15.95–16.64 min, 40% to 48% B; 16.64–18.37 min, 48% to 53% B; 18.37–22.53 min, 53% to 70% B; 22.53–22.88 min, 70% to 9% B; 22.88–25.00 min, 9% B. The injection volume was 5  $\mu\text{L}$ . The Q-TOF-MS was set for the negative mode through a mass range of 100–1000 and a resolution of 5000. The capillary and cone voltages used to record full mass spectra were 1.45 kV and 30 V, respectively. The flow rate of Helium (the cone gas) was 45 L/h, while the flow rate of the desolvation gas ( $\text{N}_2$ ) was 900 L/h. The temperature of  $\text{N}_2$  was 250 °C, the ion source temperature was 120 °C, while the collision energies needed to obtain the MS/MS spectra were set at 15, 20, and 30 V.

#### 2.5. Data Analysis

All data were obtained and processed using SCIEX OS 1.0 software. A non-target algorithm was used for peak finding. Matrix and sample specific signals were separated from true contaminations using an automatic sample-control comparison algorithm. Compound identification was done by using empirical formula finding, MS/MS library searching, and online database searching. Compound names,

peak area, retention time, similarity to metabolites in the database, and mass ( $m/z$ ) were ultimately imported into Microsoft Excel.

## 2.6. Statistical Analysis

For ACE inhibitory ability tests, all experiments were carried out in triplicates and the results were expressed as mean  $\pm$  standard deviation. The statistical analysis of data was performed using GraphPad Prism 5.0 (2007) statistical software system (GraphPad Software Inc., San Diego, CA 92037 USA).  $p < 0.05$  was considered significant as evaluated by Student's  $t$ -test.

ClustVis software (<http://biit.cs.ut.ee/clustvis/>) was used in multivariate statistical analyses, including principal component analysis (PCA) and heat maps [23]. PCA was performed to visualize the changes in metabolite composition in destarched rice, Prozyme treated destarched rice (DP), and fermented DP. Heat maps and PCA plots were drawn by using identified compounds and their peak area. We used peak areas because it is widely accepted that the peak area of an analyte in a chromatograph is directly proportional to its concentration [24–26].

## 3. Results and Discussion

Rice consists of about 90% carbohydrate, up to 8% protein, and about 2% fat [27]. These major components are bound together in the food matrix and hence, hydrolyzing rice starch with  $\alpha$ -amylase enables the release of bound proteins and other biomolecules from the food matrix, making them available for subsequent reactions.

### 3.1. ACE Inhibitory Activity of Rice Samples

Prozyme treatment significantly ( $p < 0.05$ ) increased the ACE inhibitory ability of destarched rice from  $15 \pm 5\%$  to  $45 \pm 3\%$  (Figure 1). This could be due to the release of ACE inhibitory compounds from the rice proteins during Prozyme proteolysis. Our observation agrees with earlier studies that showed that hydrolysis of rice proteins enhances the generation of ACE inhibitory hydrolysates [28]. Subsequent fermentation of the Prozyme hydrolysate with *E. faecium* EBD1 further increased the inhibitory effect up to  $75 \pm 5\%$ , while Captopril (a standard ACE inhibitory peptide) demonstrated a  $92 \pm 4\%$  inhibitory ability.

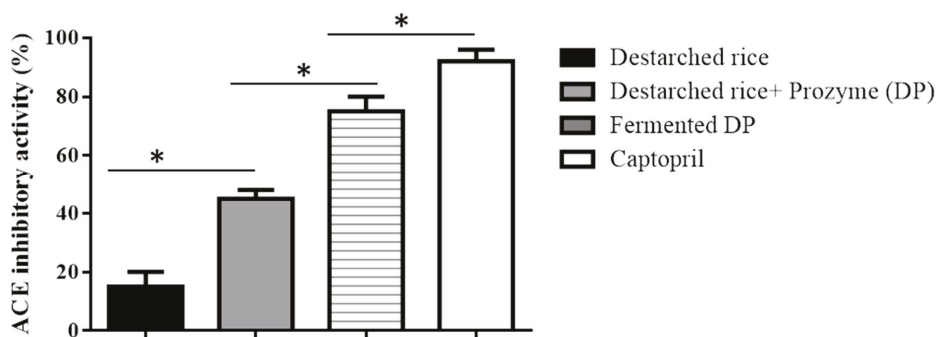


**Figure 1.** ACE inhibitory activities of destarched rice, Prozyme treated destarched rice (DP), and fermented DP. Data show mean SD ( $n = 3$ ). Each bar represents the means of three replicates  $\pm$  S.D. \* denotes a significant difference between the ACE inhibitory ability of the samples.

During lactic acid bacteria fermentation, a number of organic acids are generated from the sugars and lipids available in the growth media and this affects the flavor and pH of the final product [29]. ACE activity is best at a pH of  $\sim 8.3$  [11] and hence, the increased acidity of fermented food may contribute to inhibition of the enzyme. In this study, a total of twenty organic acids were detected in all

the rice samples (Figure 2A). Ten organic acids were detected in destarched rice, 14 in DP, and 19 in fermented DP (Table S2). Only the fermented samples contained homocitric acid, citric acid, binicotinic acid, dioxoheptanoic acid, oxobutyric acid, and hydroxybutanoic acid. Meanwhile, butyric acid [30], nicotinic acid [31], and citric acid are known antihypertensive compounds and hence, their enrichment in the fermentate makes it a potential antihypertensive functional food. Although the types and levels of organic acids in the three samples were different (Figure 2B), organic acid profiles of destarched rice and DP were similar (Figure 2C).

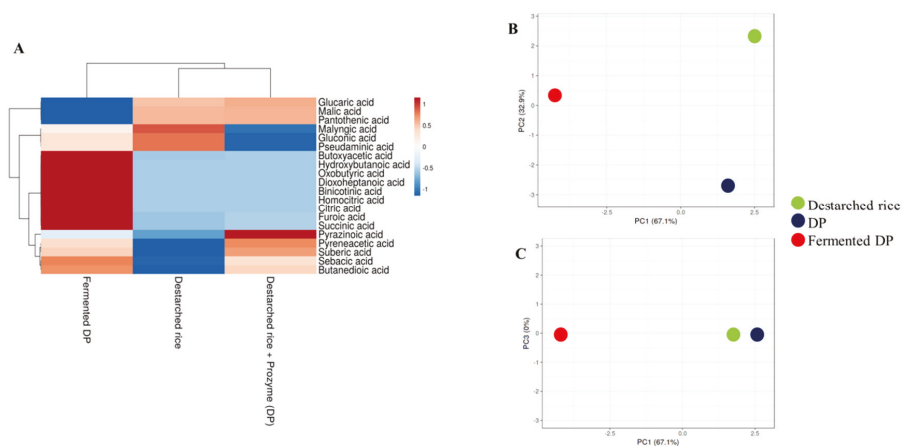


**Figure 2.** Relative levels of organic acids and volatile compounds in destarched rice, Prozyme treated destarched rice (DP), and fermented DP. (A) Heat map shows the different levels of organic acids present in the three samples. The color range from red to blue represents higher to lower levels of organic acids. (B,C) are principal component analysis (PCA) plots. (B) consists of PC1 and PC2, while (C) consists of PC1 and PC3. Red circles represent fermented DP, black represents Prozyme treated destarched rice (DP), and green represents destarched rice samples.

### 3.2. Amino Acid Levels in the Rice Samples

A total of sixteen amino acids were detected in the analyzed samples (Figure 3A, Table S3). In this study, destarched rice contained the least free amino acids contents since most of the amino acids might have remained bound to their parent proteins. Hydrolysis of rice proteins with Prozyme resulted in the cleavage and release of high amounts of essential amino acids such as phenylalanine, threonine, methionine, histidine, and tryptophan (Figure 3). The levels of these essential amino acids reduced drastically after fermentation except for histidine and methionine. Glutamine, cysteine acid, tryptophan, and pyroglutamic acid, though present in the Prozyme treated sample, were not detected in the fermented sample (Table S3) probably because they were consumed by the bacteria to meet their nitrogen requirements during the fermentation process. Meanwhile, the level of leucine (an essential amino acid) and some conditionally essential amino acids such as ornithine, arginine, and serine were increased after fermentation (Figure 3). As shown in the PCA plot (Figure 3B), the amino acid profiles of DP were similar to those of fermented DP but different from destarched rice (Figure 3C).

### 3.3. *E. faecium* EBD1fermentation Increases the Amount of Phenolic Compounds in Rice

Recent studies have shown that a strong hydrophobic interaction exists between phenolic compounds and other rice components [32]. In this study, 10 out of the 17 detected phenolic compounds were present in destarched rice, while 9 were detected after Prozyme treatment (Figure 4, Table S4). In the fermented samples however, 16 phenolic compounds were present and this implies that the fermentation process effectively enhanced the liberation of phenolic compounds that remained bound to

the rice matrix even after  $\alpha$ -amylase and Prozyme treatments. Fermentation resulted in the enrichment of strong antioxidant and antihypertensive phenolic compounds such as vanillic acid [33], eugenol [34], veratric acid [35], ethyl gallate [36], epigallocatechin [37], apigenin [38], and chrysohanol [39]. Our observation agrees with an earlier study that demonstrated that microbial fermentation increases the polyphenol contents of cereals [40,41].

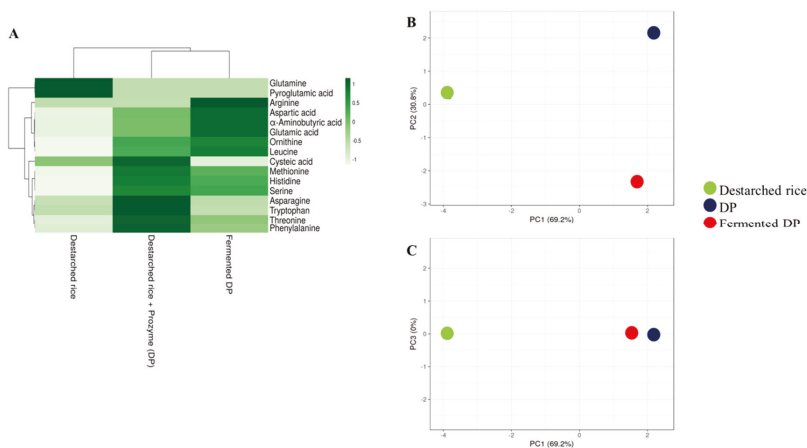


**Figure 3.** Relative levels of amino acids in destarched rice, Prozyme treated destarched rice (DP), and fermented DP. (A) Heat map shows the different levels of organic acids present in the three samples. The color range from green to white represents higher to lower levels of amino acids. (B,C) are principal component analysis (PCA) plots. (B) consists of PC1 and PC2, while (C) consists of PC1 and PC3. Red circles represent fermented DP, black represents Prozyme treated destarched rice (DP), and green represents destarched rice samples.

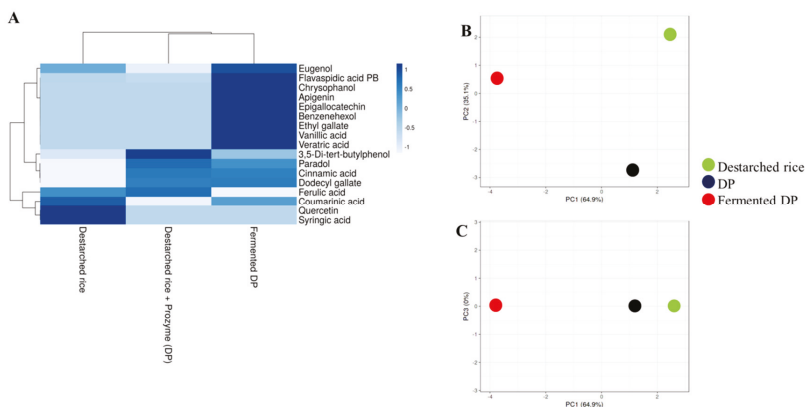


**Figure 4.** Relative levels of phenolic compounds in destarched rice, Prozyme treated destarched (DP), and fermented DP. (A) Heat map shows the different levels of phenolic compounds present in the three samples. The color range from blue to white represents higher to lower levels of phenolic compounds. (B,C) are principal component analysis (PCA) plots. (B) consists of PC1 and PC2, while (C) consists of PC1 and PC3. Red circles represent fermented DP, black represents Prozyme treated destarched rice (DP), and green represents destarched rice samples.

### 3.4. *E. faecium* EBD1fermentation Reduces Lipid Levels in Rice

Oxidation of lipids during fermentation results in the generation volatile compounds such as aldehydes and alcohols which contribute to flavor [42]. In this study, *E. faecium* EBD1fermentation caused a general reduction in the fatty acid levels in the rice sample (Figure 5). The levels of stearic acid (an antioxidant fatty acid) [43] slightly increased, while lauric acid (an antihypertensive fatty acid) [44] was still detectable in the fermentate. Our results are different from an earlier study which found no significant changes in lipid content during millet fermentation [45].

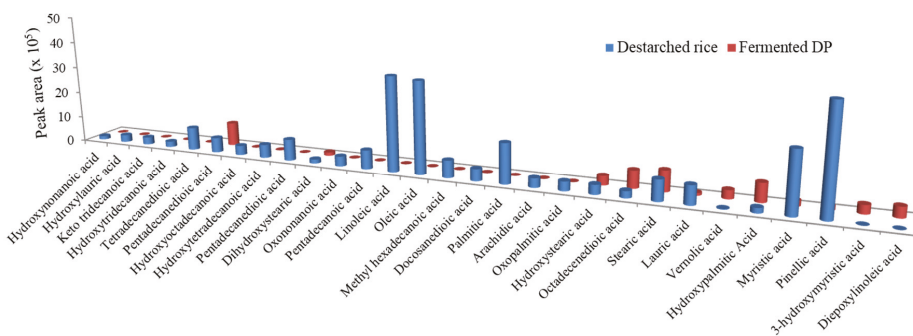


**Figure 5.** The relative levels of fatty acids in destarched rice and fermented DP.

### 3.5. *E. faecium* EBD1fermented Rice Is Enriched with Antihypertensive Peptides

Lactic acid bacteria possess cell envelop proteinases that hydrolyze proteins in media into oligopeptides after which they are absorbed to meet their nutritional needs [9]. For this reason, we analyzed the peptides generated in the fermented samples and determined their potential functions by comparing them with similar peptides already reported in literature (Table 1). In all, 32 peptides were identified in the fermented rice samples among which 16 are reported in literature as antihypertensive peptides. Nine peptides had their carboxyl or amino-terminal amino acid sequences similar to reported antihypertensive peptides, while 3 peptides, namely VPL [46], MV, and HR [47] were found to be dipeptidyl peptidase-4 (DPP IV) inhibitors. Many studies have shown the ability of DPP IV inhibitors to reduce hypertension [48,49]. One antioxidative peptide EL, was also found in the peptide profile of the fermented samples. The presence of these bioactive peptides in the fermented sample may contribute to the strong ACE inhibitory activity observed in this study. Meanwhile, functional analysis is required to confirm the antihypertensive activity of peptides in the fermented sample that contain sequences of already known antihypertensive peptides at their C and N terminals. Our findings are similar to other studies that reported that phenolic compounds [50,51] and bioactive peptides [52] in food can inhibit ACE activity.

Table 1. Peptides identified in *Enterococcus faecium* EBD1 fermented DP.

Retention Time	Peak Area	Adduct/Charge	Precursor Mass	Found at Mass	Formula Finder Results	Peptides	Similar Peptides Reported in Literature *	Peptide Function	Reference
0.93	221,600	[M-H]-	227.116	227.115	C9H16N4O3	GPC	GPC	Antihypertensive	[53]
0.97	1,227,000	[M-H]-	516.206	516.2053	C19H31N7O10	QQQD	LQQQ	Antihypertensive	[54]
1.31	506,800	[M-H]-	185.058	185.0572	C7H10N2O4	EG	EG	Antihypertensive	[55]
3.16	501,500	[M-H]-	419.121	419.1206	C18H20N4O8	GGG	GGG	Antihypertensive	[56]
8.22	292,200	[M-H]-	442.232	442.2311	C19H33N5O7	PKEA	VDKEA	Antihypertensive	[57]
8.4	219,500	[M-H]-	426.237	426.2363	C19H33N5O6	GVGVP	Not found	-	-
8.63	2,611,000	[M-H]-	227.105	227.1039	C10H16N2O4	EV	EV	Antihypertensive	[58]
9.23	1,306,000	[M-H]-	291.1	291.0989	C14H16N2O5	EY	EY	Antihypertensive	[59]
9.48	192,900	[M-H]-	544.228	544.2266	C23H31N9O7	WGGGGGG	GGG	Antihypertensive	[56]
9.87	10,460	[M-H]-	293.116	293.1143	C14H18N2O5	DF	DF	Antihypertensive	[60]
10.29	210,900	[M-H]-	326.209	326.2087	C16H29N3O4	VPL	VPL	DPP IV inhibitor	[46]
10.6	1,264,000	[M-H]-	383.231	383.2305	C18H32N4O5	PLG	PLG	Antihypertensive	[61]
11.56	195,100	[M-H]-	453.201	453.1996	C20H30N4O8	PDGA	Not found	-	-
11.61	3,821,000	[M-H]-	241.121	241.1196	C11H18N2O4	EL	EL	Antioxidative	[62]
11.81	432,500	[M-H]-	489.273	489.2725	C25H38N4O6	VLPY	VLPYP	Antihypertensive	[63]
11.84	243,600	[M-H]-	518.227	518.2263	C24H33N5O8	DISW	ISW	Antihypertensive	[64]
11.91	478,100	[M-H]-	395.195	395.1941	C18H28N4O6	YLS	YL	Antihypertensive	[65]
11.92	267,600	[M-H]-	319.135	319.1335	C13H24N2O5S	MG	MG	Antihypertensive	[66]
12.12	249,800	[M-H]-	473.209	473.2079	C20H34N4O7S	EMVP	MMVPI	Antihypertensive	[67]
12.94	1,020,000	[M-H]-	489.237	489.2361	C24H34N4O7	GPLA	GPL	Antihypertensive	[68]
13.0	471,200	[M-H]-	774.334	774.3331	C44H49N5O6S	AW	AW	Antihypertensive	[69]
13.3	187,800	[M-H]-	180.974	180.9733	C2H2N2O8	GG	GG	Antihypertensive	[58]
13.41	1,627,000	[M-H]-	496.316	496.3145	C24H43N5O6	IVPA	KPVAl	Antihypertensive	[70]
13.42	1,415,000	[M-H]-	528.284	528.2836	C27H39N5O6	FPV	GPPFIV	Antihypertensive	[70]
14.17	1,171,000	[M-H]-	510.331	510.3303	C25H45N5O6	GGGG	GGG	Antihypertensive	[56]
14.24	409,400	[M-H]-	482.263	482.2627	C22H37N5O7	VVPQ	VPO	Antihypertensive	[71]

Table 1. *Cont.*

Retention Time	Peak Area	Adduct/Charge	Precursor Mass	Found at Mass	Formula Finder Results	Peptides	Similar Peptides Reported in Literature *	Peptide Function	Reference
15.88	153.2	[M-H]-	743.35	743.3477	C33H56N6O9S2	VMV	MV	DPP IV inhibitor	[47]
17.11	14,500	[M-H]-	267.067	267.0646	C8H16N2O6S	CE	Not found	-	-
17.22	1,126,000	[M-H]-	310.165	310.1637	C12H21N7O3	HR	HR	DPP IV inhibitor	[47]
17.8	360,400	[M-H]-	457.169	457.1688	C17H34N2O8S2	CC	CCD	Antihypertensive	[72]
21.12	43,240	[M-H]-	474.264	474.2634	C22H41N3O6S	ML	RML	Antihypertensive	[73]
22.19	29,960	[M-H]-	473.284	473.2837	C19H38N8O6	KTAR	KTAP	Antihypertensive	[63]

\* Boldened alphabets represent amino acids sequences identified in this study and previous studies.

#### 4. Conclusions

Using untargeted metabolomics, we found that Prozyme treatment and subsequent fermentation enhanced the generation of organic acids (flavor compounds) and essential amino acids. The fermented DP samples also contained known antihypertensive phenolic compounds as well as antihypertensive peptides which make the sample a promising material for developing cheap antihypertensive foods. Despite the antihypertensive potential of the fermented product, further studies regarding the ability of *Enterococcus faecium* EBD1 fermented Prozyme-treated destarched rice to reduce high blood pressure in vivo is warranted.

**Supplementary Materials:** The following are available online at <http://www.mdpi.com/2304-8158/9/8/1007/s1>. Table S1: Procedure for assay of ACE activity. Table S2: Organic acids and volatile compounds in destarched rice, Prozyme treated destarched rice (DP) and fermented DP. Table S3: Amino acids in destarched rice, Prozyme treated destarched rice (DP) and fermented DP. Table S4: Phenolic compounds in destarched rice, Prozyme treated destarched rice (DP) and fermented DP.

**Author Contributions:** Conceptualization, E.B.-M.D. and D.-H.O.; Formal analysis, E.B.-M.D. and J.-R.K.; Investigation, F.K.O.; Methodology, R.C. and D.Y.; Resources, J.-H.K.; Supervision, D.-H.O.; Writing—original draft, E.B.-M.D. All authors have read and agreed to the published version of the manuscript.

**Funding:** This work was funded by the Korea Institute of Planning and Evaluation for Technology in Food, Agriculture and Forestry. Grant number 119014032SB010.

**Conflicts of Interest:** The authors declare that they have no conflict of interest. The funders had no role in study design, data collection and analysis, decision to publish, or preparation of the manuscript.

#### References

- Zhu, F. Anthocyanins in cereals: Composition and health effects. *Food Res. Int.* **2018**, *109*, 232–249. [[CrossRef](#)] [[PubMed](#)]
- Das, A.J.; Das, G.; Miyaji, T.; Deka, S.C. In vitro antioxidant activities of polyphenols purified from four plant species used in rice beer preparation in Assam India. *Int. J. Food Prop.* **2016**, *19*, 636–651. [[CrossRef](#)]
- Stagos, D. Antioxidant activity of polyphenolic plant extracts. *Antioxidants* **2020**, *9*, 19. [[CrossRef](#)] [[PubMed](#)]
- Qu, W.; Du, G.-L.; Feng, B.; Shao, H. Effects of oxidative stress on blood pressure and electrocardiogram findings in workers with occupational exposure to lead. *Int. J. Med. Res.* **2019**, *47*, 2461–2470. [[CrossRef](#)] [[PubMed](#)]
- Montezano, A.C.; Touyz, R.M. Molecular mechanisms of hypertension—Reactive oxygen species and antioxidants: A basic science update for the clinician. *Can. J. Cardiol.* **2012**, *28*, 288–295. [[CrossRef](#)] [[PubMed](#)]
- Alaaeddine, R.; Elkhatib, M.A.; Mroueh, A.; Fouad, H.; Saad, E.I.; El-Sabban, M.E.; Plane, F.; El-Yazbi, A.F. Impaired endothelium-dependent hyperpolarization underlies endothelial dysfunction during early metabolic challenge: Increased ROS generation and possible interference with NO function. *J. Pharmacol. Exp. Ther.* **2019**, *371*, 567–582. [[CrossRef](#)] [[PubMed](#)]
- Mathew, E.; Mulkadan, J. Clinical disparity of oxidative stress with blood pressure. *J. Biomed. Sci.* **2019**, *3*. [[CrossRef](#)]
- Kruger, R.; Schutte, R.; Huisman, H.; Van Rooyen, J.; Malan, N.; Fourie, C.; Louw, R.; Van der Westhuizen, F.; Van Deventer, C.; Malan, L. Associations between reactive oxygen species, blood pressure and arterial stiffness in black South Africans: The SABPA study. *J. Hum. Hypertens.* **2012**, *26*, 91–97. [[CrossRef](#)]
- Daliri, E.B.-M.; Lee, B.H.; Oh, D.H. Current perspectives on antihypertensive probiotics. *Probiotics Antimicrob. Res.* **2017**, *9*, 91–101. [[CrossRef](#)]
- Daliri, E.B.-M.; Lee, B.H.; Oh, D.H. Current trends and perspectives of bioactive peptides. *Crit. Rev. Food Sci. Nutr.* **2018**, *58*, 2273–2284. [[CrossRef](#)]
- Dong, J.; Xu, X.; Liang, Y.; Head, R.; Bennett, L. Inhibition of angiotensin converting enzyme activity by polyphenols from tea (*Camellia sinensis*) and links to processing method. *Food Funct.* **2011**, *2*, 310–319. [[CrossRef](#)] [[PubMed](#)]
- Persson, I.A.-L.; Persson, K.; Andersson, R.G. Effect of *Vaccinium myrtillus* and its polyphenols on angiotensin-converting enzyme activity in human endothelial cells. *J. Agric. Food Chem.* **2009**, *57*, 4626–4629. [[CrossRef](#)] [[PubMed](#)]

13. Al Shukor, N.; Van Camp, J.; Gonzales, G.B.; Staljanssens, D.; Struijs, K.; Zotti, M.J.; Raes, K.; Smagghe, G. Angiotensin-converting enzyme inhibitory effects by plant phenolic compounds: A study of structure activity relationships. *J. Agric. Food Chem.* **2013**, *61*, 11832–11839. [[CrossRef](#)] [[PubMed](#)]
14. Kontani, N.; Omae, R.; Kagebayashi, T.; Kaneko, K.; Yamada, Y.; Mizushige, T.; Kanamoto, R.; Ohinata, K. Characterization of Ile-His-Arg-Phe, a novel rice-derived vasorelaxing peptide with hypotensive and anorexigenic activities. *Mol. Nutr. Food Res.* **2014**, *58*, 359–364. [[CrossRef](#)] [[PubMed](#)]
15. Chen, J.; Liu, S.; Ye, R.; Cai, G.; Ji, B.; Wu, Y. Angiotensin-I converting enzyme inhibitory tripeptides from rice protein hydrolysate: Purification and characterization. *J. Funct. Foods* **2013**, *5*, 1684–1692. [[CrossRef](#)]
16. Pinciroli, M.; Aphalo, P.; Nardo, A.E.; Añón, M.C.; Quiroga, A.V. Broken rice as a potential functional ingredient with inhibitory activity of renin and angiotensin-converting enzyme. *Plant Foods Hum. Nutr.* **2019**, *74*, 405–413. [[CrossRef](#)]
17. Aluko, R.E. Antihypertensive peptides from food proteins. *Annu. Rev. Food Sci. Technol.* **2015**, *6*, 235–262. [[CrossRef](#)]
18. Oboh, G.; Ademiluyi, A.; Akindahunsi, A. Changes in polyphenols distribution and antioxidant activity during fermentation of some underutilized legumes. *Food Sci. Technol. Int.* **2009**, *15*, 41–46. [[CrossRef](#)]
19. Rubak, Y.T.; Nuraida, L.; Iswantini, D.; Prangdimurti, E. Production of antihypertensive bioactive peptides in fermented food by lactic acid bacteria—A review. *Carpath. J. Food Sci. Technol.* **2019**, *11*, 29–44.
20. Zhao, S.; Zhao, J.; Bu, D.; Sun, P.; Wang, J.; Dong, Z. Metabolomics analysis reveals large effect of roughage types on rumen microbial metabolic profile in dairy cows. *Letts. Appl. Microbiol.* **2014**, *59*, 79–85. [[CrossRef](#)]
21. Goldansaz, S.A.; Guo, A.C.; Sajed, T.; Steele, M.A.; Plastow, G.S.; Wishart, D.S. Livestock metabolomics and the livestock metabolome: A systematic review. *PLoS ONE* **2017**, *12*, e0177675. [[CrossRef](#)] [[PubMed](#)]
22. Yang, Y.; Dong, G.; Wang, Z.; Wang, J.; Zhang, Z.; Liu, J. Rumen and plasma metabolomics profiling by UHPLC-QTOF/MS revealed metabolic alterations associated with a high-corn diet in beef steers. *PLoS ONE* **2018**, *13*, e0208031. [[CrossRef](#)] [[PubMed](#)]
23. Metsalu, T.; Vilo, J. ClustVis: A web tool for visualizing clustering of multivariate data using principal component analysis and heatmap. *Nucleic Acids Res.* **2015**, *43*, W566–W570. [[CrossRef](#)] [[PubMed](#)]
24. Pinkard, B.R.; Gorman, D.J.; Rasmussen, E.G.; Maheshwari, V.; Kramlich, J.C.; Reinhall, P.G.; Novosselov, I.V. Raman spectroscopic data from formic acid decomposition in subcritical and supercritical water. *Data Brief* **2020**, *29*, 105312. [[CrossRef](#)] [[PubMed](#)]
25. Tung, L. Method of calculating molecular weight distribution function from gel permeation chromatograms. *J. Appl. Polym. Sci.* **1966**, *10*, 375–385. [[CrossRef](#)]
26. Berente, B.; De la Calle García, D.; Reichenbacher, M.; Danzer, K. Method development for the determination of anthocyanins in red wines by high-performance liquid chromatography and classification of German red wines by means of multivariate statistical methods. *J. Chromatogr. A* **2000**, *871*, 95–103. [[CrossRef](#)]
27. Zhou, Z.; Robards, K.; Helliwell, S.; Blanchard, C. Composition and functional properties of rice. *Int. J. Food Sci. Technol.* **2002**, *37*, 849–868. [[CrossRef](#)]
28. Suwannapan, O.; Wachirattanapongmetee, K.; Thawornchinsombut, S.; Katekaew, S. Angiotensin-I-converting enzyme (ACE)-inhibitory peptides from Thai jasmine rice bran protein hydrolysates. *Int. J. Food Sci.* **2020**, *55*, 2441–2450. [[CrossRef](#)]
29. Cirlini, M.; Ricci, A.; Galaverna, G.; Lazzi, C. Application of lactic acid fermentation to elderberry juice: Changes in acidic and glucidic fractions. *LWT Food Sci. Technol.* **2020**, *118*, 108779. [[CrossRef](#)]
30. Wang, L.; Zhu, Q.; Lu, A.; Liu, X.; Zhang, L.; Xu, C.; Liu, X.; Li, H.; Yang, T. Sodium butyrate suppresses angiotensin II-induced hypertension by inhibition of renal (pro)renin receptor and intrarenal renin–angiotensin system. *J. Hypertens.* **2017**, *35*, 1899–1908. [[CrossRef](#)]
31. Bays, H.E.; Maccubbin, D.; Meehan, A.G.; Kuznetsova, O.; Mitchel, Y.B.; Paolini, J.F. Blood pressure-lowering effects of extended-release niacin alone and extended-release niacin/laropiprant combination: A post hoc analysis of a 24-week, placebo-controlled trial in dyslipidemic patients. *Clin. Ther.* **2009**, *31*, 115–122. [[CrossRef](#)] [[PubMed](#)]
32. Dai, T.; Chen, J.; McClements, D.J.; Hu, P.; Ye, X.; Liu, C.; Li, T. Protein–polyphenol interactions enhance the antioxidant capacity of phenolics: Analysis of rice glutelin–procyranidin dimer interactions. *Food Func.* **2019**, *10*, 765–774. [[CrossRef](#)] [[PubMed](#)]

33. Kumar, S.; Prahalathan, P.; Raja, B. Antihypertensive and antioxidant potential of vanillic acid, a phenolic compound in L-NAME-induced hypertensive rats: A dose-dependence study. *Redox Rep.* **2011**, *16*, 208–215. [[CrossRef](#)] [[PubMed](#)]
34. Peixoto-Neves, D.; Wang, Q.; Leal-Cardoso, J.H.; Rossoni, L.V.; Jaggar, J.H. Eugenol dilates mesenteric arteries and reduces systemic BP by activating endothelial cell TRPV 4 channels. *Br. J. Pharmacol.* **2015**, *172*, 3484–3494. [[CrossRef](#)] [[PubMed](#)]
35. Saravanakumar, M.; Raja, B. Veratric acid, a phenolic acid attenuates blood pressure and oxidative stress in L-NAME induced hypertensive rats. *Eur. J. Pharmacol.* **2011**, *671*, 87–94. [[CrossRef](#)] [[PubMed](#)]
36. Jin, L.; Piao, Z.H.; Sun, S.; Liu, B.; Kim, G.R.; Seok, Y.M.; Lin, M.Q.; Ryu, Y.; Choi, S.Y.; Kee, H.J. Gallic acid reduces blood pressure and attenuates oxidative stress and cardiac hypertrophy in spontaneously hypertensive rats. *Sci. Rep.* **2017**, *7*, 1–14. [[CrossRef](#)]
37. Luo, D.; Xu, J.; Chen, X.; Zhu, X.; Liu, S.; Li, J.; Xu, X.; Ma, X.; Zhao, J.; Ji, X. (–)-Epigallocatechin-3-gallate (EGCG) attenuates salt-induced hypertension and renal injury in Dahl salt-sensitive rats. *Sci. Rep.* **2020**, *10*, 1–11. [[CrossRef](#)]
38. Sui, H.; Yan, W. Effect of apigenin on SBP of spontaneous hypertension rats and its mechanism. *J. Environ. Health* **2009**, *26*, 112–113.
39. Yusuf, M.A.; Singh, B.N.; Sudheer, S.; Kharwar, R.N.; Siddiqui, S.; Abdel-Azeem, A.M.; Fernandes Fraceto, L.; Dashora, K.; Gupta, V.K. Chrysophanol: A natural anthraquinone with multifaceted biotherapeutic potential. *Biomolecules* **2019**, *9*, 68.
40. Chandrasekara, A.; Shahidi, F. Bioaccessibility and antioxidant potential of millet grain phenolics as affected by simulated in vitro digestion and microbial fermentation. *J. Funct. Foods* **2012**, *4*, 226–237. [[CrossRef](#)]
41. Dey, T.B.; Kuhad, R.C. Enhanced production and extraction of phenolic compounds from wheat by solid-state fermentation with *Rhizopus oryzae* RCK2012. *Biotech. Rep.* **2014**, *4*, 120–127.
42. Liptáková, D.; Matejčeková, Z.; Valík, L. Lactic acid bacteria and fermentation of cereals and pseudocereals. *Ferment. Process.* **2017**, *10*, 65459.
43. Wang, Z.J.; Liang, C.L.; Li, G.M.; Yu, C.Y.; Yin, M. Stearic acid protects primary cultured cortical neurons against oxidative stress. *Acta Pharmacol. Sin.* **2007**, *28*, 315–326. [[CrossRef](#)]
44. Alves, N.F.B.; de Queiroz, T.M.; de Almeida Travassos, R.; Magnani, M.; de Andrade Braga, V. Acute treatment with lauric acid reduces blood pressure and oxidative stress in spontaneously hypertensive rats. *Basic Clin. Pharmacol. Toxicol.* **2017**, *120*, 348–353. [[CrossRef](#)] [[PubMed](#)]
45. Antony, U.; Sripriya, G.; Chandra, T. The effect of fermentation on the primary nutrients in foxtail millet (*Setaria italica*). *Food Chem.* **1996**, *56*, 381–384. [[CrossRef](#)]
46. Umezawa, H.; Aoyagi, T.; Ogawa, K.; Naganawa, H.; Hamada, M.; Takeuchi, T. Diprotins A and B, inhibitors of dipeptidyl aminopeptidase IV, produced by bacteria. *J. Antibiot.* **1984**, *37*, 422–425. [[CrossRef](#)]
47. Lan, V.T.T.; Ito, K.; Ohno, M.; Motoyama, T.; Ito, S.; Kawarasaki, Y. Analyzing a dipeptide library to identify human dipeptidyl peptidase IV inhibitor. *Food Chem.* **2015**, *175*, 66–73. [[CrossRef](#)] [[PubMed](#)]
48. Cosenso-Martin, L.N.; Giollo-Junior, L.T.; Vilela-Martin, J.F. DPP-4 inhibitor reduces central blood pressure in a diabetic and hypertensive patient: A case report. *Medicine* **2015**, *94*. [[CrossRef](#)]
49. Pacheco, B.P.; Crajoinas, R.O.; Couto, G.K.; Davel, A.P.C.; Lessa, L.M.; Rossoni, L.V.; Girardi, A.C. Dipeptidyl peptidase IV inhibition attenuates blood pressure rising in young spontaneously hypertensive rats. *Int. J. Hypertens.* **2011**, *29*, 520–528. [[CrossRef](#)]
50. Zhang, Y.; Pechan, T.; Chang, S.K.C. Antioxidant and angiotensin-I converting enzyme inhibitory activities of phenolic extracts and fractions derived from three phenolic-rich legume varieties. *J. Funct. Foods* **2018**, *42*, 289–297. [[CrossRef](#)]
51. Santos, M.C.; Toson, N.S.B.; Pimentel, M.C.B.; Bordignon, S.A.L.; Mendez, A.S.L.; Henriques, A.T. Polyphenols composition from leaves of *Cuphea* spp. and inhibitor potential, in vitro, of angiotensin I-converting enzyme (ACE). *J. Ethnopharmacol.* **2020**, *255*, 112781. [[CrossRef](#)] [[PubMed](#)]
52. Wang, X.; Chen, H.; Fu, X.; Li, S.; Wei, J. A novel antioxidant and ACE inhibitory peptide from rice bran protein: Biochemical characterization and molecular docking study. *LWT Food Sci. Technol.* **2017**, *75*, 93–99. [[CrossRef](#)]
53. Wang, X.; Wang, J.; Lin, Y.; Ding, Y.; Wang, Y.; Cheng, X.; Lin, Z. QSAR study on angiotensin-converting enzyme inhibitor oligopeptides based on a novel set of sequence information descriptors. *J. Mol. Model.* **2011**, *17*, 1599–1606. [[CrossRef](#)] [[PubMed](#)]

54. Yano, S.; Suzuki, K.; Funatsu, G. Isolation from  $\alpha$ -zein of thermolysin peptides with angiotensin I-converting enzyme inhibitory activity. *Biosci. Biotechnol. Biochem.* **1996**, *60*, 661–663. [[CrossRef](#)] [[PubMed](#)]
55. Cheung, H.-S.; Wang, F.-L.; Ondetti, M.A.; Sabo, E.F.; Cushman, D.W. Binding of peptide substrates and inhibitors of angiotensin-converting enzyme. Importance of the COOH-terminal dipeptide sequence. *J. Biol. Chem.* **1980**, *255*, 401–407. [[PubMed](#)]
56. Zhou, P.; Yang, C.; Ren, Y.; Wang, C.; Tian, F. What are the ideal properties for functional food peptides with antihypertensive effect? A computational peptidology approach. *Food Chem.* **2013**, *141*, 2967–2973. [[CrossRef](#)] [[PubMed](#)]
57. Hernández-Ledesma, B.; Recio, I.; Ramos, M.; Amigo, L. Preparation of ovine and caprine  $\beta$ -lactoglobulin hydrolysates with ACE-inhibitory activity. Identification of active peptides from caprine  $\beta$ -lactoglobulin hydrolysed with thermolysin. *Int. Dairy J.* **2002**, *12*, 805–812. [[CrossRef](#)]
58. Castellano, P.; Aristoy, M.-C.; Sentandreu, M.Á.; Vignolo, G.; Toldrá, F. Peptides with angiotensin I converting enzyme (ACE) inhibitory activity generated from porcine skeletal muscle proteins by the action of meat-borne *Lactobacillus*. *J. Proteom.* **2013**, *89*, 183–190. [[CrossRef](#)]
59. Wu, H.; He, H.-L.; Chen, X.-L.; Sun, C.-Y.; Zhang, Y.-Z.; Zhou, B.-C. Purification and identification of novel angiotensin-I-converting enzyme inhibitory peptides from shark meat hydrolysate. *Process Biochem.* **2008**, *43*, 457–461. [[CrossRef](#)]
60. Ichimura, T.; Hu, J.; Aita, D.Q.; Maruyama, S. Angiotensin I-converting enzyme inhibitory activity and insulin secretion stimulative activity of fermented fish sauce. *J. Biosci. Bioeng.* **2003**, *96*, 496–499. [[CrossRef](#)]
61. Byun, H.-G.; Kim, S.-K. Structure and activity of angiotensin I converting enzyme inhibitory peptides derived from Alaskan pollack skin. *BMB Rep.* **2002**, *35*, 239–243. [[CrossRef](#)] [[PubMed](#)]
62. Suetsuna, K.; Ukeda, H.; Ochi, H. Isolation and characterization of free radical scavenging activities peptides derived from casein. *J. Nutr. Biochem.* **2000**, *11*, 128–131. [[CrossRef](#)]
63. Kohmura, M.; Nio, N.; Kubo, K.; Minoshima, Y.; Munekata, E.; Ariyoshi, Y. Inhibition of angiotensin-converting enzyme by synthetic peptides of human  $\beta$ -casein. *Agric. Biol. Chem.* **1989**, *53*, 2107–2114.
64. Gu, Y.; Majumder, K.; Wu, J. QSAR-aided in silico approach in evaluation of food proteins as precursors of ACE inhibitory peptides. *Food Res. Int.* **2011**, *44*, 2465–2474. [[CrossRef](#)]
65. Tauzin, J.; Miclo, L.; Gaillard, J.-L. Angiotensin-I-converting enzyme inhibitory peptides from tryptic hydrolysate of bovine  $\alpha$ S2-casein. *FEBS Lett.* **2002**, *531*, 369–374. [[CrossRef](#)]
66. Nogata, Y.; Nagamine, T.; Yanaka, M.; Ohta, H. Angiotensin I converting enzyme inhibitory peptides produced by autolysis reactions from wheat bran. *J. Agric. Food Chem.* **2009**, *57*, 6618–6622. [[CrossRef](#)]
67. Escudero, E.; Sentandreu, M.A.; Arihara, K.; Toldra, F. Angiotensin I-converting enzyme inhibitory peptides generated from in vitro gastrointestinal digestion of pork meat. *J. Agric. Food Chem.* **2010**, *58*, 2895–2901. [[CrossRef](#)]
68. He, R.; Malomo, S.A.; Girgih, A.T.; Ju, X.; Aluko, R.E. Glycinylnl-histidinyl-serine (GHS), a novel rapeseed protein-derived peptide has blood pressure-lowering effect in spontaneously hypertensive rats. *J. Agric. Food Chem.* **2013**, *61*, 8396–8402. [[CrossRef](#)]
69. Nakahara, T.; Sano, A.; Yamaguchi, H.; Sugimoto, K.; Chikata, H.; Kinoshita, E.; Uchida, R. Antihypertensive effect of peptide-enriched soy sauce-like seasoning and identification of its angiotensin I-converting enzyme inhibitory substances. *J. Agric. Food Chem.* **2010**, *58*, 821–827. [[CrossRef](#)]
70. Del Mar Contreras, M.; Carrón, R.; Montero, M.J.; Ramos, M.; Recio, I. Novel casein-derived peptides with antihypertensive activity. *Int. Dairy J.* **2009**, *19*, 566–573. [[CrossRef](#)]
71. Minervini, F.; Algaron, F.; Rizzello, C.; Fox, P.; Monnet, V.; Gobbetti, M. Angiotensin I-converting-enzyme-inhibitory and antibacterial peptides from *Lactobacillus helveticus* PR4 proteinase-hydrolyzed caseins of milk from six species. *Appl. Environ. Microbiol.* **2003**, *69*, 5297–5305. [[CrossRef](#)] [[PubMed](#)]

72. Udenigwe, C.C.; Adebisi, A.P.; Doyen, A.; Li, H.; Bazinet, L.; Aluko, R.E. Low molecular weight flaxseed protein-derived arginine-containing peptides reduced blood pressure of spontaneously hypertensive rats faster than amino acid form of arginine and native flaxseed protein. *Food Chem.* **2012**, *132*, 468–475. [[CrossRef](#)] [[PubMed](#)]
73. Wu, J.; Aluko, R.E.; Nakai, S. Structural requirements of angiotensin I-converting enzyme inhibitory peptides: Quantitative structure– activity relationship study of di- and tripeptides. *J. Agric. Food Chem.* **2006**, *54*, 732–738. [[CrossRef](#)] [[PubMed](#)]



© 2020 by the authors. Licensee MDPI, Basel, Switzerland. This article is an open access article distributed under the terms and conditions of the Creative Commons Attribution (CC BY) license (<http://creativecommons.org/licenses/by/4.0/>).

Article

# Structural Characterization of Quinoa Polysaccharide and Its Inhibitory Effects on 3T3-L1 Adipocyte Differentiation

Cong Teng <sup>1</sup>, Zhenxing Shi <sup>1,2</sup>, Yang Yao <sup>1,\*</sup> and Guixing Ren <sup>1</sup>

<sup>1</sup> Institute of Crop Science, Chinese Academy of Agricultural Sciences, Beijing 100081, China; 82101172124@caas.cn (C.T.); shizhengxing@caas.cn (Z.S.); renguixing@caas.cn (G.R.)

<sup>2</sup> Laboratory of Biomass and Green Technologies, Gembloux Agro-Bio Tech, University of Liège, 5030 Gembloux, Belgium

\* Correspondence: yaoyang@caas.cn; Tel.: +86-10-6211-5595

Received: 21 July 2020; Accepted: 20 October 2020; Published: 21 October 2020

**Abstract:** Quinoa is a kind of nutritious food crop with anti-obesity activity, however, the mechanism is not unclear. In this study, we separated and purified bioactive polysaccharide from quinoa (denoted SQWP-2). The chemical structural was characterized and its effect on 3T3-L1 pre-adipocyte differentiation was evaluated. The molecular weight of SQWP-2 was found to be  $7.49 \times 10^3$  Da, and the polysaccharide consisted of fructose and glucose. The Glc-(1→, Fru-(2→, →4)-Glc-(1→, and →4,6)-Glc-(1→ glycosidic linkages were identified in SQWP-2 through gas chromatography-mass spectrometry. Nuclear magnetic resonance confirmed the monosaccharide composition and glycosidic linkage content, and a suggestion of the structural formula is provided. In Western Blotting and RT-PCR assays, treatment with SQWP-2 significantly inhibited 3T3-L1 differentiation by suppressing PPAR $\gamma$ , C/EBP $\alpha$ , C/EBP $\beta$ , C/EBP $\delta$ , SREBP1C and AP2 expression. Quinoa polysaccharide isolated here could represent an anti-obesity agent once the structures and differentiation inhibition are definitively characterized.

**Keywords:** polysaccharide purification; anti-obesity; proliferation; PPAR $\gamma$

## 1. Introduction

Obesity is a complex health disorder caused by the accumulation of adipose tissue due to increasing and enlarged fat cells [1]. Obesity is related not only to higher mortality, but also to an increased risk of cardiovascular disease, diabetes, gallbladder disease, and various cancers [2]. Therefore, finding the food trophic factors that can inhibit the condition is of high importance. As a molecular mechanism for adipogenesis, 3T3-L1 cell differentiation efficiency is an important factor associated with obesity and related diseases. This process is currently the subject of considerable research and is widely used as an adipocyte differentiation model system [3,4].

Quinoa is an important food crop, which can meet the demands of human basic nutrition according to the United Nations of Food and Agriculture Organization [5,6]. It is beneficial for human health owing to its density of nutrients including amino acids, minerals, phytochemicals, and active polysaccharides [7,8]. Previous research has demonstrated that quinoa has a significant anti-obesity effect. Farinazzi-Machado et al. reported that 30 days of consumption of quinoa candies resulted in significant reductions in body weight as well as triglycerides (TGs) and low-density lipoprotein (LDL) levels among 22 students aged 18–45 [9]. The components of quinoa identified as inducing the anti-obesity effect of the product were saponin, 20-hydroxyecdysone, and dietary fiber [9–11]. Oil red O staining and intracellular quantitation analyses confirmed that saponin from quinoa inhibits the accumulation of TG in mature adipocytes and significantly inhibits the expression

of peroxisome proliferator-activated receptor gamma (PPAR $\gamma$ ) and CCAAT/enhancer-binding protein alpha (C/EBP $\alpha$ ), which are [9] key transcription factors for messenger RNA expression and protein fat formation. Compared with high-fat (HF) mice, treated mice exhibited significantly lower mRNA levels of several markers of inflammation and insulin resistance, Foucault observed that administration of 20-hydroxyecdysone from quinoa could prevent diet-induced obesity and regulate adipocyte-specific gene expression in mice [10]. In Maha's research, the administration of quinoa dietary fiber was found to reduce levels of cholesterol components (LDL and high-density lipoprotein), TGs, and total lipids in rats [11]. Many plant polysaccharides have been reported to inhibit 3T3-L1 adipocyte differentiation within cell systems [12]. Polysaccharides from pine needles have been reported to have an anti-lipogenesis effect via regulating lipid metabolism genes encoding transcription factors and cytokines [13]. In Zhu's research, barley  $\beta$ -glucan was found to inhibit adipocyte differentiation by causing downregulation of PPAR $\gamma$ , C/EBP $\alpha$ , and Glut4 mRNA and protein expression levels [14]. Recent research has also shown that certain polysaccharides from quinoa possess antioxidant, immunoregulatory, and anticancer activities [15]. However, the anti-obesity activities of quinoa polysaccharides have not yet been studied.

Macromolecular activity is related to chemical structure [16]. Ferreira found that the immunomodulatory activity of polysaccharides main attributed to the proportion of glycosidic linkages [17]. However, the structure of quinoa polysaccharides is not entirely clear, and the exact relationship between structure and activity of quinoa polysaccharides has not been covered.

The purpose of this study was to (1) characterize the structure of quinoa polysaccharide, (2) evaluate the inhibitory effects of quinoa polysaccharide on 3T3-L1 adipocyte differentiation in vitro.

## 2. Materials and Methods

### 2.1. Plant Sample and Reagents

Quinoa seeds (Cultivar MengLi-1) were obtained from the Chinese Academy of Agricultural Sciences, Beijing, China. The seeds were crushed [9] and sifting through a 600- $\mu$ m sieve, then stored in a freezer until use, not more than 15 days after grinding.

Diethylaminoethyl (DEAE)-Sephacrose Fast Flow resin was purchased from GE Healthcare Life Sciences (Uppsala, Sweden), and 3T3-L1 cells were obtained from the Institute for Biological Sciences, Chinese Academy of Sciences, Shanghai, China. Dulbecco's modified Eagle's medium (DMEM), insulin, Fetal bovine serum (FBS), dexamethasone (DEX), 1-methyl-3-isobutylxanthine (IBMX) and  $\alpha$ -amylase were purchased from Sigma Chemical Co. (St. Louis, MO, USA).

### 2.2. Extraction and Purification

The prepared sample was extracted using 95% ethanol at a ratio of 1:8 for 3 h following centrifugation (3000 $\times$  g, 10 min). The 500 g defatted quinoa powder was collected and extracted twice using distilled water (90  $^{\circ}$ C, 4 h) at a ratio of 1:10. After centrifugation (4000 $\times$  g, 10 min), the supernatant was collected and concentrated. Chloroform-n-butanol was used to deproteinize according to the Sevage method. To remove starch, fractions were sufficiently treated with  $\alpha$ -amylase and dialyzed [18]. A polysaccharide fraction was obtained, which was then purified by chromatography using an ÄKTA Explore 100 purification system (General Electric, Stockholm, Sweden). The polysaccharide was dissolved in a Tris-HCl buffer solution at pH 7.5 with 0.1 mM CaCl<sub>2</sub>, 2.5 mM MgCl<sub>2</sub>, and 0.06% NaN<sub>3</sub> was added and stirred well, centrifuged (13,000 $\times$  g, 10 min), after which supernatant was uploaded onto a DEAE Sepharose Fast Flow column (2.6 cm  $\times$  100 cm). Fractions collected according to absorbance detected by phenol—sulfuric acid method were further purified on a Sephacryl S-300 high-resolution column (Dextran separation range 2  $\times$  10<sup>3</sup>–4  $\times$  10<sup>5</sup>) [19]. Finally, 36.1 g SQWP-2 was obtained from defatted quinoa powder. The polysaccharide purity was tested using HPLC-ELSD method equipped with a Shodex Asahipak NH2P-50 4E column (250 mm  $\times$  4.6 mm  $\times$  5  $\mu$ m, Agilent Technologies, Santa Clara, CA, USA). A solution containing acetonitrile and water (4:1) was used as the mobile phase

at a flow rate of 1.0 mL min<sup>-1</sup>, and the column oven temperature was 35 °C. Drift tube temperature was 70 °C. Spray tube temperature was 30 °C. The carrier gas flow rate was 1.1 mL min<sup>-1</sup>.

### 2.3. Evaluation of the Structure Characteristics of the Water-Soluble Polysaccharide

#### 2.3.1. Scanning Electron Microscopy

Purified bioactive polysaccharide from quinoa (denoted SQWP-2) was examined using a Sigma 300 scanning electron microscope (SEM, AMICS, Berlin, Germany). Mica surfaces were used, and 1 cm<sup>2</sup> of tape removed to expose fresh surfaces. The SQWP-2 polysaccharide powder was placed on the mica slices and samples imaged at 100- and 1000-times magnification. The surface morphology of samples was mainly revealed by secondary electron signal imaging [20].

#### 2.3.2. Molecular Weight Determination

Size exclusion chromatography was used to measure the average molecular weight (Mw) performed using two PL aquagel-OH Mixed 8- $\mu$ m columns (Tosoh Bioscience GmbH, Griesheim, Germany: 300  $\times$  7.5 mm) with a PL aquagel-OH guard protection 8- $\mu$ m precolumn for gel permeation chromatography (GPC). Eluent (0.1 M NaNO<sub>3</sub> solution) was pumped at a flow rate of 0.9 mL/min. The column was calibrated in the range of 5.8–1600 kDa using Pullan standards (British Polymer Laboratory).

#### 2.3.3. Fourier-Transform Infrared Spectroscopy

Infrared (IR) spectroscopy was performed using a Fourier-transform IR system (Bruker, Rheinstetten, Germany) with a scanning range of 4000–500 cm<sup>-1</sup>.

#### 2.3.4. Monosaccharide Composition Analysis

Acetylated derivatives were prepared by hydrolysis, reduction, and acetylation of polysaccharides for analysis using previously published methods [21]. Briefly, The RXI-5 SIL MS column (30 m  $\times$  0.25 mm  $\times$  0.25 mm) was used for gas chromatograph-mass spectrometry (GC-MS), with an initial temperature of 120 °C, final temperature of 250 °C at a flow rate of 1 mL min<sup>-1</sup>.

#### 2.3.5. Analysis of Glycosidic Linkages

Glycosidic linkages were determined by GC-MS according to the published method [22]. The sample (2 mg) was hydrolyzed with 1 mL trifluoroacetic acid (2 mol L<sup>-1</sup>) for 90 min and then the residues were dissolved into double distilled water (2 mL) and NaBH<sub>4</sub> (100 mg), respectively. One hundred microliters of glacial acetic acid was added after the reduction. The sample was dried under reduced pressure, and then acetylated with 1.0 mL acetic anhydride at 100 °C for 1 h. The acetylated derivatives were extracted with 3 mL chloroform and washed with water. The analysis was performed using a Shimadzu GCMS-QP 2010 gas chromatography-mass spectrometer.

#### 2.3.6. Nuclear Magnetic Resonance

The <sup>1</sup>H and <sup>13</sup>C spectra and DEPT135, HSQC, HMBC, NOESY spectra of the SQWP-2 were recorded at 30 °C with AV-500 MHz spectrometer (Bruker, Rheinstetten, German). Tetramethylsilane was used as an internal standard.

### 2.4. Evaluation of the Inhibition of Adipocyte Differentiation by the Water-Soluble Polysaccharide

#### 2.4.1. Cell Culture

3T3-L1 cells were cultured according to the suggested protocol from the Chinese Academy of Sciences Shanghai Cell Bank (Shanghai, China). Cells grew in DMEM supplemented with 4.5 g L<sup>-1</sup> D-glucose, 10% FBS, and 1% penicillin at 37 °C in an atmosphere containing 5% CO<sub>2</sub>.

## 2.4.2. Viability Assay

Cell viability was evaluated using the 3-(4, 5-dimethylthiazol-2-yl)-2, 5-diphenyltetrazolium bromide (MTT) method [23]. Briefly, cells were distributed into 96-well plates ( $2 \times 10^5$  cells mL<sup>-1</sup>) and cultivated overnight (37 °C, 5% CO<sub>2</sub>). After 24 h, DMEM cell medium containing SQWP-2 (0.5, 1, 2, 4, 8 mg mL<sup>-1</sup>) was added to the treated groups. Cells were cultivated for a further 24 h, after that 20 µL of MTT was added to the treated and control groups and incubation continued for 4 h. Then the MTT reagent was removed, sulfoxide (DMSO) was added (150 µL/well), and the mixture was shaken for 15 min to promote the dissolution of the purple crystals. The OD value was measured at 570 nm.

## 2.4.3. Cell Differentiation Assay

We placed 2 mL of 3T3-L1 pre-adipocytes into each well of a 12-well plate ( $2.5 \times 10^5$  cells mL<sup>-1</sup>) and cultured the cells in a treated DMEM cell medium. Cells were grown to fusion at 37 °C with 5% CO<sub>2</sub> [24]. After fusion for 48 h, cell contact was prevented (this time was defined as differentiation day 0). Cells were cultured in DMEM for 48 h (day 2), then medium replaced with DMEM containing 5 mg L<sup>-1</sup> of insulin and 10% fetal calf serum, cultured for a further 48 h (day 4). After that, the medium was changed every 48 h (using DMEM with 10% FBS), until approximately 90% of the pre-adipocytes were differentiated into adipocytes. The fat content was assessed on day 8.

## 2.4.4. Oil-Red O Staining and Measurement of Optical Density

Differentiation of the cell cultures described in Section 2.4.3 was induced on day 8. The culture solution was removed and cells were fixed with 4% paraformaldehyde for 30 min. Oil red O stain solution was added. After staining for 60 min, the solution was removed and replaced with phosphate-buffered saline (PBS). Cells were observed and photographed under an inverted microscope (Thermo Fisher Scientific, Waltham, MA, USA), then 200 µL of isopropyl alcohol added to fully dissolve oil red O in stained adipocytes and the OD measured at 492 nm.

## 2.4.5. RNA Extraction and Real-Time Reverse Transcription Polymerase Chain Reaction

Total mRNA was extracted from 3T3-L1 cells collected on day 8 using the Trizol Reagent (solarbio, Beijing, China). Total RNA was transcribed into complementary DNA (cDNA) using a large-capacity cDNA reverse transcription kit (Sangon, Shanghai, China). Gene expression was quantitatively analyzed by real-time polymerase chain reaction (PCR) using a TaqMan Fast Universal PCR Master Mix (Applied Biosystems) Primers used for PCR are shown in Table 1. The 2<sup>-ΔΔCT</sup> method was used to calculate the relative expression of each gene using β-actin as an internal standard. The relative levels of gene transcripts following exposure to SQWP-2 are expressed as fold change. Experiments were carried out in triplicate.

**Table 1.** The primer sequence is used for real-time polymerase chain reaction (PCR).

Gene Name	Forward Primer	Reverse Primer	Accession No.
C/EBPα	TTACAACAGGCCAGGTTTCC	GGCTGGCGACATACAGTACA	NM_007678
PPARγ	TTTCAAGGGTGCCAGTTTC	AATCCTTGCCCTCTGAGAT	NM_011146
C/EBPβ	CCTTTAAATCCATGGAAGTGG	GGGCTGAAGTCGATGGC	NM_005194.2
C/EBPδ	ACGACGAGAGGCCATC	TCGCCGTCGCCCAAGTC	TRCN0000013697
AP2	GGCCAAGCCCAACATGATC	CACGCCAGTTTGAAGGAAA	NM_024406
M-SREBP1c	ACAGACAAAATGCCCATCCA	GCAAGAAGCGGATGTAGTCG	NC_010454.4
β-actin	CCACAGCTGAGAGGGAAATC	AAGGAAGGCTGAAAAGAGC	X03672

## 2.4.6. Western Blot Analysis

Western blot analysis was performed according to the published method [14]. After incubated with 4 mg mL<sup>-1</sup> SQWP-2 for 24 h, 3T3-L1 cells incubated in lysis buffer (Sangon, Shanghai, China) on ice for 20 min. Cytolyte supernatant was collected and protein content was estimated after centrifugation

at  $10,000\times g$  ( $4\text{ }^{\circ}\text{C}$ , 20 min). Protein samples (10  $\mu\text{g}$ ) were separated using 10% sodium dodecyl sulfate-polyacrylamide gel electrophoresis (SDS-PAGE) and transferred to polyvinylidene fluoride (PVDF) membranes. After blocking with 5% skim milk in Tris-buffer salt containing 0.1% Tween-20 (TBST) for 1 h, anti-PPAR $\gamma$ , anti-C/EBP $\alpha$ , anti-CCAAT/enhancer-binding protein beta (C/EBP $\beta$ ), anti-CCAAT/enhancer-binding protein delta (C/EBP $\delta$ ), anti-Sterol regulatory element-binding protein-1c (SREBP1C) and anti-adipocyte protein 2 (AP2) and anti- $\beta$ -actin antibodies (Sangon, Shanghai, China) were added in combinations and the cells were incubated for 2 h at room temperature and washed with TBST. Horseradish peroxidase (HRP)-labeled secondary antibodies were added for 1 h, after which cells were washed with TBST for 10 min. Signals were detected by ELISA Pico chemiluminescent substrate (Sangon, Shanghai, China).

#### 2.4.7. Statistical Analysis

We used SPSS V.13 (SPSS Inc., Chicago, IL, USA) for all statistical analyses. One-way analysis of variance (ANOVA) and Duncan's New Multiple-Range test was used to assess statistical differences between groups. Differences were considered statistically significant at  $p < 0.05$ .

### 3. Results

#### 3.1. Extraction and Purification

The purity of QWP isolated from quinoa seeds was approximately 64.1%. Chromatographic purification enables the required fractions to be collected (Figure 1). After purification, the purity of SQWP-2 was up to 95%. In the pre-experiment, the SQWP-2 showed a higher inhibitory effect on 3T3-L1 cell differentiation than SQWP-1 (Figure S1). Therefore, SQWP-2 was further analyzed its chemical structure and reveal the mechanism of its anti-adipogenesis effect.

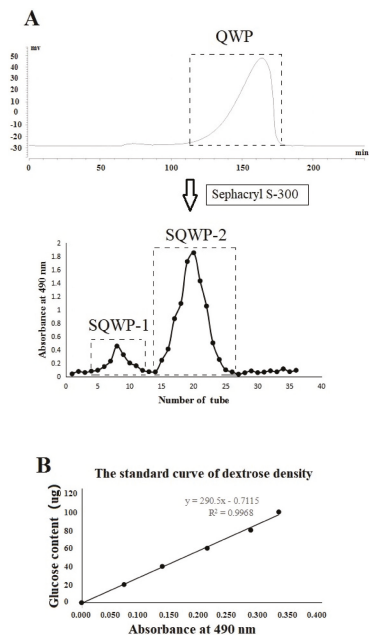


**Figure 1.** (A) Elution curve of the water-extractable (SQWP-2) on a Sepharose Flast Flow column and gel filtration chromatography; (B) standard curve of dextrose density.

### 3.2. Analysis of Surface Morphology

A representative SEM micrograph of SQWP-2 is shown in Figure 2A, SQWP-2 appeared globular in the structure at 100-times magnification. At 1000-times magnification, the surface of the polysaccharide appeared rough and dentate.

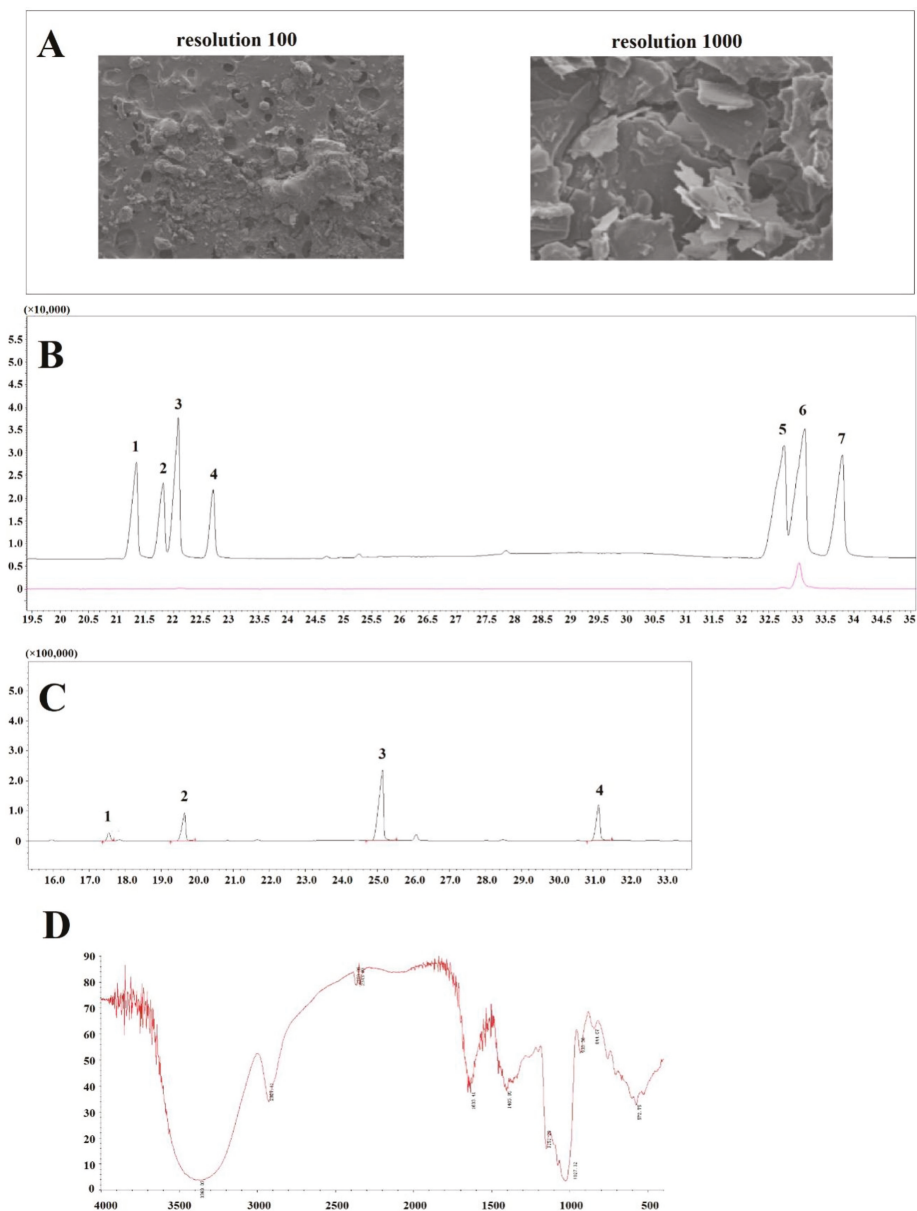


**Figure 2.** (A) Scanning electron microscopy (A  $\times$  100, B  $\times$  1000); (B) monosaccharide composition analysis by chromatograph-mass spectrometry (GC-MS). (1). Rham, (2). Fuc, (3). Ara, (4). Xyl, (5). Man, (6). Glu, (7). Gal; (C) Glycosidic linkage by methylation analysis. (1). 1,3,4,6-Me4-Glc/Manp, (2). 2,3,4,6-Me4-Glcp, (3). 2,3,6-Me3-Glcp, (4). 2,3-Me2-Glcp; (D) FT-IR spectra of SQWP-2.

### 3.3. Analysis of Monosaccharide Composition and Glycosidic Linkages

Glycosidic linkage of SQWP-2 was analyzed by GC/MS. Gas chromatography analysis indicated SQWP-2 to be composed of glucose (Figure 2B) and methylation analysis revealed the presence of four types of glycosidic linkage: 2,3,4,6-Me4-Glcp; 1,3,4,6-Me4-Glc/Manp; 2,3,6-Me3-Glcp; and 2,3-Me2-Glcp (Figure 2C). Their corresponding link way for Glc-(1→, Fru-(2→, →4)-Glcp-(1→, →4,6)-Glcp-(1→ is detailed in Table 2. The polysaccharide was found to be composed of dextran, whose main chain is →4)-Glcp-(1→ and exhibits O-6 branching.

**Table 2.** Three glycoside bonds of quinoa polysaccharide.

Methylated Sugar	Mass Fragments ( <i>m/z</i> )	Type of Linkage
2,3,4,6-Me4-Glcp	43,71,87,101,117,129,145,161,205	Glc-(1→
1,3,4,6-Me4-Glc/Manp	87,101,129,145,161	Fru-(2→
2,3,6-Me3-Glcp	43,87,99,101,113,117,129,131,161,173,233	→4)-Glcp-(1→
2,3-Me2-Glcp	43,71,85,87,99,101,117,127,159,161,201	→4,6)-Glcp-(1→

### 3.4. Fourier-Transform Infrared Spectroscopy

As Figure 2D showed, an absorption band at 3600–3200 cm<sup>-1</sup> was observed, which could be attributed to the stretching vibration absorption peak of –OH. The peak at 2927 cm<sup>-1</sup> relates to the C–H stretching vibration of polysaccharides. An absorption peak was noted at 1633 cm<sup>-1</sup> due to the asymmetric stretching vibration of C=O. Peak at 1405 cm<sup>-1</sup> could be attributed to C–H variable angular vibration. The absorption peaks between 1020 cm<sup>-1</sup> and 1160 cm<sup>-1</sup> were due to the C–O stretching vibration and the peak at 844 cm<sup>-1</sup> may be attributed to alpha-terminal radical isomerism. The specific structure of the polysaccharide needs to be confirmed by further nuclear magnetism analysis.

### 3.5. Nuclear Magnetic Spectroscopy

The <sup>1</sup>H-nuclear magnetic resonance (NMR), <sup>13</sup>C-NMR, DEPT135 of SQWP-2 were shown in Figure 3A–C, respectively. The δ 3.2–4.0 ppm signal in the hydrogen spectrum related to the proton of sugar-ring. The <sup>13</sup>C NMR spectrum (126 MHz, D<sub>2</sub>O) signals were observed to be mainly concentrated between 60 and 120 ppm. Sharp signals at 100.59, 101.82, and 105.21 ppm indicated an α configuration of the glycosidic linkages, and signals were observed in the range of δ 60–85 indicating the presence of (1→4)-α-glycosidic linkages. The results indicated that the analyzed polysaccharides were mainly composed of dextran with a small amount of fructose. The DEPT135 chromatogram revealed inverted peaks at 62.32, 62.70, and 63.91 ppm, indicating the chemical displacement of the C6 or C1 signal peak of fructose or CH<sub>2</sub> groups of either glucose or fructose.

Because the area of an absorption peak is proportional to the number of hydrogen protons, H1 of →4)-α-D-Glcp-(1→, →4,6)-α-D-Glcp-(1→, α-D-Glcp-1→, and H3 of β-D-Fru-(2→ were integrated, which were found to exist in a ratio of 3.5:1:1.4. The corresponding ratio of hydrogen protons for →4)-α-D-Glcp-(1→, →4,6)-α-D-Glcp-(1→ including α-D-Glcp-1→, and β-D-Fru-(2→ was found to be 1:1:1. Therefore, the ratio of the three types of glycosidic bonds was 3.5:1:1.4. Methylation analysis revealed the ratio of →4)-α-D-Glcp-(1→, →4,6)-α-D-Glcp-(1→, β-D-Fru-(2→, and α-D-Glcp-1→ to be 19:4:8:1.

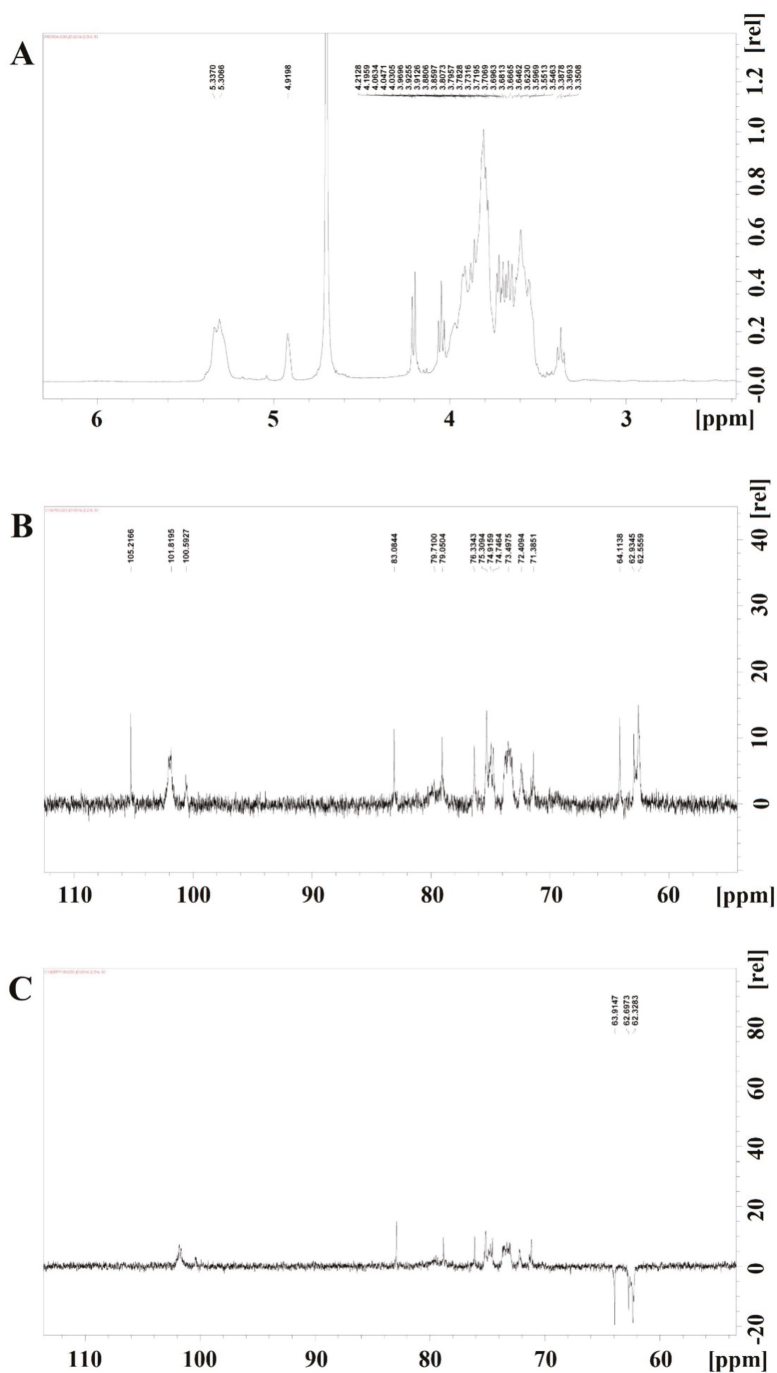


**Figure 3.** The nuclear magnetic resonance (NMR) spectra analysis of SQWP-2. (A)  $^1\text{H}$ NMR; (B)  $^{13}\text{C}$  NMR; (C) Dept135.

The 2D spectra of SQWP-2 are shown in Figure 4A–C, respectively. HSQC spectrum revealed signal of the hetero-head carbon to be  $\delta$  5.31, the corresponding hetero-head hydrogen signal to be delta 5.31, and the signal H1-2 to be 5.31/3.55. The signal of H2-3 was 3.55/3.94 and that of H3-4 was 3.94/3.57. We can infer that H1, H2, H3, and H4 are 5.32, 3.55, 3.94 and 3.57 respectively, and the corresponding C5 was 73.53.  $\delta$  62.63 for C6 and  $\delta$  3.76 for H6a. Therefore, the signal can be attributed to the  $\rightarrow$ 4)- $\alpha$ -Glc-(1 $\rightarrow$  glycosidic linkage. In addition, we observed the 105.17 ppm signal peak in the HSQC spectrum. There was no corresponding H, so we can infer that the signal relates to C2 of the Fru-2 $\rightarrow$  glycosidic linkage. We attributed this to the hydrocarbon Fru-2 $\rightarrow$  owing to the peak shape. We classified all glycosidic linkages according to the similarity rule combined with HMBC and NOESY results (Figure 4A,C; Table 3).

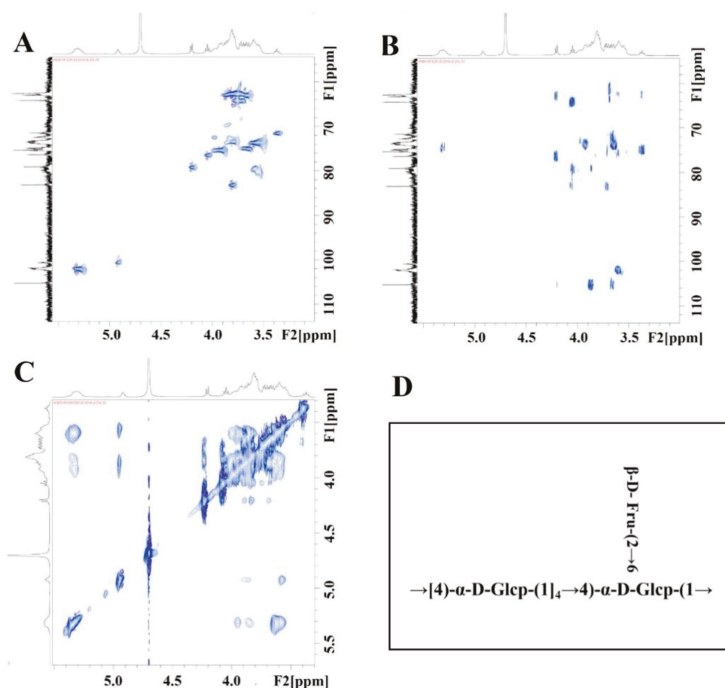


Figure 4. (A) HSQC; (B) HMBC; (C) NOESY spectra of SQWP-2; (D) Constitutional formula of SQWP-2.

Table 3. The attribution of Hydrocarbon signal.

Glycosyl Residues	H1	H2	H3	H4	H5	H6a	H6b
	C1	C2	C3	C4	C5	C6	
$\rightarrow$ 4)- $\alpha$ -D-Glc-(1 $\rightarrow$	5.31	3.55	3.94	3.57	3.78	3.76	ns
	102.01	73.57	75.31	79.58	73.52	62.63	
$\rightarrow$ 4,6)- $\alpha$ -D-Glc-(1 $\rightarrow$	4.93	3.55	3.65	3.54	3.85	3.84	ns
	100.7	73.53	74.02	78.2	74.6	69.71	
Fru-(2 $\rightarrow$	3.65/3.81		4.2	4.05	3.81	3.72/3.78	
	62.74	105.17	79.01	76.4	83.23	64.28	
$\alpha$ -D-Glc-(1 $\rightarrow$	5.26	3.36	3.66	3.95	3.98	3.6	3.82
	101.33	71.4	75.1	70.61	72.41	62.3	

Glycoside linkage signals of polysaccharides were assigned from HMBC according to the 1D-2D NMR spectra. The  $\delta$  101.14 of the  $\rightarrow$ 4)- $\alpha$ -Glc-(1 $\rightarrow$  glycoside linkage exhibited a signal peak corresponding with its H4  $\delta$ 3.55, evidencing the existence of a  $\rightarrow$ 4)- $\alpha$ -D-Glc-(1 $\rightarrow$ 4)- $\alpha$ -D-Glc-(1 $\rightarrow$

linkage. The terminal  $\alpha$ -D-Glcp-(1 $\rightarrow$  and Fru-(2 $\rightarrow$  group was found to be bonded to the main chain by O-6. The structural formula of SQWP-2 was shown in Figure 3G.

### 3.6. Cell Viability Analysis

There were no significant differences in the viability of 3T3-L1 cells exposed to 8 mg mL<sup>-1</sup> SQWP-2 compared with the control group (Figure 5A). At the maximum concentration of SQWP-2 (8 mg mL<sup>-1</sup>), a 17.1% decrease in viability was observed, suggesting that SQWP-2 did not exert a significant toxic effect on 3T3-L1 cells at this concentration. When the SQWP-2 concentration was 4 mg mL<sup>-1</sup>, its toxic effect on cells could be ruled out. Therefore, a concentration of 4 mg mL<sup>-1</sup> of SQWP-2 was used for further experiments.

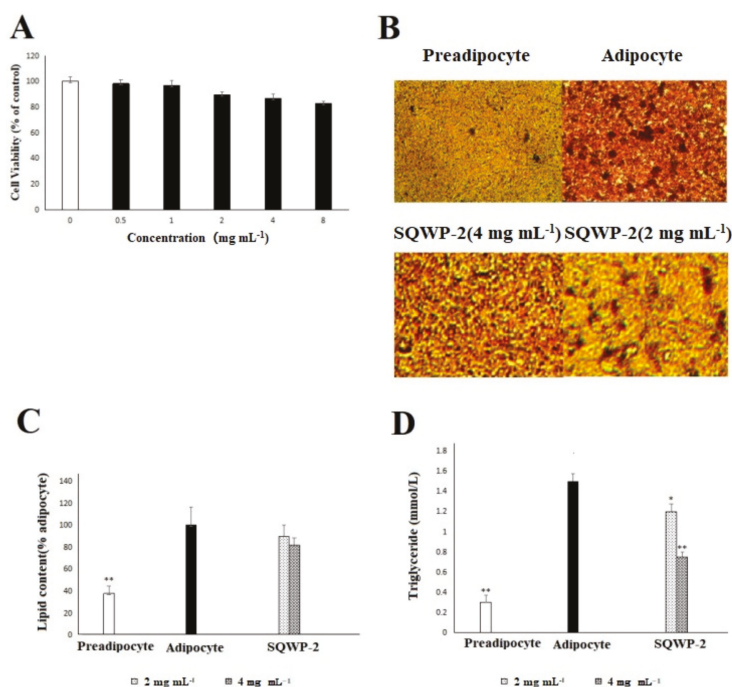


**Figure 5.** MTT cell viability of SQWP-2. Data are shown as mean  $\pm$  SD. \*  $p < 0.05$  vs. control; \*\*  $p < 0.005$  vs. control. (A) Effect of SQWP-2 on intracellular lipid accumulation in 3T3-L1 cells. Cells were treated with SQWP-2 (2 mg mL<sup>-1</sup> and 4 mg mL<sup>-1</sup>) for day 8; (B) The mature adipocytes were colored with oil-red O; (C) OD value (% adipocyte); (D) TG content (mmol L<sup>-1</sup>) were measured to quantify intracellular lipid content.

### 3.7. Effect of the Water-Soluble Polysaccharide on Intracellular Lipid Accumulation in 3T3-L1 Cells

Oil-red O staining images showed that lipid accumulation was suppressed in the experimental group with SQWP-2 (Figure 4B). Lipid content was significantly decreased in the group treated with SQWP-2 ( $p < 0.05$ , Figure 4C). These results were confirmed by TG content (Figure 4D), TG level in SQWP-2-treated (4 mg mL<sup>-1</sup>) group was reduced by 49.7% compared with the adipocyte group ( $p < 0.05$ ). From the effect of SQWP-2 on 3T3-L1 intracellular lipid accumulation, obviously, SQWP-2 with a concentration of 4 mg mL<sup>-1</sup> was significantly better than 2 mg mL<sup>-1</sup>, so the concentration of SQWP-2 in subsequent experiments was 4 mg mL<sup>-1</sup>.

### 3.8. Effect of the Water-Soluble Polysaccharide on mRNA and Protein Expression

Western Blotting revealed that protein expression reflected mRNA expression (Figure 6). The results suggested that SQWP-2 suppressed protein expression of PPAR $\gamma$ , C/EBP $\alpha$ , C/EBP $\beta$ , C/EBP $\delta$ , SREBP1C and AP2 by downregulating mRNA transcription. The expression levels of PPAR $\gamma$ , C/EBP $\alpha$ , C/EBP $\beta$ , C/EBP $\delta$ , SREBP1C and AP2 after treatment by SQWP-2 were reduced to  $0.90 \pm 0.06$ ,  $0.39 \pm 0.03$ ,  $0.86 \pm 0.06$ ,  $0.92 \pm 0.06$ ,  $0.77 \pm 0.05$  and  $0.78 \pm 0.05$  times of the control group, respectively (Figure 6B), which was consistent with the result of Western Blotting. SQWP-2 also was uncovered to suppress the mRNA expression of PPAR $\gamma$ , C/EBP $\alpha$ , C/EBP $\beta$ , C/EBP $\delta$ , SREBP1C and AP2 compared with control adipocytes. These major transcription factors work together to restrain adipocyte differentiation. The amplification curve and dissolution curve were shown in Figure S2.

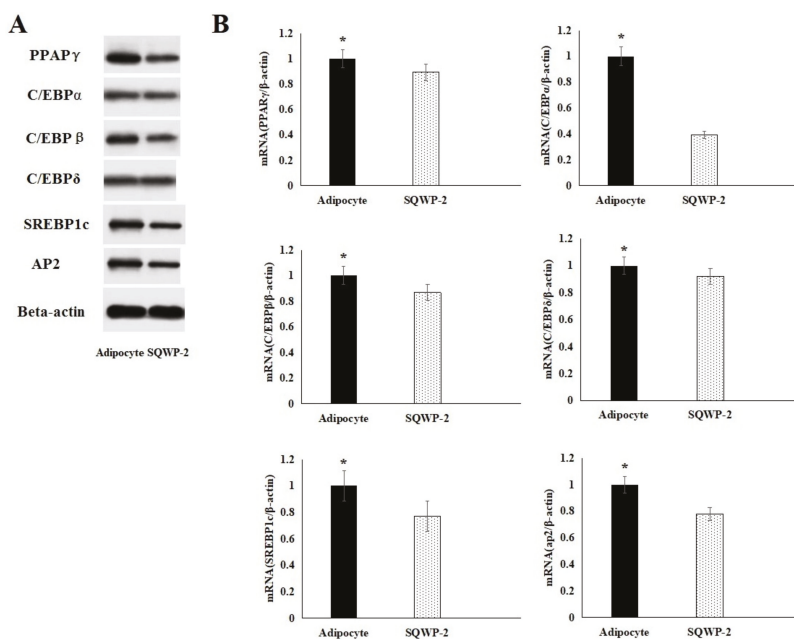


**Figure 6.** Effect of SQWP-2 on the protein levels (A) and mRNA expression (B) of related pathways in 3T3-L1 cells. Experiments were performed three times, and data are shown as mean  $\pm$  SD. Values that do not share the same letter are significantly different (\*  $p < 0.05$ ).

## 4. Discussion

Polysaccharides are the main component of grains and have been reported to possess various bioactivities. Cordeiro et al. claimed that a linear arabinan with (1  $\rightarrow$  5)-linked  $\alpha$ -L-arabinofuranosyl units of polysaccharides in quinoa showed the strongest gastroprotective activity [25]. Quinoa polysaccharide constituted of Glc and Ara with a molar ratio of 1.17:1 was proven to prevent and protect against hyperlipidaemia [26]. Quinoa is becoming popular owing to the high nutritional value of the seeds. Our previous experiments have suggested the adipogenesis inhibitory effects of crude water-soluble polysaccharides extracts from quinoa. In the present study, to identify the responsible bioactive component, two polysaccharides fractions were separated and purified from crude water-soluble polysaccharides extracts. The SQWP-2 showed a higher inhibitory effect on 3T3-L1 cells differentiation than SQWP-1 group. Structural characterization of the polysaccharide revealed SQWP-2 had an average molecular weight of  $7.49 \times 10^3$  Da and consisted mainly of mannose and glucose with a ratio of 5.1:94.9. It is worth noting that fructose is a ketose, which can isomerize to mannose and glucose in

a ratio of 52:48 during reduction. Galacturonic acid and glucose monosaccharides have been identified in a polysaccharide fraction purified from quinoa [15]. Three *Astragalus* polysaccharides prepared using different temperature treatments were found to have different chemical structures [27].

It is noteworthy that the present work is the first study to characterize glycosidic linkages using NMR spectroscopy including 1D and 2D spectra for this particular polysaccharide. The composition was found to comprise glucose, mainly dextran with a small amount of mannose. In the 1H-NMR spectrum, the prominent peak in the anomeric region indicated the presence of heterophase in Glc (p). The <sup>13</sup>C NMR spectrum revealed several abnormal carbons in the pyranosyl residues and multiple non-anomalous carbon peaks within a wide area [28]. The linkage and NMR data suggest that  $\rightarrow 4$ - $\alpha$ -Glc(p)-(1 $\rightarrow$  is the main connection unit in SQWP-2, similar to a polysaccharide isolated from *Terminalia chebula* [29]. Before this study, Cordeiro extracted the polysaccharides in quinoa and analyzed the structure and its gastroprotective activity [25]. The structure of quinoa polysaccharide in the study consisted of a linear arabinan with (1 $\rightarrow$  5)-linked  $\alpha$ -L-arabinofuranosyl units, which was different from results in this study. Two main reasons could contribute to this phenomenon. First, the source and variety of materials are different. Another is the different extraction method, 10% KOH was added in extracting polysaccharide. Due to these reasons, structural analysis and biological activity could show the difference. Research on enzymolysis and amylopectin chain-length distribution needs to be further studied to clarify the specific structural details of SQWP-2. For accuracy, we used the integral value of the proton hydrogen of each glycosidic linkage in the hydrogen spectrum to calculate the proportion of glycosidic bonds, as this exhibited good resolution without the need for processing. The glycosidic linkage  $\rightarrow 4,6$ - $\alpha$ -D-Glcp-(1 $\rightarrow$  proton coincides with Glcp-1 $\rightarrow$ . The ratio of glycosidic linkages was obtained through a methylation analysis of glycosidic linkage molar ratios.

As a nutritional supplement, quinoa has been reported to have anti-obesity activities and to have utility in the prevention and treatment of obesity [30]. Previous research has focused on the mechanism underlying the effects of quinoa in terms of increasing satiety, inhibiting digestive enzymes, and improving bacterial flora. Direct inhibition of adipocyte differentiation is another mechanism thought to contribute to the anti-obesity effects of quinoa. Polysaccharides are active compounds in many plants. In the present study, the isolated polysaccharide SQWP-2 strongly inhibited 3T3-L1 adipocyte differentiation. This can, therefore, be concluded to be one of the mechanisms explaining the anti-obesity activity of quinoa, which is a novel finding because the contribution of fullness to the anti-obesity effect has been the focus of previous research into quinoa. To further study the mechanism of SQWP-2 inhibition of differentiation of 3T3-L1 adipocytes, we studied the mRNA and protein expression of related protein factors. The protein PPAR $\gamma$  is an essential factor in adipocyte differentiation, while the expression of C/EBP $\alpha$  remains constant. This is similar to previous research results, which have shown that the morus polysaccharide effectively inhibits adipocyte differentiation [1]. The expression of SREBP1C has been reported to be similar to that of C/EBP $\beta$ , which is consistent with the results of this study. We also found that SQWP-2 strongly inhibited C/EBP $\alpha$  expression which supports previous research [31]. The transcription factor C/EBP $\alpha$  coordinates cell differentiation and growth arrest [32,33].

Polysaccharides with different structures have different biological activities. For example, the immunomodulatory activities of polysaccharides are reported to be influenced by the monosaccharides and glycosidic linkage compositions [34]. Toll-like receptor 4, an important receptor of immunomodulatory activity, is closely associated with high-glucose polysaccharides such as  $\beta$ -(1,3)-Glc,  $\beta$ -(1,4)-Glc, and  $\alpha$ -(1,4)-Glc. The main chain of polysaccharide from fungus has been reported to be composed of  $\rightarrow 3,6$ - $\beta$ -L-Man-(1 $\rightarrow$ ,  $\alpha$ -D-Glc-(1 $\rightarrow$ ,  $\rightarrow 4$ )- $\alpha$ -D-Glc-(1 $\rightarrow$ ,  $\rightarrow 3,6$ - $\beta$ -D-Gal-(1 $\rightarrow$ , and  $\rightarrow 6$ )- $\beta$ -D-Gal-(1 $\rightarrow$ , and the polysaccharide exhibits strong immunomodulatory activity [35]. Many plant polysaccharides have been demonstrated to inhibit 3T3-L1 adipocyte differentiation [12], and quinoa polysaccharides have been confirmed to have immunomodulatory functions [18]. However, the structural details and anti-obesity activity of quinoa polysaccharides are poorly studied to date. This inhibitory effect has also been demonstrated for polysaccharides isolated from Pine needles [35],

Gray Oyster mushrooms [36], and *Nannochloropsis oculata* [33], and were shown to be positively correlated with molecular weight. The anti-obesity activity of polysaccharides largely depends on their structure and the intracellular signaling pathways involved. Fucoidan has been reported to inhibit the expression of the early C/EBP $\alpha$  and PPAR $\gamma$  and the late AP2 adipose-forming transcription factors, which are crucial for the development of fat cells [31]. The present research found the presence of  $\rightarrow 4$ - $\alpha$ -D-Glcp-(1 $\rightarrow$  glycoside linkages with  $\alpha$ -D-Glcp-(1 $\rightarrow$  and Fru-(2 $\rightarrow$  to result in strong inhibition of 3T3-L1 adipocyte differentiation. Our study elucidated the mechanism of the inhibitory effects of SQWP-2 on 3T3-L1 adipocyte differentiation.

## 5. Conclusions

The isolated polysaccharide was found to consist of fructose and glucose in a ratio of 9.8:90.2 with an average molecular weight of  $7.49 \times 10^3$  Da. The main sugar residue linkages were found to be  $\rightarrow 4$ - $\alpha$ -D-Glcp-(1 $\rightarrow$ :  $\rightarrow 4,6$ )- $\alpha$ -D-Glcp-(1 $\rightarrow$ :  $\beta$ -D-Fru-(2 $\rightarrow$ :  $\alpha$ -D-Glcp-1 $\rightarrow$ , existing at a ratio of close to 19:4:8:1. The main chain connection mode of the polysaccharide was determined to be a  $\rightarrow 4$ - $\alpha$ -D-Glcp-(1 $\rightarrow$  glycoside linkage, while the terminal group of  $\alpha$ -D-Glcp-(1 $\rightarrow$  and Fru-(2 $\rightarrow$  was bonded to the main chain via O-6. The polysaccharide inhibited 3T3-L1 adipocyte differentiation, indicating that proliferation was inhibited through the promotion of PPAR $\gamma$ , C/EBP $\alpha$ , C/EBP $\beta$ , C/EBP $\delta$ , SREBP1C and AP2 expression. The expression levels were reduced to  $0.90 \pm 0.06$ ,  $0.39 \pm 0.03$ ,  $0.86 \pm 0.06$  and  $0.92 \pm 0.06$ ,  $0.77 \pm 0.05$ ,  $0.78 \pm 0.05$  times of the control group, respectively. Based on the above result, SQWP-2, as an active ingredient food, has broad application prospects due to its inhibitory effects on 3T3-L1 adipocyte differentiation.

**Supplementary Materials:** The following are available online at <http://www.mdpi.com/2304-8158/9/10/1511/s1>, Figure S1: Effects of SQWP-1 and SQWP-2 on 3T3-L1 cells inhibiting differentiation., Figure S2: Amplification curve and Dissolution curve of  $\beta$ -actin, PPAR $\gamma$ , C/EBP $\alpha$ , C/EBP $\beta$ , C/EBP $\delta$ , SREBP1C, AP2.

**Author Contributions:** Conceptualization, Y.Y. and C.T.; analysis, resources, G.R.; data curation, C.T.; writing—original draft preparation, T.C.; writing—review and editing, C.T. and Z.S.; funding acquisition, G.R. All authors have read and agreed to the published version of the manuscript.

**Funding:** This research was funded by the National Natural Science Foundation of China(31701597), Central Public-interest Scientific Institution Basal Research Fund (No. Y2020PT30), NCGRC—national crop germplasm resource center (NCGRC-2020-8) and the Agricultural Science and Technology Innovation Program of CAAS (Grant No. CAAS-ASTIP-2017-ICS).

**Acknowledgments:** We thank Amy Phillips, PhD, from Liwen Bianji, Edanz Editing China ([www.liwenbianji.cn/ac](http://www.liwenbianji.cn/ac)), for editing the English text of a draft of this manuscript.

**Conflicts of Interest:** The authors declare no conflict of interest.

## Abbreviations

PPAR $\gamma$	Peroxisome proliferator-activated receptor gamma
C/EBP $\alpha$	CCAAT/enhancer-binding protein alpha
C/EBP $\beta$	CCAAT/enhancer-binding protein beta
C/EBP $\delta$	CCAAT/enhancer-binding protein delta
AP2	Adipocyte protein 2
M-SREBP1C	Sterol regulatory element-binding protein-1c
Dept	Distortionless Enhancement Polarizationtransfer
HSQC	Heteronuclear Single Quantum Coherence
HMBC	Heteronuclear Multiple Bond Correlation
NOESY	Nuclear Overhauser Effect Spectroscopy
TG	Triglyceride

## References

- Ji, W.C.; Andriy, S.; Peter, C.; Roman, B.; Radek, P.; Yong, P. Structural analysis and anti-obesity effect of a pectic polysaccharide isolated from Korean mulberry fruit Oddi (*Morus alba* L.). *Carbohydr. Polym.* **2016**, *146*, 187–196. [[CrossRef](#)]
- James, W.P.T.; Jackson, L.R.; Mhurchu, C.N.; Kalamara, E.; Shayeghi, M.; Rigby, N.J. Overweight and obesity (high body mass index) comparative quantification of health risks: Global and regional burden of disease attributable to selected major risk factors. *World Health Organ.* **2014**, *1*, 497–596. [[CrossRef](#)]
- Ji, X.; Hou, C.; Guo, X. Physicochemical properties, structures, bioactivities and future prospective for polysaccharides from Plantago L. (Plantaginaceae): A review. *Int. J. Biol. Macromol.* **2019**, *135*, 637–646. [[CrossRef](#)] [[PubMed](#)]
- Shang, K.; Chen, D.; Lanlan, H.; Yan, B.; Tiancun, X.; Guo, J.; Su, Z.Q. The effects of COST on the differentiation of 3T3-L1 preadipocytes and the mechanism of action. *Saudi J. Biol. Sci.* **2017**, *2*, 251–255. [[CrossRef](#)]
- Sven, E.J. The worldwide potential for quinoa (*Chenopodium quinoa* Willd.). *Food Rev. Int.* **2003**, *19*, 167–177. [[CrossRef](#)]
- Antonio, M.M.F.; Monica, R.P.; Tomaz, D.S.B.; Helena, M.P.S.; Paes, C.; Jane, S.D.R.C. Quinoa: Nutritional, functional, and antinutritional aspects. *Crit. Rev. Food Sci. Nutr.* **2017**, *8*, 1618–1630. [[CrossRef](#)]
- Ogungbenle, H.N. Nutritional evaluation and functional properties of quinoa flour. *Int. J. Food Sci. Nutr.* **2003**, *54*, 153–158. [[CrossRef](#)]
- Farinazzi-Machado, F.M.V.; Barbalho, S.M.; Oshiiwa, M.R.; Goulart, O. Pessan junior use of cereal bars with quinoa (*Chenopodium quinoa* W.) to reduce risk factors related to cardiovascular diseases. *Cienc. Technol. Aliment.* **2012**, *32*, 239–244. [[CrossRef](#)]
- Yao, Y.; Zhu, Y.Y.; Gao, Y.; Shi, Z.X.; Hu, Y.B.; Ren, G.X. Suppressing effects of saponin-enriched extracts from quinoa on 3T3-L1 adipocyte differentiation. *Food Funct.* **2015**, *6*, 3282–3290. [[CrossRef](#)]
- Anne, S.F.; Véronique, M.; René, L.; Patrick, E.; Waly, D.; Stanislas, V.; Daniel, T.; Jean, F.H.; Dominique, H.; Annie, Q. Quinoa extract enriched in 20-hydroxyecdysone protects mice from diet-induced obesity and modulates adipokines expression. *Adipocyte Biol.* **2011**, *20*, 270–277. [[CrossRef](#)]
- Maha, A. Preparation of different formulae from quinoa and different sources dietary Fiber to treat obesity in rats. *Nat. Sci.* **2016**, *14*, 55–65. [[CrossRef](#)]
- Bin, K.; Xiao, K.; Xuesi, W.; Yubin, Y.; Yingjuan, H.; Jian, Q.; Chengheng, H.; Lin, S. Astragalus polysaccharides attenuates TNF- $\alpha$ -induced insulin resistance via suppression of miR-721 and activation of PPAR- $\gamma$  and PI3K/AKT in 3T3-L1 adipocytes. *Am. J. Transl. Res.* **2017**, *9*, 2195–2206.
- Liu, J.L.; Yang, L.C.; Zhu, X.J.; Wang, W.J.; Zheng, G.D. Combinational effect of pine needle polysaccharide and kudzu flavonoids on cell differentiation and fat metabolism in 3T3-L1 cells. *Food Sci. Technol. Res.* **2018**, *5*, 903–910. [[CrossRef](#)]
- Zhu, Y.Y.; Yao, Y.; Gao, Y.; Hu, Y.B.; Shi, Z.X.; Ren, G.X. Suppressing effects of barley  $\beta$ -glucans with different molecular weight on 3T3-L1 adipocyte differentiation. *J. Food Sci.* **2016**, *3*, 786–793. [[CrossRef](#)] [[PubMed](#)]
- Hu, Y.; Zhang, J.; Zou, L.; Fu, C.; Li, P.; Zhao, G. Chemical characterization, antioxidant, immune-regulating and anticancer activities of a novel bioactive polysaccharide from *Chenopodium quinoa* seeds. *Int. J. Biol. Macromol.* **2017**, *99*, 622–629. [[CrossRef](#)] [[PubMed](#)]
- Li, S.P.; Wu, D.T.; Lv, G.P.; Zhao, J. Carbohydrates analysis in herbal glycomics. *Trac Trends Anal. Chem.* **2013**, *52*, 155–169. [[CrossRef](#)]
- Ferreira, S.S.; Passos, C.P.; Madureira, P.; Vilanova, M.; Coimbra, M.A. Structure function relationships of immunostimulatory polysaccharides: A review. *Carbohydr. Polym.* **2015**, *132*, 378–396. [[CrossRef](#)]
- Yao, Y.; Zhu, Y.Y.; Ren, G.X. Immunoregulatory activities of polysaccharides from mung bean. *Carbohydr. Polym.* **2016**, *139*, 61–66. [[CrossRef](#)]
- Tatsuya, M.; Akio, M.; Norimasa, I.; Tokifumi, M.; Shin-Ichiro, N.; Yuan, C.L. Carbohydrate analysis by a phenol-sulfuric acid method in microplate format. *Anal. Biochem.* **2005**, *1*, 69–72. [[CrossRef](#)]
- Moshe, R.; Isaiah, J.K.; Yeshayahu, T. A scanning electron microscopy study of microencapsulation. *J. Food Sci.* **2010**, *50*, 139–144. [[CrossRef](#)]
- Dai, J.; Wu, Y.; Chen, S.; Zhu, S.; Yin, H.; Wang, M. Sugar compositional determination of polysaccharides from *dunaliella salina* by modified RP-HPLC method of precolumn derivatization with 1-phenyl-3-methyl-5-pyrazolone. *Carbohydr. Polym.* **2010**, *82*, 629–635. [[CrossRef](#)]

22. Pettolino, F.A.; Walsh, C.; Fincher, G.B.; Bacic, A. Determining the polysaccharide composition of plant cell walls. *Nat. Protoc.* **2012**, *7*, 1590. [[CrossRef](#)] [[PubMed](#)]
23. Meerloo, J.V.; Kaspers, G.J.L.; Cloos, J. Cell sensitivity assays: The mtt assay. *Methods Mol. Biol.* **2011**, *731*, 237–245. [[CrossRef](#)] [[PubMed](#)]
24. Zhao, X.; Hu, H.; Wang, C.; Bai, L.; Wang, Y.; Wang, W.; Wang, J. A comparison of methods for effective differentiation of the frozen-thawed 3T3-L1 cells. *Anal. Biochem.* **2019**, *568*, 57–64. [[CrossRef](#)]
25. Cordeiro, L.M.; Reinhardt, V.D.; Baggio, C.H.; Werner, M.F.; Burci, L.M.; Sasaki, G.L.; Iacomini, M. Arabinan and arabinan-rich pectic polysaccharides from quinoa (*Chenopodium quinoa*) seeds: Structure and gastroprotective activity. *Food Chem.* **2012**, *130*, 937–944. [[CrossRef](#)]
26. Cao, Y.N.; Zou, L.; Li, W.; Song, Y.; Zhao, G.; Hu, Y.C. Dietary quinoa (*Chenopodium quinoa* Willd.) polysaccharides ameliorate high-fat diet-induced hyperlipidemia and modulate gut microbiota. *Int. J. Biol. Macromol.* **2020**, *163*, 55–65. [[CrossRef](#)]
27. Yu, J.; Ji, H.; Yang, Z.; Liu, A. Relationship between structural properties and antitumor activity of Astragalus polysaccharides extracted with different temperatures. *Int. J. Biol. Macromol.* **2019**, *124*, 469–477. [[CrossRef](#)] [[PubMed](#)]
28. Cheng, H.; Neiss, T.G. Solution NMR spectroscopy of food polysaccharides. *Polym. Rev.* **2012**, *52*, 81–114. [[CrossRef](#)]
29. Hye, K.J.; Dongjoo, L.; Hong, P.K.; Seung-Hoon, B. Structure analysis and antioxidant activities of an amylopectin-type polysaccharide isolated from dried fruits of *Terminalia chebula*. *Carbohydr. Polym.* **2019**, *211*, 100–108. [[CrossRef](#)]
30. Giuliana, D.N.; Kevin, M.; Boon, P.C. Quinoa intake reduces plasma and liver cholesterol, lessens obesity-associated inflammation, and helps to prevent hepatic steatosis in obese db/db mouse. *Food Chem.* **2019**, *287*, 107–114. [[CrossRef](#)]
31. Kim, K.; Lee, O.; Lee, B. Fucoidan, a sulfated polysaccharide, inhibits adipogenesis through the mitogen-activated protein kinase pathway in 3T3-L1 preadipocytes. *Life Sci.* **2010**, *86*, 791–797. [[CrossRef](#)] [[PubMed](#)]
32. Mi-Ja, K.; Un-Jae, C.; Jin-Sil, L. Inhibitory effects of fucoidan in 3T3-L1 adipocyte differentiation. *Mar. Biotechnol.* **2009**, *11*, 557–562. [[CrossRef](#)]
33. Albalat, A.; Saera, V.A.; Capilla, E.; Gutiérrez, J.; Pérez, S.J.; Navarro, I. Insulin regulation of lipoprotein lipase (LPL) activity and expression in gilthead sea bream (*Sparus aurata*). *J. Biochem. Molecular Biol.* **2007**, *2*, 151–159. [[CrossRef](#)] [[PubMed](#)]
34. Carolina, O.P.; Élia, M.; Sónia, S.F.; Viviana, G.C.; Benedita, A.P.; Dmitry, V.E.; Angelina, S.P.; Alexandra, C.; Manuel, V.; Manuel, A.C.; et al. Structural analysis and potential immunostimulatory activity of *Nannochloropsis oculata* polysaccharides. *Carbohydr. Polym.* **2019**, *222*, 1–10. [[CrossRef](#)]
35. Ji, X.; Yan, Y.; Hou, C.; Shi, M.; Liu, Y. Structural characterization of a galacturonic acid-rich polysaccharide from *Ziziphus Jujuba* cv. Muzao. *Int. J. Biol. Macromol.* **2019**, *147*, 1–24. [[CrossRef](#)]
36. Yang, M.; Tarun, B.; Hari, P.D.; Li, L.; Zisheng, L. Trends of utilizing mushroom polysaccharides (MPs) as potent nutraceutical components in food and medicine: A comprehensive review. *Trends Food Sci. Technol.* **2019**, *92*, 94–110. [[CrossRef](#)]

**Publisher's Note:** MDPI stays neutral with regard to jurisdictional claims in published maps and institutional affiliations.



© 2020 by the authors. Licensee MDPI, Basel, Switzerland. This article is an open access article distributed under the terms and conditions of the Creative Commons Attribution (CC BY) license (<http://creativecommons.org/licenses/by/4.0/>).



Review

# Insights on Health and Food Applications of *Equus asinus* (Donkey) Milk Bioactive Proteins and Peptides—An Overview

Reda Derdak <sup>1,†</sup>, Souraya Sakoui <sup>1</sup>, Oana Lelia Pop <sup>2,3,†</sup>, Carmen Ioana Muresan <sup>2,3</sup>, Dan Cristian Vodnar <sup>2,4</sup>, Boutaina Addoum <sup>1</sup>, Romana Vulturar <sup>5,6,\*</sup>, Adina Chis <sup>5,6</sup>, Ramona Suharoschi <sup>2,3,\*</sup>, Abdelaziz Soukri <sup>1</sup> and Bouchra El Khalfi <sup>1</sup>

- <sup>1</sup> Laboratory of Physiopathology, Molecular Genetics & Biotechnology, Faculty of Sciences Ain Chock, Health and Biotechnology Research Centre, Hassan II University of Casablanca, Maarif B.P 5366, Casablanca, Morocco; reda.derdakk@gmail.com (R.D.); sakouisouraya@gmail.com (S.S.); boutaina.addoum636@gmail.com (B.A.); a\_soukri@hotmail.com (A.S.); bouchra.elkhalfi@gmail.com (B.E.K.)
  - <sup>2</sup> Department of Food Science, University of Agricultural Science and Veterinary Medicine, 3-5 Calea Mănăştur, 400372 Cluj-Napoca, Romania; oana.pop@usamvcluj.ro (O.L.P.); carmen.muresan@usamvcluj.ro (C.I.M.); dan.vodnar@usamvcluj.ro (D.C.V.)
  - <sup>3</sup> Molecular Nutrition and Proteomics Lab, CDS3, Life Science Institute, University of Agricultural Science and Veterinary Medicine, Calea Mănăştur 3-5, 400372 Cluj-Napoca, Romania
  - <sup>4</sup> Food Biotechnology and Molecular Gastronomy, CDS7, Life Science Institute, University of Agricultural Science and Veterinary Medicine, Calea Mănăştur 3-5, 400372 Cluj-Napoca, Romania
  - <sup>5</sup> Department of Molecular Sciences, 'Iuliu Hațieganu' University of Medicine and Pharmacy, Cluj-Napoca, 8 Victor Babeș, 400012 Cluj-Napoca, Romania; adinachis82@gmail.com
  - <sup>6</sup> Cognitive Neuroscience Laboratory, Department of Psychology, Babeș-Bolyai University, Cluj-Napoca, Romania, 1 Mihail Kogalniceanu, 400084 Cluj-Napoca, Romania
- \* Correspondence: romanavulturar@gmail.com (R.V.); ramona.suharoschi@usamvcluj.ro (R.S.)  
† These authors contributed equally to this work.

Received: 21 August 2020; Accepted: 11 September 2020; Published: 15 September 2020

**Abstract:** Due to its similarity with human milk and its low allergenic properties, donkey milk has long been used as an alternative for infants and patients with cow's milk protein allergy (CMPA). In addition, this milk is attracting growing interest in human nutrition because of presumed health benefits. It has antioxidant, antimicrobial, antitumoral, antiproliferative and antidiabetic activity. In addition, it stimulates the immune system, regulates the gastrointestinal flora, and prevents inflammatory diseases. Although all donkey milk components can contribute to functional and nutritional effects, it is generally accepted that the whey protein fraction plays a significant role. This review aims to highlight the active proteins and peptides of donkey milk in comparison with other types of milk, emphasizing their properties and their roles in different fields of health and food applications.

**Keywords:** donkey milk (DM); donkey colostrum (DC); mammal's milk; cow's milk protein allergy (CMPA); bioactive peptides; biologic activity; immunosenescence; health benefits

## 1. Introduction

Since ancient times, donkey milk (DM) has been known for its therapeutic properties and it was used for wound healing and for treating various diseases such as bronchitis, asthma, joint pain, gastritis [1,2]. Today, it is available on the market as a commercial product to benefit newborns, people with allergies to cow's milk proteins, and older people [1,2]. Several types of milk (from goat, dromedary, donkey, and horse) are known to have lower allergenicity than cow milk, and it has been

suggested that differences in nitrogen distribution and digestibility of milk proteins play an important role in determining the allergenic capacity of milk [3]. DM has become increasingly attractive due to its biological activities, such as anti-microbial, anti-viral, anti-inflammatory, antiproliferative [1,4], and antioxidant activity [5].

The characterization of milk's main constituents has fundamental importance according to the correlation between health and nutrition. In this context, proteins and peptides are considered important nutrients because some of them show bioactivity when they are native [2,5]. There is increasing evidence that many milk proteins and peptides (particularly peptides that are called '*bioactive peptides*') have physiological functionality. Important effects on immune modulation, cardiovascular health, tumours, bones, and teeth have been frequently reported [5,6]. It is well known that the validity of these effects and the efficacy of functional foods based on bioactive peptides remain to be fully proven in the future, and they may lead to a new class of functional foods, for example, those based on milk proteins and their products [6,7].

According to their different solubility, the DM proteins are classified into three classes: milk fat globule membrane (MFGM) proteins, caseins, and whey proteins [4,5]. The protein content of milk may vary among species, among breeds within the same species, and even among individual animals within the same breed. Furthermore, it is well known that there is a strong qualitative resemblance between the principal classes of proteins (i.e., caseins and whey proteins) in all types of milk. These whey proteins and caseins could have biomedical applications [8,9]. Due to its high nutritional and health importance, DM is rediscovered as a functional food. Most of the studies aiming to evaluate DM qualities have been carried out in Italy, and some data are published on the DM obtained from Chinese and Balkan donkey breeds [1]. Likewise, due to the increasingly global spread of food allergies, consumers have started looking for so-called "natural milk" with good taste and useful in treating of some conditions such as cow's milk protein allergy. This review aims to report published data about the proteins and peptides from DM compared with other kinds of milk (cow, goat, camel, and human milk) and, on the other hand, compared with donkey colostrum. It also shows their biological activities such as anti-microbial, anti-oxidant, anti-inflammatory, anti-allergic, anti-tumoral, anti-obesity, and anti-diabetic activity, their applications in different fields and the benefit of ingesting donkey milk proteins and peptides.

## 2. Global Composition of Donkey Milk Compared to Other Types of Milk

Due to its chemical composition, milk is considered a complete food. It consists of water, carbohydrates, fats, proteins, and other minor components such as hormones, vitamins, minerals, cytokines [1,5]. Among the constituents of milk, proteins vary between mammalian species, ranging from 1% to 24%. These proteins exist under three categories of proteins defined by their chemical composition and their physical properties: MFGM proteins, caseins, and whey proteins. In addition, the carbohydrate (lactose) milk content varies from 0.7% to 7.0% between different species of mammals. Regarding the fat content, not only the concentration varies but also the chemical composition [4,5]. Table 1 represents the global composition of the donkey, cow, camel, goat, and human milk. The amount of DM components, such as whey protein, lactose, and caseins, are similar to that of human milk, although they differ significantly compared to cow, goat, and camel milk. The only significant difference between DM and human milk is the fat content, which is very low in DM. Nevertheless, regarding the casein-to-whey protein ratio, in DM this is intermediate between human milk and cow milk.

**Table 1.** Milk composition and energy value—donkey and other species [5,10,11].

Milk Characteristics	Donkey (%)	Goat (%)	Cow (%)	Camel (%)	Human (%)
Proteins	1.74	3.41	3.43	1.80	1.64
Fat	1.21	4.62	3.46	1.80	3.38
Lactose	6.23	4.47	4.71	2.91	6.69
Dry Matter	9.61	13.23	12.38	11.30	12.43
Ashes	0.43	0.73	0.78	0.85	0.22
Water	90.39	86.77	87.62	90.60	87.57
Energy (KJ/Kg)	1939.40	3399.50	2983.00	2745.80	2855.60

### 3. Bioactive Proteins and Peptides in Donkey Milk Compared to Other Types of Milk

Table 2 shows the different protein fractions identified in cow, donkey, goat, camel, and human milk, and the g/L amount. Camel's milk, cow's milk, and the goat's type have high protein levels compared to human milk and DM. Cow's milk, camel's milk, and goat's milk have more caseins (80%) and fewer whey proteins (20%) [8]. Cow's milk, camel's milk, and goat's milk have more caseins (60%) and fewer caseins (40%) [12]. Donkey's milk has a quantity of  $\alpha$ -lactoglobulin resembling that identified in human milk and has a high level of  $\beta$ -lactoglobulin, which is not found in human milk. This  $\beta$ -lactoglobulin is the major allergen of cow's milk, besides caseins [5,8]. Another peculiarity is that lysozyme's human and donkey milk content is much higher than in cow milk:

**Table 2.** Main proteins of donkey milk compared to other types of milk [5,8,12].

	Cow (g/L)	Donkey (g/L)	Goat (g/L)	Camel (g/L)	Human (g/L)
Total protein content	31–38	13–28	25–39	25–45	9–17
Total casein	27.2	6.6	25	26.4	5.6
Total whey protein	4.5	7.5	6	6.6	8
$\alpha$ S1-casein	10–15	0.2–1	0–7	5	0.3–0.8
$\alpha$ S2-casein	3–4	0.2	4.2	2.2	n.d.
$\beta$ -casein	9–11	3.9	11–18	12.8	1.8–4
$\kappa$ -casein	3–4	n.d.	4–4.6	0.8	0.6–1
$\alpha$ -lactalbumin	1–1.5	1.8–3	1.2	3.5	1.9–2.6
$\beta$ -lactoglobulin	3.3–4	3.2–3.7	2.1	n.d.	n.d.
Lysozyme	0.00007	1	Trace	0.00015	0.04–0.2
Lactoferrin	0.1	0.08	0.02–0.2	0.22	1.7–2
Immunoglobulins	1	n.d.	1	1.54	1.1
Albumin	0.4	n.d.	0.5	0.4	0.4

n.d.—not detected.

Several research groups have been able to characterize the protein fractions of whey in DM and have demonstrated their nutraceutical properties and their beneficial properties for human health. These proteins will be described in detail below.

#### 3.1. Caseins

The caseins are organized into micelles (supramolecules of colloidal size) whose diameter varies from 30 to 600 nm. In particular,  $\alpha$ S1-,  $\alpha$ S2-,  $\beta$ -,  $\kappa$ -casein, and traces of  $\gamma$ -casein can be found. These micelles are made up of different proteins (94%) and colloidal calcium phosphate, made of calcium, phosphate, magnesium, and nitrate, comprises 6%. These different caseins have hydrophilic regions and other hydrophobic regions that are different from one casein to another [13]. Besides, the caseins are phosphoproteins. Therefore, they have phosphorylated regions at the level of the serine residues. The proline residues, uniformly distributed into the casein structure, prevent secondary structures such as  $\alpha$  helices or  $\beta$  sheets, hence the so-called open or “random coil” conformation of casein [14].  $\kappa$ -caseins have a particular role, they are first of all glycoproteins and have only one

phosphoserine group, but above all, they are stable in the presence of calcium ions and thus protect all of the caseins against precipitation and stabilize the micelles [13,15].

In mature cows' milk, caseins make up 80% (*w/w*) of all proteins, whereas, in humans [16] and equines [17], they represent only 35% and 50% of the total protein content, respectively. The DM essentially comprises  $\alpha$ S1-, and  $\beta$ -casein while  $\alpha$ S2- and  $\kappa$ -casein are minor components.  $\beta$ -casein can represent up to 80% of the total casein in human milk [18] and is also the predominant protein in the casein fraction of DM [16]. Several studies revealed that caseins and  $\beta$ -lactoglobulin are the main allergens in cow milk [19], and the low allergenicity of DM is explained by low casein content [5].

### 3.2. $\beta$ -Lactoglobulin

$\beta$ -lactoglobulin, a globular protein containing 162 amino acids that belongs to the family of lipocalin proteins, has a molecular mass of 18.36 kDa. Lipocalin molecules have pockets capable of hosting iron complexes. Iron binds to protein through iron chelators called "siderophores" [5].  $\beta$ -lactoglobulin is known for its richness in lysine, leucine, glutamic acid, and aspartic acid. Its secondary structure is mainly composed of  $\beta$  sheets ( $\approx$ 50%), but there are also  $\alpha$  helices (10%),  $\beta$  elbows (8%), and a high proportion of disordered structures (35%) [20]. Its structure is also reinforced by two disulfide bridges and a tertiary structure mainly composed of antiparallel  $\beta$  sheets. Studies showed that two different isoforms of  $\beta$ -lactoglobulin could be found in DM: the major isoform is  $\beta$ -lactoglobulin I (80%), while  $\beta$ -lactoglobulin II is encountered in lower quantities.

In DM, the  $\beta$ -lactoglobulin content of 3.75 g/L resembles that found in cow's milk [7], and is lower than that found in goat's milk, while it is absent in camel's [21] and human's milk [3]. In DM,  $\beta$ -lactoglobulins correspond to one genetic variant of  $\beta$ -LGI ( $\beta$ -LGIB), two genetic variants of  $\beta$ -LGII ( $\beta$ -LGIIB, and  $\beta$ -LGIIC), and a third minor  $\beta$ -LGII variant ( $\beta$ -LGIID) [5].

$\beta$ -lactoglobulin is known to have several functions, both nutritional and functional. One of the most studied functions is the protein's ability to bind specific nutritional interest molecules and serve as a protective matrix during digestion.  $\beta$ -lactoglobulin was shown to bind specific vitamins (D2, D3), cholesterol, particular catechins, and even mercury [20,22]. These interactions occur mainly in the protein's central area, denominated as the calyx (also known as  $\beta$ -barrel), and formed of  $\beta$  sheets. This hydrophobic cavity, which makes it possible to fix a large variety of ligands, is regulated by an EF loop, which works as a gate to the site of binding. At low pH, this loop is in the "closed" position, and interactions are impossible. When the pH increases, the loop opens, allowing the ligands to insert into the hydrophobic cavity [20]. This change in the Tanford transition structure generally occurs between pH 6.5 and 7.5 [23].

### 3.3. $\alpha$ -Lactalbumin

The  $\alpha$ -lactalbumin, a protein composed of 123 amino acid residues, with a molecular weight of 14.2 kDa, has in its tertiary structure four disulfide bridges. Native  $\alpha$ -lactalbumin is made up of two distinct domains, and a large section is produced of  $\alpha$  helices and a small  $\beta$  sheet domain. A calcium fixation loop bonds the two sections. This protein is found in DM as two isoforms with different isoelectric points (pI) values: 4.76 and 5.26.  $\alpha$ -lactalbumin content in DM is 1.8 g/L, a value very close to that found in cow and human milk [4,5].

$\alpha$ -lactalbumin is a protein recognized for its nutritional qualities, mainly for infants' nutrition. First,  $\alpha$ -lactalbumin plays an essential role in milk production in mammals because it binds to the enzyme  $\beta$ -1,4-galactosyltransferase and creates the lactose synthase essential for lactose formation. Another important nutritional element of this protein is its high tryptophan content since it is an essential amino acid. This amino acid has demonstrated positive effects on the development of newborns' brains and nervous systems and contributes to these systems' functioning as a direct precursor of serotonin or niacin (also known as vitamin B3). Studies have also shown that regular intake of  $\alpha$ -lactalbumin in adult subjects makes it possible to increase the plasma quantities of tryptophan, thus improving

certain neurological functions (such as attention, cognitive performance, and morning alertness) [24,25]. This protein also has good digestibility and a low allergenic capacity [26,27].

### 3.4. Lysozyme

Lysozyme, or muramidase, is a globular enzyme consisting of 129 amino acids and a class of hydrolases [28]. The latter consists of two domains: a domain composed essentially of  $\alpha$  helices and a  $\beta$  anti-parallel sheet and two  $\alpha$  helices. Three disulfide bridges provide the three-dimensional configuration of the molecule: two are found in the  $\alpha$ -helix domains, while one is located in the  $\beta$  sheet. Lysozyme can catalyze the hydrolysis of the glycoside 1  $\rightarrow$  4 bond of peptidoglycans in the bacterial wall and chitin present in fungi walls [1,5].

Two isoforms of lysozyme, which differ by an oxidized methionine at position 79, were described in DM: lysozyme A with a molecular weight of 14.631 kDa and lysozyme B with a molecular weight of 14.646 kDa [29,30].

Compared to human milk, donkey milk has a higher content of lysozyme (1 g/L), while in goat and cow milk, lysozyme is missing [3,5]. Due to the high amount of lysozyme [3,5] and its thermostability [29,31], the DM is resistant to alteration.

### 3.5. Lactoferrin

Lactoferrin is a glycoprotein that belongs to the transferrin family and has a molecular weight of 80 kDa. Its structure is built by two homologous domains, which bind ferric and carbonate ions. The anti-microbial activity of lactoferrin applies to a wide range of Gram-positive and Gram-negative bacteria. On the one hand, it is partly dependent on its capacity to bind iron, resulting in an environment scarce in iron, which limits the bacterial growth; on the other hand, it depends on its capacity to bind to the lipopolysaccharides of bacterial cell walls via its N-terminus, resulting in the permeabilization of the bacterial cells [5,32]. Likewise, once digested in the stomach, lactoferrin is fragmented into small peptides: lactoferrampin and lactoferricin; the second one has an important action against several bacteria, viruses, fungal pathogens, and protozoa. Moreover, this peptide has other activities, such as inhibition of tumor metastasis in mice [33] and induction of apoptosis in THP-1 human monocytic leukemic cells [34].

### 3.6. Lactoperoxidase

Lactoperoxidase (LPO) is an oxidoreductase enzyme and has a protective function against infections by microorganisms. It is found in low concentrations in fresh DM, as well as in human milk (about 100 times lower than in bovine milk) [1]. LPO can catalyze the oxidation of diverse substrates by using hydrogen peroxide. The oxidation products possess bactericidal activity against bacteria (*Mycoplasmas*), and bacteriostatic effects against *Listeria monocytogenes* [4,5]. It has been shown that immunoglobulins found in the milk exert a synergistic effect on the activity of these non-specific anti-microbial factors with LPO, whose anti-microbial activity against *Streptococcus mutans* increases considerably if the system is incubated with secretory IgA. The anti-microbial activity enhancement seems to be due to binding between LPO and immunoglobulins (IgA) [5,7]. The result of this interaction is a stabilization of the enzymatic activity of lactoperoxidase [5].

## 4. Comparison between Donkey Colostrum and Donkey Milk

Several studies have shown that milk composition is different not only between the species but also between each phase of lactation (colostrum and mature milk) [35,36]. Colostrum is the first form of milk obtained directly after the mammal's birth until the seventh day. Studies of whey proteins from different mammals (human, bovine, camel) have shown that they generally have differences between colostrum and mature milk. However, changes in the composition of DM in the course of lactation were not sufficiently studied. Recently, the compositions, comparisons, and alterations of the

proteome in mammals' milk at various lactation stages have been studied using advanced proteomics technologies [37,38].

Li et al. [37] were able to identify 300 proteins in DM and mature milk colostrum, including 13 and 12 whey proteins expressed only in donkey colostrum and mature milk, respectively (Table 3). They also showed that in the two types of milk,  $\alpha$ -lactalbumin,  $\beta$ -lactoglobulin, lysozyme, and the constant region of the heavy chains of immunoglobulins gamma 1 were the main whey proteins. The same study showed that 18 were expressed differentially between colostrum and mature milk among the proteins identified, of which neural epidermal growth factors like type 2, perilipin, thymosin beta 4, cathepsin B, and transforming factor beta, were induced. Fatty acid-binding proteins had higher levels in mature milk. Simultaneously, tetraspanin, amine oxidase, immunoglobulin gamma 1 heavy chain constant region, apolipoprotein B, prothrombin, major histocompatibility complex (MHC) class I antigen, beta-lactoglobulin II, and alphas 2 casein B were higher in colostrum [37].

**Table 3.** Uniquely expressed proteins in donkey colostrum and donkey mature milk [37,39–41].

Types of Milk	
Donkey Colostrum	Donkey's Mature Milk
Zinc-alpha-2-glycoprotein	Histone H3
Immunoglobulin lambda light chain variable region	Myristoylated lanine-rich C-kinase substrate
Thrombospondin 4	Histone H4
Peptidoglycan recognition protein 1	Multiple coagulation factor deficiency 2
Cartilage acidic protein 1	C-C motif chemokine
Peptidyl-prolyl cis-trans isomerase	Transcription factor adipocyte enhancer binding protein 1 (AEBP1)
L receptor related protein 1	Follistatin-like 1
Insulin like growth factor binding protein 7	ST6 beta-galactoside alpha-2,6-sialyltransferase 1
Major histocompatibility complex (MHC) class II associated invariant chain	Uncharacterized protein
DNA J-like protein subfamily B member 11-like protein	Multiple coagulation factor deficiency protein-like protein
Cathepsin Z	Uncharacterized protein
Uncharacterized protein	Glutathione peroxidase (Fragment)
Amino peptidase	

Other studies have also shown that there are differences between proteins and between other metabolites' (including lipids') compositions, which reveal that the composition of DM changes during lactation [39–41].

## 5. Anti-Microbial Activity of Donkey Milk

For DM, various properties were demonstrated, such as anti-bacterial, anti-viral, and anti-fungal activity. Several studies showed that DM has an anti-bacterial property against a wide range of pathogenic bacteria such as *Escherichia coli*, *Salmonella enteritidis*, *Listeria monocytogene*, *Staphylococcus aureus*, *Bacillus cereus*, *Enterococcus faecalis*, *Shigella dysenteria*, and against some yeasts [5]. The high content of lysozyme in DM is correlated with high anti-bacterial activity against *Listeria monocytogenes* and *Staphylococcus aureus* [8,42–45], making DM safer, without food-borne pathogenic bacteria, and with a longer self-life. This anti-bacterial activity is due to its high value of anti-bacterial components [46–48], mainly some whey proteins such as lysozyme and lactoferrin [44,45] (Figure 1). Since Gram negative bacteria resist lysozyme due to its lipopolysaccharide membrane, the anti-bacterial activity of DM can be explained by two mechanisms; firstly by the specific structure of lysozyme of DM (similar of equine's lysozyme), which is able to bind to calcium ions that improve its activity against Gram negative bacteria [42,49–51]; secondly by a synergistic activity of lysozyme and lactoferrin, because the latter can bind to membrane proteins of Gram negative bacteria, which disrupt the membrane and open the pores to lysozyme, which destroys the glycosidic linkage (N-acetylglucosamine and N-acetylmuramic acid) of peptidoglycans [32,44,52] (Figure 1). Other studies have shown that the immunoglobulins, IgG, IgA, and IgM [30], also contribute to the inhibition of bacterial growth, acting

in synergy with lysozyme [53,54] (Figure 1). Saric et al. (2014) [44] have shown that in addition to the immunoglobulins, some fatty acids such as linoleic acid, lauric acid, and oleic acid, when acting synergetically with lysozyme, show an important anti-bacterial activity against Gram-negative and Gram-positive bacteria.

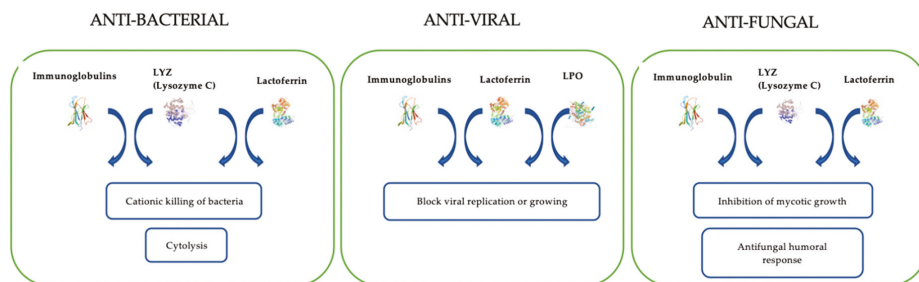


**Figure 1.** Molecular mechanism of anti-microbial activity of donkey milk (DM) proteins (protein structure is a reference to UniProtKB [55] and the Protein Data Bank—PDB [56] (LYS: Lysozyme C: (P11375); Lactoferrin (A0A3Q9HG40); Immunoglobulin (Q861S3); LPO—Lactoperoxidase (P80025))). The anti-bacterial activity of DM is mainly due to lysozyme, lactoferrin, and immunoglobulins (IgG, IgA, IgM) through two molecular mechanisms: cytolysis and the cationic killing of bacteria (LYS could act synergistically with lactoferrin, and immunoglobulins). The anti-viral capability of DM was related to synergetic action between LYS, LPO, immunoglobulins, and low abundant—low molecular weight protein fraction (<30,000 Da) through blocking viral replication or growing by binding to host cells and/or direct interaction with the viruses. The anti-fungal activity is due to the antifungal capacity of DM's proteins (lactoferrin, LYS, and immunoglobulins) within the inhibition of mycotic growth and protective cell reactions triggered in response to the fungi presence; (the arrows represent the synergistic activity of proteins).

In addition to its anti-bacterial activity, DM and its whey proteins were tested for their anti-viral activity. Brumini et al. (2013) [57] have demonstrated that they have the ability to inhibit the replication of *Echovirus type 5*, an enterovirus that affects the human gastrointestinal tract. This activity is due to high molecular weight whey proteins such as lactoferrin, LPO, and immunoglobulins (Figure 1).

Koutb et al. (2016) shown an anti-microbial activity of DM against two dermatomycotic fungi: *Trichophyton rubrum* and *Trichophyton mentagrophytes*, which are the leading causes of inflammatory tinea corporis [58]. Furthermore, the anti-fungal activity of DM has been tested and found to be effective against fungal strains which are pathogenic for humans (Figure 1). A preliminary study on four samples of DM shown that it inhibits mycotic growth, mainly of *Microsporum canis* and *Trichophyton mentagrophytes*, which are more sensitive than *Microsporum gypseum* to DM [59].

It should be mentioned that these anti-microbial factors (lysozyme, LPO, and lactoferrin) are relatively identical in different species (Table 4). Still, their quantity and importance can differ considerably. Indeed, in human milk and DM, lysozyme's content is substantially higher than that of camel, cow, and goat milk, while the LPO is present in small quantities in DM and human milk, but abundant in cow's milk. Regarding the lactoferrin, its content is higher in human milk, camel's, and goat's milk, respectively [5,8,59].

**Table 4.** Quantity of the major anti-microbial proteins found in human, bovine, camel and donkey milk [5,8,59].

Milk Type	Lysozyme (g/L)	Lactoperoxidase (g/L)	Lactoferrin (g/L)
Donkey	1.0	0.11	0.08
Human	0.12	0.77	0.3–4.2
Goat	Trace	Trace	0.02–2
Camel	0.00015	n.d.	0.22
Cow	0.00007	30–100	0.10

n.d.—not detected.

## 6. Antioxidant Activity of Donkey Milk

DM is known to have an antioxidant activity, which gives it oxidative stability, providing consumer protection. A study comparing the DM, cow milk and DM powder in terms of antioxidant activity has shown that DM has a higher antioxidant capacity than cow milk. It has a high ability to remove anionic superoxide radicals and to eliminate hydroxyl radicals, which are free radicals generated by body metabolism [60]. Simos et al. [61] were able to determine the antioxidant activity of DM using the method of oxygen radical absorbance capacity, and have shown that the principal contributors of this activity are caseins and the hydrophilic antioxidant compounds, such as uric acid and vitamin C.

## 7. Anti-Inflammatory and Anti-Tumoral Activity of Donkey Milk

Donkey milk is a matrix rich with mediators such as lactoferrin, which has anti-microbial and anti-tumoral activity, interferon  $\gamma$ , which stimulates macrophages, natural killer cells, and cytotoxic T cells [62,63]. DM can induce the release of anti-inflammatory cytokines, retaining a condition of immune homeostasis [62]. Yvon et al. (2018) [64] have demonstrated that the treatment of C57BL/6 mice (Crohn's disease model) with DM has an anti-inflammatory effect by restoring the levels of anti-microbial peptides such as  $\alpha$ -defensin and lysozyme, which help to reduce the imbalance of the microbiota. Moreover, other studies have shown that the lactic flora of DM has an anti-inflammatory effect, for example, by the production of nitric oxide by *Lactobacillus farciminis*. This anti-inflammatory activity can also be due to the synergy between this flora and the anti-microbial peptides [65,66] (Figure 2). Another study has shown that DM and colostrum stimulate the secretion of nitric oxide, a potent vasodilator, and therefore prevent atherosclerosis. They demonstrated that DM stimulates the secretion of immunoglobulins G and interleukins (IL) IL-1 $\beta$ , IL-10, and IL-12. In contrast, colostrum stimulates the secretion of immunoglobulins A. They also showed that the two types of milk stimulate the expression of CD25 and CD69 on human peripheral blood mononuclear cells (Figure 2) and thus, may be useful in the treatment of human immunological diseases [19].

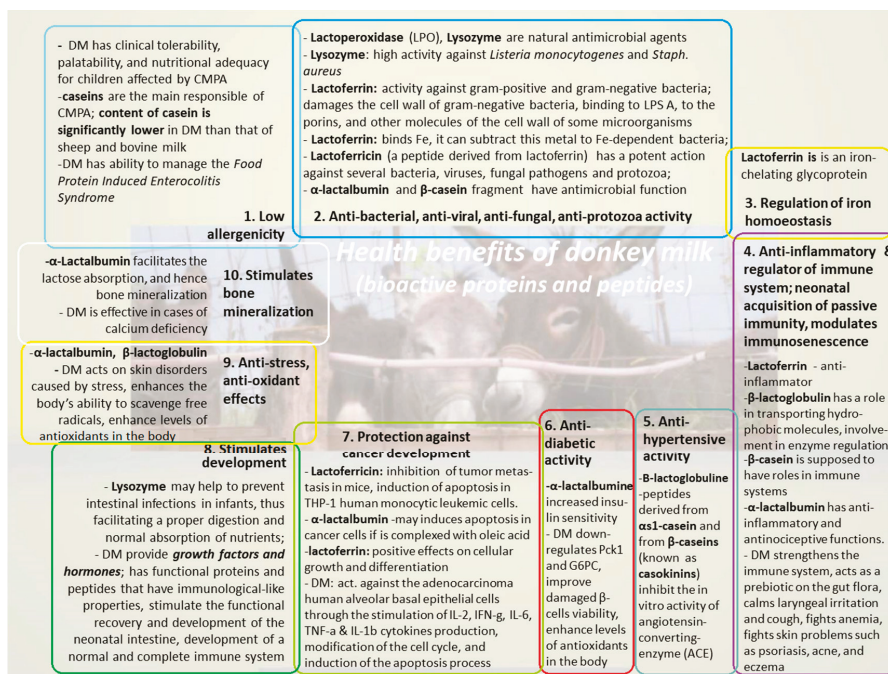


**Figure 2.** Health implications of donkey milk consumption due to bioactive proteins and peptides; the main ten health properties are listed, outlining the references and mechanisms of bioactive proteins/peptides involved in: 1. Low allergenicity [3,5,67,68]; 2. Anti-bacterial, anti-viral, anti-fungal, anti-protozoa activity [5,32,42–44,57,69,70]; 3. Regulation of iron homeostasis [5]; 4. Anti-inflammatory and regulator of immune system, neonatal acquisition of passive immunity, immunosenescence [5,20,71,72]; 5. Anti-hypertensive activity [5,73–75]; 6. Anti-diabetic activity [76]; 7. Protection against cancer development [5,77,78]; 8. Stimulate development [5,68]; 9. Anti-stress, anti-oxidant effects [5,25,65,76]; 10. Stimulate bone mineralization [5,68,79]. Abbreviations: CMPA—cow milk protein allergy, LPS A—lipopolysaccharide A, Pck1—phosphoenolpyruvate carboxykinase 1, G6PC—glucose-6-phosphatase.

Furthermore, other studies have shown that the administration of human milk or DM improves the liver’s anti-inflammatory state by improving the hepatic mitochondrial functions [80]. Trinchese et al. (2018) [81] have shown that TNF- $\alpha$  and IL-1 decreased, while IL-10 levels increased, in the serum and tissues of rats fed with DM, compared to control rats and rats fed with cow milk. The same team showed that oral supplementation with human milk and DM influences the metabolism of glucose and lipids by modulating pro- and anti-inflammatory serum and tissue mediators.

In addition to its anti-inflammatory activity, DM has other physiological functions such as immunoregulatory and anti-tumor activity [82]. Mao and his collaborators (2009) [77] have shown that many DM fractions can stimulate the production of cytokines IL-2, IFN- $\gamma$ , IL-6, TNF- $\alpha$  and IL-1 $\beta$  from lymphocytes and macrophages (Figure 2). These cytokines influence anti-proliferation by inducing apoptosis of A549 tumor cells (human lung cancer cells) and the differentiation of these A549 tumor cells into normal cells. They also showed that lysozyme has a strong anti-proliferative effect (Figure 2), and therefore, it could be a promising molecule in treating lung cancer [77].

It is well known that milk’s role is critical in developing immunosenescence mitigating strategies because bioactive milk components cannot only directly influence the aging immune physiology, but it can also act as a carrier matrix for a variety of milk products. In this regard, several authors have described the effects of goat and donkey milk consumption on healthy-aged volunteers’ serum cytokine

profiles. The authors concluded that DM consumption is useful for increasing the immune response in immunocompromised aged patients [71,72] (Figure 2). Identification of these milk-based products as antiaging agents will promote the concept of “healthy aging”.

## 8. Anti-Diabetic and Anti-Obesity Activity of Donkey Milk

In addition to its antioxidant, anti-microbial, anti-inflammatory and anti-tumoral activity, DM also has an anti-diabetic effect (Table 5) [61,76,77].

**Table 5.** Biological activity of donkey milk proteins/peptides.

Proteins/Peptide	Biological Activity	Reference
$\alpha$ S1- and $\beta$ -casein	Antihypertensive	[73]
	Inhibitor activity of Angiotensin converting enzyme (ACE) and antioxidant activity.	[5]
$\alpha$ S1- casein	Transport calcium phosphate	UniProtKB—P86272
$\alpha$ S2- casein	Transport calcium phosphate	UniProtKB—B7VGF9
Lysozyme	Anti-inflammatory properties	[63]
	Anti-tumoral properties	[77]
	Reduced incidence of diarrhea	[83]
	Anti-microbial properties	[32]
Lactoferrin	Antimicrobial properties	[57]
	Antitumor	[73]
	Antithrombotic	[74]
Lactoperoxidase	Antioxydant properties	[61]
	Anti-microbial properties	[57]
$\alpha$ -lactalbumine	Anti-diabetic properties	[76]
	Antihypertensive	[74]
$\beta$ -lactoglobuline	Antihypertensive	[74]

Type 2 diabetes, also known as non-insulin-dependent diabetes, is a metabolic disease characterized by chronic excess blood sugar (hyperglycemia). The leading causes of type 2 diabetes include obesity, dysfunction of  $\beta$  cells, and insulin resistance by peripheral tissues and cells [84]. Due to its higher whey protein content, DM could help to prevent and treat diabetes by improving glucose metabolism and insulin resistance (Figure 2). Besides the fact that DM and fermented donkey milk has a low caloric intake, the anti-obesity and anti-diabetic activity given by  $\alpha$ -lactalbumine should be correlated with triglycerides (TGL) levels—that constitute the largest group of milk lipids. The DM (like the horse milk) has only about 80–85% of total lipids, compared with the cow, sheep, and human milk for which TGL represents 97–98% of total lipids (Figure 2). An outstanding feature regarding the content of DM with effects on metabolic status of the cell is the high content in vitamin B<sub>12</sub> (cobalamin) of DM: 110 ( $\mu$ g/100 g) compared to other types of milk, i.e., 0.07 in human milk, 0.4 and 0.7 or 0.16 ( $\mu$ g/100 g) in cow, sheep or goat milk, respectively [85]. Vitamin B<sub>12</sub> is a water-soluble essential micronutrient required by all the body cells, and its deficiency in humans has been implicated in many metabolic processes, such as insulin resistance (besides hematological and neurological disorders). Likewise, Trinchese et al. [80,81] have shown that in animals (rats fed with human milk or DM), improved glucose and lipid metabolism could be identified, with modified mitochondria in adult rat skeletal muscle (compared to untreated control animals). These studies found increased muscle and liver levels of a known regulator of lipid metabolism (OEA: N-oleoylethanolamine), and this could contribute to burning fat and protecting the animals against developing certain obesity-associated metabolic and inflammatory sequelae (Figure 2). These animals had higher energy expenditures and decreased body lipid accumulation via the mitochondrial uncoupling pathway’s mild augmentation. In addition, several authors speculated that diet-associated changes in microbiota and increased levels of butyrate

(a short chain fatty acid) in human and DM-fed rats (compared with cow milk fed rats) contributed to the differences in metabolism and mitochondrial function through several as yet unknown signalling pathways [80,81,86].

Li et al., in 2020 [76], have shown that DM improves the viability of damaged pancreatic  $\beta$  cells, but does not stimulate the secretion of insulin by damaged  $\beta$  cells and that the  $\alpha$ -lactalbumin increases the insulin sensitivity of the target organs. DM has shown a better effect than metformin, an anti-diabetic drug for treating type 2 diabetes [76].

Besides, they showed that DM decreased the level of glycosylated hemoglobin and it acted positively in the treatment of diabetes by inhibiting the expression of phosphoenolpyruvate carboxykinase 1 and glucose-6-phosphatase, which are key enzymes in hepatic gluconeogenesis (Table 5).

## 9. Food and Other Applications of Donkey Milk

Considering its functional properties and its nutritional values, DM becomes an attractive product for health, technology, cosmetic industry, and others. The health effects of DM consumption are mainly related to low allergenicity [3,5,67,68], anti-microbial activity [5,32,42–44,57,69,70], regulation of iron homeostasis [5], anti-inflammatory and immune system modulation, innate immune system, immunosenescence [5,20,71,72], anti-hypertensive [5,73–75], anti-diabetic [76], anti-tumoral [5,77,78], stimulate development [5,68], anti-stress and anti-oxidant activity [5,25,65,76], and anti-osteoporosis [5,68,79] (Figure 2). DM is supplied in different forms: liquid milk, fermented products (with higher peptide content and bioavailable calcium source), freeze dried, and spray dried powders [87]. The application of new technologies such as freeze drying and microencapsulation allows better exploitation of this product [32]. Several studies have revealed that DM is an adequate alternative to children suffering from cow milk proteins allergy (CMPA) [67,88], due to its low composition of caseins, which constitute the main allergenic components of milk. Sarti et al. (2019) [67] have shown that DM has no negative influence on infants and children, and have assessed its ability to manage the “Food Protein Induced Enterocolitis Syndrome” (FPIES) caused by cow’s milk. However, cow’s milk proteins cause immune reactions mediated by immunoglobulins E (IgE), which is also managed with DM [67,88]. Donkey milk is also an important vitamin D source, which can be obtained only from diet or from exposure to sun-light. The oral source of vitamin D can be important in winter and for people who cannot be exposed to sun-light [88].

Donkey milk is a basic ingredient for the production of high-value dairy products [89]. DM lysozyme is also used in the food industry due to its stability and resistance to various technological processes such as thermic treatment [31] and digestive tract conditions such as acid pH and gastrointestinal enzymes [90].

To value the donkey, Cappola et al. (2002) [91] have investigated DM’s ability for fermentation by *Lactobacillus rhamnosus*, and showed that DM is a good base for probiotics and therapeutic food formulation. In this context, another team used *Lactobacillus casei* in addition to *Lactobacillus rhamnosus* as probiotics to produce a fermented drink made from DM, and these probiotics were able to survive in this milk up to 30 days [92]. Indeed, DM is also a base for producing yogurt products (Standard yogurt and probiotic yogurt), and yogurt supplied with probiotics showed a high antioxidant activity and a low content in lactose, which is beneficial for consumers with an allergy to cow milk proteins [93].

Because of its low fat and casein content, DM constitutes a soft gel during cheese manufacturing. Several studies have faced this situation, for example, by the addition of MTGase—a microbial transglutaminase that can enhance the texture of the curd without any effect on moisture, proteins, fats, or cheese yield [89]. Šarić et al. (2016) overcame this limitation by mixing DM with goat milk to produce a functional product with high quality [94].

Since recently, as Salimei 2016 [95] points out, donkey’s milk could thus be placed among the new generation of fermented milk drinks, such as koumiss derived from mare’s milk, and would allow for an effective combination of the advantageous properties of the raw ingredients with lactic acid

bacteria of probiotic interest. In these years, other products as ice cream, biscuits, cakes, desserts, and liqueurs have been developed from pasteurized donkey's milk, and its technological use (2%) has been successfully tested in hard cheese making, contributing to innovation in the dairy sector. Regarding the cosmetic industry, besides its potential roles in human nutrition, multipurpose applications of donkey's milk are reported in ethnomedicine, and it is used in cosmetology, most likely due to its lysozyme content, effective in smoothing skin and scalp inflammations [95].

## 10. Conclusions

Starting with fundamental importance for the correlation between health and nutrition, this review outlines the importance of the protein fraction of DM. This type of milk was used since ancient Egyptian, Greek, and Roman times, not only for its nutritional value for infants but also for its beneficial skincare properties. Later, it was recognized as a common remedy for many ailments, and in French orphanages during the late XIXth or early XXth century when infants receiving DM grew well and with lower mortality than those given cow milk, as reviewed by Carminati et al. (2017) [28], and Fantuz et al. (2016) [3]. Nowadays, DM is considered a medicinal food (or “*pharma food*”) because of its nutritional and functional properties, and because of having a composition similar to human milk when compared to other types of milk; is known that donkey's milk has a casein-to-whey protein ratio intermediate between human milk and cow milk. Donkey milk has various biological activities such as vasodilation (through the secretion of nitric oxide and therefore preventing atherosclerosis), stimulation of the immune system, and anti-diabetic, anti-inflammatory, anti-allergic, anti-obesity, anti-proliferative and anti-microbial activities. These activities are specifically attributed to whey proteins such as lactoferrin, LPO, lysozyme, and immunoglobulins. As Carminati et al. (2017) [28] mentioned, regarding the consumption of fermented DM products (with higher peptide content) by the elderly, this should be encouraged due to this excellent source of bioavailable calcium, low caloric intake, and the ability to modulate the aged immune system, including the intestinal mucosal immune response. Besides, applying certain new technologies, such as lyophilization and microencapsulation, allows better exploitation of this animal product. As a recent editorial outlined [49], although there has been a rise in consumer interest about DM (and other dairy products), it is still a ‘niche product’. The food industry should try to increase the production and availability of DM on the market; this will raise awareness and promote this sector, highlighting the food applications with multiple health benefits not only for the growing infants, but for all ages, convalescents and the elderly. For all these benefits and versatility, future production systems have to be committed to combine profitability with responsibility in protecting animal and human welfare and preventing chronic diseases (non-communicable diseases—NCDs).

**Author Contributions:** Conceptualization, R.D., O.L.P., R.S.; Funding acquisition, D.C.V., R.S.; Writing—Original Draft Preparation, R.D., O.L.P.; Visualization, R.V., R.S.; Writing—Review and Editing, S.S., O.L.P., D.C.V., C.I.M., B.A., R.V., A.C.; Supervision, B.E.K., R.S., R.V. and A.S. All authors have read and agreed to the published version of the manuscript.

**Funding:** This research was supported by ERANET 2/2018 (ProBone) and publication by (PFE)-37/2018–2020.

**Acknowledgments:** The publication was supported by funds from the National Research Development Projects to finance excellence (PFE)-37/2018–2020 granted by the Romanian Ministry of Research and Innovation.

**Conflicts of Interest:** The authors declare no conflict of interest.

## References

1. Martini, M.; Altomonte, I.; Licitra, R.; Salari, F. Nutritional and Nutraceutical Quality of Donkey Milk. *J. Equine Vet. Sci.* **2018**, *65*, 33–37. [[CrossRef](#)]
2. Karami, Z.; Akbari-adergani, B. Bioactive food derived peptides: A review on correlation between structure of bioactive peptides and their functional properties. *J. Food Sci. Technol.* **2019**, *56*, 535–547. [[CrossRef](#)]

3. Fantuz, F.; Salimei, E.; Papademas, P. Macro- and micronutrients in non-cow milk and products and their impact on human health. In *Non-Bovine Milk and Milk Products*, 1st ed.; Tsakalidou, E., Papadimitriou, K., Eds.; Elsevier Academic Press: London, UK, 2016; pp. 209–261. [\[CrossRef\]](#)
4. Aspri, M.; Economou, N.; Papademas, P. Donkey milk: An overview on functionality, technology, and future prospects. *Food Rev. Int.* **2017**, *33*, 316–333. [\[CrossRef\]](#)
5. Vincenzetti, S.; Pucciarelli, S.; Polzonetti, V.; Polidori, P. Role of proteins and of some bioactive peptides on the nutritional quality of donkey milk and their impact on human health. *Beverages* **2017**, *3*, 34. [\[CrossRef\]](#)
6. Boland, M.; Harjinder, S. *Milk Proteins: From Expression to Food*, 3rd ed.; Elsevier Academic Press: London, UK, 2020; pp. 715–730. [\[CrossRef\]](#)
7. Suharoschi, R.; Bartalici, C.I.; Petrut, R.; Semeniuc, C.A.; Rotar, A.M. Two-Dimensional gel electrophoresis of peptides as lap in bovine milk. *J. Agroalimment Process. Technol.* **2010**, *16*, 169–176.
8. Mati, A.; Senoussi-Ghezali, C.; Si Ahmed Zennia, S.; Almi-Sebbane, D.; El-Hatmi, H.; Girardet, J.-M. Dromedary camel milk proteins, a source of peptides having biological activities—A review. *Int. Dairy J.* **2017**, *73*, 25–37. [\[CrossRef\]](#)
9. Nagarajan, S.; Radhakrishnan, S.; Kalkura, S.N.; Balme, S.; Miele, P.; Bechelany, M. Overview of Protein-Based Biopolymers for Biomedical Application. *Macromol. Chem. Phys.* **2019**, *220*, 1900126. [\[CrossRef\]](#)
10. Shori, A.B. Comparative study of chemical composition, isolation and identification of micro-flora in traditional fermented camel milk products: Gariss, Suusac, and Shubat. *J. Saudi Soc. Agric. Sci.* **2012**, *11*, 79–88. [\[CrossRef\]](#)
11. Ellouze, S.; Kamoun, M. Evolution of Dromedary’s Milk Composition According to Lactation Stage. In *Rabat (Morocco), 25–27 October 1988*; CIHEAM: Montpellier, France, 1989; pp. 307–311.
12. Hazebrouck, S. Laits de chèvre, d’ânesse et de chamelle: Une alternative en cas d’allergie au lait de vache? *Innov. Agron.* **2016**, *52*, 73–84.
13. Kessler, A.; Menendez-Aguirre, O.; Hinrichs, J.; Stubenrauch, C.; Weiss, J. Alphas-casein-PE6400 mixtures: A fluorescence study. *Faraday Discuss* **2013**, *166*, 399–416. [\[CrossRef\]](#) [\[PubMed\]](#)
14. Swaisgood, H.E. Review and update of casein chemistry. *J. Dairy Sci.* **1993**, *76*, 3054–3061. [\[CrossRef\]](#)
15. Swaisgood, H.E. Chemistry of the Caseins. In *Advanced Dairy Chemistry—1 Proteins*; Springer: Boston, MA, USA, 2003; pp. 139–201. [\[CrossRef\]](#)
16. Lonnerdal, B. Nutritional and physiologic significance of human milk proteins. *Am. J. Clin. Nutr.* **2003**, *77*, 1537s–1543s. [\[CrossRef\]](#) [\[PubMed\]](#)
17. Malacarne, M.; Martuzzi, F.; Summer, A.; Mariani, P. Protein and fat composition of mare’s milk: Some nutritional remarks with reference to human and cow’s milk. *Int. Dairy J.* **2002**, *12*, 869–877. [\[CrossRef\]](#)
18. Kroening, T.A.; Mukerji, P.; Hards, R.G. Analysis of beta-casein and its phosphoforms in human milk. *Nutr. Res.* **1998**, *18*, 1175–1186. [\[CrossRef\]](#)
19. Tafaro, A.; Magrone, T.; Jirillo, F.; Martemucci, G.; D’alessandro, A.; Amati, L.; Jirillo, E. Immunological properties of donkey’s milk: Its potential use in the prevention of atherosclerosis. *Curr. Pharm. Des.* **2007**, *13*, 3711–3717. [\[CrossRef\]](#)
20. Kontopidis, G.; Holt, C.; Sawyer, L. Invited Review:  $\beta$ -Lactoglobulin: Binding Properties, Structure, and Function. *J. Dairy Sci.* **2004**, *87*, 785–796. [\[CrossRef\]](#)
21. Hinz, K.; O’Connor, P.M.; Huppertz, T.; Ross, R.P.; Kelly, A.L. Comparison of the principal proteins in bovine, caprine, buffalo, equine and camel milk. *J. Dairy Res.* **2012**, *79*, 185–191. [\[CrossRef\]](#)
22. Diarrassouba, F.; Remondetto, G.; Liang, L.; Garrat, G.; Beyssac, E.; Subirade, M. Effects of gastrointestinal pH conditions on the stability of the  $\beta$ -lactoglobulin/vitamin D3 complex and on the solubility of vitamin D3. *Food Res. Int.* **2013**, *52*, 515–521. [\[CrossRef\]](#)
23. Taulier, N.; Chalikian, T.V. Characterization of pH-induced transitions of  $\beta$ -lactoglobulin: Ultrasonic, densimetric, and spectroscopic studies. Edited by C. R. Matthews. *J. Mol. Biol.* **2001**, *314*, 873–889. [\[CrossRef\]](#)
24. Markus, C.R.; Jonkman, L.M.; Lammers, J.H.; Deutz, N.E.; Messer, M.H.; Rigtering, N. Evening intake of  $\alpha$ -lactalbumin increases plasma tryptophan availability and improves morning alertness and brain measures of attention. *Am. J. Clin. Nutr.* **2005**, *81*, 1026–1033. [\[CrossRef\]](#)
25. Markus, C.R.; Olivier, B.; de Haan, E.H. Whey protein rich in  $\alpha$ -lactalbumin increases the ratio of plasma tryptophan to the sum of the other large neutral amino acids and improves cognitive performance in stress-vulnerable subjects. *Am. J. Clin. Nutr.* **2002**, *75*, 1051–1056. [\[CrossRef\]](#) [\[PubMed\]](#)

26. Gurgel, P.V.; Carbonell, R.G.; Swaisgood, H.E. Studies of the Binding of  $\alpha$ -Lactalbumin to Immobilized Peptide Ligands. *J. Agric. Food Chem.* **2001**, *49*, 5765–5770. [[CrossRef](#)]
27. Velusamy, V.; Palaniappan, L. Compositional analysis  $\alpha$ -lactalbumin. *Am. J. Biochem. Mol. Biol* **2011**, *1*, 106–120. [[CrossRef](#)]
28. Carminati, D.; Tidona, F. Chapter 31—Nutritional Value and Potential Health Benefits of Donkey Milk. In *Nutrients in Dairy and Their Implications on Health and Disease*; Watson, R.R., Collier, R.J., Preedy, V.R., Eds.; Academic Press: London, UK, 2017; pp. 407–414. [[CrossRef](#)]
29. Vincenzetti, S.; Polidori, P.; Mariani, P.; Cammertoni, N.; Fantuz, F.; Vita, A. Donkey milk protein fractions characterization. *Food Chem.* **2008**, *10*, 640–649. [[CrossRef](#)]
30. Vincenzetti, S.; Amici, A.; Pucciarelli, S.; Vita, A.; Micozzi, D.; Carpi, F.M.; Polzonetti, V.; Natalini, P.; Polidori, P. A Proteomic Study on Donkey Milk. *Biochem. Anal. Biochem.* **2012**, *1*, 109. [[CrossRef](#)]
31. Ozturkoglu-Budak, S. Effect of different treatments on the stability of lysozyme, lactoferrin and b-lactoglobulin in donkey's milk. *Int. J. Dairy Technol.* **2016**, *71*, 36–45. [[CrossRef](#)]
32. Brumini, D.; Criscione, A.; Bordonaro, S.; Vegarud, G.E.; Marletta, D. Whey proteins and their antimicrobial properties in donkey milk: A brief review. *Dairy Sci. Technol.* **2016**, *96*, 1–14. [[CrossRef](#)]
33. Yoo, Y.C.; Watanabe, S.; Watanabe, R.; Hata, K.; Shimazaki, K.I.; Azuma, I. Bovine lactoferrin and lactoferricin, a peptide derived from bovine lactoferrin, inhibit tumor metastasis in mice. *Jpn. J. Cancer Res.* **1997**, *88*, 184–190. [[CrossRef](#)]
34. Yoo, Y.-C.; Watanabe, R.; Koike, Y.; Mitobe, M.; Shimazaki, K.-I.; Watanabe, S.; Azuma, I. Apoptosis in human leukemic cells induced by lactoferricin, a bovine milk protein-derived peptide: Involvement of reactive oxygen species. *Biochem. Biophys. Res. Commun.* **1997**, *237*, 624–628. [[CrossRef](#)]
35. Martemucci, G.; D'Alessandro, A.G. Fat content, energy value and fatty acid profile of donkey milk during lactation and implications for human nutrition. *Lipids Health Dis.* **2012**, *11*, 113. [[CrossRef](#)]
36. McGrath, B.A.; Fox, P.F.; McSweeney, P.L.H.; Kelly, A.L. Composition and properties of bovine colostrum: A review. *Dairy Sci. Technol.* **2016**, *96*, 133–158. [[CrossRef](#)]
37. Li, M.; Kang, S.; Zheng, Y.; Shao, J.; Zhao, H.; An, Y.; Cao, G.; Li, Q.; Yue, X.; Yang, M. Comparative metabolomics analysis of donkey colostrum and mature milk using ultra-high-performance liquid tandem chromatography quadrupole time-of-flight mass spectrometry. *J. Dairy Sci.* **2020**, *103*, 992–1001. [[CrossRef](#)] [[PubMed](#)]
38. Yang, M.; Cao, X.; Wu, R.; Liu, B.; Ye, W.; Yue, X.; Wu, J. Comparative proteomic exploration of whey proteins in human and bovine colostrum and mature milk using iTRAQ-coupled LC-MS/MS. *Int. J. Food Sci. Nutr.* **2017**, *68*, 671–681. [[CrossRef](#)] [[PubMed](#)]
39. Li, M.; Li, W.; Wu, J.; Zheng, Y.; Shao, J.; Li, Q.; Kang, S.; Zhang, Z.; Yue, X.; Yang, M. Quantitative lipidomics reveals alterations in donkey milk lipids according to lactation. *Food Chem.* **2020**, *310*, 125866. [[CrossRef](#)]
40. Li, W.; Li, M.; Cao, X.; Han, H.; Kong, F.; Yue, X. Comparative analysis of whey proteins in donkey colostrum and mature milk using quantitative proteomics. *Food Res. Int.* **2020**, *127*, 108741. [[CrossRef](#)]
41. Martini, M.; Altomonte, I.; Manica, E.; Salari, F. Changes in donkey milk lipids in relation to season and lactation. *J. Food Compos. Anal.* **2015**, *41*, 30–34. [[CrossRef](#)]
42. Šarić, L.; Šarić, B.; Mandić, A.; Tomić, J.; Torbica, A.; Nedeljković, N.; Ikonić, B.B. Antibacterial activity of donkey milk against Salmonella. *Agro. Food Ind. Hi. Tech.* **2014**, *25*, 30–34.
43. Šarić, L.Ć.; Šarić, B.M.; Kravić, S.Ž.; Plavšić, D.V.; Milovanović, I.L.; Gubić, J.M.; Nedeljković, N.M. Antibacterial activity of Domestic Balkan donkey milk toward *Listeria monocytogenes* and *Staphylococcus aureus*. *Food Feed Res.* **2014**, *41*, 47–54. [[CrossRef](#)]
44. Šarić, L.Ć.; Šarić, B.M.; Mandić, A.I.; Kevrešan, Ž.S.; Ikonić, B.B.; Kravić, S.Ž.; Jambrec, D.J. Role of calcium content in antibacterial activity of donkeys' milk toward *E. coli*. *Eur. Food Res. Technol.* **2014**, *239*, 1031–1039. [[CrossRef](#)]
45. Tidona, F.; Sekse, C.; Criscione, A.; Jacobsen, M.; Bordonaro, S.; Marletta, D.; Vegarud, G.E. Antimicrobial effect of donkeys' milk digested in vitro with human gastrointestinal enzymes. *Int. Dairy J.* **2011**, *21*, 158–165. [[CrossRef](#)]
46. Nazzaro, F.; Orlando, P.; Fratianni, E.; Coppola, R. Isolation of components with antimicrobial property from the donkey milk: A preliminary study. *Open Food Sci. J.* **2010**, *4*, 37–42. [[CrossRef](#)]
47. Pilla, R.; Dapra, V.; Zecconi, A.; Piccinini, R. Hygienic and health characteristics of donkey milk during a follow-up study. *J. Dairy Res.* **2010**, *77*, 392–397. [[CrossRef](#)] [[PubMed](#)]

48. Zhang, X.-Y.; Zhao, L.; Jiang, L.; Dong, M.-L.; Ren, F.-Z. The antimicrobial activity of donkey milk and its microflora changes during storage. *Food Control* **2008**, *19*, 1191–1195. [[CrossRef](#)]
49. Bruhn, O.; Grötzinger, J.; Cascorbi, I.; Jung, S. Antimicrobial peptides and proteins of the horse—Insights into a well-armed organism. *Vet. Res.* **2011**, *42*, 98. [[CrossRef](#)]
50. Šarić, L.Č.; Šarić, B.M.; Mandić, A.I.; Torbica, A.M.; Tomić, J.M.; Cvetković, D.D.; Okanović, Đ.G. Antibacterial properties of Domestic Balkan donkeys' milk. *Int. Dairy J.* **2012**, *25*, 142–146. [[CrossRef](#)]
51. Uniacke-Lowe, T.; Huppertz, T.; Fox, P.F. Equine milk proteins: Chemistry, structure and nutritional significance. *Int. Dairy J.* **2010**, *20*, 609–629. [[CrossRef](#)]
52. Benkerroum, N. Antimicrobial activity of lysozyme with special relevance to milk. *Afr. J. Biotechnol.* **2008**, *7*, 4856–4867.
53. Fratini, F.; Turchi, B.; Pedonese, F.; Pizzurro, F.; Ragolini, P.; Torracca, B.; Tozzi, B.; Galiero, A.; Nuvoloni, R. Does the addition of donkey milk inhibit the replication of pathogen microorganisms in goat milk at refrigerated condition? *Dairy Sci. Technol.* **2016**, *96*, 243–250. [[CrossRef](#)]
54. Yamauchi, K.; Wakabayashi, H.; Shin, K.; Takase, M. Bovine lactoferrin: Benefits and mechanism of action against infections. *Biochem. Cell Biol.* **2006**, *84*, 291–296. [[CrossRef](#)]
55. UniProt. Available online: <https://www.uniprot.org> (accessed on 21 August 2020).
56. PDB. Available online: <https://www.rcsb.org> (accessed on 21 August 2020).
57. Brumini, D.; Furlund, C.B.; Comi, I.; Devold, T.G.; Marletta, D.; Vegarud, G.E.; Jonassen, C.M. Antiviral activity of donkey milk protein fractions on echovirus type 5. *Int. Dairy J.* **2013**, *28*, 109–111. [[CrossRef](#)]
58. Koutb, M.; Khider, M.; Ali, E.H.; Hussein, N.A. Antimicrobial activity of donkey milk against dermatomycotic fungi and foodborne bacteria. *Int. J. Biomed. Mat. Res.* **2016**, *4*, 11–17. [[CrossRef](#)]
59. Altomonte, I.; Salari, F.; Licitra, R.; Martini, M. Donkey and human milk: Insights into their compositional similarities. *Int. Dairy J.* **2019**, *89*, 111–118. [[CrossRef](#)]
60. Li, L.; Liu, X.; Guo, H. The nutritional ingredients and antioxidant activity of donkey milk and donkey milk powder. *Food Sci. Biotechnol.* **2017**, *27*, 393–400. [[CrossRef](#)] [[PubMed](#)]
61. Simos, Y.; Metsios, A.; Verginadis, I.; D'Alessandro, A.-G.; Loiudice, P.; Jirillo, E.; Charalampidis, P.; Koumanis, V.; Boulaka, A.; Martemucci, G.; et al. Antioxidant and anti-platelet properties of milk from goat, donkey and cow: An In Vitro, Ex Vivo and In Vivo study. *Int. Dairy J.* **2011**, *21*, 901–906. [[CrossRef](#)]
62. Jirillo, E.; Magrone, T. Anti-inflammatory and anti-allergic properties of donkey's and goat's milk. *Endocr. Metab. Immune Disord. Drug Targets Former. Curr. Drug Targets-Immune Endocr. Metab. Disord.* **2014**, *14*, 27–37. [[CrossRef](#)] [[PubMed](#)]
63. Schroder, K.; Hertzog, P.J.; Ravasi, T.; Hume, D.A. Interferon-gamma: An overview of signals, mechanisms and functions. *J. Leukoc. Biol.* **2004**, *75*, 163–189. [[CrossRef](#)]
64. Yvon, S.; Olier, M.; Leveque, M.; Jard, G.; Tormo, H.; Haimoud-Lekhal, D.A.; Peter, M.; Eutamene, H. Donkey milk consumption exerts anti-inflammatory properties by normalizing antimicrobial peptides levels in Paneth's cells in a model of ileitis in mice. *Eur. J. Nutr.* **2018**, *57*, 155–166. [[CrossRef](#)]
65. Jirillo, E.; Jirillo, E.; Magrone, T. Donkey's and goat's milk consumption and benefits to human health with special reference to the inflammatory status. *Curr. Pharm. Des.* **2010**, *16*, 859–863. [[CrossRef](#)]
66. Lamine, F.; Fioramonti, J.; Bueno, L.; Nepveu, F.; Cauquil, E.; Lobysheva, I.; Eutamene, H.; Théodorou, V. Nitric oxide released by lactobacillus farciminis improves TNBS-induced colitis in rats. *Scand. J. Gastroenterol.* **2004**, *39*, 37–45. [[CrossRef](#)]
67. Sarti, L.; Martini, M.; Brajon, G.; Barni, S.; Salari, F.; Altomonte, I.; Ragona, G.; Mori, F.; Pucci, N.; Muscas, G.; et al. Donkey's Milk in the Management of Children with Cow's Milk protein allergy: Nutritional and hygienic aspects. *Ital. J. Pediatrics* **2019**, *45*, 102. [[CrossRef](#)]
68. Iacono, G.; Carroccio, A.; Cavataio, F.; Montalto, G.; Soresi, M.; Balsamo, V. Use of ass's milk in multiple food allergy. *J. Pediatr. Gastroenterol. Nutr.* **1992**, *14*, 177–181. [[CrossRef](#)] [[PubMed](#)]
69. Pelligrini, A.; Thomas, U.; Bramaz, N.; Hunziker, P.; von Fellenberg, R. Isolation and identification of three bactericidal domains in the bovine alpha-lactalbumin molecule. *Biochim. Biophys. Acta* **1999**, *1426*, 439–448. [[CrossRef](#)]
70. Cunsolo, V.; Saletti, R.; Muccilli, V.; Foti, S. Characterization of the protein profile of donkey's milk whey fraction. *J. Mass Spectrom.* **2007**, *42*, 1162–1174. [[CrossRef](#)] [[PubMed](#)]

71. Amati, L.; Marzulli, G.; Martulli, M.; Tafaro, A.; Jirillo, F.; Pugliese, V.; Martemucci, G.; D'Alessandro, A.G.; Jirillo, E. Donkey and goat milk intake and modulation of the human aged immune response. *Curr. Pharm. Des.* **2010**, *16*, 864–869. [[CrossRef](#)] [[PubMed](#)]
72. Kapila, R.; Sharma, R.; Kapila, S. *Milk and Fermented Milk Products in Alleviation of Aging Pathophysiology*; Elsevier Academic Press: London, UK, 2017; pp. 287–292. [[CrossRef](#)]
73. Hill, D.R.; Newburg, D.S. Clinical applications of bioactive milk components. *Nutr. Rev.* **2015**, *73*, 463–476. [[CrossRef](#)] [[PubMed](#)]
74. Marcone, S.; Belton, O.; Fitzgerald, D.J. Milk-derived bioactive peptides and their health promoting effects: A potential role in atherosclerosis. *Br. J. Clin. Pharmacol.* **2017**, *83*, 152–162. [[CrossRef](#)]
75. Minervini, F.; Algaron, F.; Rizzello, C.G.; Fox, P.F.; Monnet, V.; Gobetti, M. Angiotensin I-converting-enzyme-inhibitory and antibacterial peptides from *Lactobacillus helveticus* PR4 proteinase-hydrolyzed caseins of milk from six species. *Appl. Environ. Microbiol.* **2003**, *69*, 5297–5305. [[CrossRef](#)]
76. Li, Y.; Fan, Y.; Shaikh, A.S.; Wang, Z.; Wang, D.; Tan, H. Dezhou donkey (*Equus asinus*) milk a potential treatment strategy for type 2 diabetes. *J. Ethnopharmacol.* **2020**, *246*, 112221. [[CrossRef](#)]
77. Mao, X.; Gu, J.; Sun, Y.; Xu, S.; Zhang, X.; Yang, H.; Ren, F. Anti-proliferative and anti-tumour effect of active components in donkey milk on A549 human lung cancer cells. *Int. Dairy J.* **2009**, *19*, 703–708. [[CrossRef](#)]
78. Mossberg, A.K.; Hun Mok, K.; Morozova-Roche, L.A.; Svanborg, C. Structure and function of human  $\alpha$ -lactalbumin made lethal to tumor cells (HAMLET)-type complexes. *FEBS J.* **2010**, *277*, 4614–4625. [[CrossRef](#)]
79. Polidori, P.; Ariani, A.; Vincenzetti, S. Use of Donkey Milk in Cases of Cow's Milk Protein Allergies. *Int. J. Child. Health Nutr.* **2015**, *4*, 174–179. [[CrossRef](#)]
80. Trinchese, G.; Cavaliere, G.; Canani, R.B.; Matamoros, S.; Bergamo, P.; De Filippo, C.; Aceto, S.; Gaita, M.; Cerino, P.; Negri, R.; et al. Human, donkey and cow milk differently affects energy efficiency and inflammatory state by modulating mitochondrial function and gut microbiota. *J. Nutr. Biochem.* **2015**, *26*, 1136–1146. [[CrossRef](#)]
81. Trinchese, G.; Cavaliere, G.; De Filippo, C.; Aceto, S.; Prisco, M.; Chun, J.T.; Penna, E.; Negri, R.; Muredda, L.; Demurtas, A.; et al. Human Milk and Donkey Milk, Compared to Cow Milk, Reduce Inflammatory Mediators and Modulate Glucose and Lipid Metabolism, Acting on Mitochondrial Function and Oleyethanolamide Levels in Rat Skeletal Muscle. *Front. Physiol.* **2018**, *9*, 32. [[CrossRef](#)] [[PubMed](#)]
82. Ibrahim, H.R.; Aoki, T. New promises of lysozyme as immune modulator and antimicrobial agent for nutraceuticals. *Foods Food Ingrid. J. Jpn.* **2003**, *208*, 361–374.
83. Zavaleta, N.; Figueroa, D.; Rivera, J.; Sanchez, J.; Alfaro, S.; Lonnerdal, B. Efficacy of rice-based oral rehydration solution containing recombinant human lactoferrin and lysozyme in Peruvian children with acute diarrhea. *J. Pediatr. Gastroenterol. Nutr.* **2007**, *44*, 258–264. [[CrossRef](#)]
84. Weng, J.; Ji, L.; Jia, W.; Lu, J.; Zhou, Z.; Zou, D.; Guo, X. Normes de soins pour le diabète de type 2 en Chine. *Rech. et Rev. sur le Diabète Métabolisme* **2016**, *32*, 442–458.
85. Alichanidis, E.; Moatsou, G.; Polychroniadou, A. Composition and Properties of Non-cow Milk and Products. In *Non-Bovine Milk and Milk Products*; Tsakalidou, E., Papadimitriou, K., Eds.; Elsevier Academic Press: London, UK, 2016; pp. 81–116. [[CrossRef](#)]
86. Herrouin, M.; Mollé, D.; Fauquant, J.; Ballestra, F.; Maubois, J.-L.; Léonil, J. New Genetic Variants Identified in Donkey's Milk Whey Proteins. *J. Protein Chem.* **2000**, *19*, 105–116. [[CrossRef](#)]
87. Miao, W.; He, R.; Feng, L.; Ma, K.; Zhang, C.; Zhou, J.; Chen, X.; Rui, X.; Zhang, Q.; Dong, M.; et al. Study on processing stability and fermentation characteristics of donkey milk. *LWT* **2020**, *124*, 109151. [[CrossRef](#)]
88. Souroullas, K.; Aspri, M.; Papademas, P. Donkey milk as a supplement in infant formula: Benefits and technological challenges. *Food Res. Int.* **2018**, *109*, 416–425. [[CrossRef](#)]
89. D'Alessandro, A.G.; Martemucci, G.; Loizzo, P.; Faccia, M. Production of cheese from donkey milk as influenced by addition of transglutaminase. *J. Dairy Sci.* **2019**, *102*, 10867–10876. [[CrossRef](#)]
90. Tidona, F.; Criscione, A.; Devold, T.G.; Bordonaro, S.; Marletta, D.; Vegarud, G.E. Protein composition and micelle size of donkey milk with different protein patterns: Effects on digestibility. *Int. Dairy J.* **2014**, *35*, 57–62. [[CrossRef](#)]
91. Cappola, R.; Salimei, E.; Succi, M.; Sorrentino, E.; Nanni, M.; Ranieri, P.; Belli Blanes, R.; Grazia, L. Behaviour of *Lactobacillus rhamnosus* strains in ass's milk. *Ann. Microbiol.* **2002**, 55–60.
92. Chiavari, C.; Coloretto, F.; Nanni, M.; Sorrentino, E.; Grazia, L. Use of donkey's milk for a fermented beverage with lactobacilli. *Le Lait* **2005**, *85*, 481–490. [[CrossRef](#)]

93. Perna, A.; Intaglietta, I.; Simonetti, A.; Gambacorta, E. Donkey Milk for Manufacture of Novel Functional Fermented Beverages. *J. Food Sci.* **2015**, *80*, S1352–S1359. [[CrossRef](#)]
94. Šarić, L.Ć.; Šarić, B.M.; Mandić, A.I.; Hadnađev, M.S.; Gubić, J.M.; Milovanović, I.L.; Tomić, J.M. Characterization of extra-hard cheese produced from donkeys' and caprine milk mixture. *Dairy Sci. Technol.* **2016**, *96*, 227–241. [[CrossRef](#)]
95. Salimei, E. *Animals that Produce Dairy Foods: Donkey in Reference Module in Food Sciences*, 1st ed.; Elsevier Academic Press: London, UK, 2016; pp. 1–10. [[CrossRef](#)]



© 2020 by the authors. Licensee MDPI, Basel, Switzerland. This article is an open access article distributed under the terms and conditions of the Creative Commons Attribution (CC BY) license (<http://creativecommons.org/licenses/by/4.0/>).



Review

# Apitherapy for Age-Related Skeletal Muscle Dysfunction (Sarcopenia): A Review on the Effects of Royal Jelly, Propolis, and Bee Pollen

Amira Mohammed Ali <sup>1,2,\*</sup> and Hiroshi Kunugi <sup>1,3</sup>

<sup>1</sup> Department of Mental Disorder Research, National Institute of Neuroscience, National Center of Neurology and Psychiatry, Tokyo 187-0031, Japan; hkunugi@ncnp.go.jp

<sup>2</sup> Department of Psychiatric Nursing and Mental Health, Faculty of Nursing, Alexandria University, Alexandria 21527, Egypt

<sup>3</sup> Department of Psychiatry, Teikyo University School of Medicine, Tokyo 173-8605, Japan

\* Correspondence: mercy.ofheaven2000@gmail.com; Tel.: +81-042-346-1714

Received: 29 August 2020; Accepted: 22 September 2020; Published: 25 September 2020

**Abstract:** The global pandemic of sarcopenia, skeletal muscle loss and weakness, which prevails in up to 50% of older adults is increasing worldwide due to the expansion of aging populations. It is now striking young and midlife adults as well because of sedentary lifestyle and increased intake of unhealthy food (e.g., western diet). The lockdown measures and economic turndown associated with the current outbreak of Coronavirus Disease 2019 (COVID-19) are likely to increase the prevalence of sarcopenia by promoting sedentarism and unhealthy patterns of eating. Sarcopenia has multiple detrimental effects including falls, hospitalization, disability, and institutionalization. Although a few pharmacological agents (e.g., bimagrumab, sarconeos, and exercise mimetics) are being explored in different stages of trials, not a single drug has been approved for sarcopenia treatment. Hence, research has focused on testing the effect of nutraceuticals, such as bee products, as safe treatments to prevent and/or treat sarcopenia. Royal jelly, propolis, and bee pollen are common bee products that are rich in highly potent antioxidants such as flavonoids, phenols, and amino acids. These products, in order, stimulate larval development into queen bees, promote defenses of the bee hive against microbial and environmental threats, and increase royal jelly production by nurse bees. Thanks to their versatile pharmacological activities (e.g., anti-aging, anti-inflammatory, anticarcinogenic, antimicrobial, etc.), these products have been used to treat multiple chronic conditions that predispose to muscle wasting such as hypertension, diabetes mellitus, cardiovascular disorder, and cancer, to name a few. They were also used in some evolving studies to treat sarcopenia in laboratory animals and, to a limited degree, in humans. However, a collective understanding of the effect and mechanism of action of these products in skeletal muscle is not well-developed. Therefore, this review examines the literature for possible effects of royal jelly, bee pollen, and propolis on skeletal muscle in aged experimental models, muscle cell cultures, and humans. Collectively, data from reviewed studies denote varying levels of positive effects of bee products on muscle mass, strength, and function. The likely underlying mechanisms include amelioration of inflammation and oxidative damages, promotion of metabolic regulation, enhancement of satellite stem cell responsiveness, improvement of muscular blood supply, inhibition of catabolic genes, and promotion of peripheral neuronal regeneration. This review offers suggestions for other mechanisms to be explored and provides guidance for future trials investigating the effects of bee products among people with sarcopenia.

**Keywords:** apitherapy; royal jelly; propolis; bee pollen; sarcopenia; dietary interventions; muscle; skeletal; muscle wasting; physical performance; coronavirus disease 2019; COVID-19; body composition; lean body mass; insulin resistance; mitochondrial dysfunction; satellite stem cells

## 1. Introduction

While the numbers of older adults are expanding all over the world, the pandemic of sarcopenia, skeletal muscle loss/weakness is also on the rise [1]. Loss of lean body mass is a direct effect of the inflammatory and oxidative conditions that develop with aging [1,2]—described as inflammaging. Both inflammatory mediators and free radicals, which are highly expressed in older seniors and in patients with chronic diseases, such as type 2 diabetes mellitus, cause remarkable shrinkage of fast-twitch type II fibers promoting their transformation into the slow-twitch type I fibers [1,3–5].

Research indicates that muscle wasting may develop after adolescence (at the beginning of the third decade of life) as a result of sedentary lifestyle and improper diet (low protein/high fat/low fiber) [6–8]. These behavioral factors alter the composition of gut microbiota promoting gut dysbiosis, which allows the passage of bacterial endotoxins into the systemic circulation to induce inflammation and oxidative stress same as in immunological aging that occurs during old age [9,10].

Longitudinal data show that the currently-occurring global crisis, coronavirus disease 2019 (COVID-19), is likely to aggravate the development of sarcopenia in young groups by promoting unhealthy lifestyle [11]. On one hand, physical inactivity is increasing as a result of the lockdown measures and stay home strategies adopted by most governments to limit the spread of this infection [11–13]. On the other hand, food production has been seriously affected during the COVID-19 outbreak along with increase in food prices, which prompt people to consume unhealthy/processed foods since they are cheaper than fresh and healthy ones [14].

Given its high prevalence in the general population, which ranges between 5 and 40% in western countries and increases up to 50% in advanced age, sarcopenia is considered a public health problem [4,15]. It causes progressive decline of functional capacity, contributes to frailty, increases the risk of falls and hospitalization in old people [16,17], and leads to poor outcomes in patients with COVID-19 [18]. A large number of pharmacological agents are being tested as anti-sarcopenic agents such as bimagrumab (BYM338), enobasarm (GTx-024), trevogrumab (REGN1033), and sarconeos (BIO101). Most trials are in phase 1 or phase 2 [19]. In addition, outcomes of commonly used treatments (e.g., testosterone, growth hormone, and anabolic steroids) have been rather unsatisfactory [4,20–22]. Therefore, the most appropriate strategies for preventing and treating sarcopenia are limited to physical exercise and protein-rich diet [6,21]. Nevertheless, old people tend to be less compliant with physical activity programs [23,24]. Meanwhile, problems of the gastrointestinal (GI) tract that develop during advanced age (e.g., loss of teeth, taste, smell, and decreased absorption) as well as anabolic resistance of aged muscle limit potential benefits of protein-rich food in this group [25,26]. Therefore, it is of importance to search for novel preventive and curative strategies for sarcopenia, which can take into account the multifactorial nature of aging-related skeletal muscle failure.

## 2. Apitherapy as a Possible Complementary Treatment for Sarcopenia

Rock paintings from the Stone Age portray consumption of bee products by humans [27]. The first evidence of human usage of bee products for therapeutic and cosmetic purposes dates back 6000 years in ancient Egypt and later in China, Greece, and Rome [27–30]. Current research interest is directed toward the use of natural substances, including bee products, as potential pharmaceuticals to modify disease progression [31]. The term “apitherapy” describes a category of complementary and alternative medicine that comprises therapeutic use of various bee products including apilarnil (atomized drone larva) to prevent and treat illnesses [30].

Bee workers of either *Apis mellifera* or *Apis cerana* species—the former is common in Europe, Asia, Africa, and America while the latter exists only in southern and southeastern Asia—produce and store multiple bioactive substances [32]. Royal jelly, propolis, bee pollen, honey, bee venom, bee bread, and bee wax are common products of the bee hive. They all (to a varying degree) possess multiple health promoting properties due to their high content of natural antioxidants such as flavonoids, phenols, or terpenoids [28,32]. Research documents variability in contents and effects of every single bee product,

mainly due to the influence of bee species, botanical origin, geographic location, season, extraction, and handling procedures [2,28].

Several lines of evidence describe anti-aging effects of royal jelly, bee pollen, and propolis both in humans and laboratory animals [2,33–35]. These three products are widely used as dietary supplements [36–39]. In the meantime, the literature gives examples of numerous dietary supplements that could successfully prevent or alleviate the progression of muscle mass loss in old age [40–42]. Bee products represent a part of this interventional strategy. However, the extent to which bee products can affect sarcopenia as well as understanding of their underlying mechanism of action are far from being clear. Therefore, we conducted this review with the aim of investigating the anti-aging properties of these products with a focus on skeletal muscle functioning in advanced age. In this respect, we reviewed animal and human studies investigating effects of the aforementioned products on skeletal muscle aging and elaborated on different mechanisms underlying these effects. Studies included in this review were retrieved by searching PubMed and Google scholar using a combination of terminologies of “sarcopenia, muscle wasting, muscle mass, lean body mass, skeletal muscle, motor” with “royal jelly, honey, bee pollen, propolis, bee venom, bee bread, bee wax, chrysin, apamin, caffeic acid phenethyl ester”. Snow ball manual search using reference lists of retrieved studies was also conducted. This search resulted in a number of studies, which addressed muscle wasting and related dynamics through the use of three bee products, namely royal jelly, bee pollen, and propolis. Figure 1, Panel A and Panel B, summarizes the chemical composition and biological properties of these bee products while this section elaborates on these products in depth.

### 2.1. Royal Jelly: Its Constituents, Biological, and Pharmacological Activities

Royal jelly is a thick, milky, white-yellowish, acidic colloid substance secreted from the hypopharyngeal and mandibular salivary glands of young nurse honey bees (5–15 days old) [32,43]. In general, fresh royal jelly mostly consists of water (67% *w/w*) in addition to carbohydrates (16%), proteins and amino acids (12.5%), fat (5%), and many other elements [32]. However, royal jelly content of these substances noticeably varies depending on numerous factors like botanical source, bee species, bee artificial feeding, weather, season, location, method of processing, and the like [2,44].

Protein is the most copious active element in royal jelly, representing half the weight of its dry matter [2]. It vastly comprises nine 49–87 kDa water-insoluble proteins, known as major royal jelly proteins 1–9 (MRJPs1-9) [2,45]. MRJPs constitute more than 80% of royal jelly protein content, and MRJPs1–5 constitute 82–90% of all MRJPs. MRJPs contain 400–578 amino acids that contribute to the antioxidant effect of royal jelly as well as its role in cell proliferation, cell adhesion, cell growth, and immunity [46,47]. Novel non-MRJPs proteins have been newly discovered [48]. Royalisin, jelleines, and aspimin are examples of other proteins that exist in royal jelly, albeit in small amounts. These proteins as well as MRJPs demonstrate strong antimicrobial and bactericidal activities even against the most drug-resistant bacterial strains such as methicillin-resistant *Staphylococcus aureus*, *Pseudomonas aeruginosa*, *Klebsiella pneumoniae*, vancomycin-resistant *Enterococci*, as well as extended-spectrum  $\beta$ -lactamase-producing *Proteus mirabilis* and *Escherichia coli* [28,29].

Carbohydrates (e.g., fructose, glucose maltose, trehalose, melibiose, ribose, and erlose) constitute 7.5–16% or royal jelly content [49]. Reducing sugars in royal jelly are thought to contribute to its epigenetic effect through the activation of insulin-like growth factor 1 (IGF-1) and mammalian target of rapamycin (mTOR) signaling cascades. Thus, they stimulate caste differentiation of *Apis mellifera* larvae into queens by increasing intake of food and key nutrients [50].

Lipids make up 7–18% of the dry weight of royal jelly. This fraction largely comprises a group of unique and rare saturated or monounsaturated short and medium chain fatty acids that are terminally or internally hydroxylated with terminal mono- or dicarboxylic acid functions [2,28]. The vast majority of royal jelly fat content (80–85%) consists of short hydroxyl fatty acids such as trans-10-hydroxy-2-decenoic acid (10-HDA), which exists only in royal jelly; and therefore, it is known as royal jelly acid or queen bee acid [28,49,51]. 10-HDA is one of the most potent bioactive elements in

royal jelly expressing strong anti-aging, neuroprotective, antiproliferative, antimicrobial, antioxidant, anti-inflammatory, and epigenetic effects [52–58]. In addition, the lipid fraction of royal jelly contains phenolic acids (4–10%), wax (5–6%), steroids (3–4%), and phospholipids (0.4–0.8%) [49].

A wide range of minor constituents and bioactive compounds exist profusely in royal jelly such as acetylcholine, nucleotides (adenosine, guanosine, adenosine tri-phosphate (ATP), adenosine monophosphate (AMP)), minerals (iron, sodium, calcium, potassium, zinc, magnesium, manganese, and copper), amino acids (8 out of 9 essential amino acids Val, Leu, Ile, Thr, Met, Phe, Lys, and Trp), vitamins (retinol (A), ascorbic acid (C), tocopherol (E), riboflavin (B2), niacin (B3), and other B vitamins), esters, aldehydes, ketones, alcohol, and minor heterocyclic compounds [2,28,49,59–61]. It is worth noting that royal jelly loses most of its bioactive ingredients and biological properties when stored at a temperature of 5 °C or higher. Therefore, freezing is the best method to store royal jelly [62]. Enzymatic treatment of royal jelly removes allergen proteins and enhances its nutrient content in addition to improving its digestibility and absorption in the gut without altering its freshness [2,59].

Royal jelly has been historically used as a beautifying agent by famous queens such as Cleopatra, and it is still involved in the cosmetic industry [29,56]. Its rich content of bioactive compounds grants it a plethora of diverse health benefits such as antioxidant, anti-inflammatory, neurotrophic, hypotensive, antidiabetic, antilipidemic, antirheumatic, anticarcinogenic, anti-fatigue, antiadipogenic, and antimicrobial activities [43,45,63]. Therefore, it is widely used to treat multiple serious conditions including diabetes, hypertension, hyperlipidemia, cancer, skin diseases, and neurodegenerative diseases such as Alzheimer’s disease and Parkinson’s disease [2,43,46,59,64]. In addition, bee queens (which enjoy long lifespan as well as super fertility and physical qualities) consume royal jelly throughout their entire lives, and royal jelly is considered a promising anti-aging nutraceutical that can positively enhance fertility and improve body composition [2].

## 2.2. Propolis: Its Constituents, Biological, and Pharmacological Activities

Propolis, also known as bee glue, is a sticky wax-like substance that constitutes a mixture of bee salivary secretions, bee wax, and resinous sap occurring in the bark and leaf-buds of specific plants [37,65]. It comes in green, red, brown, or black colors based on the collected local flora [66]. The word propolis comprises two Greek words “pro” and “polis”, which in order mean “in front of or at the entrance to” and “community or city”. Propolis is a hive-defensive substance, which bees use to protect and repair their hives [67].

Propolis is a unique product of a complex composition that comprises more than 420 chemical substances [37,68]. Nonetheless, its composition and biological activities vary considerably depending on its botanical and geographical origins as well as the time of harvesting [38,65,67]. Propolis is rich in oxypropenylated phenylpropanoids—secondary metabolites from plants, fungi, and bacteria [69]—such as 7-isopentenylcoumarin, boropinic acid, 4-geranyloxyferulic acid, and auraptene. The last two exist in raw Italian propolis at high concentrations: 107.12 and 145.37 µg/g of dry propolis, respectively. Flavonoids, a large group of phenolic compounds, are abundant in Italian propolis, and they are differentiated into several groups including flavanones (e.g., naringenin, 4.4 mg/g), flavones (e.g., apigenin, 1.7 mg/g), flavonols (e.g., galangin, 0.9 mg/g), tannins (e.g., gallic acid 8.4 mg/g), catechins (expressed as (+)-catechin 0.4 mg/g, and caffeic acid and its esters (expressed as caffeic acid, 9.2 mg/g) [69]. The most profuse flavonoids in ethanolic extracts of Brazilian propolis are artemillin C (38.6 mg/g), coumaric acid (10.6 mg/g), and kaempferide (12.6 mg/g) [70]. Key other constituents of propolis include polyphenol (e.g., phenolic acids and aromatic esters), phenolic aldehydes, terpenoids, ketones, enzymes (e.g.,  $\alpha$ - and  $\beta$ -amylase), vitamins (e.g., thiamin (B1), riboflavin (B2), pyridoxine (B6), ascorbic acid (C), tocopherol (E)), minerals (e.g., calcium, potassium, magnesium, iron, sodium, barium) essential oils, alcohol, fatty acids,  $\beta$ -steroids, and many other elements [37,38,67,68,71].

The attention of several drug targeting studies has recently been focused on the therapeutic activities of individual bioactive compounds in propolis [65,68]. Flavonoids comprise the majority of mostly studies bioactive substances in propolis. Chrysin (5,7-dihydroxyflavone) is a flavonoid

that exists in certain mushrooms, flowers (e.g., blue passion flower), and in other bee products (e.g., honey). It expresses anti-inflammatory, antioxidant, anti-proliferative, and neuroprotective effects [72]. Caffeic acid phenethyl ester (CAPE), a derivative of hydroxycinnamic acid, expresses anti-oxidant, immunomodulatory, anti-inflammatory, antiviral, and anti-neoplastic properties [73–75]. Pinocembrin (5,7-dihydroxyflavanone) is the most copious flavonoid in propolis—1 g of balsam/an ethanolic extract from poplar propolis found in Spain contains up to 606–701 mg of pinocembrin [76]. It exists in numerous plants (e.g., Eucalyptus and Populus). It exhibits anti-inflammatory, antioxidant, antimicrobial, and antiproliferative activities [77,78].

Essential/volatile oils are major bioactive constituents of propolis, and they contribute to its special aroma [79,80]. They also, partially, contribute to the strong antimicrobial, antioxidant, and anticancer activities of propolis [79,81,82]. The volatile fraction of propolis varies in each sample even within a single country due to plant source and climate [79]. For instance, cumulative knowledge shows that volatile oils in propolis found in countries surrounding the Mediterranean depend mainly on the botanical origin. They primarily comprise poplar-derived compounds (e.g., benzoic acid and its esters and oxygenated sesquiterpene  $\beta$ -eudesmol) and conifer-derived compounds such as the hydrocarbon monoterpene  $\alpha$ -pinene [80]. Interestingly, the number of volatile compounds derived from a single type of propolis is also reported to vary according to extraction techniques. In this regard, reports from China show that traditional hydrodistillation, steam-distillation extraction, and dynamic headspace sampling could characterize around 12, 40 and 70 type of volatile components of propolis, respectively [79]. Moreover, the level of antimicrobial activity of volatile compounds of propolis greatly depends on their extent of purification [82].

Thanks to its countless bioactive elements, propolis enjoys a range of versatile biological and pharmacological properties including antimicrobial, antiviral, antifungal, antioxidant, anti-inflammatory, antineoplastic, antiaging, and cytostatic properties. In addition, it is considered a perfect natural food preservative due to its antimicrobial activity [35,38,65,66,68,71]. Because of its enormous health-promoting activities, propolis is widely used as a dietary supplement in many countries, especially in Japan [37–39].

Propolis is not suitable for use in its crude state since it may contact harmful materials e.g., asphalt from the road [68]. Using solvents like ethanol, glycerol, chloroform, ether and acetone or water is necessary to get rid of hazardous substances and to increase its yield of bioactive compounds [67,68]. Although water may be a cheap solvent, propolis has poor solubility in water. Therefore, propolis water extracts are 10-fold lower in their phenolic contents than ethanol extracts. In addition, they retain the strong flavor and aroma of propolis [68]. Moreover, propolis contains allergenic components: caffeic acids derivatives (e.g., 3-methyl-2-butenyl caffeate and phenylethyl caffeate), as well as benzyl salicylate and benzyl cinnamate [80]. Therefore, propolis use/consumption should be contraindicated in individuals with known allergies.

### 2.3. Bee Pollen: Its Constituents, Biological, and Pharmacological Activities

Bee pollen is an api-material that originally comprises male gametophytes or spermatophytes of flowers, which stick to bee body. Bee workers mix these floral pollens with honey, nectar, and bee saliva. The latter is rich in various enzymes e.g., amylase, catalase, as well as lactic acid bacteria, which cause pollen fermentation [36,83,84]. Hence, the tiny wind pollen grains collected by bees aggregate together to form granules or pellets of 1.4–4 mm in size [84].

In addition to water, which in order constitutes 20–30% and 6–8% of the content of recently collected and dried bee pollen, bee pollen contains around 200 chemical compounds. Like other bee products, its composition varies considerably according to botanical origin. Carbohydrates account for the most abundant ingredient (18.50–84.25%), and reducing sugars such as glucose, fructose, and sucrose constitute the vastest majority (13–55%). Other major elements include proteins and essential amino acids (5–60%), unsaturated and saturated fatty acids (0.15–31.26%), crude fiber (0.3–20%), nucleic acids (especially RNA), and various minerals (e.g., potassium, phosphorus, calcium, magnesium, zinc,

copper, manganese, and iron) [36,83–86]. In addition, its average total phenolic content is 30.59 mg gallic acid equivalents (GAE)/g, but again it varies considerably based on floral origin (0.69–213.20 mg GAE/g) [86]. Moreover, bee pollen is abundant in both water- and fat-soluble vitamins e.g.,  $\beta$ -carotene (vitamin A precursor), ascorbic acid (C), tocopherol (E), folic acid (B9), and other vitamin B, especially niacin. Bee pollen contains other elements that still need to be explored (2–5%) [83]. Therefore, bee pollen represents a perfect whole health-promoting food. In fact, comparisons of the percentages of nutrients in bee pollen with daily required intake of an adult individual revealed that few grams of bee pollen can meet daily human nutritional requirements [83,84].

Bee pollen demonstrates various biological properties and therapeutic activities e.g., antioxidant, anti-inflammatory, anti-lipidemic, anticancer, antiallergic, and antimicrobial [36,87]. Existing knowledge emphasizes its antiaging effects: it reduced the production of age-related pigment known as lipofuscin (induced by oral peroxidized corn oil or intravenous alloxan injection) in cardiac muscle, brain, liver, and suprarenal gland in aged mice (reviewed in [34]).

The composition of bee pollens depends primarily on its botanical source since nutrient contents (e.g., polyphenols) of pollen grains, which support their survival and fusion with female gametes, vary between different plants [83,84]. Storage conditions are of great importance were it to retain its biological activities. Bee pollen should be consumed fresh soon after collection. Most of its major elements (reducing sugars, total proteins, vitamin C, and provitamin A) are destroyed at 40 °C. Lyophilization damages its vitamin content while freezing is recommended for the storage of bee pollen since it does not affect its chemical structure [83].

Dry pollen pellets resist decay due to their tough outer coat, which comprises two layers made of cellulose and sporopollenin [88,89]. However, ingestion of bee pollen by humans may not yield its optimal nutritional value because the hard sporopollenin shell hinders access of digestive secretions to the nutrient-rich core of the pellet. Biological, chemical, and mechanical techniques are used to break bee pollen microcapsules in order to enhance its digestibility in the gut. However, these methods may be expensive or ineffective i.e., they degrade important nutrients via enzymatic activity [88,90]. Ultraviolet spectroscopy and high performance liquid chromatography-photo diode array show that processing bee pollen through the use of an edible lipid-surfactant mixture (Captex 355 and Tween 80) increases its yield of polyphenols and flavonoid aglycones [90].

#### 2.4. Safety Profile of Royal Jelly, Propolis, and Bee Pollen

Propolis exists in a plethora of commercial products that are directly consumed or used by humans e.g., lozenges, soap, toothpastes and mouth wash, creams, gels, cough syrups, wines, cakes, chewing gums, candies, shampoo, chocolate, skin lotions, processed meat, etc. [67]. In addition, royal jelly, bee pollen, and propolis are widely used as dietary supplements in many parts of the world [36–39]. Existing knowledge denotes no adverse effects from their consumption either in rodents or in humans [39,66]. The safety of pinocembrin, a flavonoid available in propolis and an approved drug in China, is documented since its elimination from the body is rapid [91]. The safety profile of bee pollen (both crude and processed) has been empirically tested. Oral consumption of bee pollen (up to 2 g/kg body weight) expressed no allergic reactions in mice including behavioral changes, salivation, diarrhea, respiratory or autonomic responses, restlessness, convulsions, tremors, or death [90]. In fact, the German Federal Board of Health acknowledges bee pollen as an official medicine [36].

Several lines of evidence support the anti-allergic effect of propolis and royal jelly. This effect involves inhibiting mast cell degranulation, suppressing cysteinyl-leukotriene release, as well as reducing serum histamine, IgG, and IgE levels in various allergic conditions by suppressing histamine H1 receptor [37,39,92]. Nevertheless, rare allergic reactions to bee products other than bee venom are documented in the literature. They are most frequent in small children [80,93]. Examples of such reactions comprise contact dermatitis in beekeepers following the handling of propolis, as well as contact stomatitis and oral mucositis after the usage of lozenges containing propolis [80]. Hence, bee products should be used with caution, especially in people with known allergies, pregnant and

lactating women, and small children [61]. In addition, bee products can be safely consumed after adequate processing. Processing involves removal of known allergens such as enzyme treatment of royal jelly and filtration of bee venom by stepped-gradient open column [2,94].

### 3. Evidence of Anti-Sarcopenia Effects of Bee Products from Preclinical and Clinical Studies

Though few animal models were used to examine the effect of bee products on sarcopenia, findings indicate that royal jelly, propolis, and bee pollen can induce both structural and symptomatic improvements and reduce behavioral dysfunctions associated with sarcopenia in rodents (Figure 1, Panel C). Both crude and protease-treated royal jelly (pRJ) significantly delayed age-related impairment of motor functions in d-galactose induced mouse model of aging [95], naturally aged sarcopenic mice [96], and in genetically heterogeneous head tilt (HET) mice—which exhibit vestibular dysfunction, imbalanced position, and inability to swim—by improving performance on grip strength, wire hang, horizontal bar, and rotarod tests [97]. Similarly, royal jelly improved physical performance in aged rodents—it significantly increased the number of crossings and swimming speed and prolonged swimming distance in water maze [96,98,99]. In addition, royal jelly decreased lipid accumulation in skeletal muscle [100], positively improved the size of muscle fibers, lowered age-related reduction of skeletal muscle weight [95–97,100], increased the differentiation and proliferation rate of muscle satellite cell, improved the regenerative capacity of injured muscle, and suppressed catabolic genes in aged mice with sarcopenia and in HET mice [96,97]. The muscle mass-accelerating effects of 10-HDA, a key fatty acid in royal jelly, were more pronounced in male animals than in females. However, 10-HDA mitigated the accumulation of adipose tissue in female mice [54]. It is note-worthy that pRJ had no effect on muscle strength and physical performance in humans aged 70 years and above [59].

The effects of other bee products on muscle mass were mostly positive. Bee pollen promoted body weight regain and increased the relative weight of the gastrocnemius muscle in eccentric exercising rats [90]. It also increased the absolute weights of plantaris and gastrocnemius muscles in malnourished old rats [36]. CAPE restored gastrocnemius muscle mass in rats on exhaustive exercise and in rats with ischemia reperfusion [101–103]. A study reported no effect of propolis ethanolic extracts (4% of diet) on the size of muscle or their level of myostatin in Nile tilapia. However, another interesting study reported significant increases in body protein deposition and body condition factor—an estimate of future growth, survival, and reproductive potential—in Nile tilapia post-larvae and fingerlings receiving 2.6 g propolis/kg of feed [104]. Nonetheless, these findings seem to be bound to fish. Interestingly, supplementing obese rats on high fat diet (HFD) with milk naturally enriched with long-chain polyunsaturated fatty acids (PUFA) and polyphenols from propolis significantly increased gastrocnemius muscle mass compared with whole milk and milk enriched with PUFA only [105]. Several molecular changes were associated with these effects. We elaborate on these changes in Section 4. Table 1 presents more details on treatments with bee products and key findings of the relevant studies.

### 4. Mechanisms of Action of Royal Jelly, Bee Pollen, and Propolis in Sarcopenia

Relatively few studies have explored the mechanism through which royal jelly, bee pollen, and propolis may be beneficial for sarcopenia. In vivo and in vitro studies included in this review uncovered a number of inter-related cellular and molecular events that underlie the effect of these bee products on skeletal muscle including suppression of catabolic genes, counteracting metabolic abnormalities, inflammation, and oxidative damages as well as enhancement of motor neuronal regeneration, promotion of stem cell function, and correction of the structure of gut microbiome (Figure 1, Panel D). These mechanisms are exclusively described in the coming paragraphs.

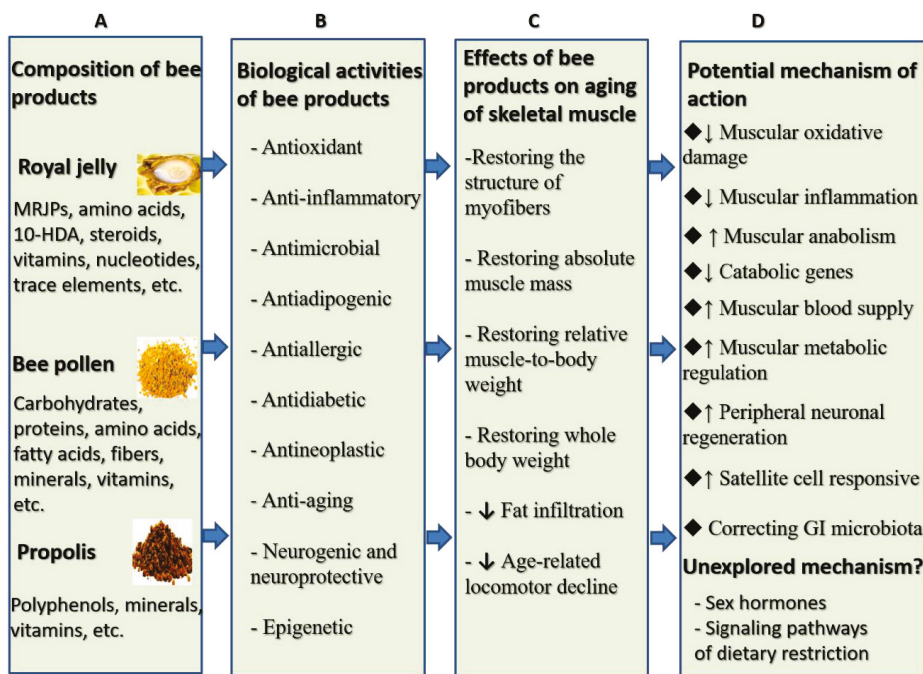


**Figure 1.** Brief summary of the chemical composition and biological activities of royal jelly, bee pollen, and propolis along with their effects on aged skeletal muscle and possible underlying mechanism. ↑ denotes increase, ↓ denotes decrease, MRJPs: major royal jelly proteins, 10-HDA: trans-10-hydroxy-2-decenoic acid, GI: gastrointestinal. Panels (A,B) describe the composition and the biological properties of royal jelly, bee pollen, and propolis. Thanks to their rich structure (which consists of proteins, polyphenols, vitamins, minerals, and trace elements) [2,28,37,49,59–61,68,80,86], these bee substances demonstrate a wide range of therapeutic activities such as counteracting inflammation and oxidative stress, in addition to many others [37–39,43,45,63,83]. Panel (C) summarizes the effects of royal jelly, bee pollen, and propolis on skeletal muscle. These products increased muscle mass [36,54,95,96] and restored muscle function in old [36,38,95–97] and exhausted [54,90,101,106] animal models. As shown in Panel (D), these effects originated from multiple molecular events that resulted in several therapeutic actions including amelioration of inflammation [36,38,90,101,107,108] and oxidative [95,106,109,110] damages, metabolic regulation [69,70,96,100,106,109,111,112], enhancements of satellite cell responsiveness [96,97], improving muscular blood supply [110], inhibition of catabolic genes [97], and promotion of peripheral neuronal regeneration [113]. However, future studies could examine the involvement of other possible mechanisms in the muscle-enhancing potential of these bee products such as the role of gut microbiome in the absorption of nutrient contents of bee products. It is not clear if these api-materials affect muscle quality via modulation of sex steroids and signaling pathways of dietary restriction, which are known to affect muscle integrity.

#### 4.1. Modulating Inflammatory Responses in Skeletal Muscle

The role that inflammation plays in skeletal muscle is not quite clear as it looks. Inflammatory mediators behave in a dual fashion in muscle cells. During injury, cytokines and chemokines stimulate muscle repair and regeneration via activation of myoblasts, a core event in muscle remodeling [108]. Similarly, serum and muscle levels of IL-6 temporarily increase following physical exercise, and IL-6 blocks the activity of catabolic cytokines such as TNF- $\alpha$ . On the other hand, chronic inflammation in muscle cells, which correlates with persistent mitochondrial dysfunction and metabolic

dyregulation, pathologically activates muscle fiber transformation and atrophy, eventually resulting in the development of sarcopenia [23,114]. It seems that bee products also act dually in skeletal muscle: they support the activity of cytokines that promote muscle remodeling [108] and suppress muscle-consuming cytokines [38,101,108]. In this regard, treating undifferentiated C2C12 myoblasts with ethanolic extracts of Brazilian propolis (100 µg/mL for 8 h) triggered the migration of RAW264 macrophage and increased their production of angiogenic factors (e.g., vascular endothelial growth factor A (VEGF-A) and metalloproteinase-12 (MMP-12)), chemokines (e.g., CCL-2 and CCL-5), and cytokines (e.g., IL-6, which increased by 40-folds). Propolis inhibited the expression of IL-1 $\beta$  and TNF- $\alpha$  at 4, 8, and 12 h of incubation. These effects were nuclear factor kappa B (NF- $\kappa$ B)-dependent given that propolis simultaneously increased nuclear translocation of p65 and p50 NF- $\kappa$ B proteins 3 h after treatment. Meanwhile, inhibiting I $\kappa$ B kinase (IKK) by BMS-345541 profoundly hindered the effect of propolis on the expression of CCL-2, CCL-5, and IL-6 by 66%, 81%, and 69%, respectively. Propolis also enhanced the expression of MAIL/I $\kappa$ B $\zeta$ . This molecule modulates chromatin and selectively induces the production of IL-6, leukemia inhibitory factor (LIF), and CCL-2 [108].

Chronic muscle tissue infiltration by inflammatory cells (e.g., leukocytes, neutrophils, and monocytes) activates oxidative and inflammatory signaling cascades that degrade cellular structures and promote necrosis such as inducible nitric oxide synthase (iNOS) and NF- $\kappa$ B [90,101,115]. CAPE and high levels (200 and 300 mg/kg) of crude and processed bee pollen reduced inflammatory cell infiltration into the gastrocnemius muscle of rats with muscle injury induced by eccentric exercise and ischemia reperfusion [90,101,102]. This effect was revealed by lower activity of myeloperoxidase, an indicator of neutrophil sequestration [101,102]. As such, CAPE and bee pollen not only suppressed lipid peroxidation (lower levels of malondialdehyde, MDA) but also inhibited the activity of myostatin and the production of muscle depleting cytokines and chemokines such as IL-1 $\beta$ ,  $\alpha$ 2-macroglobulin, and monocyte chemoattractant protein 1 (MCP-1) [36,38,90,101]. The underlying mechanism entailed downregulation of nuclear p65NF- $\kappa$ B and blockage of its consensus binding sites in skeletal muscle [101]. As a result, bee products increased muscle mass both in sarcopenic obese rat and malnourished old rats [36] and restored the structure of myofibers (despite the persistence of necrosis) compared with untreated eccentric exercising animals, which demonstrated necrotic and fragmented myofibers [90].

Royal jelly downregulated the activity of tumor necrosis factor receptor 1 (TNFR1) in the adipose tissue of aged obese rats receiving HFD [100]. TNFR1 interacts with TNFR2 to negatively regulate toll-like receptors (TLR) and Nod-like receptor signaling and stimulate excessive release of cytokines via activation of key inflammatory pathways such as NF- $\kappa$ B [107]. Mitigation of TNFR1 was associated with a significant increase of the weight of hind limb muscle and reductions in insulin levels, homeostatic model assessment of insulin resistance (HOMA-IR), serum lipids, muscle triglyceride levels, body weight gain, and abdominal fat weight. Therefore, royal jelly may protect against muscle loss in conditions involving impairment of the adipokine profile mainly through suppression of inflammatory responses associated with high fat mass, which is followed by correction of metabolic irregularities [100].

**Table 1.** Characteristics of Included Pre-Clinical and Clinical Studies Examining the Effect of Royal Jelly, Propolis, Bee Pollen, and their Constituents on Skeletal Muscle (N of studies = 24).

Bee Products/Their Constituents	Animal Model/Cell Line	Experimental Design	Outcome Measures	Results and Possible Related Mechanisms	References
<p><b>In vitro</b> Royal jelly and pRJ (500 µg/mL: 1, 2, 3, and 5 d)</p> <p><b>In vivo</b> Dietary royal jelly and pRJ (1% and 5% for 3 months)</p>	<p><b>In vitro</b> SC isolated from aged mice</p> <p><b>In vivo</b> 21-months old male C57BL/6 mice as a mouse model of sarcopenia</p>	<p><b>In vitro</b> EG1: royal jelly treated SC EG2: pRJ treated SC CG: untreated SC</p> <p><b>In vivo</b> EG1 and EG2: aged mice on 1% and 5% royal jelly, respectively EG3 and EG4: aged mice on 1% and 5% pRJ, respectively CG: untreated aged mice</p>	<p><b>In vitro</b> SC proliferation and differentiation into myotubes and AKT signaling.</p> <p><b>In vivo</b> No of SC, skeletal muscle weight, grip strength, regenerative capacity of injured muscle, and serum IGF-1.</p>	<p><b>In vitro</b> pRJ enhanced SC proliferation rate and differentiation into myotubes through activation of AKT signaling.</p> <p><b>In vivo</b> Royal jelly and pRJ significantly increased the number of SC, weight of skeletal muscle, grip strength, regenerative capacity of injured skeletal muscle, and IGF-1 serum level.</p>	[96]
<p>Intragastric 10-HDA (1.6 mM/kg body weight)</p>	<p><b>In vitro</b> L6 myotubes obtained from Osaka biobank</p> <p><b>In vivo</b> 7-weeks old male C57BL/6j mice</p>	<p><b>In vitro</b> EG: 10-HDA CG1: AICAR (1 mM) CG2: DM50 (0.1%)</p> <p><b>In vivo</b> EG: 10-HDA (1.6 mM) CG1: gum Arabic (5%)</p>	<p>Glucose uptake, AMPK signaling, and Glut4 translocation.</p>	<p>10-HDA increased glucose uptake into L6 myotubes following AMPK activation and Glut4 translocation to the plasma membrane. AMPK activation was induced by the upstream kinase Ca<sup>2+</sup>/calmodulin-dependent kinase β, independent of changes in AMP:ATP ratio and the liver kinase B1 pathway.</p>	[106]
<p>Intragastric royal jelly and pRJ (0.7 and 1.4 mg/kg body weight/d/90 d)</p>	<p>D-galactose induced mouse model of aging</p>	<p>EG1 and EG2: mice on 0.7 and 1.4 mg RJ, respectively EG3 and EG4: mice on 0.7 and 1.4 mg RJ hydrolysate, respectively CG: untreated mice</p>	<p>Antioxidant enzymes, body weight, muscular performance, memory, and learning.</p>	<p>Both doses of pRJ prevented age-related locomotor decline, preserved body weight, enhanced memory and learning, increased antioxidant enzyme activity, and inhibited the production of lipid peroxides.</p>	[95]

Table 1. *Cont.*

Bee Products/Their Constituents	Animal Model/Cell Line	Experimental Design	Outcome Measures	Results and Possible Related Mechanisms	References
Oral 10-HDA (12-60 mg/kg body weight/d/4 months)	Obese old rats and stressed mice as models of sarcopenia and depression (male and female Sprague-Dawley and 2-months old male and female BALB/c)	EG1 and EG2: aged obese rats on 10-HDA (12 or 24 mg/kg/d for 3.5 months) EG3 and EG4: stressed BALB/c mice on 10-HDA (30 or 60 mg/kg/d for 4 months) CG1 and CG2: untreated aged obese rats and untreated stressed BALB/c mice	Body weight, weight of abdominal adipose tissue, and muscle mass.	10-HDA significantly increased weight gain and weight maintenance in aged rats/mice undergoing behavioral stress without any change in diet consumption. It also significantly decreased adipose tissue in female animals and increased muscle mass in male rodents compared with untreated controls.	[54]
Dietary royal jelly and pRJ + MF powder diet (0.05% or 0.5%)	6-months old male HET mouse model of severe sarcopenia (background strains: BALB/c, C57BL/6, C3H, and DBA/2)	EG1 and EG2: HET mice on 0.05% and 0.5% royal jelly, respectively EG3 and EG4: HET mice on 0.05% and 0.5% pRJ, respectively CG1: untreated HET mice CG2: untreated young mice	No of blood cells and Pax7 SC, albumin, AST, ALT, T-CHO, TG, expression of muscle genes (MyoD, myogenin, myostatin) and catabolic genes (E3 ubiquitin ligases MuRF1, and atrogin-1). Behavioral tests: grip strength, wire hang, rotarod, and horizontal bar tests.	RJ and pRJ significantly delayed age-related impairment of motor functions, positively improved physical performance of treated mice in 4 types of tests (grip strength, wire hang, horizontal bar, and rotarod), lowered age-related muscular atrophy, increased No of Pax7 SC markers, and suppressed catabolic genes.	[97]
Intragastric royal jelly (100 mg/kg body weight/d/8 weeks)	10-months old male Sprague-Dawley on HFD as a rat model of sarcopenic obesity	EG1: aged rats on royal jelly and HFD EG2: aged rats on royal jelly CG1: untreated young rats CG2: untreated aged rats CG3: untreated old rats on HFD	Serum levels of T-CHO, TG, HDL-c, LDL-c, insulin, HOMA-IR. Skeletal muscle TC levels. Serum and adipose tissue levels of TNFR1. Percentage of weight gain of the body, abdominal fat, and tibialis anterior and hind limb muscles.	Royal jelly significantly decreased insulin levels, HOMA-IR, TNFR1 in serum and adipose tissue, serum lipids, muscle TC levels, body weight gain and abdominal fat weight and significantly increased the weight of hind limb muscle in aged rats on HFD compared with aged mice on HFD only.	[100]

Table 1. *Contd.*

Bee Products/Their Constituents	Animal Model/Cell Line	Experimental Design	Outcome Measures	Results and Possible Related Mechanisms	References
Oral royal jelly (1.0 mg/g body weight/d/3 weeks)	6–7 weeks old ICR mice	EG: endurance exercise + royal jelly CG1: sedentary rats on royal jelly CG2: endurance exercise+ distilled water CG3: sedentary rats on distilled water	CS, $\beta$ -HAD, and activities of AMPK and acetyl-CoA carboxylase in the soleus, plantaris, and tibialis anterior muscles.	Royal jelly increased CS and $\beta$ -HAD maximal activities in the soleus muscle compared with all CGs but failed to affect these enzymes in the plantaris and tibialis anterior muscles of sedentary mice compared with CG2. Royal jelly effects in the soleus muscle were mediated by AMPK and acetyl-CoA carboxylase activity.	[106]
Gavages/oral lyophilized royal jelly (50 and 100 mg/kg body weight/d/8 weeks)	18-months old (naturally aging) Wistar male rats as a model of aging	EG1 and EG2: aged rats on royal jelly 50 and 100 mg, respectively CG: aged rats on gavage solution of 0.9% NaCl.	Learning, spatial memory, and motor performance on Morris water maze.	Royal jelly improved learning, spatial memory, and motor performance e.g., increased the number of crossings, swimming speed, and swimming distance.	[98,99]
Oral pRJ (1.2 or 4.8 g/d over 1 year)	Institutionalized older adults (mean age: 78.5 $\pm$ 7.5 years, N = 199, N males = 99, N females = 95)	EG1 and EG2: pRJ (1.2 and 4.8 g/d), respectively CG: placebo	Handgrip strength, six-minute walk test, timed up and go test, and standing on one leg with eyes closed.	pRJ had no significant effect on handgrip strength, six-minute walk test, timed up and go test, and standing on one leg with eyes closed.	[59]
Brazilian propolis extract (100 $\mu$ g/mL/4–12 h)	<b>In vitro</b> Differentiated myoblast C2C12 cells and RAW264 macrophages isolated from mice	EGs: propolis (100 $\mu$ g/mL) CG1: ethanol (0.008%) CG2: DMSO (0.08%), CG3: IKK inhibitor (BMS-345541)	IL-6, LIF, CCL-2, CCL-5, CXCL-10, VEGF-A, COX2, MMP-12, migration of RAW264 macrophages, and activities of MAIL/IKK $\beta$ and NF- $\kappa$ B.	Propolis (at 8h) induced RAW264 macrophage migration, activated MAIL/IKK $\beta$ and NF- $\kappa$ B proteins p50 and p65, and increased levels of VEGF-A, COX-2, MMP-12, CCL-2, CCL-5, CCL-10, LIF, and IL-6. Propolis inhibited the production of IL-1 $\beta$ and TNF- $\alpha$ .	[108]
CAPE (1 and 10 $\mu$ M/3 min–12 h)	<b>In vitro</b> Differentiated L6 myoblast cells isolated from rats	EGs: CAPE (1, 10 $\mu$ M) CG1: insulin (100 nM) CG2: AICAR	2-Deoxyglucose uptake, AMPK and AKT signaling.	CAPE (10 $\mu$ M/1h) increased 2-Deoxyglucose uptake (same as insulin) and activated AMPK (same as AICAR, an AMPK activator). CAPE (10 $\mu$ M/3 min) activated AKT in a PI3K-dependent manner.	[111]

Table 1. *Cont.*

Bee Products/Their Constituents	Animal Model/Cell Line	Experimental Design	Outcome Measures	Results and Possible Related Mechanisms	References
Boropinic acid, 4-geranyloxyferulic acid, 7-isopentenylloxycoumarin from rats	<b>In vitro</b> Differentiated L6 myoblast cells isolated from rats	EGs: boropinic acid, 4-geranyloxyferulic acid, 7-isopentenylloxycoumarin, auroaptene (0.1, 1, 10 $\mu$ M), and propolis (0.001–1 mg/mL) CG1: insulin (0.1 $\mu$ M) CG2: DM50	GLUT4-mediated glucose uptake and GLUT4 translocation.	Propolis (1.0 and 1 mg/mL), 4-geranyloxyferulic acid, 7-isopentenylloxycoumarin, and auroaptene significantly increased glucose uptake and GLUT4 translocation.	[69]
<b>In vitro</b> A single oral dose of Brazilian propolis extract (250 mg/kg body weight) <b>In vivo</b> Artepillin C, coumaric acid, and kaempferide (1–10 <sup>4</sup> ng/mL for 15 min)	<b>In vitro</b> Differentiated L6 myoblast cells isolated from rats <b>In vivo</b> 5-weeks old male ICR mice	EGs: artepillin C, coumaric acid, and kaempferide (1, 10 $\mu$ M), and propolis (1–10 <sup>4</sup> ng/mL) CG1: insulin (100 nM) CG2: AICAR CG3: DM50	2-Deoxyglucose uptake, OGTT, maltase and sucrase-isomaltase activities in epithelial cells of the small intestinal, phosphorylation of AMPK, PI3K, AKT, AS160, IR, and GLUT4 translocation.	Polyphenols in propolis activated PI3K and AMPK signaling pathways and promoted GLUT4 translocation in L6 myotubes though only kaempferide increased glucose uptake. Propolis extract ( <b>In vitro</b> , 1 $\mu$ g) and <b>In vivo</b> significantly promoted the phosphorylation of IR, PI3K, and AMPK and increased GLUT4 translocation in rat skeletal muscle and subsequently decreased postprandial blood glucose levels. Propolis extract had no effect on $\alpha$ -glucosidase activity in the small intestine.	[70]
Gavage CAPE (5 and 10 mg/kg/d/5 d)	6-7-weeks old male adult Wistar rats	EG: CAPE + eccentric exercise CG1: normal rats + propylene glycol in saline CG2: acute eccentric treadmill exercise	Serum creatine kinase levels, IL-1 $\beta$ , MCP-1, COX-2, iNOS, leukocyte infiltration, and the extent of muscle fiber damage (vacuolization and fragmentation).	CAPE decreased serum creatine kinase, protein nitrotyrosine, PARP activity, MDA, leukocyte infiltration, skeletal muscle cell fragmentation and vacuolization, muscle levels of COX2, iNOS, IL-1 $\beta$ , MCP-1, and p65NF- $\kappa$ B activity to levels in resting CG1 compared with CG2.	[101]

Table 1. *Cont.*

Bee Products/Their Constituents	Animal Model/Cell Line	Experimental Design	Outcome Measures	Results and Possible Related Mechanisms	References
Dietary propolis (0.1% over 20 weeks)	MGO-induced muscle wasting in male C57BL/6NCR mice (4-weeks old)	EG: propolis + MGO CG1: MGO only CG2: propolis only CG3: untreated mice	Weight of EDL and soleus muscles, soleus and EDL levels of AGEs, inflammation-related molecules, and activity of glyoxalase 1.	Propolis had no effect on MGO-induced loss of EDL muscle but tended to increase the weight of the soleus muscle regardless of MGO treatment. Propolis decreased muscular levels of AGEs, IL-1 $\beta$ , IL-6, TLR4 and enhanced the activity of glyoxalase 1.	[38]
Dietary crude propolis (0.2% over 2 or 5 weeks)	HFD-induced muscle wasting in male C57BL/6 mice (4-weeks old)	EG: propolis + HFD CG1: HFD only CG2: untreated mice	16S rRNA of gut microbiota, serum levels of LPS, triacylglycerols and glucose, and skeletal muscle levels of inflammatory cytokine TLR4 expression.	Propolis (5 weeks) significantly decreased serum triacylglycerols, glucose, circulating LPS and down-regulated the expression TLR4 and inflammatory cytokine in muscle. It counteracted the effect of HFD on gut microbiota.	[116]
Oral propolis water extract (50 mg/kg body weight/d/6 weeks)	6-weeks old Sprague-Dawley rats	EG: propolis + eccentric exercise CG1: only eccentric exercise CG2: no treatment	Blood levels of glucose and insulin, MDA, SOD, GPX, and CAT in the liver and in the tissue of the liver and the gastrocnemius muscle.	Serum levels of glucose and insulin were significantly lower in EG and CG1 than CG2. Glycogen level in skeletal muscle was higher in EG and CG1 than CG2. Skeletal muscle levels of MDA were lower in EG than CG1 and CG2. Liver levels of SOD as well as gastrocnemius muscle levels of SOD, GPX and CAT were higher in EG only.	[109]
Gavage naturally-enriched milk with PUFA and propolis polyphenols (PUFA/P-M: 5 mL/kg body weight /85 d)	21-d old male Wistar rats	EG: HFD + PUFA/P-M CG1: HFD + water CG2: HFD + whole milk CG3: HFD + PUFA milk CG 4: standard chow + water N.B. All treatments were repeated in absence of HFD	Weight gain, mass of internal organs and the soleus and gastrocnemius muscles, and glucose tolerance.	Among all treatments in obese rats, only PUFA/P-m increased gastrocnemius muscle mass (tended to increase soleus muscle mass) and mesenteric fat and tended to lower LDL levels. It decreased the size of adipocytes compared with all groups except PUFA milk with no effect on body weight.	[105]

Table 1. *Cont.*

Bee Products/Their Constituents	Animal Model/Cell Line	Experimental Design	Outcome Measures	Results and Possible Related Mechanisms	References
Dietary propolis 4% (105 d)	Nile tilapia in net cages (males only)	EG: propolis rich diet CG: propolis free diet	Muscle morphometry and myostatin gene expression.	Propolis diet had no effect on muscle growth or myostatin gene expression at 35, 70, and 105 d.	[117]
Dietary propolis (1, 2, 3 and 4 g/kg of feed/45 d)	Nile tilapia post-larvae and fingerlings in tanks	EG: propolis rich diet CG: propolis free diet	Final weight, total and standard body length, survival, body composition, and intestinal villus height.	Propolis supplementation had no effect on weight, total and standard length, survival, and intestinal villus height. However, 2.6 g propolis/kg of feed significantly improved body protein deposition and body condition factor—an estimate of future growth.	[104]
Intraperitoneal CAPE (10 µM/kg 1 h before ischemia reperfusion)	Adult male Wistar rats undergoing ischemia reperfusion	EG: ischemia reperfusion + CAPE CG1: ischemia reperfusion CG2: sham	Neutrophil infiltration, serum creatine kinase, serum and gastrocnemius muscle levels of protein carbonyl, xanthine oxidase, and adenosine deaminase.	CAPE reduced neutrophil infiltration and serum creatine kinase as well as protein carbonyl, xanthine oxidase, and adenosine deaminase levels in the blood and gastrocnemius muscle.	[102,103]
Gavage propolis (1 g/kg body weight/d/2 weeks)	Adult male Wistar rats with 2-week hind limb unloading (HU)	EG: HU rats + propolis CG1: normal rats + propolis CG2: normal rats CG3: untreated HU rats	Soleus muscle weight, FCSA, myofiber number, apoptosis of endothelial cells, capillary to muscle fiber ratio, capillary number, luminal diameter, and capillary volume, levels of ROS, SOD-1, anti-angiogenic factors, and pro-angiogenic factors.	Propolis had no effect on soleus muscle weight or FCSA. However, the relative soleus muscle-to-body weight and the capillary to muscle fiber ratio of the soleus muscle were significantly higher in EG than in CG3. Propolis decreased the number of apoptotic endothelial cells, improved levels of SOD-1, ROS, and VEGF leading to increased capillary number, luminal diameter, and capillary volume in the EG to the levels of CG1 and CG2, which were all significantly different from CG3.	[110]
Gavage propolis (200-mg/kg body weight/d/28 d)	Adult female Wistar rats undergoing crush injuries of the sciatic nerve	EG: propolis CG1: curcumin CG2: methylprednisolone CG3: sham rats CG4: untreated rats with sciatic nerve injury	Gastrocnemius muscle mass, motor function, nerve fiber myelination, and nerve conduction.	Propolis and curcumin significantly restored gastrocnemius muscle mass, improved walking, nerve fiber myelination, and motor conduction to the gastrocnemius muscle compared with CG4.	[113]

Table 1. *Contd.*

Bee Products/Their Constituents	Animal Model/Cell Line	Experimental Design	Outcome Measures	Results and Possible Related Mechanisms	References
Dietary fresh monofloral bee pollen 5% or 10% (3 weeks)	Malnourished old male Wistar rats (22-month-old)	EG1 and EG2: refeeding diet + bee pollen 5% and 10%, respectively CG1: refeeding diet CG2: no treatment CG3: untreated normal weight rats	Body weight and composition, muscle mass, muscle protein synthesis rate, plasma cytokines, mitochondrial enzyme activity, and mTOR/p70S6kinase/4eBP1 signaling;	Bee pollen restored visceral and subcutaneous adipose tissues and increased plantaris and gastrocnemius muscle mass. 10% pollen restored the levels of cytokines to normal, boosted muscle protein synthesis, and increased complex IV activity while both 5% and 10% increased the activity CS and the phosphorylation of mTOR/p70S6kinase/4eBP1 signaling.	[36]
Oral crude and processed monofloral Indian mustard bee pollen (100, 200, and 300 mg/kg body weight/4 weeks)	Adult male Wistar rats and Swiss albino mice	EG1: neat bee pollen + acute eccentric swimming EG2: processed bee pollen + acute eccentric swimming CG1: no treatment CG2: bee pollen only CG3: acute eccentric swimming + vehicle gum acacia	Body weight, relative weight of the gastrocnemius muscle, SOD, GSH, MDA, NO, total protein content, lipid peroxidation, myostatin mRNA, $\beta$ -actin, mitochondrial complex I, II, III, and IV enzyme activity.	Crude (300 mg/kg) and processed (200 and 300 mg/kg) bee pollen prevented myofiber fragmentation and restored body weight and the relative weight of the gastrocnemius muscle as well as mitochondrial complex-I, -II, -III, and -IV enzyme activity to normal (CG1 and CG2) compared with CG3. Both bee pollen treatments decreased MDA, NO, total protein content, lipid peroxidation, and myostatin and increased SOD and GSH in skeletal muscle.	[90]

N.B. All studies were conducted in vivo unless otherwise indicated. pRfJ: protease-treated royal jelly. No: number. SC: Satellite cells. EG: experimental group. CG: control group. min: minute, d: day, h: hour, IGF-1: Insulin growth factor 1, AKT: Serine/threonine protein kinase, AS160: AKT substrate of 160 kDa, BALB/c: Bagg albino, 10-HDA: 10-Hydroxy-decanoic acid, ROS: reactive oxygen species, HET: genetically heterogeneous mice, AST: aspartate aminotransferase, ALT: alanine aminotransferase, T-CHO: total cholesterol, TLR4: toll-like receptors 4, TG: triglyceride, HFD: high fat diet, LPS: lipopolysaccharide, HDL: high density lipoprotein, LDL: low density lipoprotein, HOMA-IR: homeostatic model assessment of insulin resistance, PUFA: polyunsaturated fatty acids, TNFR1: tumor necrosis factor receptor 1, HU: hind limb unloading, IKK: I $\kappa$ B kinase, DMSO: dimethyl sulfoxide, AICAR: 5-aminoimidazole-4-carboxamide ribonucleoside, CAPE: caffeic acid phenethyl ester, AGEs: advanced glycation end products, MMP-12: metalloproteinase-12, MyoD: myogenic differentiation 1; VEGF: vascular endothelial growth factor, NF- $\kappa$ B: nuclear factor kappa B, MDA: malondialdehyde, SOD: superoxide dismutase, CAT: catalase, and GPX: glutathione peroxidase, LIF: leukemia inhibitory factor, CXCL-10: chemokine (C-X-C motif) ligand 10, CCL: C-C chemokine ligand, MCP-1: monocyte chemoattractant protein-1, COX-2: cyclooxygenase-2, iNOS: inducible nitric oxide synthase, PARP: poly (ADP-ribose) polymerase, AMPK: adenosine monophosphate activated protein kinase, P3K: phosphatidylinositol 3-kinase, IR: insulin receptor, GLUT4: glucose transporter 4, OGTT: Oral Glucose Tolerance Test, FCSA: fiber cross-sectional area, mTOR: mammalian target of rapamycin, p70S6kinase: p70 ribosomal proteins S6 kinase, 4eBP1: eukaryotic translation initiation 4E-binding protein 1, SOD: superoxide dismutase, GSH: glutathione, MDA: malonaldehyde, NO: nitric oxide, MGO: methylglyoxal, EDL: extensor digitorum longus, IL-6: interleukin-6, IL-1 $\beta$ : interleukin-1 $\beta$ , TLR4: toll-like receptor 4, CS: citrate synthase,  $\beta$ -HAD:  $\beta$ -hydroxyacyl coenzyme A dehydrogenase.

#### 4.2. Counteracting Oxidative Stress in Skeletal Muscle

High production of reactive oxygen species (ROS) in skeletal muscle tissues has serious destructive effects, which alter the integrity of skeletal muscle resulting into fatigue, muscle wasting, and muscle weakness [90,101]. Sources of intramuscular ROS are numerous including mitochondrial dysfunction (e.g., alteration of mitochondrial enzymes in the respiratory chain as well as enzymes responsible for  $\beta$ -oxidation), neutrophil infiltration, and the activity of cytokines and major muscle degrading molecules such as myostatin [21,36,38,101,102,118]. Oxidative and nitrosative damages in skeletal muscle tissues are mediated by the activity of numerous pro-oxidant enzymes that are associated with inflammatory processes such as cyclooxygenase-2 (COX-2) and iNOS [101]. ROS triggers the activity of corrosive molecules such as poly (ADP-ribose) polymerase (PARP), xanthine oxidase, and adenosine deaminase, which contribute to DNA damage, lipid peroxidation (e.g., increased MDA), and protein nitrotyrosylation as well as ATP catabolism in muscle tissues [101,102].

Royal jelly enhanced the activity of antioxidant enzymes and suppressed lipid peroxidation in a d-galactose induced model of aging [95]. Two weeks of propolis treatment in rats undergoing hind limb unloading significantly reduced nuclear ROS levels and numbers of apoptotic endothelial cells in the soleus muscle to levels similar to normal rats [110]. Moreover, propolis significantly suppressed MDA activity in skeletal muscle and increased liver levels of SOD as well as gastrocnemius muscle levels of SOD, glutathione peroxidase and catalase in rats on eccentric exercise training (70%  $\text{VO}_2\text{max}$  treadmill running exercise for 60 min) compared with rats receiving exercise alone or no treatment [109]. In addition, intraperitoneal pre-administration of CAPE (60 min before induction of ischemia reperfusion) significantly ameliorated the effects associated with high ROS levels, which accompany acute ischemia such as protein peroxidation and ATP catabolism in the gastrocnemius muscle [102].

Bee products probably reduced ROS production via regulation of the activity of mitochondrial enzymes. Royal jelly increased the maximal activity of citrate synthase (CS) and  $\beta$ -hydroxyacyl coenzyme A dehydrogenase ( $\beta$ -HAD) in the soleus muscle of rats on endurance training [106]. Bee pollen restored mitochondrial complex-I, -II, -III, and -IV enzyme activity to normal, increased SOD and glutathione, and reduced MDA, NO, and total protein content in the gastrocnemius muscle of rats on exhaustive exercise [90]. It also increased the activity of CS and complex IV in malnourished old rats via a mechanism that involved activation of mTOR [36]. mTOR is a major signaling pathway that regulates various signaling cascades involved in metabolism and autophagy such nuclear respiratory factor 2 (NRF2) [2]. Therefore, it is possible that the antioxidant activity demonstrated by bee products, particularly that expressed in the mitochondria, is associated with their metabolic and hypoglycemic activities. For instance, 10-HDA increased expression of peroxisome proliferator-activated receptor- $\gamma$  coactivator-1 $\alpha$  (PGC-1 $\alpha$ ) in skeletal muscle of diabetic mice [112,119]. Similarly, aged mice treated with amino acids similar to those found in royal jelly demonstrated improved size of muscle fiber by increasing PGC-1 $\alpha$  mRNA levels. PGC-1 $\alpha$  functions as a key regulator of sirtuin 1, which limits ROS production through stimulation of mitochondrial biogenesis and ROS defense system, thus protecting metabolically active tissues against oxidative damage [120]. Mechanistically, when PGC-1 $\alpha$  gets activated, it interacts with other bioactive molecules such as muscle-specific transcription factors to stimulate the expression of genes that induce mitochondrial oxidative metabolism in brown fat and fiber-type switching in skeletal muscle [121].

The antioxidant activity of royal jelly and CAPE might be related to their strong capacity to activate the master redox-active NRF2 signaling pathway [73,122], which stimulates the production of internal antioxidants such as heme oxygenase-1 (HO-1), which scavenge free radicals [123]. Meanwhile, NRF2 and HO-1 block ROS production indirectly via suppression of inflammatory reactions [122]. In this context, CAPE reduced degenerative myopathy in rats on eccentric exercise via a complex mechanism that involved inhibition of NF- $\kappa$ B and its downstream pro-oxidant COX-2 and iNOS [101]. Correspondingly, CAPE decreased markers of oxidative cellular damages (protein carbonyl, protein nitrosylation, xanthine oxidase, and adenosine deaminase) associated with ischemia reperfusion

and eccentric exercise in the gastrocnemius muscle [101–103]. In this regard, CAPE operated via a mechanism that involved inhibition of neutrophil and leukocyte infiltration into the gastrocnemius muscle, which was associated with decreased levels of myeloperoxidase. Myeloperoxidase contributes to excessive production of ROS and oxidative organ damage through a mechanism that embroils increased synthesis of hypochlorous acid [101,102]. Furthermore, CAPE accelerated purine salvage for ATP synthesis and inhibited ROS-induced lipid peroxidation via attenuation of the activity of adenosine deaminase [102].

In summary, the reported antioxidant effects of bee products were multifaceted involving increased production of antioxidant enzymes [90,95,109,110], and decreased ROS production [90,101–103,110] (secondary to reduction of inflammatory cell infiltration into skeletal muscle) [90,101–103], and restoration of mitochondrial activity [36,90,106].

#### 4.3. Metabolic Regulation

Skeletal muscle is the main tissue that utilizes insulin for glucose uptake. Insulin regulates mitochondrial oxidative phosphorylation of proteins in human skeletal muscle and contributes to calcium mobilization from the sarcoplasmic-endoplasmic reticulum to mitochondria to stimulate the translocation of glucose transporter 4 (GLUT4) to the cell surface for glucose uptake. This process improves muscle protein synthesis in healthy people when the delivery of amino acids to skeletal muscle is increased, eventually leading to increased muscular mass [124–126]. Insulin resistance and glucose intolerance increase with old age evoking muscle loss. In this respect, hypoglycemic agents such as metformin can improve skeletal muscle metabolism via activation of adenosine monophosphate activated protein kinase (AMPK) [21].

AMPK, a heterotrimeric complex that consists of a catalytic subunit and two regulatory subunits, is an intracellular energy sensor that regulates glucose and lipid metabolism. It gets activated when cellular energy is depleted through allosteric binding of AMP or phosphorylation by AMPK kinase at Thr172 of the catalytic subunit by AMPK kinase. Upregulated AMPK activates signaling pathways that generate ATP from glucose and fatty acid oxidation, and it simultaneously blocks signaling that contributes to the synthesis of cholesterol, fatty acid, and triacylglycerol [111]. In addition, AMPK masters numerous signaling cascades such as Forkhead Box O transcription factor (FOXO) and AKT/mTOR, which regulate the expression of genes associated with inflammation, oxidative stress, mitochondrial function, autophagy, metabolism, and apoptosis [127,128].

The molecular events involved in the effect of bee products on catabolic genes and anabolic resistance in skeletal muscle could be much related to their hypoglycemic effects, which positively affect the quality of skeletal muscle. Evidence signifies a positive effect of royal jelly acid (10-HDA) on inflammation and autophagy via upregulation of AMPK, which subsequently alters NF- $\kappa$ B and NLRP3 inflammasome-IL1 $\beta$  signaling [129]. Positive effects of whole royal jelly on skeletal muscle are associated with improved insulin signaling [96,100]. In one study, royal jelly improved serum IGF-1 levels in aged rats and increased AKT signaling in satellite cells extracted from aged rats in a separate *in vitro* investigation [96]. In another study, royal jelly decreased fat mass and improved anabolic resistance in the skeletal muscle of old obese rats on HFD via downregulation of inflammatory responses in adipose tissue as indicated by downregulation of TNFR1. This effect was associated with enhanced sensitivity to insulin—portrayed by reduction of serum insulin level and HOMA-IR [100].

Japanese researchers proved that oral consumption of royal jelly and 10-HDA induced mitochondrial adaptation in the soleus muscle when accompanied with endurance training. These compounds also enhanced glucose uptake in skeletal muscle by inducing the phosphorylation of AMPK [106,112], an effect that was mediated by the upstream kinase Ca<sup>2+</sup>/calmodulin-dependent kinase $\beta$ —independently of changes in AMP:ATP ratio and the liver kinase B1 pathway. Activation of AMPK was followed by translocation of GLUT4 to the plasma membrane of L6 myotubes [106]. It is note-worthy that effects of royal jelly on mitochondrial biogenesis under endurance training were muscle-specific. In this respect, neither endurance training nor royal jelly alone had an effect on the

maximal activities of CS and  $\beta$ -HAD—the enzyme that catalyzes the rate-limiting step of  $\beta$ -oxidation of long-chain fatty acids—in the soleus muscle, which comprises type I fiber (around 35–45%) and type IIa (around 35–50%). On the other hand, royal jelly enhanced the activity of these enzymes in the soleus muscle of mice on endurance training. Of interest, endurance training increased the activity of CS and  $\beta$ -HAD in the plantaris and tibialis anterior muscles (which are mainly type II fiber with a total percentage of type IIb and type IIx fiber types of 90%) while royal jelly failed to exert an effect on these muscles in sedentary mice [106]. Nonetheless, the observed effects of royal jelly in the soleus muscle represent a merit. This is mainly because the oxidative type I fibers (e.g., soleus muscle) naturally undergo higher protein turnover (especially degradation), which makes them unable to grow in size or respond properly to insufficient nutrient intake [130].

Several lines of evidence indicate that propolis may affect muscle quality through the regulation of glucose metabolism [69,70,109,111]. This effect was vividly depicted *in vivo* by increased glycogen level in skeletal muscle and reduced serum levels of glucose and insulin [109]. Same as insulin, ethanolic extracts of propolis and CAPE induced glucose uptake [69,70,111] and potentiated insulin-mediated AKT activation and glucose uptake in differentiated L6 myoblast cells [111]. Likewise, Italian propolis at concentrations of 0.1 and 1 mg/mL as well as 4-geranyloxyferulic acid and auraptene (2 oxypropenylated phenylpropanoids, which are abundant in propolis) remarkably increased GLUT4 translocation to the plasma membrane and accelerated GLUT4-mediated glucose uptake in L6 skeletal myoblasts. The effect of propolis at a concentration of 11 mg/mL was significantly superior to the effect of insulin (0.1  $\mu$ M), which was used as a positive control [69].

Similar to royal jelly, the effects of propolis (1  $\mu$ g/mL), CAPE (10  $\mu$ M), artepillin C, coumaric acid, and kaempferide on glucose metabolism occurred via activation of AMPK. These effects were comparable to those of 5-aminoimidazole-4-carboxamide ribonucleoside (AICAR), a potent AMPK activator. In the meantime, co-treatment with inhibitors of AMPK (e.g., compound C) and of phosphatidylinositol 3-kinase (PI3K) (e.g., LY-294002) blocked the effects of CAPE [70,111]. Phosphorylation of AMPK results in activation of the insulin receptor (IR) and subsequent phosphorylation of PI3K followed by activation of AKT and protein kinase C (PKC) leading to GLUT4 translocation and subsequent activation of several molecules that modulate insulin-stimulated glucose transport, eventually leading to glucose influx into cells of several tissues such as skeletal muscle and adipose tissue [69,70,111]. It is worth noting that the effects of CAPE on AMPK and AKT were quick (within 1 h and 3 min, respectively), and they vanished quickly (both molecules returned back to their basal levels within 12 h and 30 min, respectively) [111].

#### 4.4. Enhancement of Muscle Protein Synthesis

Imbalance between muscle protein synthesis and degradation is associated with low protein intake and altered efficiency of the GI tract in old age, which triggers skeletal muscle loss and poor physical performance [36,40], given that proteins are the main building blocks of muscle myofibers. Moreover, transmembrane proteins and micro-peptides (e.g., myomixer and myomaker/Tmem8c) contribute to the formation of myofibers by promoting myoblast fusion via a mechanism that involves appropriate localization of Tmem8c at the plasma membrane of myoblasts allowing trafficking related to palmitoylation of C-terminal cysteine residues and C-terminal leucine [17]. Amino acid supplements (e.g., leucine, a master dietary regulator of muscle protein turnover, and its metabolite  $\beta$ -hydroxy  $\beta$ -methylbutyrate) and early refeeding with high protein diet (especially fast digestive proteins) can preserve muscle mass and function, revert sarcopenia, and enhance mobility and quality of life (QoL) by correcting age-related nutritional deficiencies, muscle protein turnover, and immune dysregulation—these effects are even greater when combined with other nutrients like vitamin D or omega 3 fatty acids as well as with physical exercise [6,131–138].

Research indicates that age-related skeletal muscle wasting results mainly from insufficient delivery of amino acids to skeletal muscle due to dysregulations in the activity of mTORC1- and activating transcription factor-4 (ATF4)-mediated amino acid sensing pathways. Meanwhile, interventions that

ameliorate age-related damages in skeletal muscle operate primarily by reversing alterations in the delivery of amino acids to skeletal muscle via upregulation of mTORC1 and/or ATF4 [139]. mTORC1 is a nutrient sensing protein that acts as a core regulator of protein metabolism. It is sensitive to amino acids, energy status (ATP), stress (e.g., oxidative stress), and growth factors (e.g., insulin), which all can regulate its signaling [2,136]. Nevertheless, bioavailability of amino acids is necessary for growth factors to effectively activate mTORC1. Even more, amino acids on their own can adequately activate mTORC1 [136]. Evidence from preclinical and human studies confirms that ingestion of essential amino acids (similar to those found in royal jelly and bee pollen such as valine) increases cellular bioavailability of amino acids, which is associated with activation of the endothelial nitric oxide synthase (eNOs) pathway. eNOs further upregulates mTORC1 kinase. Translocation of mTORC1 from the cytosol to the surface of lysosomes is associated with improved mitochondrial biogenesis and cellular oxidative capacity in skeletal muscle due to activation of its substrates: P70 ribosomal proteins S6 kinase (S6K) and eukaryotic translation initiation 4E-binding protein 1 (eIF4E, also known as 4eBP1) [120,135,136].

As shown in Table 1, royal jelly and 10-HDA significantly increased muscle mass [54,96,100] and improved motor performance in aged rats [95,98,99]. In addition, dietary supplementation with monofloral bee pollen significantly improved the rate of muscle protein synthesis and restored muscle mass in emaciated old rats via upregulation of mTOR and two related downstream controllers of protein translation: p70S6k and 4eBP1, which were suppressed in malnourished old rats [36]. Although propolis improved various muscle-related parameters, its effect on muscle mass in rodents was limited—relative to royal jelly and bee pollen. However, it fostered muscle protein deposition in post-larva Nile tilapia [104]. Moreover, milk naturally enriched with PUFA and polyphenols from propolis remarkably increased the weight of the gastrocnemius muscle of growing obese rats while whole milk and milk enriched with PUFA only could not express any effect on skeletal muscle [105]. Therefore, this finding denotes that propolis could have enhanced the delivery of amino acids available in milk to skeletal muscle leading to its growth. Altogether, it is likely that the observed anabolic effects of royal jelly and bee pollen are associated with their high content of proteins and amino acids [32,36,83–86].

#### 4.5. Suppression of Catabolic Activity in Skeletal Muscle

Skeletal muscle tissues represent the largest protein store in the human body (30–45% of total protein). Muscular mass, strength, and functions are greatly governed by the rates of muscle protein synthesis and turnover [124]. Muscle protein metabolism is regulated by the interaction of a wide range of genes. Aging is associated with various stresses, which increase the expression of catabolic genes such as E3 ubiquitin ligases MuRF1 and atrogin-1 (MAFbx). These genes heighten the occurrence of age-related muscular atrophy [97]. Oral consumption of royal jelly by aged HET mice resulted in lower levels of catabolic genes (e.g., MuRF1 and MAFbx), which were similar to those in young mice. In the meantime, the expression of these genes in the control mice was high indicating that royal jelly can delay age-related muscular apoptosis by suppressing the activity of catabolic genes [97]. Two other studies reported that CAPE suppressed catabolism that contributed to degenerative myopathy in the gastrocnemius muscle of rats undergoing eccentric exercising or femoral artery ligation as reflected by decreased serum levels of creatine kinase, a marker of muscular proteolysis [101–103]. Apart from skeletal muscle, CAPE was reported to protect heart muscle against age-related deteriorations such as accumulation of lipofuscin, nuclear irregularity, mitochondrial degeneration, and myofilament disorganization and disruption [33].

The molecular mechanism underlying blockage of muscle proteolysis by bee products in sarcopenic rodents involves an interplay of various signaling pathways. Royal jelly and bee pollen activated mTOR and its substrate AKT, which are suggested to inhibit muscular proteolysis [36,96]. Similar to the effect of royal jelly on catabolic genes in HET mice, treating both L6 myoblasts and rats with propolis, CAPE, and kaempferide resulted in potent activation of AKT in a PI3K-dependent manner [111], in addition

to phosphorylation of IR, PI3K, and AMPK [70]. AKT, a key substrate of mTORC2, is a conserved serine/threonine nutrient sensing protein kinase that belongs to the PI3k-related protein kinase family. Upon presence of growth factors, PI3k gets activated by IR substrate resulting in stimulation of a series of signaling cascades that involve activation of AKT, which leads to further activation of mTORC1. mTORC1 activates the phosphorylation of two main regulators of cap-dependent protein synthesis: S6K and eIF4E [2,140]. In addition, mTORC1 contributes to autophagy—a turnover process that involves clearance of dysfunctional organelles and long-lived protein aggregations with provision of energy and macromolecular precursors in return—by binding with AMPK resulting in phosphorylation of autophagy genes such as Unc51-like kinase 1 at different sites [140]. In fact, royal jelly is reported to fine-tune the transcriptional activity of the FOXO through modulating the activity of insulin/IGF-1 signaling [141]. FOXO plays a major role in the activation of AKT pathway, which implicates regulation of multiple stress–response pathways such as ROS detoxification and DNA repair and translation. In addition, the FOXOs family exerts a direct effect on certain muscle atrophy genes such as MUSA1 and a formerly uncharacterized ligase known as Specific of Muscle Atrophy and Regulated by Transcription (SMART) [142].

#### 4.6. Enhancement of Stem Cell Function

Reduction of the number and functional capacity of the muscle satellite cells is considered a core contributor to the development of age-related muscular dysfunction [96]. Induction of myogenesis via *in vivo* reprogramming of muscle satellite cells is a currently studied strategy that has not been successfully used for sarcopenia treatment yet [143]. On the other hand, treating sarcopenic rats with both royal jelly and pRJ was reported to increase the number of Pax7-positive satellite cells *in vivo* and *in vitro* (pRJ only). pRJ induced self-renewal of satellite cells via activation of AKT signaling [96,97]. AKT activity was associated with activation of IGF-1 as indicated by increased serum levels of IGF-1. IGF-1 plays a crucial role in the activation of various signaling pathways; it is believed to be a major mediator of muscle growth and repair that functions by stimulating the proliferation and differentiation of satellite cells into myotubes, albeit the exact mechanism is not clear yet [96]. Similarly, pRJ activated AKT-signaling pathway in satellite cells culture, which was associated with increased proliferation of myosatellite cells and their differentiation into myotubes—an effect that is contradictory to muscle loss. AKT is thought to contribute to the synthesis of muscular proteins and inhibition of muscle proteolysis [96].

#### 4.7. Counteracting Glycation Stress

Oxidative stress, inflammation, and insensitivity to insulin, which accompany advanced age, contribute to the production of advanced glycation end products (AGEs) via enhancement of the activity of the Receptor for Advanced Glycation End products (RAGE) [144,145]. AGEs destroy the protein and lipid ingredients of muscle tissues by promoting the production of destructive molecules such as free radicals and inflammatory cytokines [101,102,113]. Thanks to their potent antioxidant properties, polyphenolic compounds exert multifaceted anti-glycation functions. On one hand, they scavenge free-radicals and chelate transition metals that are involved in the synthesis of dicarbonyl intermediates subsequently resulting in inhibition of the formation of AGEs. On the other hand, polyphenolic compounds antagonize AGE receptors, mainly RAGE, and facilitate the removal of already formed  $\alpha,\beta$ -dicarbonyl intermediates such as methylglyoxal, promoting the degradation of AGEs [37,38,146]. Royal jelly is reported to downregulate the activity of RAGE, the main receptor for AGEs, in an aged model of cognitive impairment [147]. However, its anti-glycation effect has not been investigated in skeletal muscle yet. Propolis exhibits strong anti-AGE properties, which are superior to those of quercetin or chlorogenic acid, well-known natural AGE inhibitors. Its flavonoid fraction potentially impedes the synthesis of AGEs by trapping dicarbonyl intermediates [37]. Table 1 shows that propolis accelerated AGEs clearance in a model of muscle aging induced by administration of a precursor of AGEs (methylglyoxal) via activation of glyoxalase 1, an enzyme that eliminates

dicarbonyl compounds (key elements of AGEs) [38]. CAPE inhibited the production of AGEs-related molecules such as protein carbonyl in the gastrocnemius muscle of rats via blockage of the activity of xanthine oxidase and adenosine deaminase [101–103]. The latter negatively affects insulin signaling and promotes the development of hyperglycemia, which represents a favorable condition for the production of AGEs [148]. However, propolis could not counteract the wasting effects of AGEs that already occurred in the extensor digitorum longus muscle though it tended to restore soleus muscle mass. This finding denotes that different muscle tissues respond differently to treatment, probably based on their ratio of type I to type II fibers. It also signifies the importance of early use of bee products (e.g., propolis) for the prevention of AGEs formation in skeletal muscle in people with high risk for AGEs formation such as diabetics [38].

#### 4.8. Neuronal Regeneration

Neuronal denervation is a key factor that contributes to skeletal muscle loss, and it is related to a plethora of pathological conditions [3,149]. Experimental induction of oxidative stress and inflammation results in skeletal muscle atrophy through induction of denervation e.g., of sciatic nerve [150]. Injuries of peripheral nerves (e.g., sciatic nerve) interrupt mechanical transmission and microvasculature of the nerve and induce reperfusion. Reperfusion involves pooling of oxygen and nutrients promoting high emission of free radicals, which attack protein and lipid contents surrounding the injury site resulting in excessive tissue loss [113]. Likewise, alterations in gut microbiome in aged rats are associated with alterations in serum level of vitamin B12 and fat metabolism as well as reductions in the gastrocnemius muscle mass and sciatic response amplitude [151]. Furthermore, dysregulation of insulin-mediated GLUT4 activity in certain areas of the central nervous system impairs neuronal metabolism and plasticity [69]. Meanwhile, activation of PGC-1 $\alpha$ , a core regulator of mitochondrial content and oxidative metabolism, increases muscle fiber resistance to denervation and atrophy through downregulation of two ubiquitin-ligases involved in the ubiquitin-proteasome pathway: MuRF1 and Atrogin-1 [1,152].

Propolis treatment for four weeks restored gastrocnemius muscle weight and improved functional performance (e.g., walking) in rats with crush injury of the sciatic nerve. Effects of propolis were associated with increased nerve healing and regeneration as depicted by faster healing of the myelin sheath and ultra-structurally normal unmyelinated axons and Schwann cells. Investigations of motor conduction from the sciatic nerve to the gastrocnemius muscle indicated that nerve recovery induced by propolis treatment promoted optimal physical functioning by allowing motor conduction to reach the gastrocnemius muscle [113]. Neuroprotective effects of propolis in motor neurons are documented in the literature. Both kaempferide and kaempferol protected motor neurons against atrophy induced by the toxic copper-zinc superoxide dismutase in amyotrophic lateral sclerosis—a serious neurodegenerative disease that involves selective and progressive loss of motor neurons [65]. In addition, orally administered chrysin (a flavonoid that is copious in propolis) to rats intoxicated by 6-hydroxidopamine showed neuroprotective effects by mitigating neuroinflammation, enhancing levels of neurotrophins and neuronal recovery factors (e.g., brain derived neurotrophic factor and glial cell line-derived neurotrophic factor), and maintaining integrity of dopaminergic neurons resulting in better motor performance [72].

The release of acetylcholine (a neurotransmitter that regulates cognition) at the synaptic cleft of the neuromuscular junction is essential for motor neurotransmission, which controls excitation-contraction coupling and cell size. However, free radicals, cytokines, and AGEs impair neurotransmission by altering the production of acetylcholine [6,21,149,153]. On the other hand, upregulation of acetylcholine receptors improves neurotransmission [154]. Treatment with royal jelly may correct acetylcholine neurotransmission given its high content of acetylcholine (4–8 mM) [60]. In addition, royal jelly, propolis, and bee pollen are rich in antioxidant elements that have a potential to scavenge ROS and mitigate other pathologies that contribute to acetylcholine deficiency (e.g., neuroinflammation) [73,101–103]. In this respect, treatment of experimental models of carrageenan-induced hind paw edema with

hydroalcoholic extract of red propolis and its biomarker, formononetin, is reported to inhibit leukocyte migration and ameliorate inflammatory neurogenic pain induced by injections of formalin and glutamate [115]. However, investigations of the action of bee products on neurotransmission are very scarce.

#### 4.9. Improving Muscular Blood Supply

Aging is associated with higher onset of atherosclerosis and restenosis, which involve vascular and microvascular damages that result from hyperproliferation of vascular smooth muscle cells (VSMCs) [155]. Muscle unloading (e.g., in sedentary lifestyle) involves chronic neuromuscular inactivity, which results in reductions in capillary number, luminal diameter, and capillary volume as well as heightened production of anti-angiogenic factors, such as p53 and TSP-1 in skeletal muscle [110]. Microvascular alterations and impaired nitric oxide (NO) production are key causes of decreased blood flow to the skeletal muscle. Poor muscular blood supply induces muscle wasting via a mechanism that entails impaired glucose metabolism and suboptimal protein anabolism [156,157]. In addition, ischemic injury in skeletal muscle is associated with high ROS release from polymorphonuclear leukocytes, which infiltrate muscle tissues. Free radicals alter cellular structure and function by attacking lipid and protein biomolecules that exist in the structure of biological membranes, enzymes, and transport proteins [102]. Therefore, improving vascularization and blood supply to skeletal muscle is a possible mechanism for the prevention of muscle wasting.

Mitchell and colleagues examined changes in microvascular blood volume, microvascular flow velocity, and microvascular blood flow in the quadriceps muscle following treatment with 15 g of amino acids in young and old subjects (20–70 years old). They detected improvements in all the 3 parameters only in young groups, and those effects were associated with proper insulin activity. Thus, the authors suggested that refeeding effects on muscular blood supply may be hindered by dysfunctions in postprandial circulation and glucose dysregulation [157]. Bee products such as bee pollen and propolis have a potential to boost microcirculation and correct pathologies that contribute to vascular dysfunction such as hyperglycemia and dyslipidemia [36,155]. In this context, CAPE, one of the basic constituents of propolis, was reported to combat vascular damages by counteracting the proliferative activity of platelet-derived growth factor. The molecular mechanism involved inducing cell-cycle arrest in VSMCs via activation of p38mitogen-activated protein kinase (MAPK), which was associated with accumulation of hypoxia-inducible factor (HIF)-1 $\alpha$ —mainly due to inhibition of HIF prolylhydroxylase, a key contributor to proteasomal degradation of HIF-1 $\alpha$ —and subsequent induction of HO-1 [155]. In the same regard, supplementing rats undergoing capillary regression (resulting from two weeks of hind limb unloading) in the soleus muscle with two daily intragastric doses of propolis for two weeks restored capillary number, capillary structure, capillary volume, and capillary to muscle fiber ratio through a mechanism that involves inhibition of anti-angiogenic factors and activation of pro-angiogenic factors (e.g., VEGF). The relative muscle-to-body weight in treated animals was higher than in the unloaded control animals, and the number of TUNEL-positive apoptotic endothelial cells in the soleus muscle was similar to that in the normal control animals [110]. Likewise, bee pollen (both neat and processed) increased blood vessels in the gastrocnemius muscle of rats undergoing muscle injury because of vigorous exercise [90]. Treating C2C12 myoblasts with propolis ethanolic extract increased VEGF production [108]. VEGF is a pro-angiogenic factor that contributes to angiogenesis by recruiting endothelial cells and promoting their differentiation to form new vascular networks. VEGF protects skeletal muscle undergoing unloading against the progression of capillary regression [110]. Its expression in skeletal muscle and associated angiogenic response increase following exercise due to change in the activity of HIF-1 $\alpha$  and AMPK. It promotes the generation of ATP following mitochondrial biogenesis in order to meet oxygen demand [158]. Altogether, these reports signify that bee products and endurance exercise share common mechanisms to produce their vitality effects in skeletal muscle.

#### 4.10. Improving the Composition of Gut Microbiome

Bee products such as royal jelly and propolis display potent antifungal, bactericidal, microbicidal, anti-inflammatory, antioxidant, and healing effects [2,66]. Most bee products investigated in this review were administered orally. Therefore, it is likely that their therapeutic effects may start locally within the GI tract, which frequently undergoes propagation of harmful endobacteria, inflammation, aberrations, and permeability in advanced age [10,24,152]. In this respect, Roquette and colleagues [116] supplemented C57BL/6 mice on HFD with crude propolis (0.2%) for two and five weeks. HFD increased the proportion of the phylum Firmicutes as well as levels of circulating lipopolysaccharide (LPS) and inflammatory biomarkers. DNA sequencing for the 16S rRNA of the gut microbiota revealed that five weeks of propolis treatment rendered the microbiota profile almost normal. Compared with untreated mice, propolis-supplemented animals demonstrated lower levels of serum triacylglycerols, glucose, and circulating LPS, along with reduced expression of TLR4 and inflammatory cytokines in skeletal muscle [116].

Lactic acid bacteria profusely exist in bee saliva and all bee products [36,83,84]. Various species of lactic acid bacteria have been experimentally used to correct GI dysbiosis and related muscle wasting [159,160]. Moreover, oligosaccharides have been chemically isolated from bee products [32,161]. These api-materials are classified as prebiotics, fermented non-digestible compounds that promote the proliferative activity of health-promoting bacteria [24,161]. Supplementing frail old adults with fructooligosaccharides expressed positive effects on skeletal muscle strength (handgrip) and endurance (exhaustion) [162]. On the other side, microbiome of the gut can affect the biological activity of bee products. The literature shows that certain endobacteria transform dietary polyphenols into phenolic acids, which can easily access the circulation and then cross the blood brain barrier to produce therapeutic effects [163]. Hence, it is important that future investigations of bee products among sarcopenic subjects examine the effect of these products on the composition of GI microbial population and its association with muscle-related outcomes.

## 5. Discussion

Age-related deteriorations in skeletal muscle are multifactorial in nature, which contributes to the high failure rates of drugs designed to target sarcopenia. Thus, there is a strong need for new therapeutic agents that express multidimensional effects in order to provide physically frail elders a chance to restore their health and QoL [21]. Given the scarcity of human trials using bee products among physically frail and sarcopenic subjects, cell culture and animal studies may provide useful information about the effect of bee products on skeletal muscle and help identifying their probable mechanism of action. Both in vivo and in vitro studies indicate that substances produced by honey bees such as royal jelly, bee pollen, and propolis can positively modulate basic cellular functions of myoblasts as well as mature myocytes. These products seem to be promising anti-sarcopenic agents because they can promote muscle protein synthesis [36,104], decrease mitochondrial oxidative stress [36,90,106], mitigate inflammation [38,90,101,108,115], improve muscular blood supply [102,110], enhance peripheral motor conduction [113], accelerate the removal of AGEs [38], counteract catabolism, and decrease markers of skeletal muscle atrophy [97,101–103].

One of the major pathologies underlying age-related skeletal muscle failure is insulin resistance, which alters glucose metabolism [3,4,21,118,130,164]. Numerous studies signify that bee products may protect against muscle wasting by correcting metabolic dysregulations in skeletal muscle via activation of some of the key nutrient sensing molecules [69,96,100,106,109,111]. In this respect, bee pollen permitted mTORC1 to mitigate anabolic resistance through the regulation of muscle protein and muscle growth in malnourished sarcopenic old rats [36]. Royal jelly and CAPE restored muscle mass and metabolism through activation of AKT, a substrate of mTOR [96,111]. Polyphenols in propolis [70], CAPE [111], and 10-HDA [106] activated AMPK resulting in enhanced skeletal muscle glucose uptake. In the meantime, royal jelly improved mitochondrial biogenesis in skeletal muscle via activation of AMPK [106]. AMPK and mTOR are master regulators of metabolism and autophagy [2,165]; they keep

muscle integrity by stimulating protein synthesis [21,22]. Accordingly, all these findings denote that bee products represent a promising nutritional strategy that can tackle skeletal muscle wasting in old age by correcting its underlying metabolic causes. However, the detailed physiological processes involved still need to be deeply unraveled in further investigations.

The activity of mTOR depends mainly on the bioavailability of essential amino acids in addition to many other molecules in the cellular microenvironment [136]. Evidence from preclinical and human studies confirms that ingestion of essential amino acids increases their cellular bioavailability, which is associated with upregulation of the activity of the nutrient sensing mTORC1 kinase following its translocation from the cytosol to the surface of lysosomes [135,136]. Research shows that ingestion of small amounts of essential amino acids (6.8 g) by healthy older adults could stimulate muscle protein synthesis by activating mTORC1 signaling even without involvement in resistance exercise training [137]. Other factors affect the capacity of essential amino acids to stimulate muscle protein synthesis. Amino acid bioavailability depends to a great extent on the bacterial strains of resident gut microbiome, which can either promote amino acid loss by degrading them or substantially contribute to their availability by producing some of them e.g., lysine [152]. Furthermore, amino acid supplements in old age do not enhance muscle protein metabolism, combat anabolic resistance, or improve muscle condition under sedentary conditions [25,166].

According to Table 1, different models of skeletal muscle injury (e.g., natural aging [96], sarcopenic obesity [54], AGE-induced muscle wasting [38], malnutrition-related muscle loss [36], exhaustive exercise [90,109], etc.) were used to evaluate the effect of bee products on skeletal muscle. The effects of bee products on muscle mass varied considerably: some studies reported that bee products increased muscle mass [36,54,90,96,100,105,113] and improved physical performance [95–99] while others could not or did not depict any significant change in muscle mass [38,102–104,110,117]. However, the latter revealed major beneficial effects related to the biology of skeletal muscle aging such as improved muscle protein deposition [104], enhanced activity of mitochondrial enzymes [106], decreased muscle infiltration by inflammatory cells, decreased muscle proteolysis, lowered lipid peroxidation and protein carbonylation [102,103], increased microvascular blood supply, heightened production of antioxidants [110], and increased clearance of AGEs from skeletal muscle [38]. These findings suggest that bee products may prevent the development of sarcopenia if supplemented earlier before the occurrence of muscle atrophy. In this regard, supplementing young football players with royal jelly for two months resulted in a significant increase in muscle and bone mass compared with control players who did not receive royal jelly [167].

As for the effect of bee products on sarcopenia in humans, we could locate only one randomized control trial (RCT), which examined the effect of pRJ (1.2 g/d or 4.8 g/d over 1 year) on muscle strength among institutionalized aged population. This study revealed no significant effect of pRJ on the tested muscular functions: handgrip strength, six-minute walk test, timed up and go test, and standing on one leg with eyes closed [59]. Nonetheless, such outcome indexes may not be sufficient to evaluate the overall effect of royal jelly on muscular performance and quality. In addition, the literature documents gut microbiome alterations-related to muscle loss in institutionalized old adults compared with older adults living in the community, which might affect the efficacy of nutritional therapies in this particular group [164,168,169].

The relation between muscle mass or strength and physical function in old people is not as direct or clear as originally presumed. Existing knowledge indicates that muscle strength may be intact in people with muscle loss. Likewise, decreased muscle strength may not necessarily alter physical performance [21,170]. Research notes that selection of interventions that merely increase muscle mass and/or strength entails ignoring valuable therapies that contribute to various biological processes of muscle recovery by interfering with pathologies conducive to muscle loss. More, combining functional measures of muscle performance with different comprehensive biomarkers (e.g., of metabolism, inflammation, oxidative stress, etc.) in skeletal muscle and the whole body may identify therapies that can positively affect muscle qualities independent of mass increase [21]. In support of this argument,

treating sarcopenic elderly with oral amino acids (which represent only one ingredient of royal jelly or bee pollen) significantly increased whole-body lean mass 6 and 18 months after treatment as indicated by dual-energy X-ray absorptiometry. This effect was attributed to enhancement of insulin sensitivity and anabolism as portrayed by significant reductions in fasting blood glucose, serum insulin, HOMA-IR, and serum tumor necrosis factor- $\alpha$  (TNF- $\alpha$ ) as well as increase of serum level of IGF-1 and IGF-1/TNF- $\alpha$  ratio [171]. Animal studies lend further support to those reports. For instance, royal jelly had no effect on muscle differentiation genes (myogenic differentiation 1 (MyoD), myogenin, myostatin) in sarcopenic mice, indicating that royal jelly may not improve age-related deterioration of muscle strength—once it occurs. On the other hand, royal jelly significantly reduced the progression of muscle atrophy by decreasing the expression of catabolism genes E3 ubiquitin ligases MuRF1 and atrogin-1 in old mice to levels similar to those in young mice [97]. Royal jelly also stimulated the differentiation of satellite stem cells both *in vivo* and *in vitro* and improved the regenerative capacity of injured muscle [96,97]. Therefore, royal jelly treatment might reduce the progression of age-related muscular atrophy [59]. Future RCTs that evaluate the effect of bee products on muscle qualities and motor performance in humans should be properly designed to include biological markers of motor functioning along with behavioral measures.

Multifactorial conditions such as sarcopenia should be addressed by multimodal interventions. Nutrition and physical exercise are key strategies that can preserve muscle mass and function in older adults both in clinical and community settings [21]. Thus, it might be helpful to compare the effect of combining bee products with other conventional treatments such as other dietary elements and exercise given that factors such as physical activity and diet can interfere with or promote the effect of bee products on muscle qualities and disorders that underlie muscle weakness [105,106]. Fat mass increases with age, especially after age-related hormonal decline (e.g., after menopause), and it activates inflammatory processes that disturb body physiology [172]. In this regard, supplementing obese rats with milk naturally enriched with PUFA and polyphenols from propolis increased gastrocnemius muscle mass and tended to increase the mass of the soleus muscle. It decreased the diameter of adipocytes and tended to decrease serum levels of low-density lipoprotein. These findings suggest a role of propolis-enriched milk in the mitigation of sarcopenic obesity, albeit it had no effect on body weight [105]. On the other side, many studies show that exercise has significantly improved muscle mass and strength in sarcopenic seniors [4,42,132,173]. Propolis treatment of undifferentiated L6 myoblast selectively stimulated IL-6 production and inhibited pathological cytokines such as interleukin (IL)-1 $\beta$  and TNF- $\alpha$  [108]. This interesting *in vitro* investigation indicates that propolis can mimic the mechanism through which exercise induces skeletal muscle remodeling [23,114]. Evidence from preclinical studies shows that concurrent treatment of rats on endurance training with royal jelly enhanced mitochondrial adaptation in muscles that combine both type I and type II fibers such as the soleus muscle whereas neither royal jelly alone nor exercise alone could influence the activity of mitochondrial enzymes in that muscle [106]. Moreover, bee pollen and propolis treatment of rats on exhaustive exercise increased the production of antioxidant enzymes, blocked the production of free radicals, promoted glycogen use in the skeletal muscle and liver, and restored muscle fiber structure [90,109].

In most studies, whole royal jelly, bee pollen, and propolis were used. However, these products appeared in different forms e.g., neat vs processed bee pollen [90], water [109] vs ethanolic extracts [110] of propolis, lyophilized [98,99] and crude [97] vs enzyme-treated [59,95–97] royal jelly. Both processed bee pollen [36] and pRJ [97,106] had better effects compared with crude bee pollen and royal jelly. In addition, a large group of constituents of royal jelly and propolis were used such as 10-HDA [54,106], CAPE [69,101–103], artemillin C, coumaric acid, kaempferide [70], boropinic acid, 4-geranyloxyferulic acid, 7-isopentenylcoumarin, and auraptene [69]. 10-HDA was the only element in royal jelly that was tested in skeletal muscle. It enhanced glucose uptake via AMPK phosphorylation [106]. It also restored body weight, restored skeletal muscle mass (only in males), and reduced fat mass (only in females) in aged rats undergoing chronic stress [54]. CAPE is one of the most investigated

compounds in propolis: it enhanced skeletal muscle glucose uptake [111], inhibited cytokine and ROS production, prevented protein carbonylation, lipid peroxidation, and muscle proteolysis [101–103]. The effects of whole ethanolic extracts of propolis and CAPE on glucose uptake in skeletal muscle were comparable to those of insulin [69,109,111]. More, investigations of the effect of flavonoids and oxyprenylated phenylpropanoids abundant in ethanolic extracts of propolis on glucose uptake in skeletal muscle revealed superior effects of kaempferide [70], 4-geranyloxyferulic acid, and auraptene. Among 5 oxyprenylated phenylpropanoids derived from propolis, auraptene most potently activated GLUT4 translocation and accelerated glucose influx into skeletal muscle cells. Measurement of the incorporated amounts of these compounds into myotubes indicated that auraptene had the highest bioavailability among other effective compounds [69].

Matters concerning dosage and duration of treatment remain issues of concern should these compounds be used to prevent and treat sarcopenia. In addition, the effect of other active ingredients of bee products on skeletal muscle pathologies is worth investigation. For instance, MRJPs are reported to contribute to most therapeutic properties of royal jelly due to their rich amino acid content (up to 578 amino acids) [47]. In the meantime, the literature documents a potent regulatory effect of amino acids on skeletal muscle protein turnover [6,131,132]. Nonetheless, the effect of MRJPs on skeletal muscle were not studied until now.

Despite the details illustrated in this review, many questions remain unanswered. The most important question among all is which bee product or bee component can produce the best benefits against skeletal muscle senescence and under which circumstances? Sarcopenia is the result of several interrelated factors such as neuromuscular dysfunction, oxidative stress, metabolic alterations, poor blood supply, hormonal deficiencies (e.g., sex hormones), chronic inflammation, and lifestyle choices (e.g., physical inactivity and unhealthy diet) [21]. The effect of bee products on some of these factors are underaddressed (e.g., neuromuscular dysfunction, muscle blood supply, and gut microbiome) while some other have not been explored yet (e.g., sex steroids and their association with muscular function).

## 6. Conclusions

All animal studies discussed above indicate that royal jelly, propolis, and bee pollen as well as their key ingredients such as 10-HDA and CAPE might counteract age-related muscular decline, especially in early stages. These products operate by modulating most mechanisms that contribute to sarcopenia such as metabolic dysregulation, inflammation, oxidative stress, etc. However, more studies are needed to examine the specific cellular and molecular mechanisms of these products and other major ingredients that were not explored, such as MRJPs in royal jelly. Among all bee products, royal jelly has been used to improve muscular performance in humans, though at a small scale, without any reported side effects. Future RCTs that examine the effect of bee products on sarcopenia should consider individual variations (e.g., gender, general health, activity level, diet, etc.) and combine functional and subjective outcome measures with sound predictive biomarkers.

**Author Contributions:** Conceptualization, A.M.A.; methodology, A.M.A.; software, A.M.A.; validation, A.M.A.; writing—original draft preparation, A.M.A.; writing—review and editing, H.K.; supervision, H.K.; project administration, H.K.; funding acquisition, H.K. All authors have read and agreed to the published version of the manuscript.

**Funding:** This study was supported by the Strategic Research Program for Brain Sciences from Japan Agency for Medical Research and development, AMED, Japan (Grant No. 18dm0107100h0003).

**Conflicts of Interest:** The authors declare no conflict of interest.

## Abbreviations

4eBP1/eIF4E	Eukaryotic translation initiation 4E-binding protein 1
10-HDA	trans-10-hydroxy-2-decenoic acid
AGEs	Advanced glycation end products
AKT	A serine/threonine nutrient sensing protein kinase
AMP	Adenosine monophosphate
AMPK	Adenosine monophosphate activated protein kinase
ARE	Antioxidant response element
ATF4	Activating transcription factor-4
ATP	Adenosine tri-phosphate
COX	Cyclooxygenase
eNOs	Endothelial nitric oxide synthase
ER	Endoplasmic reticulum
FOXO	Forkhead box O
GI	Gastrointestinal
GLUT4	Glucose transporter 4
HET	Heterogeneous head tilt
HFD	High fat diet
HIF	Hypoxia-inducible factor
HO-1	Heme oxygenase 1
HOMA-IR	Homeostatic model assessment of insulin resistance
IKK	I $\kappa$ B kinase
IGFs	Insulin-like growth factors
IL	Interleukin
iNOS	Inducible nitric oxide synthase
IR	Insulin receptor
LESM	Lower extremity skeletal muscle mass
MAPK	Mitogen-activated protein kinase
MDA	Malondialdehyde
mTOR	Mammalian target of rapamycin
MMP-12	Metalloproteinase-12
MCP-1	Monocyte chemotactic protein 1
MRJPs	Major royal jelly proteins
MyoD	Myogenic differentiation 1
NF- $\kappa$ B	Nuclear factor kappa-B
NRF2	Nuclear factor erythroid 2/Nuclear respiratory factor 2
PGC-1 $\alpha$	Peroxisome proliferator-activated receptor gamma coactivator 1 alpha
PI3k	Phosphoinositide-3 kinase
PUFA	Polyunsaturated fatty acids
PKC	Protein kinase C
pRJ	Protease-treated royal jelly
QOL	Quality of life
RAGE	Receptor for Advanced Glycation End products
RCT	Randomized control trial
ROS	Reactive oxygen species
SDs	Standard deviations
S6K	P70 ribosomal proteins S6 kinase
SMART	Specific of Muscle Atrophy and Regulated by Transcription
TNF	Tumor necrosis factor
TNFR1	Tumor necrosis factor receptor 1
VEGF-A	Vascular endothelial growth factor A
VSMCs	Vascular smooth muscle cells

## References

1. Miljkovic, N.; Lim, J.Y.; Miljkovic, I.; Frontera, W.R. Aging of skeletal muscle fibers. *Ann. Rehabil. Med.* **2015**, *39*, 155–162. [[CrossRef](#)] [[PubMed](#)]
2. Kunugi, H.; Ali, A.M. Royal Jelly and Its Components Promote Healthy Aging and Longevity: From Animal Models to Humans. *Int. J. Mol. Sci.* **2019**, *20*, 4662. [[CrossRef](#)] [[PubMed](#)]
3. Welch, A.A.; Hayhoe, R.P.G.; Cameron, D. The relationships between sarcopenic skeletal muscle loss during ageing and macronutrient metabolism, obesity and onset of diabetes. *Proc. Nutr. Soc.* **2020**, *79*, 158–169. [[CrossRef](#)] [[PubMed](#)]
4. Keller, K. Sarcopenia. *Wien. Med. Wochenschr.* **2019**, *169*, 157–172. [[CrossRef](#)]
5. Wilkinson, D.J.; Piasecki, M.; Atherton, P.J. The age-related loss of skeletal muscle mass and function: Measurement and physiology of muscle fibre atrophy and muscle fibre loss in humans. *Ageing Res. Rev.* **2018**, *47*, 123–132. [[CrossRef](#)] [[PubMed](#)]
6. Liguori, I.; Russo, G.; Aran, L.; Bulli, G.; Curcio, F.; Della-Morte, D.; Gargiulo, G.; Testa, G.; Cacciatore, F.; Bonaduce, D.; et al. Sarcopenia: Assessment of disease burden and strategies to improve outcomes. *Clin. Interv. Aging* **2018**, *13*, 913–927. [[CrossRef](#)] [[PubMed](#)]
7. Perikias, S.; Vandewoude, M. Where frailty meets diabetes. *Diabetes Metab. Res.* **2016**, *32*, 261–267. [[CrossRef](#)] [[PubMed](#)]
8. Vandewoude, M.F.; Alish, C.J.; Sauer, A.C.; Hegazi, R.A. Malnutrition-sarcopenia syndrome: Is this the future of nutrition screening and assessment for older adults? *J. Aging Res.* **2012**, *2012*, 651570. [[CrossRef](#)]
9. O'Toole, P.W.; Shiels, P.G. The role of the microbiota in sedentary lifestyle disorders and ageing: Lessons from the animal kingdom. *J. Intern. Med.* **2020**, *287*, 271–282. [[CrossRef](#)]
10. Bleau, C.; Karelis, A.D.; St-Pierre, D.H.; Lamontagne, L. Crosstalk between intestinal microbiota, adipose tissue and skeletal muscle as an early event in systemic low-grade inflammation and the development of obesity and diabetes. *Diabetes Metab. Res. Rev.* **2015**, *31*, 545–561. [[CrossRef](#)]
11. Zheng, C.; Huang, W.Y.; Sheridan, S.; Sit, C.H.; Chen, X.K.; Wong, S.H. COVID-19 Pandemic Brings a Sedentary Lifestyle in Young Adults: A Cross-Sectional and Longitudinal Study. *Int. J. Environ. Res. Public Health* **2020**, *17*, 6035. [[CrossRef](#)] [[PubMed](#)]
12. Langhammer, B.; Sagbakken, M.; Kvaal, K.; Ulstein, I.; Näden, D.; Rognstad, M.K. Music Therapy and Physical Activity to Ease Anxiety, Restlessness, Irritability, and Aggression in Individuals With Dementia With Signs of Frontotemporal Lobe Degeneration. *J. Psychosoc. Nurs. Ment. Health Serv.* **2019**, *57*, 29–37. [[CrossRef](#)] [[PubMed](#)]
13. Zhai, L.; Zhang, Y.; Zhang, D. Sedentary behaviour and the risk of depression: A meta-analysis. *Br. J. Sports Med.* **2014**, *49*, 1–6. [[CrossRef](#)]
14. Bhasker, A.G.; Greve, J.W. Are Patients Suffering from Severe Obesity Getting a Raw Deal During COVID-19 Pandemic? *Obes. Surg.* **2020**, *1–2*. [[CrossRef](#)]
15. Mori, H.; Kuroda, A.; Ishizu, M.; Ohishi, M.; Takashi, Y.; Otsuka, Y.; Taniguchi, S.; Tamaki, M.; Kurahashi, K.; Yoshida, S.; et al. Association of accumulated advanced glycation end-products with a high prevalence of sarcopenia and dynapenia in patients with type 2 diabetes. *J. Diabetes Investig.* **2019**, *10*, 1332–1340. [[CrossRef](#)]
16. Gensous, N.; Bacalini, M.G.; Franceschi, C.; Meskers, C.G.M.; Maier, A.B.; Garagnani, P. Age-Related DNA Methylation Changes: Potential Impact on Skeletal Muscle Aging in Humans. *Front. Physiol.* **2019**, *10*, 996. [[CrossRef](#)]
17. Rong, S.; Wang, L.; Peng, Z.; Liao, Y.; Li, D.; Yang, X.; Nuessler, A.K.; Liu, L.; Bao, W.; Yang, W. The mechanisms and treatments for sarcopenia: Could exosomes be a perspective research strategy in the future? *J. Cachexia Sarcopenia Muscle* **2020**, *11*, 348–365. [[CrossRef](#)] [[PubMed](#)]
18. Laviano, A.; Koverech, A.; Zanetti, M. Nutrition support in the time of SARS-CoV-2 (COVID-19). *Nutrition* **2020**, *74*, 110834. [[CrossRef](#)] [[PubMed](#)]
19. Rooks, D.; Roubenoff, R. Development of Pharmacotherapies for the Treatment of Sarcopenia. *J. Frailty Aging* **2019**, *8*, 120–130. [[CrossRef](#)]
20. Morley, J.E. Treatment of sarcopenia: The road to the future. *J. Cachexia Sarcopenia Muscle* **2018**, *9*, 1196–1199. [[CrossRef](#)]

21. Hardee, J.P.; Lynch, G.S. Current pharmacotherapies for sarcopenia. *Expert Opin. Pharmacother.* **2019**, *20*, 1645–1657. [[CrossRef](#)] [[PubMed](#)]
22. Consitt, L.A.; Clark, B.C. The Vicious Cycle of Myostatin Signaling in Sarcopenic Obesity: Myostatin Role in Skeletal Muscle Growth, Insulin Signaling and Implications for Clinical Trials. *J. Frailty Aging* **2018**, *7*, 21–27. [[CrossRef](#)] [[PubMed](#)]
23. Vatic, M.; von Haehling, S.; Ebner, N. Inflammatory biomarkers of frailty. *Exp. Gerontol.* **2020**, *133*, 110858. [[CrossRef](#)] [[PubMed](#)]
24. Grosicki, G.J.; Fielding, R.A.; Lustgarten, M.S. Gut Microbiota Contribute to Age-Related Changes in Skeletal Muscle Size, Composition, and Function: Biological Basis for a Gut-Muscle Axis. *Calcif. Tissue Int.* **2018**, *102*, 433–442. [[CrossRef](#)]
25. Latham, C.M.; Wagner, A.L.; Urschel, K.L. Effects of dietary amino acid supplementation on measures of whole-body and muscle protein metabolism in aged horses. *J. Anim. Physiol. Anim. Nutr.* **2019**, *103*, 283–294. [[CrossRef](#)] [[PubMed](#)]
26. Tsintzas, K.; Jones, R.; Pabla, P.; Mallinson, J.; Barrett, D.A.; Kim, D.H.; Cooper, S.; Davies, A.; Taylor, T.; Gaffney, C.; et al. Effect of acute and short-term dietary fat ingestion on postprandial skeletal muscle protein synthesis rates in middle-aged, overweight and obese men. *Am. J. Physiol. Endocrinol. Metab.* **2020**, *318*, E417–E429. [[CrossRef](#)]
27. Kieliszek, M.; Piwowarek, K.; Kot, A.M.; Błażej, S.; Chlebowska-Śmigiel, A.; Wolska, I. Pollen and bee bread as new health-oriented products: A review. *Trends Food Sci. Technol.* **2018**, *71*, 170–180. [[CrossRef](#)]
28. Kocot, J.; Kielczykowska, M.; Luchowska-Kocot, D.; Kurzepa, J.; Musik, I. Antioxidant Potential of Propolis, Bee Pollen, and Royal Jelly: Possible Medical Application. *Oxid. Med. Cell. Longev.* **2018**, *2018*, 7074209. [[CrossRef](#)]
29. Fratini, F.; Cilia, G.; Mancini, S.; Felicioli, A. Royal Jelly: An ancient remedy with remarkable antibacterial properties. *Microbiol. Res.* **2016**, *192*, 130–141. [[CrossRef](#)]
30. Nitecka-Buchta, A.; Buchta, P.; Tabenska-Bosakowska, E.; Walczynska-Dragon, K.; Baron, S. Myorelaxant effect of bee venom topical skin application in patients with RDC/TMD Ia and RDC/TMD Ib: A randomized, double blinded study. *BioMed Res. Int.* **2014**, *2014*, 296053. [[CrossRef](#)]
31. Alvarez-Fischer, D.; Noelker, C.; Vulinovic, F.; Grunewald, A.; Chevarin, C.; Klein, C.; Oertel, W.H.; Hirsch, E.C.; Michel, P.P.; Hartmann, A. Bee venom and its component apamin as neuroprotective agents in a Parkinson disease mouse model. *PLoS ONE* **2013**, *8*, e61700. [[CrossRef](#)] [[PubMed](#)]
32. Cornara, L.; Biagi, M.; Xiao, J.; Burlando, B. Therapeutic Properties of Bioactive Compounds from Different Honeybee Products. *Front. Pharmacol.* **2017**, *8*, 412. [[CrossRef](#)] [[PubMed](#)]
33. Eşrefoğlu, M.; Gül, M.; Ateş, B.; Erdoğan, A. The effects of caffeic acid phenethyl ester and melatonin on age-related vascular remodeling and cardiac damage. *Fundam. Clin. Pharmacol.* **2011**, *25*, 580–590. [[CrossRef](#)] [[PubMed](#)]
34. Rzepecka-Stojko, A.; Stojko, J.; Kurek-Górecka, A.; Górecki, M.; Kabała-Dzik, A.; Kubina, R.; Moździerz, A.; Buszman, E. Polyphenols from Bee Pollen: Structure, Absorption, Metabolism and Biological Activity. *Molecules* **2015**, *20*, 21732–21749. [[CrossRef](#)] [[PubMed](#)]
35. Ebadi, P.; Fazeli, M. Anti-photoaging potential of propolis extract in UVB-irradiated human dermal fibroblasts through increasing the expression of FOXO3A and NGF genes. *Biomed. Pharmacother.* **2017**, *95*, 47–54. [[CrossRef](#)]
36. Salles, J.; Cardinaut, N.; Patrac, V.; Berry, A.; Giraudet, C.; Collin, M.L.; Chanet, A.; Tagliaferri, C.; Denis, P.; Pouyet, C.; et al. Bee pollen improves muscle protein and energy metabolism in malnourished old rats through interfering with the Mtor signaling pathway and mitochondrial activity. *Nutrients* **2014**, *6*, 5500–5516. [[CrossRef](#)]
37. Boisard, S.; Shahali, Y.; Aumond, M.-C.; Derbré, S.; Blanchard, P.; Dadar, M.; Le Ray, A.-M.; Richomme, P. Anti-AGE activity of poplar-type propolis: Mechanism of action of main phenolic compounds. *Int. J. Food Sci.* **2020**, *55*, 453–460. [[CrossRef](#)]
38. Egawa, T.; Ohno, Y.; Yokoyama, S.; Yokokawa, T.; Tsuda, S.; Goto, K.; Hayashi, T. The Protective Effect of Brazilian Propolis against Glycation Stress in Mouse Skeletal Muscle. *Foods* **2019**, *8*, 439. [[CrossRef](#)]
39. Shaha, A.; Mizuguchi, H.; Kitamura, Y.; Fujino, H.; Yabumoto, M.; Takeda, N.; Fukui, H. Effect of Royal Jelly and Brazilian Green Propolis on the Signaling for Histamine H1 Receptor and Interleukin-9 Gene Expressions Responsible for the Pathogenesis of the Allergic Rhinitis. *Biol. Pharm. Bull.* **2018**, *41*, 1440–1447. [[CrossRef](#)]

40. Cruz-Jentoft, A.J.; Kiesswetter, E.; Drey, M.; Sieber, C.C. Nutrition, frailty, and sarcopenia. *Aging Clin. Exp. Res.* **2017**, *29*, 43–48. [[CrossRef](#)]
41. Perna, S.; Alalwan, T.A.; Al-Thawadi, S.; Negro, M.; Parimbelli, M.; Cerullo, G.; Gasparri, C.; Guerriero, F.; Infantino, V.; Diana, M.; et al. Evidence-Based Role of Nutrients and Antioxidants for Chronic Pain Management in Musculoskeletal Frailty and Sarcopenia in Aging. *Geriatrics* **2020**, *5*, 16. [[CrossRef](#)] [[PubMed](#)]
42. Ticinesi, A.; Lauretani, F.; Milani, C.; Nouvenne, A.; Tana, C.; Del Rio, D.; Maggio, M.; Ventura, M.; Meschi, T. Aging Gut Microbiota at the Cross-Road between Nutrition, Physical Frailty, and Sarcopenia: Is There a Gut-Muscle Axis? *Nutrients* **2017**, *9*, 1303. [[CrossRef](#)] [[PubMed](#)]
43. Ramanathan, A.N.K.G.; Nair, A.J.; Sugunan, V.S. A review on Royal Jelly proteins and peptides. *J. Funct. Foods* **2018**, *44*, 255–264. [[CrossRef](#)]
44. Virgiliou, C.; Kanelis, D.; Pina, A.; Gika, H.; Tananaki, C.; Zotou, A.; Theodoridis, G. A targeted approach for studying the effect of sugar bee feeding on the metabolic profile of Royal Jelly. *J. Chromatogr. A* **2019**, *460783*. [[CrossRef](#)] [[PubMed](#)]
45. Qiu, W.; Chen, X.; Tian, Y.; Wu, D.; Du, M.; Wang, S. Protection against oxidative stress and anti-aging effect in *Drosophila* of royal jelly-collagen peptide. *Food Chem. Toxicol.* **2020**, *135*, 110881. [[CrossRef](#)]
46. Alu'datt, M.H.; Rababah, T.; Sakandar, H.A.; Imran, M.; Mustafa, N.; Alhamad, M.N.; Mhaidat, N.; Kubow, S.; Tranchant, C.; Al-Tawaha, A.R.; et al. Fermented Food-Derived Bioactive Compounds with Anticarcinogenic Properties: Fermented Royal Jelly as a Novel Source for Compounds with Health Benefits. In *Anticancer plants: Properties and Application*; Akhtar, M., Swamy, M., Eds.; Springer: Singapore, 2018.
47. Xin, X.-X.; Chen, Y.; Chen, D.; Xiao, F.; Parnell, L.D.; Zhao, J.; Liu, L.; Ordovas, J.M.; Lai, C.-Q.; Shen, L.-R. Supplementation with Major Royal-Jelly Proteins Increases Lifespan, Feeding, and Fecundity in *Drosophila*. *J. Agric. Food Chem.* **2016**, *64*, 5803–5812. [[CrossRef](#)]
48. Hossen, M.S.; Nahar, T.; Gan, S.H.; Khalil, M.I. Bioinformatics and Therapeutic Insights on Proteins in Royal Jelly. *Curr. Proteom.* **2019**, *16*, 84–101. [[CrossRef](#)]
49. Xue, X.; Wu, L.; Wang, K. Chemical Composition of Royal Jelly. In *Bee Products—Chemical and Biological Properties*; Alvarez-Suarez, J.M., Ed.; Springer International Publishing: Cham, Switzerland, 2017; pp. 181–190. [[CrossRef](#)]
50. Buttstedt, A.; Ihling, C.H.; Pietzsch, M.; Moritz, R.F.A. Royalactin is not a royal making of a queen. *Nature* **2016**, *537*, E10. [[CrossRef](#)]
51. Ali, A.M.; Hendawy, A.O. Royal Jelly Acid, 10-Hydroxy-Trans-2-Decenoic Acid, for Psychiatric and Neurological Disorders: How helpful could it be?! *Edelweiss J. Food Sci. Technol.* **2019**, *1*, 1–4.
52. Chen, Y.F.; Wang, K.; Zhang, Y.Z.; Zheng, Y.F.; Hu, F.L. In Vitro Anti-Inflammatory Effects of Three Fatty Acids from Royal Jelly. *Mediat. Inflamm.* **2016**, *2016*, 3583684. [[CrossRef](#)]
53. Yang, Y.C.; Chou, W.M.; Widowati, D.A.; Lin, I.P.; Peng, C.C. 10-hydroxy-2-decenoic acid of royal jelly exhibits bactericide and anti-inflammatory activity in human colon cancer cells. *BMC Complement. Altern. Med.* **2018**, *18*, 202. [[CrossRef](#)] [[PubMed](#)]
54. Weiser, M.J.; Grimshaw, V.; Wynalda, K.M.; Mohajeri, M.H.; Butt, C.M. Long-Term Administration of Queen Bee Acid (QBA) to Rodents Reduces Anxiety-Like Behavior, Promotes Neuronal Health and Improves Body Composition. *Nutrients* **2017**, *10*, 13. [[CrossRef](#)] [[PubMed](#)]
55. Hattori, N.; Nomoto, H.; Fukumitsu, H.; Mishima, S.; Furukawa, S. Royal jelly-induced neurite outgrowth from rat pheochromocytoma PC12 cells requires integrin signal independent of activation of extracellular signal-regulated kinases. *Biomed. Res.* **2007**, *28*, 139–146. [[CrossRef](#)] [[PubMed](#)]
56. Peng, C.C.; Sun, H.T.; Lin, I.P.; Kuo, P.C.; Li, J.C. The functional property of royal jelly 10-hydroxy-2-decenoic acid as a melanogenesis inhibitor. *BMC Complement. Altern. Med.* **2017**, *17*, 392. [[CrossRef](#)]
57. Zheng, J.; Lai, W.; Zhu, G.; Wan, M.; Chen, J.; Tai, Y.; Lu, C. 10-Hydroxy-2-decenoic acid prevents ultraviolet A-induced damage and matrix metalloproteinases expression in human dermal fibroblasts. *J. Eur. Acad. Dermatol. Venereol.* **2013**, *27*, 1269–1277. [[CrossRef](#)]
58. Wang, J.G.; Ruan, J.; Li, C.Y.; Wang, J.M.; Li, Y.; Zhai, W.T.; Zhang, W.; Ye, H.; Shen, N.H.; Lei, K.F.; et al. Connective tissue growth factor, a regulator related with 10-hydroxy-2-decenoic acid down-regulate MMPs in rheumatoid arthritis. *Rheumatol. Int.* **2012**, *32*, 2791–2799. [[CrossRef](#)]
59. Meng, G.; Wang, H.; Pei, Y.; Li, Y.; Wu, H.; Song, Y.; Guo, Q.; Guo, H.; Fukushima, S.; Tatefuji, T.; et al. Effects of protease-treated royal jelly on muscle strength in elderly nursing home residents: A randomized, double-blind, placebo-controlled, dose-response study. *Sci. Rep.* **2017**, *7*, 11416. [[CrossRef](#)]

60. Wessler, I.; Gartner, H.A.; Michel-Schmidt, R.; Brochhausen, C.; Schmitz, L.; Anspach, L.; Grunewald, B.; Kirkpatrick, C.J. Honeybees Produce Millimolar Concentrations of Non-Neuronal Acetylcholine for Breeding: Possible Adverse Effects of Neonicotinoids. *PLoS ONE* **2016**, *11*, e0156886. [[CrossRef](#)]
61. Ahmad, S.; Campos, M.G.; Fratini, F.; Altaye, S.Z.; Li, J. New Insights into the Biological and Pharmaceutical Properties of Royal Jelly. *Int. J. Mol. Sci.* **2020**, *21*, 382. [[CrossRef](#)]
62. Ramadan, M.F.; Al-Ghamdi, A. Bioactive compounds and health-promoting properties of royal jelly: A review. *J. Funct. Foods* **2012**, *4*, 39–52. [[CrossRef](#)]
63. Pan, Y.; Xu, J.; Jin, P.; Yang, Q.; Zhu, K.; You, M.; Chen, M.; Hu, F. Royal Jelly Ameliorates Behavioral Deficits, Cholinergic System Deficiency, and Autonomic Nervous Dysfunction in Ovariectomized Cholesterol-Fed Rabbits. *Molecules* **2019**, *24*, 1149. [[CrossRef](#)] [[PubMed](#)]
64. Ali, A.M.; Kunugi, H. Apitherapy for Parkinson's disease: A focus on the effects of propolis and royal jelly. *Oxid. Med. Cell. Longev.* **2020**, accepted.
65. Ueda, T.; Inden, M.; Shirai, K.; Sekine, S.I.; Masaki, Y.; Kurita, H.; Ichihara, K.; Inuzuka, T.; Hozumi, I. The effects of Brazilian green propolis that contains flavonols against mutant copper-zinc superoxide dismutase-mediated toxicity. *Sci. Rep.* **2017**, *7*, 2882. [[CrossRef](#)] [[PubMed](#)]
66. Rufatto, L.C.; dos Santos, D.A.; Marinho, F.; Henriques, J.A.P.; Roesch Ely, M.; Moura, S. Red propolis: Chemical composition and pharmacological activity. *Asian Pac. J. Trop. Biomed.* **2017**, *7*, 591–598. [[CrossRef](#)]
67. Anjum, S.I.; Ullah, A.; Khan, K.A.; Attaullah, M.; Khan, H.; Ali, H.; Bashir, M.A.; Tahir, M.; Ansari, M.J.; Ghramh, H.A.; et al. Composition and functional properties of propolis (bee glue): A review. *Saudi J. Biol. Sci.* **2019**, *26*, 1695–1703. [[CrossRef](#)]
68. Pobiega, K.; Kraśniewska, K.; Gniewosz, M. Application of propolis in antimicrobial and antioxidative protection of food quality—A review. *Trends Food Sci. Technol.* **2019**, *83*, 53–62. [[CrossRef](#)]
69. Genovese, S.; Ashida, H.; Yamashita, Y.; Nakgano, T.; Ikeda, M.; Daishi, S.; Epifano, F.; Taddeo, V.A.; Fiorito, S. The interaction of auraptene and other oxyprenylated phenylpropanoids with glucose transporter type 4. *Phytomedicine* **2017**, *32*, 74–79. [[CrossRef](#)]
70. Ueda, M.; Hayashibara, K.; Ashida, H. Propolis extract promotes translocation of glucose transporter 4 and glucose uptake through both PI3K- and AMPK-dependent pathways in skeletal muscle. *Biofactors* **2013**, *39*, 457–466. [[CrossRef](#)]
71. Sung, S.H.; Choi, G.H.; Lee, N.W.; Shin, B.C. External Use of Propolis for Oral, Skin, and Genital Diseases: A Systematic Review and Meta-Analysis. *Evid. Based Complement. Alternat. Med.* **2017**, *2017*, 8025752. [[CrossRef](#)]
72. Goes, A.T.R.; Jesse, C.R.; Antunes, M.S.; Lobo Ladd, F.V.; Lobo Ladd, A.A.B.; Luchese, C.; Paroul, N.; Boeira, S.P. Protective role of chrysin on 6-hydroxydopamine-induced neurodegeneration a mouse model of Parkinson's disease: Involvement of neuroinflammation and neurotrophins. *Chem. Biol. Interact.* **2018**, *279*, 111–120. [[CrossRef](#)]
73. Havermann, S.; Chovolou, Y.; Humpf, H.U.; Watjen, W. Caffeic acid phenethyl ester increases stress resistance and enhances lifespan in *Caenorhabditis elegans* by modulation of the insulin-like DAF-16 signalling pathway. *PLoS ONE* **2014**, *9*, e100256. [[CrossRef](#)] [[PubMed](#)]
74. Zaitone, S.A.; Ahmed, E.; Elsherbiny, N.M.; Mehanna, E.T.; El-Kherbetawy, M.K.; ElSayed, M.H.; Alshareef, D.M.; Moustafa, Y.M. Caffeic acid improves locomotor activity and lessens inflammatory burden in a mouse model of rotenone-induced nigral neurodegeneration: Relevance to Parkinson's disease therapy. *Pharmacol. Rep.* **2019**, *71*, 32–41. [[CrossRef](#)] [[PubMed](#)]
75. Noelker, C.; Bacher, M.; Gocke, P.; Wei, X.; Klockgether, T.; Du, Y.; Dodel, R. The flavanoid caffeic acid phenethyl ester blocks 6-hydroxydopamine-induced neurotoxicity. *Neurosci. Lett.* **2005**, *383*, 39–43. [[CrossRef](#)] [[PubMed](#)]
76. Escriche, I.; Juan-Borrás, M. Standardizing the analysis of phenolic profile in propolis. *Food Res. Int.* **2018**, *106*, 834–841. [[CrossRef](#)] [[PubMed](#)]
77. Wang, H.; Wang, Y.; Zhao, L.; Cui, Q.; Wang, Y.; Du, G. Pinocembrin attenuates MPP(+)-induced neurotoxicity by the induction of heme oxygenase-1 through ERK1/2 pathway. *Neurosci. Lett.* **2016**, *612*, 104–109. [[CrossRef](#)]
78. Wang, Y.; Gao, J.; Miao, Y.; Cui, Q.; Zhao, W.; Zhang, J.; Wang, H. Pinocembrin protects SH-SY5Y cells against MPP(+)-induced neurotoxicity through the mitochondrial apoptotic pathway. *J. Mol. Neurosci.* **2014**, *53*, 537–545. [[CrossRef](#)]

79. Chi, Y.; Luo, L.; Cui, M.; Hao, Y.; Liu, T.; Huang, X.; Guo, X. Chemical Composition and Antioxidant Activity of Essential Oil of Chinese Propolis. *Chem. Biodivers.* **2020**, *17*, e1900489. [[CrossRef](#)]
80. El-Guendouz, S.; Lyoussi, B.; Miguel, M.G. Insight on Propolis from Mediterranean Countries: Chemical Composition, Biological Activities and Application Fields. *Chem. Biodivers.* **2019**, *16*, e1900094. [[CrossRef](#)]
81. Hochheim, S.; Pacassa Borges, P.; Boeder, A.M.; Scharf, D.R.; Simionatto, E.L.; Yamanaka, C.N.; Alberton, M.D.; Guedes, A.; de Cordova, C.M.M. A Bioguided Approach for the Screening of Antibacterial Compounds Isolated From the Hydroalcoholic Extract of the Native Brazilian Bee's Propolis Using Mollicutes as a Model. *Front. Microbiol.* **2020**, *11*, 558. [[CrossRef](#)]
82. Rivero-Cruz, J.F.; Granados-Pineda, J.; Pedraza-Chaverri, J.; Pérez-Rojas, J.M.; Kumar-Passari, A.; Diaz-Ruiz, G.; Rivero-Cruz, B.E. Phytochemical Constituents, Antioxidant, Cytotoxic, and Antimicrobial Activities of the Ethanol Extract of Mexican Brown Propolis. *Antioxidants* **2020**, *9*, 70. [[CrossRef](#)]
83. Campos, M.G.R.; Bogdanov, S.; de Almeida-Muradian, L.B.; Szczesna, T.; Mancebo, Y.; Frigerio, C.; Ferreira, F. Pollen composition and standardisation of analytical methods. *J. Apic. Res.* **2008**, *47*, 154–161. [[CrossRef](#)]
84. Denisow, B.; Denisow-Pietrzyk, M. Biological and therapeutic properties of bee pollen: A review. *J. Sci. Food Agric.* **2016**, *96*, 4303–4309. [[CrossRef](#)] [[PubMed](#)]
85. Themelis, T.; Gotti, R.; Orlandini, S.; Gatti, R. Quantitative amino acids profile of monofloral bee pollens by microwave hydrolysis and fluorimetric high performance liquid chromatography. *J. Pharm. Biomed. Anal.* **2019**, *173*, 144–153. [[CrossRef](#)] [[PubMed](#)]
86. Thakur, M.; Nanda, V. Composition and functionality of bee pollen: A review. *Trends Food Sci. Technol.* **2020**, *98*, 82–106. [[CrossRef](#)]
87. Li, Q.-Q.; Wang, K.; Marcucci, M.C.; Sawaya, A.C.H.F.; Hu, L.; Xue, X.-F.; Wu, L.-M.; Hu, F.-L. Nutrient-rich bee pollen: A treasure trove of active natural metabolites. *J. Funct. Foods* **2018**, *49*, 472–484. [[CrossRef](#)]
88. Zhang, D.; Shi, J.; Yang, X. Role of Lipid Metabolism in Plant Pollen Exine Development. *Subcell. Biochem.* **2016**, *86*, 315–337. [[CrossRef](#)] [[PubMed](#)]
89. Diego-Taboada, A.; Beckett, S.T.; Atkin, S.L.; Mackenzie, G. Hollow pollen shells to enhance drug delivery. *Pharmaceutics* **2014**, *6*, 80–96. [[CrossRef](#)]
90. Ketkar, S.; Rathore, A.; Kandhare, A.; Lohidasan, S.; Bodhankar, S.; Paradkar, A.; Mahadik, K. Alleviating exercise-induced muscular stress using neat and processed bee pollen: Oxidative markers, mitochondrial enzymes, and myostatin expression in rats. *Integr. Med. Res.* **2015**, *4*, 147–160. [[CrossRef](#)]
91. Shen, X.; Liu, Y.; Luo, X.; Yang, Z. Advances in Biosynthesis, Pharmacology, and Pharmacokinetics of Pinocembrin, a Promising Natural Small-Molecule Drug. *Molecules* **2019**, *24*, 2323. [[CrossRef](#)]
92. Guendouz, M.; Haddi, A.; Grar, H.; Kheroua, O.; Saidi, D.; Kaddouri, H. Preventive effects of royal jelly against anaphylactic response in a murine model of cow's milk allergy. *Pharm. Biol.* **2017**, *55*, 2145–2152. [[CrossRef](#)]
93. Cifuentes, L. Allergy to honeybee ... not only stings. *Curr. Opin. Allergy Clin. Immunol.* **2015**, *15*, 364–368. [[CrossRef](#)] [[PubMed](#)]
94. Lee, Y.; Kim, S.G.; Kim, I.S.; Lee, H.D. Standardization of the Manufacturing Process of Bee Venom Pharmacopuncture Containing Melittin as the Active Ingredient. *Evid. Based Complement. Alternat. Med.* **2018**, *2018*, 2353280. [[CrossRef](#)] [[PubMed](#)]
95. Ji, W.Z.; Zhang, C.P.; Wei, W.T.; Hu, F.L. The in vivo antiaging effect of enzymatic hydrolysate from royal jelly in d-galactose induced aging mouse. *J. Chin. Inst. Food Sci. Technol.* **2016**, *16*, 18–25.
96. Niu, K.; Guo, H.; Guo, Y.; Ebihara, S.; Asada, M.; Ohru, T.; Furukawa, K.; Ichinose, M.; Yanai, K.; Kudo, Y.; et al. Royal jelly prevents the progression of sarcopenia in aged mice in vivo and in vitro. *J. Gerontol. A Biol. Sci. Med. Sci.* **2013**, *68*, 1482–1492. [[CrossRef](#)] [[PubMed](#)]
97. Okumura, N.; Toda, T.; Ozawa, Y.; Watanabe, K.; Ikuta, T.; Tatefuji, T.; Hashimoto, K.; Shimizu, T. Royal Jelly Delays Motor Functional Impairment During Aging in Genetically Heterogeneous Male Mice. *Nutrients* **2018**, *10*, 1191. [[CrossRef](#)]
98. Pyrzanowska, J.; Piechal, A.; Blecharz-Klin, K.; Graikou, K.; Widy-Tyszkiewicz, E.; Chinou, I. Chemical analysis of Greek royal jelly—Its influence of the long-term administration on spatial memory in aged rats. *Planta Med.* **2012**, *78*. [[CrossRef](#)]

99. Pyrzanowska, J.; Piechal, A.; Blecharz-Klin, K.; Joniec-Maciejak, I.; Graikou, K.; Chinou, I.; Widy-Tyszkiewicz, E. Long-term administration of Greek Royal Jelly improves spatial memory and influences the concentration of brain neurotransmitters in naturally aged Wistar male rats. *J. Ethnopharmacol.* **2014**, *155*, 343–351. [[CrossRef](#)]
100. Metwally Ibrahim, S.E.L.; Kosba, A.A. Royal jelly supplementation reduces skeletal muscle lipotoxicity and insulin resistance in aged obese rats. *Pathophysiology* **2018**, *25*, 307–315. [[CrossRef](#)]
101. Shen, Y.C.; Yen, J.C.; Liou, K.T. Ameliorative effects of caffeic acid phenethyl ester on an eccentric exercise-induced skeletal muscle injury by down-regulating NF-kappaB mediated inflammation. *Pharmacology* **2013**, *91*, 219–228. [[CrossRef](#)]
102. Ozyurt, B.; Iraz, M.; Koca, K.; Ozyurt, H.; Sahin, S. Protective effects of caffeic acid phenethyl ester on skeletal muscle ischemia-reperfusion injury in rats. *Mol. Cell. Biochem.* **2006**, *292*, 197–203. [[CrossRef](#)]
103. Ozyurt, H.; Ozyurt, B.; Koca, K.; Ozgocmen, S. Caffeic acid phenethyl ester (CAPE) protects rat skeletal muscle against ischemia-reperfusion-induced oxidative stress. *Vascul. Pharmacol.* **2007**, *47*, 108–112. [[CrossRef](#)] [[PubMed](#)]
104. Santos, L.D.D.; Zadelino, I.V.; Silva, L.; Zilli, R.L.; Barreiros, M.A.B.; Mauerwerk, M.T.; Meurer, F. Alcoholic extract of propolis in Nile tilapia post-larvae and fingerlings' diets: Effects on production performance, body composition and intestinal histology. *An. Acad. Bras. Cienc.* **2019**, *91*, e20180297. [[CrossRef](#)] [[PubMed](#)]
105. Santos, N.W.; Yoshimura, E.H.; Mareze-Costa, C.E.; Machado, E.; Agostinho, B.C.; Pereira, L.M.; Brito, M.N.; Brito, N.A.; Zeoula, L.M. Supplementation of cow milk naturally enriched in polyunsaturated fatty acids and polyphenols to growing rats. *PLoS ONE* **2017**, *12*, e0172909. [[CrossRef](#)] [[PubMed](#)]
106. Takikawa, M.; Kumagai, A.; Hirata, H.; Soga, M.; Yamashita, Y.; Ueda, M.; Ashida, H.; Tsuda, T. 10-Hydroxy-2-decenoic acid, a unique medium-chain fatty acid, activates 5'-AMP-activated protein kinase in L6 myotubes and mice. *Mol. Nutr. Food Res.* **2013**, *57*, 1794–1802. [[CrossRef](#)]
107. Edilova, M.I.; Abdul-Sater, A.A.; Watts, T.H. TRAF1 Signaling in Human Health and Disease. *Front. Immunol.* **2018**, *9*, 2969. [[CrossRef](#)]
108. Washio, K.; Kobayashi, M.; Saito, N.; Amagasa, M.; Kitamura, H. Propolis Ethanol Extract Stimulates Cytokine and Chemokine Production through NF-kappaB Activation in C2C12 Myoblasts. *Evid. Based Complement. Alternat. Med.* **2015**, *2015*, 349751. [[CrossRef](#)]
109. Kwon, T.D.; Lee, M.W.; Kim, K.H. The effect of exercise training and water extract from propolis intake on the antioxidant enzymes activity of skeletal muscle and liver in rat. *J. Exerc. Nutr. Biochem.* **2014**, *18*, 9–17. [[CrossRef](#)]
110. Tanaka, M.; Kanazashi, M.; Maeshige, N.; Kondo, H.; Ishihara, A.; Fujino, H. Protective effects of Brazilian propolis supplementation on capillary regression in the soleus muscle of hindlimb-unloaded rats. *J. Physiol. Sci.* **2019**, *69*, 223–233. [[CrossRef](#)]
111. Lee, E.S.; Uhm, K.O.; Lee, Y.M.; Han, M.; Lee, M.; Park, J.M.; Suh, P.G.; Park, S.H.; Kim, H.S. CAPE (caffeic acid phenethyl ester) stimulates glucose uptake through AMPK (AMP-activated protein kinase) activation in skeletal muscle cells. *Biochem. Biophys. Res. Commun.* **2007**, *361*, 854–858. [[CrossRef](#)]
112. Takahashi, Y.; Hijikata, K.; Seike, K.; Nakano, S.; Banjo, M.; Sato, Y.; Takahashi, K.; Hatta, H. Effects of Royal Jelly Administration on Endurance Training-Induced Mitochondrial Adaptations in Skeletal Muscle. *Nutrients* **2018**, *10*, 1735. [[CrossRef](#)]
113. Yuce, S.; Cemal Gokce, E.; Iskdemir, A.; Koc, E.R.; Cemil, D.B.; Gokce, A.; Sargon, M.F. An experimental comparison of the effects of propolis, curcumin, and methylprednisolone on crush injuries of the sciatic nerve. *Ann. Plast. Surg.* **2015**, *74*, 684–692. [[CrossRef](#)]
114. Miko, A.; Poto, L.; Matrai, P.; Hegyi, P.; Furedi, N.; Garami, A.; Illes, A.; Solymar, M.; Vincze, A.; Balasko, M.; et al. Gender difference in the effects of interleukin-6 on grip strength—A systematic review and meta-analysis. *BMC Geriatr.* **2018**, *18*, 107. [[CrossRef](#)] [[PubMed](#)]
115. Lima Cavendish, R.; de Souza Santos, J.; Belo Neto, R.; Oliveira Paixao, A.; Valeria Oliveira, J.; Divino de Araujo, E.; Berretta, E.S.A.A.; Maria Thomazzi, S.; Cordeiro Cardoso, J.; Zanardo Gomes, M. Antinociceptive and anti-inflammatory effects of Brazilian red propolis extract and formononetin in rodents. *J. Ethnopharmacol.* **2015**, *173*, 127–133. [[CrossRef](#)] [[PubMed](#)]
116. Roquette, A.R.; Monteiro, N.E.S.; Moura, C.S.; Toreti, V.C.; de Pace, F.; Santos, A.D.; Park, Y.K.; Amaya-Farfan, J. Green propolis modulates gut microbiota, reduces endotoxemia and expression of TLR4 pathway in mice fed a high-fat diet. *Food Res. Int.* **2015**, *76*, 796–803. [[CrossRef](#)] [[PubMed](#)]

117. Buck, E.L.; Mizubuti, I.Y.; Alfieri, A.A.; Otonel, R.A.; Buck, L.Y.; Souza, F.P.; Prado-Calixto, O.P.; Poveda-Parra, A.R.; Alexandre Filho, L.; Lopera-Barrero, N.M. Effect of propolis ethanol extract on myostatin gene expression and muscle morphometry of Nile tilapia in net cages. *Genet. Mol. Res.* **2017**, *16*. [[CrossRef](#)]
118. Sriram, S.; Subramanian, S.; Sathiakumar, D.; Venkatesh, R.; Salerno, M.S.; McFarlane, C.D.; Kambadur, R.; Sharma, M. Modulation of reactive oxygen species in skeletal muscle by myostatin is mediated through NF-kappaB. *Aging Cell* **2011**, *10*, 931–948. [[CrossRef](#)]
119. Watadani, R.; Kotoh, J.; Sasaki, D.; Someya, A.; Matsumoto, K.; Maeda, A. 10-Hydroxy-2-decenoic acid, a natural product, improves hyperglycemia and insulin resistance in obese/diabetic KK-Ay mice, but does not prevent obesity. *J. Vet. Med. Sci.* **2017**, *79*, 1596–1602. [[CrossRef](#)]
120. D'Antona, G.; Ragni, M.; Cardile, A.; Tedesco, L.; Dossena, M.; Bruttini, F.; Caliaro, F.; Corsetti, G.; Bottinelli, R.; Carruba, M.O.; et al. Branched-chain amino acid supplementation promotes survival and supports cardiac and skeletal muscle mitochondrial biogenesis in middle-aged mice. *Cell Metab.* **2010**, *12*, 362–372. [[CrossRef](#)]
121. Puigserver, P.; Spiegelman, B.M. Peroxisome proliferator-activated receptor-gamma coactivator 1 alpha (PGC-1 alpha): Transcriptional coactivator and metabolic regulator. *Endocr. Rev.* **2003**, *24*, 78–90. [[CrossRef](#)]
122. Inoue, Y.; Hara, H.; Mitsugi, Y.; Yamaguchi, E.; Kamiya, T.; Itoh, A.; Adachi, T. 4-Hydroperoxy-2-decenoic acid ethyl ester protects against 6-hydroxydopamine-induced cell death via activation of Nrf2-ARE and eIF2 $\alpha$ -ATF4 pathways. *Neurochem. Int.* **2018**, *112*, 288–296. [[CrossRef](#)]
123. Kobayashi, E.H.; Suzuki, T.; Funayama, R.; Nagashima, T.; Hayashi, M.; Sekine, H.; Tanaka, N.; Moriguchi, T.; Motohashi, H.; Nakayama, K.; et al. Nrf2 suppresses macrophage inflammatory response by blocking proinflammatory cytokine transcription. *Nat. Commun.* **2016**, *7*, 11624. [[CrossRef](#)]
124. Abdulla, H.; Smith, K.; Atherton, P.J.; Idris, I. Role of insulin in the regulation of human skeletal muscle protein synthesis and breakdown: A systematic review and meta-analysis. *Diabetologia* **2016**, *59*, 44–55. [[CrossRef](#)] [[PubMed](#)]
125. Guillet, C.; Boirie, Y. Insulin resistance: A contributing factor to age-related muscle mass loss? *Diabetes Metab.* **2005**, *31*, 5520–5526. [[CrossRef](#)]
126. Tubbs, E.; Chanon, S.; Robert, M.; Bendridi, N.; Bidaux, G.; Chauvin, M.-A.; Ji-Cao, J.; Durand, C.; Gauvrit-Ramette, D.; Vidal, H.; et al. Disruption of Mitochondria-Associated Endoplasmic Reticulum Membrane (MAM) Integrity Contributes to Muscle Insulin Resistance in Mice and Humans. *Diabetes* **2018**, *67*, 636–650. [[CrossRef](#)] [[PubMed](#)]
127. Salminen, A.; Kaarniranta, K. AMP-activated protein kinase (AMPK) controls the aging process via an integrated signaling network. *Ageing Res. Rev.* **2012**, *11*, 230–241. [[CrossRef](#)]
128. Salminen, A.; Kauppinen, A.; Kaarniranta, K. AMPK activation inhibits the functions of myeloid-derived suppressor cells (MDSC): Impact on cancer and aging. *J. Mol. Med.* **2019**, *97*, 1049–1064. [[CrossRef](#)]
129. You, M.; Miao, Z.; Tian, J.; Hu, F. Trans-10-hydroxy-2-decenoic acid protects against LPS-induced neuroinflammation through FOXO1-mediated activation of autophagy. *Eur. J. Nutr.* **2019**, *59*, 2875–2892. [[CrossRef](#)]
130. Argiles, J.M.; Campos, N.; Lopez-Pedrosa, J.M.; Rueda, R.; Rodriguez-Manas, L. Skeletal Muscle Regulates Metabolism via Interorgan Crosstalk: Roles in Health and Disease. *J. Am. Med. Direct. Assoc.* **2016**, *17*, 789–796. [[CrossRef](#)]
131. Landi, F.; Calvani, R.; Tosato, M.; Martone, A.M.; Ortolani, E.; Savera, G.; D'Angelo, E.; Sisto, A.; Marzetti, E. Protein Intake and Muscle Health in Old Age: From Biological Plausibility to Clinical Evidence. *Nutrients* **2016**, *8*, 295. [[CrossRef](#)]
132. Chen, L.K.; Liu, L.K.; Woo, J.; Assantachai, P.; Auyeung, T.W.; Bahyah, K.S.; Chou, M.Y.; Chen, L.Y.; Hsu, P.S.; Krairit, O.; et al. Sarcopenia in Asia: Consensus report of the Asian Working Group for Sarcopenia. *J. Am. Med. Direct. Assoc.* **2014**, *15*, 95–101. [[CrossRef](#)]
133. Walrand, S.; Gryson, C.; Salles, J.; Giraudet, C.; Migne, C.; Bonhomme, C.; Le Ruyet, P.; Boirie, Y. Fast-digestive protein supplement for ten days overcomes muscle anabolic resistance in healthy elderly men. *Clin. Nutr.* **2016**, *35*, 660–668. [[CrossRef](#)] [[PubMed](#)]
134. Boirie, Y.; Guillet, C. Fast digestive proteins and sarcopenia of aging. *Curr. Opin. Clin. Nutr. Metab. Care* **2018**, *21*, 37–41. [[CrossRef](#)] [[PubMed](#)]
135. Graber, T.G.; Borack, M.S.; Reidy, P.T.; Volpi, E.; Rasmussen, B.B. Essential amino acid ingestion alters expression of genes associated with amino acid sensing, transport, and mTORC1 regulation in human skeletal muscle. *Nutr. Metab.* **2017**, *14*, 35. [[CrossRef](#)] [[PubMed](#)]

136. Ham, D.J.; Lynch, G.S.; Koopman, R. Amino acid sensing and activation of mechanistic target of rapamycin complex 1: Implications for skeletal muscle. *Curr. Opin. Clin. Nutr. Metab. Care* **2016**, *19*, 67–73. [[CrossRef](#)]
137. Moro, T.; Brightwell, C.R.; Deer, R.R.; Graber, T.G.; Galvan, E.; Fry, C.S.; Volpi, E.; Rasmussen, B.B. Muscle Protein Anabolic Resistance to Essential Amino Acids Does Not Occur in Healthy Older Adults Before or After Resistance Exercise Training. *J. Nutr.* **2018**, *148*, 900–909. [[CrossRef](#)]
138. Osowska, S.; Duchemann, T.; Walrand, S.; Paillard, A.; Boirie, Y.; Cynober, L.; Moinard, C. Citrulline modulates muscle protein metabolism in old malnourished rats. *Am. J. Physiol. Endocrinol. Metab.* **2006**, *291*, E582–E586. [[CrossRef](#)]
139. Moro, T.; Ebert, S.M.; Adams, C.M.; Rasmussen, B.B. Amino Acid Sensing in Skeletal Muscle. *Trends Endocrinol. Metab.* **2016**, *27*, 796–806. [[CrossRef](#)]
140. Zhu, Z.; Yang, C.; Iyaswamy, A.; Krishnamoorthi, S.; Sreenivasmurthy, S.G.; Liu, J.; Wang, Z.; Tong, B.C.; Song, J.; Lu, J.; et al. Balancing mTOR Signaling and Autophagy in the Treatment of Parkinson’s Disease. *Int. J. Mol. Sci.* **2019**, *20*, 728. [[CrossRef](#)]
141. Wang, X.; Cook, L.F.; Grasso, L.M.; Cao, M.; Dong, Y. Royal Jelly-Mediated Prolongevity and Stress Resistance in *Caenorhabditis elegans* Is Possibly Modulated by the Interplays of DAF-16, SIR-2.1, HCF-1, and 14-3-3 Proteins. *J. Gerontol. A Biol.* **2015**, *70*, 827–838. [[CrossRef](#)]
142. Milan, G.; Romanello, V.; Pescatore, F.; Armani, A.; Paik, J.-H.; Frasson, L.; Seydel, A.; Zhao, J.; Abraham, R.; Goldberg, A.L.; et al. Regulation of autophagy and the ubiquitin–proteasome system by the FoxO transcriptional network during muscle atrophy. *Nat. Commun.* **2015**, *6*, 6670. [[CrossRef](#)]
143. Chiche, A.; Le Roux, I.; von Joest, M.; Sakai, H.; Aguin, S.B.; Cazin, C.; Salam, R.; Fiette, L.; Alegria, O.; Flamant, P.; et al. Injury-Induced Senescence Enables In Vivo Reprogramming in Skeletal Muscle. *Cell Stem Cell* **2017**, *20*, 407–414.e404. [[CrossRef](#)]
144. Sharman, M.J.; Verdile, G.; Kirubakaran, S.; Münch, G. Inflammation in Alzheimer’s Disease, and Prevention with Antioxidants and Phenolic Compounds—What Are the Most Promising Candidates? In *Neurodegeneration and Alzheimer’s Disease: The Role of Diabetes, Genetics, Hormones, and Lifestyle*; Martins, R.N., Brennan, C.S., Fernando, B., Brennan, M.A., Fuller, S.J., Eds.; JohnWiley & Sons Ltd.: Hoboken, NJ, USA, 2019; pp. 233–266. [[CrossRef](#)]
145. MacLean, M.; Derk, J.; Ruiz, H.H.; Juranek, J.K.; Ramasamy, R.; Schmidt, A.M. The Receptor for Advanced Glycation End Products (RAGE) and DIAPH1: Implications for vascular and neuroinflammatory dysfunction in disorders of the central nervous system. *Neurochem. Int.* **2019**, *126*, 154–164. [[CrossRef](#)] [[PubMed](#)]
146. Chenet, A.L.; Duarte, A.R.; de Almeida, F.J.S.; Andrade, C.M.B.; de Oliveira, M.R. Carvacrol Depends on Heme Oxygenase-1 (HO-1) to Exert Antioxidant, Anti-inflammatory, and Mitochondria-Related Protection in the Human Neuroblastoma SH-SY5Y Cells Line Exposed to Hydrogen Peroxide. *Neurochem. Res.* **2019**, *44*, 884–896. [[CrossRef](#)] [[PubMed](#)]
147. Pan, Y.; Xu, J.; Chen, C.; Chen, F.; Jin, P.; Zhu, K.; Hu, C.W.; You, M.; Chen, M.; Hu, F. Royal Jelly Reduces Cholesterol Levels, Ameliorates A $\beta$  Pathology and Enhances Neuronal Metabolic Activities in a Rabbit Model of Alzheimer’s Disease. *Front. Aging Neurosci.* **2018**, *10*, 50. [[CrossRef](#)] [[PubMed](#)]
148. Bottini, N.; Gloria-Bottini, F.; Borgiani, P.; Antonacci, E.; Lucarelli, P.; Bottini, E. Type 2 diabetes and the genetics of signal transduction: A study of interaction between adenosine deaminase and acid phosphatase locus 1 polymorphisms. *Metabolism* **2004**, *53*, 995–1001. [[CrossRef](#)]
149. Anagnostou, M.E.; Hepple, R.T. Mitochondrial Mechanisms of Neuromuscular Junction Degeneration with Aging. *Cells* **2020**, *9*, 197. [[CrossRef](#)]
150. Sharma, B.; Dutt, V.; Kaur, N.; Mittal, A.; Dabur, R. *Tinospora cordifolia* protects from skeletal muscle atrophy by alleviating oxidative stress and inflammation induced by sciatic denervation. *J. Ethnopharmacol.* **2020**, *254*, 112720. [[CrossRef](#)]
151. Siddharth, J.; Chakrabarti, A.; Pannerec, A.; Karaz, S.; Morin-Rivron, D.; Masoodi, M.; Feige, J.N.; Parkinson, S.J. Aging and sarcopenia associate with specific interactions between gut microbes, serum biomarkers and host physiology in rats. *Aging* **2017**, *9*, 1698–1720. [[CrossRef](#)]
152. Bindels, L.B.; Delzenne, N.M. Muscle wasting: The gut microbiota as a new therapeutic target? *Int. J. Biochem. Cell Biol.* **2013**, *45*, 2186–2190. [[CrossRef](#)]

153. Genin, E.C.; Madji Hounoum, B.; Bannwarth, S.; Fragaki, K.; Lacas-Gervais, S.; Mauri-Crouzet, A.; Lespinasse, F.; Neveu, J.; Ropert, B.; Auge, G.; et al. Mitochondrial defect in muscle precedes neuromuscular junction degeneration and motor neuron death in CHCHD10(S59L/+) mouse. *Acta Neuropathol.* **2019**, *138*, 123–145. [[CrossRef](#)]
154. Xiao, Y.; Zhang, J.; Shu, X.; Bai, L.; Xu, W.; Wang, A.; Chen, A.; Tu, W.Y.; Wang, J.; Zhang, K.; et al. Loss of mitochondrial protein CHCHD10 in skeletal muscle causes neuromuscular junction impairment. *Hum. Mol. Genet.* **2019**, *29*, 1784–1796. [[CrossRef](#)] [[PubMed](#)]
155. Roos, T.U.; Heiss, E.H.; Schwaiberger, A.V.; Schachner, D.; Sroka, I.M.; Oberan, T.; Vollmar, A.M.; Dirsch, V.M. Caffeic acid phenethyl ester inhibits PDGF-induced proliferation of vascular smooth muscle cells via activation of p38 MAPK, HIF-1alpha, and heme oxygenase-1. *J. Nat. Prod.* **2011**, *74*, 352–356. [[CrossRef](#)] [[PubMed](#)]
156. Ticinesi, A.; Meschi, T.; Narici, M.V.; Lauretani, F.; Maggio, M. Muscle Ultrasound and Sarcopenia in Older Individuals: A Clinical Perspective. *J. Am. Med. Direct. Assoc.* **2017**, *18*, 290–300. [[CrossRef](#)] [[PubMed](#)]
157. Mitchell, W.K.; Phillips, B.E.; Williams, J.P.; Rankin, D.; Smith, K.; Lund, J.N.; Atherton, P.J. Development of a new Sonovue contrast-enhanced ultrasound approach reveals temporal and age-related features of muscle microvascular responses to feeding. *Physiol. Rep.* **2013**, *1*, e00119. [[CrossRef](#)]
158. Menzies, K.; Zaldivar-Jolissaint, J.F.; Auwerx, J. Sirtuins as Metabolic Modulators of Muscle Plasticity. In *Sirtuins, Proteins and Cell Regulation*; Houtkooper, R., Ed.; Springer: Dordrecht, The Netherlands, 2016; Volume 10.
159. Chen, Y.M.; Wei, L.; Chiu, Y.S.; Hsu, Y.J.; Tsai, T.Y.; Wang, M.F.; Huang, C.C. Lactobacillus plantarum TWK10 Supplementation Improves Exercise Performance and Increases Muscle Mass in Mice. *Nutrients* **2016**, *8*, 205. [[CrossRef](#)]
160. Bindels, L.B.; Beck, R.; Schakman, O.; Martin, J.C.; De Backer, F.; Sohet, F.M.; Dewulf, E.M.; Pachikian, B.D.; Neyrinck, A.M.; Thissen, J.P.; et al. Restoring specific lactobacilli levels decreases inflammation and muscle atrophy markers in an acute leukemia mouse model. *PLoS ONE* **2012**, *7*, e37971. [[CrossRef](#)]
161. Ali, A.M.; Kunugi, H. Bee honey protects astrocytes against oxidative stress: A preliminary in vitro investigation. *Neuropsychopharmacol. Rep.* **2019**, *39*, 312–314. [[CrossRef](#)]
162. Buigues, C.; Fernandez-Garrido, J.; Pruijboom, L.; Hoogland, A.J.; Navarro-Martinez, R.; Martinez-Martinez, M.; Verdejo, Y.; Mascaros, M.C.; Peris, C.; Cauli, O. Effect of a Prebiotic Formulation on Frailty Syndrome: A Randomized, Double-Blind Clinical Trial. *Int. J. Mol. Sci.* **2016**, *17*, 932. [[CrossRef](#)]
163. Wang, D.; Ho, L.; Faith, J.; Ono, K.; Janle, E.M.; Lachcik, P.J.; Cooper, B.R.; Jannasch, A.H.; D’Arcy, B.R.; Williams, B.A.; et al. Role of intestinal microbiota in the generation of polyphenol-derived phenolic acid mediated attenuation of Alzheimer’s disease beta-amyloid oligomerization. *Mol. Nutr. Food Res.* **2015**, *59*, 1025–1040. [[CrossRef](#)]
164. Picca, A.; Ponziani, F.R.; Calvani, R.; Marini, F.; Biancolillo, A.; Coelho-Junior, H.J.; Gervasoni, J.; Primiano, A.; Putignano, L.; Del Chierico, F.; et al. Gut Microbial, Inflammatory and Metabolic Signatures in Older People with Physical Frailty and Sarcopenia: Results from the BIOSPHERE Study. *Nutrients* **2019**, *12*, 65. [[CrossRef](#)]
165. Hindupur, S.K.; González, A.; Hall, M.N. The opposing actions of target of rapamycin and AMP-activated protein kinase in cell growth control. *Cold Spring Harb. Perspect. Biol.* **2015**, *7*, a019141. [[CrossRef](#)] [[PubMed](#)]
166. Jeejeebhoy, K.N. Malnutrition, fatigue, frailty, vulnerability, sarcopenia and cachexia: Overlap of clinical features. *Curr. Opin. Clin. Nutr. Metab. Care* **2012**, *15*, 213–219. [[CrossRef](#)] [[PubMed](#)]
167. Joksimović, A.; Stanković, D.; Joksimović, I.; Molnar, S.; Joksimović, S. Royal jelly as a supplement for young football players. *Sport Sci.* **2009**, *2*, 62–67.
168. Claesson, M.J.; Jeffery, I.B.; Conde, S.; Power, S.E.; O’Connor, E.M.; Cusack, S.; Harris, H.M.; Coakley, M.; Lakshminarayanan, B.; O’Sullivan, O.; et al. Gut microbiota composition correlates with diet and health in the elderly. *Nature* **2012**, *488*, 178–184. [[CrossRef](#)]
169. Jeffery, I.B.; Lynch, D.B.; O’Toole, P.W. Composition and temporal stability of the gut microbiota in older persons. *ISME J.* **2016**, *10*, 170–182. [[CrossRef](#)]
170. Fragala, M.S.; Alley, D.E.; Shardell, M.D.; Harris, T.B.; McLean, R.R.; Kiel, D.P.; Cawthon, P.M.; Dam, T.T.; Ferrucci, L.; Guralnik, J.M.; et al. Comparison of Handgrip and Leg Extension Strength in Predicting Slow Gait Speed in Older Adults. *J. Am. Geriatr. Soc.* **2016**, *64*, 144–150. [[CrossRef](#)]

171. Solerte, S.B.; Gazzaruso, C.; Bonacasa, R.; Rondanelli, M.; Zamboni, M.; Basso, C.; Locatelli, E.; Schifino, N.; Giustina, A.; Fioravanti, M. Nutritional supplements with oral amino acid mixtures increases whole-body lean mass and insulin sensitivity in elderly subjects with sarcopenia. *Am. J. Cardiol.* **2008**, *101*, 69e–77e. [[CrossRef](#)]
172. Ali, A.M.; Ahmed, A.H.; Smail, L. Psychological Climacteric Symptoms and Attitudes toward Menopause among Emirati Women. *Int. J. Environ. Res. Public Health* **2020**, *17*, 5028. [[CrossRef](#)]
173. Landi, F.; Camprubi-Robles, M.; Bear, D.E.; Cederholm, T.; Malafarina, V.; Welch, A.A.; Cruz-Jentoft, A.J. Muscle loss: The new malnutrition challenge in clinical practice. *Clin. Nutr.* **2019**, *38*, 2113–2120. [[CrossRef](#)]



© 2020 by the authors. Licensee MDPI, Basel, Switzerland. This article is an open access article distributed under the terms and conditions of the Creative Commons Attribution (CC BY) license (<http://creativecommons.org/licenses/by/4.0/>).

Review

# Bioactive Compounds and Bioactivities of Ginger (*Zingiber officinale* Roscoe)

Qian-Qian Mao <sup>1</sup>, Xiao-Yu Xu <sup>1</sup>, Shi-Yu Cao <sup>1</sup>, Ren-You Gan <sup>2,\*</sup>, Harold Corke <sup>2</sup>, Trust Beta <sup>3,4</sup> and Hua-Bin Li <sup>1,\*</sup>

- <sup>1</sup> Guangdong Provincial Key Laboratory of Food, Nutrition and Health, Department of Nutrition, School of Public Health, Sun Yat-sen University, Guangzhou 510080, China; maoqq@mail2.sysu.edu.cn (Q.-Q.M.); xuxy53@mail2.sysu.edu.cn (X.-Y.X.); caoshy3@mail2.sysu.edu.cn (S.-Y.C.)
- <sup>2</sup> Department of Food Science & Technology, School of Agriculture and Biology, Shanghai Jiao Tong University, Shanghai 200240, China; hcorke@sjtu.edu.cn
- <sup>3</sup> Department of Food & Human Nutritional Sciences, University of Manitoba, Winnipeg, MB R3T 2N2, Canada; Trust.Beta@umanitoba.ca
- <sup>4</sup> Richardson Centre for Functional Foods and Nutraceuticals, University of Manitoba, Winnipeg, MB R3T 2N2, Canada
- \* Correspondence: renyougan@sjtu.edu.cn (R.-Y.G.); lihuabin@mail.sysu.edu.cn (H.-B.L.); Tel.: +86-21-3420-8517 (R.-Y.G.); +86-20-873-323-91 (H.-B.L.)

Received: 12 May 2019; Accepted: 28 May 2019; Published: 30 May 2019

**Abstract:** Ginger (*Zingiber officinale* Roscoe) is a common and widely used spice. It is rich in various chemical constituents, including phenolic compounds, terpenes, polysaccharides, lipids, organic acids, and raw fibers. The health benefits of ginger are mainly attributed to its phenolic compounds, such as gingerols and shogaols. Accumulated investigations have demonstrated that ginger possesses multiple biological activities, including antioxidant, anti-inflammatory, antimicrobial, anticancer, neuroprotective, cardiovascular protective, respiratory protective, antiobesity, antidiabetic, anti-nausea, and antiemetic activities. In this review, we summarize current knowledge about the bioactive compounds and bioactivities of ginger, and the mechanisms of action are also discussed. We hope that this updated review paper will attract more attention to ginger and its further applications, including its potential to be developed into functional foods or nutraceuticals for the prevention and management of chronic diseases.

**Keywords:** phytochemicals; antioxidant; anti-nausea; antiobesity; anticancer; anti-inflammatory

## 1. Introduction

Ginger (*Zingiber officinale* Roscoe), which belongs to the Zingiberaceae family and the *Zingiber* genus, has been commonly consumed as a spice and an herbal medicine for a long time [1]. Ginger root is used to attenuate and treat several common diseases, such as headaches, colds, nausea, and emesis. Many bioactive compounds in ginger have been identified, such as phenolic and terpene compounds. The phenolic compounds are mainly gingerols, shogaols, and paradols, which account for the various bioactivities of ginger [2]. In recent years, ginger has been found to possess biological activities, such as antioxidant [3], anti-inflammatory [4], antimicrobial [5], and anticancer [6] activities. In addition, accumulating studies have demonstrated that ginger possesses the potential to prevent and manage several diseases, such as neurodegenerative diseases [7], cardiovascular diseases [8], obesity [9], diabetes mellitus [10], chemotherapy-induced nausea and emesis [11], and respiratory disorders [12]. In this review, we focus on the bioactive compounds and bioactivities of ginger, and we pay special attention to its mechanisms of action.

## 2. Bioactive Components and Bioactivities of Ginger

### 2.1. Bioactive Components

Ginger is abundant in active constituents, such as phenolic and terpene compounds [13]. The phenolic compounds in ginger are mainly gingerols, shogaols, and paradols. In fresh ginger, gingerols are the major polyphenols, such as 6-gingerol, 8-gingerol, and 10-gingerol. With heat treatment or long-time storage, gingerols can be transformed into corresponding shogaols. After hydrogenation, shogaols can be transformed into paradols [2]. There are also many other phenolic compounds in ginger, such as quercetin, zingerone, gingerenone-A, and 6-dehydrogingerdione [14,15]. Moreover, there are several terpene components in ginger, such as  $\beta$ -bisabolene,  $\alpha$ -curcumene, zingiberene,  $\alpha$ -farnesene, and  $\beta$ -sesquiphellandrene, which are considered to be the main constituents of ginger essential oils [16]. Besides these, polysaccharides, lipids, organic acids, and raw fibers are also present in ginger [13,16].

### 2.2. Antioxidant Activity

It has been known that overproduction of free radicals, such as reactive oxygen species (ROS), plays an important part in the development of many chronic diseases [17]. It has been reported that a variety of natural products possess antioxidant potential, such as vegetables, fruits, edible flowers, cereal grains, medicinal plants, and herbal infusions [18–24]. Several studies have found that ginger also has high antioxidant activity [14,25].

The antioxidant activity of ginger has been evaluated *in vitro* via ferric-reducing antioxidant power (FRAP), 2,2-diphenyl-1-picrylhydrazyl (DPPH), and 2,2'-azinobis-(3-ethylbenzothiazoline-6-sulfonic acid) (ABTS) methods. The results revealed that dried ginger exhibited the strongest antioxidant activity, because the number of phenolic compounds was 5.2-, 1.1-, and 2.4-fold higher than that of fresh, stir-fried, and carbonized ginger, respectively. The antioxidant activity of different gingers had a tendency to be the following: dried ginger > stir-fried ginger > carbonized ginger > fresh ginger. This was mainly associated with their polyphenolic contents. When fresh ginger was heated, dried ginger with higher antioxidant activity was obtained, because fresh ginger contains a higher moisture content. However, when dried ginger was further heated to obtain stir-fried ginger and carbonized ginger, the antioxidant activity decreased, because the processing could change gingerols into shogaols [26]. Additionally, a fraction of the dried ginger powder abundant in polyphenols showed high antioxidant activity based on data from FRAP, oxygen radical absorbance capacity, and cellular antioxidant activity assays [27]. Besides, the type of extraction solvent could have an effect on the antioxidant activity of ginger. An ethanolic extract of ginger showed high Trolox-equivalent antioxidant capacity and ferric-reducing ability, and an aqueous extract of ginger exhibited strong free radical scavenging activity and chelating ability [16]. Moreover, ethanolic, methanolic, ethyl acetate, hexane, and water extracts of ginger respectively inhibited 71%, 76%, 67%, 67%, and 43% of human low-density lipoprotein (LDL) oxidation induced by  $\text{Cu}^{2+}$  [28]. Results from a xanthine/xanthine oxidase system showed that an ethyl acetate extract and an aqueous extract had higher antioxidant properties than ethanol, diethyl ether, and *n*-butanol extracts did [3].

Several studies have indicated that ginger was effective for protection against oxidative stress. The underlying mechanisms of antioxidant action were investigated in cell models [14,29]. Ginger extract showed antioxidant effects in human chondrocyte cells, with oxidative stress mediated by interleukin-1 $\beta$  (IL-1 $\beta$ ). It stimulated the expression of several antioxidant enzymes and reduced the generation of ROS and lipid peroxidation [30]. Additionally, ginger extract could reduce the production of ROS in human fibrosarcoma cells with  $\text{H}_2\text{O}_2$ -induced oxidative stress [31]. In stressed rat heart homogenates, ginger extract decreased the content of malondialdehyde (MDA), which was related to lipid peroxidation [29]. Ginger and its bioactive compounds (such as 6-shogaol) exhibited antioxidant activity via the nuclear factor erythroid 2-related factor 2 (Nrf2) signaling pathway (Figure 1) [32]. In human colon cancer cells, 6-shogaol increased intracellular glutathione/glutathione

disulfide (GSH/GSSG) and upregulated Nrf2 target gene expression, such as with heme oxygenase-1 (*HO-1*), metallothionein 1 (*MT1*), aldo-keto reductase family 1 member B10 (*AKR1B10*), ferritin light chain (*FTL*), and  $\gamma$ -glutamyltransferase-like activity 4 (*GGTLA4*). Besides, 6-shogaol also enhanced the expression of genes involved in glutathione synthesis, such as the glutamate-cysteine ligase catalytic subunit (*GCLC*) and the glutamate-cysteine ligase modifier subunit (*GCLM*). Further analysis revealed that 6-shogaol and its metabolite activated Nrf2 via the alkylation of cysteine residues of Kelch-like ECH-associated protein 1 (Keap1) [33]. Moreover, ginger phenylpropanoids improved Nrf2 activity and enhanced the levels of glutathione S-transferase P1 (GSTP1) as well as the downstream effector of the Nrf2 antioxidant response element in foreskin fibroblast cells [15]. In a human mesenchymal stem cell model, ginger oleoresin was investigated for its effects on injuries that were induced by ionizing radiation. The treatment of oleoresin could decrease the level of ROS by translocating Nrf2 to the cell nucleus and activating the gene expression of *HO-1* and *NQO1* (nicotinamide adenine dinucleotide phosphate (NADPH) quinone dehydrogenase 1) [14].

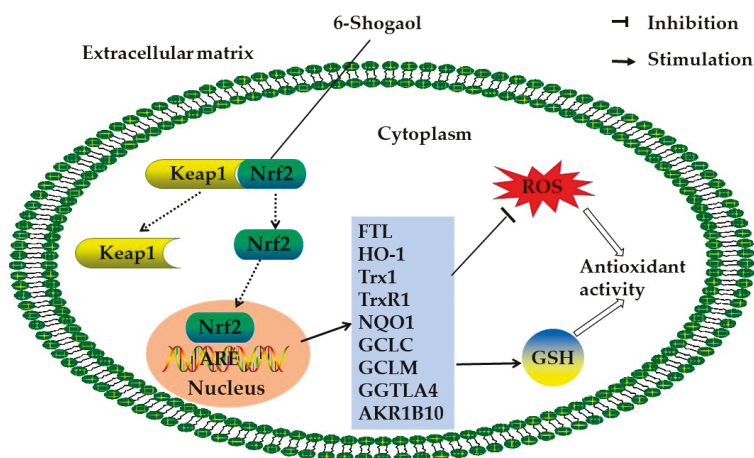


**Figure 1.** The potential mechanism for the antioxidant action of 6-shogaol: 6-shogaol leads to the translocation of Nrf2 into the nucleus and increases the expression of Nrf2 target genes by modifying Keap1 and preventing Nrf2 from proteasomal degradation. Thus, the level of GSH increases, and the level of ROS decreases. Abbreviations: Nrf2, nuclear factor erythroid 2-related factor 2; Keap1, Kelch-like ECH-associated protein 1; *NQO1*, nicotinamide adenine dinucleotide phosphate (NADPH) quinone dehydrogenase 1; *HO-1*, heme oxygenase-1; *GCLC*, glutamate-cysteine ligase catalytic subunit; *GCLM*, glutamate-cysteine ligase modifier subunit; *Trx1*, thioredoxin 1; *TrxR1*, thioredoxin reductase 1; *AKR1B10*, Aldo-keto reductase family 1 member B10; *FTL*, ferritin light chain; *GGTLA4*,  $\gamma$ -glutamyltransferase-like activity 4; ROS, reactive oxygen species; GSH, glutathione; ARE, antioxidant response element.

An animal model has also been used to investigate the antioxidant properties of ginger and its bioactive compounds in vivo. There, 6-shogaol exhibited antioxidant potential by inducing the expression of Nrf2 target genes such as *MT1*, *HO-1*, and *GCLC* in the colon of wild-type mice, but not *Nrf2*<sup>-/-</sup> mice [33]. In addition, rats with a gastric ulcer induced by diclofenac sodium were treated with the butanol extract of ginger. It could prevent an increase in the level of MDA and a decrease in catalase activity as well as the level of glutathione [34]. Moreover, the 6-gingerol-rich fraction from ginger could reduce the levels of H<sub>2</sub>O<sub>2</sub> and MDA, enhance antioxidant enzyme activity, and increase glutathione in rats with oxidative damage induced by chlorpyrifos [25]. Furthermore, treatment with ginger extract elevated the contents of antioxidants and testosterone in serum and protected rat testes from injuries in chemotherapy with cyclophosphamide [35].

Overall, *in vitro* and *in vivo* studies have demonstrated that ginger and its bioactive compounds, such as 6-shogaol, 6-gingerol, and oleoresin, possess strong antioxidant activity (Table 1). Moreover, the activation of the Nrf2 signaling pathway is crucial to the underlying mechanisms of action. It should also be pointed out that the overproduction of ROS in the human body is considered to be a cause of many diseases. Theoretically, antioxidants should be effective. However, several factors, such as health conditions, individual differences, the lifestyles of people, other dietary factors, and the dosage, solubility, and oral intake of antioxidants could affect the bioaccessibility and bioavailability of antioxidants, leading to low blood concentrations overall, which probably could explain why most antioxidants do not work in the real world.

### 2.3. Anti-Inflammatory Activity

A series of studies showed that ginger and its active constituents possessed anti-inflammatory activity (Table 2), which could protect against inflammation-related diseases such as colitis [4,36]. The anti-inflammatory effects were mainly related to phosphatidylinositol-3-kinase (PI3K), protein kinase B (Akt), and the nuclear factor kappa light chain-enhancer of activated B cells (NF- $\kappa$ B).

In addition, 6-shogaol showed protective effects against tumor necrosis factor  $\alpha$  (TNF- $\alpha$ )-induced intestinal barrier dysfunction in human intestinal cell models. It also prevented the upregulation of Claudin-2 and the disassembly of Claudin-1 via the suppression of signaling pathways involved with PI3K/Akt and NF- $\kappa$ B [37]. In addition, 6-dehydroshogaol was more potent than 6-shogaol and 6-gingerol in reducing the generation of proinflammatory mediators such as nitric oxide (NO) and prostaglandin E<sub>2</sub> (PGE<sub>2</sub>) in mouse macrophage RAW 264.7 cells [36]. Besides, ginger extract and zingerone inhibited NF- $\kappa$ B activation and decreased the level of IL-1 $\beta$  in the colons of mice, which alleviated colitis induced by 2, 4, 6-trinitrobenzene sulfonic acid [38]. Ginger also protected against anti-CD3 antibody-induced enteritis in mice, and ginger could reduce the production of TNF- $\alpha$  as well as the activation of Akt and NF- $\kappa$ B [39]. Moreover, nanoparticles derived from edible ginger (GDNPs 2) could prevent intestinal inflammation by increasing the levels of anti-inflammatory cytokines such as interleukin-10 (IL-10) and IL-22 and decreasing the levels of proinflammatory cytokines such as TNF- $\alpha$ , IL-6, and IL-1 $\beta$  in mice with acute colitis and chronic colitis [4]. In addition, nanoparticles loaded with 6-shogaol were found to attenuate colitis symptoms and improve colitis wound repair in mice with dextran sulfate sodium-induced colitis [40]. Moreover, microRNAs of ginger exosome-like nanoparticles (GELN) ameliorated mouse colitis by inducing the production of IL-22, a barrier function improvement factor [41]. Additionally, a fraction rich in 6-gingerol prevented an increase in inflammatory markers such as myeloperoxidase, NO, and TNF- $\alpha$  in the brain, ovaries, and uterus of rats treated with chlorpyrifos [25]. Furthermore, 28 male endurance runners consumed capsules of 500 mg of ginger powder. The results showed that the treatment could attenuate the post-exercise elevation of several cytokines that promote inflammation, such as plasma IL-1 $\beta$ , IL-6, and TNF- $\alpha$  [42].

In general, ginger and its active compounds have been found to be effective in alleviating inflammation, especially in inflammatory bowel diseases. The anti-inflammatory mechanisms of ginger are probably associated with the inhibition of Akt and NF- $\kappa$ B activation, an enhancement in anti-inflammatory cytokines, and a decline in proinflammatory cytokines. Notably, the application of ginger nanoparticles has the potential to improve the prevention of and therapy for inflammatory bowel disease.

Table 1. The antioxidant activity and potential mechanisms of ginger.

Constituent	Study Type	Subjects	Dose	Potential Mechanisms	Ref.
6-shogaol	In vivo	HCT-116 human colon cancer cells	20 $\mu$ M	Increasing the intracellular GSH/GSSG ratio; decreasing the level of ROS; upregulating the expression of <i>AKR1B10</i> , <i>FTL</i> , <i>GGTLA4</i> , <i>HO-1</i> , <i>MT1</i> , <i>GCLC</i> , and <i>GCLM</i> genes	[33]
Ginger oleoresin	In vitro	Wild-type and <i>Nrf2</i> <sup>-/-</sup> C57BL/6J mice	100 mg/kg	Upregulating the expression of <i>MT1</i> , <i>HO-1</i> , and <i>GCLC</i>	
Ginger phenylpropanoids	In vitro	Human mesenchymal stem cells	100 $\mu$ g/mL	Reducing ROS production; inducing the translocation of <i>Nrf2</i> to the cell nucleus; activating <i>HO-1</i> and <i>NQO1</i> gene expression	[14]
6-gingerol-rich fraction	In vitro	BJ foreskin fibroblasts	40 $\mu$ g/mL	Increasing <i>Nrf2</i> activity and the level of <i>GSTP1</i>	[15]
Ginger extract	In vivo	Female Wistar rats	50 and 100 mg/kg	Reducing the levels of $H_2O_2$ and MDA; increasing the activities of antioxidant enzymes and the level of GSH	[25]
	In vivo	Male Wistar albino rats	100 mg/kg	Reducing the level of MDA; preventing the depletion of catalase activity and GSH content	[34]
	In vitro	C28I2 human chondrocyte cells	5 and 25 $\mu$ g/mL	Increasing the gene expression of antioxidant enzymes; reducing the content of ROS and lipid peroxidation	[30]
	In vitro	HT1080 human fibrosarcoma cells	200 and 400 $\mu$ g/mL	Reducing the generation of ROS	[31]
	In vitro	Rat heart homogenates	78–313 $\mu$ g/mL	Decreasing the level of MDA	[29]

GSSG, glutathione disulfide; *MT1*, metallothionein 1; *GSTP1*, glutathione S-transferase P1; MDA, malondialdehyde; Ref, reference.

Table 2. Anti-inflammatory activity and potential mechanisms of ginger.

Constituent	Study Type	Subjects	Dose	Potential Mechanisms	Ref.
6-shogaol	In vitro	HT-29/B6 and Caco-2 human intestinal epithelial cells	100 $\mu$ M	Inhibiting the PI3K/Akt and NF- $\kappa$ B signaling pathways	[37]
6-shogaol and 6-gingerol, 6-dehydroshogaol	In vitro	RAW 264.7 mouse macrophage cells	2.5, 5, and 10 $\mu$ M	Inhibiting the production of NO and PGE <sub>2</sub>	[36]
6-gingerol-rich fraction	In vivo	Female Wistar rats	50 and 100 mg/kg	Increasing the levels of myeloperoxidase, NO, and TNF- $\alpha$	[25]
GDNPs 2	In vivo	Female C57BL/6 FVB/NJ mice	0.3 mg	Increasing the levels of IL-10 and IL-22; decreasing the levels of TNF- $\alpha$ , IL-6, and IL-1 $\beta$	[4]
Ginger extract and zingerone	In vivo	Female BALB/c mice	0.1, 1, 10, and 100 mg/kg	Inhibiting NF- $\kappa$ B activation and decreasing the level of IL-1 $\beta$	[38]
Ginger extract	In vivo	C57BL/6J mice	50 mg/mL	Inhibiting the production of TNF- $\alpha$ ; Activating Akt and NF- $\kappa$ B	[39]

NO, nitric oxide; PGE<sub>2</sub>, prostaglandin E<sub>2</sub>; TNF- $\alpha$ , tumor necrosis factor  $\alpha$ ; GDNPs 2, nanoparticles derived from edible ginger.

## 2.4. Antimicrobial Activity

The spread of bacterial, fungal, and viral infectious diseases has been a major public threat due to antimicrobial resistance. Several herbs and spices have been developed into natural effective antimicrobial agents against many pathogenic microorganisms [43]. In recent years, ginger has been reported to show antibacterial, antifungal, and antiviral activities [44,45].

Biofilm formation is an important part of infection and antimicrobial resistance. One result found that ginger inhibited the growth of a multidrug-resistant strain of *Pseudomonas aeruginosa* by affecting membrane integrity and inhibiting biofilm formation [46]. In addition, treatment with ginger extract blocked biofilm formation via a reduction in the level of bis-(3'-5')-cyclic dimeric guanosine monophosphate (c-di-GMP) in *Pseudomonas aeruginosa* PA14 [47]. Moreover, a crude extract and methanolic fraction of ginger inhibited biofilm formation, glucan synthesis, and the adherence of *Streptococcus mutans* by downregulating virulence genes. Consistent with the in vitro study, a reduction in caries development caused by *Streptococcus mutans* was found in a treated group of rats [48]. Furthermore, an in vitro study revealed that gingerenone-A and 6-shogaol exhibited an inhibitory effect on *Staphylococcus aureus* by inhibiting the activity of 6-hydroxymethyl-7, 8-dihydropterin pyrophosphokinase in the pathogen [49].

The compounds in ginger essential oil possess lipophilic properties, making the cell wall as well as the cytoplasmic membrane more permeable and inducing a loss of membrane integrity in fungi [50]. An in vitro study revealed that ginger essential oil effectively inhibited the growth of *Fusarium verticillioides* by reducing ergosterol biosynthesis and affecting membrane integrity. It could also decrease the production of fumonisin B<sub>1</sub> and fumonisin B<sub>2</sub> [51]. In addition, ginger essential oil had efficacy in suppressing the growth of *Aspergillus flavus* as well as aflatoxin and ergosterol production [50]. Moreover, the  $\gamma$ -terpinene and citral in ginger essential oil showed potent antifungal properties against *Aspergillus flavus* and reduced the expression of some genes related to aflatoxin biosynthesis [44]. Furthermore, fresh ginger was found to inhibit plaque formation induced by human respiratory syncytial virus (HRSV) in respiratory tract cell lines. Ginger was effective in blocking viral attachment and internalization [52]. In a clinical trial, ginger extract decreased hepatitis C virus (HCV) loads, the level of  $\alpha$ -fetoprotein (AFP), and markers relevant to liver function, such as aspartate aminotransferase (AST) and alanine aminotransferase (ALT), in Egyptian HCV patients [53].

Therefore, ginger has been demonstrated to inhibit the growth of different bacteria, fungi, and viruses. These effects could be mainly related to the suppression of bacterial biofilm formation, ergosterol biosynthesis, and viral attachment and internalization (Table 3).

**Table 3.** Antimicrobial activity and potential mechanisms of ginger.

Constituent	Study Type	Subjects	Dose	Potential Mechanisms	Ref.
Ginger essential oil	In vitro	<i>Fusarium verticillioides</i>	500, 1000, 2000, 3000, 4000, and 5000 $\mu$ g/mL	Reducing ergosterol biosynthesis; affecting membrane integrity; decreasing the production of fumonisin B <sub>1</sub> and fumonisin B <sub>2</sub>	[51]
	In vitro	<i>Aspergillus flavus</i>	5, 10, 15, 20, 25, 50, 100, and 150 $\mu$ g/mL	Reducing ergosterol biosynthesis; affecting membrane integrity; inhibiting the production of aflatoxin	[50]
Gingerenone-A and shogaol	In vitro	<i>Staphylococcus aureus</i>	25, 50, and 75 $\mu$ g/mL	Inhibiting the activity of 6-hydroxymethyl-7, 8-dihydropterin pyrophosphokinase	[49]
Ginger extract	In vitro	<i>Pseudomonas aeruginosa</i>	50, 100, 150, and 200 $\mu$ g/mL	Affecting membrane integrity; inhibiting biofilm formation	[46]
	In vitro	<i>Streptococcus mutans</i>	8, 16, 32, 64, and 128 $\mu$ g/mL	Inhibiting biofilm formation, glucan synthesis, and adherence	[48]
	In vitro	HEp-2 human larynx epidermoid carcinoma cells and A549 human lung carcinoma cells with HRSV	10, 30, 100, and 300 $\mu$ g/mL	Blocking viral attachment and internalization	[52]

HRSV, human respiratory syncytial virus.

## 2.5. Cytotoxicity

Cancer is documented to be a dominant cause of death, and there were approximately 9.6 million cases of death in 2018 [54]. Several research works have demonstrated that natural products such as fruits and medicinal plants possess anticancer activity [55,56]. Recently, ginger has been widely investigated for its anticancer properties against different cancer types, such as breast, cervical, colorectal, and prostate cancer [4,57,58]. The potential mechanisms of action involve the inhibition of proliferation and the induction of apoptosis in cancer (Figure 2) [59,60].

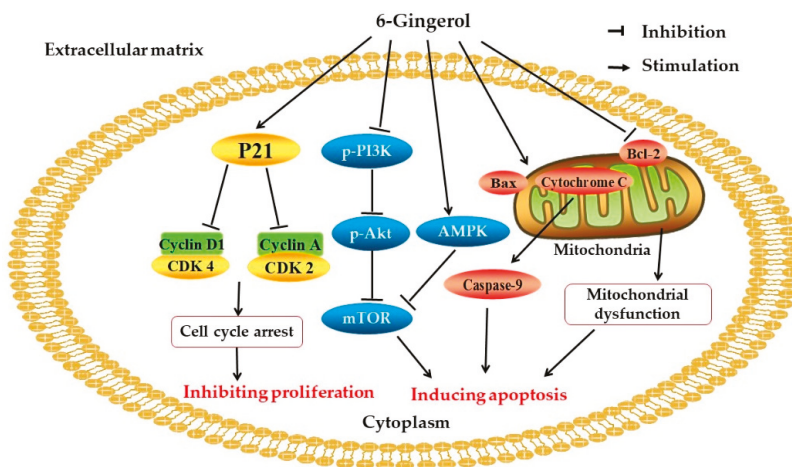


**Figure 2.** Several signaling pathways are involved in the anticancer mechanisms of 6-gingerol. CDK: Cyclin-dependent kinase; PI3K: Phosphoinositide 3-kinase; Akt: Protein kinase B; mTOR: Mammalian target of rapamycin; AMPK: 5'adenosine monophosphate-activated protein kinase; Bax: Bcl-2-associated X protein; Bcl-2: B-cell lymphoma 2.

Several investigations have demonstrated that ginger and its bioactive compounds can interfere with the carcinogenic processes of colorectal cancer. It was observed in an in vitro study that a fraction rich in the polyphenols of dried ginger powder suppressed the proliferation of colorectal cancer cells and gastric adenocarcinoma cells [27]. Besides, treatment with ginger extract promoted apoptosis by decreasing the expression of genes involved with the Ras/extracellular signal-regulated kinase (ERK) and PI3K/Akt pathways, such as the v-Ki-ras2 Kirsten rat sarcoma viral oncogene homolog (*KRAS*), *ERK*, *Akt*, and B-cell lymphoma-extralarge (*Bcl-xL*). It also increased the expression of caspase 9, which promoted apoptosis in HT-29 colorectal cancer cells [60]. In rats with 1,2-dimethylhydrazine-induced colon cancer, ginger extract loading with coated alginate beads increased the activities of NADH dehydrogenase and succinate dehydrogenase [61]. In addition, GDNPs 2 treatment decreased tumor numbers and tumor loads in mice with colitis-associated cancer induced by azoxymethane and dextran sodium sulfate. The levels of proinflammatory cytokines were decreased, and intestinal epithelial cell proliferation was inhibited [4]. In a pilot, randomized, and controlled trial, ginger extract supplementation decreased proliferation and increased apoptosis in the colonic mucosa of patients with a high risk of colorectal cancer. Ginger extract supplementation induced a decrease in the expression of two markers of cell proliferation, telomerase reverse transcriptase (hTERT) and MIB-1 (epitope of Ki-67), and increased the expression of pro-apoptotic gene Bcl-2-associated X (*Bax*) [6]. In subjects with a high risk of colorectal cancer, ginger supplementation decreased cyclooxygenase-1 (COX-1) expression, a key enzyme in the production of PGE<sub>2</sub>, which indicated the preventive potential of ginger in colorectal cancer [62].

The cytotoxic effects and underlying mechanisms of ginger in prostate cancer were evaluated both in vivo and in vitro. It was found that 6-gingerol, 10-gingerol, 6-shogaol, and 10-shogaol

showed an antiproliferative effect on human prostate cancer cells via a downregulation of the protein expression of multidrug resistance associated protein 1 (MRP1) and glutathione-S-transferase (GST $\pi$ ) [59]. In addition, binary combinations of ginger phytochemicals, such as 6-gingerol, 8-gingerol, 10-gingerol, and 6-shogaol, synergistically inhibited the proliferation of PC-3 prostate cancer cells [63]. An *in vivo* study investigated the effect of ginger on athymic nude mice with human prostate tumor xenografts. A natural ginger extract showed a 2.4-fold higher inhibitory effect on the growth of tumors than an artificial mixture of 6-shogaol, 6-gingerol, 8-gingerol, and 10-gingerol [64]. Additionally, 6-shogaol could be more significant than 6-gingerol and 6-paradol in reducing cell survival and inducing apoptosis in human and mouse prostate cancer cells. It worked mainly through the suppression of signal transducer and activator of transcription 3 (STAT3) and NF- $\kappa$ B signaling. It also decreased the expression of *cyclinD1*, *survivin*, *c-Myc*, and B-cell lymphoma 2 (*Bcl-2*), and enhanced *Bax* expression [56].

Ginger also exhibits cytotoxic activity against other types of cancer, such as breast, cervical, liver, and pancreatic cancer. An *in vitro* study revealed that 6-gingerol could inhibit the growth of HeLa human cervical adenocarcinoma cells, and it induced cell cycle arrest in the G<sub>0</sub>/G<sub>1</sub>-phase by decreasing the protein levels of cyclin A and cyclin D1. Apoptosis in HeLa cells was induced by increasing the expression of caspase and inhibiting mammalian target of rapamycin (mTOR) signaling [65]. Besides, ginger extract protected against breast cancer in mice through the activation of 5' adenosine monophosphate-activated protein kinase (AMPK) and the downregulation of cyclin D1. The extract promoted apoptosis via an increase in the expression of the tumor suppressor gene *p53* and a decrease in the level of NF- $\kappa$ B in tumor tissue [58]. Additionally, 10-gingerol was found to be potent in inhibiting human and mouse breast carcinoma cell growth. It reduced cell division and induced S phase cell cycle arrest and apoptosis [66]. Moreover, fluorescent carbon nanodots (C-dots) prepared from ginger effectively controlled tumor growth in nude mice, where the tumor was caused by HepG2 human hepatocellular carcinoma cells. The *in vitro* experiment found that C-dots increased the content of ROS in the HepG2 cells, which upregulated the expression of *p53* and promoted apoptosis [67]. Furthermore, ginger extract and 6-shogaol suppressed the growth of human pancreatic cancer cells and led to ROS-mediated and caspase-independent cell death. Ginger extract suppressed tumor growth from pancreatic cancer in both a peritoneal dissemination model and an orthotopic model of mice without serious adverse effects [68].

Experimental studies have demonstrated that ginger can prevent and treat several types of cancer, such as colorectal, prostate, breast, cervical, liver, and pancreatic cancer (Table 4). The anticancer mechanisms mainly involve the induction of apoptosis and the inhibition of the proliferation of cancer cells.

## 2.6. Neuroprotection

Some individuals, especially elderly people, have a high risk for neurodegenerative diseases, such as Alzheimer's disease (AD) and Parkinson's disease (PD) [69]. Recently, many investigations have revealed that ginger positively affects memory function and exhibits anti-neuroinflammatory activity, which might contribute to the management and prevention of neurodegenerative diseases [70,71].

The results from a lipopolysaccharide (LPS)-activated BV2 microglia culture model revealed that 10-gingerol was responsible for the strong anti-neuroinflammatory capacity of fresh ginger. It inhibited the expression of proinflammatory genes by blocking NF- $\kappa$ B activation, which led to a decline in the levels of NO, IL-1 $\beta$ , IL-6, and TNF- $\alpha$  [7]. Additionally, in mice with scopolamine-induced memory deficits, ginger extract could ameliorate the cognitive function of mice, which was assessed by a novel object recognition test. Further experiments in mouse hippocampi and rat C6 glioma cells revealed that ginger extract promoted the formation of synapses in the brain through the activation of extracellular signal-regulated kinase (ERK) induced by nerve growth factor (NGF) and cyclic AMP response element-binding protein (CREB) [69]. Another study found that 6-shogaol exhibited neuroprotective activity by activating Nrf2, scavenging free radicals, and elevating the levels of several phase II antioxidant molecules, such as NQO1 and HO-1, in neuron-like rat pheochromocytoma PC12

cells [32]. In addition, 6-dehydrogingerdione exhibited cytoprotection against neuronal cell damage induced by oxidative stress. It could effectively scavenge various free radicals in PC12 cells [72].

**Table 4.** Cytotoxic activity and potential mechanisms of ginger.

Constituent	Study Type	Subjects	Dose	Potential Mechanisms	Ref.
6-shogaol	In vitro	LNCaP, DU145, and PC-3 human prostate cancer cells	10, 20, and 40 $\mu$ M	Inducing apoptosis; inhibiting STAT3 and NF- $\kappa$ B signaling; downregulating the expression of <i>cyclin D1</i> , <i>survivin</i> , <i>c-Myc</i> , and <i>Bcl2</i>	[57]
6-gingerol	In vitro	HeLa human cervical adenocarcinoma cells	60, 100, and 140 $\mu$ M	Inducing cell cycle arrest in the G <sub>0</sub> /G <sub>1</sub> -phase; decreasing the levels of cyclin A, cyclin D1, and cyclin E1; increasing the expression of caspase; inhibiting the mTOR signaling pathway	[65]
10-gingerol	In vitro	Human and mouse breast carcinoma cells	50, 100, and 200 $\mu$ M	Inhibiting cell growth; reducing cell division; inducing S phase cell cycle arrest and apoptosis	[66]
6-gingerol, 10-gingerol, 6-shogaol, and 10-shogaol	In vitro	PC-3 human prostate cancer cells	1,10, and 100 $\mu$ M	Inhibiting prostate cancer cell proliferation; downregulating the expression of MRP1 and GST $\pi$	[59]
GDNPs 2	In vivo	Female C57BL/6 mice	0.3 mg	Suppressing the expression of cyclin D1; inhibiting intestinal epithelial cell proliferation	[4]
Ginger extract	In vitro	HT29 human colorectal adenocarcinoma cells	2–10 mg/mL	Promoting apoptosis; upregulating the caspase 9 gene; downregulating <i>KRAS</i> , <i>ERK</i> , <i>Akt</i> , and <i>Bcl-xL</i>	[60]
	In vivo	Female Swiss albino mice	100 mg/kg	Activating AMPK; decreasing the expression of cyclin D1 and the level of NF- $\kappa$ B;	[58]
Ginger extract with alginate beads	In vivo	Male Wistar rats	50 mg/kg	increasing the expression of <i>p53</i>	[61]
Ginger extract-based fluorescent carbon nanodots	In vitro	HepG2 human hepatocellular carcinoma cells	1.11 mg/mL	Increasing the activity of NADH dehydrogenase and succinate dehydrogenase	[67]

STAT3, signal transducer and activator of transcription 3; Bcl-2, B-cell lymphoma 2; mTOR, mammalian target of rapamycin; MRP1, multidrug resistance associated protein 1; GST $\pi$ , glutathione-S-transferase; AMPK, 5'adenosine monophosphate-activated protein kinase; NF- $\kappa$ B, nuclear factor kappa light chain-enhancer of activated B cells.

In a mouse model of AD induced by amyloid  $\beta_{1-42}$  plaque, fermented ginger ameliorated memory impairment by protecting neuronal cells in mouse hippocampi, and it increased the levels of presynaptic and postsynaptic proteins [71]. In addition, ginger extract had protective effects against AD in rats, and a high dose of ginger extract decreased latency in showing significant memory deficits, as well as the levels of NF- $\kappa$ B, IL-1 $\beta$ , and MDA [73]. Moreover, 6-shogaol could alleviate cognitive dysfunction in mice with AD by inhibiting inflammatory responses, upregulating the level of NGF, and enhancing synaptogenesis in the brain [74]. Furthermore, in rat mesencephalic cells treated with 1-methyl-4-phenylpyridinium (MPP<sup>+</sup>), 6-shogaol improved the amount of tyrosine hydroxylase-immunoreactive (TH-IR) neurons and inhibited the levels of TNF- $\alpha$  and NO. Treatment with 6-shogaol ameliorated motor coordination and bradykinesia in vivo in PD [70].

The above studies found that ginger and its bioactive compounds, such as 10-gingerol, 6-shogaol, and 6-dehydrogingerdione, exhibited protective effects against AD and PD. The antioxidant and anti-inflammatory activities of ginger contributed to neuroprotection.

## 2.7. Cardiovascular Protection

Cardiovascular diseases have been considered to be a leading cause of premature death, and 17.9 million people die per year [75]. Dyslipidemia and hypertension are known to be risk

factors for cardiovascular diseases, including stroke and coronary heart disease [8,76]. A series of studies has shown that ginger can decrease the levels of blood lipids and blood pressure [77,78], contributing to protection from cardiovascular diseases.

Ginger extract reduced the body weight of rats fed a high-fat diet and enhanced the level of serum high-density lipoprotein-cholesterol (HDL-C), a protective factor against coronary heart disease. Besides, ginger extract increased the levels of apolipoprotein A-1 and lecithin-cholesterol acyltransferase mRNA in the liver, which was related to high-density lipoprotein (HDL) formation [79]. Additionally, total cholesterol (TC) and LDL concentrations were decreased by ginger extract in rats fed a high-fat diet, and the level of HDL increased through the combined application of aerobic exercise and ginger extract [76]. Moreover, ginger extract could reduce the levels of plasma TC, triglyceride (TG), and very low-density lipoprotein (VLDL) cholesterol in high-fat diet rats. The mechanism was related to higher liver expression of peroxisome proliferator-activated receptors (PPAR $\alpha$  and PPAR $\gamma$ ), which were related to atherosclerosis [78].

Vascular smooth muscle cell proliferation is a process in the pathogenesis of cardiovascular diseases. In an *in vitro* study, 6-shogaol exerted antiproliferative effects through increasing the number of cells in the G<sub>0</sub>/G<sub>1</sub> phase and activating the Nrf2 and HO-1 pathways [80]. In addition, ginger decreased the activities of angiotensin-1 converting enzyme (ACE) and arginase and increased the level of NO, a well-known vasodilator molecule. Thus, blood pressure decreased in hypertensive rats pretreated with ginger [8]. Besides, ginger protected against hypertension-derived complications by decreasing platelet adenosine deaminase (ADA) activity and increasing the level of adenosine, which prevented platelet aggregation and promoted vasodilation in hypertensive rats [77]. Moreover, ginger extract exhibited vasoprotective effects on porcine coronary arteries by suppressing NO synthase and cyclooxygenase [81]. Furthermore, a cross-sectional study found that the probability of hypertension and coronary heart disease declined when a daily intake of ginger was increased [82].

Generally, ginger has exhibited cardiovascular protective effects by attenuating hypertension and ameliorating dyslipidemia, such as in the improvement of HDL-C, TC, LDL, TG, and VLDL.

### 2.8. Antiobesity Activity

Obesity is a risk factor for many chronic diseases, such as diabetes, hypertension, and cardiovascular diseases [83]. Several studies have reported that ginger is effective in the management and prevention of obesity [9,84].

In 3T3-L1 preadipocyte cells, gingerone A exhibited a greater inhibitory effect on adipogenesis and lipid accumulation than gingerols and 6-shogaol. Gingerone A could also modulate fatty acid metabolism via the activation of AMPK *in vivo*, attenuating diet-induced obesity [9]. In cultured skeletal muscle myotubes, 6-shogaol and 6-gingerol could increase peroxisome proliferator-activated receptor  $\delta$  (PPAR $\delta$ )-dependent gene expression, and this resulted in the enhancement of cellular fatty acid catabolism [83]. In addition, both ginger and orlistat reduced the body weight and lipid profile of high-fat diet rats, while ginger had a greater effect on increasing the level of HDL-C than orlistat did [84]. In a randomized, double-blind, and placebo-controlled study, obese women receiving 2 g of ginger powder daily had a decreased body mass index (BMI) [85]. Moreover, the intake of dried ginger powder could reduce respiratory exchange ratios and promote fat utilization by increasing fat oxidation in humans [86].

Ginger and its bioactive constituents, including gingerone A, 6-shogaol, and 6-gingerol, have shown antiobesity activity, with the mechanisms mainly related to the inhibition of adipogenesis and the enhancement of fatty acid catabolism.

### 2.9. Antidiabetic Activity

Diabetes mellitus is known as a severe metabolic disorder caused by insulin deficiency and/or insulin resistance, resulting in an abnormal increase in blood glucose. Prolonged hyperglycemia could accelerate protein glycation and the formation of advanced glycation end products (AGEs) [87].

Many research works have evaluated the antidiabetic effect of ginger and its major active constituents [88].

An *in vitro* experiment resulted in both 6-shogaol and 6-gingerol preventing the progression of diabetic complications, and they inhibited the production of AGEs by trapping methylglyoxal (MGO), the precursor of AGEs [87]. Additionally, 6-gingerol reduced the levels of plasma glucose and insulin in mice with high-fat diet-induced obesity. N $\epsilon$ -carboxymethyl-lysine (CML), a marker of AGEs, was decreased by 6-gingerol through Nrf2 activation [88]. In 3T3-L1 adipocytes and C2C12 myotubes, 6-paradol and 6-shogaol promoted glucose utilization by increasing AMPK phosphorylation. In addition, in a mouse model fed a high-fat diet, 6-paradol significantly reduced the level of blood glucose [10]. In another study, 6-gingerol facilitated glucose-stimulated insulin secretion and ameliorated glucose tolerance in type 2 diabetic mice by increasing glucagon-like peptide 1 (GLP-1). Besides, 6-gingerol treatment activated glycogen synthase 1 and increased cell membrane presentation of glucose transporter type 4 (GLUT4), which increased glycogen storage in skeletal muscles [89]. Furthermore, the consumption of ginger could reduce the levels of fasting plasma glucose, glycated hemoglobin A (HbA<sub>1c</sub>), insulin, TG, and TC in patients with type 2 diabetes mellitus (DM2) [90]. Moreover, ginger extract treatment improved insulin sensitivity in rats with metabolic syndrome, which might have been relevant to the energy metabolism improvement induced by 6-gingerol [91]. In addition, ginger extract alleviated retinal microvascular changes in rats that had diabetes induced by streptozotocin. Ginger extract could reduce the levels of NF- $\kappa$ B, TNF- $\alpha$ , and vascular endothelial growth factor in the retinal tissue [92]. In a randomized, double-blind, and placebo-controlled trial, the ingestion of ginger decreased the levels of insulin, low-density lipoprotein cholesterol (LDL-C), and TG; decreased the homeostasis model assessment index; and increased the quantitative insulin sensitivity check index in patients with DM2 [93].

The studies have demonstrated that ginger and its bioactive compounds could protect against diabetes mellitus and its complications, probably by decreasing the level of insulin, but increasing the sensitivity of insulin.

#### 2.10. Antinausea and Antiemetic Activities

Ginger has been traditionally used to treat gastrointestinal symptoms, and recent research has demonstrated that ginger could effectively alleviate nausea and emesis [11,94,95].

In a clinical trial, inhaling ginger essence could attenuate nausea intensity and decrease emesis episodes two and six hours after a nephrectomy in patients [96]. In addition, dried ginger powder treatment reduced episodes of intraoperative nausea in elective cesarean section patients [97]. Moreover, nausea and emesis are common side effects of chemotherapy [98]. The activation of vagal afferent mediated by serotonin (5-HT) is crucial in the mechanism of emesis. An *in vitro* experiment revealed that 6-shogaol, 6-gingerol, and zingerone inhibited emetic signal transmission in vagal afferent neurons by suppressing the 5-HT receptor, and 6-shogaol had the strongest inhibitory efficacy [99]. Furthermore, ginger extract alleviated chemotherapy-induced nausea and emesis by suppressing the activation of 5-HT receptors in enteric neurons [11]. In a double-blind, randomized, and placebo-controlled trial, supplementation with ginger could improve the nausea-related quality of life in patients after chemotherapy [94]. Moreover, ginger alleviated the nausea induced by antituberculosis drugs and antiretroviral therapy, and it reduced the frequency of mild, moderate, and severe episodes of nausea in patients [100,101].

Previous results have shown that ginger could attenuate pregnancy-induced nausea and emesis and motion sickness, while recent studies have focused on the preventive efficacy of ginger on postoperative and chemotherapy-induced nausea and emesis [102].

### 2.11. Protective Effects against Respiratory Disorders

Natural herbal medicines have a long history of application in the treatment of respiratory disorders such as asthma, and ginger is one of these remedies [12,103]. Ginger and its bioactive compounds have exhibited bronchodilating activity and antihyperactivity in several studies [104].

Ginger induced significant and rapid relaxation in the isolated human airway smooth muscle. In results from guinea pig and human tracheas models, 6-gingerol, 8-gingerol, and 6-shogaol could lead to the rapid relaxation of precontracted airway smooth muscle. The nebulization of 8-gingerol attenuated airway resistance via a reduction in  $Ca^{2+}$  influx in mice [12]. In another study, 6-gingerol, 8-gingerol, and 6-shogaol promoted  $\beta$ -agonist-induced relaxation in human airway smooth muscle via the suppression of phosphodiesterase 4D [103]. In addition, ginger ameliorated allergic asthma by reducing allergic airway inflammation and suppressed Th2-mediated immune responses in mice with ovalbumin-induced allergic asthma [105]. Moreover, the water-extracted polysaccharides of ginger could decrease times of coughing, which was induced through citric acid in guinea pigs [106]. Besides, ginger oil and its bioactive compounds, including citral and eucalyptol, inhibited rat tracheal contraction induced by carbachol in rats [104]. Furthermore, in patients with acute respiratory distress syndrome (ARDS), an enteral diet with rich ginger contributed to gas exchange and reduced the duration of mechanical ventilation [107].

The above results indicate that ginger and its bioactive constituents, including 6-gingerol, 8-gingerol, 6-shogaol, citral, and eucalyptol, have protective effects against respiratory disorders, at least mediating them through the induction of relaxation in airway smooth muscle and the attenuation of airway resistance and inflammation.

### 2.12. Other Bioactivities of Ginger

Apart from the bioactivities mentioned above (Figure 3), ginger has other beneficial effects, such as hepatoprotective and antiallergic effects [108,109].

In a rat nephropathy model induced by gentamicin, gingerol dose-dependently ameliorated renal function and reduced lipid peroxidation and nitrosative stress. Gingerol also increased the levels of GSH and the activity of superoxide dismutase (SOD) [110]. Additionally, ginger extract ameliorated histological and biochemical alterations in the radiation-induced kidney damage of rats through antioxidant and anti-inflammatory activities [111]. Furthermore, liver histological results showed that ginger essential oil reduced lipid accumulations in the liver of obese mice fed a high-fat diet. Ginger essential oil could protect against steatohepatitis by enhancing antioxidant capacity and reducing inflammatory responses in the liver [109]. In another study with mice fed an alcohol-containing liquid diet, ginger essential oil ameliorated alcoholic fatty liver disease by decreasing the levels of AST, ALT, TG, and TC and increasing liver antioxidant enzyme activity, such as catalase and SOD [112]. To our knowledge, there has been no literature reporting the liver toxicity of ginger up to now. Additionally, in a mouse model of allergic rhinitis induced by ovalbumin (OVA), a ginger diet attenuated the severity of sneezing and nasal rubbing and inhibited the infiltration of mast cells into nasal mucosa as well as the secretion of serum immunoglobulin E. The *in vitro* study indicated that 6-gingerol could alleviate allergic rhinitis by reducing cytokine production for T cell activation and inhibiting the activation of B cells and mast cells [108]. Moreover, treatment with ginger could reduce blood loss in women with heavy menstrual bleeding [113]. In a double-blinded randomized clinical trial, treatment with ginger powder alleviated a common migraine attack and had fewer clinical adverse effects than the clinical medicine sumatriptan [114].

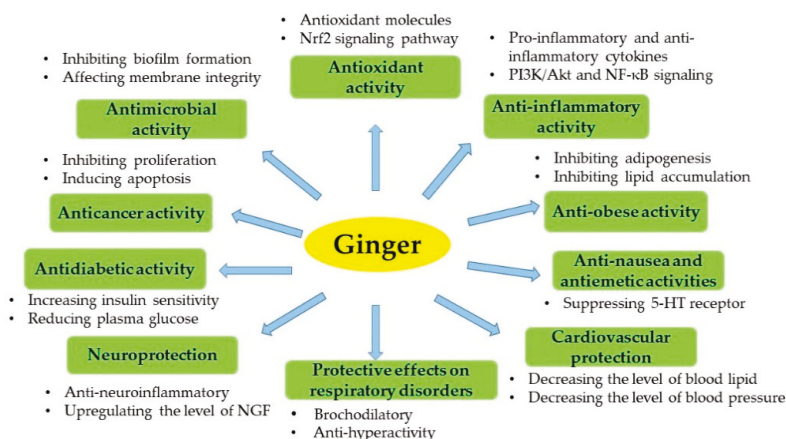


Figure 3. An overview of the bioactivities of ginger.

It is interesting to note that several plants in Zingiberaceae have also attracted increasing attention, such as *Curcuma longa* L. (turmeric), *Zingiber officinale* Roscoe (ginger), and *Alpinia zerumbet* (shell ginger) [115]. In a previous paper, we reviewed the bioactivities of curcumin (main active component of *Curcuma longa*) [116], and a comparison between ginger and shell ginger is given in Table 5. Shell ginger has exhibited similar biological activities to ginger, including antioxidant, anti-inflammatory, antimicrobial, anticancer, cardiovascular protective, antiobesity, and antidiabetic activities [115]. Differently, ginger has also been reported to have neuroprotective, respiratory protective, antinausea, and antiemetic activities, while shell ginger might contribute to longevity. In particular, shell ginger has been found to play an important contributory role in the longevity of people in Okinawa [115].

Table 5. The comparison between ginger and shell ginger.

Items	Ginger	Shell Ginger	Ref.
Scientific name	<i>Zingiber officinale</i> Roscoe	<i>Alpinia zerumbet</i> (Pers.) B.L. Burtt & R.M. Sm.	[115,117]
Family and genus	Zingiberaceae family and <i>Zingiber</i> genus	Zingiberaceae family and <i>Alpinia</i> genus	[115,117]
Edible parts	Rhizomes	Leaves and rhizomes	[8,115]
Bioactive compounds	Gingerols, shogaols, paradols, and essential oils	Dihydro-5,6-dehydrokawain, 5,6-dehydrokawain, essential oils, and flavonoids	[2,44,115]
Biological activities	Antioxidant, anti-inflammatory, antimicrobial, anticancer, cardiovascular protective, antiobesity, antidiabetic, neuroprotective, respiratory protective, antinausea, and antiemetic activities	Antioxidant, anti-inflammatory, antimicrobial, anticancer, cardiovascular protective, antiobesity, antidiabetic activities, longevity	[3–12,115]

### 3. Conclusions

In conclusion, ginger contains diverse bioactive compounds, such as gingerols, shogaols, and paradols, and possesses multiple bioactivities, such as antioxidant, anti-inflammatory, and antimicrobial properties. Additionally, ginger has the potential to be the ingredient for functional foods or nutraceuticals, and ginger could be available for the management and prevention of several diseases such as cancer, cardiovascular diseases, diabetes mellitus, obesity, neurodegenerative diseases, nausea, emesis, and respiratory disorders. In the future, more bioactive compounds in ginger could be isolated and clearly identified, and their biological activities and related mechanisms of action should be further investigated. Notably, well-designed clinical trials of ginger and its various bioactive compounds are warranted to prove its efficacy against these diseases in human beings.

**Author Contributions:** Conceptualization, Q.-Q.M., R.-Y.G., and H.-B.L.; writing—original draft preparation, Q.-Q.M. and X.-Y.X.; writing—review and editing, X.-Y.X., S.-Y.C., R.-Y.G., H.C., T.B., and H.-B.L.; supervision, R.-Y.G. and H.-B.L.; funding acquisition, R.-Y.G., H.C., and H.-B.L.

**Funding:** This study was supported by the National Key R&D Program of China (2017YFC1600100), the Shanghai Basic and Key Program (18JC1410800), the Agri-X Interdisciplinary Fund of Shanghai Jiao Tong University (Agri-X2017004), and the Key Project of the Guangdong Provincial Science and Technology Program (2014B020205002).

**Conflicts of Interest:** The authors declare no conflicts of interest.

## References

- Han, Y.A.; Song, C.W.; Koh, W.S.; Yon, G.H.; Kim, Y.S.; Ryu, S.Y.; Kwon, H.J.; Lee, K.H. Anti-inflammatory effects of the *Zingiber officinale* Roscoe constituent 12-dehydrogingerdione in lipopolysaccharide-stimulated raw 264.7 cells. *Phytother. Res.* **2013**, *27*, 1200–1205. [\[CrossRef\]](#)
- Stoner, G.D. Ginger: Is it ready for prime time? *Cancer Prev. Res.* **2013**, *6*, 257–262. [\[CrossRef\]](#)
- Nile, S.H.; Park, S.W. Chromatographic analysis, antioxidant, anti-inflammatory, and xanthine oxidase inhibitory activities of ginger extracts and its reference compounds. *Ind. Crop. Prod.* **2015**, *70*, 238–244. [\[CrossRef\]](#)
- Zhang, M.; Viennois, E.; Prasad, M.; Zhang, Y.; Wang, L.; Zhang, Z.; Han, M.K.; Xiao, B.; Xu, C.; Srinivasan, S.; et al. Edible ginger-derived nanoparticles: A novel therapeutic approach for the prevention and treatment of inflammatory bowel disease and colitis-associated cancer. *Biomaterials* **2016**, *101*, 321–340. [\[CrossRef\]](#)
- Kumar, N.V.; Murthy, P.S.; Manjunatha, J.R.; Bettadaiah, B.K. Synthesis and quorum sensing inhibitory activity of key phenolic compounds of ginger and their derivatives. *Food Chem.* **2014**, *159*, 451–457. [\[CrossRef\]](#)
- Citronberg, J.; Bostick, R.; Ahearn, T.; Turgeon, D.K.; Ruffin, M.T.; Djuric, Z.; Sen, A.; Brenner, D.E.; Zick, S.M. Effects of ginger supplementation on cell-cycle biomarkers in the normal-appearing colonic mucosa of patients at increased risk for colorectal cancer: Results from a pilot, randomized, and controlled trial. *Cancer Prev. Res.* **2013**, *6*, 271–281. [\[CrossRef\]](#) [\[PubMed\]](#)
- Ho, S.; Chang, K.; Lin, C. Anti-neuroinflammatory capacity of fresh ginger is attributed mainly to 10-gingerol. *Food Chem.* **2013**, *141*, 3183–3191. [\[CrossRef\]](#)
- Akinyemi, A.J.; Thome, G.R.; Morsch, V.M.; Stefanello, N.; Goularte, J.F.; Bello-Klein, A.; Oboh, G.; Chitolina Schetinger, M.R. Effect of dietary supplementation of ginger and turmeric rhizomes on angiotensin-1 converting enzyme (ACE) and arginase activities in L-NAME induced hypertensive rats. *J. Funct. Foods* **2015**, *17*, 792–801. [\[CrossRef\]](#)
- Suk, S.; Kwon, G.T.; Lee, E.; Jang, W.J.; Yang, H.; Kim, J.H.; Thimmesgowda, N.R.; Chung, M.; Kwon, J.Y.; Yang, S.; et al. Gingerone A, a polyphenol present in ginger, suppresses obesity and adipose tissue inflammation in high-fat diet-fed mice. *Mol. Nutr. Food Res.* **2017**, *61*, 1700139. [\[CrossRef\]](#)
- Wei, C.; Tsai, Y.; Korinek, M.; Hung, P.; El-Shazly, M.; Cheng, Y.; Wu, Y.; Hsieh, T.; Chang, F. 6-Paradol and 6-shogaol, the pungent compounds of ginger, promote glucose utilization in adipocytes and myotubes, and 6-paradol reduces blood glucose in high-fat diet-fed mice. *Int. J. Mol. Sci.* **2017**, *18*, 168. [\[CrossRef\]](#)
- Walstab, J.; Krueger, D.; Stark, T.; Hofmann, T.; Demir, I.E.; Ceyhan, G.O.; Feistel, B.; Schemann, M.; Niesler, B. Ginger and its pungent constituents non-competitively inhibit activation of human recombinant and native 5-HT3 receptors of enteric neurons. *Neurogastroent. Motil.* **2013**, *25*, 439–447. [\[CrossRef\]](#)
- Townsend, E.A.; Siviski, M.E.; Zhang, Y.; Xu, C.; Hoonjan, B.; Emala, C.W. Effects of ginger and its constituents on airway smooth muscle relaxation and calcium regulation. *Am. J. Resp. Cell Mol.* **2013**, *48*, 157–163. [\[CrossRef\]](#)
- Prasad, S.; Tyagi, A.K. Ginger and its constituents: role in prevention and treatment of gastrointestinal cancer. *Gastroent. Res. Pract.* **2015**, *2015*, 142979. [\[CrossRef\]](#)
- Ji, K.; Fang, L.; Zhao, H.; Li, Q.; Shi, Y.; Xu, C.; Wang, Y.; Du, L.; Wang, J.; Liu, Q. Ginger oleoresin alleviated gamma-ray irradiation-induced reactive oxygen species via the Nrf2 protective response in human mesenchymal stem cells. *Oxid. Med. Cell. Longev.* **2017**, *2017*, 1480294. [\[CrossRef\]](#)
- Schadich, E.; Hlavac, J.; Volna, T.; Varanasi, L.; Hajduch, M.; Dzubak, P. Effects of ginger phenylpropanoids and quercetin on Nrf2-ARE pathway in human BJ fibroblasts and HaCaT keratinocytes. *Biomed Res. Int.* **2016**, *2016*, 2173275. [\[CrossRef\]](#)

16. Yeh, H.; Chuang, C.; Chen, H.; Wan, C.; Chen, T.; Lin, L. Bioactive components analysis of two various gingers (*Zingiber officinale* Roscoe) and antioxidant effect of ginger extracts. *LWT-Food Sci. Technol.* **2014**, *55*, 329–334. [[CrossRef](#)]
17. Poprac, P.; Jomova, K.; Simunkova, M.; Kollar, V.; Rhodes, C.J.; Valko, M. Targeting free radicals in oxidative stress-related human diseases. *Trends Pharmacol. Sci.* **2017**, *38*, 592–607. [[CrossRef](#)]
18. Li, S.; Li, S.; Gan, R.; Song, F.; Kuang, L.; Li, H. Antioxidant capacities and total phenolic contents of infusions from 223 medicinal plants. *Ind. Crop. Prod.* **2013**, *51*, 289–298. [[CrossRef](#)]
19. Deng, G.; Lin, X.; Xu, X.; Gao, L.; Xie, J.; Li, H. Antioxidant capacities and total phenolic contents of 56 vegetables. *J. Funct. Foods* **2013**, *5*, 260–266. [[CrossRef](#)]
20. Deng, G.; Xu, X.; Guo, Y.; Xia, E.; Li, S.; Wu, S.; Chen, F.; Ling, W.; Li, H. Determination of antioxidant property and their lipophilic and hydrophilic phenolic contents in cereal grains. *J. Funct. Foods* **2012**, *4*, 906–914. [[CrossRef](#)]
21. Fu, L.; Xu, B.; Gan, R.; Zhang, Y.; Xu, X.; Xia, E.; Li, H. Total phenolic contents and antioxidant capacities of herbal and tea infusions. *Int. J. Mol. Sci.* **2011**, *12*, 2112–2124. [[CrossRef](#)] [[PubMed](#)]
22. Fu, L.; Xu, B.; Xu, X.; Gan, R.; Zhang, Y.; Xia, E.; Li, H. Antioxidant capacities and total phenolic contents of 62 fruits. *Food Chem.* **2011**, *129*, 345–350. [[CrossRef](#)]
23. Guo, Y.; Deng, G.; Xu, X.; Wu, S.; Li, S.; Xia, E.; Li, F.; Chen, F.; Ling, W.; Li, H. Antioxidant capacities, phenolic compounds and polysaccharide contents of 49 edible macro-fungi. *Food Funct.* **2012**, *3*, 1195–1205. [[CrossRef](#)]
24. Song, F.; Gan, R.; Zhang, Y.; Xiao, Q.; Kuang, L.; Li, H. Total phenolic contents and antioxidant capacities of selected chinese medicinal plants. *Int. J. Mol. Sci.* **2010**, *11*, 2362–2372. [[CrossRef](#)]
25. Abolaji, A.O.; Ojo, M.; Afolabi, T.T.; Arowoogun, M.D.; Nwawolor, D.; Farombi, E.O. Protective properties of 6-gingerol-rich fraction from *Zingiber officinale* (ginger) on chlorpyrifos-induced oxidative damage and inflammation in the brain, ovary and uterus of rats. *Chem. Biol. Interact.* **2017**, *270*, 15–23. [[CrossRef](#)] [[PubMed](#)]
26. Li, Y.; Hong, Y.; Han, Y.; Wang, Y.; Xia, L. Chemical characterization and antioxidant activities comparison in fresh, dried, stir-frying and carbonized ginger. *J. Chromatogr. B* **2016**, *1011*, 223–232. [[CrossRef](#)]
27. Sakulnarmrat, K.; Srzednicki, G.; Konczak, I. Antioxidant, enzyme inhibitory and antiproliferative activity of polyphenolic-rich fraction of commercial dry ginger powder. *Int. J. Food Sci. Tech.* **2015**, *50*, 2229–2235. [[CrossRef](#)]
28. Gunathilake, K.D.P.P.; Rupasinghe, H.P.V. Inhibition of human low-density lipoprotein oxidation in vitro by ginger extracts. *J. Med. Food* **2014**, *17*, 424–431. [[CrossRef](#)]
29. Akinyemi, A.J.; Ademiluyi, A.O.; Oboh, G. Aqueous extracts of two varieties of ginger (*Zingiber officinale*) inhibit angiotensin I-converting enzyme, iron(II), and sodium nitroprusside-induced lipid peroxidation in the rat heart *in vitro*. *J. Med. Food* **2013**, *16*, 641–646. [[CrossRef](#)]
30. Hosseinzadeh, A.; Juybari, K.B.; Fatemi, M.J.; Kamarul, T.; Bagheri, A.; Tekiyehmaroof, N.; Sharifi, A.M. Protective effect of ginger (*Zingiber officinale* Roscoe) extract against oxidative stress and mitochondrial apoptosis induced by interleukin-1 beta in cultured chondrocytes. *Cells Tissues Organs* **2017**, *204*, 241–250. [[CrossRef](#)]
31. Romero, A.; Forero, M.; Sequeda-Castaneda, L.G.; Grismaldo, A.; Iglesias, J.; Celis-Zambrano, C.A.; Schuler, I.; Morales, L. Effect of ginger extract on membrane potential changes and AKT activation on a peroxide-induced oxidative stress cell model. *J. King Saud Univ. Sci.* **2018**, *30*, 263–269. [[CrossRef](#)]
32. Peng, S.; Yao, J.; Liu, Y.; Duan, D.; Zhang, X.; Fang, J. Activation of Nrf2 target enzymes conferring protection against oxidative stress in PC12 cells by ginger principal constituent 6-shogaol. *Food Funct.* **2015**, *6*, 2813–2823. [[CrossRef](#)]
33. Chen, H.; Fu, J.; Chen, H.; Hu, Y.; Soroka, D.N.; Prigge, J.R.; Schmidt, E.E.; Yan, F.; Major, M.B.; Chen, X.; et al. Ginger compound [6]-shogaol and its cysteine-conjugated metabolite (M2) activate Nrf2 in colon epithelial cells *in vitro* and *in vivo*. *Chem. Res. Toxicol.* **2014**, *27*, 1575–1585. [[CrossRef](#)]
34. Saiah, W.; Halzoune, H.; Djaziri, R.; Tabani, K.; Koceir, E.A.; Omari, N. Antioxidant and gastroprotective actions of butanol fraction of *Zingiber officinale* against diclofenac sodium-induced gastric damage in rats. *J. Food Biochem.* **2018**, *42*, e12456. [[CrossRef](#)]
35. Mohammadi, F.; Nikzad, H.; Taghizadeh, M.; Taherian, A.; Azami-Tameh, A.; Hosseini, S.M.; Moravveji, A. Protective effect of *Zingiber officinale* extract on rat testis after cyclophosphamide treatment. *Andrologia* **2014**, *46*, 680–686. [[CrossRef](#)]

36. Zhang, G.; Nitteranon, V.; Chan, L.Y.; Parkin, K.L. Glutathione conjugation attenuates biological activities of 6-dehydroshogaol from ginger. *Food Chem.* **2013**, *140*, 1–8. [[CrossRef](#)]
37. Luettig, J.; Rosenthal, R.; Lee, I.M.; Krug, S.M.; Schulzke, J.D. The ginger component 6-shogaol prevents TNF-alpha-induced barrier loss via inhibition of PI3K/Akt and NF-kappa B signaling. *Mol. Nutr. Food Res.* **2016**, *60*, 2576–2586. [[CrossRef](#)]
38. Hsiang, C.; Lo, H.; Huang, H.; Li, C.; Wu, S.; Ho, T. Ginger extract and zingerone ameliorated trinitrobenzene sulphonic acid-induced colitis in mice via modulation of nuclear factor-kappa B activity and interleukin-1 beta signalling pathway. *Food Chem.* **2013**, *136*, 170–177. [[CrossRef](#)]
39. Ueno, N.; Hasebe, T.; Kaneko, A.; Yamamoto, M.; Fujiya, M.; Kohgo, Y.; Kono, T.; Wang, C.; Yuan, C.; Bissonnette, M.; et al. TU-100 (Daikenchuto) and ginger ameliorate anti-CD3 antibody induced T cell-mediated murine enteritis: microbe-independent effects involving Akt and Nf-kappa b suppression. *PLoS ONE* **2014**, *9*, e97456. [[CrossRef](#)] [[PubMed](#)]
40. Zhang, M.; Xu, C.; Liu, D.; Han, M.K.; Wang, L.; Merlin, D. Oral delivery of nanoparticles loaded with ginger active compound, 6-shogaol, attenuates ulcerative colitis and promotes wound healing in a murine model of ulcerative colitis. *J. Crohns Colitis.* **2018**, *12*, 217–229. [[CrossRef](#)]
41. Teng, Y.; Ren, Y.; Sayed, M.; Hu, X.; Lei, C.; Kumar, A.; Hutchins, E.; Mu, J.; Deng, Z.; Luo, C.; et al. Plant-derived exosomal micrnas shape the gut microbiota. *Cell Host Microbe* **2018**, *24*, 637–652. [[CrossRef](#)] [[PubMed](#)]
42. Zehsaz, F.; Farhangi, N.; Mirheidari, L. The effect of *Zingiber officinale* R. rhizomes (ginger) on plasma pro-inflammatory cytokine levels in well-trained male endurance runners. *Cent. Eur. J. Immunol.* **2014**, *39*, 174–180. [[CrossRef](#)]
43. Awan, U.A.; Ali, S.; Shah Nawaz, A.M.; Shafique, I.; Zafar, A.; Khan, M.A.R.; Ghous, T.; Saleem, A.; Andleeb, S. Biological activities of *Allium sativum* and *Zingiber officinale* extracts on clinically important bacterial pathogens, their phytochemical and FT-IR spectroscopic analysis. *Pak. J. Pharm. Sci.* **2017**, *30*, 729–745.
44. Moon, Y.; Lee, H.; Lee, S. Inhibitory effects of three monoterpenes from ginger essential oil on growth and aflatoxin production of *Aspergillus flavus* and their gene regulation in aflatoxin biosynthesis. *Appl. Biol. Chem.* **2018**, *61*, 243–250. [[CrossRef](#)]
45. Nassan, M.A.; Mohamed, E.H. Immunopathological and antimicrobial effect of black pepper, ginger and thyme extracts on experimental model of acute hematogenous pyelonephritis in albino rats. *Int. J. Immunopath. Ph.* **2014**, *27*, 531–541. [[CrossRef](#)]
46. Chakotiya, A.S.; Tanwar, A.; Narula, A.; Sharma, R.K. *Zingiber officinale*: Its antibacterial activity on *Pseudomonas aeruginosa* and mode of action evaluated by flow cytometry. *Microb. Pathogenesis.* **2017**, *107*, 254–260. [[CrossRef](#)] [[PubMed](#)]
47. Kim, H.; Park, H. Ginger extract inhibits biofilm formation by *Pseudomonas aeruginosa* PA14. *PLoS ONE* **2013**, *8*, e76106. [[CrossRef](#)]
48. Hasan, S.; Danishuddin, M.; Khan, A.U. Inhibitory effect of *Zingiber officinale* towards *Streptococcus mutans* virulence and caries development: in vitro and in vivo studies. *BMC Microbiol.* **2015**, *15*, 1. [[CrossRef](#)] [[PubMed](#)]
49. Rampogu, S.; Baek, A.; Gajula, R.G.; Zeb, A.; Bavi, R.S.; Kumar, R.; Kim, Y.; Kwon, Y.J.; Lee, K.W. Ginger (*Zingiber officinale*) phytochemicals-gingerenone-A and shogaol inhibit SaHPPK: molecular docking, molecular dynamics simulations and in vitro approaches. *Ann. Clin. Microb. Anti.* **2018**, *17*, 16. [[CrossRef](#)]
50. Nerilo, S.B.; Rocha, G.H.O.; Tomoike, C.; Mossini, S.A.G.; Grespan, R.; Mikcha, J.M.G.; Machinski, M., Jr. Antifungal properties and inhibitory effects upon aflatoxin production by *Zingiber officinale* essential oil in *Aspergillus flavus*. *Int. J. Food Sci. Tech.* **2016**, *51*, 286–292. [[CrossRef](#)]
51. Garcia Yamamoto-Ribeiro, M.M.; Grespan, R.; Kohiyama, C.Y.; Ferreira, F.D.; Galerani Mossini, S.A.; Silva, E.L.; de Abreu Filho, B.A.; Graton Mikcha, J.M.; Machinski Junior, M. Effect of *Zingiber officinale* essential oil on *Fusarium verticillioides* and fumonisin production. *Food Chem.* **2013**, *141*, 3147–3152. [[CrossRef](#)] [[PubMed](#)]
52. Chang, J.S.; Wang, K.C.; Yeh, C.F.; Shieh, D.E.; Chiang, L.C. Fresh ginger (*Zingiber officinale*) has anti-viral activity against human respiratory syncytial virus in human respiratory tract cell lines. *J. Ethnopharmacol.* **2013**, *145*, 146–151. [[CrossRef](#)] [[PubMed](#)]
53. Abdel-Moneim, A.; Morsy, B.M.; Mahmoud, A.M.; Abo-Seif, M.A.; Zanaty, M.I. Beneficial therapeutic effects of *Nigella sativa* and/or *Zingiber officinale* in HCV patients in Egypt. *Excli J.* **2013**, *12*, 943–955. [[PubMed](#)]

54. Bray, F.; Ferlay, J.; Soerjomataram, I.; Siegel, R.L.; Torre, L.A.; Jemal, A. Global cancer statistics 2018: GLOBOCAN estimates of incidence and mortality worldwide for 36 cancers in 185 countries. *CA Cancer J. Clin.* **2018**, *68*, 394–424. [[CrossRef](#)] [[PubMed](#)]
55. Li, F.; Li, S.; Li, H.; Deng, G.; Ling, W.; Wu, S.; Xu, X.; Chen, F. Antiproliferative activity of peels, pulps and seeds of 61 fruits. *J. Funct. Foods* **2013**, *5*, 1298–1309. [[CrossRef](#)]
56. Li, F.; Li, S.; Li, H.; Deng, G.; Ling, W.; Xu, X. Antiproliferative activities of tea and herbal infusions. *Food Funct.* **2013**, *4*, 530–538. [[CrossRef](#)]
57. Saha, A.; Blando, J.; Silver, E.; Beltran, L.; Sessler, J.; DiGiovanni, J. 6-Shogaol from dried ginger inhibits growth of prostate cancer cells both in vitro and in vivo through inhibition of STAT3 and NF-kappa B signaling. *Cancer Prev. Res.* **2014**, *7*, 627–638. [[CrossRef](#)]
58. El-Ashawy, N.E.; Khedr, N.F.; El-Bahrawy, H.A.; Mansour, H.E.A. Ginger extract adjuvant to doxorubicin in mammary carcinoma: study of some molecular mechanisms. *Eur. J. Nutr.* **2018**, *57*, 981–989. [[CrossRef](#)]
59. Liu, C.; Kao, C.; Tseng, Y.; Lo, Y.; Chen, C. Ginger phytochemicals inhibit cell growth and modulate drug resistance factors in docetaxel resistant prostate cancer cell. *Molecules* **2017**, *22*, 1477. [[CrossRef](#)]
60. Tahir, A.A.; Sani, N.F.A.; Murad, N.A.; Makpol, S.; Ngah, W.Z.W.; Yusof, Y.A.M. Combined ginger extract & Gelam honey modulate Ras/ERK and PI3K/AKT pathway genes in colon cancer HT29 cells. *Nutr. J.* **2015**, *14*, 31.
61. Deol, P.K.; Kaur, I.P. Improving the therapeutic efficiency of ginger extract for treatment of colon cancer using a suitably designed multiparticulate system. *J. Drug Target* **2013**, *21*, 855–865. [[CrossRef](#)] [[PubMed](#)]
62. Jiang, Y.; Turgeon, D.K.; Wright, B.D.; Sidahmed, E.; Ruffin, M.T.; Brenner, D.E.; Sen, A.; Zick, S.M. Effect of ginger root on cyclooxygenase-1 and 15-hydroxyprostaglandin dehydrogenase expression in colonic mucosa of humans at normal and increased risk for colorectal cancer. *Eur. J. Cancer Prev.* **2013**, *22*, 455–460. [[CrossRef](#)]
63. Brahmabhatt, M.; Gundala, S.R.; Asif, G.; Shamsi, S.A.; Aneja, R. Ginger phytochemicals exhibit synergy to inhibit prostate cancer cell proliferation. *Nutr. Cancer* **2013**, *65*, 263–272. [[CrossRef](#)]
64. Gundala, S.R.; Mukkavilli, R.; Yang, C.; Yadav, P.; Tandon, V.; Vangala, S.; Prakash, S.; Aneja, R. Enterohepatic recirculation of bioactive ginger phytochemicals is associated with enhanced tumor growth-inhibitory activity of ginger extract. *Carcinogenesis* **2014**, *35*, 1320–1329. [[CrossRef](#)] [[PubMed](#)]
65. Zhang, F.; Zhang, J.; Qu, J.; Zhang, Q.; Prasad, C.; Wei, Z. Assessment of anti-cancerous potential of 6-gingerol (Tongling white ginger) and its synergy with drugs on human cervical adenocarcinoma cells. *Food Chem. Toxicol.* **2017**, *109*, 910–922. [[CrossRef](#)] [[PubMed](#)]
66. Bernard, M.M.; McConnery, J.R.; Hoskin, D.W. [10]-Gingerol, a major phenolic constituent of ginger root, induces cell cycle arrest and apoptosis in triple-negative breast cancer cells. *Exp. Mol. Pathol.* **2017**, *102*, 370–376. [[CrossRef](#)]
67. Li, C.; Ou, C.; Huang, C.; Wu, W.; Chen, Y.; Lin, T.; Ho, L.; Wang, C.; Shih, C.; Zhou, H.; et al. Carbon dots prepared from ginger exhibiting efficient inhibition of human hepatocellular carcinoma cells. *J. Mater. Chem. B* **2014**, *2*, 4564–4571. [[CrossRef](#)]
68. Akimoto, M.; Iizuka, M.; Kanematsu, R.; Yoshida, M.; Takenaga, K. Anticancer effect of ginger extract against pancreatic cancer cells mainly through reactive oxygen species-mediated autotic cell death. *PLoS ONE* **2015**, *10*, e0126605. [[CrossRef](#)]
69. Lim, S.; Moon, M.; Oh, H.; Kim, H.G.; Kim, S.Y.; Oh, M.S. Ginger improves cognitive function via NGF-induced ERK/CREB activation in the hippocampus of the mouse. *J. Nutr. Biochem.* **2014**, *25*, 1058–1065. [[CrossRef](#)]
70. Park, G.; Kim, H.G.; Ju, M.S.; Ha, S.K.; Park, Y.; Kim, S.Y.; Oh, M.S. 6-Shogaol, an active compound of ginger, protects dopaminergic neurons in Parkinson's disease models via anti-neuroinflammation. *Acta Pharmacol. Sin.* **2013**, *34*, 1131–1139. [[CrossRef](#)] [[PubMed](#)]
71. Huh, E.; Lim, S.; Kim, H.G.; Ha, S.K.; Park, H.; Huh, Y.; Oh, M.S. Ginger fermented with *Schizosaccharomyces pombe* alleviates memory impairment via protecting hippocampal neuronal cells in amyloid beta(1-42) plaque injected mice. *Food Funct.* **2018**, *9*, 171–178. [[CrossRef](#)] [[PubMed](#)]
72. Yao, J.; Ge, C.; Duan, D.; Zhang, B.; Cui, X.; Peng, S.; Liu, Y.; Fang, J. Activation of the phase II enzymes for neuroprotection by ginger active constituent 6-dehydrogingerdione in PC12 cells. *J. Agric. Food Chem.* **2014**, *62*, 5507–5518. [[CrossRef](#)] [[PubMed](#)]
73. Zeng, G.; Zhang, Z.; Lu, L.; Xiao, D.; Zong, S.; He, J. Protective effects of ginger root extract on Alzheimer disease-induced behavioral dysfunction in rats. *Rejuv. Res.* **2013**, *16*, 124–133. [[CrossRef](#)]

74. Moon, M.; Kim, H.; Choi, J.G.; Oh, H.; Lee, P.K.J.; Ha, S.K.; Kim, S.Y.; Park, Y.; Huh, Y.; Oh, M.S. 6-Shogaol, an active constituent of ginger, attenuates neuroinflammation and cognitive deficits in animal models of dementia. *Biochem. Biophys. Res. Commun.* **2014**, *449*, 8–13. [[CrossRef](#)]
75. Du, H.; Li, L.; Bennett, D.; Guo, Y.; Key, T.J.; Bian, Z.; Sherliker, P.; Gao, H.; Chen, Y.; Yang, L.; et al. Fresh fruit consumption and major cardiovascular disease in China. *New Engl. J. Med.* **2016**, *374*, 1332–1343. [[CrossRef](#)]
76. Khosravani, M.; Azarbayjani, M.A.; Abolmaesoomi, M.; Yusof, A.; Abidin, N.Z.; Rahimi, E.; Feizolah, F.; Akbari, M.; Seyedjalali, S.; Dehghan, F. Ginger extract and aerobic training reduces lipid profile in high-fat fed diet rats. *Eur. Rev. Med. Pharmacol.* **2016**, *20*, 1617–1622.
77. Akinyemi, A.J.; Thome, G.R.; Morsch, V.M.; Bottari, N.B.; Baldissarelli, J.; de Oliveira, L.S.; Goularte, J.F.; Bello-Klein, A.; Obboh, G.; Chitolina Schetinger, M.R. Dietary supplementation of ginger and turmeric rhizomes modulates platelets ectionucleotidase and adenosine deaminase activities in normotensive and hypertensive rats. *Phytother. Res.* **2016**, *30*, 1156–1163. [[CrossRef](#)] [[PubMed](#)]
78. De Las Heras, N.; Valero-Munoz, M.; Martin-Fernandez, B.; Ballesteros, S.; Lopez-Farre, A.; Ruiz-Roso, B.; Lahera, V. Molecular factors involved in the hypolipidemic and insulin-sensitizing effects of a ginger (*Zingiber officinale* Roscoe) extract in rats fed a high-fat diet. *Appl. Physiol. Nutr. Metab.* **2017**, *42*, 209–215. [[CrossRef](#)]
79. Oh, S.; Lee, M.; Jung, S.; Kim, S.; Park, H.; Park, S.; Kim, S.; Kim, C.; Jo, Y.; Kim, I.; et al. Ginger extract increases muscle mitochondrial biogenesis and serum HDL-cholesterol level in high-fat diet-fed rats. *J. Funct. Foods* **2017**, *29*, 193–200. [[CrossRef](#)]
80. Liu, R.; Heiss, E.H.; Sider, N.; Schinkovitz, A.; Groblacher, B.; Guo, D.; Bucar, F.; Bauer, R.; Dirsch, V.M.; Atanasov, A.G. Identification and characterization of [6]-shogaol from ginger as inhibitor of vascular smooth muscle cell proliferation. *Mol. Nutr. Food Res.* **2015**, *59*, 843–852. [[CrossRef](#)]
81. Wu, H.; Horng, C.; Tsai, S.; Lee, Y.; Hsu, S.; Tsai, Y.; Tsai, F.; Chiang, J.; Kuo, D.; Yang, J. Relaxant and vasoprotective effects of ginger extracts on porcine coronary arteries. *Int. J. Mol. Med.* **2018**, *41*, 2420–2428. [[CrossRef](#)]
82. Wang, Y.; Yu, H.; Zhang, X.; Feng, Q.; Guo, X.; Li, S.; Li, R.; Chu, D.; Ma, Y. Evaluation of daily ginger consumption for the prevention of chronic diseases in adults: A cross-sectional study. *Nutrition* **2017**, *36*, 79–84. [[CrossRef](#)]
83. Misawa, K.; Hashizume, K.; Yamamoto, M.; Minegishi, Y.; Hase, T.; Shimotoyodome, A. Ginger extract prevents high-fat diet-induced obesity in mice via activation of the peroxisome proliferator-activated receptor delta pathway. *J. Nutr. Biochem.* **2015**, *26*, 1058–1067. [[CrossRef](#)] [[PubMed](#)]
84. Mahmoud, R.H.; Elnour, W.A. Comparative evaluation of the efficacy of ginger and orlistat on obesity management, pancreatic lipase and liver peroxisomal catalase enzyme in male albino rats. *Eur. Rev. Med. Pharmacol.* **2013**, *17*, 75–83.
85. Attari, V.E.; Ostadrahimi, A.; Jafarabadi, M.A.; Mehrizadeh, S.; Mahluji, S. Changes of serum adipocytokines and body weight following *Zingiber officinale* supplementation in obese women: A RCT. *Eur. J. Nutr.* **2016**, *55*, 2129–2136. [[CrossRef](#)]
86. Miyamoto, M.; Matsuzaki, K.; Katakura, M.; Hara, T.; Tanabe, Y.; Shido, O. Oral intake of encapsulated dried ginger root powder hardly affects human thermoregulatory function, but appears to facilitate fat utilization. *Int. J. Biometeorol.* **2015**, *59*, 1461–1474. [[CrossRef](#)]
87. Zhu, Y.; Zhao, Y.; Wang, P.; Ahmedna, M.; Sang, S. Bioactive ginger constituents alleviate protein glycation by trapping methylglyoxal. *Chem. Res. Toxicol.* **2015**, *28*, 1842–1849. [[CrossRef](#)] [[PubMed](#)]
88. Sampath, C.; Rashid, M.R.; Sang, S.; Ahmedna, M. Specific bioactive compounds in ginger and apple alleviate hyperglycemia in mice with high fat diet-induced obesity via Nrf2 mediated pathway. *Food Chem.* **2017**, *226*, 79–88. [[CrossRef](#)]
89. Bin Samad, M.; Bin Mohsin, M.N.A.; Razu, B.A.; Hossain, M.T.; Mahzabeen, S.; Unnoor, N.; Muna, I.A.; Akhter, F.; Ul Kabir, A.; Hannan, J.M.A. [6]-Gingerol, from *Zingiber officinale*, potentiates GLP-1 mediated glucose-stimulated insulin secretion pathway in pancreatic beta-cells and increases RAB8/RAB10-regulated membrane presentation of GLUT4 transporters in skeletal muscle to improve hyperglycemia in Lepr(db/db) type 2 diabetic mice. *BMC Complement. Altern. M.* **2017**, *17*, 395.
90. Arablou, T.; Aryaeian, N.; Valizadeh, M.; Sharifi, F.; Hosseini, A.; Djalali, M. The effect of ginger consumption on glycemic status, lipid profile and some inflammatory markers in patients with type 2 diabetes mellitus. *Int. J. Food Sci. Nutr.* **2014**, *65*, 515–520. [[CrossRef](#)]

91. Li, Y.; Tran, V.H.; Kota, B.P.; Nammi, S.; Duke, C.C.; Roufogalis, B.D. Preventative effect of *Zingiber officinale* on insulin resistance in a high-fat high-carbohydrate diet-fed rat model and its mechanism of action. *Basic Clin. Pharmacol.* **2014**, *115*, 209–215. [[CrossRef](#)]
92. Dongare, S.; Gupta, S.K.; Mathur, R.; Saxena, R.; Mathur, S.; Agarwal, R.; Nag, T.C.; Srivastava, S.; Kumar, P. *Zingiber officinale* attenuates retinal microvascular changes in diabetic rats via anti-inflammatory and antiangiogenic mechanisms. *Mol. Vis.* **2016**, *22*, 599–609.
93. Mahluji, S.; Attari, V.E.; Mobasser, M.; Payahoo, L.; Ostadrahimi, A.; Golzari, S.E.J. Effects of ginger (*Zingiber officinale*) on plasma glucose level, HbA1c and insulin sensitivity in type 2 diabetic patients. *Int. J. Food Sci. Nutr.* **2013**, *64*, 682–686. [[CrossRef](#)]
94. Marx, W.; McCarthy, A.L.; Ried, K.; McKavanagh, D.; Vitetta, L.; Sali, A.; Lohning, A.; Isenring, E. The effect of a standardized ginger extract on chemotherapy-induced nausea-related quality of life in patients undergoing moderately or highly emetogenic chemotherapy: A double blind, randomized, placebo controlled trial. *Nutrients* **2017**, *9*, 867. [[CrossRef](#)]
95. Bossi, P.; Cortinovis, D.; Fatigoni, S.; Rocca, M.C.; Fabi, A.; Seminara, P.; Ripamonti, C.; Alfieri, S.; Granata, R.; Bergamini, C.; et al. A randomized, double-blind, placebo-controlled, multicenter study of a ginger extract in the management of chemotherapy-induced nausea and vomiting (CINV) in patients receiving high-dose cisplatin. *Ann. Oncol.* **2017**, *28*, 2547–2551. [[CrossRef](#)]
96. Adib-Hajbaghery, M.; Hosseini, F.S. Investigating the effects of inhaling ginger essence on post-nephrectomy nausea and vomiting. *Complement. Ther. Med.* **2015**, *23*, 827–831. [[CrossRef](#)]
97. Kalava, A.; Darji, S.J.; Kalstein, A.; Yarmush, J.M.; SchianodiCola, J.; Weinberg, J. Efficacy of ginger on intraoperative and postoperative nausea and vomiting in elective cesarean section patients. *Eur. J. Obstet. Gyn. R. B.* **2013**, *169*, 184–188. [[CrossRef](#)]
98. Marx, W.M.; Teleni, L.; McCarthy, A.L.; Vitetta, L.; McKavanagh, D.; Thomson, D.; Isenring, E. Ginger (*Zingiber officinale*) and chemotherapy-induced nausea and vomiting: a systematic literature review. *Nutr. Rev.* **2013**, *71*, 245–254. [[CrossRef](#)]
99. Jin, Z.; Lee, G.; Kim, S.; Park, C.; Park, Y.S.; Jin, Y. Ginger and its pungent constituents non-competitively inhibit serotonin currents on visceral afferent neurons. *Korean J. Physiol. Pha.* **2014**, *18*, 149–153. [[CrossRef](#)]
100. Dabaghzadeh, F.; Khalili, H.; Dashti-Khavidaki, S.; Abbasian, L.; Moeinifard, A. Ginger for prevention of antiretroviral-induced nausea and vomiting: a randomized clinical trial. *Expert Opin. Drug Saf.* **2014**, *13*, 859–866. [[CrossRef](#)]
101. Emrani, Z.; Shojaei, E.; Khalili, H. Ginger for prevention of antituberculosis-induced gastrointestinal adverse reactions including hepatotoxicity: A randomized pilot clinical trial. *Phytother. Res.* **2016**, *30*, 1003–1009. [[CrossRef](#)]
102. Palatty, P.L.; Haniadka, R.; Valder, B.; Arora, R.; Baliga, M.S. Ginger in the prevention of nausea and vomiting: A review. *Crit. Rev. Food Sci.* **2013**, *53*, 659–669. [[CrossRef](#)]
103. Townsend, E.A.; Zhang, Y.; Xu, C.; Wakita, R.; Emala, C.W. Active components of ginger potentiate beta-agonist-induced relaxation of airway smooth muscle by modulating cytoskeletal regulatory proteins. *Am. J. Resp. Cell Mol.* **2014**, *50*, 115–124.
104. Mangprayool, T.; Kupittayanant, S.; Chudapongse, N. Participation of citral in the bronchodilatory effect of ginger oil and possible mechanism of action. *Fitoterapia* **2013**, *89*, 68–73. [[CrossRef](#)]
105. Khan, A.M.; Shahzad, M.; Asim, M.B.R.; Imran, M.; Shabbir, A. *Zingiber officinale* ameliorates allergic asthma via suppression of Th2-mediated immune response. *Pharm. Biol.* **2015**, *53*, 359–367. [[CrossRef](#)]
106. Bera, K.; Nosalova, G.; Sivova, V.; Ray, B. Structural elements and cough suppressing activity of polysaccharides from *Zingiber officinale* rhizome. *Phytother. Res.* **2016**, *30*, 105–111. [[CrossRef](#)]
107. Shariatpanahi, Z.V.; Mokhtari, M.; Taleban, F.A.; Alavi, F.; Surmaghi, M.H.S.; Mehrabi, Y.; Shahbazi, S. Effect of enteral feeding with ginger extract in acute respiratory distress syndrome. *J. Crit. Care.* **2013**, *28*, 217.e6. [[CrossRef](#)]
108. Kawamoto, Y.; Ueno, Y.; Nakahashi, E.; Obayashi, M.; Sugihara, K.; Qiao, S.; Iida, M.; Kumasaka, M.Y.; Yajima, I.; Goto, Y.; et al. Prevention of allergic rhinitis by ginger and the molecular basis of immunosuppression by 6-gingerol through T cell inactivation. *J. Nutr. Biochem.* **2016**, *27*, 112–122. [[CrossRef](#)]

109. Lai, Y.; Lee, W.; Lin, Y.; Ho, C.; Lu, K.; Lin, S.; Panyod, S.; Chu, Y.; Sheen, L. Ginger essential oil ameliorates hepatic injury and lipid accumulation in high fat diet-induced nonalcoholic fatty liver disease. *J. Agric. Food Chem.* **2016**, *64*, 2062–2071. [[CrossRef](#)]
110. Rodrigues, F.A.P.; Prata, M.M.G.; Oliveira, I.C.M.; Alves, N.T.Q.; Freitas, R.E.M.; Monteiro, H.S.A.; Silva, J.A.; Vieira, P.C.; Viana, D.A.; Liborio, A.B.; et al. Gingerol fraction from *Zingiber officinale* protects against gentamicin-induced nephrotoxicity. *Antimicrob. Agents Ch.* **2014**, *58*, 1872–1878. [[CrossRef](#)]
111. Saberi, H.; Keshavarzi, B.; Shirpoor, A.; Gharalari, F.H.; Rasmi, Y. Rescue effects of ginger extract on dose dependent radiation-induced histological and biochemical changes in the kidneys of male Wistar rats. *Biomed. Pharmacother.* **2017**, *94*, 569–576. [[CrossRef](#)] [[PubMed](#)]
112. Liu, C.; Raghu, R.; Lin, S.; Wang, S.; Kuo, C.; Tseng, Y.J.; Sheen, L. Metabolomics of ginger essential oil against alcoholic fatty liver in mice. *J. Agric. Food Chem.* **2013**, *61*, 11231–11240. [[CrossRef](#)]
113. Kashefi, F.; Khajehei, M.; Alavinia, M.; Golmakani, E.; Asili, J. Effect of ginger (*Zingiber officinale*) on heavy menstrual bleeding: a placebo-controlled, randomized clinical trial. *Phytother. Res.* **2015**, *29*, 114–119. [[CrossRef](#)]
114. Maghbooli, M.; Golipour, F.; Esfandabadi, A.M.; Yousefi, M. Comparison between the efficacy of ginger and sumatriptan in the ablative treatment of the common migraine. *Phytother. Res.* **2014**, *28*, 412–415. [[CrossRef](#)]
115. Teschke, R.; Xuan, T.D. Viewpoint: A contributory role of shell ginger (*Alpinia zerumbet*) for human longevity in Okinawa, Japan? *Nutrients* **2018**, *10*, 166. [[CrossRef](#)]
116. Xiao-Yu, X.; Xiao, M.; Sha, L.; Ren-You, G.; Ya, L.; Hua-Bin, L. Bioactivity, health benefits, and related molecular mechanisms of curcumin: Current progress, challenges, and perspectives. *Nutrients* **2018**, *10*, 1553.
117. Li, H.L.; Huang, M.J.; Tan, D.Q.; Liao, Q.H.; Zou, Y.; Jiang, Y.S. Effects of soil moisture content on the growth and physiological status of ginger (*Zingiber officinale* Roscoe). *Acta Physiol. Plant.* **2018**, *40*, 125. [[CrossRef](#)]



© 2019 by the authors. Licensee MDPI, Basel, Switzerland. This article is an open access article distributed under the terms and conditions of the Creative Commons Attribution (CC BY) license (<http://creativecommons.org/licenses/by/4.0/>).



Article

# Melanoidins from Chinese Distilled Spent Grain: Content, Preliminary Structure, Antioxidant, and ACE-Inhibitory Activities In Vitro

Shiqi Yang, Wenlai Fan \* and Yan Xu

Key Laboratory of Industrial Biotechnology of Ministry of Education, Laboratory of Brewing Microbiology and Applied Enzymology, School of Biotechnology, Jiangnan University, 1800 Lihu Ave, Wuxi 214122, Jiangsu, China; shiqiyang\_jiangnan@163.com (S.Y.); yxu@jiangnan.edu.cn (Y.X.)

\* Correspondence: wenlaifan@jiangnan.edu.cn; Tel.: +86-510-85197082

Received: 24 September 2019; Accepted: 16 October 2019; Published: 18 October 2019

**Abstract:** Distilled spent grain (DSG), as the major by-product of baijiu making, contains melanoidins generated via the Maillard reaction. In this study, four melanoidin fractions (RF1–RF4) were isolated successively from dried DSG (DDSG) using sodium hydroxide solution and water as extractants, and the content, preliminary structure, and ACE-inhibitory activities in vitro of melanoidins were first investigated. The antioxidant activity was also evaluated. The results indicated that the total content of melanoidins was 268.60 mg/g DDSG dry weight (dw) using a model system of glucose and serine as standard, and RF4 showed the highest content of melanoidins (174.30 mg/g DDSG dw). Functional groups like C=O, N-H, C-N, O-H, C-H, C-O, C-C, and -C-CO-C- were present in the structure of melanoidins from RF4, as determined by Fourier transform infrared (FT-IR) assay. The highest antioxidant activities, as assessed by 2,2'-azino-bis (3-ethylbenzothiazoline-6-sulfonic acid) (ABTS<sup>•+</sup>), ferric-reducing antioxidant power (FRAP), and 1,1-diphenyl-2-picrylhydrazyl radical (DPPH) assays, and the highest angiotensin-converting enzyme (ACE) inhibitory activity (95.92% at 2 mg RF4/mL) were also exhibited by RF4. The RF4 was further fractionated by ultrafiltration based on molecular weight (MW). The more than 100 kDa melanoidins (RF4-6) exhibited the highest yield and antioxidant activity. The 3–10 kDa melanoidins (RF4-2) were more efficient in ACE-inhibitory activity. Our study could raise awareness of the DDSG as a value-added resource.

**Keywords:** dried distilled spent grain (DDSG); melanoidins; content; structure; antioxidant activity; ACE-inhibitory activity

## 1. Introduction

Distilled spent grain (DSG), the sorghum residue obtained after solid state fermentation and distillation, is the biggest byproduct in baijiu (Chinese liquor) production. The output of DSG amounted to 30 million tons in 2018. DSG is rich in carbohydrates (5.71–11.34% *w/w*), protein (5.0–13.8% *w/w*), crude fiber (10.05–10.20% *w/w*), and crude lipids (1.31–3.24% *w/w*) [1]. DSG rots easily and causes serious environmental pollution due to the high water content (60–70%) and acidity. To date, DSG was mainly used for biogas production [2], livestock feeding [3], and single-cell protein production [4], etc.

In recent years, lots of studies have begun to focus on foods rich in bioactive compounds with the ability to promote benefits for human health [5]. Melanoidins from DSG, generated by the Maillard reaction of the baijiu-making process, are also bioactive compounds.

Melanoidins, a class of brown hydrophilic nitrogen-containing polymers, are formed in the last stage of the Maillard reaction, and they are widely found in coffee, cocoa, toast, dark beer, malt, honey, and other foods [6]. Apart from their role in the aroma and color as well as texture of thermally processed food, a lot of research on melanoidins has been carried out in recent years

due to their potential nutritional, biological, and functional implications such as antioxidant [7], antihypertensive [8], prebiotic activity [9], and antimicrobial [10] properties.

The structure of melanoidins is complicated due to the strong influence of starting materials and reaction conditions [11]. The exact structure of melanoidins has remained unknown until now. There were three main proposals for the structure of melanoidins: (a) Melanoidins were polymers consisting of repeating units of furans and/or pyrroles [12]; (b) High molecular weight melanoidins were formed by the cross-linking of proteins with low molecular weight chromophores [13]; (c) The sugar degradation product, as the skeleton of melanoidins, could be linked to amino compounds to form melanoidins [14]. In model systems, it has been demonstrated that linear and branched melanoidin-like polymers in which bridging carbons link furan and pyrrole units exist [12] (Figure 1). Moreover, some compounds (mainly furans) accompanied by carbonyl compounds, pyrroles, pyrazines, pyridines, and some oxazoles were detected by thermal degradation in the glucose/glycine melanoidins [15] (Figure 2). As for real food, polysaccharides, proteins, and chlorogenic acids were reported to be involved in the formation of coffee melanoidins [16].

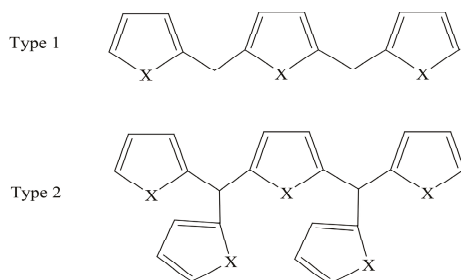


**Figure 1.** Proposed structures for melanoidin polymers, X = NR or O [12].

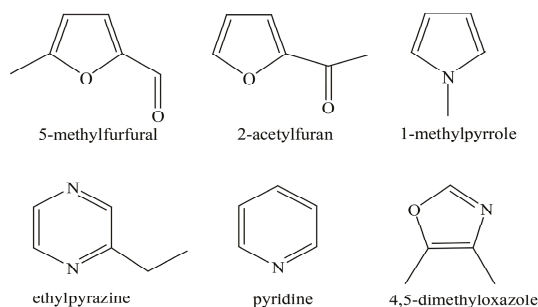


**Figure 2.** Structures of some representative compounds identified in the glucose/glycine melanoidins [15].

Some information about melanoidins from the spent grain of the brewing/liquor-making industry was available in brewers' spent grain (BSG) and DSG. High molecular weight (MW) melanoidin (>10 kDa) extracts from black BSG was found to have relevance, with a high phenolic content, protein content, metal-chelating activity, and antioxidant activity [17]. The melanoidins from DSG have also been reported to possess antioxidant activity [18]. Up to now, few studies concerning the content, chemical composition, structure, and other biological activities of DSG melanoidins have been published.

The purpose of this article was to study the content, preliminary structure, chemical properties, antioxidant, and angiotensin-converting enzyme (ACE) inhibitory activity of melanoidins from dried DSG (DDSG) *in vitro*. Our research may raise awareness of the DDSG as a value-added resource.

## 2. Materials and Methods

### 2.1. Materials

DSG samples used in this study were kindly provided by Golden Seed Distillery Co., Ltd. (Fuyang, China) and stored at  $-20\text{ }^{\circ}\text{C}$  until use.

D-glucose, gallic acid, bovine serum albumin, methanol, and 1,1-diphenyl-2-picrylhydrazyl radical (DPPH) were bought from Sigma-Aldrich (Shanghai, China). Total Antioxidant Capacity Assay Kits with a rapid 2,2'-azino-bis (3-ethylbenzothiazoline-6-sulfonic acid) (ABTS) and ferric-reducing antioxidant power (FRAP) were purchased from Beyotime Biotechnology Co., Ltd (Shanghai, China). ACE Kit-WST was obtained from Dojindo Inc. (Kumamoto, Japan). Other chemicals were analytical grade.

### 2.2. Melanoidin Extraction and Ultrafiltration

DSG was removed from  $-20\text{ }^{\circ}\text{C}$ , thawed, and oven-dried at  $70\text{ }^{\circ}\text{C}$  for 24 h to a constant weight, and then the husk was removed. DDSG was crushed with a high-speed multipurpose grinder (RY-280A, Yongkang Ruiyi Electromechanical Co., Ltd, JinHua, China) and then filtered through a 0.25 mm mesh screen (Sinopharm Chemical Reagent Co., Ltd., Hefei, China).

The method of extracting melanoidins from DDSG was carried out according to previous studies [17,19] with some modifications. The extraction steps are schematically outlined in Figure 3. All centrifugation steps were carried out under the conditions of  $2700\times g$  at  $10\text{ }^{\circ}\text{C}$  for 20 min, and then all supernatants (RF1–RF4) were adjusted to pH 7.0 using 2 N NaOH or 2 N HCl as required. RF4 was further separated into different MW fractions by ultrafiltration using centrifugal tubes (Millipore Co., Ltd. Shanghai, China) equipped with 3, 10, 30, 50, and 100 kDa nominal MW cut-off membranes (MWCOs). All samples were centrifuged at  $4000\times g$  for 20 min. The retentate was washed with distilled water 3–5 times. Melanoidin fractions with different MWs were named as RF4-1 (<3 kDa), RF4-2 (3–10 kDa), RF4-3 (10–30 kDa), RF4-4 (30–50 kDa), RF4-5 (50–100 kDa), and RF4-6 (>100 kDa).

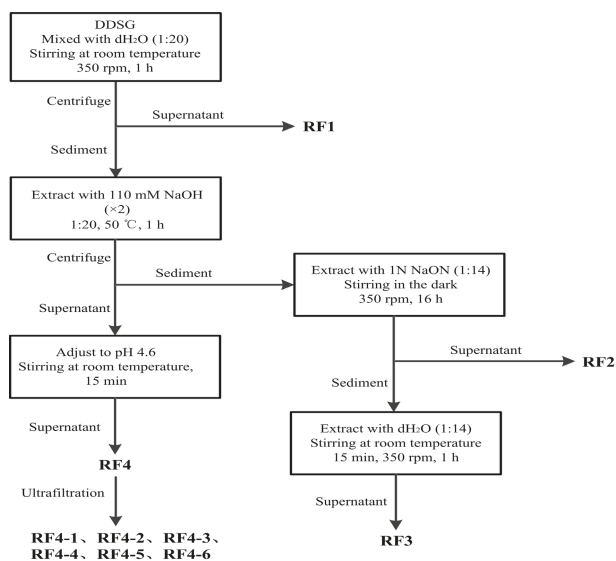


**Figure 3.** Flowchart for extraction melanoidins from dried distilled spent grain (DDSG). Four supernatants (RF1–RF4) containing melanoidins were obtained, and six different molecular weight (MW) fractions named RF4-1 (<3 kDa), RF4-2 (3–10 kDa), RF4-3 (10–30 kDa), RF4-4 (30–50 kDa), RF4-5 (50–100 kDa), and RF4-6 (>100 kDa) were obtained by ultrafiltration.

### 2.3. Preliminary Structural Identification

The preliminary structure of melanoidins from RF4 was identified by ultraviolet–visible absorption spectroscopy (UV-VIS) and Fourier transform infrared (FT-IR) spectra. UV-VIS was determined using a MAPADA P7 spectrophotometer (Mapada Instruments Co., Ltd., Shanghai, China) at room temperature with a scanning wavelength ranging from 200 to 800 nm. The FT-IR spectra were obtained by a FT-IR spectrometer (NEXUS470, NICOLET instruments co., Ltd., Madison, WI, USA) in the frequency range of 4000–600  $\text{cm}^{-1}$ . Lyophilizates of RF4 and six different MW fractions (RF4-1–RF4-6) were made into potassium bromide flakes at similar weight concentrations before FT-IR analysis.

### 2.4. Color Analysis

The color analysis of melanoidin fractions was carried out by recording the absorbance using A380 spectrophotometer (AOYI instruments co., Ltd., Shanghai, China) with a 1-cm path length cell at 420 nm [20]. Distilled water was used as a blank.

### 2.5. Total Phenolic, Protein, and Carbohydrate Content

The total phenolic content (TPC) of melanoidin fractions (aqueous solutions of 1 mg/mL) was determined by the Folin-Ciocalteu procedures [21]. The TPC was calculated using a calibration curve with gallic acid (final assay concentration, 2–50  $\mu\text{g/mL}$ ) as standard. The results were expressed as mg gallic acid equivalents per g dry weight of DDSG (mg GAE/g DDSG dw).

The protein content of melanoidin fractions (aqueous solutions of 1 mg/mL) was measured by the Bradford method [22]. Bovine serum albumin was used as standard (0.01–0.5 mg/mL). The results were expressed as mg bovine serum albumin equivalents per g dry weight of DDSG (mg BSA/g DDSG dw).

The carbohydrate content of melanoidin fractions (aqueous solutions of 1 mg/mL) was estimated using the phenol-sulfuric acid method [23]. A standard curve was plotted with glucose (0.01–0.8 mg/mL) as standard. The results were expressed as mg glucose equivalents per g dry weight of DDSG (mg GE/g DDSG dw).

### 2.6. Total Antioxidant Capacity In Vitro

DPPH radical-scavenging capacity. The DPPH radical-scavenging capacity was measured in accordance with the described method [24]. Aliquots of 0.2 mL of sample solution (1 mg/mL) were added to 3.0 mL of DPPH solution (0.72 mM) prepared in methanol, then vortexed and allowed to stand in the dark for 30 min at room temperature, and the absorbance at 516 nm was read by a microplate reader (Cytation 3, BioTek Instruments, Inc., Winooski, VT, USA). The results were expressed as DPPH (%). The DPPH radical-scavenging rate (%) was calculated using Equation (1).

$$\text{DPPH (\%)} = \frac{A_{\text{control}} - A_{\text{sample}}}{A_{\text{control}}} \times 100 \quad (1)$$

$A_{\text{sample}}$  is the absorbance of the sample solution, while  $A_{\text{control}}$  represents the absorbance of the blank in which 0.2 mL methanol replaced the sample solution.

Ferric-reducing antioxidant power (FRAP). The FRAP assay was achieved with the kit mentioned in the materials section. Briefly, aqueous solutions of  $\text{FeSO}_4 \cdot 7\text{H}_2\text{O}$  (0.15–1.5 mM) and a FRAP working solution were prepared prior to the assay. The FRAP working solution was obtained by mixing 150  $\mu\text{L}$  of 2,4,6-tri(2-pyridyl)-s-triazine (TPTZ) diluent, 15  $\mu\text{L}$  of TPTZ solution, and 15  $\mu\text{L}$  of detection buffer sequentially for one measurement. When testing, an aliquot of 180  $\mu\text{L}$  of FRAP working solution was added to each test well. Aliquots of 5  $\mu\text{L}$  of sample solution (1 mg/mL) were added to sample wells, in blank wells was added 5  $\mu\text{L}$  of distilled water instead, and 5  $\mu\text{L}$  of  $\text{FeSO}_4 \cdot 7\text{H}_2\text{O}$  was added to the wells for the standard curve. All of the wells were incubated at 37 °C for 3–5 min. The absorbance was read at 593 nm. The results were expressed as mmol  $\text{FeSO}_4$  equivalents per g dry weight of DDSG (mmol FE/g DDSG dw).

ABTS<sup>•+</sup> assay. The ABTS<sup>•+</sup> assay was conducted using the kit mentioned in the materials section. The Trolox solution (0.15–1.5 mM) used to make the standard curve and ABTS<sup>•+</sup> working solution were prepared prior to testing. The ABTS<sup>•+</sup> working solution consisted of 152 µL of assay buffer, 10 µL of ABTS<sup>•+</sup> solution, and 8 µL of 1/1000 hydrogen peroxide solution for one measurement. An aliquot of 20 µL of peroxidase working solution was added to each test well. Then, 10 µL of the sample solution (1 mg/mL) was added to the sample well while 10 µL of distilled water was added to the blank well, and 10 µL of a different concentration of Trolox solution was added to the well of the standard curve. Finally, 170 µL of ABTS<sup>•+</sup> working solution was added to each well and incubated at 37 °C for 3–5 min at room temperature. The absorbance was recorded at 414 nm. The antioxidant capacity as measured with the ABTS<sup>•+</sup> assay was expressed as mmol Trolox equivalents per g dry weight of DDSG (mmol TE/g DDSG dw).

### 2.7. ACE-Inhibitory Activity In Vitro

The determination of ACE-inhibitory activity was performed using a 96-well plate colorimetric detection system as previously described [25]. Each sample well contained the following solution: 20 µL of sample solution (2 mg/mL), 20 µL of substrate buffer, and 20 µL of enzyme working solution. Blank 1 consisted of 20 µL of distilled water, 20 µL of substrate buffer, and 20 µL of enzyme working solution. Blank 2 contained 40 µL of distilled water and 20 µL of substrate buffer. All of these wells were incubated at 37 °C for 1 h. Aliquots of 200 µL of the indicator working solution were added to each well and further incubated for 10 min. Then the absorbance was measured at 450 nm using a microplate reader. The formula for calculating the ACE inhibition rate was Equation (2).

$$\text{ACE inhibition rate (\%)} = \frac{A_{\text{blank1}} - A_{\text{sample}}}{A_{\text{blank1}} - A_{\text{blank2}}} \times 100 \quad (2)$$

$A_{\text{blank1}}$  is the absorbance without adding sample solution,  $A_{\text{blank2}}$  is the value without adding enzyme working solution, and  $A_{\text{sample}}$  represents the absorbance of the sample solution.

### 2.8. Calculation of Melanoidin Content

The method for calculating melanoidin content was performed according to [20] with some modification. The aliquot of 0.05 mol glucose and serine was fully dissolved with an appropriate amount of distilled water and freeze-dried to constant weight. The lyophilizate was placed in an oven at 90 °C for 1 h. Once reacted, brown solid was taken out and immediately cooled to room temperature then ground to fine powder, 5 g of which was dissolved in 200 mL distilled water. The solution was stirred for 12 h at 4 °C. After filtration, the content of melanoidins was calculated using the calibration curve obtained by using the filtrate as standard (0.1–5 mg/mL). The absorbance of the melanoidin standard was recorded at 420 nm.

### 2.9. Statistical Analysis

All tests in this study were measured at least in triplicate, and all statistical analyses were performed using IBM SPSS Statistics 22.0 (IBM, Armonk, NY, USA) software. Differences in mean were detected by one-way analysis of variance (ANOVA) after testing for normal distribution (Shapiro–Wilk test) and homogeneous variance (Levene’s test). Tukey’s test was then carried out, and values of  $p < 0.05$  were considered to indicate significant difference.

## 3. Results and Discussion

### 3.1. The Content of Melanoidins in DDSG

Simulation of melanoidin standard is a method for estimating the amount of melanoidins in real foods. Model systems consisting of glucose and L-aspartic acid or glucose and glycine have served as

standards of barley melanoidins [20,26]. Comparing the FT-IR spectra of the freeze-dried RF4 with model systems comprised of 20 amino acids and glucose respectively, the model system comprised of glucose and serine was selected as the standard of DDSG melanoidins.

Melanoidins can be rich in DDSG. The total amount of melanoidins in DDSG was 268.60 mg/g DDSG dw (Table 1), which was higher than the content in roasted barley malt (67.90 mg/g) [20], roasted coffee (72.00 mg/g), dry biscuit crusts (120.00 mg/g), and sliced bread crusts (180.00 mg/g) [27].

**Table 1.** Content of melanoidins in four fractions obtained by alkaline solution (RF2 and RF4) and distilled water (RF1 and RF3) extraction of dried distilled spent grain (DDSG).

Fractions	Content (mg/g DDSG Dry Weight (dw)) <sup>1</sup>
RF1	9.69 ± 1.85 <sup>d</sup>
RF2	72.40 ± 3.67 <sup>b</sup>
RF3	12.20 ± 1.59 <sup>c</sup>
RF4	174.30 ± 5.80 <sup>a</sup>
total	268.60

<sup>1</sup> The results are shown as mean ± standard deviation (SD) ( $n = 3$ ). Differences in mean were detected by one-way analysis of variance (ANOVA) after testing for normal distribution (Shapiro–Wilk test) and homogeneous variance (Levene’s test). Values in the same column with different letters are significantly different ( $p < 0.05$ ).

The content of melanoidins in four fractions (RF1–RF4) was significantly different ( $p < 0.05$ ) (Table 1). RF1 represented the fraction obtained by an initial aqueous extraction of DDSG (Figure 3). RF4 was the fraction obtained using 110 mM NaOH extraction followed by isoelectric precipitation of proteins, and RF2 was the fraction obtained by extracting sediment with 1 N NaOH after 110 mM NaOH extraction, whereas RF3 was the fraction obtained by thoroughly aqueous washing of the precipitate extracted with 1 N NaOH. The amount of melanoidins in RF4 (174.30 mg/g DDSG dw) and RF2 (72.40 mg/g DDSG dw) were significantly higher than that of the other two fractions (Table 1), RF1 and RF3, suggesting that the fractions isolated by alkaline solution had a higher amount of melanoidins than fractions extracted by water.

### 3.2. The Preliminary Structure of Melanoidins

UV-VIS spectroscopy can provide certain information for the internal structure of organic compounds, and FT-IR assay is an ideal method for exploring protein–carbohydrate systems [28], both of which have been successfully implemented in the structural analysis of melanoidins [29,30].

RF4 was submitted to structural analysis due to having the highest amount of melanoidins. The UV-VIS spectrum (Figure 4) showed that the absorbance decreased with increasing wavelength, which was very similar to the descriptions previously reported [29,31,32]. The absorption peak at 280 nm indicated the possible presence of protein, and 420 nm was the characteristic absorption wavelength of melanoidins [33,34]. The absorption peaks were present both in ultraviolet and visible regions, suggesting that the structure of melanoidins contains a conjugated system.

The FT-IR spectrum (Figure 5) was similar to that of Chinese huangjiu (yellow wine) melanoidins [35]. The absorption peak at 1651.35  $\text{cm}^{-1}$  refers to C=O stretching vibration, N–H bending vibration, and C–N stretching vibration, which represents the amide I band of protein [36,37]. There were few peaks at 1540  $\text{cm}^{-1}$  (amide II) and 1300–1200  $\text{cm}^{-1}$  (amide III). That was probably because the Maillard reaction changed the structure of protein. A wide and strong absorption band of O–H stretching appeared around 3376.30  $\text{cm}^{-1}$ , indicating that alcohol could be present in the structure of melanoidins. The characteristic absorption band near 2926.64  $\text{cm}^{-1}$  is assigned to the saturated C–H stretching vibration, and the group is most likely to be  $-\text{CH}_2-$  under this wave number. A weak absorption peak at 1402.67  $\text{cm}^{-1}$  could be generated by C–N stretching vibration. The absorption peak at 1042.23  $\text{cm}^{-1}$  was generated by C–O stretching vibration, C–C stretching vibration, and C–H bending vibration. The absorption peak around 565.13  $\text{cm}^{-1}$  could be generated by the in-plane bending vibration of the aliphatic ketone  $-\text{C}-\text{CO}-\text{C}-$  having a substituent at the  $\alpha$ -position.

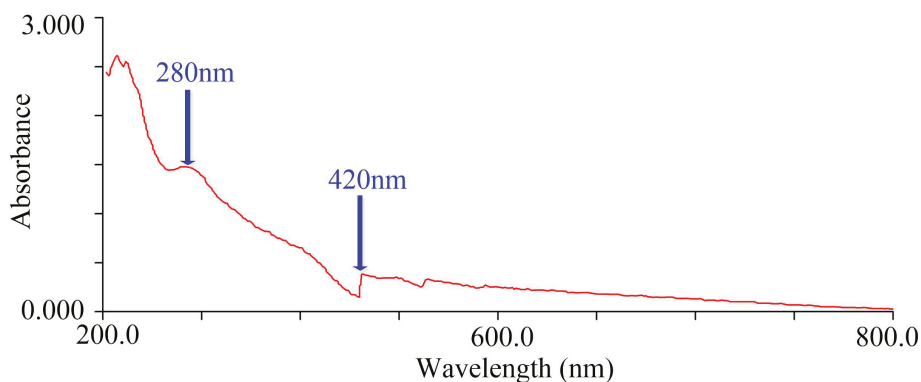


**Figure 4.** Ultraviolet-visible absorption spectroscopy (UV-VIS) spectrum of RF4. The aqueous solutions of RF4 was 1 mg/mL.

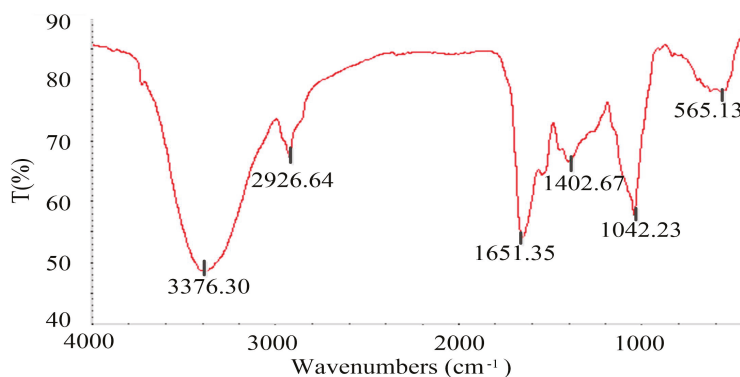


**Figure 5.** Fourier transform infrared (FT-IR) spectrum of RF4. The wavenumbers corresponding to the important absorption peaks were marked in the figure.

The FT-IR spectrum showed the possible presence of C=O, N-H, C-N, O-H, C-H, C-O, C-C, and -C-CO-C-groups in the structure of DDSG melanoidins. To the best of our knowledge, the structure of DDSG melanoidins was first investigated in this study. Further structure analysis will be performed by thermal degradation, liquid chromatography-mass spectrometry (LC-MS), and nuclear magnetic resonance (NMR).

### 3.3. Color and Chemical Properties of Melanoidins

#### 3.3.1. Color Analysis

Brown is a typical external characteristic of melanoidins and might be caused by multiple chromophores [38]. The absorbance of four fractions (RF1-RF4, aqueous solution of 1 mg/mL) was measured at 420 nm (Table 2). The RF4 exhibited the highest level of absorbance (0.507), followed by RF2 (0.188), RF3 (0.150), and RF1 (0.132).

**Table 2.** Absorbance of RF1–RF4 at 420 nm <sup>1</sup>.

Fractions	RF1	RF2	RF3	RF4
Absorbance	0.132 ± 0.02	0.188 ± 0.06	0.150 ± 0.05	0.507 ± 0.08

<sup>1</sup> The absorbances of four fractions were recorded at aqueous solutions of 1 mg/mL, and the results are shown as mean ± SD (*n* = 3).

### 3.3.2. Chemical Properties Analysis

Phenols and protein as well as carbohydrate were considered to be the three major components of melanoidins [39–41]. The TPC and protein content of RF4 exhibited the highest levels (18.31 mg GAE/g DDSG dw and 88.98 mg BSA/g DDSG dw, respectively), followed by RF2 (8.73 mg GAE/g DDSG dw and 59.58 mg BSA/g DDSG dw) (Table 3). The fact that RF4 and RF2 possessed higher levels of phenols and protein is possibly due to the reason that alkaline extraction contributed to the release of phenolic compounds [42] and extraction of protein [43]. In addition, RF4 showed the highest carbohydrate content (164.30 mg GE/g DDSG dw). The higher levels of phenols and protein as well as carbohydrate exhibited by RF4 could be attributed to the presence of more melanoidins in RF4.

**Table 3.** Content of total phenols, protein, and carbohydrate in four fractions <sup>1</sup>.

Fractions	Total Phenols (mg GAE/g DDSG dw)	Protein (mg BSA/g DDSG dw)	Carbohydrate (mg GE/g DDSG dw)
RF1	5.23 ± 0.07 <sup>c</sup>	14.15 ± 0.64 <sup>d</sup>	131.90 ± 4.62 <sup>b</sup>
RF2	8.73 ± 0.10 <sup>b</sup>	59.58 ± 2.41 <sup>b</sup>	61.84 ± 2.02 <sup>c</sup>
RF3	5.56 ± 0.13 <sup>c</sup>	50.01 ± 4.99 <sup>c</sup>	32.93 ± 1.04 <sup>d</sup>
RF4	18.31 ± 1.23 <sup>a</sup>	88.98 ± 3.89 <sup>a</sup>	164.30 ± 3.27 <sup>a</sup>

<sup>1</sup> The determinations were performed at the aqueous solutions of 1 mg/mL. The results are shown as mean ± SD (*n* = 3). Differences in mean were detected by ANOVA after conducting a Shapiro–Wilk test and Levene’s test. Values in the same column with different letters are significantly different (*p* < 0.05).

It is worth noting that there is no obvious absorption peak of phenol present in the FT-IR spectrum (Figure 5), and this could be due to the phenolic content of RF4 (18.31 mg GAE/g DDSG dw) being too low to be detected.

## 3.4. The Antioxidant and ACE-Inhibitory Activity of Melanoidins In Vitro

### 3.4.1. Antioxidant Activity

Different methods used for antioxidant measurement could exhibit different experimental data, and two or more determined methods are needed herein to evaluate the antioxidant activity of melanoidins. Thus, ABTS<sup>•+</sup>, FRAP, and DPPH assays were chosen for determination. The results obtained by these three assays were similar in the RF1–RF4 fractions, of which RF4 showed higher antioxidant capacity (ABTS<sup>•+</sup>, 1.03 mmol TE/g DDSG dw; FRAP, 0.33 mmol FE/g DDSG dw; DPPH, 20.57% at 1 mg RF4/mL) than the other three fractions (Table 4). The ability of RF4 to inhibit ABTS<sup>•+</sup> oxidation was 38 times higher than the biscuits’ melanoidins [44] and 7 times higher than lightly roasted coffee melanoidins [7]. The antioxidant activity of RF4 as determined by the FRAP assay was higher than straw wine melanoidins (0.15–0.26 mmol FE/g) [45]. However, the ability of RF4 to scavenge DPPH radicals (20.57%) was about one-third that of BSG melanoidins (59.50%) [19].

**Table 4.** Antioxidant activity of RF1–RF4<sup>1</sup>.

Fractions	ABTS <sup>•+</sup> (mmol TE/g DDSG dw)	FRAP (mmol FE/g DDSG dw)	DPPH (%)
RF1	0.88 ± 0.01 <sup>b</sup>	0.04 ± 0.02 <sup>c</sup>	4.90 ± 0.02 <sup>c</sup>
RF2	0.89 ± 0.02 <sup>b</sup>	0.11 ± 0.04 <sup>b</sup>	10.63 ± 0.39 <sup>b</sup>
RF3	0.87 ± 0.01 <sup>b</sup>	0.04 ± 0.03 <sup>c</sup>	5.88 ± 0.26 <sup>c</sup>
RF4	1.03 ± 0.03 <sup>a</sup>	0.33 ± 0.03 <sup>a</sup>	20.57 ± 0.92 <sup>a</sup>

<sup>1</sup> The aqueous fractions used in ABTS<sup>•+</sup>, FRAP, and DPPH assays were 1 mg/mL. The results are shown as mean ± SD (*n* = 3). Differences in mean were detected by ANOVA after conducting a Shapiro–Wilk test and Levene’s test. Values in the same column with different letters are significantly different (*p* < 0.05).

Melanoidins from DDSG could be used as a functional ingredient in the production of food due to its strong antioxidant activity.

### 3.4.2. ACE-Inhibitory Activity

ACE (EC 3.4.15.1), a zinc-containing dipeptide carboxypeptidase, converts angiotensin I into angiotensin II in plasma, along with strengthening the contraction of the myocardium and increasing blood pressure. The inhibitory activity of ACE plays an important role in lowering blood pressure [46]. As shown in Table 5, RF4 exhibited the highest ACE-inhibitory activity, with a value of 95.92% at 2 mg RF4/mL. The ACE-inhibitory activity of RF4 was obviously stronger than that of melanoidins in coffee (lightly roasted coffee, 36.80%; medium-roasted coffee, 43.10%; dark-roasted coffee, 45.10%) [8], vinegar (15.75–43.68%) [47], and black brewer’s spent grain (75.18%) at 2 mg/mL [17]. It has been reported that the ACE-inhibitory activity of melanoidins is related to antioxidant activity [48]. It would be interesting to study whether the ACE-inhibitory activity of melanoidins from DDSG is related to its high antioxidant activity under ABTS<sup>•+</sup> and FRAP assays.

**Table 5.** Angiotensin-converting enzyme (ACE)-inhibitory activity of RF1–RF4<sup>1</sup>.

Fractions	RF1	RF2	RF3	RF4
ACE inhibition rate (%)	86.43 ± 3.42	63.83 ± 5.18	88.28 ± 3.59	95.92 ± 4.86

<sup>1</sup> The aqueous fractions used in the assay of ACE inhibition rate were 2 mg/mL. The results are shown as mean ± SD (*n* = 3).

### 3.5. Preliminary Structure and Properties of Different MW Melanoidin Fractions from RF4

RF4 had the deepest color, the highest content, the strongest antioxidant capacity and ACE-inhibitory ability of melanoidins compared to the other three fractions. The different MW subfractions of RF4, RF4-1 (<3 kDa), RF4-2 (3–10 kDa), RF4-3 (10–30 kDa), RF4-4 (30–50 kDa), RF4-5 (50–100 kDa), and RF4-6 (>100 kDa), were obtained by ultrafiltration for further analysis of the structure and properties.

#### 3.5.1. Yield of RF4 Subfractions

The yields of RF4 subfractions are presented in Table 6, and it is obviously observed that RF4-6 (>100 kDa) had the highest yield (12.76% of the DDSG dw), suggesting that most of the melanoidins in RF4 from DDSG were >100 kDa compounds. The more than 100 kDa melanoidins have also been reported in real foods like coffee [49], roasted malt [50], and bread crusts [6]. Furthermore, the formation of high MW melanoidins (MW > 10 kDa) was related to an intense heating temperature and long reaction time [51]. Therefore, the formation of melanoidins in DDSG could be derived from the higher temperature daqu, the higher temperature stacking of fermenting grains, and distillation processes.

**Table 6.** Yields of melanoidin fractions with different molecular weights (MWs).<sup>1</sup>

Fractions	Yield (%)
RF4-1 <sup>2</sup>	0.64
RF4-2	2.46
RF4-3	0.06
RF4-4	0.37
RF4-5	0.94
RF4-6	12.76

<sup>1</sup> The yields were calculated on a DDSG dw basis. <sup>2</sup> RF4-1: <3 kDa, RF4-2: 3–10 kDa, RF4-3: 10–30 kDa, RF4-4: 30–50 kDa, RF4-5: 50–100 kDa, RF4-6: >100 kDa.

### 3.5.2. Color and Chemical Properties of RF4

The RF4 subfractions were characterized in terms of their color, phenolic content, protein content, and carbohydrate content (Table 7). RF4-6 exhibited the darkest color (0.633, 1 mg RF4-6/mL), the highest content of phenols (4.66 mg GAE/g DDSG dw), carbohydrate (61.48 mg GE/g DDSG dw), and protein (34.17 mg BSA/g DDSG dw), followed by RF4-5 and RF4-4. RF4-1 had the lightest color (0.128), lowest phenols (1.41 mg GAE/g DDSG dw), carbohydrate (5.41 mg GE/g DDSG dw), and protein content (2.40 mg BSA/g DDSG dw). The higher absorbance exhibited by higher MW fractions, except for RF4-2, which is indicative of an increase in color contribution as MW increased. This phenomenon was in accordance with previous work [30]. The total phenols and protein content, as well as carbohydrate content, were more concentrated in RF4-6, which had the highest yield of melanoidins, further proving the inference mentioned above, that these three compositions could be involved in the melanoidin structure.

**Table 7.** Absorbance, total phenolic, carbohydrate, and protein content of different MW fractions <sup>1</sup>.

Fractions	Absorbance	Total Phenols (mg GAE/g DDSG dw)	Carbohydrate (mg GE/g DDSG dw)	Protein (mg BSA/g DDSG dw)
RF4-1 <sup>2</sup>	0.128 ± 0.01 <sup>d</sup>	1.41 ± 0.06 <sup>e</sup>	5.41 ± 0.71 <sup>f</sup>	2.40 ± 0.38 <sup>e</sup>
RF4-2	0.144 ± 0.01 <sup>d</sup>	1.93 ± 0.38 <sup>d</sup>	11.62 ± 0.65 <sup>e</sup>	4.09 ± 0.52 <sup>de</sup>
RF4-3	0.135 ± 0.02 <sup>d</sup>	1.76 ± 0.13 <sup>de</sup>	15.44 ± 0.87 <sup>d</sup>	7.41 ± 0.98 <sup>d</sup>
RF4-4	0.302 ± 0.01 <sup>c</sup>	2.50 ± 0.38 <sup>c</sup>	28.70 ± 2.86 <sup>c</sup>	16.12 ± 1.06 <sup>c</sup>
RF4-5	0.359 ± 0.03 <sup>b</sup>	3.03 ± 0.43 <sup>b</sup>	40.13 ± 3.05 <sup>b</sup>	23.85 ± 0.82 <sup>b</sup>
RF4-6	0.633 ± 0.05 <sup>a</sup>	4.66 ± 0.13 <sup>a</sup>	61.48 ± 5.15 <sup>a</sup>	34.17 ± 3.31 <sup>a</sup>

<sup>1</sup> Determinations were carried out on different aqueous fractions of 1 mg/mL, and the results are shown as mean ± SD (*n* = 3). Differences in mean were detected by ANOVA after conducting a Shapiro-Wilk test and Levene's test. Values in the same column with different letters are significantly different (*p* < 0.05). <sup>2</sup> RF4-1: <3 kDa, RF4-2: 3–10 kDa, RF4-3: 10–30 kDa, RF4-4: 30–50 kDa, RF4-5: 50–100 kDa, RF4-6: >100 kDa.

### 3.5.3. Preliminary Structure of RF4 Subfractions

At the wavelength of 200–800 nm, the UV-VIS spectra of RF4 subfractions showed similar shapes but different absorbance (Figure 6), suggesting that different MW melanoidin fractions had similar characteristics in terms of structure but different amounts of chromophores.

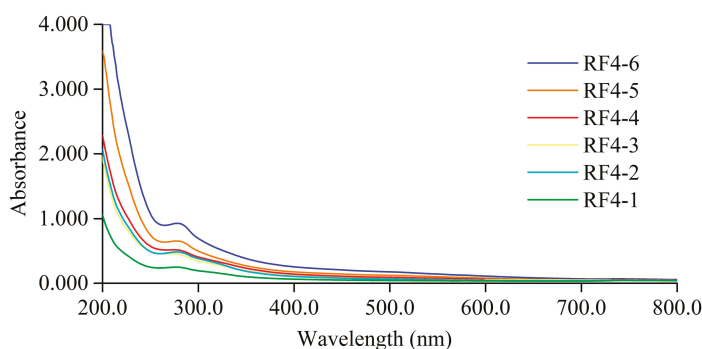


**Figure 6.** UV-VIS spectrum of different MW fractions obtained from RF4 by ultrafiltration. The aqueous solutions of fractions were 0.2 mg/mL.

The FT-IR assay of different MW melanoidin fractions showed that the structure of these MW fractions could be similar, except for RF4-6 (Figure 7). It was speculated that different MW melanoidin fractions contained the same functional groups (C=O, N-H, C-N, O-H, C-H, C-O, C-C, and -C-CO-C-), except for RF4-6. RF4-6 had an obvious absorption peak at 1519  $\text{cm}^{-1}$ , which could be caused by the presence of a benzene ring according to previous research on the structure of melanoidins [16].

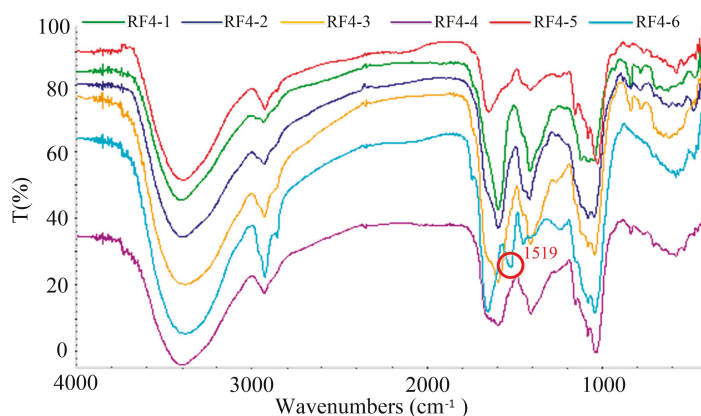


**Figure 7.** FT-IR spectrum of different MW fractions obtained from RF4 by ultrafiltration.

### 3.5.4. Physiological Activity of RF4 Subfractions In Vitro

The antioxidant capacity of different MW fractions was investigated under ABTS<sup>•+</sup>, FRAP (Figure 8a), and DPPH assays (Figure 8b). Except for the similar antioxidant capacity of RF4-2 and RF4-3, the other MW fractions have statistically significant differences ( $p < 0.05$ ). On the whole, the antioxidant capacity of RF4 subfractions increased with the increase in MW. RF4-6 showed the highest antioxidant capacity, while RF4-1 had the lowest. The ability of RF4-6 to scavenge ABTS<sup>•+</sup> (0.23 mmol TE/g DDSC dw) was 1.8 times higher, FRAP (0.13 mmol FE/g DDSC dw) was 2.5 times higher, and the DPPH radical-scavenging rate (39.52% at 1 mg RF4-6/mL) was 26 times higher compared with RF4-1. RF4-2 with lower MW had higher antioxidant activity than RF4-3, possibly because RF4-2 contained more phenols. The phenols of melanoidins can show high antioxidant activity by binding to melanoidin skeletons with non-covalent bonds [33]. In the case of the DPPH radical-scavenging rate, the fractions with MW < 30 kDa had little scavenging activity, and DPPH radical-scavenging rate of MW > 100 kDa fractions could reach about 40%.

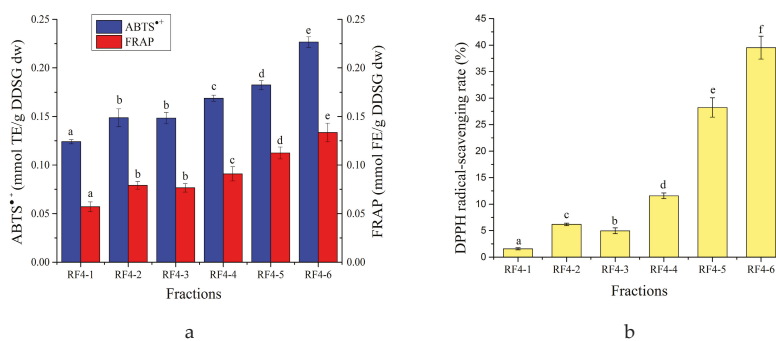


**Figure 8.** The antioxidant capacity of different MW fractions assessed by ABTS<sup>•+</sup> (a), FRAP (a), and DPPH assay (b). The aqueous solutions of fractions were 1 mg/mL. Differences in mean were detected by ANOVA after conducting a Shapiro-Wilk test and Levene's test. Different letters in the same assay represent significant differences ( $p < 0.05$ ).

The ACE-inhibition rate of different MW fractions ranged from 54.64% to 92.74% (Figure 9). For fractions with MW > 3 kDa, the ACE-inhibitory activity gradually decreased with the increase of MW, which was contrary to the phenomenon previously observed for antioxidant activity. The fractions with MW 3–10 kDa (RF4-2) had the strongest ACE-inhibitory activity, at 92.74%.

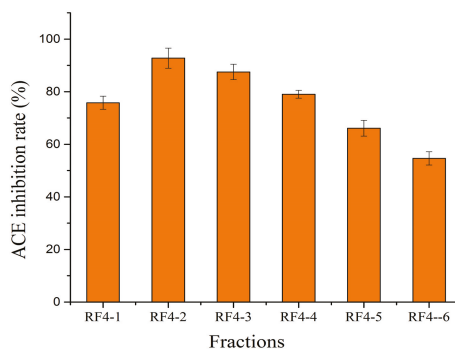


**Figure 9.** The ACE-inhibitory activity assay of different MW fractions. The aqueous solutions of fractions were 2 mg/mL.

#### 4. Conclusions

In this work, preliminary explorations of the content, structure, antioxidant capacity, and ACE-inhibitory activity of DDSG melanoidins were reported. The determination of content was achieved through a model system of serine and glucose. The total content of melanoidins was 268.60 mg/g DDSG dw, and melanoidins of DDSG mainly comprised >100 kDa compounds (12.76% of the DDSG dw). Functional groups such as C=O, N-H, C-N, O-H, C-H, C-O, C-C, and -C-CO-C- were present in the structure of melanoidins. In addition, DDSG melanoidins were proven to possess strong FRAP, ABTS<sup>•+</sup> scavenging capacity, and ACE-inhibitory activity. The large availability of DSG and the health benefits of melanoidins suggested herein could provide new possibilities for its high value-added utilization. Future work on the main production stage of DSG melanoidins and changes in the baijiu-making process is worth carrying out.

**Author Contributions:** Conceptualization, W.F.; Methodology, S.Y.; Data curation, W.F.; Writing—Original draft preparation, S.Y.; Writing—Review and editing, W.F. and Y.X.; Supervision, W.F.; Funding acquisition, Y.X.

**Funding:** This research was funded by the National Key R&D Program of China under grant no. 2016YFD0400503 and the national first-class discipline program of Light Industry Technology and Engineering (LITE2018-12).

**Acknowledgments:** The authors thank Golden Seed Winery Co., Ltd. for the DSG donation.

**Conflicts of Interest:** The authors declare no conflict of interest.

## References

1. Wei, D.; Fan, W.; Xu, Y. In Vitro Production and Identification of Angiotensin Converting Enzyme (ACE) Inhibitory Peptides Derived from Distilled Spent Grain Prolamin Isolate. *Foods* **2019**, *8*, 390. [[CrossRef](#)] [[PubMed](#)]
2. Xing, Y.; Lin, S.L.; Shi, Y.; Ren, G.X. Aerogenic Characteristics of Anaerobic Fermentation Using Vinasse and Marc. *J. Henan Agric. Sci.* **2011**, *40*, 88–90. (In Chinese)
3. Tan, Z.L.; Liu, J.H.; Ma, K.; Chen, D.D. New Technologies for Comprehensive Utilization of Distillers Grains. *Guangdong Chem. Ind.* **2015**, *42*, 72–73. (In Chinese)
4. Niu, G.J.; Liu, J.; Sun, D.W. Study on the Production of Single Cell Protein with Liquor Lees. *Liquor Mak.* **2010**, *37*, 28–30. (In Chinese)
5. Martins, S.; Mussatto, S.I.; Martínez-Avila, G.; Montañez-Saenz, J.; Aguilar, C.N.; Teixeira, J.A. Bioactive phenolic compounds: Production and extraction by solid-state fermentation. A review. *Biotechnol. Adv.* **2011**, *29*, 365–373. [[CrossRef](#)]
6. Lindenmeier, M.; Faist, V.; Hofmann, T. Structural and Functional Characterization of Pronyl-lysine, a Novel Protein Modification in Bread Crust Melanoidins Showing in Vitro Antioxidative and Phase I/II Enzyme Modulating Activity. *J. Agric. Food Chem.* **2002**, *50*, 6997–7006. [[CrossRef](#)]
7. Rosa, C.B.; Attilio, V.; Carmela, M.; Monica, A.; Vincenzo, F. Chemical characterization and antioxidant properties of coffee melanoidins. *J. Agric. Food Chem.* **2002**, *50*, 6527–6533.
8. Rufián-Henares, J.A.; Morales, F.J. Angiotensin-I Converting Enzyme Inhibitory Activity of Coffee Melanoidins. *J. Agric. Food Chem.* **2007**, *55*, 1480–1485. [[CrossRef](#)]
9. Borrelli, R.C.; Fogliano, V. Bread crust melanoidins as potential prebiotic ingredients. *Mol. Nutr. Food Res.* **2010**, *49*, 673–678. [[CrossRef](#)]
10. Rufián-Henares, J.A.; Morales, F.J. Microtiter plate-based assay for screening antimicrobial activity of melanoidins against E-coli and S-aureus. *Food Chem.* **2008**, *111*, 1069–1074. [[CrossRef](#)]
11. Cammerer, B.; Kroh, L.W. Investigation on the influence of reaction conditions on the elementary composition of melanoidins. *Food Chem.* **1995**, *53*, 55–59. [[CrossRef](#)]
12. Tressl, R.; Wondrak, G.T.; Garbe, L.A.; Krüger, R.P.; Rewicki, D. Pentoses and hexoses as sources of new melanoidin-like Maillard polymers. *J. Agric. Food Chem.* **1998**, *46*, 1765–1776. [[CrossRef](#)]
13. Hofmann, T. Studies on melanoidin-type colorants generated from the Maillard reaction of protein-bound lysine and furan-2-carboxaldehyde-chemical characterisation of a red coloured domain. *Z. Lebensmittelunters. Forsch.* **1998**, *206*, 251–258. [[CrossRef](#)]
14. Kato, H.; Tsuchida, H. Estimation of melanoidin structure by pyrolysis and oxidation. *Prog. Food Nutr. Sci.* **1981**, *5*, 147–156.
15. Adams, A.; Abbaspour, T.K.; Kersiene, M.; Venskutions, R.; Kimpe, N.D. Characterization of Model Melanoidins by the Thermal Degradation Profile. *J. Agric. Food Chem.* **2003**, *51*, 4338–4343. [[CrossRef](#)]
16. Moreira, A.S.; Nunes, F.M.; Domingues, M.R.; Coimbra, M.A. Coffee melanoidins: Structures, mechanisms of formation and potential health impacts. *Food Funct.* **2012**, *3*, 903–915. [[CrossRef](#)]
17. Piggott, C.O.; Connolly, A.; Fitzgerald, R.J. Application of ultrafiltration in the study of phenolic isolates and melanoidins from pale and black brewers' spent grain. *Int. J. Food Sci. Technol.* **2014**, *49*, 2252–2259. [[CrossRef](#)]
18. Zheng, J.J. Extraction and Purification Techniques of Melanoidin from Distillers' Grains. Master's Thesis, Shandong Agricultural University, Shandong, China, 2015.
19. Connolly, A.; Piggott, C.O.; Fitzgerald, R.J. Characterisation of protein-rich isolates and antioxidative phenolic extracts from pale and black brewers' spent grain. *Int. J. Food Sci. Technol.* **2013**, *48*, 1670–1681. [[CrossRef](#)]
20. Carvalho, D.O.; Correia, E.; Lopes, L.; Guido, L.F. Further insights into the role of melanoidins on the antioxidant potential of barley malt. *Food Chem.* **2014**, *160*, 127–133. [[CrossRef](#)]

21. Singleton, V.; Rossi, J.A. Colorimetry of Total Phenolics with Phosphomolybdic-Phosphotungstic Acid Reagents. *Am. J. Enol. Vitic.* **1965**, *16*, 144–158.
22. Bradford, M.M. A rapid and sensitive method for the quantitation of microgram quantities of protein utilizing the principle of protein-dye binding. *Anal. Biochem.* **1976**, *72*, 248–254. [[CrossRef](#)]
23. Dubois, M.; Gilles, K.A.; Hamilton, J.K.; Rebers, P.A.; Smith, F. Colorimetric Method for Determination of Sugars and Related Substances. *Anal. Chem.* **1956**, *28*, 350–356. [[CrossRef](#)]
24. Gizdavic-Nikolaidis, M.; Travas-Sejdic, J.; Bowmaker, G.A.; Cooney, R.P.; Thompson, C.; Kilmartin, P.A. The antioxidant activity of conducting polymers in biomedical applications. *Curr. Appl. Phys.* **2004**, *4*, 347–350. [[CrossRef](#)]
25. So, P.B.T.; Rubio, P.; Lirio, S.; Macabeo, A.P.; Huang, H.Y.; Corpuz, M.J.A.T.; Villaflores, O.B. In vitro angiotensin I converting enzyme inhibition by a peptide isolated from *Chiropsalmus quadrigatus* Haeckel (box jellyfish) venom hydrolysate. *Toxicon* **2016**, *119*, 77–83. [[CrossRef](#)] [[PubMed](#)]
26. Milic, B.L.; Grujic-Injac, B.; Piletic, M.V.; Lajsic, S.; Kolarov, L.A. Melanoidins and carbohydrates in roasted barley. *J. Agric. Food Chem.* **1975**, *23*, 960–963. [[CrossRef](#)]
27. Fogliano, V.; Morales, F.J. Estimation of dietary intake of melanoidins from coffee and bread. *Food Funct.* **2011**, *2*, 117–123. [[CrossRef](#)]
28. Farhat, I.A.; Orset, S.; Moreau, P.; Blanshard, J.M.V. FTIR Study of Hydration Phenomena in Protein–Sugar Systems. *J. Colloid Interface Sci.* **1998**, *207*, 200–208. [[CrossRef](#)]
29. Coca, M.; García, M.T.; González, G.; Peña, M.; García, J.A. Study of coloured components formed in sugar beet processing. *Food Chem.* **2004**, *86*, 421–433. [[CrossRef](#)]
30. Mohsin, G.F.; Schmitt, F.J.; Kanzler, C.; Epping, J.D.; Flemig, S.; Hornemann, A. Structural characterization of melanoidin formed from D-glucose and L-alanine at different temperatures applying FTIR, NMR, EPR, and MALDI-ToF-MS. *Food Chem.* **2018**, *245*, 761–767. [[CrossRef](#)]
31. Kim, J.S.; Lee, Y.S. Effect of reaction pH on enolization and racemization reactions of glucose and fructose on heating with amino acid enantiomers and formation of melanoidins as result of the Maillard reaction. *Food Chem.* **2008**, *108*, 582–592. [[CrossRef](#)]
32. Wang, H.S.; Pan, Y.M.; Tang, X.J.; Huang, Z.Q. Isolation and characterization of melanin from *Osmanthus fragrans* seeds. *Lwt-Food Sci. Technol.* **2006**, *39*, 496–502. [[CrossRef](#)]
33. Brands, C.M.J.; Wedzicha, B.L.; Boekel, M.A.J.S. Van. Quantification of melanoidin concentration in sugar-casein systems. *J. Agric. Food Chem.* **2002**, *50*, 1178–1183. [[CrossRef](#)] [[PubMed](#)]
34. Brudzynski, K.; Miotto, D. The recognition of high molecular weight melanoidins as the main components responsible for radical-scavenging capacity of unheated and heat-treated Canadian honeys. *Food Chem.* **2011**, *125*, 570–575. [[CrossRef](#)]
35. Zhang, H.J.; Qiu, C.; Tian, Q.; Hui, M. Extraction, Composition and Spectral Properties of Melanoidins from Chinese Rice Wine. *J. Henan Univ. Technol.* **2016**, *37*, 57–62.
36. Gu, F.L.; Kim, J.M.; Abbas, S.; Zhang, X.M.; Xia, S.Q.; Chen, Z.X. Structure and antioxidant activity of high molecular weight Maillard reaction products from casein-glucose. *Food Chem.* **2010**, *120*, 505–511. [[CrossRef](#)]
37. Oliver, C.M.; Kher, A.; McNaughton, D.; Augustin, M.A. Use of FTIR and mass spectrometry for characterization of glycosylated caseins. *J. Dairy Res.* **2009**, *76*, 105–110. [[CrossRef](#)]
38. Liggett, R.W.; Deitz, V.R. Color and Turbidity of Sugar Products. *Adv. Carbohydr. Chem.* **1954**, *9*, 247–283.
39. Brudzynski, K.; Miotto, D. Honey melanoidins: Analysis of the compositions of the high molecular weight melanoidins exhibiting radical-scavenging activity. *Food Chem.* **2011**, *127*, 1023–1030. [[CrossRef](#)]
40. Coelho, C.; Ribeiro, M.; Cruz, A.C.S.; Domingues, M.R.M.; Coimbra, M.A.; Bunzel, M.; Nunes, F.M. Nature of Phenolic Compounds in Coffee Melanoidins. *J. Agric. Food Chem.* **2014**, *62*, 7843–7853. [[CrossRef](#)]
41. Mesías, M.; Delgado-Andrade, C. Melanoidins as a potential functional food ingredient. *Curr. Opin. Food Sci.* **2017**, *14*, 37–42. [[CrossRef](#)]
42. Oracz, J.; Nebesny, E.; Zyzelewicz, D. Identification and quantification of free and bound phenolic compounds contained in the high-molecular weight melanoidin fractions derived from two different types of cocoa beans by UHPLC-DAD-ESI-HR-MSn. *Food Res. Int.* **2019**, *115*, 135–149. [[CrossRef](#)] [[PubMed](#)]
43. Qin, F.; Johansen, A.Z.; Mussatto, S.I. Evaluation of different pretreatment strategies for protein extraction from brewer's spent grains. *Ind. Crops Prod.* **2018**, *125*, 443–453. [[CrossRef](#)]

44. Borrelli, R.C.; Mennella, C.; Barba, F.; Russo, M.; Russo, G.L.; Krome, K.; Erbersdobler, H.F.; Faist, V.; Fogliano, V. Characterization of coloured compounds obtained by enzymatic extraction of bakery products. *Food Chem. Toxicol.* **2003**, *41*, 1367–1374. [[CrossRef](#)]
45. Goulas, V.; Nicolaou, D.; Botsaris, G.; Barbouti, A. Straw Wine Melanoidins as Potential Multifunctional Agents: Insight into Antioxidant, Antibacterial, and Angiotensin-I-Converting Enzyme Inhibition Effects. *Biomedicines* **2018**, *6*, 83. [[CrossRef](#)]
46. Corvol, P.; Williams, T.A.; Soubrier, F. Peptidyl dipeptidase—Angiotensin I converting enzyme. *Methods Enzymol.* **1995**, *248*, 283–305.
47. Lu, X. Research on Antioxidant Effect and Anti-ACE Activity of Shanxi Aged Vinegar. Master's Thesis, Shanxi University, Shanxi, China, 2015.
48. Jin, W.N.; Hwang, I.G.; Kim, H.Y.; Lee, Y.R.; Woo, K.S.; Bang, Y.H.; Chang, S.J.; Lee, J.; Jeong, H.S. Free radical scavenging, angiotensin I-converting enzyme (ACE) inhibitory, and in vitro anticancer activities of ramie (*Boehmeria nivea*) leaves extracts. *Food Sci. Biotechnol.* **2010**, *19*, 383–390.
49. Bekedam, E.K.; Schols, H.A.; Van Boekel, M.A.J.S.; Smit, G. High molecular weight melanoidins from coffee brew. *J. Agric. Food Chem.* **2006**, *54*, 7658–7666. [[CrossRef](#)]
50. Faist, V.; Lindenmeier, M.; Geisler, C.; Erbersdobler, H.F.; Hofmann, T. Influence of molecular weight fractions isolated from roasted malt on the enzyme activities of NADPH-cytochrome c-reductase and glutathione-S-transferase in caco-2 cells. *J. Agric. Food Chem.* **2002**, *50*, 602–606. [[CrossRef](#)]
51. Bekedam, E.K.; Loots, M.J.; Schols, H.A.; Van Boekel, M.A.; Smit, G. Roasting effects on formation mechanisms of coffee brew melanoidins. *J. Agric. Food Chem.* **2008**, *56*, 7138–7145. [[CrossRef](#)]



© 2019 by the authors. Licensee MDPI, Basel, Switzerland. This article is an open access article distributed under the terms and conditions of the Creative Commons Attribution (CC BY) license (<http://creativecommons.org/licenses/by/4.0/>).



Article

# Valorisation of Grape Stems as a Source of Phenolic Antioxidants by Using a Sustainable Extraction Methodology

Juan Antonio Nieto <sup>1</sup>, Susana Santoyo <sup>1</sup>, Marin Prodanov <sup>1</sup>, Guillermo Reglero <sup>1,2</sup> and Laura Jaime <sup>1,\*</sup>

<sup>1</sup> Institute of Food Science Research (CIAL), Universidad Autónoma de Madrid (CEI, UAM-CSIC), 28049 Madrid, Spain; juan.nieto@uam.es (J.A.N.); susana.santoyo@uam.es (S.S.); marin.prodanov@uam.es (M.P.); guillermo.reglero@uam.es (G.R.)

<sup>2</sup> IMDEA-Food Institute, Campus de Cantoblanco, 28049 Madrid, Spain

\* Correspondence: laura.jaime@uam.es; Tel.: +34-910017900

Received: 7 April 2020; Accepted: 4 May 2020; Published: 8 May 2020

**Abstract:** Pressurized liquid extraction with ethanol:water mixtures was proposed for obtaining phenolic antioxidants from grape stems. The optimal extraction conditions were elucidated by using a central composite rotatable design (solvent ( $X_1$ , 0–100% ethanol:water *v/v*), temperature ( $X_2$ , 40–120 °C) and time ( $X_3$ , 1–11 min)). Response surface methodology determined 30% ethanol:water, 120 °C and 10 min as the optimal extraction conditions regarding total phenolic content (TPC) ( $185.3 \pm 2.9$  mg gallic acid/g of extract) and antioxidant activity ( $3.55 \pm 0.21$  mmol Trolox/g,  $1.22 \pm 0.06$  mmol Trolox/g and  $1.48 \pm 0.17$  mmol Trolox/g of extract in ABTS, DPPH and ORAC methodologies, respectively). The antioxidant activity was attributed to total polymer procyanidins and flavan-3-ol monomers and oligomers, although other phenolic compound contributions should not be ruled out. Forty-two phenolic compounds were identified in the optimal extract, mainly polymer procyanidins and, to a lesser extent, monomers and oligomers of flavan-3-ols, quercetin-3-*O*-glucuronide,  $\epsilon$ -viniferin, gallic and caftaric acid. Ethyl gallate, ellagic acid, protocatechuic aldehyde, delphinidin-7-*O*-glucoside and cyanidin-3-*O*-glucoside were reported for the first time in grape stem extracts. In conclusion, this study highlights the use of this winery side stream as a source of antioxidants within a sustainable food system.

**Keywords:** grape stem; phenolic compounds; central composite rotatable design; antioxidant activity; sustainable food systems; pressurized liquid extraction; side streams valorisation

## 1. Introduction

Nowadays, there is increasing concern about the sustainability of food production, including an environmentally friendly use of food by-products. In this context, one of the main goals of FAO is the promotion of sustainable food systems [1]. Accordingly, the exploitation of vegetable by-products as a source of bioactive compounds represents a promising opportunity to obtain added-value products for food or pharma industries. Particularly, wine production generates thousands of tons of solid organic waste, where grape stems represent up to 5% (*w/w*) of the processed grapes, being approximately 25% of the total by-products generated by the wine industry [2].

Whereas several studies have been focused on *Vitis vinifera* L. grape skins and seeds, less attention has been paid to grape stems as source of useful bioproducts [3,4]. Research papers focused on stem phenolic composition pointed out the presence of a high content of flavan-3-ol monomers (catechin and epicatechin) and, to a lesser extent, stilbenes (mainly resveratrol and  $\epsilon$ -viniferin), as well as different phenolic acids and flavonols [5–7]. These compounds are known for their important biological

activities; therefore, the use of stem by-products as a source of bioactive compounds has become a great opportunity to obtain functional ingredients in a sustainable way [4,8]. Nevertheless, there is a lack of studies with a comprehensive description of the phenolic composition of grape stem extracts. Thus, some studies are only focused on stilbene compounds [9,10], flavan-3-ol composition [11], their main phenolic constituents [3,6], or other specific groups [12,13]. However, there is scarce information about the proanthocyanidin fraction [12,14].

Extraction procedure is an important step to consider in recovery of bioactive compounds from plant sources. As conventional solid–liquid extraction (SLE) procedures usually have different drawbacks (such as long extraction time, intensive labour procedures, large volumes of solvents needed, and low extraction yields), many alternative techniques have been emerged in the last two decades [15]. In this regard, pressurized liquid extraction (PLE), ultrasound assisted extraction (UAE), microwave assisted extraction (MAE) and supercritical fluid extraction (SFE) have been proposed for extraction of bioactive compounds. Specifically, PLE has been used for extraction of phenolic compounds from a wide range of plant materials, e.g., hops, aromatic plants, grapes, as well as microalgae. Methanol, water, ethanol, acetone or their aqueous mixtures have been commonly used up to 170 °C in a light- and oxygen-free environment, with a greater efficiency than SLE procedures [16,17]. Development of an extraction methodology implies the establishment of optimal extraction conditions for a specific compound or group of compounds. For this purpose, the use of experimental designs, along with response surface methodology (RSM), has been proposed as a useful tool that enables the analysis of the influence of different extraction factors and allows reducing the number of experimental trials. Accordingly, it has been successfully used for improving phenolic extraction procedures from vegetable materials [12,13].

Regarding grape stem by-products, SLE with organic solvents has been commonly used for extraction of phenolic compounds [18]. However, alternative extraction techniques such as UAE [19], SFE [20], MAE [21] and PLE [22] have been scarcely studied. Moreover, only a few studies have focused on the use of green solvents, such as pure sub- and supercritical ethanol [23] or aqueous-ethanol mixtures with conventional SLE [12,13].

Therefore, to the best of our knowledge, a green extraction procedure based on the application of PLE to extraction of phenolic antioxidants from grape stems has not been established yet. Moreover, the relationship between phenolic composition and antioxidant activity should be established.

Hence, the aim of the present study was to develop a sustainable extraction procedure for valorisation of grape stems as a source of phenolic antioxidant compounds by using PLE and ethanol:water mixtures as green solvents. For this purpose, an experimental design along with RSM was used to optimize the extraction procedure (extraction solvent, temperature and time). Additionally, an extensive analysis of the phenolic composition of the extracts was done.

## 2. Materials and Methods

### 2.1. Chemicals and Reagents

Acetonitrile and formic acid, HPLC quality, were supplied by Labscan (Dublin, Ireland) and Acros Organic (Belgium), respectively. Protocatechuic acid, vanillic acid, syringic acid, caffeic acid, p-coumaric acid, 3-coumaric acid, ethyl gallate, 3,5,4'-trihydroxystilbene-3-O- $\beta$ -D-glucoside (*trans*-piceid), (+)-catechin, (–)-epicatechin, epicatechin gallate, procyanidin B<sub>1</sub>, procyanidin B<sub>2</sub>, procyanidin B<sub>3</sub>, quercetin-3-O-galactoside, quercetin-3-O-rutinoside, quercetin-3-O-glucuronide, quercetin-3-O-glucoside, quercetin dihydrate, delphinidin-3-O-glucoside, cyanidin-3-O-glucoside and malvidin-3-O-glucoside were purchased from Extrasynthèse (Genay, France). Gallic acid, 4-hydroxybenzoic acid, *trans*-caftaric acid, *trans*-ferulic acid, ellagic acid, protocatechuic aldehyde, *trans*-resveratrol, 6-hydroxy-2,5,7,8-tetramethylchromane-2-carboxylic acid (Trolox), potassium persulfate, 2,2'-azinobis(3-ethylbenzothiazoline-6-sulphonic acid) diammonium salt (ABTS), 2,2-diphenyl-1-picrylhydrazyl (DPPH), 1 M phosphate buffer, fluorescein sodium and

2,2'-azobis(2-methylpropionamidine) dihydrochloride (AAPH) were obtained from Sigma-Aldrich (Madrid, Spain). Disodium carbonate, Folin–Ciocalteu reagent, methanol and ethanol were from Panreac (Barcelona, Spain).

## 2.2. Plant Material

Grape stems (*Vitis vinifera* L. cv. Merlot) were provided by Instituto Madrileño de Investigación y Desarrollo Rural, Agrario y Alimentario (IMIDRA, Spain). Stems were separated manually. Raw fresh stems were dried at 40 °C for 48 h in an air bath Stuart S150 (Stuart, UK). Thereafter, dried material was ground in a blender and the resulting powder was sieved to a  $\leq 1$  mm particle size and stored in a closed bag at  $-20$  °C until further use.

## 2.3. Experimental Design

A central composite rotatable design (CCRD) was used to evaluate the influence of three independent variables (factors), i.e., solvent composition ( $X_1$ , 0%–100% ethanol), extraction temperature ( $X_2$ , 40–120 °C) and extraction time ( $X_3$ , 1–11 min) on the yield, antioxidant activity (ABTS, DPPH), total phenolic content (TPC) and flavan-3-ols content (mono-oligomers and polymers), measured by means of NP-HPLC, after PLE extraction. Therefore, a total of 19 experimental conditions were established at five levels ( $2^3$  points of the full factorial design + 6 star points + 5 central points) (Table 1). To determine the influence of the different experimental factors, response surface methodology (RSM) was used, and regression analysis of the response variable data was performed and fitted to a quadratic polynomial model as shown in the following equation:

$$Y = \beta_0 + \beta_1Et + \beta_2T + \beta_3t + \beta_{1,1}Et^2 + \beta_{2,2}T^2 + \beta_{3,3}t^2 + \beta_{1,2}EtT + \beta_{1,3}Ett + \beta_{2,3}Tt + \varepsilon, \quad (1)$$

where  $Y$  is the response variable;  $\beta_0$  the independent term;  $\beta_1$ ,  $\beta_2$  and  $\beta_3$  the linear coefficients;  $\beta_{1,1}$ ,  $\beta_{2,2}$  and  $\beta_{3,3}$  the quadratic coefficients;  $\beta_{1,2}$ ,  $\beta_{1,3}$  and  $\beta_{2,3}$  the interaction factor coefficients and  $\varepsilon$  the experimental error. The goodness of fit was evaluated according to the determination coefficient ( $R^2$ ), the residual standard deviation (RSD), and the lack of fit test provided by the analysis of variance (ANOVA).

**Table 1.** Coded levels and experimental values of the factors used in the central composite rotatable design.

Factor	Coded Symbol	Coded Levels				
		−1.68	−1	0	1	1.68
Ethanol concentration (%)	Et	0	20	50	80	100
Temperature (°C)	T	40	56	80	104	120
Time (min)	t	1	3	6	9	11

## 2.4. PLE

Extractions were performed by using an ASE 350 extractor from Dionex Corporation (Sunnyvale, CA, USA). Dry stem powder (1 g) was mixed in a ceramic mortar with 1 g of diatomaceous earth (Dionex, Sunnyvale, CA, USA). The solid mixture was loaded in an 11-mL extraction cell. Two cellulose filters (Dionex, Sunnyvale, CA, USA) were placed at the bottom of the cell to prevent the clogging of the system. The cell was automatically filled with the proper solvent to a pressure of 1500 psi. The extraction cell heat-up time was fitted according to the applied extraction temperature (e.g., 5 min, when the extraction temperature was 40 °C). Subsequently, a static extraction was performed. Afterwards, the cell was rinsed (60% cell volume) and solvent was purged from the cell with pressurized  $N_2$  gas for 90 s. A rinse of the complete system was made between extractions. Ethanol from all extracts was removed by vacuum evaporation at 37 °C in an IKA RV 10 control (IKA, Staufen, Germany), followed

by freeze-drying (Telstar Lyobeta 15 equipment; Telstar, Madrid, Spain). Powder extracts were kept at  $-20\text{ }^{\circ}\text{C}$  until analysis.

### 2.5. Identification and Quantification of Phenolic Compounds by RP-HPLC-PAD-MS

Individual phenolics were determined by reversed-phase high-performance liquid chromatography (RP-HPLC) as described by Grases et al. [24], adapted for grape stems. Chromatographic analyses were carried out in a C18 ACE RP18-AR (150 mm  $\times$  4.6 mm, 3  $\mu\text{m}$  particle size) (Symta, Madrid, Spain) protected by a guard column ACE 3 C18-AR (7 mm  $\times$  13 mm) packed with the same stationary phase. The column oven was set at  $30\text{ }^{\circ}\text{C}$  and sample injection volume was 40  $\mu\text{L}$ . A gradient consisting of 1% aqueous formic acid (solvent A) and acetonitrile containing 1% formic acid (solvent B) was used at a flow rate of 0.6 mL/min. The elution programme was applied as follows: 0 min, 0% B; 80 min, 20% B; 115 min, 28% B; 125 min, 50% B; 135 min, 100% B; 145 min, 100% B; and finally 10 min to recover initial chromatographic conditions. Chromatographic separation was carried out in an Agilent HPLC 1260 series equipped with a photodiode array detector (PAD) coupled online to an ion trap mass selective detector with an electrospray ionization source (Agilent Technologies Inc., Santa Clara, CA, USA). The system was controlled by ChemStation software (Agilent, vers. 6.8). Chromatograms were recorded at 280, 320, 360 and 520 nm. The electrospray ionization (ESI) parameters were as follows: drying gas ( $\text{N}_2$ ) flow and temperature, at  $11\text{ L min}^{-1}$  and  $350\text{ }^{\circ}\text{C}$ , respectively; nebulizer pressure 65.0 psi; and capillary voltage 4 kV. The full-scan mass covered the range from  $m/z$  100 to 2000  $\text{u.m.a}$ . Mass spectrometry data were acquired in positive ionisation mode for anthocyanins and negative ionisation mode for the other phenolic compounds. Prior to injection, all samples were diluted in 1 mL of ultrapure water:methanol (1:1) mixture and then filtered by a 0.45  $\mu\text{m}$  PVDF membrane filter.

Phenolic compounds were identified according to their retention time, mass-to-charge ratio ( $m/z$ ) of their molecular ions and UV/Vis spectrum by chromatographic comparison with analytical reference substances. Procyanidin dimers  $\text{B}_4$  and  $\text{B}_7$  were purified from natural extracts by high-speed countercurrent chromatography (HSCCC) as described in Grases et al. [24]. Procyanidin trimer  $\text{C}_1$  was identified by the use of a purified OPC-rich extract from cocoa as a complex reference substance, according to Prodanov et al. [25]. The rest of phenolic compounds were tentatively identified on base of their peak retention time,  $m/z$  of their molecular ions and diagnostic fragments, UV/Vis spectrum and/or data from Scifinder database and literature.

For quantification purposes, PAD was used. Chromatographic conditions were similar to those already described for identification purposes. Phenolic compounds were quantified by calibration curves of their respective reference solutions, except for procyanidin oligomers, apart from  $\text{B}_2$ , and resveratrol derivatives that were quantified from procyanidin  $\text{B}_1$  and resveratrol calibration curves, respectively. Hydroxybenzoic acids and flavan-3-ols were quantified at 280 nm, hydroxycinnamic acids and stilbenes at 320 nm, flavonols at 360 nm and anthocyanins at 520 nm. Samples were analysed at least in triplicate.

### 2.6. Analysis of Total Flavan-3-ol Monomers and Oligomers and Total Polymers by NP-HPLC

Analyses of total flavan-3-ol monomers and oligomers and total polymers, based on increasing order of their molecular masses (degree of polymerization), were performed by NP-HPLC following Muñoz-Labrador et al. [26] elution programme. A Kromasil 60 DIOL column (250 mm  $\times$  4.6 mm, 5  $\mu\text{m}$  particle size; AzkoNobel, Amsterdam, Netherland) was used with a security guard Lichrospher Diol-5 (7 mm  $\times$  13 mm) cartridge packed with the same material. Column temperature was kept at  $35\text{ }^{\circ}\text{C}$ . Solvent (A) was 2% acetic acid in acetonitrile, solvent (B) was methanol containing 2% acetic acid and 3% water, and solvent C was a 2% aqueous acetic acid. A constant flow rate of  $0.8\text{ mL min}^{-1}$  was used. Volume sample injection was 10  $\mu\text{L}$ . Chromatographic analyses were performed using an Agilent Infinity 1260 liquid chromatograph system.

Flavan-3-ol monomer and oligomers were identified according to their retention time and UV/Vis spectrum in comparison with a purified flavan-3-ol oligomer from cocoa-rich extract, used here as a complex reference substance for oligomer procyanidins of up to octamers. Total polymer procyanidins eluted as a singular peak at the end of the chromatogram [26]. Both mono- and oligomers and total polymers were quantified by means of catechin calibration curve at 280 nm. The results were expressed as mg of catechin equivalent (CE)/g extract. All analyses were done in triplicate.

### 2.7. Determination of Mean Degree of Procyanidin Polymerization (mDP)

Flavan-3-ol procyanidins were isolated in a minicolumn assembly-line system (minicolumn cartridge C18 Sep-Pack and tC18 Sep-Pack from Waters, Milford, MA, USA) as previously described by Sun et al. [27]. After that, degradation of isolated procyanidins was done by acid-catalysed degradation using toluene- $\alpha$ -tiol. Quantification of degradation products and mDP were conducted by RP-HPLC-PAD. All analyses were done in triplicate.

### 2.8. Total Phenolic Content (TPC)

Total phenolic content was determined according to the Folin–Ciocalteu reagent method [28]. The results were expressed as mg of gallic acid equivalents (GAE)/g extract. All analyses were done in triplicate.

### 2.9. Antioxidant Activity

ABTS<sup>+</sup> and DPPH radical scavenging assays were carried out according to the original method described by Re et al. [29] and Brand-Williams et al. [30], respectively, and both results were expressed as TEAC value (mmol Trolox/g extract).

ORAC assay was carried out using the method of Huang et al. [31] with some modifications. Briefly, 150  $\mu$ L of fluorescein solution ( $8 \times 10^{-8}$  M fluorescein in 0.075 M phosphate buffer) was mixed with 25  $\mu$ L of sample, phosphate buffer (blank) or Trolox solution (100, 80, 60, 40, 20 and 10  $\mu$ molar solution), or 50  $\mu$ L of phosphate buffer (control) in a 96 wells plate. The reaction was carried out by adding 25  $\mu$ L of a fresh AAPH solution (165.94 mmol AAPH in phosphate buffer) at 37 °C, except for control wells. The mixture was shaken for 8 s and fluorescence intensity was monitored for 120 min (485 nm and 520 nm for excitation and emission wavelength, respectively). ORAC values were expressed as mmol Trolox/g extract.

Antioxidant analyses were done in triplicate.

### 2.10. Statistical Analyses

The statistical analysis of CCR experimental design data was carried out by RSM with the statistical program Statgraphics Centurion XVI (Statistical Graphics Corp., Warrenton, VA, USA). Correlation coefficients between the different experimental data were performed using Pearson's test ( $p \leq 0.05$ ). Moreover, a principal component analysis (PCA) was conducted for correlation between response variables.

## 3. Results and Discussion

### 3.1. Experimental Model Fitting

The present study was conducted to evaluate the optimal conditions for the extraction of phenolic antioxidants from Merlot's grape stems (*Vitis vinifera* L.). This variety is one of the most representative grape varieties as it is one of the most widespread cultivars. For this purpose, a central composite rotatable design was applied as displayed in Table 2. Three independent variables or factors, namely, ethanol concentration ( $X_1$ , 0–100%), temperature ( $X_2$ , 40 °C–120 °C) and time ( $X_3$ , 1–11 min), were studied to assess their influence on antioxidant activity, flavan-3-ol monomers and oligomers, polymer procyanidins and total phenolic compounds. These factors are considered as the

main extraction-independent variables, at the expense of others less significant, such as solid–solvent ratio or solvent pH [13,32]. Aqueous methanol has been proposed as the most suitable solvent for the extraction of phenolic compounds from grape products [11,22]. Nevertheless, this toxic solvent is currently being replaced by aqueous ethanol [6,12]. Its high efficiency and GRAS status makes it suitable for food or pharmaceutical applications [12]. Heating up to 200 °C has been commonly used in PLE extractions, since higher temperatures lead to a greater extraction yield [23]. Nevertheless, values above 120 °C should be avoided as they may cause degradation of phenolic compounds [16]. Accordingly, the maximal temperature value was set at 120 °C in the present study. Moreover, the extraction time variable was limited in low values, since higher extraction time may promote phenolic degradation without an enhancement of extraction yields [17,32]. Table 2 shows response variable data corresponding to each experimental condition.

**Table 2.** Experimental design and experimental response variable data.

Run	Factor			Response Variables					
	X <sub>1</sub> , Ethanol	X <sub>2</sub> , Temperature	X <sub>3</sub> , Time	Yield	Total Phenolic Compounds (TPC)	ABTS	DPPH	Total Flavan-3-ol Mono- and Oligomers	Total Polymer Procyanidins
	(%)	(°C)	(min)	(g Extract/100 g Stem)	(mg GAE/g Extract)	(mmol Trolox/g Extract)	(mmol Trolox/g Extract)	(mg catechin/g Extract)	(mg catechin/g Extract)
1	20	56	3	21.5	118.1	2.06	0.65	19.53	30.02
2	80	56	3	9.4	114.0	1.89	0.55	52.72	14.55
3	20	104	3	27.5	164.0	2.89	0.97	24.48	42.64
4	80	104	3	23.3	145.9	2.50	0.81	31.51	32.10
5	20	56	9	21.0	148.7	2.63	0.86	27.16	41.97
6	80	56	9	10.3	113.2	1.94	0.56	69.97	21.26
7	20	104	9	28.5	178.7	3.33	1.19	26.59	44.58
8	80	104	9	14.8	135.2	2.42	0.72	52.64	19.65
9	0	80	6	24.9	147.8	2.54	0.87	17.81	21.68
10	100	80	6	12.4	87.4	1.39	0.29	98.73	4.06
11	50	40	6	18.8	129.4	2.24	0.77	30.67	34.53
12	50	120	6	30.6	186.6	3.43	1.22	26.51	49.78
13	50	80	1	21.2	147.8	2.60	0.88	26.26	38.42
14	50	80	11	24.8	172.7	2.96	1.06	27.73	44.51
15	50	80	6	22.8	167.6	2.98	1.00	47.45	22.05
16	50	80	6	25.0	171.8	3.00	1.05	45.43	21.62
17	50	80	6	24.3	167.9	2.94	1.03	45.67	21.30
18	50	80	6	24.1	169.7	2.95	0.98	45.34	21.82
19	50	80	6	24.0	160.2	2.77	1.01	46.65	21.48

The regression coefficients of linear, quadratic and interaction terms of the experimental factors were calculated by fixing the experimental values of response variables to a quadratic linear regression model. The effect of each term in the model and its statistical significance on the response variables were analysed from the standardized Pareto chart (data not shown). The quadratic and interaction terms not significantly different from zero ( $p \leq 0.05$ ) were excluded from the model, and the mathematical model was refitted by multiple linear regression (MLR), resulting in the polynomial equations shown in Table 3.

These equations suggest that RSM was successfully applied for the optimisation of the considered variables. The models did not show significant lack of fit ( $p > 0.05$ ), indicating well-fitting models for yield, TPC, ABTS and DPPH, opposite to flavan-3-ol monomers and oligomers, and polymer procyanidin behaviour. However, determination coefficients ( $R^2$ ) for all the studied variables were over 0.90. Therefore, the proposed models could be used as an approach to the real behaviour of these compounds regarding these extraction parameters. Concerning extraction yields, the obtained data exhibited a very good fit for a quadratic model. Moreover, all the experimental factors were significant, mainly ethanol proportion in a quadratic manner (Table 3). In addition, some significant interaction factors were found. Response surface plot showed that an increase of ethanol proportion caused an extraction yield rise of up to almost 25% (Figure 1). Therefore, higher and lower ethanol:water ratios led to a decrease in the extraction yield, more markedly at high ethanol proportions (Figure 1A,B).

Moreover, temperature caused a linear effect, that is, extraction yield was enhanced linearly when temperature increased (Figure 1A). On the other hand, a weak quadratic influence of extraction time was noticed.

**Table 3.** Polynomial equations and statistical parameters of the fitted models obtained for response variables.

Variable	Polynomial Equation of Fitted Model	R <sup>2</sup>	Lack-of-Fit (p-Value)
Yields (g extract/g stem)	$Y = -2.05097 + 0.188423(Et) + 0.24681(T) + 2.91554(t) - 0.00271887(Et)^2 - 0.0115812(Et \times t) - 0.0144409(T \times t) - 0.0984341(t)^2$	0.951	0.15
TPC (mg GAE/g extract)	$Y = -15.954 + 2.10974(Et) + 1.94514(T) + 10.808(t) - 0.0212643(Et)^2 - 0.0807058(Et \times t) - 0.00779276(T)^2 - 0.408779(t)^2$	0.97	0.21
ABTS (mmol Trolox/g extract)	$Y = 0.578714 + 0.0369343(Et) + 0.0142628(T) + 0.112674(t) - 0.000382393(Et)^2 - 0.00147263(Et \times t)$	0.97	0.33
DPPH (mmol Trolox/g extract)	$Y = -0.238343 + 0.0209687(Et) + 0.00766806(T) + 0.0851506(t) - 0.000183361(Et)^2 - 0.0000407129(Et \times T) - 0.00071712(Et \times t) - 0.00273786(t)^2$	0.98	0.19

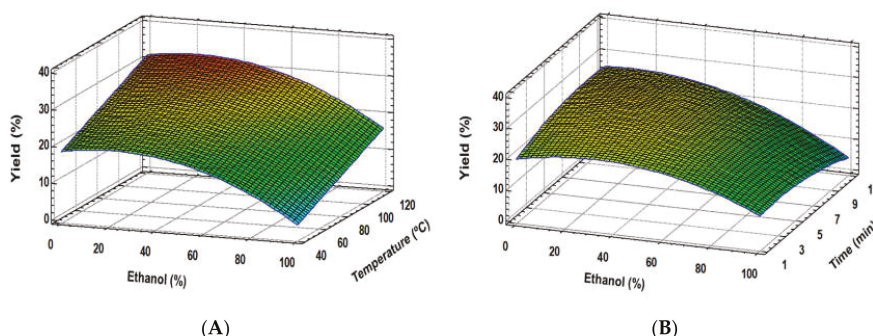


**Figure 1.** Response surface plots of the extraction yield as affected by independent factors; ethanol (%) vs. temperature (A), ethanol (%) vs. time (B).

Similar results were found regarding the total phenolic content (TPC) and antioxidant activity (ABTS, DPPH), where good fitting models for these response variables were established (Table 3). Furthermore, extraction solvent was the most important factor, showing a quadratic effect, together with a linear effect of temperature (Figures 2A, 3A and 4A). Although time and some interaction factors resulted in meaningful effects, a lower contribution to response variables was determined for these parameters (Figures 2B, 3B and 4B), where extraction time significance is generally linked to temperature [32]. The optimum ethanol concentration effect was determined to be close to 30%; meanwhile, 120 °C allowed reaching the highest response variable values. Similar results were found in other studies, where ethanol:water mixtures’ behaviour was analysed [12,13]. These authors indicated that extraction solvent was the main factor for both antioxidant activity and TPC of the extracts, showing a quadratic main effect. The optimum ethanol concentration in ethanol:water mixtures to achieve the maximum phenolic extraction, and therefore the greatest antioxidant capacity, is generally observed between 30% and 80% [4,12,13]. In accordance with the present study, the optimization of conventional solid–liquid extraction for two grape stem samples through RSM determined that ethanol and temperature were the main factors during phenolic extractions. The optimum ethanol:water

concentration was determined as 57.9% and 63.8%. Although a strong negative and quadratic effect was also observed in these studies for ethanol concentration effect, noticeably higher amounts of ethanol were found [12]. The lower optimum ethanol content in the PLE extraction solvent of the present study (30%) is probably due to the improvement extraction capacities of the solvents because of the pressure and higher temperatures applied during the extraction process. Moreover, PLE modified the extraction capacities of solvents by reducing their polarity [17] and enhancing the extraction of low polar compounds, such as phenolic compounds. Therefore, PLE reduces the required ethanol:water proportion compared to conventional solid–liquid extraction [12,13] or ultrasound extraction [4]. Besides, temperature increase is generally associated with enhancements of phenolic compound extraction [12,13]. Since PLE allows increasing the temperature over the solvent boiling point, the extraction capacity of the used solvents is generally enhanced [17]. Because of that, optimum extraction time is reduced when PLE is used in comparison with conventional extraction [12,13].

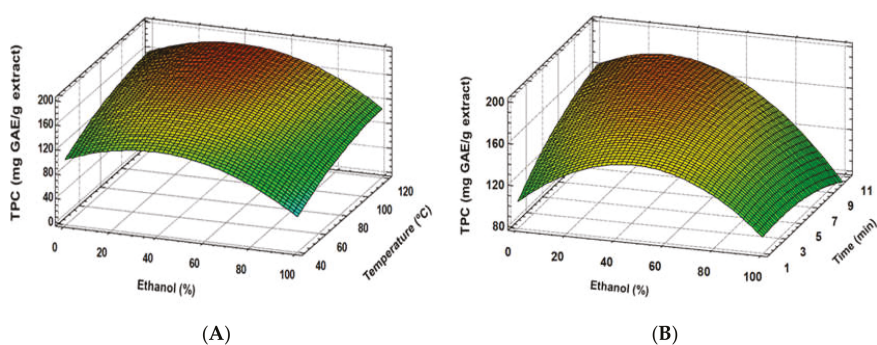


**Figure 2.** Response surface plots of the TPC as affected by independent factor; ethanol (%) *vs.* temperature (A), ethanol (%) *vs.* time (B).

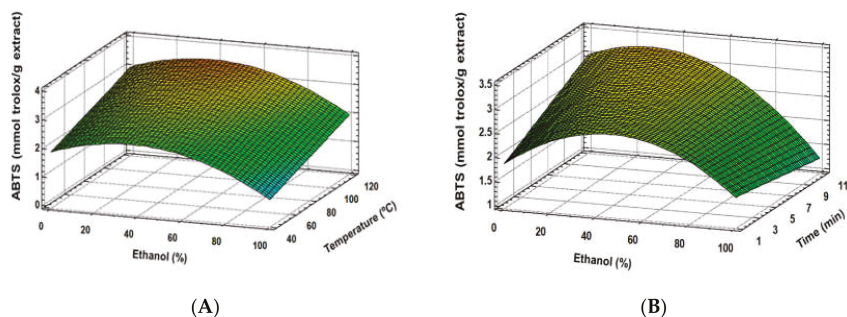


**Figure 3.** Response surface plots of the ABTS as affected by independent factors; ethanol (%) *vs.* temperature (A), ethanol (%) *vs.* time (B).

Furthermore, temperature was found to be an important but controversial factor, regarding phenolic compound extraction and antioxidant activity. In general, a high extraction temperature is correlated with an increase in the solubility of phenolic compounds from the matrix [33], as it reduces solvent viscosity and enhances solvent penetration [34]. On the other hand, high temperatures may lead to breakdown of thermolabile compounds [13]. Nevertheless, this shortcoming could be avoided by using high extraction temperatures (100–120 °C) at a short extraction time [35]. Accordingly, in the present study, a short extraction time (up to 10 min) at 120 °C avoided thermal degradation of some phenolic compounds.

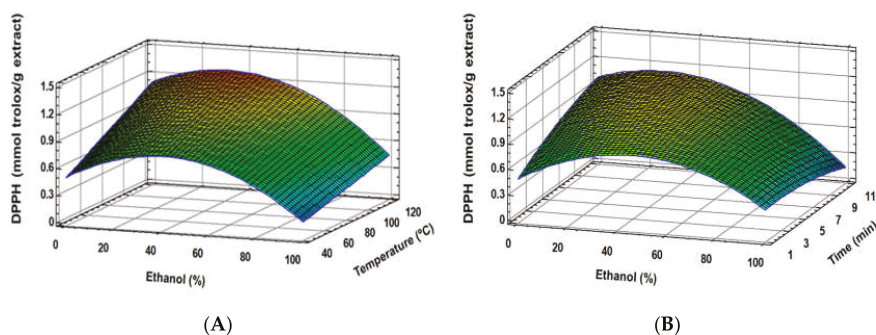


**Figure 4.** Response surface plots of the DPPH as affected by independent factors; ethanol (%) vs. temperature (A), ethanol (%) vs. time (B).

Regarding total flavan-3-ol monomers and oligomers or total polymers of procyanidin content, experimental data did not fit with the quadratic proposed model, suggesting more complex behaviour. Nevertheless, according to response surface plots, extraction solvent resulted as the main factor in the total mono-oligomer demeanour, whereas temperature and time were remarkably less meaningful. Ethanol seems to enhance flavanol-3-ol monomer and oligomer extraction (Figure 5A), while temperature or time influences are less clear (Figure 5A,B). Opposite to that, higher ethanol proportions seem to reduce the extraction of total polymer procyanidins, while temperature increased their extraction yield (Figure 6A). In this case, although extraction time turned out to show a positive tendency, an important interaction between time and the rest of studied factors distorted the effect of time into an overall negative trend (Figure 6A,B). Moreover, temperature increase resulted in a higher extraction of polymers, while ethanol had a suppressive effect, but enhanced the flavan-3-ol monomer and oligomer yield. Sun and Spranger [36] indicated that temperature allowed higher proanthocyanidin extraction rates if the temperature did not reach a degradation point. Likewise, solvent mixtures with higher polarities improve the extraction of these compounds, disrupting the bonds between phenolic compounds and the matrix. In this sense, Karvela et al. [13] found that greater flavanol monomers contents were reached at 60% of ethanol:water, whereas oligomers and polymer proanthocyanidins were achieved at 44% and 55%, respectively.

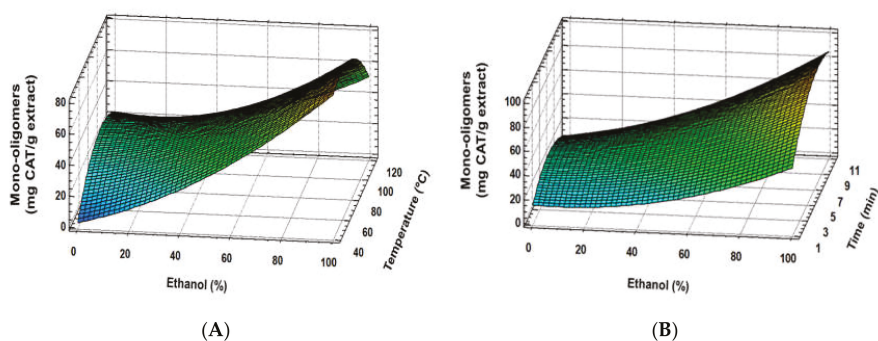


**Figure 5.** Response surface plots of flavan-3-ol monomer and oligomer content as affected by independent factors; ethanol (%) vs. temperature (A), ethanol (%) vs. time (B).

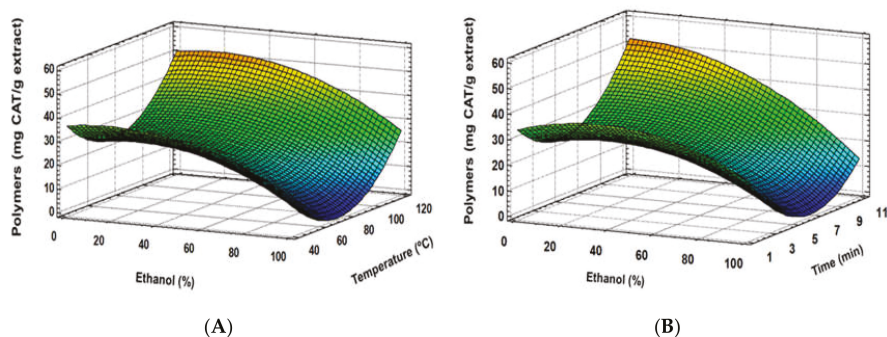


**Figure 6.** Response surface plots of polymer procyanidins content as affected by independent factors; ethanol (%) vs. temperature (A), ethanol (%) vs. time (B).

Nevertheless, it is important to highlight that, in all cases, individual optimisation of extraction conditions is required as grape variety, agro- and weather conditions or plant material are other factors that are not taken into consideration and can have significant influence on phenol recovery [12].

### 3.2. Optimal Conditions and Validation of the Developed Model

Optimal experimental conditions were achieved for extraction yield, TPC and antioxidant activity since these response variables were fitted to the proposed model. As can be seen in Table 4, only slight differences were found regarding the optimal conditions of these variables. A tight range of ethanol concentrations (22%–30%) was found as the optimum, while the highest temperature (120 °C) was optimal in every response variable. Moreover, high extraction time showed better results, except for extraction yield and TPC, where a slight decrease was shown at 11 min. Therefore, 30% ethanol, 120 °C and 10 min were selected as the most suitable extraction conditions in order to obtain an extract with the highest contents of phenolic antioxidants (optimum extract) by PLE from Merlot grape stem.

**Table 4.** Optimal extraction conditions, experimental and estimated values for response variables in the optimum extract.

	Optimal Conditions			Optimal Extract Values (30% Et, 120 °C, 10 min)	
	Et (%)	T (°C)	T (min)	Experimental	Estimated
Yields (g extract/100 g stem)	25	120	4.5	28.9	29.2
TPC (mg GAE/g extract)	30	120	10	187.3	192.4
ABTS (mmol Trolox/g extract)	27	120	11	3.69	3.81
DPPH (mmol Trolox/g extract)	22	120	11	1.32	1.37

Under such optimal conditions, the statistical model predicted an extraction yield of 29.2%, 192.4 mg GAE/g extract (TPC), and TEAC values of 3.81 and 1.31 mmol Trolox/g extract regarding the ABTS and DPPH methods, respectively. To corroborate these values, additional extractions were made at the optimal extraction conditions (Table 4). The results display that optimum extract showed values very close to the predicted ones, validating the proposed model. In addition, ORAC assay was carried out in order to perform a deeper antioxidant characterization of this optimum extract, with an ORAC value of  $1.48 \pm 0.17$  mmol Trolox/g extract. Moreover,  $26.8 \pm 0.4$  mg of mono-oligomers and  $79.17 \pm 1.36$  mg of proanthocyanidin polymers were quantified in this extract.

These optimal experimental conditions allowed obtaining an extraction yield, TPC and antioxidant activity in agreement with the wide range of values determined by González-Centeno et al. [22] for

several grape stem varieties of *Vitis vinifera*, or even slightly higher results regarding PLE Merlot extract. However, it should be noted that these authors proposed substantially different extraction conditions.

Experimental designs have been proposed previously to find optimal extraction conditions for grape stems [12,13]. In these studies, ethanol:water mixtures, time, temperature or pH were studied as experimental factor using SLE. Slightly higher TPC, along with greater TEAC values, was found in the present study. It is worth mentioning that a lower ethanol:water proportion was required at optimal extraction conditions compared to SLE [12,13]. As has been mentioned before, even if the grape variety or environmental conditions should affect this behaviour, this result could be ascribed to an electric constant decrease in the extraction solvent at high pressure [37]. Furthermore, shorter extraction time and less consumption of solvents were used for PLE than for SLE.

Moreover, similar or lower values of TPC and antioxidant activity were observed when data presented in this study were compared with other SLE or PLE extracts from grape stems [8,18,22]. However, regarding these parameters, the few data in the literature concerning grape stem extracts show a wide range of values. In this regard, differences caused by ripening stage, grape variety, geographic factors, climatological factors or oenological practices, as well as different extraction procedures applied, should be considered [38,39].

### 3.3. Correlation between Response Variables

Correlations between TPC and TEAC values (ABTS and DPPH) were established in order to confirm the influence of phenolic compounds on the antioxidant activity of the extracts. Antioxidant activity, measured by two methods in the present study (ABTS and DPPH) resulted in a strong correlation with TPC, achieving  $r = 0.993$  and  $r = 0.987$ , respectively ( $p \leq 0.001$ ). Besides, antioxidant activities obtained by both methods showed a high correlation between them ( $r = 0.993$ ;  $p \leq 0.001$ ). This confirms that phenolic compounds are the main factor responsible for the extract antioxidant activity, according to the similar optimal conditions predicted by RSM models. In addition, Pearson's test indicated a good correlation between TPC and the two fractions of phenolic compounds, flavan-3-ol monomers and oligomers ( $r = 0.557$ ;  $p \leq 0.05$ ) and polymers ( $r = 0.586$ ;  $p \leq 0.01$ ). Furthermore, statistical correlations between antioxidant activity and flavan-3-ol monomers and oligomers were found ( $r = 0.571$ ;  $p \leq 0.05$  for ABTS method, and  $r = 0.617$ ;  $p \leq 0.01$  for DPPH method). However, correlations turned out to be stronger with polymer procyanidins, being  $r = 0.621$  ( $p \leq 0.01$ ) for ABTS and  $r = 0.637$  ( $p \leq 0.05$ ) for the DPPH method. These results reveal that the antioxidant activity of the grape stem extracts could be ascribed to their general phenolic content [38], although particular contributions of phenolic groups, such as polymer proanthocyanidins, could be higher [13].

Additionally, a PCA was carried out to understand correlations between procyanidins and antioxidant activity. The principal component of the analysis explains a 90.79% of the samples. The antioxidant activity, determined using the ABTS method, was mainly explained by PC1 (76.48%) whereas PC2 contributed to a lesser extent (14.32%) (Figure 7A). Therefore, PCA analyses showed a strong correlation between the polymer content and the total antioxidant activity of the samples. Therefore, those samples characterised by higher amounts of polymers, being samples 7, 12 and the optimum extract, showed greater antioxidant activity. These samples were characterised by the use of high temperatures during PLE extraction (104 °C, 120 °C and 120 °C, respectively), being in concordance with the polynomial equations of the fitted models (Table 3). Additionally, the proximity of samples 3 and 14 in the PCA graph, as well as sample 7, evidences the influence of the extraction time. Similar results were observed when PCA analysis was conducted for DPPH values (Figure 7B), explaining 89.65% of the samples.

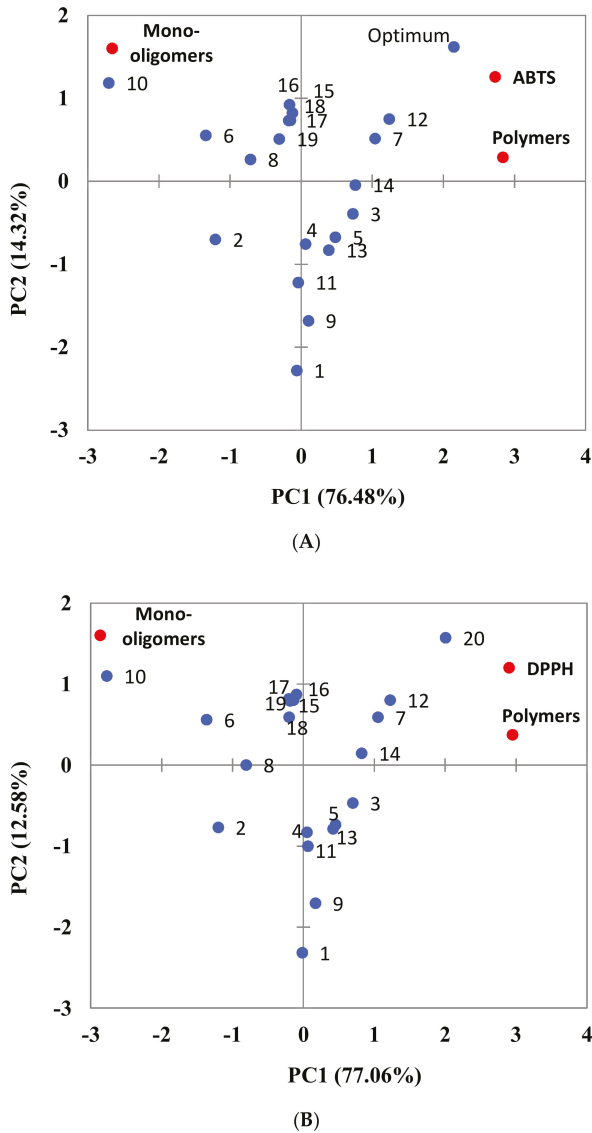


**Figure 7.** Principal components analysis (PCA) of response variables. Projections of the variables and samples (Biplot) for ABTS (A) and DPPH values (B).

### 3.4. Phenolic Composition of the Optimum Extract

Forty-two phenolic compounds were identified by HPLC-PAD-MS. Optimal PLE grape stem extract showed a complex composition of phenolic compounds, including phenolic acids, stilbenes, flavonols and, especially, flavanols (Table 5). Regarding phenolic acids, gallic and caftaric acids were the main hydroxybenzoic and hydroxycinnamic acids of the extract, followed by vanillic and syringic acid [19]. In addition, stilbenes were identified, including *trans*-resveratrol,  $\epsilon$ -viniferin, *trans*-resveratrol-glucoside (piceid), along with different dimmers and trimers of *trans*- and *cis*-resveratrol [9,10,40].

**Table 5.** HPLC-PAD-ESI-MS phenolic analysis of the optimal grape stem extracts (mg compound/g dry extract).

Phenolic Compound	UV-Vis Max.	[M – H] <sup>-1</sup>	[M + H] <sup>+1</sup>	MS/MS Fragments	mg/g dry Extract
No Flavonoids					
Hydroxybenzoic acids					
Gallic acid	270	169		125	0.541 ± 0.029
Protocatechuic acid	260/290	153		117	0.008 ± 0.000
Monogalloyl glucoside	257/298	331		169	<LOQ
4-Hydroxybenzoic acid					
Vanillic acid	256	137			0.048 ± 0.001
Syringic acid	259/292	167		153	0.224 ± 0.010
Ethyl gallate	278	197		183	0.202 ± 0.015
Ellagic acid	277	197		169	0.010 ± 0.001
Ellagic acid	256/353	301		229	0.073 ± 0.004
Hydroxycinnamic acids					
<i>trans</i> -caftaric acid	296/328	311		179	0.357 ± 0.003
<i>trans</i> -caffeic acid	300/324	179		161	0.006 ± 0.000
4-Coumaric acid	290/310	163		119	0.004 ± 0.000
3-Coumaric acid	289/309	163		119	0.003 ± 0.000
Coumaroyl- <i>O</i> -glucoside	280/308	325		163,119	0.003 ± 0.000
<i>trans</i> -ferulic acid	298/322	193		149	0.008 ± 0.000
Stilbenes					
<i>trans</i> -Piceid	295/324	389		227	0.016 ± 0.000
<i>trans</i> -Resveratrol	303/328	227		185	0.141 ± 0.003
$\epsilon$ -viniferin	262/308/322	453		359	0.879 ± 0.065
<i>cis</i> -resveratrol trimer	286	679		585	0.031 ± 0.002
<i>trans</i> -resveratrol trimer	296/320	679		587,575	0.012 ± 0.001
<i>trans</i> -resveratrol trimer	288/326	679		587,575	0.042 ± 0.003
<i>trans</i> -resveratrol tetramer	306/316	905		811	0.136 ± 0.011
<i>trans</i> -resveratrol tetramer	306/316	905		811	0.086 ± 0.007
<i>cis</i> -resveratrol tetramer	284	905		811,717	0.038 ± 0.003
<i>trans</i> -resveratrol tetramer	306/318	905		811,799	<LOQ
Flavonoids					
Flavan-3-ols					
Catechin	278	289		245	2.422 ± 0.034
Epicatechin	278	289		245	1.293 ± 0.039
Epicatechin gallate	280	441		289,169	0.245 ± 0.005
Procyanidin B1	278	577		425	1.410 ± 0.034
Procyanidin B2	278	577		425	0.015 ± 0.003
Procyanidin B3	278	577		425	0.349 ± 0.025
Procyanidin B4	279	577		425	0.036 ± 0.002
Procyanidin B7	280	577		425	0.025 ± 0.003
Procyanidin C1	280	865		577	0.016 ± 0.001
Flavonols					
Kaempferol-3- <i>O</i> -glucoside	287/358	447		285	<LOQ
Quercetin-3- <i>O</i> -galactoside	256/354	463		301	0.047 ± 0.000
Quercetin-3- <i>O</i> -rutinoside	256/354	609		301	0.029 ± 0.000
Quercetin-3- <i>O</i> -glucuronide	252/354	477		301	1.425 ± 0.001
Quercetin-3- <i>O</i> -glucoside	254/354	463		301	0.106 ± 0.004
Quercetin	256/368	301			0.005 ± 0.000
Anthocyanins					
Delphinidin-3- <i>O</i> -glucoside	292/535		465	303	<LOQ
Cyanidin-3- <i>O</i> -glucoside	290/530		449	287	0.010 ± 0.001
Malvidin-3- <i>O</i> -glucoside	293/537		493	331	0.079 ± 0.002

LOQ: limit of quantification

Numerous flavan-3-ols were also determined, including monomers, dimers and oligomers [40]. Catechin was the main monomeric compound, followed by epicatechin, whereas dimer B<sub>1</sub> turned out to be the highest dimer compound [11].

Moreover, different flavonols were quantified, mainly as quercetin derivatives. The most remarkable compound corresponded to quercetin-3-*O*-glucuronide, followed by quercetin-3-*O*-glucoside [40]. These forms of quercetin are the main flavonols of grape stems, along with others such as quercetin-3-*O*-rutinoside and quercetin-3-*O*-galactoside [8,19,40]. In addition, low quantities of different anthocyanins were detected in the extract, malvidin-3-*O*-glucoside being the most abundant of this group [8].

It is remarkable that, as far as we know, it is the first time that compounds such as ethyl gallate, ellagic acid, delphinidin-7-*O*-glucoside or cyanidin-3-*O*-glucoside have been identified in grape stem extracts, although ethyl gallate has been previously reported in grape seed extracts [25].

Just a few articles depict the composition of proanthocyanidin fraction in grape stem extracts. In the present study, 80 mg of CE/g extract was quantified as procyanidins according to the procedure of Sun et al. [27]. Procyanidin characterization revealed a mDP of 12 units. Structural composition showed catechin as a predominant terminal unit and epicatechin as a principal extension unit, where approximately 12% of the total constituent units of procyanidins were galloylated (Table 6). Focusing on general composition, epicatechin was the main monomer unit (72.3%), followed by catechin (14.6%), epicatechin gallate (12.4%) and, to a lesser extent, epigallocatechin (0.7%). All these results are consistent with the stem proanthocyanidin fraction described in literature [14,22], and particularly with Merlot's proanthocyanidins [7]. Nevertheless, slightly higher mDP was found in the present study. This result might be attributable to the effect of pressure extraction conditions used in this study, allowing a higher penetration of the solvent during extraction process.

**Table 6.** Characteristics and structural composition (percent in moles) of procyanidin fraction from optimal stem PLE extract.

Terminal Units (%)			Extension Units (%)				mDP	Galloylated Units (%)
Cat	EC	ECG	Cat	EC	ECG	EGC		
6.32	1.07	0.81	8.27	71.27	11.59	0.68	12.22	12.40

#### 4. Conclusions

Ethanol:water mixture (30%), 120 °C and 10 min turn out to be the optimal extraction conditions of the environmentally friendly PLE process carried out in this study. These conditions lead to obtaining an extract with a high phenolic content and a remarkable antioxidant activity from Merlot grape stems. This methodology allows reducing solvent volume, ethanol concentration and extraction time compared to conventional solid–liquid extraction. This study shows that this by-product is an interesting and undervalued source of procyanidins, and to a lesser extent, stilbene and flavonol derivatives. Moreover, although the contribution of polymer procyanidins to the antioxidant activity of the extract is established, the role played by other phenolics should not be ruled out. Therefore, the present study highlights the valorisation of this side stream as a source of natural phenolic antioxidants by using a green extraction technology as part of a sustainable food system.

**Author Contributions:** Conceptualization, L.J. and S.S.; Methodology, J.A.N., L.J. and M.P.; Validation, J.A.N., M.P. and L.J.; Formal analysis, J.A.N., L.J. and M.P.; Investigation, J.A.N.; writing—original draft preparation, J.A.N. and L.J.; Supervision, L.J. and S.S.; writing—review and editing, L.J., M.P. and S.S.; Project administration, G.R.; funding acquisition, G.R. All authors have read and agreed to the published version of the manuscript.

**Funding:** This research was funded by Comunidad Autónoma de Madrid (ALIBIRD, project number P2013/ABI2728).

**Acknowledgments:** The authors would like to thank Félix Cabello from IMIDRA for the kind supply of grapes.

**Conflicts of Interest:** The authors declare no conflict of interest.

## References

1. Food and Agriculture Organization of the United Nations (FAO). 2019. Available online: <http://www.fao.org/faostat/en/#home> (accessed on 11 April 2019).
2. Gouvinhas, I.; Queiroz, M.; Rodrigues, M.; Barros, A.I. Evaluation of the Phytochemistry and Biological Activity of Grape (*Vitis vinifera* L.) Stems: Toward a Sustainable Winery Industry. In *Polyphenols in Plants*; Watson, R.R., Ed.; Academic Press Inc.: San Diego, CA, USA, 2019; pp. 381–394.
3. Barros, A.I.; Gouvinhas, I.; Machado, N.; Pinto, J.; Cunha, M.; Rosa, E.; Domínguez-Perles, R. New grape stems-based liqueur: Physicochemical and phytochemical evaluation. *Food Chem.* **2016**, *190*, 896–903. [[CrossRef](#)] [[PubMed](#)]
4. Ruiz-Moreno, M.J.; Raposo, R.; Cayuela, J.M.; Zafrilla, P.; Piñeiro, Z.; Moreno-Rojas, J.M.; Mulero, J.; Puertas, B.; Girón, F.; Guerrero, R.F.; et al. Valorization of grape stems. *Ind. Crop. Prod.* **2015**, *63*, 152–157. [[CrossRef](#)]
5. Goutzourelas, N.; Stagos, D.; Spanidis, Y.; Liosi, M.; Apostolou, A.; Priftis, A.; Haroutounian, S.; Spandidos, D.A.; Tsatsakis, A.M.; Kouretas, D. Polyphenolic composition of grape stem extracts affects antioxidant activity in endothelial and muscle cells. *Mol. Med. Rep.* **2015**, *12*, 5846–5856. [[CrossRef](#)] [[PubMed](#)]
6. Silva, V.; Igrejas, G.; Falco, V.; Santos, T.P.; Torres, C.; Oliveira, A.M.P.; Pereira, J.E.; Amaral, J.S.; Poeta, P. Chemical composition, antioxidant and antimicrobial activity of phenolic compounds extracted from wine industry by-products. *Food Control.* **2018**, *92*, 516–522. [[CrossRef](#)]
7. Souquet, J.M.; Labarbe, B.; Le Guernevé, C.; Cheynier, V.Y. Phenolic composition of grape stems. *J. Agric. Food. Comp. Chem.* **2000**, *48*, 1076–1080. [[CrossRef](#)] [[PubMed](#)]
8. Barros, A.; Gironés-Vilaplana, A.; Teixeira, A.; Collado-González, J.; Moreno, D.A.; Gil-Izquierdo, A.; Rosa, E.; Domínguez-Perles, R. Evaluation of grape (*Vitis vinifera* L.) stems from Portuguese varieties as a resource of (poly)phenolic compounds: A comparative study. *Food Res. Int.* **2014**, *65*, 375–384. [[CrossRef](#)]
9. Pugajeva, I.; Perkons, I.; Górnas, P. Identification and determination of stilbenes by Q-TOF in grape skins, seeds, juice and stems. *J. Food Compos. Anal.* **2018**, *74*, 44–52. [[CrossRef](#)]
10. Püssa, T.; Floren, J.; Kuldeke, P.; Raal, A. Survey of grape wine stem polyphenols by liquid chromatography–diode array detection tandem mass spectrometry. *J. Agric. Food Chem.* **2006**, *54*, 7488–7994. [[CrossRef](#)]
11. Luo, L.; Cui, Y.; Zhang, S.; Li, L.; Suo, H.; Sun, B. Detailed phenolic composition of Vidal grape pomace by ultrahigh-performance liquid chromatography–tandem mass spectrometry. *J. Chromatogr. B* **2017**, *1068*, 201–209. [[CrossRef](#)]
12. Domínguez-Perles, R.; Teixeira, A.; Rosa, E.; Barros, A. Assessment of (poly)phenols in grape (*Vitis vinifera* L.) stems by using food/pharma industry compatible solvents and response surface methodology. *Food Chem.* **2014**, *164*, 339–346.
13. Karvela, E.; Makris, D.P.; Kalogeropoulou, N.; Karathanosa, V.T. Deployment of response surface methodology to optimize recovery of grape (*Vitis vinifera*) stem and seed polyphenols. *Procedia Food Sci.* **2011**, *1*, 1686–1693. [[CrossRef](#)]
14. Llaudy, M.C.; Canals, R.; Canals, J.M.; Zamora, F. Influence of ripening stage and maceration length on the contribution of grape skins, seeds and stems to phenolic composition and astringency in wine-simulated macerations. *Eur. Food Res. Technol.* **2008**, *226*, 337–344. [[CrossRef](#)]
15. Choi, M.P.K.; Chan, K.K.C.; Leung, H.W.; Huie, C.W. Pressurized liquid extraction of active ingredients (ginsenosides) from medicinal plants using non-ionic surfactant solutions. *J. Chromatogr. A* **2003**, *983*, 153–162. [[CrossRef](#)]
16. Arapitsas, P.; Turner, C. Pressurized solvent extraction and monolithic column HPLC/DAD analysis of anthocyanins in red cabbage. *Talanta* **2008**, *74*, 1218–1223. [[CrossRef](#)]
17. Wijngaard, H.; Hossain, M.B.; Rai, D.K.; Brunton, N. Techniques to extract bioactive compounds from food by-products of plant origin. *Food Res. Int.* **2012**, *46*, 505–513. [[CrossRef](#)]

18. Llobera, A. Study on the Antioxidant Activity of Grape Stems (*Vitis vinifera*). A Preliminary Assessment of Crude Extracts. *Food Nutr. Sci.* **2012**, *3*, 500–504.
19. Anastasiadi, M.; Pratsinis, H.; Kletsas, D.; Skaltsounis, A.; Haroutounian, S.A. Grape stem extracts: Polyphenolic content and assessment of their in vitro antioxidant properties. *Lwt Food Sci. Technol.* **2012**, *48*, 316–322. [[CrossRef](#)]
20. Casas, L.; Mantell, C.; Rodríguez, M.; Martínez de la Ossa, E.J.; Roldán, A.; De Ory, I.; Caro, I.; Blandino, A. Extraction of resveratrol from the pomace of Palomino fino grapes by supercritical carbon dioxide. *J. Food Eng.* **2010**, *96*, 304–308. [[CrossRef](#)]
21. Piñeiro, Z.; Marrufo-Curtido, A.; Vela, C.; Palma, M. Microwave-assisted extraction of stilbenes from woody vine material. *Food Bioprod. Process.* **2017**, *103*, 18–26. [[CrossRef](#)]
22. González-Centeno, M.R.; Jourdes, M.; Femenia, A.; Simal, S.; Rosselló, C.; Teissedre, P.L. Proanthocyanidin composition and antioxidant potential of the stem winemaking byproducts from 10 different grape varieties (*Vitis vinifera* L.). *J. Agric. Food Chem.* **2012**, *60*, 11850–11858.
23. Wenzel, J.; Storer-Samaniego, C.; Wang, L.; Nelson, L.; Ketchum, K.; Ammerman, M.; Zand, A. Superheated liquid and supercritical denatured ethanol extraction of antioxidants from Crimson red grape stems. *Food Sci. Nutr.* **2015**, *3*, 569–576. [[CrossRef](#)] [[PubMed](#)]
24. Grases, F.; Prieto, R.M.; Fernández-Cabot, R.A.; Costa-Bauzá, A.; Sánchez, A.M.; Prodanov, M. Effect of consuming a grape seed supplement with abundant phenolic compounds on the oxidative status of healthy human volunteers. *Nutr. J.* **2015**, *14*, 94–101. [[CrossRef](#)] [[PubMed](#)]
25. Prodanov, M.; Vacas, V.; Hernández, T.; Estrella, I.; Amador, B.; Winterhalter, P. Chemical characterisation of Malvar grape seeds (*Vitis vinifera* L.) by ultrafiltration and RP-HPLC-PAD-MS. *J. Food Comp. Anal.* **2013**, *31*, 284–292. [[CrossRef](#)]
26. Muñoz-Labrador, A.; Prodanov, M.; Villamiel, M. Effects of high intensity ultrasound on disaggregation of a macromolecular procyanidin-rich fraction from *Vitis vinifera* L. seed extract and evaluation of its antioxidant activity. *Ultrason. Sonochem.* **2019**, *50*, 74–81. [[CrossRef](#)]
27. Sun, B.S.; Leandro, M.C.; Ricardo-da-Silva, J.M.; Spranger, M.I. Separation of grape and wine proanthocyanidins according to their degree of polymerisation. *J. Agric. Food Chem.* **1998**, *46*, 1390–1396. [[CrossRef](#)]
28. Singleton, V.L.; Orthofer, R.; Lamuela-Raventós, R.M. Analysis of total phenols and other oxidation substrates and antioxidants by means of Folin-Ciocalteu Reagent. *Methods Enzym.* **1999**, *299*, 152–178.
29. Re, R.; Pellegrini, N.; Proteggente, A.; Pannala, A.; Yang, M.; Rice-Evans, C. Antioxidant activity applying an improved ABTS radical cation decolorization assay. *Free Radic. Biol. Med.* **1999**, *26*, 1231–1237. [[CrossRef](#)]
30. Brand-Williams, W.; Cuveleir, M.E.; Berset, C. Use of a free radical method to evaluate antioxidant activity. *Lwt-Food Sci. Technol.* **1995**, *28*, 25–30. [[CrossRef](#)]
31. Huang, D.J.; Ou, D.X.; Hampsch-Woodill, M.; Flanagan, J.A.; Prior, R.L. High-throughput assay of oxygen radical absorbance capacity (ORAC) using a multichannel liquid handling system coupled with a microplate fluorescence reader in 96-well format. *J. Agric. Food Chem.* **2002**, *50*, 4437–4444. [[CrossRef](#)]
32. Li, Y.; Skouroumounis, J.K.; Elsey, G.M.; Taylor, D.K. Microwave-assistance provides very rapid and efficient extraction of grape seed polyphenols. *Food Chem.* **2011**, *129*, 570–576. [[CrossRef](#)]
33. Silva, E.M.; Rogez, H.; Larondelle, Y. Optimization of extraction of phenolic from *Inga edulis* leaves using response surface methodology. *Sep. Purif. Technol.* **2007**, *55*, 381–387. [[CrossRef](#)]
34. Mandal, V.; Mohan, Y.; Hemalatha, S. Microwave assisted extraction-an innovative and promising extraction tool for medicinal plant research. *Pharm. Rev.* **2007**, *1*, 7–18.
35. Aliakbarian, B.; Fathi, A.; Perego, P.; Dehghani, F. Extraction of antioxidants from winery wastes using subcritical water. *J. Supercrit. Fluids* **2012**, *65*, 18–24. [[CrossRef](#)]
36. Sun, B.; Spranger, M.I. Changes in phenolic composition of Tinta Miúda red wines after 2 years of ageing in bottle: effect of winemaking technologies. *Eur. Food Res. Technol.* **2005**, *221*, 305–312. [[CrossRef](#)]
37. Hawthorne, S.B.; Yang, Y.; Miller, D.J. Extraction of organic pollutants from environmental solids with subcritical and supercritical water. *Anal. Chem.* **1994**, *66*, 2912–2920. [[CrossRef](#)]
38. Makris, D.P.; Boskou, G.; Andrikopoulos, K. Recovery of antioxidant phenolics from white vinification solid by-products employing water/ethanol mixtures. *Bioresour. Technol.* **2007**, *98*, 2963–2967. [[CrossRef](#)]

39. Mulero, J.; Martínez, G.; Oliva, J.; Cermeño, S.; Cayuela, J.M.; Zafrilla, P.; Martínez-Cachá, A.; Barba, A. Phenolic compounds and antioxidant activity of red wine made from grapes treated with different fungicides. *Food Chem.* **2015**, *180*, 25–31. [[CrossRef](#)]
40. Marchante, L.; Loarce, L.; Izquierdo-Cañas, M.P.; Alañón, M.E.; García-Romero, E.; Pérez-Coello, M.S.; Díaz-Maroto, M.C. Natural extracts from grape seed and stem by-products in combination with colloidal silver as alternative preservatives to SO<sub>2</sub> for white wines: Effects on chemical composition and sensorial properties. *Food Res. Int.* **2019**, 108594. [[CrossRef](#)]



© 2020 by the authors. Licensee MDPI, Basel, Switzerland. This article is an open access article distributed under the terms and conditions of the Creative Commons Attribution (CC BY) license (<http://creativecommons.org/licenses/by/4.0/>).



Article

# Improving the Functional Activities of Curcumin Using Milk Proteins as Nanocarriers

Soad Taha <sup>1,\*</sup>, Ibrahim El-Sherbiny <sup>2</sup>, Toshiki Enomoto <sup>3</sup>, Aida Salem <sup>4</sup>, Emiko Nagai <sup>3</sup>, Ahmed Askar <sup>5</sup>, Ghada Abady <sup>4</sup> and Mahmoud Abdel-Hamid <sup>1</sup>

<sup>1</sup> Dairy Science Department, Faculty of Agriculture, Cairo University, Giza 12613, Egypt; mahmoud.mohamed@agr.cu.edu.eg

<sup>2</sup> Nanomaterials Lab, Center of Material Science (CMS), Zewail City of Science and Technology, 6th of October, Giza 12588, Egypt; ielsherbiny@zewailcity.edu.eg

<sup>3</sup> Department of Food Science, Ishikawa Prefectural University, Nonoichi, Ishikawa 921-8836, Japan; enomoto@ishikawa-pu.ac.jp (T.E.); nagai.e1025@gmail.com (E.N.)

<sup>4</sup> Dairy Technology Department, Animal Production Research Institute, Agricultural Research Center, Giza 12618, Egypt; aidas\_salem@hotmail.com (A.S.); ghabady@hotmail.com (G.A.)

<sup>5</sup> Botany and Microbiology Department, Faculty of Science (Boys), Al-Azhar University, Nasr City, Cairo 11884, Egypt; drahmed\_askar@azhar.edu.eg

\* Correspondence: soad.taha@agr.cu.edu.eg

Received: 6 July 2020; Accepted: 23 July 2020; Published: 24 July 2020

**Abstract:** Curcumin is one of the most common spices worldwide. It has potential benefits, but its poor solubility and bioavailability have restricted its application. To overcome these problems, this study aimed to assess the efficacy of sodium caseinate (SC),  $\alpha$ -lactalbumin ( $\alpha$ -La),  $\beta$ -lactoglobulin ( $\beta$ -lg), whey protein concentrate (WPC) and whey protein isolate (WPI) as nanocarriers of curcumin. Furthermore, the antioxidant, anticancer and antimicrobial activities of the formed nanoparticles were examined. The physicochemical characteristics of the formed nanoparticles as well as the entrapment efficiency (%) and the in vitro behavior regarding the release of curcumin (%) were examined. The results showed that the formation of curcumin–milk protein nanoparticles enhanced both the entrapment efficiency and the in vitro behavior release of curcumin (%). Cur/ $\beta$ -lg nanoparticles had the highest antioxidant activity, while SC and WPC nanoparticles had the highest anticancer effect. The antimicrobial activity of the formed nanoparticles was much higher compared to curcumin and the native milk proteins.

**Keywords:** curcumin; milk proteins; nanoparticles; antioxidant; anticancer; antimicrobial activities

## 1. Introduction

Curcumin is a bright yellow powder produced from *Curcuma longa* plants. It is the principal curcuminoid of turmeric (*Curcuma longa*), which is used as an herbal supplement, cosmetics ingredient, food flavoring and food coloring [1]. Curcumin has been reported to display several biological activities, such as antioxidant, antibacterial, anti-inflammatory, anti-amyloid and anticancer activities in addition to wound healing and antibiofilm properties [1,2]. However, the practical application of curcumin in functional food formulations is limited due its poor water solubility and bioavailability and rapid degradation under neutral and alkaline pH conditions [3]. Many attempts have been made to enhance the solubility and bioavailability of curcumin, including the use of emulsions, liposomes and nanoparticles [3]. The application of nanotechnology is an important tool to improve the solubility and bioavailability of curcumin [4]. A variety of nanoparticle formulations has been developed to improve the functional characteristics of curcumin [5,6]. In this context, various nanocarriers, generally made of biodegradable substances, such as proteins (including milk proteins), liposomes, carbohydrates and polysaccharides (i.e., chitosan), have been used [7–9].

Milk proteins have a specific structural and functional diversity which allows their utilization as agents of encapsulation and for the transport of bioactive molecules. Milk proteins can be used as carriers of hydrophobic molecules or ions, and they are excellent interfacial agents, meaning that they are used in the formation and stabilization of emulsions containing hydrophobic molecules. Furthermore, milk proteins are able to form covalent or electrostatic complexes with molecules of interest and to entrap bioactives through the formation of gels. Furthermore, milk proteins are able to self-assemble or co-assemble to form supra-structures that allow the encapsulation and the transport of a diversity of small molecules [10]. In this context, using  $\beta$ -lg as carrier for curcumin significantly enhanced the water solubility, resistance to pepsin, and pH stability of curcumin [11]. In addition, a complex of whey protein isolate with curcumin increased the solubility of curcumin 180-fold [12]. Furthermore, a whey protein isolate microgel loaded with curcumin had higher antioxidant activity compared to curcumin dissolved in water [13]. The encapsulation of curcumin in camel beta-casein increased the solubility of curcumin 2500-fold. Moreover, the antioxidant activity and cytotoxicity to the human leukemia cell line of curcumin were higher than both camel beta-casein and curcumin [14]. Bovine serum albumin (BSA)-dextran-curcumin nanoparticles exhibited a cellular antioxidant activity in Caco-2 cells that was higher than free curcumin [15].

Consequently, the aim in this study was to evaluate the efficacy of different milk proteins as nanocarriers of curcumin. Furthermore, the antioxidant, anticancer and antimicrobial activities of the developed milk protein-curcumin nanoparticles were assessed.

## 2. Materials and Methods

### 2.1. Materials

Sodium caseinate (SC) was kindly provided by Friesland Campina DMV, Nederland. Whey protein concentrate (WPC 80%) was kindly provided by Onalaska Wisconsin, USA. Whey protein isolate (WPI),  $\alpha$ -lactalbumin ( $\alpha$ -La 97.46% protein) and  $\beta$ -lactoglobulin ( $\beta$ -lg 97.8% protein) were kindly provided by Davisco Foods International, USA. Low molecular weight chitosan (Cs) and sodium tripolyphosphate (TPP) were purchased from Acros Organics, New Jersey, USA. Curcumin (Cur  $\geq$  96.1% purity) was purchased from Kolorjet Chemicals Pvt Ltd., Mumbai, Maharashtra, India. 1,1-diphenyl-2-picrylhydrazyl (DPPH), tetracycline, amphotericin B, nutrient agar medium and Czapek's Dox agar medium (for antifungal activity) were purchased from Sigma Chemical Company St. Louis, MO, USA. Human hepatocellular carcinoma (HepG2), human breast adenocarcinoma (MCF-7), Gram-positive (*Bacillus subtilis* ATCC 6633, *Staphylococcus aureus* ATCC 29213) and Gram-negative bacteria (*Pseudomonas aeruginosa* ATCC 27853, *Escherichia coli* ATCC 25922) and *Candida albicans* (ATCC10231) were obtained from the American Type Culture Collection (ATCC) Manassas, Virginia, USA. Roswell Park Memorial Institute (RPMI) 1640 medium was purchased from Genetix Biotech, Asia Pvt. Ltd., India. 3-(4,5-Dimethyl-2-thiazolyl)-2,5-diphenyl-2H-tetrazolium-bromide (MTT) was purchased from SERVA Electrophoresis GmbH, Heidelberg, Germany. Phosphate buffered saline (PBS) tablets were purchased from Fountain Pkwy, Solon, USA. All other chemicals used were of analytical grade.

### 2.2. Experimental Procedures and Methods of Analysis

#### 2.2.1. Preparation and Characterization of Milk Protein-Chitosan Nanocomposite

Nanocomposites of milk protein-chitosan were prepared by the ionotropic gelation method [16]. Briefly, 1 mL of protein solution (10%) was added to 50 mL chitosan solution (0.2% prepared in 1% acetic acid) under mild stirring. Then, 15 mL sodium tripolyphosphate solution (TPP 0.5%) was added drop-wise to the mixture. The overall mixture was stirred for 30 min at 25 °C. The resulting particles were collected by centrifugation (Avanti j-301 Beckman, CA, USA) at 25,000 rpm for 30 min at 4 °C, washed twice with distilled water and then freeze-dried (Labconco freeze dryer, USA).

## 2.2.2. Preparation of Curcumin-Loaded Milk Proteins

Curcumin solution was prepared separately by dissolving curcumin (100 mg) in ethanol until the solution became clear; then, the solution was added to the milk protein–chitosan nanosuspension (without freeze drying) and stirred for 30 min at 25 °C, followed by centrifugation at 25,000 rpm for 30 min at 4 °C. The resulting curcumin-loaded nanoparticles (NPs) were washed twice with distilled water and then freeze-dried.

## 2.3. Characterizations of Nanoparticles

### 2.3.1. Particle Size and Zeta Potential Measurements

The size distribution and zeta potential of the resultant nanoparticles were determined using a zetasizer (Nano-ZS, Malvern, UK) [17]. The measurements were performed at 25 °C after the appropriate dilution of samples with water (1:400). The zeta potential was measured using a disposable zeta cuvette.

### 2.3.2. Physicochemical Characterization

The Fourier-transform infrared spectroscopy (FTIR) spectra of native and curcumin-loaded milk proteins nanoparticles were examined by an FTIR spectrometer (NICOLET iS10, Thermo Scientific Inc., USA) in the attenuated total reflection (ATR) mode [18]. The spectra were recorded in the wavenumber range of 600–4000  $\text{cm}^{-1}$ .

The morphology of curcumin-loaded milk protein nanoparticles was imaged using transmission electron microscopy (TEM) (JEOL, JEM1400, Japan) according to Swed et al. [19]. Drops of aqueous suspension of nanoparticles suspended in distilled water were deposited in carbon-coated copper grids and then dried at room temperature before examination.

## 2.4. Determination of the Entrapment Efficiency (EE %) and In Vitro Release %

The entrapment efficiency (EE %) was determined according to Sadeghi et al. [20]. The amount of curcumin encapsulated into the developed nanoformulations was obtained by determining the difference between the total amount of curcumin added initially into the preparation medium and the amount which remained in the supernatant after centrifugation. The free curcumin present in the supernatant was determined spectrophotometrically at 426 nm using a UV–Vis spectrophotometer (Evolution UV 600, Thermo Scientific, USA). The EE% was calculated using the following equation:

$$\text{EE}(\%) = \frac{\text{Initial amount of curcumin} - \text{free curcumin in supernatant}}{\text{Initial amount of curcumin}} \times 100$$

The method of Teng et al. [21] was adapted to determine the in vitro release percentage of curcumin from the nanoparticles. Curcumin-loaded milk protein nanoparticles (5 mg) were mixed with 2 mL of PBS at pH 7.4. The blend was placed into a dialysis bag (MW cutoff 10 kDa) which was then put in 45 mL falcon tubes containing 20 mL of PBS with 0.5% Tween 20. The falcon tubes were incubated in a shaking bath (Thermo Scientific, MaxQ4450, USA) at 37 °C under constant shaking at 110 rpm. Afterwards, a 1 mL aliquot of the PBS medium was withdrawn at specific intervals of 0.25, 0.50, 1, 2, 4, 6, 24 and 48 h and replaced by a fresh medium. The absorbance was measured at 426 nm, which was converted to the mass of released curcumin using a linear standard curve ( $R^2 = 0.9976$ ). The concentration of curcumin at different time intervals was monitored, and then calculated using the following equation:

$$C_n = C_{n \text{ means}} + A/V \cdot \sum_{S=1}^{n-1} C_{S \text{ means}}$$

where  $C_n$  is the expected theoretical sample concentration,  $C_{n \text{ means}}$  is the measured concentration,  $A$  is the volume of withdrawn aliquot (20 mL),  $V$  is the volume of the dissolution medium (2 mL),  $n-1(20-1)$

is the total volume of all the previously withdrawn samples before the currently measured sample and  $C_s$  is the total concentration of all previously measured samples before the currently measured sample. The in vitro release % of curcumin from the resultant nanocarriers was measured in triplicate, and the cumulative release percentage was plotted against time.

### 2.5. Antioxidant Activity

The antioxidant activity (radical scavenging activity %) was measured using DPPH (1,1-diphenyl-2-picrylhydrazyl) [22]. In brief, 1.5 mL of the tested materials at concentrations of 1.25, 2.5 and 5 mg/mL was mixed with 1.5 mL of 0.1 mM DPPH in ethanol. The mixtures were vortexed and incubated in the dark for 30 min at room temperature, and then the absorbance was measured at 517 nm.

$$\text{Radical scavenging activity(\%)} = (A_0 - A_1 / A_0) \times 100$$

where  $A_0$  is the absorbance of the control without samples (DPPH solution) and  $A_1$  is the absorbance of the tested materials.

### 2.6. Anticancer Activity

The cytotoxicity of the tested materials on HepG2 and MCF-7 cell lines was determined by MTT assay [23]. The cells were plated ( $1 \times 10^5$  cells/mL) in 96 well plates and incubated at 37 °C for 24 h to develop a complete monolayer sheet. The plates were washed with phosphate buffered saline (pH 7.4) and then incubated at 37 °C for 24 h in the presence of 0.1 mL of the tested material solutions (2.5, 5 and 10 mg/mL) in Roswell Park Memorial Institute (RPMI) medium (maintenance medium). Then, 20  $\mu$ L/well of MTT in buffered saline solution (5 mg/mL) was added, and the plates were incubated at 37 °C in a CO<sub>2</sub> incubator for 1–5 h to allow the MTT to be metabolized, forming formazan. The optical density at 560 nm and 620 nm (subtract background) was measured. The effect of the tested materials on the proliferation of human cancer cells is expressed as the cell viability % using the following formula:

$$\text{Cell viability(\%)} = \text{absorbance of treated cells} / \text{absorbance of control cells} \times 100$$

### 2.7. Antimicrobial Activity

The antimicrobial activity of all tested materials were examined against Gram-positive (*Bacillus subtilis* and *Staphylococcus aureus*) and Gram-negative bacteria (*Pseudomonas aeruginosa* and *Escherichia coli*) as well as *Candida albicans* using the agar well diffusion method [24]. All strains (individually) were grown in 10 mL of nutrient broth and adjusted to a count of  $10^8$  cells/mL for bacteria or  $10^5$  cells/mL for fungi using a spectrophotometer. Tested strains (100  $\mu$ L) were added to the growth medium and allowed to solidify. One milliliter of each tested material (500  $\mu$ g/mL) was added to each well. The plates were incubated at 37 °C for 24 h for bacteria and at 27 °C for 72 h for fungi. After incubation, the growth of microorganisms was observed. The antimicrobial activity was evaluated by measuring the diameter of the zone of transparent inhibition against tested microorganisms. Tetracycline was used as a standard antibacterial drug, while amphotericin B was used as a standard antifungal drug.

### 2.8. Statistical Analysis

A randomized complete block design with two factors (factor A: concentration. and factor B: treatments) was employed. For the other parameters, we used a randomized complete block design with one factor, with three replications for each parameter. The treatment means were compared by the least significant difference (L.S.D.) [25].

### 3. Results and Discussion

#### 3.1. Characterizations of Nanoparticles

##### 3.1.1. Particle Size

The data in Table 1 show that the average particle size of the milk protein–chitosan nanocomposite ranged from 275.33 to 334.90 nm with non-significant differences between all treatments except for Cs/WPI NPs. After loading curcumin, the average particle sizes decreased in the case of casein,  $\alpha$ -La and  $\beta$ -Lg nanoparticles with non-significant differences and reached 278.10, 290.83 and 274.80 nm, respectively, while the sizes significantly increased in the case of WPI and WPC nanoparticles, reaching 462.80 and 439.90 nm, respectively, which may be due to the formation of large aggregates via nonspecific interactions [26]. All nanoparticles—either without or with curcumin—are the under nano-scale, which agreed with the data reported by Singh et al. [27] and Arroyo-Maya et al. [28].

**Table 1.** Particle size, zeta potential and entrapment efficiency (EE %) of curcumin-loaded milk protein nanoparticles.

Treatments	Particle Size (nm)	Zeta Potential	EE%	pH
Cs/SCNPs	328.67 <sup>b</sup> ± 47.55	−12.73 <sup>cd</sup> ± 0.87	-	5.00
Cs/ $\alpha$ -LaNPs	334.90 <sup>b</sup> ± 5.84	−12.70 <sup>cd</sup> ± 0.44	-	5.21
Cs/ $\beta$ -lgNPs	310.53 <sup>bc</sup> ± 13.17	−11.13 <sup>c</sup> ± 0.64	-	5.00
Cs/WPI NPs	275.33 <sup>c</sup> ± 30.89	17.30 <sup>b</sup> ± 1.90	-	4.30
Cs/WPC NPs	318.17 <sup>bc</sup> ± 33.98	−14.03 <sup>d</sup> ± 1.21	-	5.30
Cur-Cs/SCNPs	278.10 <sup>c</sup> ± 16.89	−12.63 <sup>cd</sup> ± 2.11	72.27 <sup>e</sup> ± 0.13	5.20
Cur-Cs/ $\alpha$ -La NPs	290.83 <sup>bc</sup> ± 47.17	−19.50 <sup>e</sup> ± 0.17	74.67 <sup>c</sup> ± 0.06	5.31
Cur-Cs/ $\beta$ -lg NPs	274.80 <sup>c</sup> ± 8.84	−14.83 <sup>d</sup> ± 2.58	73.97 <sup>d</sup> ± 0.12	5.30
Cur-Cs/WPI NPs	462.80 <sup>a</sup> ± 6.15	−13.57 <sup>d</sup> ± 3.23	76.30 <sup>b</sup> ± 0.10	5.42
Cur-Cs/WPC NPs	439.90 <sup>a</sup> ± 2.95	27.73 <sup>a</sup> ± 0.81	77.27 <sup>a</sup> ± 0.06	4.20

Different superscripts (a–e) in the same column are significantly different ( $p < 0.05$ ). SCNPs: sodium caseinate nanoparticles; WPI: whey protein isolate; WPC: whey protein concentrate; NPs: nanoparticles.

##### 3.1.2. Zeta Potential

Zeta potential values ranged from −11.13 to −14.03 mV (pH 5.3) for milk protein–chitosan nanocomposites, with the exception of Cs-WPI nanocomposite, where the value was −17.30 mV (pH 4.3), with significant differences with other treatments. In case of curcumin-loaded milk protein nanoparticles, the zeta potential ranged from −12.63 to −19.5 (pH 5.2–5.42), while it changed to be highly positive for Cur-Cs/WPC, at +27.73 mV (pH 4.2). Significant differences were noticed between all curcumin NPs (Table 1). These findings are in agreement with Awad et al. [29] and Sangeetha et al. [17].

##### 3.1.3. Fourier-Transform Infrared Spectroscopy (FTIR)

FTIR spectra of native and curcumin-loaded nanoparticles explain any structural differences between pure compounds and the different developed nanoparticle systems. As shown in Figure 1, the spectrum of native sodium caseinate (SC) had four characteristic peaks at 3273, 2960, 1635 and 1515  $\text{cm}^{-1}$  attributed to  $\text{NH}_2/\text{OH}$ , C-H stretching, C=O stretching and  $\text{NH}_2$  bending, respectively, while for  $\alpha$ -La, the four characteristic peaks of the FTIR spectra appeared at 3273, 2960, 1650 and 1500  $\text{cm}^{-1}$ , attributed to  $\text{NH}_2/\text{OH}$ , CH stretching, C=O and  $\text{NH}_2$  bending, respectively. Furthermore, the FTIR spectra of native  $\beta$ -Lg showed four characteristic absorbance peaks at 3271, 2957, 1633 and 1515  $\text{cm}^{-1}$ , attributed to  $\text{NH}_2/\text{OH}$ , CH stretching,  $\text{NH}/\text{C}=\text{O}$  and  $\text{NH}_2$  bending of the amide group respectively. With respect to WPC and WPI, similar results were found in terms of their FTIR spectra, which exhibited three characteristic absorbance peaks at 2957, 1633 and 1532  $\text{cm}^{-1}$ , which correspond to CH stretching,  $\text{NH}/\text{C}=\text{O}$  and  $\text{N}=\text{O}$ , respectively. It is also clear that the spectrum of chitosan showed three characteristic absorbance peaks. One peak at 3354  $\text{cm}^{-1}$  corresponds to the combined peaks of

NH and OH groups in chitosan, while the peaks at 1592 and 1377  $\text{cm}^{-1}$  correspond to the N-H bending of the amide group (N-acetylated residues) and symmetrical  $\text{CH}_3$ , respectively. The FTIR spectrum of curcumin exhibited three strong peaks at 3272, 1505 and 1625  $\text{cm}^{-1}$ , attributed to  $\text{CH}/\text{NH}_2$ , OH and  $\text{N}=\text{O}$ , respectively (Figure 1). The characteristic absorbance peak at 3507  $\text{cm}^{-1}$ , which corresponds to the CH stretching vibration of curcumin, disappeared after encapsulation. Furthermore, there was a shift in the band peak from 1625 and 1505 to 1633 and 1520  $\text{cm}^{-1}$  after nanoparticles were loaded with curcumin (Cur-NPs). These peaks shifted slightly toward a higher wavenumber, and new absorption bands appeared ( $\text{C}=\text{O}$  and  $\text{N}=\text{O}$ ). This may be due to the structural changes of curcumin during the encapsulation process. In general, it was clear from these results that NPs were formed due to the interaction between the carboxyl group ( $-\text{COO}^-$ ) of the protein and amino groups of chitosan. In addition, there was an interaction between milk protein–chitosan nanocomposites and curcumin; the same spectra were found for curcumin milk protein–chitosan nanoparticles with slight shifting (Figure 1), and this may be a result of the electrostatic interactions during the formation of curcumin-loaded milk protein nanoparticles (Cur-NPs). These results are in line with those of Udompormmongkol and Chiang [30].

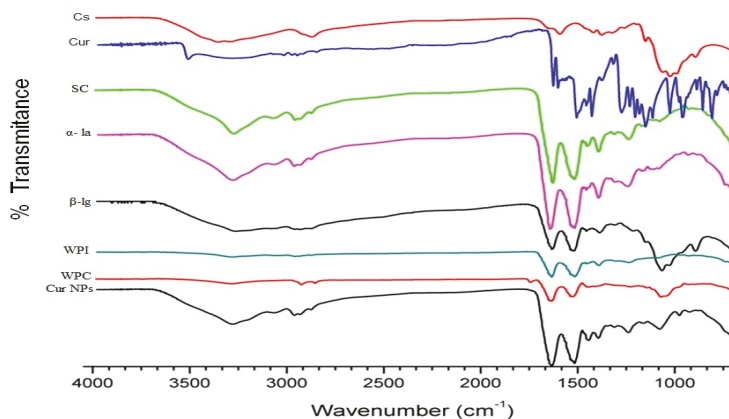


**Figure 1.** Fourier-transform infrared (FTIR) spectra of chitosan (Cs), curcumin (Cur), Sod. caseinate (SC),  $\alpha$ -lactalbumin ( $\alpha$ -La),  $\beta$ -lactoglobulin ( $\beta$ -Ig), whey protein isolate (WPI), whey protein concentrate (WPC) and curcumin loaded nanoparticles (Cur NPs).

#### 3.1.4. Transmission Electron Microscopy (TEM)

Figure 2 shows the morphological characteristics of the prepared nanoparticles from the various treatments. The prepared nanoparticles were regular and spherical in shape, with sizes under the nano-scale. The average size matched that observed in the dynamic light scattering DLS values. The loading of curcumin resulted in an increase in the particle size, particularly with WPI and WPC, which matched the DLS values.

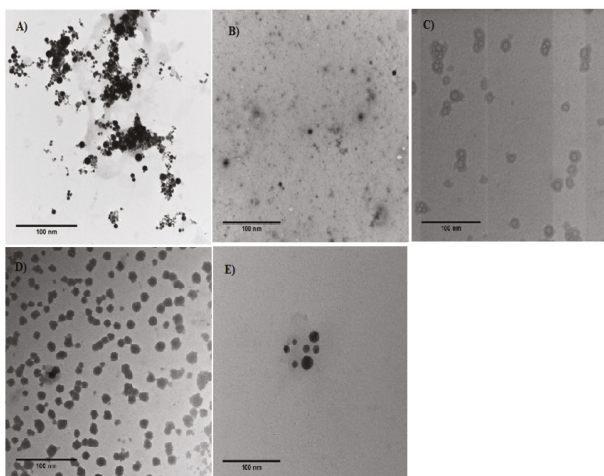


**Figure 2.** Transmission electron microscope (TEM) images of curcumin-loaded milk protein nanoparticles. (A) Cur-SC NPs, (B) Cur- $\alpha$ -La NPs, (C) Cur- $\beta$ -Ig NPs, (D) Cur-WPI NPs, (E) Cur-WPC NPs.

### 3.2. Entrapment (Encapsulation) Efficiency (EE %)

The EE% ranged from 72.27–77.27% with significant differences between all treatments (Table 1). Both Cur-Cs/WPI NPs and Cur-Cs/WPC NPs had the highest EE% values, at 76.30% and 77.27%, respectively, while the lowest EE% was achieved for SC, at 72.27%, which may be due to the presence of more binding sites on WPC and WPI than other types of proteins. These results are in line with those reported by Chen and Subirade [31], Pan et al. [32] and El-Sayed et al. [33].

### 3.3. The In Vitro Behavior Release of Curcumin (%)

In general, the in vitro behavior release of curcumin (%) increased gradually in all treatments as the experimental time increased, and this was the highest for curcumin-loaded casein nanoparticles (Figure 3). In the first 2 h, about 50% of the encapsulated curcumin was released from casein,  $\alpha$ -la and WPC, while this value ranged from 31.45% to 36.21% in the first 15 min and gradually increased with time to reach 96.33–97.83% after 48 h. The obtained results indicated that milk proteins can be successfully considered to be carriers for curcumin. The release of curcumin was controlled by its dissociation from the porous polymer matrix and particle size; a smaller size led to a faster release due to the increase in the surface area [34].

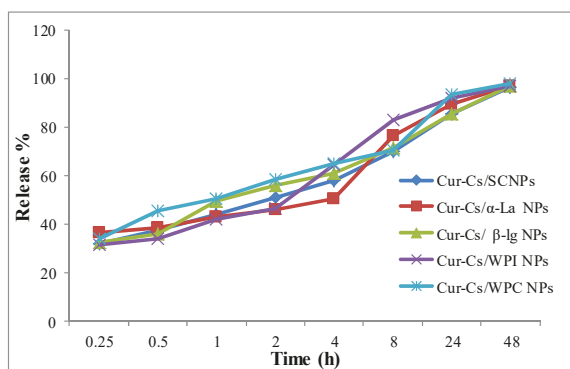


**Figure 3.** In vitro release profiles of curcumin from curcumin–milk protein nanoparticles.

### 3.4. Antioxidant Activity (%)

As shown in Table 2, the antioxidant activity was dependent on concentration. Furthermore, the antioxidant activity of all native proteins was significantly lower than that of both of chitosan or curcumin, except for both  $\beta$ -lg and WPI, whose antioxidant activities were slightly higher or close to curcumin. The antioxidant activity ranged from 46.12% to 60.32% and 41.60% to 62.13% for chitosan and curcumin, respectively, while it ranged from 36.30% to 43.70% for native milk proteins at the level of 1.25 mg/mL and from 52.80% to 61.03% at the level of 5 mg/mL. It is obvious that the antioxidant activity of all curcumin-loaded milk protein nanoparticles is significantly higher than that of chitosan, curcumin and all native proteins or nanocomposites with chitosan. The antioxidant activity of curcumin–milk protein nanoparticles can be arranged in descending order as follows: Cur/ $\beta$ -lg > Cur/WPI > Cur/SC > Cur  $\alpha$ -la > Cur/WPC. These results are consistent with Yi et al. [35], who reported that the DPPH scavenging activity of curcumin encapsulated with milk proteins such as  $\alpha$ -La was dramatically enhanced due to the increased water solubility and greater surface area, which facilitated the interaction between curcumin and radicals. Previous studies have demonstrated that WPI alone exhibits antioxidant activity, while the WPI–curcumin microparticles showed higher antioxidant activity than curcumin or native WPI [36]. Furthermore, the use of  $\beta$ -casein as a carrier of curcumin enhanced its solubility and as a result improved the functional activities of curcumin nanoparticles [14].

**Table 2.** Antioxidant activity (radical scavenging activity %) of different concentrations of native milk proteins, chitosan–milk protein nanocomposite and curcumin-loaded milk protein nanoparticles.

Treatments	Concentration (mg/mL)			Mean
	2.5	5	10	
Chitosan	46.12 ± 2.9	54.08 ± 3.9	60.32 ± 6.7	53.51 ± 4.5
Curcumin	41.60 ± 3.5	54.02 ± 4.0	62.13 ± 2.9	52.58 ± 3.5
SC	39.18 ± 3.0	42.75 ± 3.3	52.28 ± 3.7	44.74 ± 3.3
CS/SCNPs	39.97 ± 2.7	50.48 ± 2.7	66.90 ± 3.5	52.45 ± 3.0
Cur-Cs/SCNPs	49.17 ± 4.4	60.61 ± 4.4	67.54 ± 3.5	59.11 ± 4.1
$\alpha$ -La	36.15 ± 1.7	48.38 ± 3.6	56.55 ± 2.1	47.03 ± 2.5
CS/ $\alpha$ -LaNPs	47.06 ± 2.8	56.90 ± 2.5	62.51 ± 3.0	55.49 ± 2.7
Cur-CS/ $\alpha$ -La NPs	53.82 ± 2.0	59.35 ± 2.9	66.44 ± 1.9	59.87 ± 2.3
$\beta$ -lg	43.70 ± 2.9	53.51 ± 2.0	60.49 ± 2.8	52.57 ± 2.6
CS/ $\beta$ lgNPs	46.86 ± 3.1	54.14 ± 3.3	65.90 ± 1.2	55.63 ± 2.5
Cur-Cs/ $\beta$ lg NPs	48.08 ± 2.8	61.62 ± 2.9	69.05 ± 3.5	59.58 ± 3.1
WPI	43.26 ± 3.1	50.52 ± 6.8	60.92 ± 1.9	51.57 ± 3.9
Cs/WPI NPs	51.10 ± 3.8	55.10 ± 2.4	66.49 ± 2.5	57.56 ± 2.9
Cur-Cs/WPINPs	50.11 ± 3.3	55.08 ± 1.6	68.57 ± 2.5	57.92 ± 2.5
WPC	36.30 ± 2.0	52.44 ± 2.4	61.03 ± 4.8	49.92 ± 3.1
Cs/WPC NPs	47.03 ± 3.9	57.26 ± 2.9	65.40 ± 2.7	56.56 ± 3.2
Cur-Cs/WPCNPs	49.03 ± 4.2	56.20 ± 3.1	63.30 ± 2.6	56.18 ± 3.3
Mean	45.21 ± 3.1	54.26 ± 3.2	63.28 ± 3.0	

Least significant difference (L.S.D.) value at 0.05: concentrations: 0.72, treatments: 1.72, interaction: 2.98.

### 3.5. Anticancer Activity

The data presented in Tables 3 and 4 show the anticancer activity of all tested materials against human hepatocarcinoma (HepG2) and human breast carcinoma cells (MCF-7). It is generally evident that as the concentration of the tested materials increased and that the anticancer activity significantly increased [37].

**Table 3.** Anticancer activity of different concentrations of native proteins, chitosan–milk protein nanocomposite and curcumin-loaded milk protein nanoparticles against HepG2 cell lines.

Treatments	Anticancer Activity %/Concentrations (mg/mL)			Mean
	2.5	5	10	
Chitosan	34.97 ± 1.03	73.35 ± 2.25	91.79 ± 1.96	66.70 ± 1.75
Curcumin	54.06 ± 1.94	81.08 ± 2.32	95.07 ± 2.93	76.74 ± 2.40
SC	33.71 ± 1.29	71.33 ± 2.12	93.05 ± 2.95	66.03 ± 2.12
CS/SCNPs	40.4 ± 3.35	82.95 ± 3.35	95.29 ± 1.71	72.88 ± 2.80
Cur-Cs/SCNPs	46.49 ± 2.64	86.36 ± 2.64	97.31 ± 2.04	76.72 ± 2.44
α-La	36.75 ± 1.75	70.70 ± 2.40	92.04 ± 1.36	66.50 ± 1.84
CS/α-La NPs	38.23 ± 1.77	76.67 ± 1.43	94.11 ± 1.89	69.67 ± 1.70
Cur-Cs/α-La NPs	45.9 ± 1.40	81.79 ± 1.19	96.80 ± 3.30	74.83 ± 1.96
βIg	17.55 ± 2.55	48.36 ± 4.64	83.58 ± 2.42	49.83 ± 3.20
CS/βIgNPs	40.88 ± 2.12	70.84 ± 2.56	92.55 ± 2.45	68.09 ± 2.38
Cur-Cs/βIg NPs	43.27 ± 1.73	85.54 ± 1.37	95.80 ± 2.20	74.87 ± 1.77
WPI	18.59 ± 1.41	53.91 ± 1.19	76.64 ± 1.66	49.71 ± 1.42
CS/WPINPs	43.03 ± 1.53	81.69 ± 1.91	93.81 ± 1.19	72.84 ± 1.54
Cur-Cs/WPINPs	49.9 ± 1.10	82.20 ± 2.79	96.31 ± 2.81	76.14 ± 2.23
WPC	30.63 ± 2.37	81.29 ± 3.71	93.68 ± 2.18	68.53 ± 2.75
Cs/WPC NPs	42.74 ± 2.26	82.53 ± 1.07	95.27 ± 3.23	73.51 ± 2.19
Cur-Cs/WPCNPs	48.68 ± 4.32	80.36 ± 3.06	98.07 ± 3.07	75.70 ± 3.48
Mean	39.16 ± 2.03	75.94 ± 2.35	93.01 ± 2.31	

L.S.D. value at 0.05: concentrations: 0.69, treatments: 1.63, interaction: 2.83.

**Table 4.** Anticancer activity of different concentrations of native proteins, chitosan–milk protein nanocomposite and curcumin-loaded milk protein nanoparticles against MCF7 cell lines.

Treatments	Anticancer Activity (%) / Concentrations (mg/mL)			Mean
	2.5	5	10	
Chitosan	33.22 ± 1.7	67.21 ± 1.6	92.21 ± 2.8	64.21 ± 2.0
Curcumin	33.4 ± 1.7	73.27 ± 2.0	93.52 ± 2.0	66.73 ± 1.9
SC	25.25 ± 2.1	71.27 ± 2.6	92.93 ± 2.1	63.15 ± 2.3
CS/SCNPs	35.86 ± 3.9	75.91 ± 3.9	93.33 ± 1.8	68.37 ± 3.7
Cur-Cs/SCNPs	50.84 ± 2.9	78.15 ± 2.9	96.88 ± 5.5	75.29 ± 3.7
α-La	30.27 ± 2.8	71.27 ± 2.0	93.25 ± 1.8	64.93 ± 2.2
CS/α-La NPs	41.61 ± 3.1	75.13 ± 4.1	94.78 ± 3.7	70.51 ± 3.6
Cur-Cs/α-La NPs	51.26 ± 2.3	77.18 ± 2.2	98.31 ± 1.8	75.58 ± 2.1
βIg	19.24 ± 1.8	50.98 ± 3.1	85.37 ± 4.2	51.86 ± 3.0
CS/βIgNPs	44.08 ± 2.9	61.58 ± 2.5	91.93 ± 2.1	65.86 ± 2.5
Cur-Cs/βIg NPs	53.63 ± 2.6	74.61 ± 3.4	98.47 ± 3.5	75.57 ± 3.5
WPI	16.63 ± 2.5	48.80 ± 4.1	83.17 ± 2.8	49.53 ± 3.1
CS/WPINPs	41.65 ± 2.4	74.78 ± 3.8	94.2 ± 1.3	70.21 ± 2.5
Cur-Cs/WPINPs	52.43 ± 2.8	77.87 ± 5.9	98.48 ± 5.5	76.26 ± 4.7
WPC	17.87 ± 2.1	62.24 ± 2.6	76.30 ± 3.0	52.14 ± 2.6
Cs/WPC NPs	33.26 ± 2.2	74.79 ± 3.3	93.86 ± 2.3	67.30 ± 2.6
Cur-Cs/WPCNPs	50.03 ± 1.5	75.96 ± 2.9	98.06 ± 2.5	74.68 ± 2.3
Mean	37.09 ± 2.4	70.06 ± 3.2	89.12 ± 2.9	

L.S.D. value at 0.05: concentrations: 1.15, treatments: 2.73, interaction: 4.7.

As for HepG2 cancer cells, as shown in Table 3, it is evident that the anticancer activity of curcumin is considerably greater than that of chitosan, which is in agreement with Senft et al. [38] and Gupta et al. [39] who reported that curcumin has a higher toxic effect on tumor cells owing to the capability of curcumin to interfere with several biochemical pathways involved in the proliferation and survival of cancer cells. Furthermore, Bouhenna et al. [40] stated that the anticancer activity of chitosan may be due to the interactions between the charged groups of chitosan molecules and tumor cells.

The anticancer activity of the native milk proteins ranged from 17.55% to 36.75% (at the level of 2.5 mg/mL). Native  $\beta$ -lg had the lowest effect, while  $\alpha$ -la tended to have the highest effect. The mechanism of action of WP on tumor development is due to increased concentrations of tissue glutathione, which detoxifies free radicals and improves the immune response [41]. Additionally, the anticancer activity of curcumin-loaded milk protein nanoparticles is significantly higher than that of the native milk proteins or chitosan–milk protein nanocomposite. The inhibitory activity % of SC and WPC in all forms was the highest compared to the other tested materials, which confirmed the work of Pan et al. [42], who reported that the entrapment of curcumin in casein nanoparticles resulted in higher antioxidant activity and cytotoxicity against cancer cells compared to free curcumin. This may be due to the antimutagenic properties of the casein structure, which can control the mutagen rather than its amino acid composition. Furthermore, Krissansen [43] noted that whey protein concentrate could play a potential role in cancer treatments as it increased baicalein's cytotoxicity to the HepG2 cell line.

As regards the MCF-7 cancer cells, as previously mentioned, the anticancer activity of all tested materials increased significantly as their concentration increased. Both chitosan and curcumin had almost the same anticancer activity (Table 4). It is apparent that native milk proteins (SC and  $\alpha$ -La) had almost the same anticancer activity (at the level of 10 mg/mL) as both chitosan and curcumin, and they also had the highest effect compared to the other milk proteins. The inhibition % of the native milk proteins ranged from 16.63% (WPI) to 30.27% ( $\alpha$ -la) with significant differences between the native proteins at the level of 2.5 mg/mL, while it increased to 76.30% (WPC) and 93.25% ( $\alpha$ -la) at the level of 10 mg/mL. The inhibitory effect of whey proteins may be due to its content of sulfur amino acids which enhanced the glutathione bioavailability and reduced oxidative stress, leading to cancer prevention [44]. The anticancer activity of the milk protein–chitosan nanocomposite was higher than native proteins. These findings also implied that curcumin-loaded milk protein nanoparticles showed the highest anticancer activity relative to all the tested materials. These results are in line with Adahoun et al. [45], who reported that curcumin NPs had a much stronger antiproliferative impact on cancer cells compared to native curcumin due to their ability to inhibit specific molecular signaling pathways involved in carcinogenesis. Tabatabaei et al. [46] proved that curcumin-loaded poly(lactide-co-glycolide)-poly(ethylene glycol) (PLGA-PEG) has more cytotoxic effects on the MCF-7 breast cancer cell line due to the enhancement of its water solubility as well as its bioavailability and functionality compared to curcumin.

### 3.6. Antimicrobial Activity

As shown in Table 5, the antibacterial effect of curcumin was slightly higher, with non-significant differences compared to chitosan. The inhibition zone ranged from 16.00 to 23.00 mm for curcumin, while it ranged from 14.00 to 21.00 mm for chitosan. Furthermore, it is notable that *B.subtilis* was more sensitive to curcumin and chitosan compared to the other strains. Additionally, all tested materials displayed variable antibacterial activity. All native forms of milk proteins had almost no effect on all tested strains, except SC; its antibacterial effect was higher than that of both of chitosan or curcumin. Its inhibition zone ranged from 15.00 to 26.00 mm. The inhibitory effect of curcumin may be due to cell membrane damage causing membrane permeabilization [47], while the key mechanism of chitosan is due to its cationic nature and the electrostatic interaction between positively charged chitosan groups and negatively charged sites on the microbial cell and its penetration into the bacteria cell wall, which is linked to the microorganism DNA inhibiting the transcription and consequently the translation process [48].

**Table 5.** Antimicrobial activity of native proteins, chitosan–milk protein nanocomposite and curcumin-loaded milk protein nanoparticles.

Treatments	Inhibition Zone (mm)				
	<i>E. Coli</i>	<i>Staph. aureus</i>	<i>B. subtilis</i>	<i>P. aeruginosa</i>	<i>C. albicans</i>
Chitosan	15 <sup>g</sup> ± 4	19 <sup>bcd</sup> ± 2	21 <sup>fg</sup> ± 3	14 <sup>f</sup> ± 4	12 <sup>e</sup> ± 2
Curcumin	16 <sup>fg</sup> ± 3	20 <sup>bc</sup> ± 3	23 <sup>ef</sup> ± 2	16 <sup>ef</sup> ± 3	21 <sup>bc</sup> ± 3
SC	19 <sup>efg</sup> ± 2	25 <sup>a</sup> ± 2	26 <sup>cde</sup> ± 4	15 <sup>f</sup> ± 3	14 <sup>e</sup> ± 2
CS/SCNPs	22 <sup>cde</sup> ± 3	17 <sup>cde</sup> ± 3	28 <sup>bcd</sup> ± 3	20 <sup>cde</sup> ± 3	20 <sup>cd</sup> ± 4
Cur-Cs/SCNPs	27 <sup>ab</sup> ± 3	21 <sup>b</sup> ± 4	31 <sup>ab</sup> ± 4	25 <sup>ab</sup> ± 4	28 <sup>a</sup> ± 3
α-La	0 <sup>h</sup> ± 0	0 <sup>f</sup> ± 0	0 <sup>h</sup> ± 0	0 <sup>g</sup> ± 0	20 <sup>cd</sup> ± 3
CS/α-LaNPs	20 <sup>def</sup> ± 3	15 <sup>e</sup> ± 4	25 <sup>def</sup> ± 3	25 <sup>ab</sup> ± 2	22 <sup>bc</sup> ± 3
Cur-Cs/α-La NPs	24 <sup>bcd</sup> ± 3	20 <sup>bc</sup> ± 3	30 <sup>abc</sup> ± 3	28 <sup>a</sup> ± 3	25 <sup>ab</sup> ± 2
Blg	0 <sup>h</sup> ± 0	0 <sup>f</sup> ± 0	0 <sup>h</sup> ± 0	0 <sup>g</sup> ± 0	0 <sup>f</sup> ± 0
CS/βlgNPs	25 <sup>bc</sup> ± 2	19 <sup>bcd</sup> ± 2	30 <sup>abc</sup> ± 3	24 <sup>abc</sup> ± 3	16 <sup>de</sup> ± 3
Cur-Cs/βlgNPs	30 <sup>a</sup> ± 3	22 <sup>ab</sup> ± 3	33 <sup>a</sup> ± 2	26 <sup>ab</sup> ± 3	21 <sup>bc</sup> ± 3
WPI	0 <sup>h</sup> ± 0	0 <sup>f</sup> ± 0	0 <sup>h</sup> ± 0	0 <sup>g</sup> ± 0	0 <sup>f</sup> ± 0
Cs/WPI NPs	20 <sup>def</sup> ± 3	14 <sup>e</sup> ± 3	28 <sup>bcd</sup> ± 3	15 <sup>f</sup> ± 2	16 <sup>de</sup> ± 3
Cur-Cs/WPI NPs	28 <sup>ab</sup> ± 3	20 <sup>bc</sup> ± 3	32 <sup>ab</sup> ± 3	22 <sup>bcd</sup> ± 3	21 <sup>bc</sup> ± 3
WPC	0 <sup>h</sup> ± 0	0 <sup>f</sup> ± 0	16 <sup>g</sup> ± 1	0 <sup>g</sup> ± 0	0 <sup>f</sup> ± 0
Cs/WPC NPs	24 <sup>b-d</sup> ± 3	16 <sup>de</sup> ± 3	22 <sup>ef</sup> ± 3	18 <sup>def</sup> ± 3	15 <sup>e</sup> ± 3
Cur-Cs/WPC NPs	31 <sup>a</sup> ± 4	22 <sup>ab</sup> ± 3	28 <sup>bcd</sup> ± 3	20 <sup>cde</sup> ± 3	23 <sup>bc</sup> ± 2

Different superscripts (a–g) in the same column are significantly different ( $p < 0.05$ ).

The formation of nanoparticles of milk proteins with chitosan or curcumin (in most cases) significantly enhanced the inhibitory effect compared to chitosan, curcumin and native milk proteins. It is also noticeable that all curcumin-loaded milk protein nanoparticles had increased activity against *E. coli* and *B. subtilis*. The inhibition zone ranged from 24 to 31 mm and from 28 to 33 mm, respectively, as compared to the other tested strains. *P. aeruginosa* and *Staph. aureus* were less sensitive to the tested curcumin-loaded nanoparticles (Table 5). The inhibition zone ranged from 20 mm (Cur-Cs/α-La NPs and Cur-Cs/WPI NPs) to 22 mm (Cur-Cs/βlgNPs and Cur-Cs/WPC NPs) for *Staph. aureus*, and from 20 mm (Cur-Cs/WPC NPs) to 28 mm (Cur-Cs/α-La NPs) for *P. aeruginosa*. These results are in line with those of Deka et al. [49] who reported that the water solubility and antimicrobial activity of curcumin were significantly improved by curcumin nanoparticle formation compared to curcumin alone.

*Candida albicans* is a major fungal pathogen of humans, affecting millions of people and causing death worldwide [50]. The antifungal activity of curcumin is significantly higher than that of chitosan, at 21 vs. 12 mm (Table 5). The antifungal effect of curcumin against *C. albicans* was due to the disruption of the cell wall [51]; for chitosan, the positive charge of chitosan can interact with the negatively charged microbial cell surface and disrupt the anion–cation balance, thereby exerting an inhibitory effect [52].

Only native SC and α-La had an antifungal effect similar to chitosan, and this was significantly lower than curcumin (Table 5). The formation of nanocomposite and curcumin-loaded milk protein nanoparticles enhanced the antifungal effect more than the native forms. Cur-Cs/SCNPs were most effective against *C. albicans* compared to the other tested materials. The diameter of the inhibition zone ranged from 21 mm (Cur-Cs/WPINPs) to 28 mm (Cur-Cs/SCNPs). It was also remarkable that the inhibitory effect of the tested nanoparticles in most cases was higher than that of the used standard antibiotics, which agreed with the results of Paul et al. [53], who reported that curcumin–silver nanoparticles displayed antifungal activity against different isolates of candida species as compared to curcumin and AgNO<sub>3</sub> solutions. The inhibitory effect of the nanoparticles can be arranged in descending order as follows: Cur/SC > Cur/α-La > Cur/WPC > Cur/βlg > Cur/WPI.

#### 4. Conclusions

The obtained results revealed that all milk proteins used had a proven efficiency as nanocarriers for curcumin. All curcumin-loaded milk protein nanoparticles exhibited antioxidant and anticancer activity on both HepG2 and MCF-7 cell lines due to the enhanced solubility and bioavailability of curcumin. This effect was dose-dependent. Curcumin nanoparticles with  $\alpha$ -lactalbumin showed the highest antioxidant activity at a concentration of 2.5 mg/mL. Furthermore, curcumin nanoparticles with WPI had the highest anticancer activity against HepG2 cell line, while curcumin nanoparticles with  $\beta$ -lactoglobulin exhibited the highest anticancer activity against MCF-7 cell line. Moreover, all nanoparticles displayed antibacterial and anticandida effects. It is worth noting that curcumin nanoparticles with  $\beta$ -lactoglobulin and WPC showed the highest antimicrobial activity against all tested strains. These results allow and encourage the use of these compounds in the food and medical sectors.

**Author Contributions:** Conceptualization, Data Analysis, Original Draft Preparation, Review & Editing S.T.; Data Analysis, Review & Editing I.E.-S., A.S. and M.A.-H.; Sample Preparation, Sample Analysis A.A. and G.A.; Funding the publication fee, Review & Editing T.E. and E.N. All authors have read and agreed to the published version of the manuscript.

**Funding:** This research received no external funding.

**Conflicts of Interest:** No potential conflict of interest was reported by the authors.

#### References

- Xu, X.-Y.; Meng, X.; Li, S.; Gan, R.-Y.; Li, Y.; Li, H.-B. Bioactivity, health benefits, and related molecular mechanisms of curcumin: Current progress, challenges, and perspectives. *Nutrients* **2018**, *10*, 1553. [[CrossRef](#)] [[PubMed](#)]
- Da Silva, A.C.; De Freitas Santos, P.D.; Do Prado Silva, J.T.; Leimann, F.V.; Bracht, L.; Gonçalves, O.H. Impact of curcumin nanoformulation on its antimicrobial activity. *Trends Food Sci. Technol.* **2018**, *72*, 74–82. [[CrossRef](#)]
- Kumar, D.D.; Mann, B.; Pothuraju, R.; Sharma, R.; Bajaj, R. Formulation and characterization of nanoencapsulated curcumin using sodium caseinate and its incorporation in ice cream. *Food Funct.* **2016**, *7*, 417–424. [[CrossRef](#)] [[PubMed](#)]
- Jahangirian, H.; Lemraski, E.G.; Webster, T.J.; Rafiee-Moghaddam, R.; Abdollahi, Y. A review of drug delivery systems based on nanotechnology and green chemistry: Green nanomedicine. *Int. J. Nanomed.* **2017**, *12*, 2957. [[CrossRef](#)] [[PubMed](#)]
- Rai, M.; Pandit, R.; Gaikwad, S.; Yadav, A.; Gade, A. Potential applications of curcumin and curcumin nanoparticles: From traditional therapeutics to modern nanomedicine. *Nanotechnol. Rev.* **2015**, *4*, 161–172. [[CrossRef](#)]
- Rai, M.; Pandit, R.; Paralikar, P.; Nagaonkar, D.; Rehman, F.; Dos Santos, C.A. Pharmaceutical applications of curcumin-loaded nanoparticles. In *Nanotechnology Applied to Pharmaceutical Technology*; Springer: Cham, Switzerland, 2017; pp. 139–154.
- Liu, W.; Chen, X.D.; Cheng, Z.; Selomulya, C. On enhancing the solubility of curcumin by microencapsulation in whey protein isolate via spray drying. *J. Food Eng.* **2016**, *169*, 189–195. [[CrossRef](#)]
- Khodabandehloo, H.; Zahednasab, H.; Hafez, A.A. Nanocarriers usage for drug delivery in cancer therapy. *Iran. J. Cancer Prev.* **2016**, *9*, e3966. [[CrossRef](#)]
- Li, J.; Cai, C.; Li, J.; Li, J.; Sun, T.; Wang, L.; Wu, H.; Yu, G. Chitosan-based nanomaterials for drug delivery. *Molecules* **2018**, *23*, 2661. [[CrossRef](#)]
- Livney, Y.D. Milk proteins as vehicles for bioactives. *Curr. Opin. Colloid Interface Sci.* **2010**, *15*, 73–83. [[CrossRef](#)]
- Li, M.; Cui, J.; Ngadi, M.O.; Ma, Y. Absorption mechanism of whey-protein-delivered curcumin using caco-2 cell monolayers. *Food Chem.* **2015**, *180*, 48–54. [[CrossRef](#)]
- Mohammadian, M.; Salami, M.; Momen, S.; Alavi, F.; Emam-Djomeh, Z.; Moosavi-Movahedi, A.A. Enhancing the aqueous solubility of curcumin at acidic condition through the complexation with whey protein nanofibrils. *Food Hydrocoll.* **2019**, *87*, 902–914. [[CrossRef](#)]

13. Mohammadian, M.; Salami, M.; Momen, S.; Alavi, F.; Emam-Djomeh, Z. Fabrication of curcumin-loaded whey protein microgels: Structural properties, antioxidant activity, and in vitro release behavior. *LWT* **2019**, *103*, 94–100. [[CrossRef](#)]
14. Esmaili, M.; Ghaffari, S.M.; Moosavi-Movahedi, Z.; Atri, M.S.; Sharifzadeh, A.; Farhadi, M.; Yousefi, R.; Chobert, J.-M.; Haertlé, T.; Moosavi-Movahedi, A.A. Beta casein-micelle as a nano vehicle for solubility enhancement of curcumin; food industry application. *Lwt-Food Sci. Technol.* **2011**, *44*, 2166–2172. [[CrossRef](#)]
15. Fan, Y.; Yi, J.; Zhang, Y.; Yokoyama, W. Fabrication of curcumin-loaded bovine serum albumin (bsa)-dextran nanoparticles and the cellular antioxidant activity. *Food Chem.* **2018**, *239*, 1210–1218. [[CrossRef](#)]
16. Calvo, P.; Remunan-Lopez, C.; Vila-Jato, J.L.; Alonso, M. Novel hydrophilic chitosan-polyethylene oxide nanoparticles as protein carriers. *J. Appl. Polym. Sci.* **1997**, *63*, 125–132. [[CrossRef](#)]
17. Sangeetha, K.S.S.; Umamaheswari, S.; Reddy, C.U.M.; Kalkura, S.N. Chrysin loaded chitosan nanoparticle: Formulation and in-vitro characterization. *Int. J. Pharm. Sci. Res.* **2017**, *8*, 1102–1109.
18. Chopra, M.; Jain, R.; Dewangan, A.K.; Varkey, S.; Mazumder, S. Design of curcumin loaded polymeric nanoparticles-optimization, formulation and characterization. *J. Nanosci. Nanotechnol.* **2016**, *16*, 9432–9442. [[CrossRef](#)]
19. Swed, A.; Cordonnier, T.; Fleury, F.; Boury, F. Protein encapsulation into plga nanoparticles by a novel phase separation method using non-toxic solvents. *J. Nanomed. Nanotechnol.* **2014**, *5*, 241.
20. Sadeghi, R.; Moosavi-Movahedi, A.A.; Emam-Jomeh, Z.; Kalbasi, A.; Razavi, S.H.; Karimi, M.; Kokini, J. The effect of different desolvating agents on bsa nanoparticle properties and encapsulation of curcumin. *J. Nanopart Res.* **2014**, *16*, 2565. [[CrossRef](#)]
21. Teng, Z.; Li, Y.; Wang, Q. Insight into curcumin-loaded  $\beta$ -lactoglobulin nanoparticles: Incorporation, particle disintegration, and releasing profiles. *J. Agric. Food Chem.* **2014**, *62*, 8837–8847. [[CrossRef](#)]
22. Asouri, M.; Ataei, R.; Ahmadi, A.A.; Amini, A.; Moshaei, M.R. Antioxidant and free radical scavenging activities of curcumin. *Asian J. Chem.* **2013**, *25*, 7593–7595. [[CrossRef](#)]
23. Vidhyalakshmi, R.; Vallinachiyar, C. Apoptosis of human breast cancer cells (mcf-7) induced by polysaccharides produced by bacteria. *J. Cancer Sci. Ther.* **2013**, *5*, 031–034.
24. Cappuccino, J.G.; Sherman, N. *Microbiology. A Laboratory Manual*; Pearson Education, Inc.: New Delhi, India, 2004; pp. 282–283.
25. Snedecor, G.W.; Cochran, W.G. *Statistical Methods*, 6th ed.; Ames, Iowa, Iowa State College Press: Iowa City, IA, USA, 1976.
26. Athira, G.K.; Jyothi, A.N. Preparation and characterization of curcumin loaded cassava starch nanoparticles with improved cellular absorption. *Int. J. Pharm. Pharm. Sci.* **2014**, *6*, 171–176.
27. Singh, H.D.; Wang, G.; Uludağ, H.; Unsworth, L.D. Poly-l-lysine-coated albumin nanoparticles: Stability, mechanism for increasing in vitro enzymatic resilience, and sirna release characteristics. *Acta Biomater.* **2010**, *6*, 4277–4284. [[CrossRef](#)]
28. Arroyo-Maya, I.J.; Rodiles-López, J.; Cornejo-Mazon, M.; Gutierrez-Lopez, G.F.; Hernández-Arana, A.; Toledo-Núñez, C.; Barbosa-Cánovas, G.; Flores-Flores, J.; Hernandez-Sanchez, H. Effect of different treatments on the ability of  $\alpha$ -lactalbumin to form nanoparticles. *J. Dairy Sci.* **2012**, *95*, 6204–6214. [[CrossRef](#)]
29. Awad, R.; Hassan, Z.; Farrag, A.; El-Sayed, M.; Soliman, T. The use of whey portien isolate in microencapsulation of curcumin. *Int. J. Food Nutr. Sci.* **2015**, *4*, 125–131.
30. Udornpornmongkol, P.; Chiang, B.H. Curcumin-loaded polymeric nanoparticles for enhanced anti-colorectal cancer applications. *J. Biomater. Appl.* **2015**, *30*, 537–546. [[CrossRef](#)]
31. Chen, L.; Subirade, M. Chitosan/ $\beta$ -lactoglobulin core-shell nanoparticles as nutraceutical carriers. *Biomaterials* **2005**, *26*, 6041–6053. [[CrossRef](#)]
32. Pan, K.; Zhong, Q.; Baek, S.J. Enhanced dispersibility and bioactivity of curcumin by encapsulation in casein nanocapsules. *J. Agric. Food Chem.* **2013**, *61*, 6036–6043. [[CrossRef](#)]
33. El-Sayed, M.; Hassan, Z.; Awad, M.; Salama, H. Chitosan-whey protein complex (cs-wp) as delivery systems to improve bioavailability of iron. *Int. J. Appl. Pure Sci. Agric.* **2015**, *1*, 34–46.
34. Farnia, P.; Mollaei, S.; Bahrami, A.; Ghassempour, A.; Velayati, A.A.; Ghanavi, J. Improvement of curcumin solubility by polyethylene glycol/chitosan-gelatin nanoparticles (cur-peg/cs-g-nps). *Biomed. Res.* **2016**, *27*, 659–665.

35. Yi, J.; Fan, Y.; Zhang, Y.; Wen, Z.; Zhao, L.; Lu, Y. Glycosylated  $\alpha$ -lactalbumin-based nanocomplex for curcumin: Physicochemical stability and dpph-scavenging activity. *Food Hydrocoll.* **2016**, *61*, 369–377. [\[CrossRef\]](#)
36. Kerasioti, E.; Stagos, D.; Priftis, A.; Aivazidis, S.; Tsatsakis, A.M.; Hayes, A.W.; Kouretas, D. Antioxidant effects of whey protein on muscle c2c12 cells. *Food Chem.* **2014**, *155*, 271–278. [\[CrossRef\]](#)
37. Akalya, V.; Rajeshwari, M.; Sivasurya, R.V.; Manivasagan, N.G.; Ramesh, B.; Karthikeyan, S. Antimicrobial and anticancer activity of curcumin on hepg2 cells. *Int. J. Res. Appl. Sci. Eng. Technol. (Ijrasnet)* **2017**, *5*, 1188–1194.
38. Senft, C.; Polacin, M.; Priester, M.; Seifert, V.; Kögel, D.; Weissenberger, J. The nontoxic natural compound curcumin exerts anti-proliferative, anti-migratory, and anti-invasive properties against malignant gliomas. *BMC Cancer* **2010**, *10*, 491. [\[CrossRef\]](#) [\[PubMed\]](#)
39. Gupta, S.C.; Kismali, G.; Aggarwal, B.B. Curcumin, a component of turmeric: From farm to pharmacy. *Biofactors* **2013**, *39*, 2–13. [\[CrossRef\]](#) [\[PubMed\]](#)
40. Bouhenna, M.; Salah, R.; Bakour, R.; Drouiche, N.; Abdi, N.; Grib, H.; Lounici, H.; Mameri, N. Effects of chitin and its derivatives on human cancer cells lines. *Environ. Sci. Pollut. Res.* **2015**, *22*, 15579–15586. [\[CrossRef\]](#)
41. Bounous, G.; Batist, G.; Gold, P. Whey proteins in cancer prevention. *Cancer Lett.* **1991**, *57*, 91–94. [\[CrossRef\]](#)
42. Pan, K.; Luo, Y.; Gan, Y.; Baek, S.J.; Zhong, Q. Ph-driven encapsulation of curcumin in self-assembled casein nanoparticles for enhanced dispersibility and bioactivity. *Soft Matter* **2014**, *10*, 6820–6830. [\[CrossRef\]](#)
43. Krissansen, G.W. Emerging health properties of whey proteins and their clinical implications. *J. Am. Coll. Nutr.* **2007**, *26*, 713S–723S. [\[CrossRef\]](#)
44. Zarogoulidis, P.; Tsakiridis, K.; Karapantou, C.; Lampaki, S.; Kioumis, I.; Pitsiou, G.; Papaiwannou, A.; Hohenforst-Schmidt, W.; Huang, H.; Kesisis, G.; et al. Use of proteins as biomarkers and their role in carcinogenesis. *J. Cancer* **2015**, *6*, 9–18. [\[CrossRef\]](#)
45. Adahoun, M.A.; Al-Akhras, M.-A.H.; Jaafar, M.S.; Bououdina, M. Enhanced anti-cancer and antimicrobial activities of curcumin nanoparticles. *Artif. CellsNanomed. Biotechnol.* **2017**, *45*, 98–107. [\[CrossRef\]](#) [\[PubMed\]](#)
46. Tabatabaei Mirakabad, F.S.; Akbarzadeh, A.; Milani, M.; Zarghami, N.; Taheri-Anganeh, M.; Zeighamian, V.; Badrzadeh, F.; Rahmati-Yamchi, M. A comparison between the cytotoxic effects of pure curcumin and curcumin-loaded plga-peg nanoparticles on the mcf-7 human breast cancer cell line. *Artif. CellsNanomed. Biotechnol.* **2016**, *44*, 423–430. [\[CrossRef\]](#)
47. Tyagi, P.; Singh, M.; Kumari, H.; Kumari, A.; Mukhopadhyay, K. Bactericidal activity of curcumin i is associated with damaging of bacterial membrane. *PLoS ONE* **2015**, *10*, e0121313. [\[CrossRef\]](#) [\[PubMed\]](#)
48. Kim, S. Competitive biological activities of chitosan and its derivatives: Antimicrobial, antioxidant, anticancer, and anti-inflammatory activities. *Int. J. Polym. Sci.* **2018**. [\[CrossRef\]](#)
49. Deka, C.; Aidew, L.; Devi, N.; Buragohain, A.K.; Kakati, D.K. Synthesis of curcumin-loaded chitosan phosphate nanoparticle and study of its cytotoxicity and antimicrobial activity. *J. Biomater. Sci. Polym. Ed.* **2016**, *27*, 1659–1673. [\[CrossRef\]](#) [\[PubMed\]](#)
50. Pfaller, M.; Diekema, D. Epidemiology of invasive candidiasis: A persistent public health problem. *Clin. Microbiol. Rev.* **2007**, *20*, 133–163. [\[CrossRef\]](#)
51. Lee, W.; Lee, D. An antifungal mechanism of curcumin lies in membrane-targeted action within candida albicans. *Iubmb Life* **2014**, *66*, 780–785. [\[CrossRef\]](#)
52. Martínez-Camacho, A.; Cortez-Rocha, M.; Ezquerro-Brauer, J.; Graciano-Verdugo, A.; Rodríguez-Félix, F.; Castillo-Ortega, M.; Yépiz-Gómez, M.; Plascencia-Jatomea, M. Chitosan composite films: Thermal, structural, mechanical and antifungal properties. *Carbohydr. Polym.* **2010**, *82*, 305–315. [\[CrossRef\]](#)
53. Paul, S.; Mohanram, K.; Kannan, I. Antifungal activity of curcumin-silver nanoparticles against fluconazole-resistant clinical isolates of candida species. *Ayu* **2018**, *39*, 182. [\[CrossRef\]](#)



Article

# Modifications of Gut Microbiota after Grape Pomace Supplementation in Subjects at Cardiometabolic Risk: A Randomized Cross-Over Controlled Clinical Trial

Sara Ramos-Romero <sup>1,2</sup>, Daniel Martínez-Maqueda <sup>3,†</sup>, Mercè Hereu <sup>1</sup>, Susana Amézqueta <sup>4</sup>, Josep Lluís Torres <sup>1</sup> and Jara Pérez-Jiménez <sup>3,\*</sup>

<sup>1</sup> Institute of Advanced Chemistry of Catalonia (IQAC-CSIC), Jordi Girona 18-26, 08034 Barcelona, Spain; sara.ramosromero@ub.edu (S.R.-R.); merce.hereu@iqac.csic.es (M.H.); josepluis.torres@iqac.csic.es (J.L.T.)

<sup>2</sup> Department of Cell Biology, Physiology & Immunology, Faculty of Biology, University of Barcelona, Avinguda Diagonal 643, 08028 Barcelona, Spain

<sup>3</sup> Department of Metabolism and Nutrition, Institute of Food Science, Technology and Nutrition (ICTAN-CSIC), José Antonio Novais 10, 28040 Madrid, Spain; daniel.martinez.maqueda@madrid.org

<sup>4</sup> Departament d'Enginyeria Química i Química Analítica, Institut de Biomedicina (IBUB), Universitat de Barcelona, Carrer de Martí i Franquès, 1-11, 08028 Barcelona, Spain; samezqueta@ub.edu

\* Correspondence: jara.perez@ictan.csic.es; Tel.: +34-915-492-300

† Current affiliation: Department of Agrifood Research, Madrid Institute for Rural, Agricultural and Food Research and Development (IMIDRA), A-2 Km. 38.2, 28805 Alcalá de Henares (Madrid), Spain.

Received: 30 July 2020; Accepted: 7 September 2020; Published: 11 September 2020

**Abstract:** Polyphenols are dietary bioactive compounds able to induce modifications in the gut microbiota profile, although more clinical studies are needed. With this aim, a randomized cross-over clinical trial was conducted, where 49 subjects at cardiometabolic risk (exhibiting at least two metabolic syndrome factors) were supplemented with a daily dose of 8 g of grape pomace (GP) for 6 weeks, with an equivalent control (CTL) period. The levels of total bacteria and Bacteroidetes, Firmicutes, Lactobacillales, *Bacteroides* and *Prevotella* were estimated in fecal DNA by quantitative real-time PCR (qPCR), while fecal short-chain fatty acids (SCFAs) were assessed by gas chromatography. Several cardiometabolic markers were evaluated in blood samples. GP reduced insulin levels only in half of the participants (responders). GP supplementation did not cause significant modifications in the microbiota profile of the whole group, except for a tendency ( $p = 0.059$ ) towards a decrease in the proportion of Lactobacillales, while it increased the proportion of *Bacteroides* in non-responder subjects. The reduction of insulin levels in subjects at cardiometabolic risk upon GP supplementation appears not to be induced by changes in the major subgroups of gut microbiota. Further studies at the species level may help to elucidate the possible role of microbiota in GP-induced insulinemic status.

**Keywords:** metabolic syndrome; microbiota; insulin sensitivity; polyphenols; grape pomace

## 1. Introduction

Colonic microbiota has emerged as a key player in the crosstalk between diet and health. Increasing evidence connects unbalances in gut microbiota (dysbiosis) with pathologies, such as cancer [1] or Parkinson's disease [2]. Dysbiosis appears to be particularly decisive in the development of risk factors for cardiometabolic disease. It has been shown that the profile of gut microbiota in subjects presenting obesity [3], impaired glucose tolerance [4], or hypertension [5] are different to those of healthy subjects. Metabolic syndrome (MetS) is a combination of cardiometabolic risk factors (central obesity, high blood glucose and triglycerides, low HDL cholesterol, hypertension) arising from underlying pathophysiological processes such as insulin resistance (IR) [6], sub-clinical inflammation [7], or oxidative stress (OS) [8].

Since the prevalence of MetS is increasing, there is growing interest in further exploring the role of dysbiosis as well as the opportunities gut microbiota may offer for dietary interventions [9].

Polyphenols, a wide group of secondary metabolites widely distributed in foods of vegetal origin, may be effective against MetS-associated risk factors, particularly low HDL-cholesterol [10]. More robust clinical trials are still needed [11]. Polyphenols may exert their action by different mechanisms: improvement of insulin and adiponectin signaling pathways; inhibition of inflammation signaling pathways; stimulation of endogenous antioxidant systems; repression of intestinal lipid absorption; decrease of triglyceride content in skeletal muscle; inhibition of chylomicron/VLDL secretion; stimulation of nitric oxide production [12–19]. Polyphenols may exert some of their effects through the modulation of oral and gut microbiota. The limited evidence currently available from in vitro, pre-clinical and clinical studies is suggesting that some of the effects of polyphenols against colorectal cancer and cardiovascular disease may be related to changes in the relative populations of bacterial subgroups such as *Bacteriodes*, *Lactobacillus*, and *Bifidobacterium* [20,21].

Another important aspect in the health effects of dietary bioactive compounds is the inter-individual variability. Not all subjects exhibit the same response to supplementation (e.g., with polyphenols) [22]. The action of microbiota is probably a major determinant of inter-individual variability as polyphenols are extensively transformed by several bacterial species, which generate a great variety of bioactive absorbable metabolites [23]. Indeed, the concept of metabotypes, i.e., groups of subjects with a tendency to originate certain combinations of circulating polyphenol metabolites as compared to other groups not able to generate them, has become a key concept in the field of dietary polyphenols [24].

Grape pomace (GP) is generated during wine making being commonly discarded or underutilized. This product is very rich in both dietary fiber and polyphenols (particularly the so-called non-extractable polyphenols, associated with dietary fiber [25]), thus, being suggested as a new food ingredient in multiple products [26]. Indeed, some studies have reported that the intake of GP or derived extracts improved blood pressure, fasting glucose, fasting or postprandial insulin and lipid profile [27–31]. Several in vitro, preclinical, and clinical studies have evaluated the changes induced by different grape-derived products in the populations of gut microbiota as well as their associated beneficial effects [32]. A clinical trial with healthy women supplemented with a GP extract for 3 weeks did not find any modification in gut microbiota profile [28]. As far as we know, no clinical trial has explored whether the sustained intake of whole GP may affect microbiota profile.

Dried GP supplementation at nutritional doses (8 g daily) for 6 weeks in subjects at high cardiometabolic risk led to a significant improvement in insulin sensitivity in a randomized cross-over clinical trial [29]. This study explored the potential modifications in microbiota profile induced by GP supplementation, exploring specifically the possible ways in which GP supplementation might have differentially induced a reduction of insulin secretion in responder individuals, with particular attention to changes in representative gut bacterial populations.

## 2. Experimental Materials

### 2.1. Composition of Grape Pomace

In this study, subjects were daily supplemented with freeze-dried and milled GP (*Vitis vinifera* L. cv. Tempranillo) provided in monodoses (8 g). To ensure safety, standard microbiological and metal analysis were performed in the product.

Detailed composition of the product has been provided elsewhere [29]. Its main constituent was dietary fiber (68.2%), being insoluble fraction a 98% of it. The next major constituent were polyphenols (29.6%), with 66% of them being non-extractable polymeric proanthocyanidins. Protein content was 11.6%, fat content was 10.3% and ash content was 5.7%. Simple sugars content in GP was 2.5%.

This study was a randomized cross-over controlled clinical trial. Permissions were obtained from the Ethics Subcommittee of the Spanish National Research Council (CSIC), Madrid, Spain (2016/12/13), and the Ethics Committee for Clinical Research of the University Hospital Puerta de

Hierro-Majadahonda, Majadahonda, Spain (2016/12/02). It was registered in the Clinical Trials database with the identifier NCT03076463, where whole trial protocol is available. Recruitment for the study took place between December 2016 and March 2017, while the study was conducted between March 2017 and July 2017. A written informed consent was requested to participate in the study.

Details on this clinical trial have been already reported, together with CONSORT flow diagram [29]. Briefly, participants were aged 18–70 years with at least two of the factors requested for MetS diagnosis [33], without diagnosis or medication for cardiometabolic pathologies. Exclusion criteria were: pregnancy, lactation, current or close participation in any other dietary intervention study. Although it was not an exclusion criterion, subjects were asked about dietary supplement consumption and none of them was consuming probiotics. The number of subjects was fixed in 50; for this, a 30% decrease in HOMA-IR (homeostatic model assessment for insulin resistance) index was fixed as primary outcome, based on previous nutritional clinical trials [34]. For a statistical power of 95% and an alpha value of 0.05, a number of 40 subjects was obtained, which was increased to 50 foreseeing potential withdrawals from the study. Subject were recruited by mailing and public advertisement in the Madrid region.

The study had a cross-over design, where subjects were randomly assigned (based on recruitment date) either to supplementation with GP (suspended in water) or to the C arm (since no valid placebo was found for this period, they followed their usual diet and had the same controls as in the GP period). Each period had a duration of 6 weeks, separated by a 4 week wash-out. At the beginning of the GP period, the subjects received the doses for the six weeks and were instructed to keep them frozen, as well as not to modify their dietary habits. Nevertheless, three days before each visit (at the beginning and at the end of each period) they had to follow a low polyphenol diet, for which specific instructions were provided. Random allocation sequence, participant recruitment and participant assignment to interventions were performed by the same researchers.

When each period started and finished, fasting blood and urine samples were collected. In these visits, the volunteers also provided a fecal sample from the previous 24 h. Additionally, at the beginning and at the end of the GP period, half of the participants were subjected to a fasting OGTT (oral glucose tolerance test). After ingesting 75 g of glucose in 200 mL of water, blood samples were collected at 0, 30, 60, and 120 min. Centrifugation was applied at 1000 g for 15 min in order to obtain serum and plasma samples. All biological samples were stored at  $-80^{\circ}\text{C}$ . Fasting samples were used to assess the primary outcome, as well as the other cardiometabolic markers described below. Postprandial samples were used to evaluate glucose and insulin concentration.

Once the study was finished, and after observing that GP caused a significant decrease in fasting plasma insulin, a more detailed analysis of data for this parameter was performed. It was found that in 23 of the subjects this reduction was of at least 10% (responders, GP-R) while in 26 of the subjects there was an increase (non-responder, GP-NR). This classification was then used to evaluate the modifications in other cardiometabolic markers, microbiota composition and fecal short-chain fatty acids (SCFAs).

## 2.2. Cardiometabolic Markers

The markers measured by an automatic analyzer (ADVIA Chemistry XPT System, Siemens Healthineers, Tarrytown, NY, USA) were: serum total cholesterol, HDL cholesterol, LDL cholesterol, triglycerides and high-sensitive plasma C reactive protein. Plasma insulin was determined by a commercial ELISA kit (Merck-Millipore, Burlington, MS, USA), according to the manufacturer instructions. Commercial kits were used for plasma and urine uric acid (Spinreact S.A., Sant Esteve de Bas, Spain) and urine creatinine concentration (Cromatest Linear Chemicals S.L., Montgat, Spain), used to normalize urinary determinations. The enzyme electrode method was used to assess blood glucose (in fasting and postprandial state) with a Free Style Optimum Neo blood glucose meter from Abbott (Chicago, IL, USA).

For blood pressure, mean values for two measurements made between 8:00 and 10:00 h in a quiet temperature-controlled room using an automated digital oscillometric device (Omron model M6 Comfort, Omron Corporation, Tokyo, Japan) were obtained. Height, body weight, and abdominal

perimeter were measured. Total body fat and abdominal fat were assessed by using a tetrapolar bioimpedance system (Tanita BC601, Arlington heights, IL, USA).

### 2.3. Fecal Microbiota

The levels of total bacteria and Bacteroidetes, Firmicutes, Lactobacillales, and *Bacteroides* and *Prevotella* were estimated from fecal DNA by quantitative real-time PCR (qPCR). First, a DNA extraction from the feces was performed using QIAamp DNA StoolMini Kit from Qiagen (Hilden, Germany) and then a Nanodrop 8000 Spectrophotometer (Thermo Scientific, Waltham, MA, USA) was used for quantification. A dilution to 20 ng/ $\mu$ L was performed in all DNA samples. A LightCycler 480 II (Roche, Basel, Switzerland) was employed for the qPCR experiments, performed in triplicate. The samples contained DNA (2  $\mu$ L) and a master mix (18  $\mu$ L) made of 2XSYBR (10  $\mu$ L), the corresponding forward and reverse primer (1  $\mu$ L each), and water (6  $\mu$ L). All reactions were paralleled by analysis of a non-template control (water) and a positive control. The identified regions of the 16S rRNA gene were previously tested [35–39]. They were predicted to be highly conserved amongst each studied bacterial subgroup and specific for them. The primers and annealing temperatures are detailed in Table 1.

**Table 1.** Quantitative real-time PCR (qPCR) primers and conditions.

Target Bacteria	Annealing Temperature (°C)	Sequences (5'-3')	Positive Control	Reference
Total Bacteria	65	F: ACT CCT ACG GGA GGC AGC AGT R: ATT ACC GCG GCT GCT GGC	( <sup>a</sup> )	[35]
Bacteroidetes	62	F: ACG CTA GCT ACA GGC TTA A R: ACG CTA CTT GGC TGG TTC A	<i>Bacteroides fragilis</i>	[36]
Firmicutes	52	F: CTG ATG GAG CAA CGC CGC GT R: ACA CYT AGY ACT CAT CGT TT	<i>Ruminococcus productus</i>	[37]
Lactobacillales	60	F: AGC AGT AGG GAA TCT TCC A R: CAC CGC TAC ACA TGG AG	<i>Lactobacillus acidophilus</i>	[38]
<i>Bacteroides</i>	60	F: GGT TCT GAG AGG AGG TCC C R: GCT GCC TCC CGT AGG AGT	<i>Bacteroides fragilis</i>	[39]
<i>Prevotella</i>	60	F: CAG CAG CCG CGG TAA TA R: GGC ATC CAT CGT TTA CCG T	<i>Prevotella copri</i>	[39]

<sup>a</sup> Positive control of total bacteria was the same as those the result was rated with.

The qPCR cycling conditions were: 10 s at 95 °C, then 45 cycles of 5 s at 95 °C, 30 s at primer-specific annealing temperature (Table 1), and 30 s at 72 °C (extension). Next to amplification, the specificity of the qPCR was evaluated, for which melting curve analysis was carried out by treatment for 2 s at 95 °C, 15 s at 65 °C followed by continuous increase of temperature up to 95 °C (0.11 °C/s) with five fluorescence recordings per degree Celsius. The relative DNA abundances for the different genes were calculated from the second derivative maximum of their respective amplification curves ( $C_p$ , calculated in triplicate) by considering  $C_p$  values to be proportional to the dual logarithm of the inverse of the specific DNA concentration. For this, this equation: was applied:  $[DNAa]/[DNAb] = 2^{C_{pb}-C_{pa}}$  [40]. Total bacteria was normalized as 16S rRNA gene copies per mg of wet feces (copies per mg).

### 2.4. Fecal Short-Chain Fatty Acids

SCFAs were analyzed in feces by gas chromatography. For this, a previously described method [39] was applied, incorporating several validated changes. First, the freeze-dried fecal samples were weighed (~50 mg dry matter) and a solution (1.5 mL) providing the internal standard 2-ethylbutiric acid (6.67 mg/L) and oxalic acid (2.97 g/L) in acetonitrile/water 3:7 was added. Then, SCFAs were extracted for 10 min using a rotating mixer. The suspension was centrifuged (5 min, 12,880 g) in a 5810R centrifuge (Eppendorf, Hamburg, Germany) and the supernatant filtered through a 0.45  $\mu$ m nylon filter. From this, an aliquot (0.7 mL) was diluted with acetonitrile/water 3:7 up to 1 mL. The equipment used for SCFAs analysis was a Trace 2000 gas chromatograph coupled to a flame ionization detector

(ThermoFinnigan, Waltham, MA, USA). The column was an Innowax 30 m × 530 μm × 1 μm capillary column (Agilent, Santa Clara, CA, USA). Chrom-Card software was used for data analysis.

### 2.5. Statistical Analysis

Graph Pad Prism 5 (Graph Pad Software, Inc., San Diego, CA, USA) software was used for statistical analysis. Results are provided as mean values accompanied by standard errors (SEM). For cardiometabolic markers, the variations in NR and R subjects were compared by Kruskal-Wallis test, since they did not follow a normal distribution. For microbiota composition and fecal SCFAs, normal distributions and heterogeneity of the data were evaluated, and the statistical significance was determined by Student's *t* test. Differences were considered significant when  $p < 0.05$ .

## 3. Results

### 3.1. Subject Characteristics

The study was completed by a total of 49 participants aged 20–65 with a mean age of 42.6 (SEM 1.6). The proportion of male participants was 55%. Since they must fulfill a minimum of two MetS factors, it was found that 63% already fulfilled all criteria for official MetS diagnoses. Besides overweight/obesity, 67% of the subjects exhibited hypertension and 57% of them presented glycaemia (both factors were present in 24% of total population). The less common MetS factor was hypertriglyceridemia, found in 12% of the subjects. Basal individual values for MetS factors are provided as Supplementary Material Table S1.

### 3.2. Evolution in Cardiometabolic Markers

No significant differences in the cardiometabolic markers were observed during the control (CTL) period (data not shown). Regarding the GP period, basal values for the different cardiometabolic markers, together with the variation observed in NR and R subjects, are shown in Table 2. As expected, significant differences ( $p < 0.00001$ ) were observed between NR and R subjects for plasma insulin values, since this was the criterium (insulin decrease of at least 10% due to GP supplementation) used to classify the subjects as R or NR. In R subjects, median variation (−42%) was close to mean value, while in NR subjects, the median variation (49.3%) was far from mean value, evidencing a higher dispersion in the data. Nevertheless, the mean and median increase in NR subjects would show that, in this group, insulin was not only not reduced by GP supplementation, but even increased by it. For the other parameters, significant differences were not found between R and NR subjects.

**Table 2.** Evolution in cardiometabolic parameters in subjects at high cardiometabolic risk participating in the clinical trial on grape pomace (GP) supplementation, classified according to their modifications in insulin response.

Parameter	Pre-GP Supplementation		Post-GP Supplementation (Variation, %)				p-Value *
	Whole Sample (n = 49)		Non-Responders (n = 26)		Responders (n = 23)		
	Mean	S.E.M.	Mean	S.E.M.	Mean	S.E.M.	
Body mass index (kg/m <sup>2</sup> )	31	1	−0.2	0.3	−0.1	0.2	0.618
Abdominal perimeter (cm)	103	2	0.2	0.4	−0.5	0.6	0.591
Total body fat (%)	31	1	0.1	0.8	−1.7	0.9	0.249
Abdominal fat (%)	103	2	−0.3	1.1	0.1	0.8	0.880
Systolic blood pressure (mm Hg)	120	17	−2	3	2	2	0.322
Diastolic blood pressure (mm Hg)	84	12	−1	3	2	2	0.809
Glucose (mg/dL)	98	2	7	2	1	2	0.540
Insulin (μU/mL)	8.9	1.9	82	10	−40	4	<b>&lt;0.00001</b>
HOMA-IR	2.1	0.4	100	10	−40	4	<b>&lt;0.00001</b>
Triglycerides (mg/dL)	147	21	22	8	−2	5	0.595
Total cholesterol (mg/dL)	341	48	−3	2	−5	2	0.353
HDL cholesterol (mg/dL)	47	7	0.0	2	4	2	0.200
LDL cholesterol (mg/dL)	121	17	−6	2	−8	2	0.873
Fibrinogen (mg/dL)	340	50	−0.4	2	−4	2	0.567
Plasma uric acid (mg/dL)	6	1	3	2	−0.3	1	0.548
Urine uric acid (mg/g creatinine)	490	70	−5	7	5	6	0.318

\* significant differences (<0.05) marked in bold; S.E.M., standard error of the mean.

3.3. Fecal Microbiota and SCFAs

The proportions of selected bacterial phyla, order, and genus of gut microbiota were evaluated at the beginning and the end of the supplementation (Figures 1 and 2). There were no differences between the groups in the Bacteroidetes and Firmicutes phyla. The GP supplementation tended to reduce ( $p = 0.059$ ) the proportion of the order Lactobacilliales (Figure 1E) with respect to the CTL period, while these proportions were similar in GP-R and GP-NR groups.

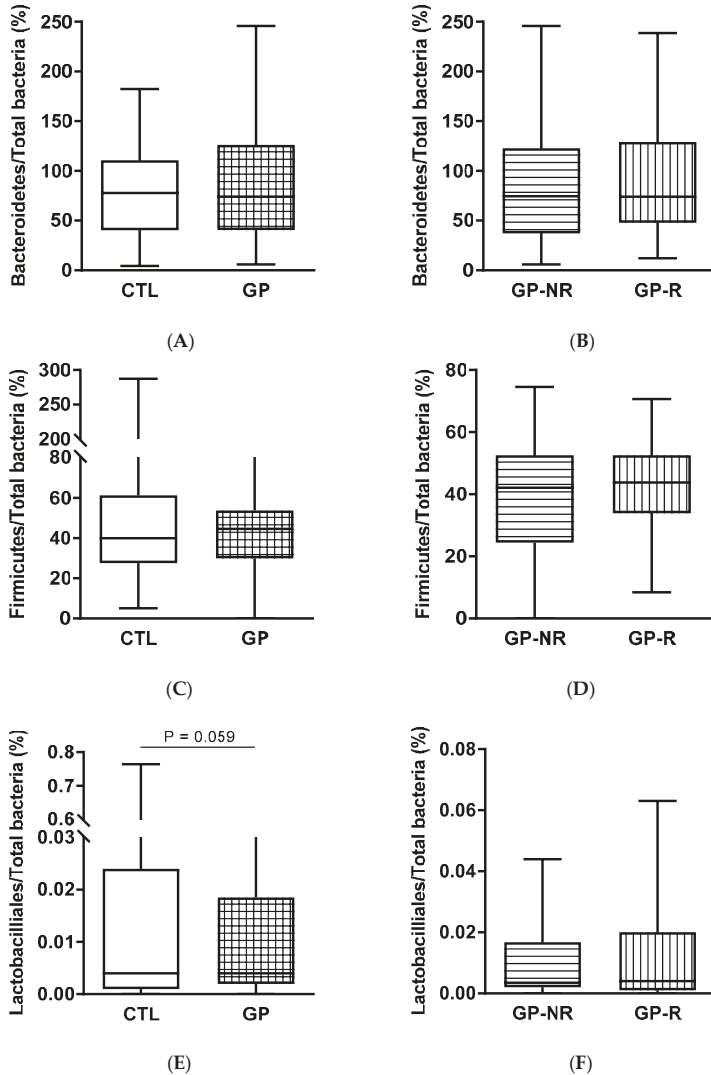


**Figure 1.** Excreted gut bacteria expressed as percentages of total bacteria in feces from subjects at high cardiometabolic risk participating in the clinical trial on grape pomace (GP) supplementation: CTL, control period without supplementation; GP, after GP supplementation; GP-NR, non-responders to GP supplementation; GP-R, responders to GP supplementation. (A,B): Bacteroidetes; (C,D): Firmicutes; (E,F): Lactobacilliales.

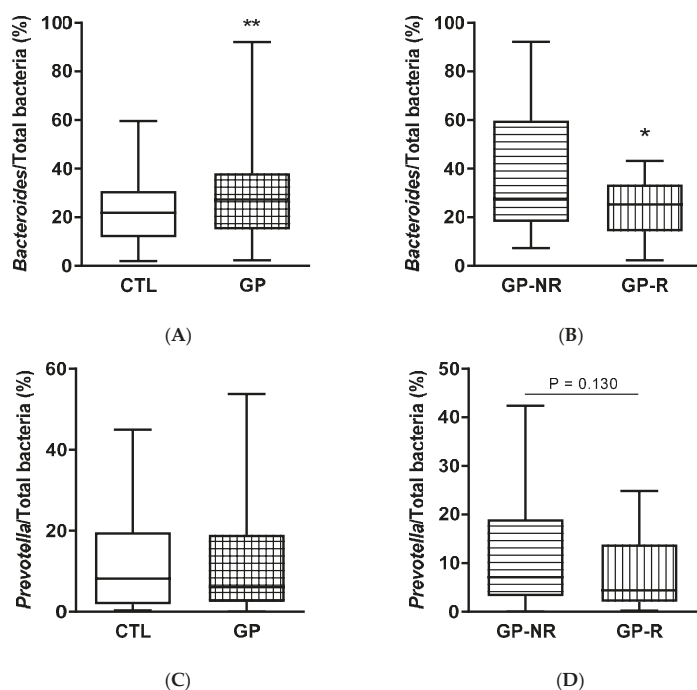


**Figure 2.** Excreted gut bacteria expressed as percentages of total bacteria in feces from subjects at high cardiometabolic risk participating in the clinical on grape pomace (GP) supplementation: CTL, control period without supplementation; GP, after GP supplementation; GP-NR, non-responders to GP supplementation; GP-R, responders to GP supplementation. (A,B): *Bacteroides*; (C,D): *Prevotella*. \*, *p*-value < 0.05; \*\*, *p*-value < 0.01.

The population of the genus *Bacteroides* was significantly (*p* < 0.01) increased by the GP intervention (Figure 2A). This difference is attributable exclusively to the GP-NR group, as the proportion of *Bacteroides* in the GP-R group was significantly (*p* < 0.05) lower than that in the GP-NR group (Figure 2B) and similar to that in the CTL period. The proportions of the genus *Prevotella* were similar between the CTL and GP periods, while there was a tendency (*p* = 0.130) to a reduction in the proportion of *Prevotella* in the R group (Figure 2D).

Fecal concentration of SCFAs were similar between periods, with the exception of isovaleric acid, that was significantly (*p* < 0.05) lower after GP supplementation than in CTL period (Table 3).

**Table 3.** Short-chain fatty acid (SCFA) concentration in feces from subjects at high cardiometabolic risk participating in the clinical trial on GP supplementation: CTL, control period without supplementation; GP, after GP supplementation; GP-NR, non-responders to GP supplementation; GP-R, responders to GP supplementation.

Compound	CTL		GP		<i>p</i> -Value	GP-NR		GP-R		<i>p</i> -Value
	Mean	SEM	Mean	SEM		Mean	SEM	Mean	SEM	
Acetic acid	120	20	120	10	0.602	110	20	118	20	0.879
Propionic acid	55	8	56	7	0.972	60	10	49	9	0.438
Isobutyric acid	6.9	0.5	6.9	0.7	0.940	6.8	0.6	7.1	1.4	0.852
Butyric acid	38	5	31.6	4.1	0.352	31	6	32	6	0.943
Isovaleric acid	7.1	0.5	5.7	0.4	<b>0.023</b> *	6.0	0.6	5.2	0.6	0.344
Valeric acid	6.8	0.8	5.8	0.7	0.435	6.1	1.0	5.6	1.1	0.731

\* significant differences (<0.05) marked in bold.

#### 4. Discussion

Polyphenols are dietary bioactive compounds able to induce subtle modifications in many physiological processes [41]. When associated with insoluble dietary fibers as it occurs in GP, their effects may be additive to those of the dietary fiber [42]. This diversity of mechanisms of action makes it difficult to elucidate the processes eventually involved in the health effects associated with polyphenol-rich dietary fibers such as GP. Gut microbiota may play a prominent role in the action of GP. As clinical trials in the field of polyphenols and microbiota are still scarce, we explored the effect of GP supplementation (a polyphenol-rich product containing both extractable and non-extractable polyphenols) on the populations of some significant subgroups of gut microbiota in subjects at cardiometabolic risk.

As observed in a previous study, where a GP extract was administered to healthy women [28], GP did not cause significant modifications in the major microbiota subgroups tested in subjects supplemented for 6 weeks. This suggests that the observed reduction of insulin levels in overweight subjects at cardiometabolic risk by GP was not induced by changes in the major subgroups of gut microbiota. A tendency ( $p = 0.059$ ) towards a decrease in the proportion of Lactobacilliales was observed after the supplementation. Although this effect may seem surprising according to the expected beneficial effects of GP and the traditional consideration of this order as a whole as beneficial bacteria, several studies have shown that this relationship is not so unequivocal. Thus, an increase in the Lactobacillaceae family was observed in mice fed industrially-generated trans-fatty acids, an effect further confirmed by in vitro fermentation of these compounds by the family Lactobacillaceae and the genus *Lactobacillus* [43]. A tendency towards an increase in Lactobacilliales was observed in subjects with Behcet's syndrome, a systemic inflammatory condition [44] and, recently, an increase in the genus *Lactobacillus* has been reported in diabetic rats, being significantly associated with an increase in body weight and adverse modification in biomarkers of glucose homeostasis and inflammation [45]. While it is still not clear whether the increase in Lactobacilliales in these adverse situations is a cause or a consequence, after observing an increase in several *Lactobacillus* spp. in an animal model of steatohepatitis, the authors suggested that this was due to their involvement in bile acid metabolism [46]. Further studies on the health effects of specific bacterial species belonging to Lactobacilliales are thus needed.

GP supplementation did not show any significant effect on the major phyla (Bacteroidetes and Firmicutes) of gut microbiota. Then, we examined the populations of the main genera within Bacteroidetes, *Prevotella* and *Bacteroides*, because the ratio between these two subgroups has been related to the intake of dietary fiber [47]. The populations of *Prevotella* were also similar in the controls and supplemented groups while *Bacteroides* significantly increased after GP supplementation. Similarly, the populations of *Bacteroides* were increased by other grape-derived products such as grape seed proanthocyanidins [48] and wine [49]. *Bacteroides* are particularly well-adapted to harsh environments through several biochemical tools, such as enzymes capable of metabolizing many diet- and host-derived polysaccharides, cytochrome bd oxidase to tolerate oxygen, and glycosyl transferases that generate a vast number of cell surface structures [50]. Our results are suggesting that *Bacteroides* are particularly equipped to degrade and use GP to foster their growth while *Prevotella* spp. remain mostly irresponsive. One of the main mediators that link gut microbiota and host metabolism are the SCFA, by fermenting indigestible dietary constituents. The changes in gut microbiota are consistent with the outcome of SCFA analysis (Table 3), which did not show any significant difference between groups.

A closer observation of the results from the human experiment revealed that the increase in the relative population of *Bacteroides* was only evident in the GP-NR group (Figure 2B). The subjects in the GP-NR group were those with significantly lower fasting plasma insulin concentration compared to those in the GP-R group, which upon GP supplementation had their insulin levels reduced (Ramos-Romero et al., *submitted*). These results evidence that the possible relationship between the *Bacteroides* sensitivity to GP and insulin responsiveness deserves further attention, including a more thorough examination at the species level.

The main limitations of this study arise from the lack of an appropriate placebo in the study design, as well as microbiota evaluation at species level. Future studies using next-generation sequencing techniques could complete the presented results. In contrast, the main strengths of the study are a cross-over design focused on overweight or obese subjects at cardiometabolic risk, as well as the comparative evaluation of microbiota between responders and non-responders to GP supplementation.

## 5. Conclusions

Results from a randomized cross-over clinical trial suggest that a reduction of insulin levels in overweight subjects at cardiometabolic risk by GP is not induced by changes in the major subgroups of gut microbiota. Those subjects non-responsive to GP supplementation experienced a significant increase in the relative population of the genus *Bacteroides*. Further studies at the species level should shed more light on the biological significance of the changes induced by GP in the gut microbiota.

**Supplementary Materials:** The following are available online at <http://www.mdpi.com/2304-8158/9/9/1279/s1>, Table S1: Basal individual values for Metabolic Syndrome factor in subjects at high cardiometabolic risk participating in the clinical trial on grape pomace supplementation.

**Author Contributions:** Conceptualization, S.R.-R., J.P.-J. and J.L.T.; Methodology, S.A., S.R.-R., J.P.-J. and J.L.T.; Investigation, M.H., D.M.-M., S.R.-R. and J.P.-J.; Resources, J.P.J. and J.L.T.; Data Curation, M.H., D.M.-M., S.R.-R. and J.P.-J.; Writing—Original Draft Preparation, S.R.-R., J.P.-J. and J.L.T.; Writing—Review & Editing, S.A., D.M.-M., S.R.-R., J.P.-J. and J.L.T.; Visualization, J.P.-J. and S.R.-R.; Supervision, S.R.-R., J.P.-J. and J.L.T.; Project Administration, S.R.-R., J.P.-J. and J.L.T.; Funding Acquisition, J.P.J. and J.L.T. All authors have read and agreed to the published version of the manuscript.

**Funding:** Funding provided by the Spanish Ministry of Science and Innovation (MINECO-FEDER grant AGL2014-55102-JIN and MINECO grant AGL2017-83599-R).

**Acknowledgments:** Roquesan Wineries are thanked for providing grape pomace. The authors are grateful to the volunteers for participating in the clinical trial. The sponsors had no role in the design, execution, interpretation, or writing of the study.

**Conflicts of Interest:** The authors declare no conflict of interest.

## Abbreviations

HOMA-IR	homeostatic model assessment for insulin resistance
MetS	metabolic syndrome
OGT	oral glucose tolerance test
GP	grape pomace

## References

- Roy, S.; Trinchieri, G. Microbiota: A key orchestrator of cancer therapy. *Nat. Rev. Cancer* **2017**, *17*, 271–285. [[CrossRef](#)] [[PubMed](#)]
- Sampson, T.R.; Debelius, J.W.; Thron, T.; Janssen, S.; Shastri, G.G.; Ilhan, Z.E.; Challis, C.; Schretter, C.E.; Rocha, S.; Gradinaru, V.; et al. Gut microbiota regulate motor deficits and neuroinflammation in a model of Parkinson’s disease. *Cell* **2016**, *167*, 1469–1480. [[CrossRef](#)]
- Ridaura, V.K.; Faith, J.J.; Rey, F.E.; Cheng, J.; Duncan, A.E.; Kau, A.L.; Griffin, N.W.; Lombard, V.; Henrissat, B.; Bain, J.R.; et al. Gut microbiota from twins discordant for obesity modulate metabolism in mice. *Science* **2013**, *341*, 1241241. [[CrossRef](#)]
- Zhang, X.; Shen, D.; Fang, Z.; Jie, Z.; Qiu, X.; Zhang, C.; Chen, Y.; Ji, L. Human gut microbiota changes reveal the progression of glucose intolerance. *PLoS ONE* **2013**, *8*. [[CrossRef](#)] [[PubMed](#)]
- Lee, S.T.M.; Kahn, S.A.; Delmont, T.O.; Shaiber, A.; Esen, O.C.; Hubert, N.A.; Morrison, H.G.; Antonopoulos, D.A.; Rubin, D.T.; Eren, A.M. Tracking microbial colonization in fecal microbiota transplantation experiments via genome-resolved metagenomics. *Microbiome* **2017**, *5*. [[CrossRef](#)] [[PubMed](#)]
- Guo, S. Insulin signaling, resistance, and metabolic syndrome: Insights from mouse models into disease mechanisms. *J. Endocrinol.* **2014**, *220*, T1–T23. [[CrossRef](#)] [[PubMed](#)]

7. Esser, N.; Legrand-Poels, S.; Piette, J.; Scheen, A.J.; Paquot, N. Inflammation as a link between obesity, metabolic syndrome and type 2 diabetes. *Diabetes Res. Clin. Pract.* **2014**, *105*, 141–150. [[CrossRef](#)] [[PubMed](#)]
8. Bonomini, F.; Rodella, L.F.; Rezzani, R. Metabolic syndrome, aging and involvement of oxidative stress. *Aging Dis.* **2015**, *6*, 109–120. [[CrossRef](#)]
9. Aguilar, M.; Bhuket, T.; Torres, S.; Liu, B.; Wong, R.J. Prevalence of the metabolic syndrome in the United States, 2003–2012. *JAMA J. Am. Med. Assoc.* **2015**, *313*, 1973–1974. [[CrossRef](#)]
10. Castro-Barquero, S.; Tresserra-Rimbau, A.; Vitelli-Storelli, F.; Domènech, M.; Salas-Salvadó, J.; Martín-Sánchez, V.; Rubín-García, M.; Buil-Cosiales, P.; Corella, D.; Fitó, M.; et al. Dietary polyphenol intake is associated with HDL-cholesterol and a better profile of other components of the metabolic syndrome: A PREDIMED-plus sub-study. *Nutrients* **2020**, *12*, 689. [[CrossRef](#)]
11. Chiva-Blanch, G.; Badimón, L. Effects of polyphenol intake on metabolic syndrome: Current evidences from human trials. *Oxidative Med. Cell. Longev.* **2017**. [[CrossRef](#)] [[PubMed](#)]
12. Álvarez-Cilleros, D.; Ramos, S.; Goya, L.; Martín, M.A. Colonic metabolites from flavanols stimulate nitric oxide production in human endothelial cells and protect against oxidative stress-induced toxicity and endothelial dysfunction. *Food Chem. Toxicol.* **2018**, *115*, 88–97. [[CrossRef](#)] [[PubMed](#)]
13. Barrett, A.; Ndou, T.; Hughey, C.A.; Straut, C.; Howell, A.; Dai, Z.; Kaletunc, G. Inhibition of alpha-amylase and glucoamylase by tannins extracted from cocoa, pomegranates, cranberries, and grapes. *J. Agric. Food Chem.* **2013**, *61*, 1477–1486. [[CrossRef](#)] [[PubMed](#)]
14. Blade, C.; Arola, L.; Salvadó, M.-J. Hypolipidemic effects of proanthocyanidins and their underlying biochemical and molecular mechanisms. *Mol. Nutr. Food Res.* **2010**, *54*, 37–59. [[CrossRef](#)]
15. Castell-Auvi, A.; Cedo, L.; Pallarés, V.; Blay, M.T.; Pinent, M.; Motilva, M.J.; García-Vallve, S.; Pujadas, G.; Maechler, P.; Ardèvol, A. Procyanidins modify insulinemia by affecting insulin production and degradation. *J. Nutr. Biochem.* **2012**, *23*, 1565–1572. [[CrossRef](#)]
16. Chou, E.J.; Keevil, J.G.; Aeschlimann, S.; Wiebe, D.A.; Folts, J.D.; Stein, J.H. Effect of ingestion of purple grape juice on endothelial function in patients with coronary heart disease. *Am. J. Cardiol.* **2001**, *88*, 553–555. [[CrossRef](#)]
17. Fraga, C.G.; Galleano, M.; Verstraeten, S.V.; Oteiza, P.I. Basic biochemical mechanisms behind the health benefits of polyphenols. *Mol. Asp. Med.* **2010**, *31*, 435–445. [[CrossRef](#)]
18. Medjakovic, S.; Jungbauer, A. Pomegranate: A fruit that ameliorates metabolic syndrome. *Food Funct.* **2013**, *4*, 19–39. [[CrossRef](#)]
19. Pan, M.-H.; Lai, C.-S.; Ho, C.-T. Anti-inflammatory activity of natural dietary flavonoids. *Food Funct.* **2010**, *1*, 15–31. [[CrossRef](#)]
20. Cueva, C.; Silva, M.; Pinillos, I.; Bartolomé, B.; Moreno-Arribas, M.V. Interplay between dietary polyphenols and oral and gut microbiota in the development of colorectal cancer. *Nutrients* **2020**, *12*, 625. [[CrossRef](#)]
21. Moorthy, M.; Chaikunapruk, N.; Jacob, S.A.; Palanisamy, U.D. Prebiotic potential of polyphenols, its effect on gut microbiota and anthropometric/clinical markers: A systematic review of randomised controlled trials. *Trends Food Sci. Technol.* **2020**, *99*, 634–649. [[CrossRef](#)]
22. Manach, C.; Milenkovic, D.; Van de Wiele, T.; Rodríguez-Mateos, A.; de Roos, B.; García-Conesa, M.T.; Landberg, R.; Gibney, E.R.; Heinonen, M.; Tomás-Barberán, F.; et al. Addressing the inter-individual variation in response to consumption of plant food bioactives: Towards a better understanding of their role in healthy aging and cardiometabolic risk reduction. *Mol. Nutr. Food Res.* **2017**, *61*. [[CrossRef](#)] [[PubMed](#)]
23. Cortés-Martín, A.; Selma, M.V.; Tomás-Barberán, F.A.; González-Sarrias, A.; Espín, J.C. Where to look into the puzzle of polyphenols and health? The postbiotics and gut microbiota associated with human metabolotypes. *Mol. Nutr. Food Res.* **2020**. [[CrossRef](#)]
24. García-Villalba, R.; Vissenaekens, H.; Pitart, J.; Romo-Vaquero, M.; Espín, J.C.; Grootaert, C.; Selma, M.V.; Raes, K.; Smagghe, G.; Possemiers, S.; et al. Gastrointestinal simulation model TWIN-SHIME shows differences between human urolithin-metabolotypes in gut microbiota composition, pomegranate polyphenol metabolism, and transport along the intestinal tract. *J. Agric. Food Chem.* **2017**, *65*, 5480–5493. [[CrossRef](#)] [[PubMed](#)]
25. Pérez-Jiménez, J.; Arranz, S.; Saura-Calixto, F. Proanthocyanidin content in foods is largely underestimated in the literature data: An approach to quantification of the missing proanthocyanidins. *Food Res. Int.* **2009**, *42*, 1381–1388. [[CrossRef](#)]

26. Bordiga, M.; Travaglia, F.; Locatelli, M. Valorisation of grape pomace: An approach that is increasingly reaching its maturity-A review. *Int. J. Food Sci. Technol.* **2019**, *54*, 933–942. [[CrossRef](#)]
27. Costabile, G.; Vitale, M.; Luongo, D.; Naviglio, D.; Vetrani, C.; Ciciola, P.; Tura, A.; Castello, F.; Mena, P.; Del Rio, D.; et al. Grape pomace polyphenols improve insulin response to a standard meal in healthy individuals: A pilot study. *Clin. Nutr.* **2019**, *38*, 2727–2734. [[CrossRef](#)]
28. Gil-Sánchez, I.; Esteban-Fernández, A.; de Llano, D.G.; Sanz-Buenhombre, M.; Guadarrana, A.; Salazar, N.; Gueimonde, M.; de los Reyes-Gavilán, C.G.; Gómez, L.M.; Bermejo, M.L.G.; et al. Supplementation with grape pomace in healthy women: Changes in biochemical parameters, gut microbiota and related metabolic biomarkers. *J. Funct. Foods* **2018**, *45*, 34–46. [[CrossRef](#)]
29. Martínez-Maqueda, D.; Zapatera, B.; Gallego-Narbón, A.; Vaquero, M.P.; Saura-Calixto, F.; Pérez-Jiménez, J. A 6-week supplementation with grape pomace to subjects at cardiometabolic risk ameliorates insulin sensitivity, without affecting other metabolic syndrome markers. *Food Funct.* **2018**, *9*, 6010–6019. [[CrossRef](#)] [[PubMed](#)]
30. Pérez-Jiménez, J.; Serrano, J.; Tabernero, M.; Arranz, S.; Díaz-Rubio, M.E.; García-Diz, L.; Goni, I.; Saura-Calixto, F. Effects of grape antioxidant dietary fiber in cardiovascular disease risk factors. *Nutrition* **2008**, *24*, 646–653. [[CrossRef](#)] [[PubMed](#)]
31. Urquiaga, I.; D'Acuna, S.; Pérez, D.; Dicenta, S.; Echeverria, G.; Rigotti, A.; Leighton, F. Wine grape pomace flour improves blood pressure, fasting glucose and protein damage in humans: A randomized controlled trial. *Biol. Res.* **2015**. [[CrossRef](#)] [[PubMed](#)]
32. Zorraquín, I.; Sánchez-Hernández, E.; Ayuda-Durán, B.; Silva, M.; Gonález-Paramás, A.M.; Santos-Buelga, C.; Moreno-Arribas, M.V.; Bartolomé, B. Current and future experimental approaches in the study of grape and wine polyphenols interacting gut microbiota. *J. Sci. Food Agric.* **2020**, *100*, 3789–3802. [[CrossRef](#)] [[PubMed](#)]
33. Alberti, K.; Eckel, R.H.; Grundy, S.M.; Zimmet, P.Z.; Cleeman, J.I.; Donato, K.A.; Fruchart, J.C.; James, W.P.T.; Loria, C.M.; Smith, S.C. Harmonizing the metabolic syndrome. A joint interim statement of the International Diabetes Federation task force on epidemiology and prevention; National Heart, Lung, and Blood Institute; American Heart Association; World Heart Federation; International Atherosclerosis Society; and International Association for the Study of Obesity. *Circulation* **2009**, *120*, 1640–1645. [[CrossRef](#)] [[PubMed](#)]
34. Grassi, D.; Desideri, G.; Necozione, S.; Lippi, C.; Casale, R.; Properzi, G.; Blumberg, J.B.; Ferri, C. Blood pressure is reduced and insulin sensitivity increased in glucose-intolerant, hypertensive subjects after 15 days of consuming high-polyphenol dark chocolate. *J. Nutr.* **2008**, *138*, 1671–1676. [[CrossRef](#)]
35. Hartman, A.L.; Lough, D.M.; Barupal, D.K.; Fiehn, O.; Fishbein, T.; Zasloff, M.; Eisen, J.A. Human gut microbiome adopts an alternative state following small bowel transplantation. *Proc. Natl. Acad. Sci. USA* **2009**, *106*, 17187–17192. [[CrossRef](#)]
36. Ismail, N.A.; Ragab, S.H.; Elbaky, A.A.; Shoeib, A.R.; Alhosary, Y.; Fekry, D. Frequency of Firmicutes and Bacteroidetes in gut microbiota in obese and normal weight Egyptian children and adults. *Arch. Med. Sci.* **2011**, *7*, 501–507. [[CrossRef](#)]
37. Haakensen, M.; Dobson, C.M.; Deneer, H.; Ziola, B. Real-time PCR detection of bacteria belonging to the Firmicutes Phylum. *Int. J. Food Microbiol.* **2008**, *125*, 236–241. [[CrossRef](#)]
38. Walter, J.; Hertel, C.; Tannock, G.W.; Lis, C.M.; Munro, K.; Hammes, W.P. Detection of *Lactobacillus*, *Pediococcus*, *Leuconostoc*, and *Weissella* species in human feces by using group-specific PCR primers and denaturing gradient gel electrophoresis. *Appl. Environ. Microbiol.* **2001**, *67*, 2578–2585. [[CrossRef](#)]
39. Schwertz, A.; Taras, D.; Schafer, K.; Beijer, S.; Bos, N.A.; Donus, C.; Hardt, P.D. Microbiota and SCFA in lean and overweight healthy subjects. *Obesity* **2010**, *18*, 190–195. [[CrossRef](#)] [[PubMed](#)]
40. Pfaffl, M.W. A new mathematical model for relative quantification in real-time RT-PCR. *Nucleic Acids Res.* **2001**. [[CrossRef](#)]
41. De Pascual-Teresa, S.; Clifford, M.N. Advances in polyphenol research: A journal of agricultural and food chemistry virtual issue. *J. Agric. Food Chem.* **2017**, *65*, 8093–8095. [[CrossRef](#)]
42. Holscher, H.D. Dietary fiber and prebiotics and the gastrointestinal microbiota. *Gut Microbes* **2017**, *8*, 172–184. [[CrossRef](#)] [[PubMed](#)]
43. Ge, Y.; Liu, W.; Tao, H.; Zhang, Y.; Liu, L.; Liu, Z.; Qiu, B.; Xu, T. Effect of industrial trans-fatty acids-enriched diet on gut microbiota of C57BL/6 mice. *Eur. J. Nutr.* **2019**, *58*, 2625–2638. [[CrossRef](#)] [[PubMed](#)]

44. Consolandi, C.; Turrone, S.; Emmi, G.; Severgnini, M.; Fiori, J.; Peano, C.; Biagi, E.; Grassi, A.; Rampelli, S.; Silvestri, E.; et al. Behcet's syndrome patients exhibit specific microbiome signature. *Autoimmun. Rev.* **2015**, *14*, 269–276. [[CrossRef](#)] [[PubMed](#)]
45. Álvarez-Cilleros, D.; Ramos, S.; López-Oliva, M.E.; Escrivá, F.; Álvarez, C.; Fernández-Millán, E.; Martín, M.A. Cocoa diet modulates gut microbiota composition and improves intestinal health in Zucker diabetic rats. *Food Res. Int.* **2020**. [[CrossRef](#)]
46. Zeng, H.; Liu, J.; Jackson, M.I.; Zhao, F.-Q.; Yan, L.; Combs, G.F., Jr. Fatty liver accompanies an increase in Lactobacillus species in the hind gut of C57BL/6 mice fed a high-fat diet. *J. Nutr.* **2013**, *143*, 627–631. [[CrossRef](#)]
47. Wu, G.D.; Chen, J.; Hoffmann, C.; Bittinger, K.; Chen, Y.-Y.; Keilbaugh, S.A.; Bewtra, M.; Knights, D.; Walters, W.A.; Knight, R.; et al. Linking Long-Term Dietary Patterns with Gut Microbial Enterotypes. *Science* **2011**, *334*, 105–108. [[CrossRef](#)]
48. Casanova-Martí, A.; Serrano, J.; Portune, K.J.; Sanz, Y.; Blay, M.T.; Terra, X.; Ardèvol, A.; Pinent, M. Grape seed proanthocyanidins influence gut microbiota and enteroendocrine secretions in female ratst. *Food Funct.* **2018**, *9*, 1672–1682. [[CrossRef](#)]
49. Queipo-Ortuño, M.I.; Boto-Ordóñez, M.; Murri, M.; Gómez-Zumaquero, J.M.; Clemente-Postigo, M.; Estruch, R.; Cardona-Díaz, F.; Andrés-Lacueva, C.; Tinahones, F.J. Influence of red wine polyphenols and ethanol on the gut microbiota ecology and biochemical biomarkers. *Am. J. Clin. Nutr.* **2012**, *95*, 1323–1334. [[CrossRef](#)]
50. Wexler, A.G.; Goodman, A.L. An insider's perspective: Bacteroides as a window into the microbiome. *Nat. Microbiol.* **2017**, *2*, 17026. [[CrossRef](#)]



© 2020 by the authors. Licensee MDPI, Basel, Switzerland. This article is an open access article distributed under the terms and conditions of the Creative Commons Attribution (CC BY) license (<http://creativecommons.org/licenses/by/4.0/>).

MDPI  
St. Alban-Anlage 66  
4052 Basel  
Switzerland  
Tel. +41 61 683 77 34  
Fax +41 61 302 89 18  
[www.mdpi.com](http://www.mdpi.com)

*Foods* Editorial Office  
E-mail: [foods@mdpi.com](mailto:foods@mdpi.com)  
[www.mdpi.com/journal/foods](http://www.mdpi.com/journal/foods)





MDPI  
St. Alban-Anlage 66  
4052 Basel  
Switzerland

Tel: +41 61 683 77 34  
Fax: +41 61 302 89 18

[www.mdpi.com](http://www.mdpi.com)



ISBN 978-3-0365-1157-3